

**Ventilation for Energy Efficiency and Optimum
Indoor Air Quality
13th AIVC Conference, Nice, France
15-18 September 1992**

Paper 2

**Healthy Building: An Energy Efficient Air
Conditioned Office With Good Indoor Air Quality.**

Don Dickson* and Peter Collins**

*** EA Technology, Capenhurst, Chester, CH1 6ES,
UK**

*** NORWEB HQ, Talbot Road, Manchester, M16
0HQ, UK**

Healthy Building: An energy efficient air conditioned office with good indoor air quality.

Synopsis

The NORWEB Headquarters in Manchester, UK, is an air conditioned energy efficient office building of unusual design, completed in 1988. It has three stories with overhanging canopies providing solar shading and 21% solar control glazing. The open plan interior is ventilated by a displacement system with three twist outlets in the floor to each desk position.

A detailed questionnaire survey showed this to be one of the 'healthiest' buildings tested so far, with a very low 'building sickness symptom score'.

Air temperature, humidity, air speed, fresh air, noise, dust and lighting were monitored and found to lie within accepted guidelines. Fine dust levels were lower than outside.

Energy costs monitored over three years proved to be low for a building of this type.

The achievement of good indoor air quality combined with energy efficiency is attributed to good passive design features, the displacement ventilation system, a limited smoking policy and active participation of the end user at all stages of the design, construction and management of the building.

1 Introduction

1.1 Building design

The NORWEB Headquarters in Manchester is a purpose built office building which was completed in 1988. The plan, Figure 1, comprises a central core with two wings per floor which are mainly open plan. The three floors progressively decrease in area providing balconies and walkways which give solar shading, access for maintenance and a striking external appearance.

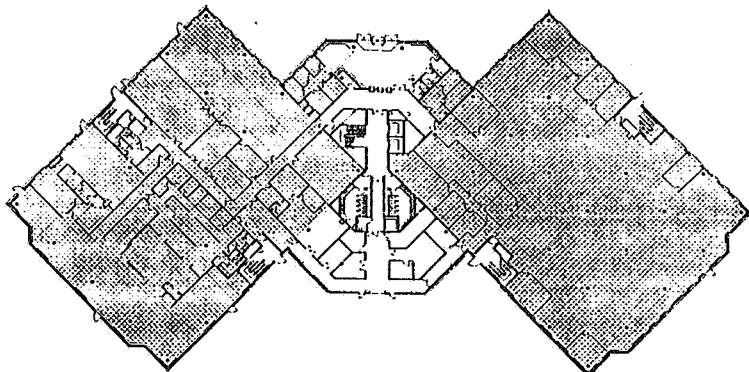


Figure 1 Norweb HQ floor plan.

The design brief was for an all electric building which would provide the best possible working conditions combined with operational flexibility, ease of maintenance and energy efficiency. The plan had to accommodate present and future information technology requirements

The original brief also included an instruction to include energy conservation features which had a payback period of three years or less.

1.2 Passive design features

The main structure is of reinforced concrete providing a long thermal time constant. 21% of the wall area is glazed with solar control double glazing (U-value $1.6 \text{ W/m}^2\text{K}$). This moderate window area provides a useful degree of contact with the outside without causing problems for the heating and ventilating system. Solar shading is provided by overhanging canopies to all floors, while balconies provide access for maintenance, as shown in Figure 2.

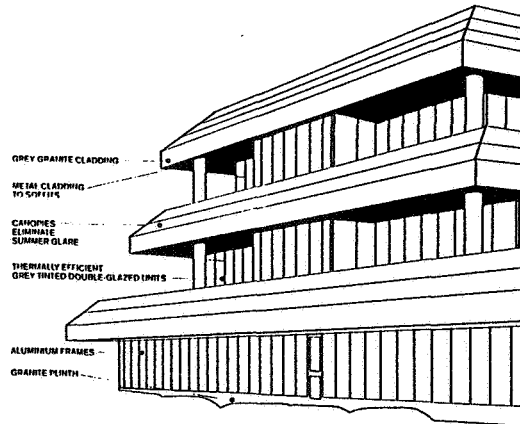


Figure2 Overhanging canopies and balconies.

1.3 Thermal Performance

Walls, floor and roof are insulated to U-values of 0.48 , 0.12 , and $0.28 \text{ W/m}^2 \text{ K}$ respectively. The design day (-4 C) heat loss is 443 kW equivalent to $45.5 \text{ Watts/square metre}$ of floor area.

The number of occupants is 540 , equivalent to a thermal contribution of about 65 kW . The net usable space allocation overall is about $9.75 \text{ square metres}$ per person and in the open plan areas the space per person, is about $6.5 \text{ square metres}$.

2. Heating and ventilating system

2.1 Air conditioning

The open plan areas are provided with air at a fixed flow rate. Nominally 25% of this is fresh outside air, the rest being recycled. The total air flow rate is nominally $8 \text{ air changes/hour}$. Tracer decay tests showed that the actual fresh air ventilation rate in the open plan areas was $1 \text{ air change/hour}$. This is equivalent to $10\text{-}14 \text{ litre/second per}$

person, which is generous compared to the CIBSE and ASHRAE guidelines of 8-10 litres/second per person.

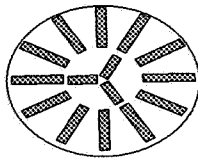
Exhaust air passes through heat recovery coils with heat pumps transferring heat to the low pressure hot water system as preheat for the building hot water services. The chillers for the air conditioning plant reject heat which cannot be used for heating other parts of the building to an open cooling tower on the roof. To reduce running costs, the chilled water temperature is controlled between 10 and 20°C depending on the cooling load requirements.

2.2 Heating

The heating system consists of two water to water heat pumps each electrically loaded at 135 kW, incorporating double bundle condensers. Heat is extracted from the cooling coils within each extract plant in sequence.

Heat to the main heater batteries and volume control box reheat coils is supplied in sequence from the heating condenser and hot water storage vessels with a total stored volume of 35000 litres at a temperature of 135 C. The two megatherm boilers, each rated at 234 kW, are supplied with night electricity using the cheapest 14 half hour periods between 2200 and 0630 daily.

2.3 Air distribution



The air is supplied via an under floor plenum to 'twist' outlet grilles Figure 3, nominally three per desk which provide a rapidly decaying spiral of air at low speed. The air speed in the vicinity of the grilles has dropped to the low ambient level of 0.1 m/s within a radius of 0.25m and a height of 0.6m. Air return is through the light fittings.

Figure 3 Twist outlet.

The underfloor plenum also acts as an easily accessible services distribution duct; the floor is in easily removable sections 600x600mm. This also makes it easy to reposition the twist outlets when desks have been moved.

With cool air being supplied at low speed at floor level, and ceiling extract, the system acts in a displacement ventilation mode.

2.4 Control system

Each open plan office area is controlled in 2 central zones (east and west) plus a perimeter, and control is by two averaging thermostats operating the individual heater or cooler batteries. Overall control is through a computer energy management system which monitors and controls all the main plant, flow and return temperatures. The plant

is switched off, to minimise energy usage, when:

- (a) the building is unoccupied,
- or (b) when predetermined conditions are reached.

The preheat/building response time is automatically adjusted by optimisers in the energy management system. The longest pre-heat period occurred in the worst of the four winters, on a Monday morning after being switched off all weekend, when the system switched on at 0100 for an 0800 occupancy.

3 Lighting

3.1 Design

In general, the lighting installation in the offices was designed to use fluorescent luminaires of the air handling type incorporating high frequency low-loss electronic ballast equipment, and low brightness diffusers complying with TM6, the CIBSE Lighting Guide for Visual Display Units (now LG3).

The design encompassed the three main human working requirements of comfort, satisfaction and performance. The office complex supports a diverse operation including all aspects of office work such as reading/writing reports, drawing office, transferring information from documents at computer terminals, full time word processing at VDU screens, desk top publishing, electricity utilisation/environmental design work and planning the electricity supply network.

Task lighting is supplied where needed.

3.2 Operation

The lighting load is 136 kW, i.e 14 Watts/square metre, with 7 kW of emergency lighting. Control is by localised manual switching and also by the computer energy management system.

The illumination levels in the office areas are between 500 and 600 lux at desk level with a mean of 525 lux and a standard deviation of 100 lux. Subjectively, a questionnaire survey showed that over 90% of all the office staff were satisfied with their lighting scheme.

4 Water heating

Hot water to the kitchen and toilets is heated electrically by day and night (cheap rate) immersion heaters, after the cold water feed has been pre-heated by a loop off the low pressure hot water heat recovery coils.

5 Environmental assessment

5.1 Subjective survey

A self completion questionnaire survey of the occupants was carried out in two open plan wings of the building . The questionnaire was one developed for studies in offices by Building Use Studies Ltd, who also carried out the survey for EA Technology. The questions covered type of work, smoking habits, VDU usage, environmental comfort, and the various symptoms which have come to be associated with sick building syndrome. 166 questionnaires were distributed and 147 returned.

Respondents were presented with a list of eight symptoms associated with Sick Building Syndrome; the most common symptom experienced was lethargy, followed in turn by headache, stuffy nose, dry throat, dry eyes, itching eyes, flu-like symptoms and runny nose. A symptom was counted if experienced on more than two occasions in the past year and improved on leaving the building. The 'building sickness score' is the average number of symptoms per person, i.e. the lower the score the 'healthier' the building. A survey [1] of over 4000 workers in 47 buildings carried out on 1985/86 found building sickness scores between 1.25 and 5.25 depending mainly on the type of building; mean values were as follows:

- 2.18 in mechanically ventilated buildings
- 2.49 in naturally ventilated buildings
- 3.41 in centrally air conditioned
- 3.81 in those with local air conditioning.

The building sickness score for this building was 1.68 making it the best air conditioned building found by ourselves so far. 38% of the sample reported no symptoms at all; in common with other buildings those who did suffer did so frequently, on most days

The most common response on environmental comfort factors (i.e. thermal comfort, ventilation, noise and lighting) was the neutral point of a seven point scale, except for noise. Most people found the conditions satisfactory:

	1	2	3	4	5	6	7
%	satisfactory			neutral	unsatisfactory		
thermal comfort		56		31		13	
ventilation		49		31		20	
noise level		40		24		36	
lighting		53		31		16	

Satisfaction with the noise level was lower than for other comfort factors and, in reply to a supplementary question, 56% of respondents judged the noise level to be loud and intrusive.

Two thirds of the sample were to some degree dissatisfied with the privacy at their desks, most people felt that they had little or no control over their environmental conditions and found their job fairly stressful. These factors did not relate to number of symptoms reported.

The number of symptoms was significantly related to dissatisfaction with environmental comfort factors. Women clerical workers experienced more symptoms than other categories of workers.

The sample consisted of mainly professional males (47%) and clerical females (25%) with 59% of them under 40 years old. Only 13% were current smokers, compared with 22% in the Office Environment Survey. The office has a no-smoking policy at desks so that there is virtually no passive smoking in the building. Most people use a VDU regularly, but usually less than 3 hours per day.

5.2 Physical survey

A measurement survey of environmental factors was carried out at the same time as the subjective survey.

Air temperature was found to be very uniform in space and time. During a week in September, when the outside temperature was 12 C, the temperature at sitting head height (1.2m) was 23 ± 0.5 C falling to 22 C over the weekend and rising to 24 C on some afternoons. Ankle temperatures were generally 0.5 C cooler; ceiling temperatures up to 1 C warmer. Relative humidity was $50 \pm 5\%$.

Air speeds were generally about 0.1m/s, and always less than 0.2m/s.

At the occupancy found during the survey (carried out on a normal working day in September), the fresh air rate as measured by tracer decay was of the order 14 l/s per person. This generous fresh air rate was reflected in the relatively low carbon dioxide concentration, which showed a peak of 560 ppm mid-morning and mid-afternoon.

The equivalent continuous sound level L_{eq} was nearly 60 dBA which would generally be considered too noisy for sedentary workers. The CIBSE Guide [2] recommends NR45 (equivalent to about 51dBA) for a landscaped office.

The indoor dust level in the particle size range 0.25 to 8 microns was less than outside, particularly in the range 1 to 2 microns where the ratio of indoor to outdoor dust was 1:20. However the dust level for particles larger than 8 microns was greater than outside.

5.3 Microbiological survey

Samples of water were taken from the mains tap in the kitchen, cold water storage tanks, humidifiers, calorifiers, cooling tower distribution troughs. All systems were free of legionellae. All water systems were found to be in excellent condition and very clean, although the bacteria counts in the calorifiers and cooling towers were higher than elsewhere.

Air sampling inside the building showed a yeast and mould count lower than outside.

6 Energy analysis

The building is all-electric with a sub-station on site serving two 800kVA transformers. The high voltage input is metered, with low voltage submetering on each transformer, chiller and megatherm boiler, and also the plant room, sports/social club and kitchen. Lighting and general power are deduced as the difference between total and submetered loads.

The monthly energy consumption has been monitored over the three years since the building was commissioned. The sports and social club is in a separate building and the kitchen is excluded as not being part of the office for the purpose of this paper.

To allow for different month lengths, and variations in date of meter readings, the monthly kWh figures have been converted into daily mean power data in Watts/m² by dividing by (number of days x 24 x floor area). Figure 4 shows the itemised figures together with the appropriate monthly degree day data to base 15.5 C for Manchester.

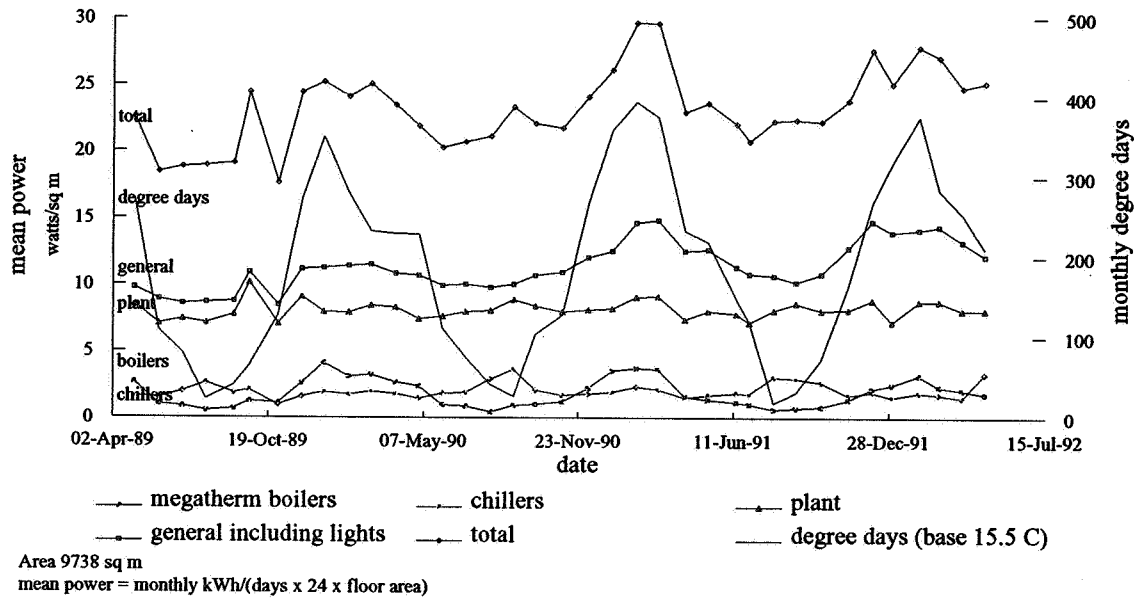


Figure 4 Monthly mean power data

The corresponding annual (1st April to 31st March) energy consumptions in kWh/m² are:

year	boilers	chillers	plant	general and lighting	total energy	corrected total energy
1989/90	17.1	15.7	69.7	86.9	189.4	172
1990/91	16.3	18.3	71.4	100.6	206.6	188
1991/92	14.2	17.7	71.1	109.3	212.3	193

For comparison with other offices, allowance must be made for the length of the working day. Since moving into this new building, owing to changes brought about by

privatisation of the Electricity Supply Industry in the UK, staff office hours have been longer than normal office hours and the building has been in use for 12 to 14 hours per day (for 5 days pr week) rather than the usual commercial working day of 10 hours. A factor of 1.1 has been applied to the energy figures to allow for this. The degree days for the three yearly periods are 2089, 2044 and 2045 respectively.

Figures collected by the UK Energy Efficiency Office [3] show that energy consumption in offices varies from 100 to 1000 kWh per year per square metre of treated floor area. A typical prestige 'good practice' air conditioned office runs at about 400 kWh/m². The figures for the Norweb office are seen to be about half this value.

7 Indoor air quality and energy efficiency

By all the normal measures of indoor air quality, and by subjective assessment the environment inside this air conditioned building, the conditions are very acceptable. The general impression of a comfortable pleasant office is reflected in the low incidence of 'building sickness' symptoms. If there were any complaints it was that it was sometimes slightly too warm, dry rather than humid and perhaps somewhat noisy. However the majority were comfortable. The no-smoking policy assists in achieving good indoor air quality.

Energy efficiency has been achieved by attention to detail at all stages of the design construction and operation. The occupiers were intimately involved throughout. Passive design features are mainly modest glazing and solar shading. Aesthetically the building is interesting both inside and out. Design decisions which contribute to the success are the underfloor plenum and associated displacement ventilation system; this provides efficient ventilation and a services duct which is easily accessible. The building and its systems are well managed by staff who understand them.

8 Conclusions

In a deep plan air conditioned office it is possible to achieve good indoor air quality and energy efficiency. Appropriate design decisions for the building shell (glazing and shading) plus wise choice of heating and ventilating plant (displacement ventilation) combined with good management, and involvement of the end users at all stages of the project explain the success of this building.

9 References

1. Wilson S and Hedge A. "A study of building sickness "
The Office Environment Survey. Building Use Studies, May 1987.
2. CIBSE Guide Volume A. The Chartered Institution of Building Service Engineers.
- 3 Energy Efficiency Office (UK). Energy consumption guide 19:
Energy efficiency in offices (October 1991).

**Ventilation for Energy Efficiency and Optimum
Indoor Air Quality
13th AIVC Conference, Nice, France
15-18 September 1992**

Poster 8

**Practical Guidelines for Using Tracer Gases for the
Evaluation of Ventilation Systems.**

R A Grot

**Lagus Applied Technology, 18159 Village Mart
Drive, Suite 242, Olney, MD 20832, USA**

Abstract
13th AVIC Conference
Nice, France

Practical Guidelines for Using Tracer Gases for the Evaluation of Ventilation Systems

Richard A. Grot
Lagus Applied Technology
18159 Village Mart Dr. Suite 242
Olney, MD 20832
USA

Over the years there has been significant advance in the development of experimental methods and analysis for the use of tracer gases in the evaluation of ventilation systems. As a rule, these advances have been in the direction of greater complexity and more sophisticated data analysis methods. Most of these advances are difficult for buildings researchers to understand, not to mention the confusion they have created for practitioners. This paper will attempt to return to basics and give guidelines for the practical application of tracer gas methods for the evaluation of building ventilation systems. Methods which can be applied in a period of several hours without the use of sophisticated equipment will be emphasized. Simple but accurate data analysis methods will be presented including how to analyze data when equilibrium or steady state is not obtained. The guidelines will include: simple methods to inject tracer into a building and obtain good mixing, methods to gather integral tracer gas samples, strategies for selecting the location of injection, the location of sampling, the time interval between samples, the duration of the test and the selection of appropriate analysis methods. Examples will be given from the author's experience in evaluating commercial and industrial facilities.

**Ventilation for Energy Efficiency and Optimum
Indoor Air Quality
13th AIVC Conference, Nice, France
15-18 September 1992**

Poster 2

**Air Movements & Air Change Rates Within Nucleus
Hospitals.**

R E Edwards, C Irwin

**Dept of Building Engineering, UMIST, P O Box 88,
Sackville Street, Manchester, M60 1QD**

Abstract

The Nucleus Hospital programme has been progressed by the Department of Health for over a decade. The Maidstone District General Hospital was the first project which involved the construction of a complete hospital using the Nucleus design concept. Within a hospital, air movement patterns and air change rates are a prime concern in the case of Maidstone, the interest in these parameters was much greater in view of the fact that a natural ventilation strategy had been chosen for ward units.

This paper describes a series of measurements made at Maidstone using the UMIST PCS multiple tracer gas system, and discusses the results obtained.

Introduction

The Department of Health has had a long standing interest in the Nucleus system of hospital design. Under this system, the main medical services are located within the core of the hospital, whilst ward units spread out from the central core; in effect, the Nucleus system is modular, with clear advantages in terms of simplicity of layout and ease of extension. The first prototype ward was constructed at Pinderfields Hospital, Wakefield, whilst the first stand alone hospital unit was built at Maidstone, Kent.

It was intended that the fresh air requirements of ward units be met by natural ventilation. Because of this, the Department of Health was keen to quantify the relative contributions of various air leakage paths to the total air leakage rate, and also to determine the nature and magnitude of air movement routes from ward units to adjacent cells within the building envelope. To this end, the Department of Building Engineering at UMIST was commissioned to undertake a series of fan pressurisation and multiple tracer gas tests within a ward unit at the Maidstone Hospital.

Experimental details

1) Test ward

The ward unit tested is situated on the first floor of the hospital (Figure 1), and lies on the east face of the building. It communicates with the adjacent corridor via double self-closing doors on the north side of the ward, whilst the adjacent ward on the south side is connected by means of double fire escape doors which are normally kept closed. The ward has a suspended T-frame ceiling with lightweight vein finished tiles spring-clipped into position. The roof void above the suspended ceiling is ventilated by means of a continuous ventilation opening at ridge height.

As has been previously mentioned, ward units within the Maidstone Hospital were so designed as to be ventilated naturally. The test ward has three louvred windows within the east facing wall: in addition, three remotely controlled opening roof lights are available to provide high level ventilation.

2) Tests performed

The schedule of tests performed can be conveniently divided into five groups:

- Group 1: air leakage testing to determine the contributions of a range of fabric components to background air leakage. These tests were undertaken using standard fan pressurisation equipment;
- Group 2: tracer gas decay tests to determine air infiltration rates within the ward, and to demonstrate the effects of door opening, window opening, and the influence of air infiltration through the suspended ceiling;
- Group 3: tracer gas tests to determine the air flows from ward to ceiling void;
- Group 4: tracer gas tests to determine air movements between the ward and the adjacent corridor, and to demonstrate the effects of door and window opening;
- Group 5: tracer gas tests to determine air movements between the ward ceiling void and the ceiling void over the adjacent corridor, and to demonstrate the effect of opening the ward windows.

All the tests in Groups 2 to 4 were performed using the parallel column system (PCS) tracer gas equipment developed at UMIST. This equipment is well documented in the literature (for example, reference 1) and will not be described here.

Results and Discussion

The results of the group 1 tests are summarised in Table 1. It should be noted that the upper limit of the range of applied pressure differentials used during the test programme was limited to approximately 30 Pascals, due to the suspended ceiling showing signs of buckling. Values of Q_{50} have been obtained by using the extrapolation procedure described by Kronvall (2).

The results show that the ceiling construction provides 41% of the air leakage paths within the ward fabric. Cracking around doors provides 27% of the total, whilst the remaining

31% can be attributed to the external fabric, gaps around windows, service duct and pipe entries, and light fittings in the ceiling.

The results of the Group 2 tests are shown in Figure 2, plotted against mean wind velocity at roof height. (Internal/external pressure differences and temperature differences were also recorded during the study, but are not considered here). Unsealing the suspended ceiling increases the air change rate within the ward by approximately 50%; when the doors are unsealed, the ward air change rate increases on average by approximately 52%. The results for the ceiling unsealed case correlated very closely with the air leakage tests in Group 1. This is not the case for the data generated with the ceiling and doors unsealed. It should be noted, however, that the mean wind speeds experienced during these latter tests were rather higher than for the former. Pressure data taken during these tests show a positive pressure difference of between 2 and 4 Pascals between the outside face of the building and the ward, and a negative pressure difference of between 0.05 and 0.3 Pascals between the ceiling void and the ward. The existence of the positive pressure difference across the leeward face of the building probably owes its existence to a vortex in the courtyard adjacent to the ward. The negative pressure difference between ward ceiling void and ward is almost certainly caused by the continuous ridge ventilator. No low level openings are provided to encourage cross-flow ventilation. In the light of the recommendations given in reference 3, it is highly likely that the use of high level ventilation on its own is resulting in depressurisation of the ceiling void.

The results of the Group 3 tests are shown in Figure 3. With the door and window shut a 35–45m³/hr air flow exists between ward to ward ceiling void; in other words, approximately 50% of the air leaving the ward does so through the suspended ceiling. When the doors and windows are opened, the proportion of air leaving the ward via the suspended ceiling drops to between 20% and 40%.

Group 4 test results are presented in Figure 4. It is apparent that a two directional air flow exists between the ward and the adjacent corridor, and that the relative sizes of the two air flow components are dependent upon window and door openings. When the doors and windows are closed, the outflow from ward to corridor is between 64 and 80m³/hr, and the

inflow from corridor to ward is between 14 and 36m³/hr. When the doors to the corridor and the ward windows are opened, the outflow increases to between 107 and 150m³/hr, whilst the inflow falls to between 6.5 and 10m³/hr.

Consideration of subsidiary data not presented in this paper reveals that ward and corridor air temperatures are essentially the same, whilst a positive pressure difference of between 3 and 9 Pascals exists between the ward and corridor. The test data is broadly in agreement with the work of Shaw (4, 5) and Lidwell (6); careful study to these three references is commended to any reader interested in the influence of pressure and temperature differentials upon two-way air flows through openings.

The results for the Group 5 tests (Figure 5) are interesting, since they reveal that a one-directional air flow exists between the ward ceiling void and the ceiling void above the adjacent corridor. The magnitude of the air flow is influenced very strongly by the opening of ward windows. With the windows closed the air flow is between 60 and 85m³/hr; with the windows open, the air flow increases to between 81 and 118m³/hr. Inspection of pressure data relevant to the test periods show increased positive pressure differences between ward and ward ceiling void, and between ward ceiling void and corridor ceiling void. Inspection of the partition wall between the two ceiling voids reveals potential air flow paths in the form of large gaps around service pipes. Although time constraints curtailed suitable tracer gas tests from being performed, it is the opinion of the authors that better sealing around service pipe penetrations would significantly reduce the air flow.

Conclusions

The air flows between interconnected cells within the Maidstone Nucleus Hospital have been shown to be influenced by wind speed, wind direction, temperature differences and door/window opening patterns. The clearest finding is that the suspended ceiling constitutes an extremely important air leakage path, and that the nature of the void above not only results in the flow of air from the ward upwards, but also from the void to the adjacent corridor roof void.

Acknowledgement

This programme of work was commissioned by the NHS Estates Agency of the Department of Health and this paper is published with their permission.

References

- 1) C Irwin and R E Edwards, "The measurement of air flows using a rapid response tracer gas technique", BSER&T, Vol. 6, No. 4, pp145-152, 1985
- 2) J Kronvall, PhD Thesis, 1981.
- 3) British Standards Institution, "Control of Condensation in Buildings", BS 5250, 1989.
- 4) B H Shaw, "Heat and mass transfer by natural convection and combined natural convection with forced air flow through a large rectangular opening in a vertical partition", Institute of Mechanical Engineers Conference, Volume C819, 1972.
- 5) B H Shaw and W Whyte, "Air movement through doorways", Building Services Engineer, Vol. 42, 1974.
- 6) O M Lidwell, "Airborne infection in a fully air conditioned hospital", Journal of Hygiene, 75, p.141, 1977.

Table 1: Results of pressurisation tests performed at Maidstone Hospital.

Test No.	Condition	Leakage rate
45	Doors and ceiling sealed	0.667m ³ /s at 50 Pa
46	Doors only sealed	1.567m ³ /s at 50 Pa
47	Ceiling sealed, doors unsealed	1.083m ³ /s at 50 Pa
48	No sealing	2.133m ³ /s at 50 Pa

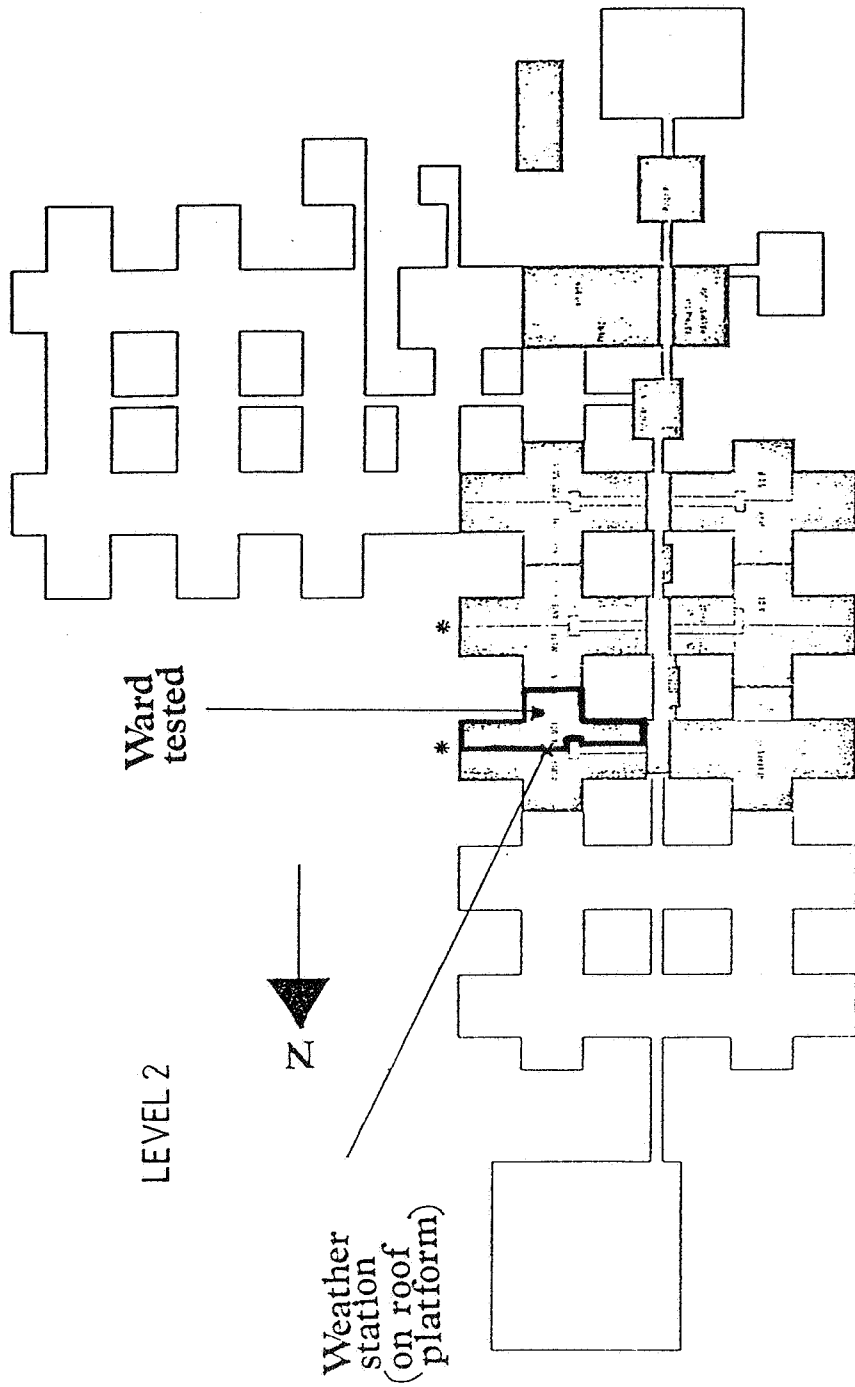


FIGURE 1

WEST WIND

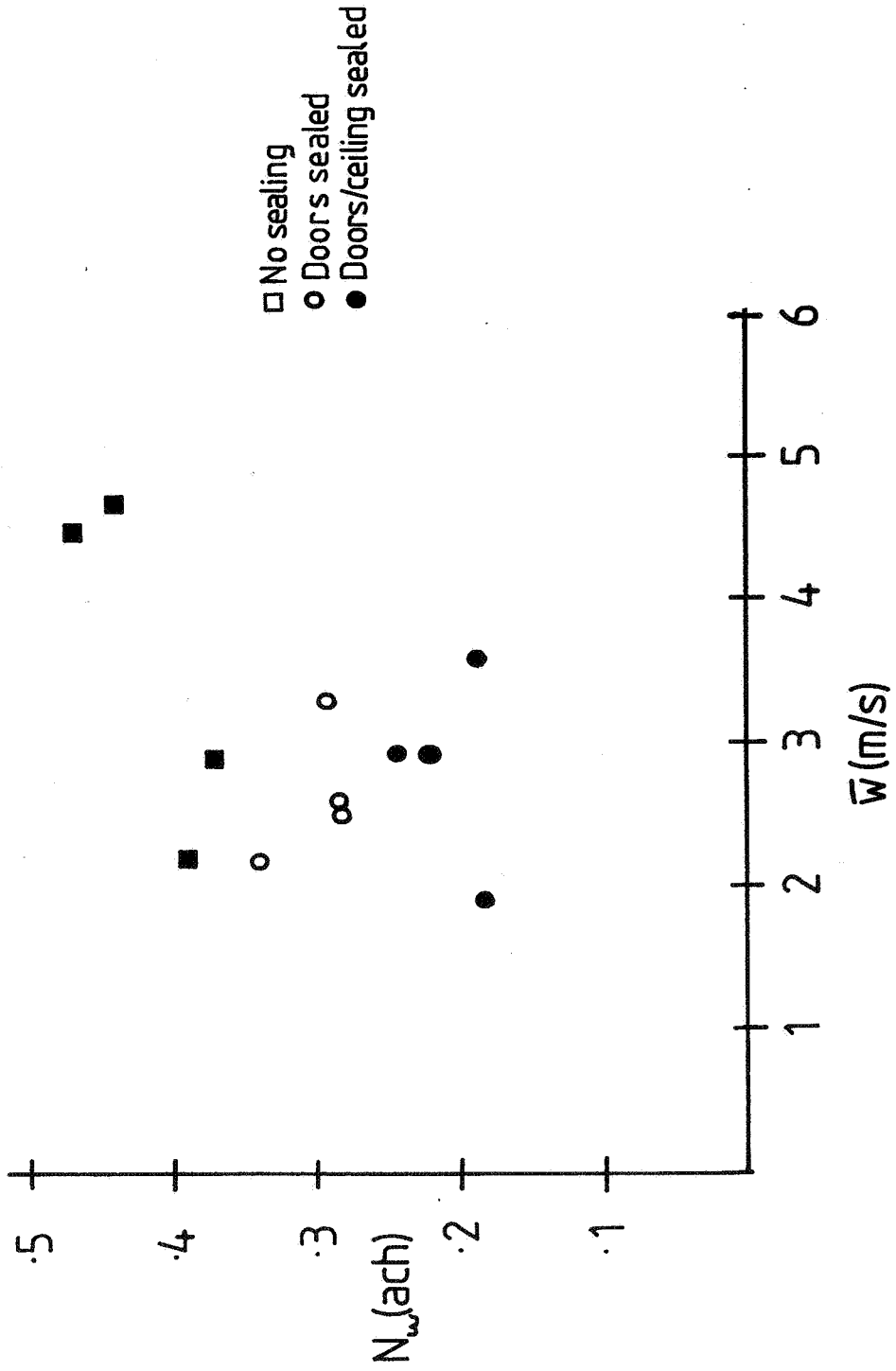


FIGURE 2

NORTH-EAST WIND

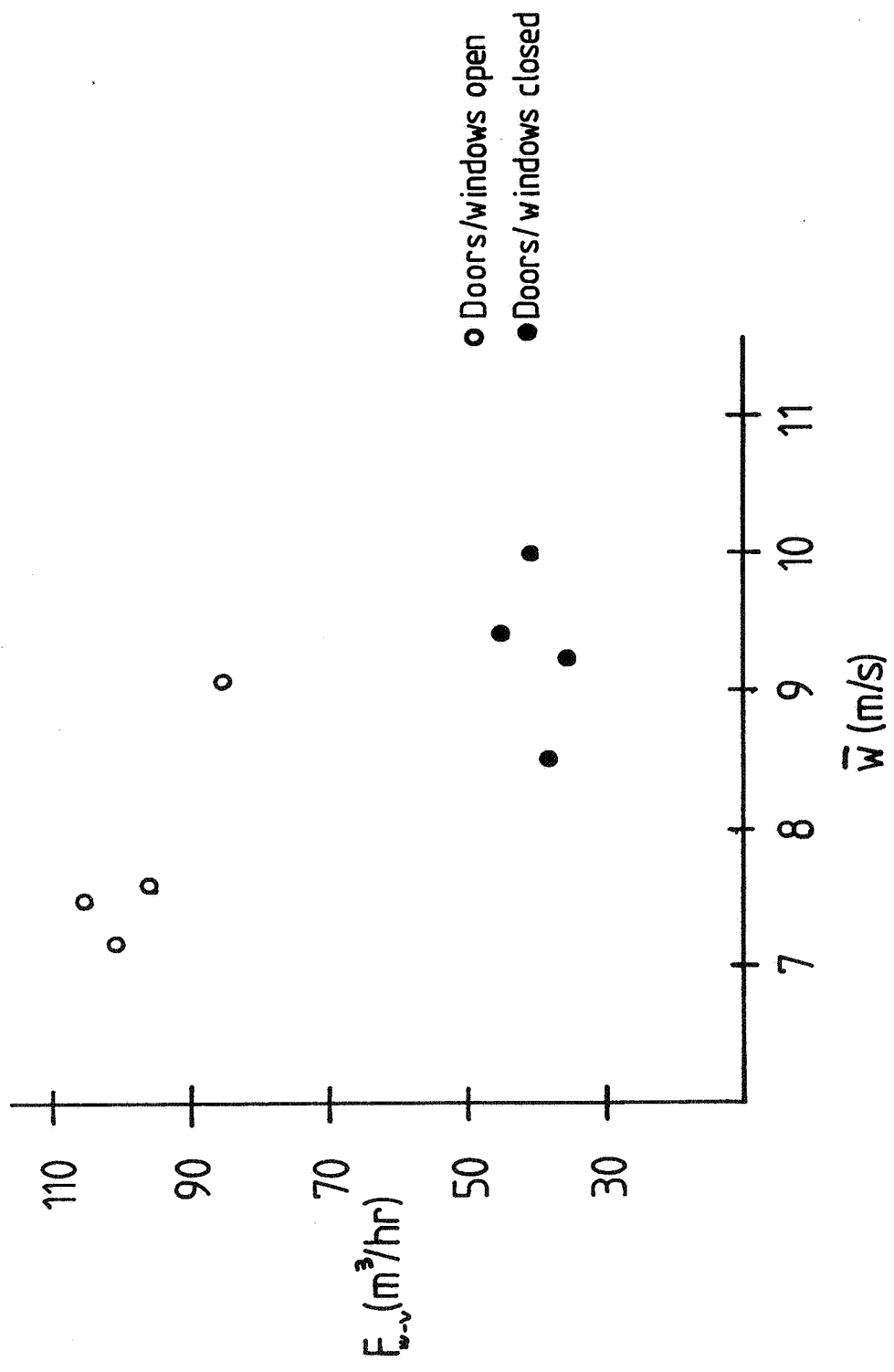


FIGURE 3

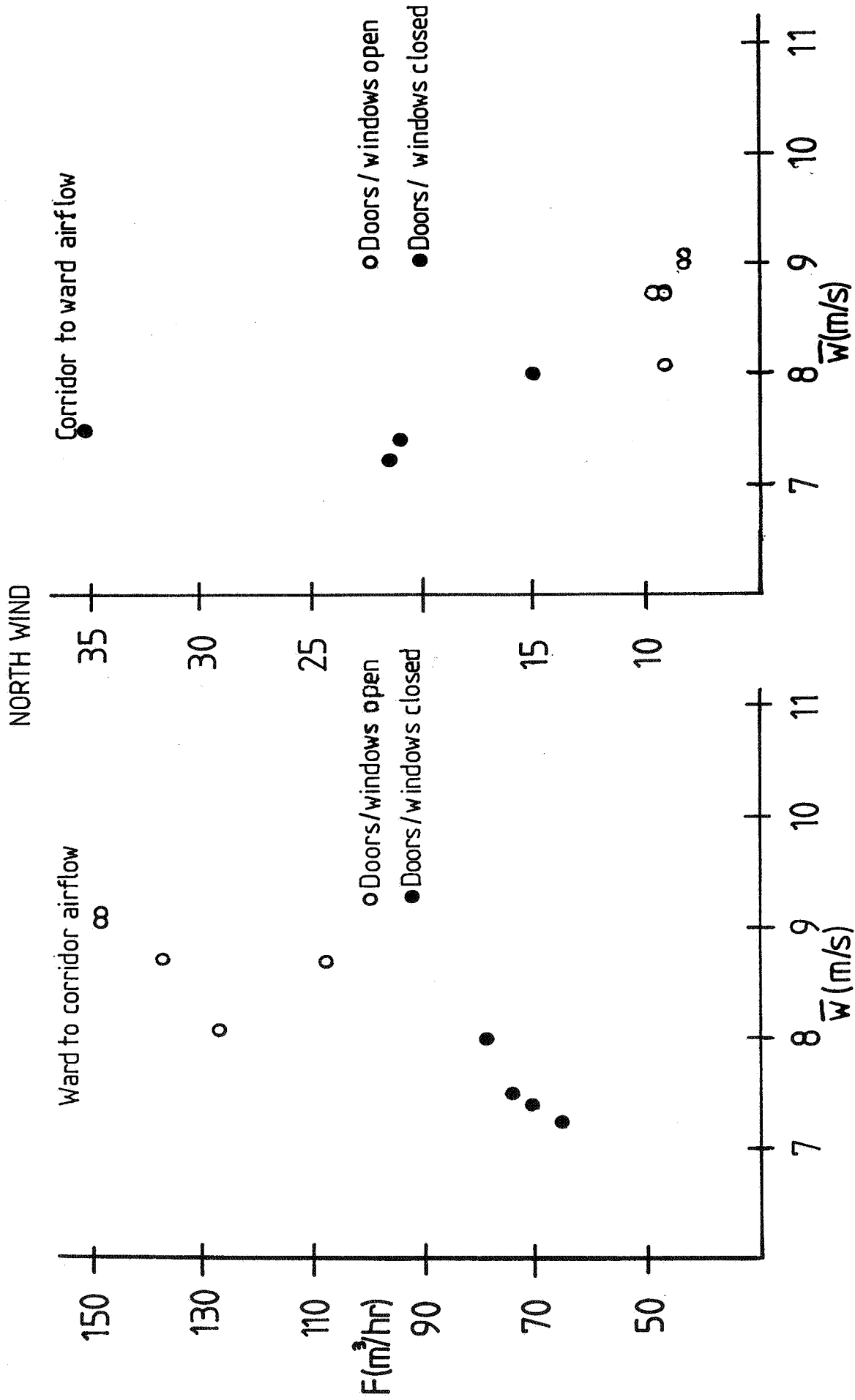


FIGURE 4

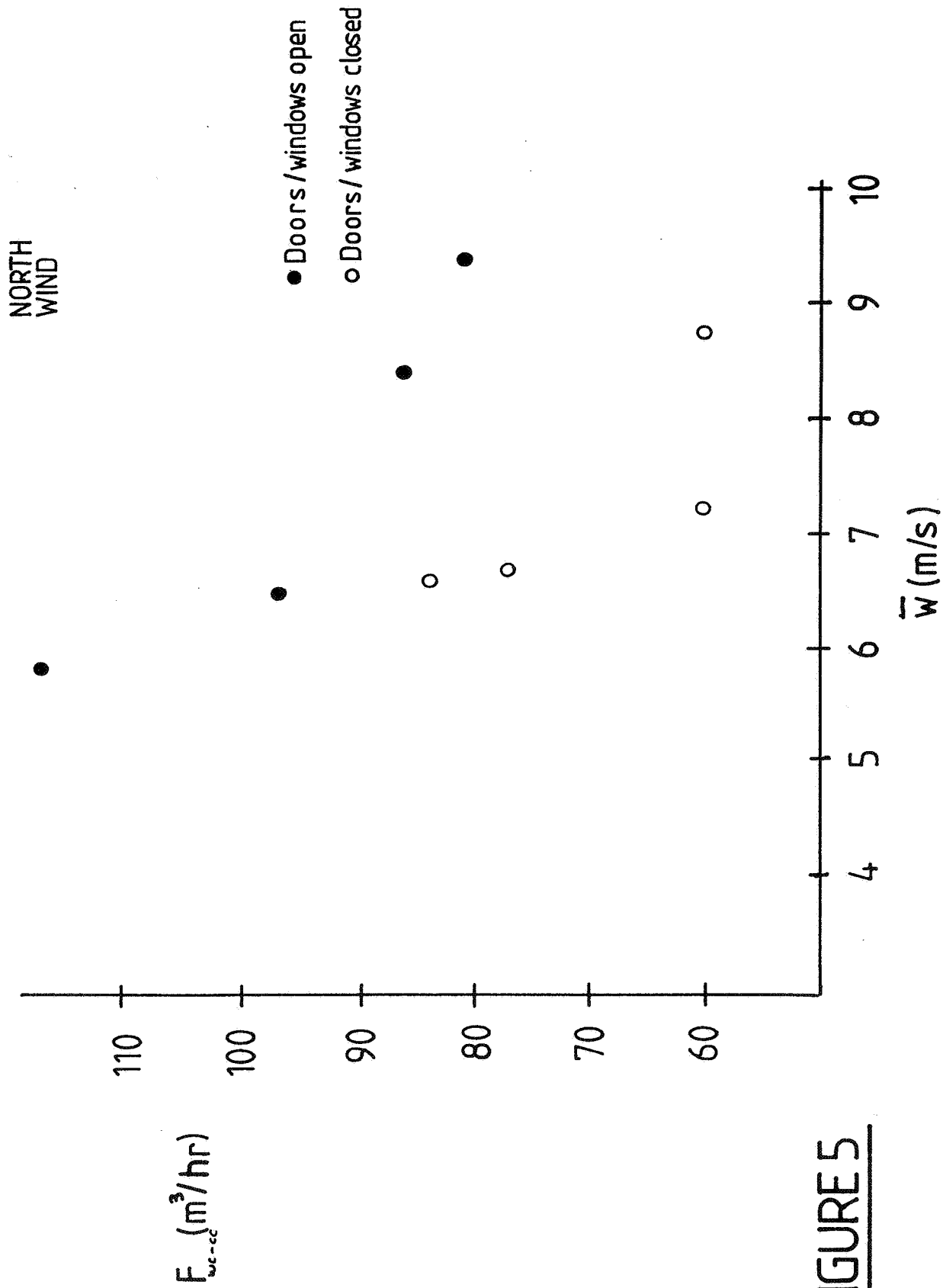


FIGURE 5

**Ventilation for Energy Efficiency and Optimum
Indoor Air Quality
13th AIVC Conference, Nice, France
15-18 September 1992**

Poster 32

**Measured Air Flows Across the Ceiling in Typical
Residential Assemblies.**

W.B. Rose

**Building Research Council, University of Illinois, 1
East St. Mary's Road, Champaign, IL 61801, USA.**

Synopsis

A laboratory for the study of residential attic performance under natural conditions has been constructed. In one of the test cells, with a flat ceiling, white shingles, and venting devices at the soffit and ridge, measurements were taken of air flow through the plane of the ceiling. A ceiling "hole" was constructed in the otherwise tight ceiling, consisting of a PVC tube, an anemometer and a direction sensor. Data were collected for a six-month period. The velocity data have been compared to the recorded values taken at the site for outdoor air temperature and wind (resolved to a north/south wind component).

The results show that up to half of the variance in the air velocity measurements can be accounted for using these two variables. Of the two variables, outdoor air temperature is the more important. The air flow through the ceiling into the attic is considerably greater during the winter than during the summer months. There is a strong correlation between air pressure differences and air velocities through the ceiling hole.

Aim

The intent of this paper is to present measured values for air flow between an indoor space and the attic in a typical residential assembly. The data results from a research project, the Attic Performance Project, which has the larger aim of describing overall attic performance in residential assemblies typical of North American construction under natural conditions.

There are several factors which affect attic performance, including wind, temperature, humidity, construction detailing, and building use. Two construction details appear to be particularly important for attic performance: ceiling airtightness and attic ventilation. Of these two, ceiling airtightness appears to be the more critical. Ceiling

airtightness is also the attic performance parameter which has a significant impact on overall building performance.

Measured values for air flow are important in that they will assist any estimation of moisture flow and heat flow across the ceiling plane. Recent work has highlighted the moisture impact of air flows through building cavities (TenWolde 1992).

Test Setup

In 1989, a laboratory building was constructed for the field study of the performance of typical residential attic assemblies under natural conditions. The building is situated on a slight rise, 150m from the nearest tree line. The building contains eight test cells. Each of the test cells has similar construction, and each is maintained at similar temperature and humidity.

The attics are of varied construction. Five of the bays are framed of wood trusses forming a flat ceiling, as shown in **Figure 1**. Three of the bays are framed with dimension lumber, forming a "cathedral ceiling".

The principal data from this paper is data from Bay 1. This test cell has a flat ceiling, fiberglass batt insulation, truss framing, sheathing of oriented strand board, felt roofing underlayment and white-colored asphalt shingles. The bay has ventilation devices, as shown in **Figure 1**, namely, perforated vinyl panels at the soffits and a ridge vent device at the ridge. Above the top wall plate, a polystyrene air chute is used to ensure that air can flow between the soffit area and the attic volume.

A "hole" was placed in the ceiling of each of the study bays, as shown in **Figures 1** and **2**. The hole is actually a length of PVC plumbing pipe, 1 1/2" (38mm) diameter, that extends through the ceiling gypsum board and through the ceiling insulation. The hole can be capped or opened. An anemometer is used to measure air speed through the hole. The interior of each test bay was designed to be tight. Using air pressurization testing and tracer gas testing, the entire indoor enclosure was

found to have a leakage area of less than 2 sq. in. (129 mm²) (CMHC 1990). A port was provided through the wall on the north side to provide makeup air for air flowing through the ceiling.

Instrumentation

Ceiling air flows are measured using a heated thermistor anemometer, shown in **Figure 2**. The anemometer contains an excitation circuit, a heated thermistor in the air stream, a temperature compensating thermistor protected from the air stream, and a voltage output circuit. The anemometers were calibrated in a wind tunnel down to approximately 0.1 m/s. The anemometers are practically omnidirectional--a plastic framework shields the thermistors on two sides.

Thermometry was used to determine air flow direction through the pipe opening in the ceiling. A thermocouple was installed in the pipe opening at the midpoint of the insulation. The data acquisition equipment permits the temperature at that point to be compared to the attic temperature and the indoor temperature. If the pipe temperature was found to be closer to the indoor temperature than to the attic temperature, then a positive value was assigned to the air flow magnitude, indicating flow upward through the ceiling. Conversely, if the pipe temperature was found to be closer to the attic temperature, a negative value was assigned to the air flow, indicating flow downward. This technique was found to be very reliable.

Pressure difference measurements were made across the ceiling plane using a sensitive electronic manometer. The manometer was calibrated to a 0.25 Pa pressure difference against a Wahlen Gauge (ASHRAE 1985, Willard 1921).

Outdoor air temperature was taken using a resistance temperature detector in a standard weather station enclosure. Wind direction and wind speed were taken at 5m using standard weather station anemometry. The wind vector was resolved into its north/south and east/west components. The north/south wind component was used in this analysis in that it is the component acting perpendicular to the length of the building, the soffit

vents and the ridge vent. This component was selected as a variable, after a preliminary analysis showed very little correlation of ceiling air velocity with scalar (directionless) wind speed.

Data were sampled at 4 minute intervals and hourly averages were kept. The data for this study are for the period from January 1992 to June 1992.

Findings

Six months of data were compiled to illustrate performance during 1) January and February 1992 ("winter" data), 2) March and April 1992 ("spring" data) and 3) May and June 1992 ("summer" data). Measurements of air velocity through the hole in the ceiling were compared to the outdoor air temperature, and to the north/south wind component. The results are shown in **Figure 3** through **Figure 8**. These charts include plots of the hourly data points, together with interval means and standard deviations within the interval. A simple multivariate regression were performed and the results are shown in **Table 1**.

An air velocity of 1 m/s through the pipe can be seen during periods of cold temperature or during periods of high winds. The section area of the pipe is 11.3 cm². If the flow were uniform through the pipe, this velocity would indicate a volume flow rate of 4 m³/hr.

The results show considerable scatter, which is common in any measurement of convective effects. The correlation coefficient (R^2) is less than .5, indicating that less than half of the total variance of the data points is explained by these two variables.

The comparison of the ceiling air velocity with the outdoor air temperatures indicates a clear trend for increased air flows at lower temperatures. This is a simple illustration of bouyancy. With the coming of spring, high outdoor (and attic) temperatures instigated downward air flows, which appear as negative velocity values in the accompanying figures. Flows at temperatures above 20 degC indicate downward flow during spring and relatively

strong upward flow in the summer data set. Both of these effects should be attributed to unexplained variation. If the data sets are combined, the effects are seen to cancel one another, and the trend toward zero net flow at that temperature is evident.

The first line of **Table 1** shows that the mean velocity for the entire data period is considerably higher in the winter (0.85 m/s) than in the summer months (0.36 m/s).

There is a slight trend for greater air flows at higher outdoor wind speeds (north/south component). The correlation of ceiling air flows with north/south wind component is clearly seen in **Figures 4, 6, and 8**. **Table 1** shows the weakness of wind as an explanatory variable. The t-value is the ratio of the regression coefficient to the standard error for that coefficient. In this case, given the lack of cross-correlation between outdoor air temperature and north/south wind speed, the relative size of these numbers may serve as an indicator of their relative importance as explanatory variables.

Results from pressure difference testing were compared to the ceiling air velocity during a two week period in January 1992. Those results are shown in **Figure 9**. In this case the correlation coefficient (R^2) is 0.79, indicating rather close agreement. Thus, close estimates of rates of air flow could be deduced from measurement of pressure differences across the ceiling plane.

Conclusions

Measurements of air velocity through a ceiling hole were taken for three seasons in a laboratory containing test cells under natural conditions. The velocities during the winter are considerably higher than they are during the summer months. The effects of outdoor air temperature and wind speed on ceiling air velocities can be seen, though these variables together explain no more than half of the total variance in the velocity data. Of the two variables, outdoor air temperature is more important. In this test cell, ceiling air velocity correlated closely with measured values for air pressure difference across the ceiling.

Acknowledgement

The author would like to express his gratitude to CertainTeed Corporation for their generous sponsorship of this research.

References

ASHRAE

Handbook of Fundamentals 1989

CANADIAN MORTGAGE AND HOUSING CORPORATION (CMHC).

"Survey of moisture levels in attics."

Prepared by Buchan, Lawton, Parent Ltd. Ottawa 1991.

TENWOLDE, A., CARLL, C.

"Effect of Cavity Ventilation on Moisture in Walls and Roofs"

Prepared for publication in *Proceedings of ASHRAE Conference Thermal Performance of Building Envelopes V*, December 1992.

WILLARD, A.C., KRATZ, A.P., DAY, V.S

Investigation of warm-air furnaces and heating systems.

University of Illinois Engineering Experiment Station Bulletin No. 120, Vol. XVIII, No. 29, March 1921.

Table 1

statistic	Jan/Feb	Mar/April	May/June
mean air velocity			
(m/s)	0.85	0.73	0.36
R ² _{ns}	.06	.03	.09
R ² _{ato}	.12	.42	.12
R ² _{ns,ato}	.18	.47	.21
t-value _{ns}	9.2	9.6	11.7
t-value _{ato}	12.8	29.0	13.4

Note: R² is the correlation coefficient computed for the individual variables: ns for north/south wind component, and ato for outdoor air temperature. The statistic t-value is the ratio of the regression coefficient to the standard error for that coefficient in multivariate regression. Higher values of R² and t-value indicate relative importance of that variable.

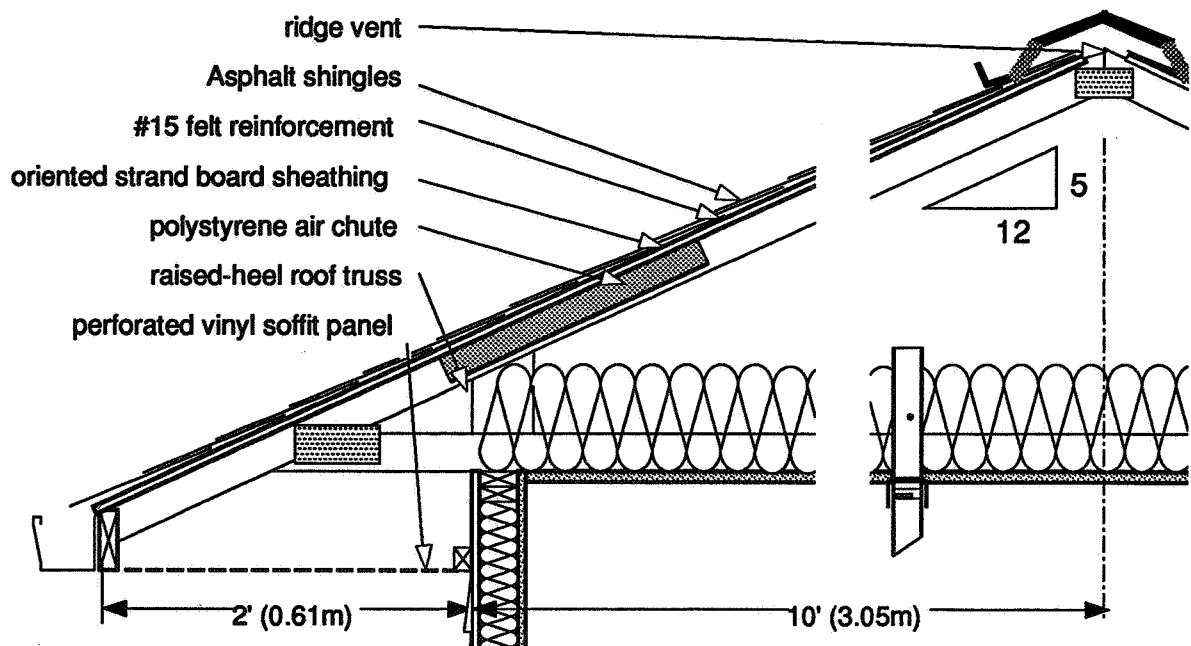


Figure 1. Detail section of the research laboratory attic. The assembly shown is a flat-ceilinged, vented attic, with perforated vinyl soffit panels and a ridge vent.

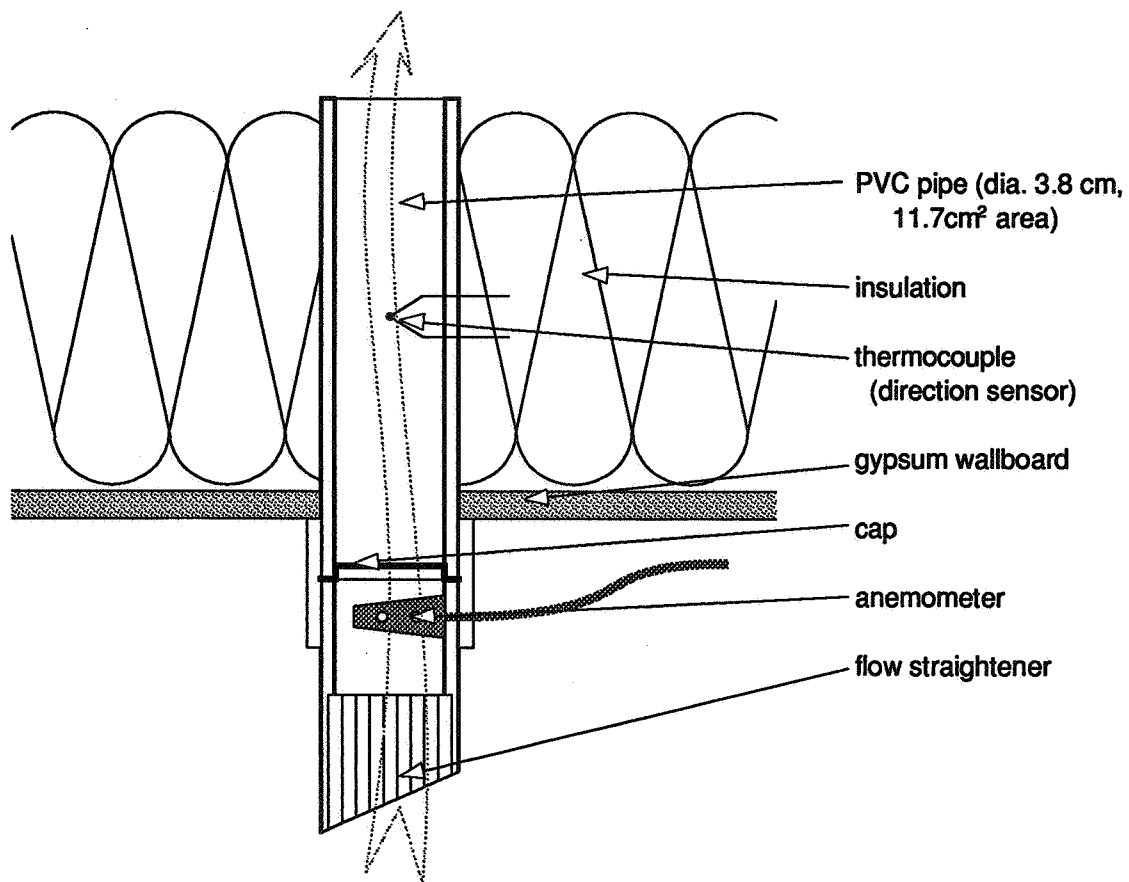


Figure 2. Schematic drawing of PVC pipe used as ceiling hole, showing placement of heated thermistor anemometer, cap (which can be opened for measurement) and thermocouple used as a direction sensor.

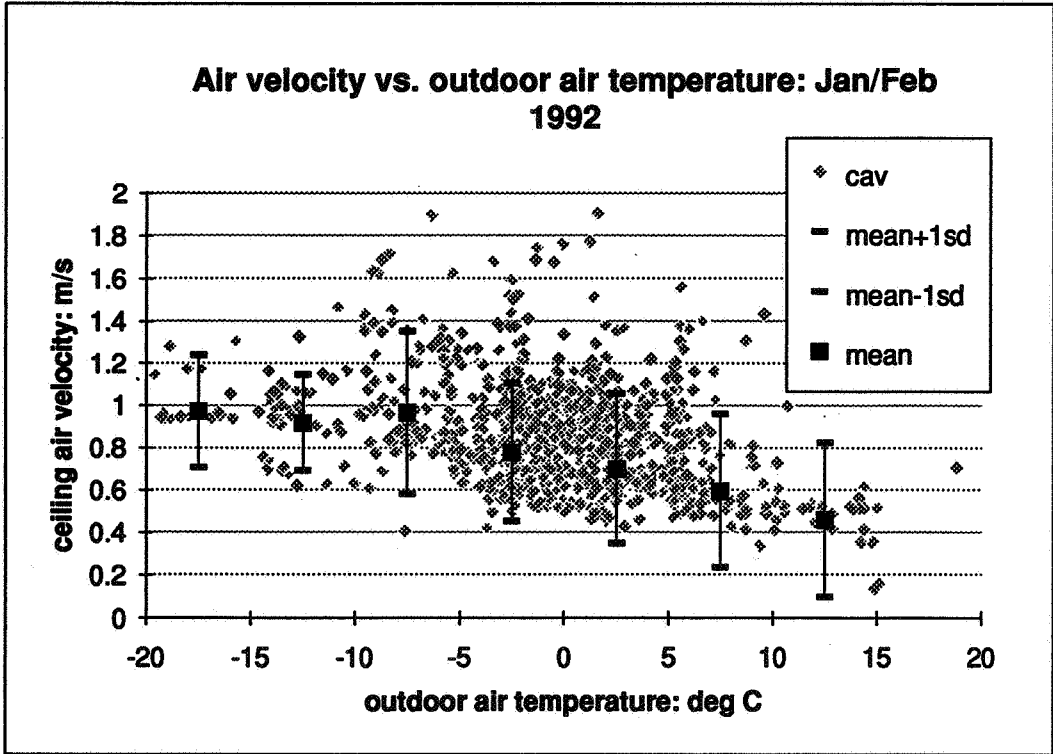


Figure 3. Winter comparison of ceiling air velocity with outdoor air temperature. Confidence band of 1 standard deviation is shown. Trend toward reduced ceiling flow at lower temperatures is evident.

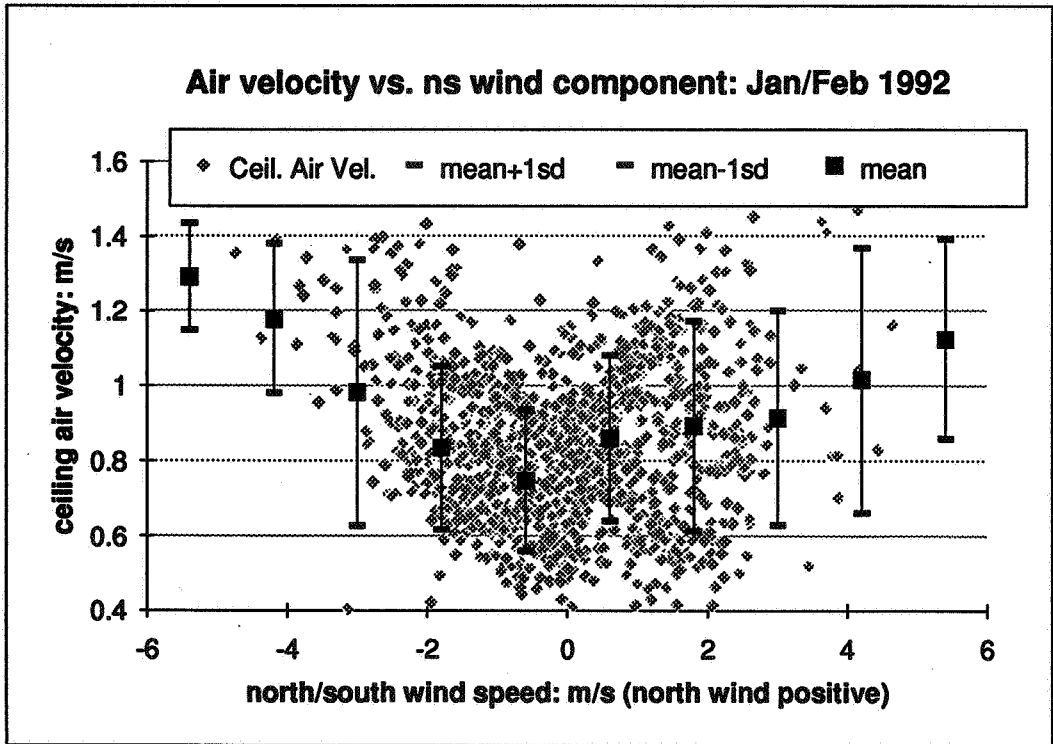


Figure 4. Winter comparison of ceiling air velocity with north/south wind speed. Effect of both north and south winds on ceiling air flows is evident.

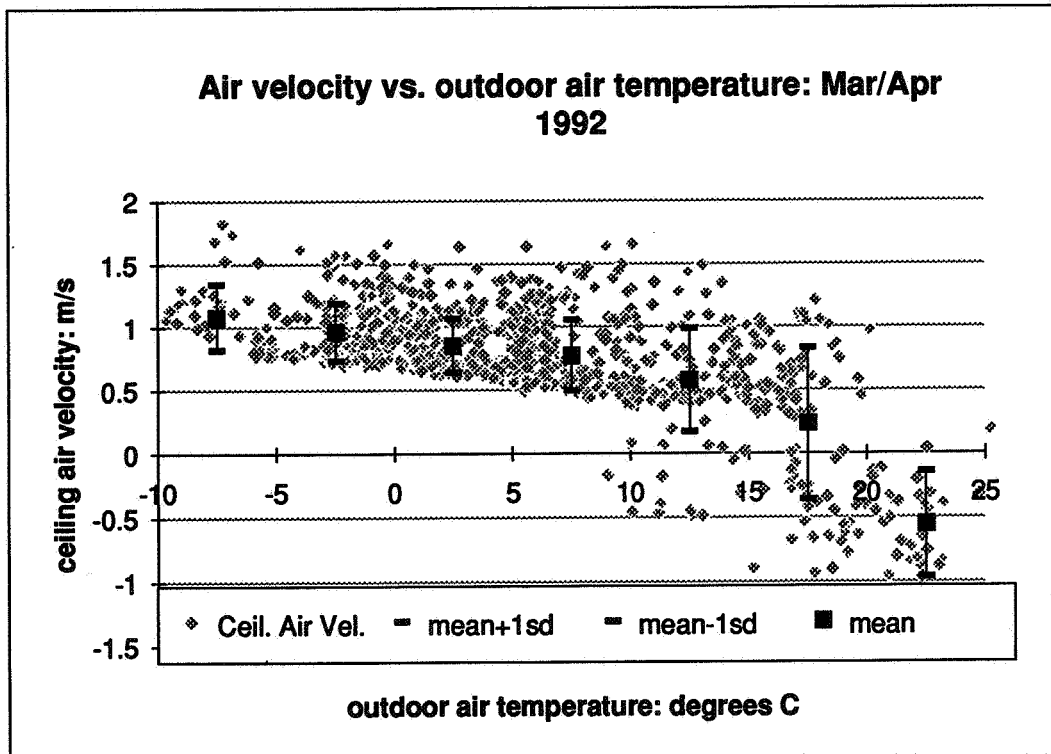


Figure 5. Spring comparison of ceiling air velocity with outdoor air temperature. Results above 20 degC conflict with findings from following months.

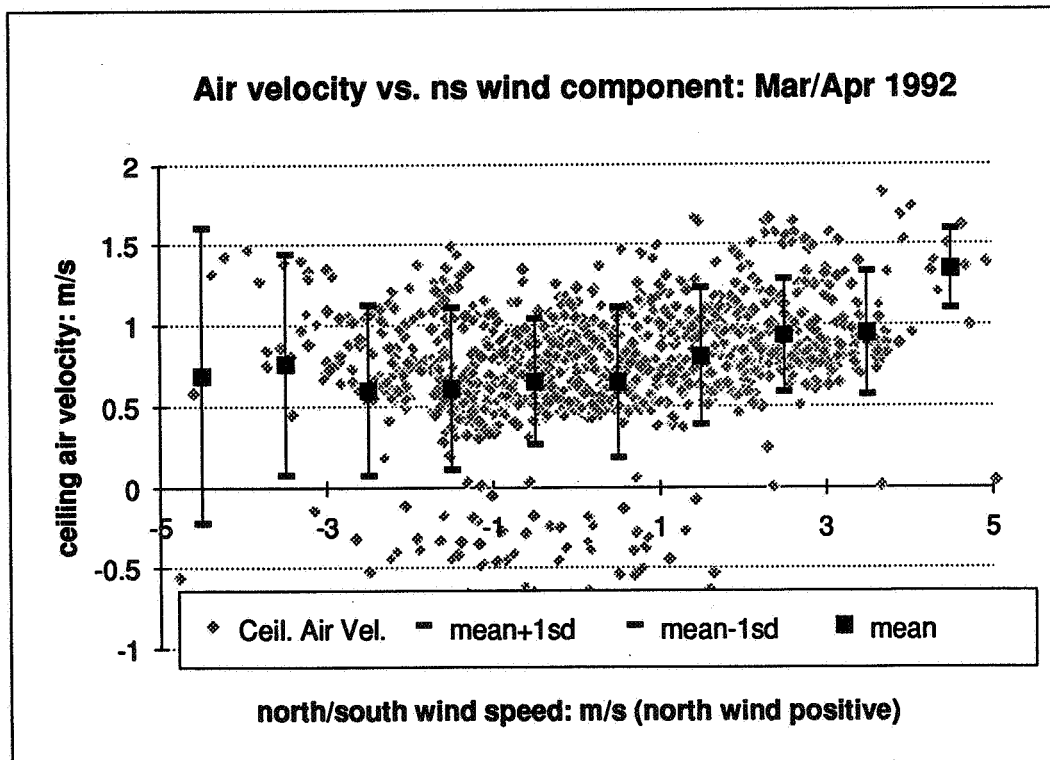


Figure 6. Spring comparison of ceiling air velocity with north/south wind speed. Effect of wind speed is less visible than during winter.

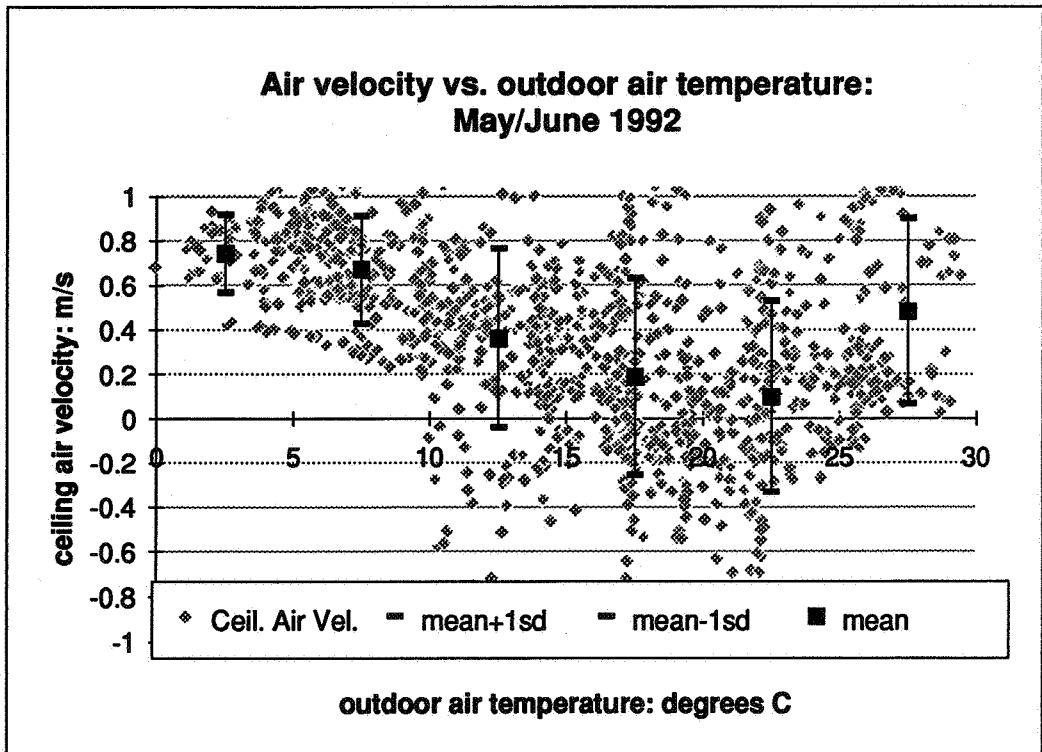


Figure 7. Summer comparison of ceiling air velocity with outdoor air temperature.

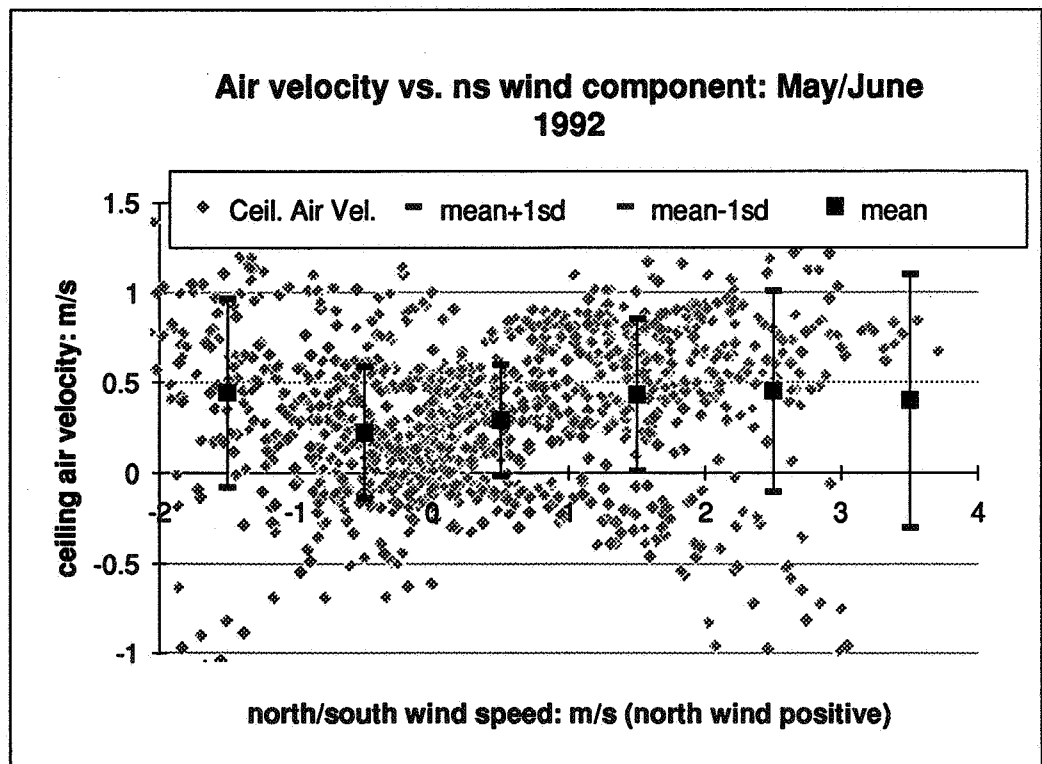


Figure 8. Summer comparison of ceiling air velocity with north/south wind speed.

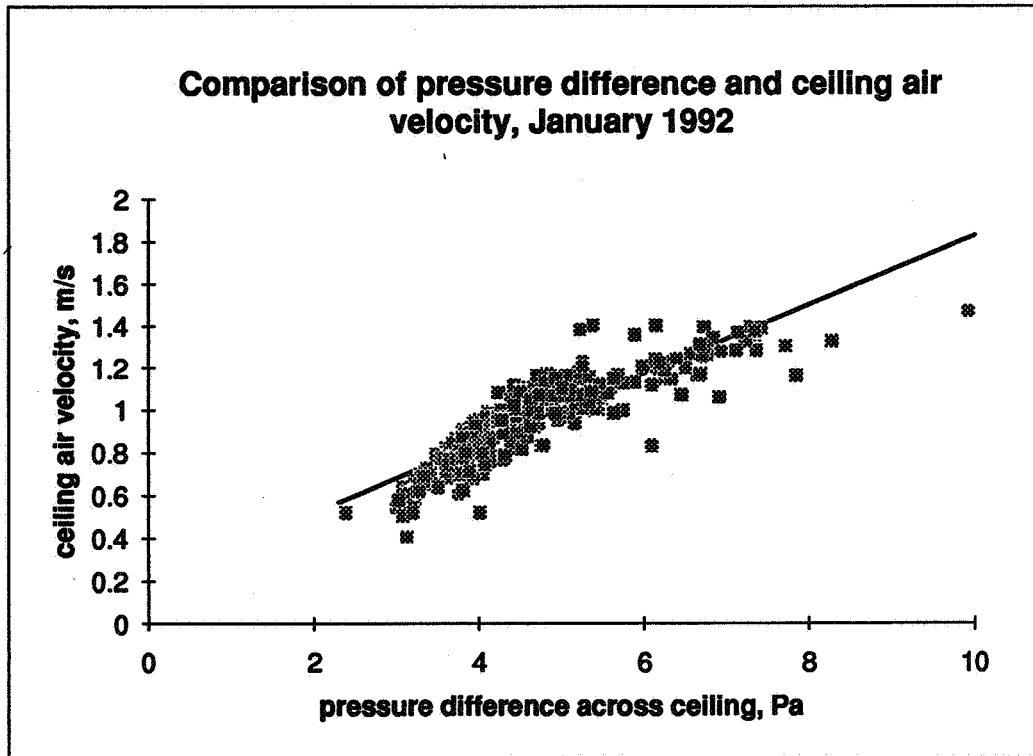


Figure 9. Comparison of ceiling air velocity with air pressure difference. Pressure difference values are hourly averages of 15 samples. Correlation coefficient is 0.79.

**Ventilation for Energy Efficiency and Optimum
Indoor Air Quality
13th AIVC Conference, Nice, France
15-18 September 1992**

Poster 30

Air Flow In A Cavity Wall

H-G R. Kula, I.C. Ward

**Building Science Unit, School of Architectural
Studies, University of Sheffield, P O Box 595, The
Arts Tower, Western Bank, Sheffield, S10 2UJ,
United Kingdom**

ABSTRACT

The external facade of a nine storey office building has been reclad with a ventilated cavity structure with a length to height ratio greater than forty. As there is little published information regarding the likely air flows within such cavities a research programme has been set-up to investigate the ventilation and energy performance of this structure. This paper will address the cavity air flows through both theoretical and full scale measurements.

Theoretical predictions were calculated using the COMIS infiltration simulation programme utilising different pressure profiles from around the building. A detailed wind tunnel study [1] was carried out prior to this in order to obtain accurate wind pressure distribution profiles for the building.

The experimental measurements were carried out on the cavity wall structure on the second (west facing) floor of the building. Using a N₂O tracer gas detector system, the flow velocity and the air flow volume were deduced from the measurements and compared with the theoretical prediction. The comparison of the two sets of results show good agreement, considering the varying wind and temperature conditions which are difficult to simulate. The maximum difference between the calculated and the predicted airflows, for the tests carried out is in the range of 30 %.

Air flow pattern and mixing of the tracer gas were demonstrated using a 2.44 metre long segment of the wall structure under laboratory conditions.

INTRODUCTION

As part of the updating policy of the University of Sheffield the external facade of a nine storey office building has been reclad with a ventilated cavity wall structure. This recladding was to prevent deterioration of the building due to moisture penetration through the original glass curtain wall cladding. The cavity on each floor on the west and the east facades measures 1.2 metre in height and extends 46 metres along the length of the building. The new cavity wall structure consists of a brick layer, an air cavity of 10 cm followed by 5 cm of cavity insulation and the original concrete structure with plaster on the inside wall of the building. To prevent moisture built-up and condensation problems, 98 weep hole devices were installed along the wall to ventilate the cavity. As little can be found in the literature on the performance of these weep hole devices a pressurisation test to determine the "crack" flow characteristics of the weep hole device was carried out. The coefficients were calculated from a standard statistical package using the measured data and found to be $k_1=0.00015329$ and $k_2=0.4105174$. Using this data the occurring airflows in the cavity due to wind pressure difference in and around the wall structure were investigated using COMIS.

The pressure profiles used as input data to the model were obtained from a detailed wind tunnel study of the building within its surroundings [1].

THEORETICAL PREDICTIONS

To calculate the air flow in the ventilated cavity the infiltration simulation programme COMIS was used. The infiltration modelling programme COMIS was developed as a multizone model on a modular base. COMIS can be used as a stand alone infiltration model with input and output features or as an infiltration module for thermal building simulation programmes[2,3]. The two parts of the COMIS programme used for this work were the COMIN and COMVEN programme routines. The input file was created using the COMIN programme entering all the available data of the wall structure necessary to perform the simulation. These specific input data are described in table 1 below:

Description	Input values
Wind speed	3,7,10,15 [m/s]
Cavity volume per zone	0.2326 [m ³]
Weep hole devices zone 1,25	bottom 1 per zone
Weep hole devices zone 2-24	bottom 2 per zone
Weep hole devices zone 1-25	top 2 per zone
Cavity temperature	20 deg C
Crack temperature	20 deg C
Outside temperature	-10 and 20 deg C
Cp-values	from wind tunnel study [1]
Crack flow characteristics	from de-pressurisation test k1=0.00015329 k2=0.4105174

The wind pressure coefficients chosen from the wind tunnel study characterise wind from the north-west. Calculations using the COMVEN programme were only carried out for the 2nd floor on the west facing facade. The overall air flow from zone to zone and the contribution of each weep hole device to that air flow was calculated.

The results for the 4 different wind speeds are presented in figures 1.

Theoretical Airflow

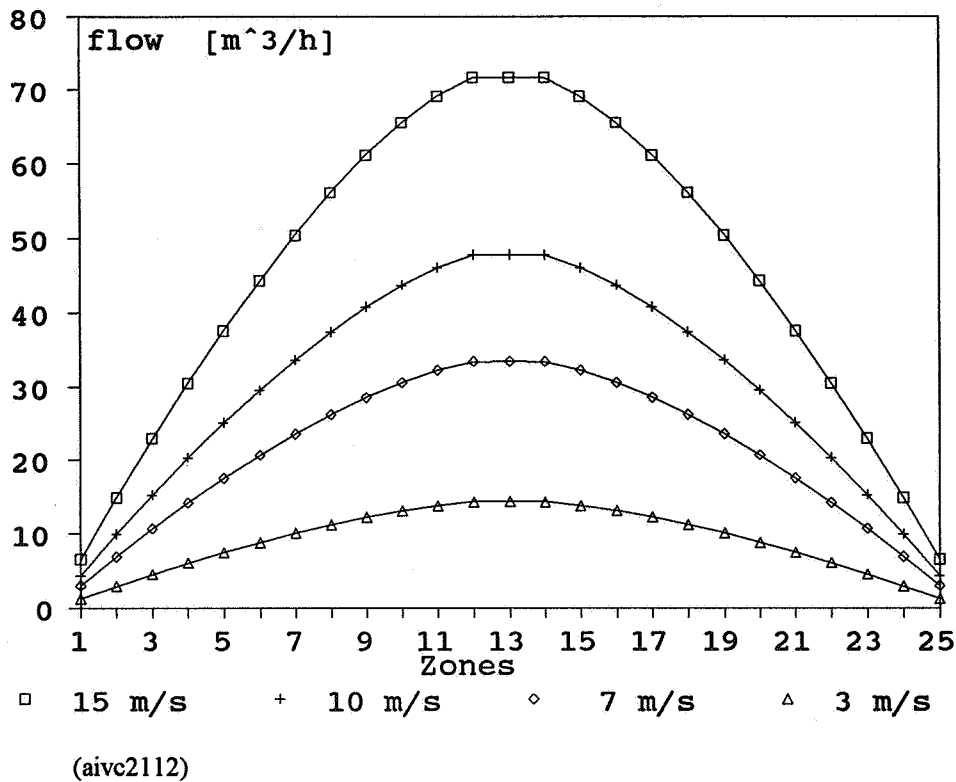


Figure 1: Theoretical predictions of air flow at various wind speeds

LABORATORY TESTS

To be able to control the ambient conditions during the experiments, a segment of the wall, 2.44 metre in length, was built in the laboratory. The wall segment has four built-in weep hole devices, of which two were covered with flow hoods connected to a pressurisation system used to simulate the in-going air flow. The air flow was measured with a standard 40 mm orifice plate. For the experiments carried out, the tracer gas was injected at a constant flow rate either into the top or the bottom flow hood. Eighteen sampling points were used to trace the flow occurring in the cavity due to the imposed flow. Where using tracer gases to determine the flow between zones, it is essential to reach a homogeneous mixture of the gases with the air anywhere in the zone, otherwise significant errors may arise [4]. The following experiments were conducted to show that reasonable mixing occurs in the cavity. For the first test the gas was injected into the top weep hole device. The injected gas concentration was first measured directly behind the inlet. After 10 minutes, allowing for the flow patterns to stabilise, the 18 sample points were connected, one after the other, to the gas analyser. The sampling time at each point was two minutes and 30 seconds. Between the two tests the cavity was flushed with fresh air to eliminate gas pockets that might have accumulated in corners of the laboratory set-up during the previous test. The imposed air flow and the N₂O gas flow were kept at a constant rate of 94 L/min and 0.5 L/min respectively. The procedure for

the second test was similar, however the gas was injected in the bottom weep hole flow hood.

The results of the two tests performed show that the top and the bottom weep hole devices in this wall configuration create slightly different flow patterns. Due to the constant supply of tracer gas stable flow patterns should build-up at the 18 sampling points (figure 2) giving information of these two flow patterns.

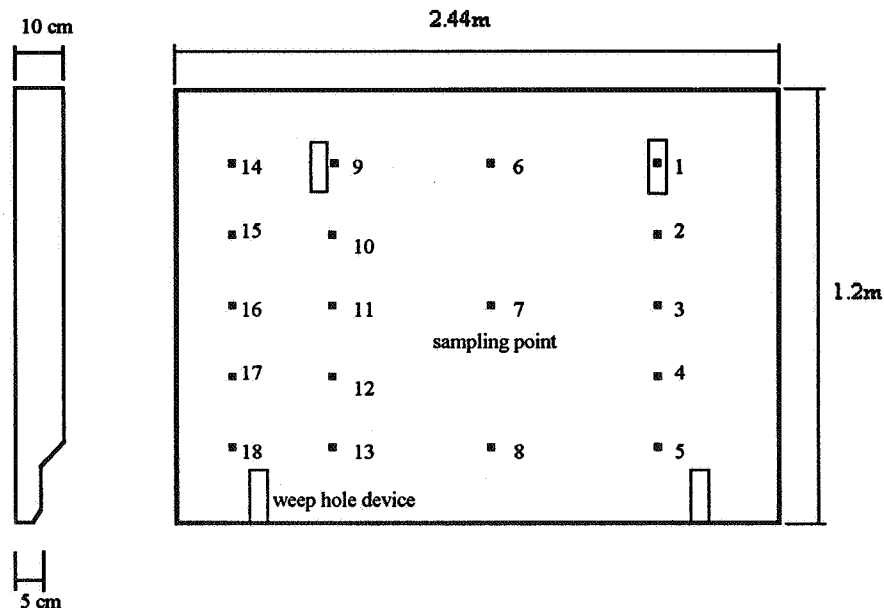


Figure 2: Sampling points in the laboratory wall segment

For the first test (figure 3), with the tracer gas being injected in the top flow hood the tracer gas concentration decreases in the vertical plane from sample point 1 to 5 and 6 to 8. In the horizontal plane the tracer gas concentration decreases from the initial inlet concentration by 25 % at point 6 and stabilises at this value for the remaining sampling points 9 to 18. This result shows that good vertical and horizontal mixing occurs approximately 1 metre from the injection point.

The gas concentrations measured during the second test (figure 4), with the tracer gas being injected in the bottom flow hood, show that only very little of the injected gas flows to the top part of the cavity, represented by sampling points 1,2,6,9,10,14 and 15. However, in the centre of the cavity the gas concentration stabilises at 30 % below the gas concentration measured at the inlet weep hole. This phenomenon can be explained by the different area configuration at the bottom of the cavity wall, where the width of the cavity is only half (figure 2).

Further tests simulating the real situation were carried out on the laboratory set-up to determine the flows. A known constant airflow of 96.95 L/min was imposed on the cavity via the two flow hoods. After the initial waiting period of ten minutes, allowing for the flow pattern to stabilise the tracer gas was injected at a constant rate of 0.5 L/min into the top weep hole device. The aim of this was to measure the travelling time. It took the tracer gas 98.5 sec to travel the distance a 1.25 metre to the second top weep hole

where the sampling tube, connected to the gas analyser was fixed. This corresponds to an average velocity of 0.01269 m/s, resulting in an airflow of 91.4 L/min. This test was carried out several times to show reproducibility and the differences between the imposed flows and the deduced flows were in the range of less than (+-)7% which indicates good agreement.

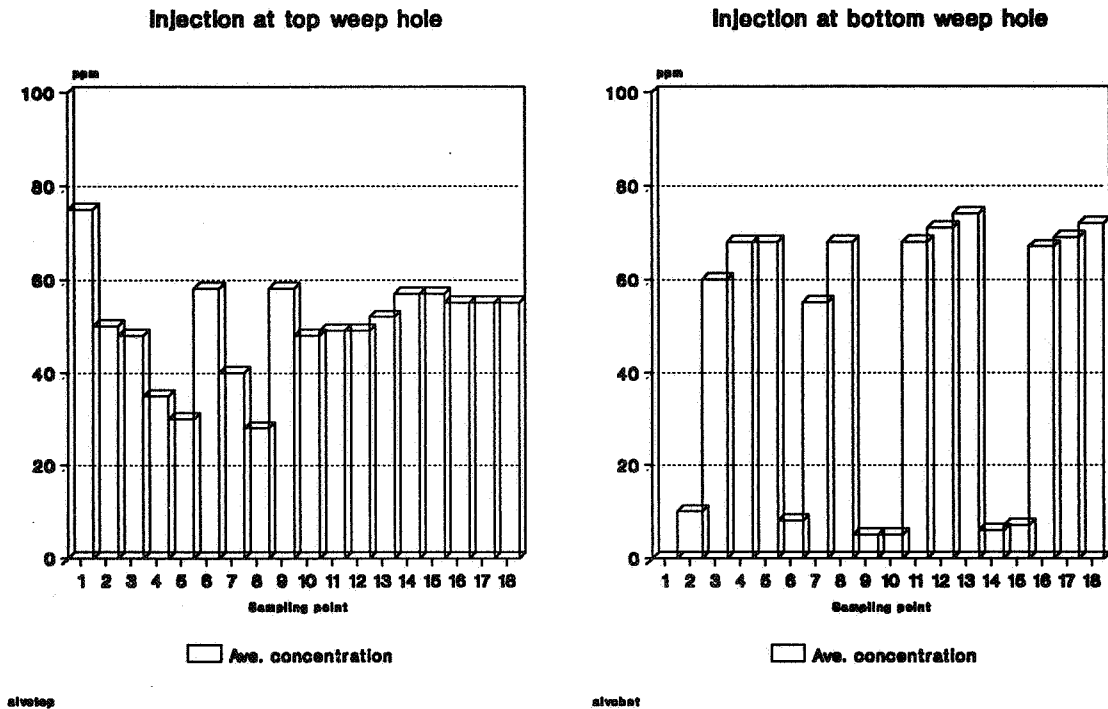


Figure 3 and 4: Average gas concentration measured at the 18 sampling points

HICKS BUILDING EXPERIMENTS

The procedure for the experiments carried out on the 2nd floor of the building were more complex. First, the wind direction and the wind speed had to be determined in order to predict the flow direction in the cavity according to the wind pressure profiles obtained from the wind tunnel study [1]. The tracer gas was then injected into the top weep hole nearest to the centre, whereas the sampling tube was inserted into the second weep hole into the cavity opposite the centreline of the building. The distance between these two points measured 2.89 m. The aim was to measure the time necessary for the injected tracer gas to travel to the sampling point. Due to the known area configuration of the cavity, the amount of air flow can then be determined.

Several tests with different wind direction and wind velocities to check the technique were carried out. For a calm day with an average wind velocity of 1 m/s the first record of the tracer gas were detected after 3.5 minutes. Five minutes after the start of the tracer gas injection a more reliable record of the gas was detected. The travelling time i.e. the travelling speed of the tracer gas and the known area of the cavity allowed the air flow volume at this point in the cavity to be calculated. The first record of the tracer gas

Buildings were in good agreement for the cases considered. The maximum difference between the calculated and the measured airflows was up to 30 % which may be explained by the varying wind and temperature conditions during the full scale measurements.

These results show that as the wind speed increases there is better agreement between the measurements and the simulations. This indicates that at low wind speeds convective currents within the cavity may be dominant.

FUTURE WORK

This paper reported the first step of a research project aimed at investigating the overall thermal and ventilation performance of a ventilated cavity wall structure. Future steps will include the calculation and measurement of the ventilation efficiency, the heat flux through the wall and the moisture behaviour of the wall.

The effect of the airflow on the thermal and moisture behaviour will be investigated in the second part of this project.

ACKNOWLEDGEMENTS

The authors would like to acknowledge the support of the SERC Council (Grant No. Gr / F 28397).

REFERENCES

1. KULA, H.-G.R. and WARD, I.C.
"The Hicks Building in Sheffield, A Wind Tunnel Study"
Internal Report, Building Science Unit, University of Sheffield, June 1992
2. FEUSTEL, H.E. et.al.
"Fundamentals of the multizone air flow model - COMIS"
Technical Note TN 29
AIVC 1990
3. FEUSTEL, H.E. and RAYNER-HOOSON, A. (Editors)
"COMIS User Guide"
Lawrence Berkeley Laboratory, Feb. 1991
4. SHERMAN, M.H.
"Air Infiltration Measurements"
Lawrence Berkeley Laboratory Report 27656
Aug. 1989

would indicate a flow velocity of 0.01376 m/s, the more reliable record, after five minutes results in 0.00963 m/s. These velocities correspond to a deducted air flow of 0.0016512 m³/s and 0.001156 m³/s respectively.

Measurements in the cavity, with a wind velocity of 1.5 m/s from the Southwest resulted in an air flow rate of 0.00211 m³/s. With a wind velocity of 4 m/s from the SSW the air flow rate was 0.0029 m³/s.

The highest air flow measured for West wind with a wind velocity of 3.5 m/s and 5 m/s in gusts was 0.0048 m³/s.

COMPARISON OF THE RESULTS

Considering that the computer simulations were carried out using constant "set" temperatures for the cavity air, the outside air and the crack temperature, as well as the wind direction and wind speed the results from the simulation with the COMIS programme and the measurements on the cavity structure in the Hicks Building compare reasonably well. Table 2 shows the results of the simulations and measurements carried out.

	wind direction	wind velocity	COMIS	measured
1	calm	< 1 m/s	0.001645 [m ³ /s]	0.00165; 0.00156 [m ³ /s]
2	SSW	4 m/s	0.00262 [m ³ /s]	0.0029 [m ³ /s]
3	West	5 m/s	0.00473 [m ³ /s]	0.0048 [m ³ /s]

At a wind speed of 1 m/s using the appropriate wind pressure coefficients the result of the simulation at the centre line of the cavity give an air flow of 0.001645 m³/s. The measurement with the same, but averaged wind velocity give an air flow between 0.0016512 m³/s and 0.001156 m³/s. The first record of the tracer gas is in good agreement with the prediction. However, the more reliable second record of the tracer gas indicates an airflow being 30 % below the predicted.

The simulation results for the wind direction SSW were calculated for 4 m/s. The resulting airflow in the centre of the building is 0.002622m³/s, which is 10 % less than the deducted airflow from the measurements.

The simulation results for the last test for West wind with a velocity of 4 m/s is 0.00379m³/s which under predicts. However, the simulation results for a wind velocity of 5 m/s were 0.004738 m³/s and were in good agreement with the measurement which was 0.0048m³/s.

CONCLUSION

The results of the laboratory tests show that mixing occurs in this wall configuration suggesting that the tracer gas method adopted to deduct the airflow from the travelling time of the tracer gas in the cavity can be applied on the wall structure.

The comparison of the numerical prediction calculated with COMIS and the tracer gas measurements carried out on the cavity wall structure on the second floor of the Hicks

**Ventilation for Energy Efficiency and Optimum
Indoor Air Quality
13th AIVC Conference, Nice, France
15-18 September 1992**

Poster 29

**Modelling and Predicting of Pollutant Transfer in
Multizone Buildings Coupled with Ventilation
Networks.**

A.C. Megri, F. Allard, G. Krauss

**CETHIL-URA CNRS 1372, Bât 307 - INSA, 69621
Villeurbanne Cedex, France**

**Ventilation for Energy Efficiency and Optimum
Indoor Air Quality
13th AIVC Conference, Nice, France
15-18 September 1992**

**MODELING AND PREDICTING OF POLLUTANT
TRANSFER IN MULTIZONE BUILDINGS
COUPLED WITH VENTILATION NETWORKS.**

A.C. MEGRI , F. ALLARD , G. KRAUSS

CETHIL - URA CNRS 1372, Bât 307 - INSA
69621 Villeurbanne Cedex (FRANCE)

Air flow modeling and contaminant dispersion in multizone buildings is still a hard task which has motivated the COMIS and then annex 23 projects.

During the last two years, CETHIL has contributed to these joint projects by developing the COMIS code in order to predict on the one hand the coupled behavior of multizone buildings equipped of their complete ventilation network and on the other hand the resulting transfer of contaminants.

In a first step we present here some results obtained in simulating a multizone building coupled with a ventilation network.

In a second step, an air quality index for multizone buildings is proposed. By coupling the ventilation code with a pollutant transfer model, we are then able to predict and qualify the ventilation efficiency of a multizone building coupled with a ventilation network.

1.- Introduction :

A literature review shows that the actual trends to prediction of air flow in multizone buildings are not only due to economical reasons but mainly to indoor air quality, acoustical and thermal comfort improvements.

During the last decade, almost fifty models have been developed in eight countries [1]-[4]. Except some models the analysis of interaction between HVAC systems and building infiltration is seldom studied [5].

In this paper our first objective is the study of a building coupled with HVAC systems, in order to find out some complex phenomena resulting from coupling the building with its ventilation network.

Our second objective is to qualify the ventilation efficiency of a multizone building coupled with a ventilation network by an air quality index, and to provide guidance to occupations on ways to reduce their exposure to pollutants.

2.- Modeling principles :

We use COMIS model as a support [4]. In COMIS, the building and HVAC systems are represented by nodes connected by different kind of links (cracks, fans, ducts, large openings, etc); every node represents a zone at thermodynamical equilibrium and represented by its state variables (temperature and reference pressure).

The building and the HVAC systems are coupled by using simple laws between flow and pressure. For different components (cracks,fans,etc), these relationships are based on the same physical principle.

In order to identify the law between flow and pressure, three steps are necessary:

- calculate the coefficient of these laws,
- calculate the pressure difference through each component, using Bernoulli equations,
- correct these relationships, according to the real conditions.

3.- Component Modeling :

3.1.- Ducts and Duct Fittings :

We consider two types of ducts :

- Straight ducts characterized by their dimensions and a friction factor.
- Duct fittings characterized by their type, their geometry and a local loss coefficient.

In order to integrate ducts and duct fittings into the general network, their

behavior is represented by power law functions (orifice laws).

$$Q=C(\Delta P)^N$$

C and N are identified by simulating at first the behavior of the duct for various flow regimes, using its characteristic friction factor (for ducts) or local loss coefficient (for duct fittings) to calculate the pressure loss [6]-[8].

The results can be drawn as a flow function and C and N are obtained by numerical regression.

Then the flow in the duct is corrected as a function of the real thermophysical characteristics in each duct.

3.2.- The junction of a Tee :

The junction is represented by three pressure nodes and treated as a particular pressure node by COMIS. It means that the static pressure of the node with the big flow is iteratively calculated by the solver. With this pressure and using the relation of pressure loss, we deduce the other two pressures. Figure 1 represents one case of the six cases existing (Table 1)

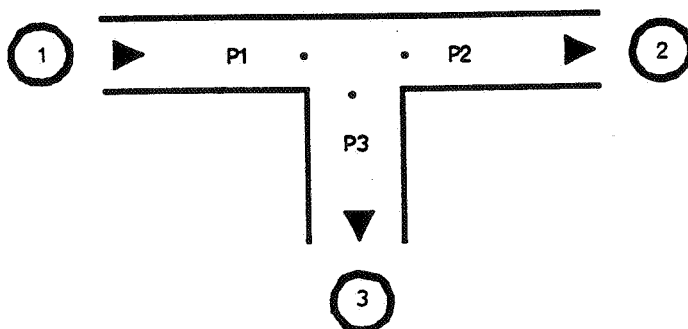


Figure 1 : Pressures at a Junction of a Tee

Table 1 : Different configurations of a Tee Junction.

Configuration	Diagram
T splitting	
T gathering	
straight stream gathering	
lateral stream gathering	
straight stream splitting	
lateral stream splitting	

3.3.- Fans :

Fan is modeled via a polynomial function for every rotating speed. In our model, we use the polynomial ($Q = f(\Delta P)$) instead of ($\Delta P = f(Q)$) given experimentally or by the constructor. Out of the definite range $[\Delta P_{\min}, \Delta P_{\max}]$, we assume a linear behavior of the fan; this curve passes through the two points $(\Delta P_{\min}, Q_{\max})$ and $(\Delta P_{\max}, Q_{\min})$.

This characteristic curve is then corrected if we consider the effect of density and rotating speed. Figure 2 gives an example of fan model.

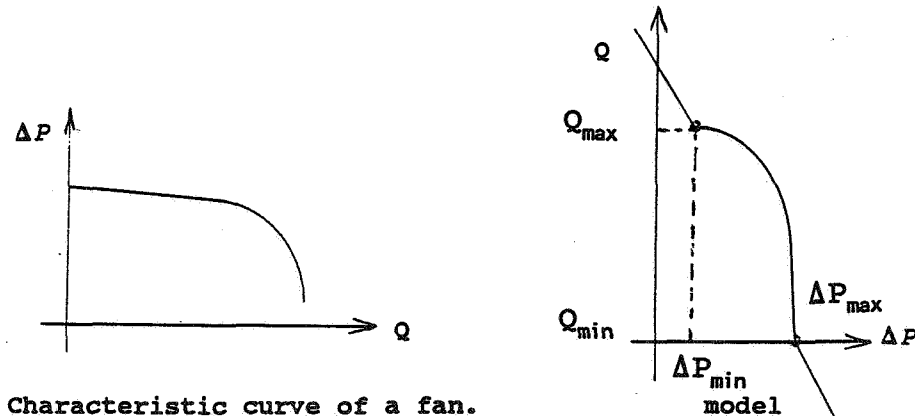


Figure 2 : Fan model.

3.4.- Flow controllers :

Flow controllers represent most of the available dampers or regulators used in a ventilation network. The basic premise of flow controllers is that they have a flap or valve which may throttle the flow by gradually closing the opening when the pressure increases.

A flow controller is called ideal if after a first pressure threshold it delivers a constant flow rate when the pressure increases.

Furthermore, a flow controller is called symmetrical if it has exactly the same behavior for both positive and negative pressure drops.

Figures 3 presents the 4 combinations we can find between this two definitions.

F1 : Symmetrical ideal flow controllers.

F2 : Non symmetrical ideal flow controllers.

F3 : Symmetrical non ideal flow controllers.

F4 : Non symmetrical non ideal flow controllers.

For each category we can represent the behavior of any flow controller by power law functions (range 1+ and 1-) and polynomial laws (range 2+, 2- and 3+, 3-).

In the case of self-controlled air inlets, the aim is to limit the crossing air flow in the building. This phenomenon of crossing air flow becomes more important in a building with a double exposition and a high wind velocity [9].

One application of the self-controlled air inlets is to automatically control the ventilation as a function of the concentration of different zones. If the concentration is less than the peak, the damper is closed, the air is exhausted by a fixed orifice.

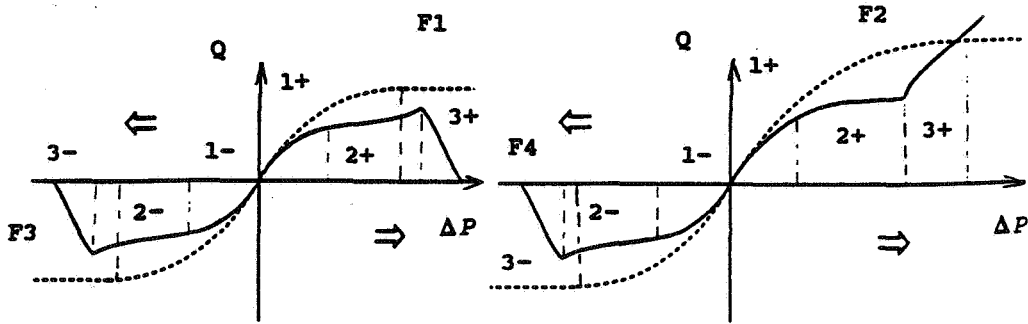


Figure 3 : Characteristic curves of flow controllers.

4.- Pollutant transport and IAQ evaluation :

Furthermore, a pollutant transport module already existed in COMIS [10], this module has been extended and coupled with an evaluation procedure of indoor air quality using the ventilation effectiveness concept in order to qualify the quality of ventilation in a multizone building [11]-[13].

Ventilation Effectiveness is a measure of how quickly an air-borne contaminant is removed from the room.

$$\varepsilon^c = \frac{C_e(\infty)}{\langle C(\infty) \rangle}$$

with :

$C_e(\infty)$: contaminant concentration in exhaust air at time ∞

$\langle C(\infty) \rangle$: room mean concentration of contaminant

$$C_e(\infty) = \frac{\sum_{i=1}^{i=Nz} F_{i0} C_i}{\sum_{i=1}^{i=Nz} F_{i0}}$$

$$\langle C(\infty) \rangle = \frac{\sum_{i=1}^{i=Nz} C_i V_i}{\sum_{i=1}^{i=Nz} V_i}$$

F_{i0} : air flow rate from zone i through the exhaust duct to outside [m^3/s].

C_i : Contaminant concentration in zone i.

V_i : Room volume [m³]

The Contaminant Removal Efficiency is derived from the ventilation effectiveness.

$$\eta^c = \frac{\epsilon^c}{1 + \epsilon^c}$$

We define the instantaneous exposure, E, to a pollutant at time t as the concentration, C(t), in the zone with the person at time t :

$$E = C(t)$$

The cumulative exposure from t_1 to t_2 is given by :

$$E_c = \int_{t_1}^{t_2} C(t) dt$$

E_c may be obtained by numerical integration of the calculated contaminant concentration curve.

5.- Test case :

The test building is a five zone single family house presented in Figure 4.

This building is characterized by 26 flow paths (doors, windows, cracks of internal and external walls...), 4 identical self-controlled air inlets located on living room walls and a mechanical exhaust system (fan, duct fittings, duct straights, such as elbow, diffuser, and flow controllers). Figure 5 gives a general scheme of this network. Each component is described by its characteristic curves (see figures 6 to 8).

We consider in this example a typical winter day, with a south blowing wind.

Outdoor temperature : -2°C

Outdoor pressure : 101300 Pa

Outdoor Relative Humidity : 60 %

Indoor temperatures : Living room and Kitchen : 20°C

Bathroom : 22°C

Toilets : 19°C

Attic : 10°C

Indoor Relative humidity : 50%

The Cp-values used for the calculation are given in Table 1.

Table 2 : Cp-Values for each wall

South façade	West and East façades	North façade	South roof	North roof	End of exhaust duct
+ 0.25	- 0.70	- 0.50	- 0.55	- 0.60	- 0.75

5.1.- Wind Speed Influence :

We vary the wind speed from 0 to 12 m/s; according to the wind velocity, the building ventilation works as explained next:

- At zero wind velocity, the air goes through the two façades (windward and upwind façades). The air change rate is equal to the specific flow of ventilation (i.e. the flow is controlled by the fan).

- At a low wind velocity, the air still goes through the two façades with an increased flow at the windward and a decreased flow at the upwind façade. The total air change rate is identical.

- At a given wind velocity (6 m/s in our case), named the protection level, the air flows through the windward façade. The total air change rate is higher than previously. A flow going through the windward facade, which is a function of the façade infiltration and the wind velocity, is added to the specific flow (flow of the fan). The crossing air flow is zero up to the protection level. After this threshold, it continuously increases the total ventilation rate up to 64 % at 12 m/s (Figure 9).

5.2.- Indoor Air Quality :

At first we consider an oven located in the kitchen (its power is 3 kW and its CO₂ emissive power is 0.0981g/s) and a CO₂ source pollutant in the living room (its CO₂ emissive power is 0.01g/s, which is equivalent to two person emission). The resulting Ventilation Effectiveness is 2.75, and the Contaminant Removal Efficiency is 0.73. Figure 10 presents the evolution of CO₂ concentration in different rooms with a 1 m/s wind. In this case, the mechanical exhaust system appears to be a good solution, the concentration in the living room is lower.

Secondly, we consider two persons, with different activity patterns, and we calculate the exposure of every one to different sources of CO₂ pollutants. The first person is in the kitchen during 10 minutes, moves to the outdoor during 4 hours and 40 minutes (we suppose that the outdoor concentration is zero), then prepares the lunch in the kitchen for 1 hour, after goes outdoor for 4 hours, returns in the kitchen during 10 minutes, then leaves the building for 1 hour and 50 minutes, prepares the dinner for 1 hour and finally he stays in the living room. The second person stays in the living room during 24 hours. The instantaneous and cumulative exposures (during one day) to the pollutant CO₂ for the two persons separately are given in figures 11 and 12. We notice that, while the instantaneous exposure for the first person is some times (initial instantaneous exposure and when he uses the kitchen) much higher than for the second person, the cumulative exposure for the first person is very low.

6.- Conclusion :

The actual version of COMIS code may be used as the core of a design tool of a multizone building and enables diagnosis of its defective ventilation network. An interface allowing pre and post processing of data and results is essential to use such

a code in a research organization.

The case study presented in this paper is only given as an illustrative example, it demonstrates the feasibility of our project developed within the frame of an international effort coordinated by the International Energy Agency, Annex 23.

This is only the first step of the study and characterization of a building from the air quality point of view. In order to enable a real air management introduction of new components which pollution level is dealing with their behavior with time is now necessary.

References :

- [1] **B. MALO, P. VALTON**, "Etudes des modèles de ventilation et simulation du renouvellement d'air dans les locaux". Rapport final, convention A.F.M.E /Co.S.T.I.C, juin 1987
- [2] **M. W. LIDDAMENT - C. ALLEN** " The validation and comparaison of mathematical models of air infiltration. A.I.C.- TN11- September 1983.
- [3] **H.E. FEUSTEL, Juergen Dieris**, " A survey of airflow models for multizone Structures", Energy and Building, Volume 18, Number 2, 1992.
- [4] **F. ALLARD et alii**, "Technical Note AIVC 29. Fundamentals of the multizone. Air Flow Model-COMIS", May 1990
- [5] **G.N. WALTON**. 1989. "A computer algorithm for predicting infiltration and interroom airflows". ASHRAE Transactions, Vol.90, Part 1.
- [6] **A.C. MEGRI, G. KRAUSS, F. ALLARD**, "Modélisation de réseaux de distribution d'air couplés à des bâtiments multizones", GEVRA, Lyon les 21 et 22 Mars 1991
- [7] **A.C. MEGRI, F. ALLARD, G. KRAUSS** " Coupling Ventilation Network and HVAC systems to multizone infiltration models", Proceedings of the Ninth International PLEA Conference, Seville, Spain, September 24-27 1991
- [8] **R.J. Tsal, H.F. Behls, R.Mangel** " T-Method Duct Design, Part III : Simulation " ASHRAE, 1989
- [9] **Pierre JARDINIER** " Appareillage de ventilation pour le bâtiment. Seminaire spécialisé 19 et 20 Septembre 1989.
- [10] **E. A. Rodriguez, F. Allard**, " Coupling COMIS airflow model with other transfer phenomena, Energy and Buildings, Volume 18, Number 2, 1992.
- [11] **R.K. Clayton, E.E. Stephenson, M.D. Jackson and L.E. Sparks** (1988) " EPA's indoor air quality test house 3. Mothcake studies," Proc. of the 1988 EPA/APCA Int. Sympos. Measurement of Toxic and Related Air Pollutants.
- [12] **E.A.B. Maldonado**, (1982) " A method to characterize air exchange in residences for evaluation of indoor air quality," Ph.D. Dissertation in Mechanical Engineering, Iowa State University, Ames, IA.
- [13] **B.A. Tichenor, L.E. Sparks, J.B. White and M.D. Jackson** (1990) "Evaluating sources of indoor air pollution.

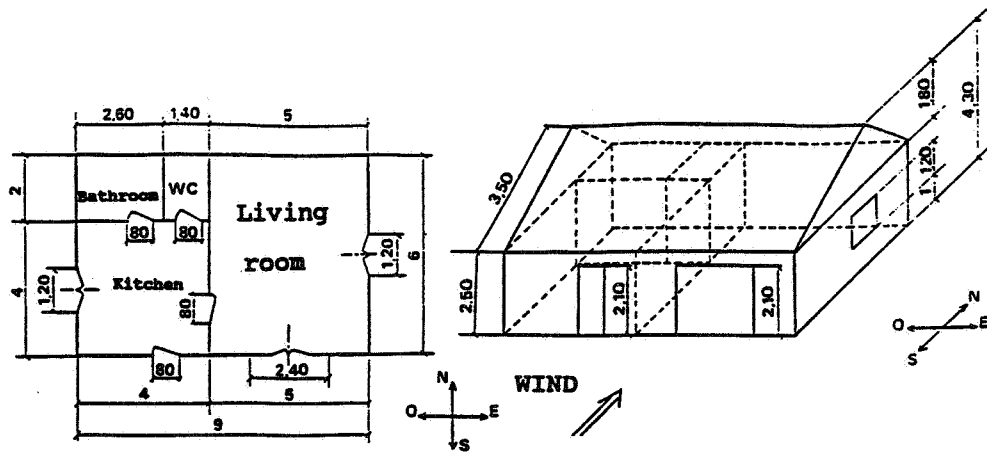


Figure 4 : Test Case.

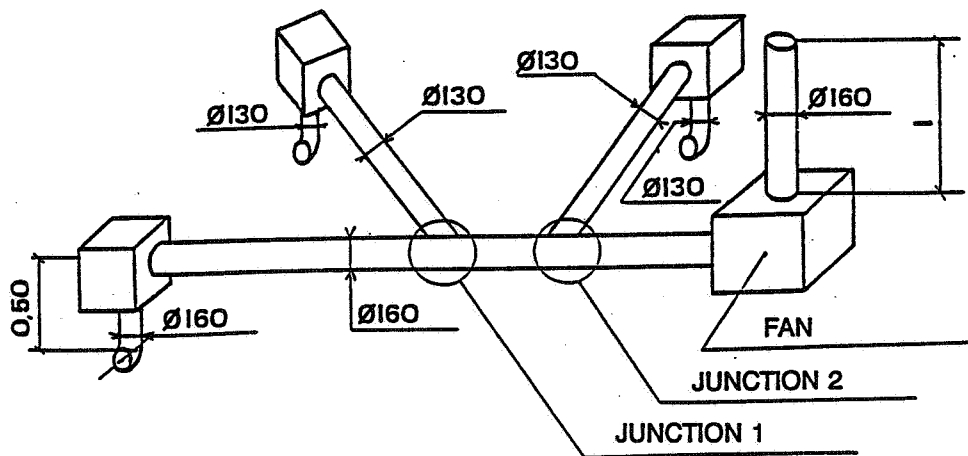


Figure 5 : General description of the ventilation network.

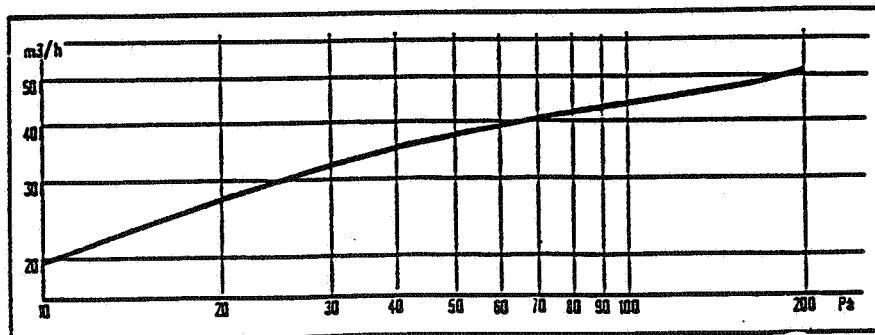


Figure 6 : Characteristic curve of the air inlets.

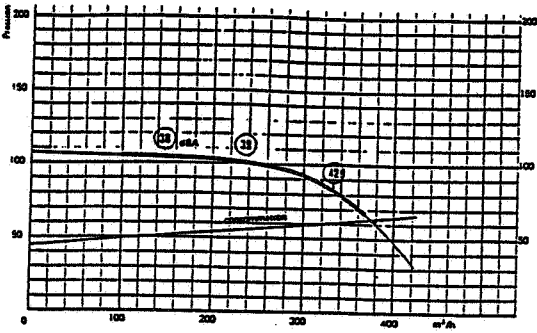


Figure 7 : Characateristic curve of the fan.

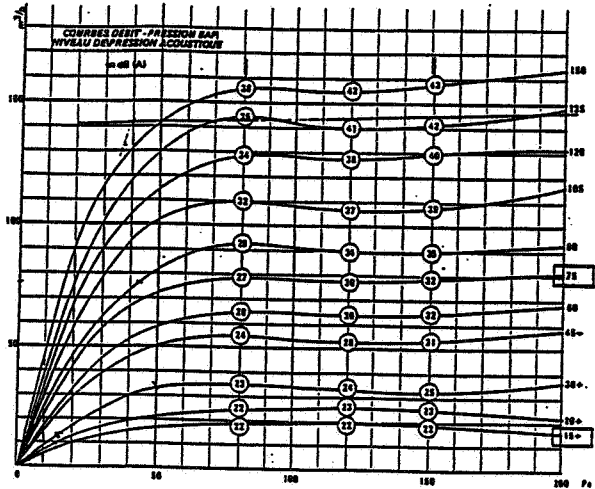


Figure 8 : Characteristic curve of the exhaust grids.

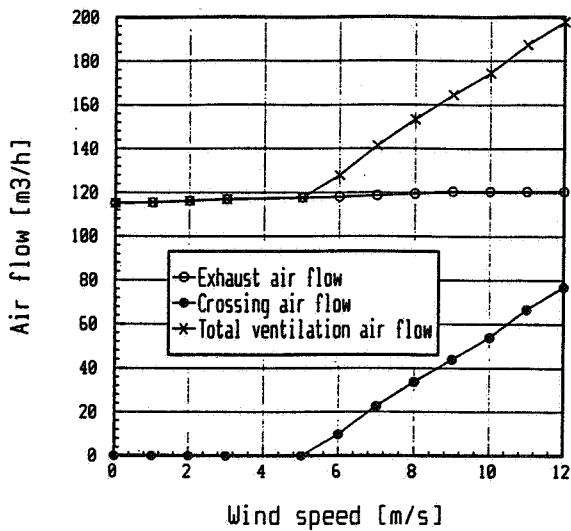


Figure 9 : Wind Speed Influence.

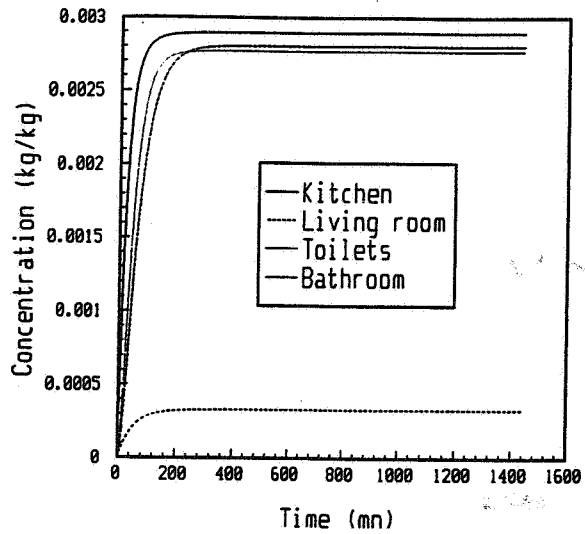


Figure 10 : Evolution in time of CO₂ concentration in different rooms.

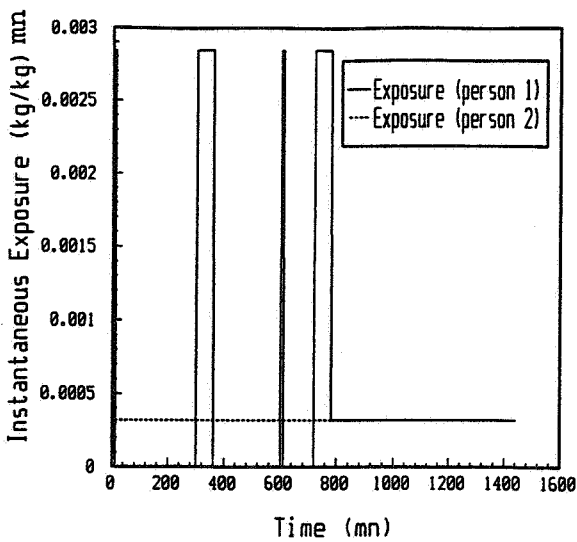


Figure 11 : Instantaneous exposure.

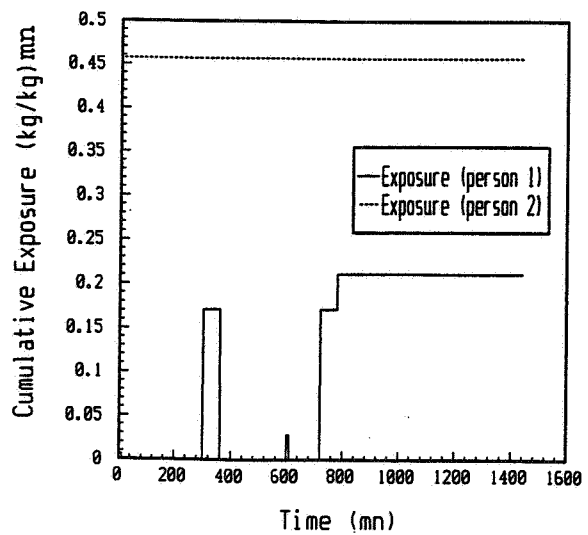
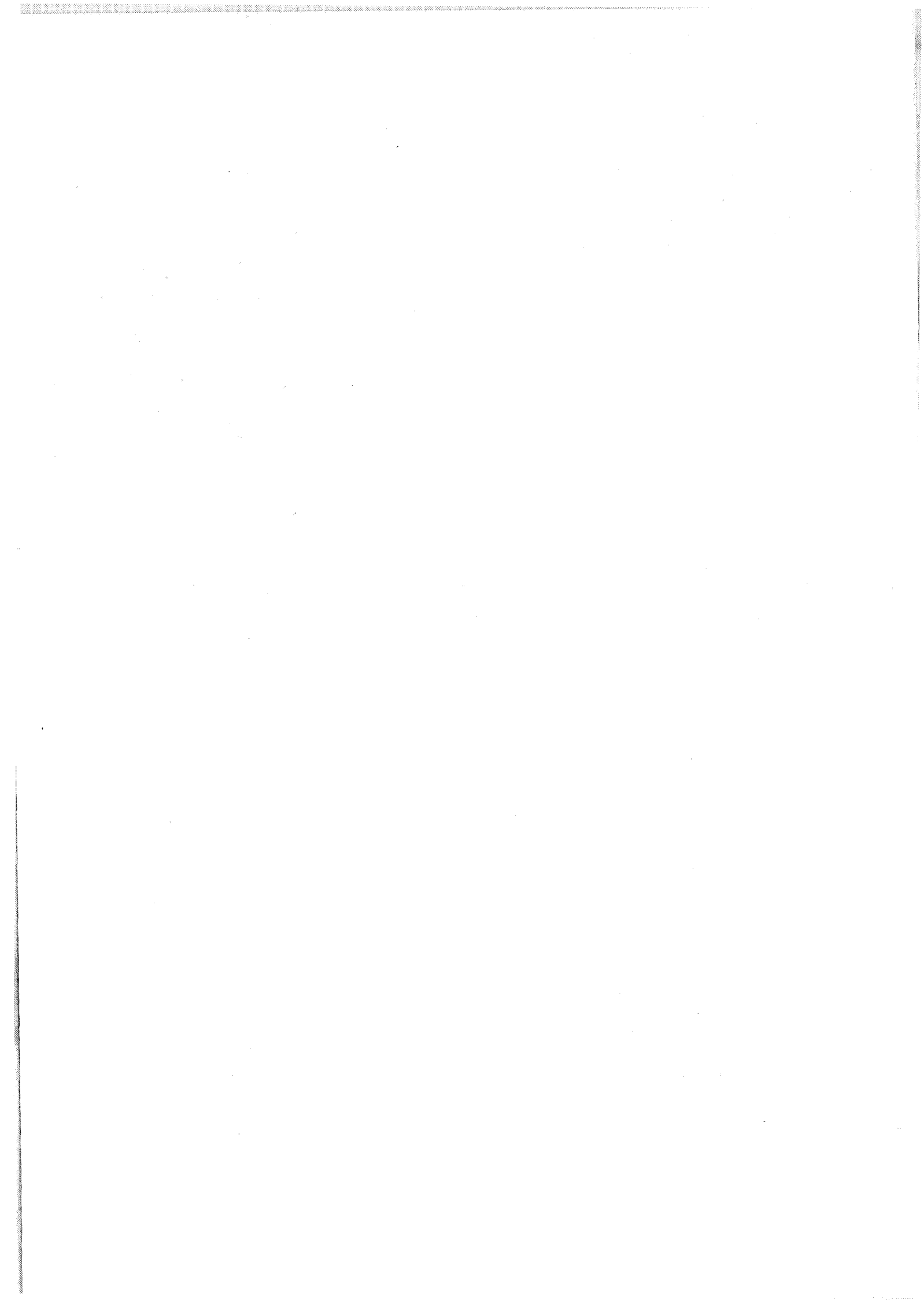


Figure 12 : Cumulative exposure.



**Ventilation for Energy Efficiency and Optimum
Indoor Air Quality
13th AIVC Conference, Nice, France
15-18 September 1992**

Poster 28

**Experimental and Numerical Investigations within a
Post-Annex-20-Model**

B. Hanel, E. Richter, P. Vogel

**Technische Universität Dresden, Institut für
Strömungsmechanik, Lehrgebiet
Thermofluidodynamik, Mommsenstr.13, O-8027
Dresden, Germany**

1. Introduction and aims

A small test room has been build which is five times smaller than the so called Annex-20- room (Figure 1 and 4). Different kinds of tracers have been used for visualizing of flow patterns (/1/). Velocities, concentrations and mass transfer coefficients have been measured. The measuring instrumentation is based on thermal anemometry (hot wire probes) and a special ammonia-mass transfer method, respectively, in order to estimate the heat flux coefficient at the walls. The values measured and the flow patterns have been applied in order to compare and to evaluate a computer code developed in Dresden to simulate three dimensional flows. This code is based on a finite-volume-discritization for the transport equations (Navier-Stokes- with k-ε-model) solved with a new iteration technique including a multi grid solver.

2. Measuring Equipment

A test room was constructed at a scale of 1:5 to the test room (/2/,/3/), specified by the international project IEA ANNEX 20 (/4/,/5/). A lot of measuring and computational results are available for this problem. The dimensions of our test room are (L x W x H)=(0,84m x 0,6m x 0,5m). The inlet device has a width of 0,155m and a height of 0,042m. The dimensions of the outlet device are (w x h)=(0,06m x 0,039m). The walls are transparent to make flow visualization possible. At present a maximum velocity of 2m/s can be applied due to the installed equipment. That leads to a Reynolds number relating to the inlet of $Re=5500$ and an air change rate of $n=186$ 1/h. The flow within the test room is isothermal and visualized by means of several kinds of tracers (e.g. so-called 'disco fog', incense, glycerine-water mixture). A system consisting of light sheet equipment and a CCD camera is applied to get a snapshot of the flow pattern in a specified plane. Averaged velocities and turbulent quantities are measured by means of hot wire anemometry (DANTEC 55M). A unit made by construction elements (ISEL automation) is used to move the probe to the measuring position controlled by the computer. Placing the probe at 100 locations takes about 15 minutes including 2s integration time at every measuring point. It is taken approximately 2000 values for time averaging for each measuring point. Figure 2 shows the special calibration equipment (/5/) used to calibrate the probe right beside the test room within a range of 0,1 to 2,0 m/s.

As mentioned above, heat transfer coefficients are determined by means of the ammonia transfer method (7/) using the analogy between heat and mass transfer and a computer aided image processing system (Figure 3, /8/). Small quantities of ammonia are added to the supplied air. That causes a chemical reaction at foils moistened with a reaction substance. The colouring of this foils indicates the intensity of the mass transfer. Using the analogy between heat and mass transfer the heat transfer coefficients can be calculated by

$$\alpha = \frac{\beta_{\text{NH}_3} \cdot \lambda}{D_{\text{NH}_3-\text{L}}} \cdot \left(\frac{\text{Pr}}{\text{Sc}} \right)^n$$

3. Mathematical Model

As basic equations we consider the time averaged transport equations for an incompressible fluid. By means of Boussinesq's concept, Boussinesq's approximation of buoyancy and a k-ε turbulence model, the following system of differential equations is formed by :

$$\frac{\partial \bar{U}_i}{\partial t} + \bar{U}_j \frac{\partial \bar{U}_i}{\partial x_j} - \frac{\partial}{\partial x_j} \left[\nu \left(\frac{\partial \bar{U}_i}{\partial x_j} + \frac{\partial \bar{U}_j}{\partial x_i} \right) \right] + \frac{1}{\rho} \frac{\partial \bar{p}}{\partial x_i} = \frac{\bar{f}_i}{\rho} - \frac{\partial \overline{u'_j u'_i}}{\partial x_j}$$

$$\frac{\partial \bar{U}_i}{\partial x_i} = 0$$

$$\frac{\partial \bar{T}}{\partial t} + \bar{U}_j \frac{\partial \bar{T}}{\partial x_j} - \frac{\partial}{\partial x_j} \left[a \frac{\partial \bar{T}}{\partial x_j} \right] = \overline{q^v} - \frac{\partial \overline{u'_j T'}}{\partial x_j}$$

$$\frac{\partial k}{\partial t} + \bar{U}_j \frac{\partial k}{\partial x_j} - \frac{\partial}{\partial x_j} \left[\left(\nu + \frac{\nu_t}{\text{Pr}_k} \right) \frac{\partial k}{\partial x_j} \right] =$$

$$\nu_t \frac{\partial \bar{U}_i}{\partial x_j} \left(\frac{\partial \bar{U}_i}{\partial x_j} + \frac{\partial \bar{U}_j}{\partial x_i} \right) - \epsilon + g_j \cdot \gamma \frac{\nu_t}{\text{Pr}_t} \frac{\partial \bar{T}}{\partial x_j}$$

$$\frac{\partial \varepsilon}{\partial t} + \overline{U}_j \frac{\partial \varepsilon}{\partial x_j} - \frac{\partial}{\partial x_j} \left[\left(\nu + \frac{\nu_t}{Pr_\varepsilon} \right) \frac{\partial \varepsilon}{\partial x_j} \right] = + C_1 \nu_t \frac{\varepsilon}{k} \frac{\partial \overline{U}_i}{\partial x_j} \left(\frac{\partial \overline{U}_i}{\partial x_j} + \frac{\partial \overline{U}_j}{\partial x_i} \right) - C_2 \frac{\varepsilon^2}{k} + C_1 g_j \gamma \frac{\nu}{Pr_t} \frac{\partial T}{\partial x_j}$$

with $\nu_t = C_D \cdot k^2/\varepsilon$ and $a_t = \nu_t / Pr_t$

In addition, appropriate initial and boundary conditions have to be specified. Details are given by Rösler (/9/). The set of constants of the turbulence model is shown in the table below.

C_D	C_1	C_2	Pr_t	Pr_ε	Pr_k
0,09	1,44	1,92	0,77	1,3	1,0

Instead of solving the fully discretized and linearized equation system we are using an explicit velocity-pressure iteration which is based on the algorithm of the Marker and Cell Method. Our strategy of solution will be presented in the paper /10/.

4.Results

Figure 5 shows the first of the experimental and numerical results of mean air velocities at a Reynolds number of $Re=2238$ and an air change rate of $n=75$ at the symmetry plane.

Experimental data have been averaged in time and space, given by

$$|\bar{u}| = \sqrt{\bar{u}^2 + \bar{v}^2} .$$

The numerically predicted velocity profiles are in a good agreement with the measured ones. Notice that the velocities are given as absolute values. Therefore the velocities close to outlet device have the same direction like the inlet device velocities. Furthermore, results like flow patterns, mass concentrations at the walls and therefrom heat flux coefficients and turbulent quantities will be shown at the poster because some pictures have a good quality only in the original state.

5. Conclusions

A 1:5 scaled test room was built to estimate and validate a simulation code of three-dimensional indoor air flows by experimental investigations. First results show that the constructed test room is suitable for this task.

Reynolds number, geometry of in- and outlet device, turbulence intensity and direction of supplied air will be varied in further experiments. An improvement of numerical results is expected by using a Low-Reynolds-Number turbulence model.

In addition, it is planned to compare these results with data available from others ANNEX20 participants (3/).

6. Acknowledgement

The research was supported by the Bundesministerium für Forschung und Technologie under the contract 0329016D.

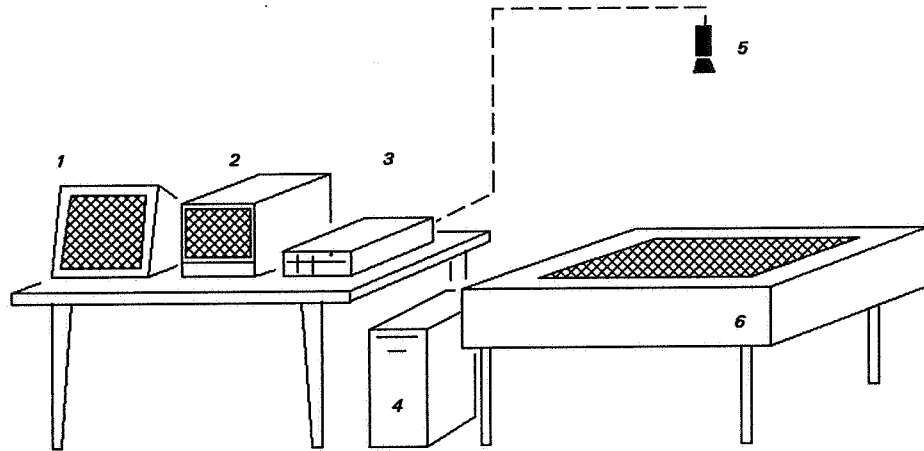
7. Photographs , graphs and diagrams

Photograph not available for Conference Proceedings.

Figure 1: The model "post-annex-20-room" with the moving system for the probes (author : P. Vogel)

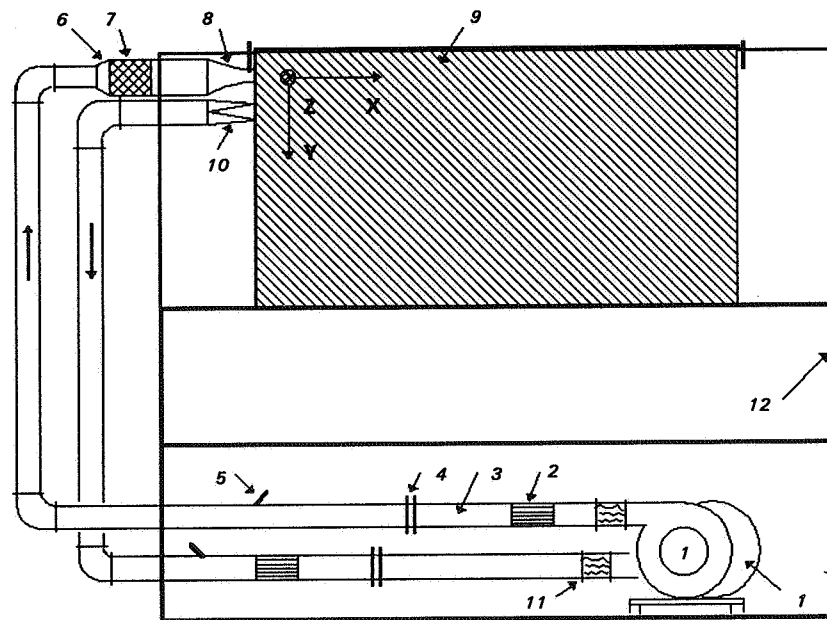
Photograph not available for Conference Proceedings.

Figure 2: The special calibration equipment which is used to calibrate the hot wire probes (author P. Vogel)



- | | |
|------------------------|-----------------------------------------------|
| 1 ... Computer monitor | 4 ... AT 486/33 with a grabber card AT-Chroma |
| 2 ... Camera monitor | 5 ... CCD-camera FK 6512 IQ |
| 3 ... Control system | 6 ... Light table |

Figure 3: Picture processing system IMPAC/PiPS



- | | |
|-----------------------------------------------------|------------------------------|
| 1 ... ventilator | 7 ... heat exchanger |
| 2 ... rectifier | 8 ... air supply inlet |
| 3,4 . air supply pipe with mass measuring equipment | 9 ... model room |
| 5 ... temperature measuring point | 10 ... outlet |
| 6 ... transition piece | 11 ... vibration compensator |
| | 12 ... chassis |

Figure 4: The model "post-annex-20-room"

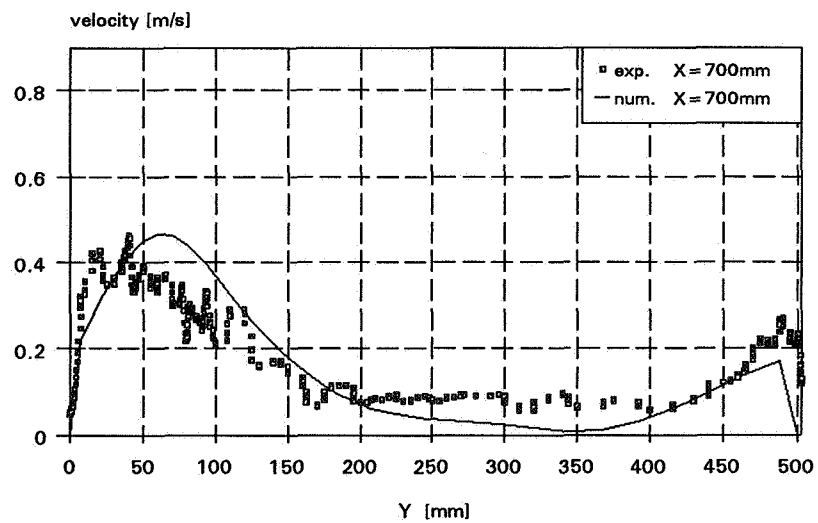
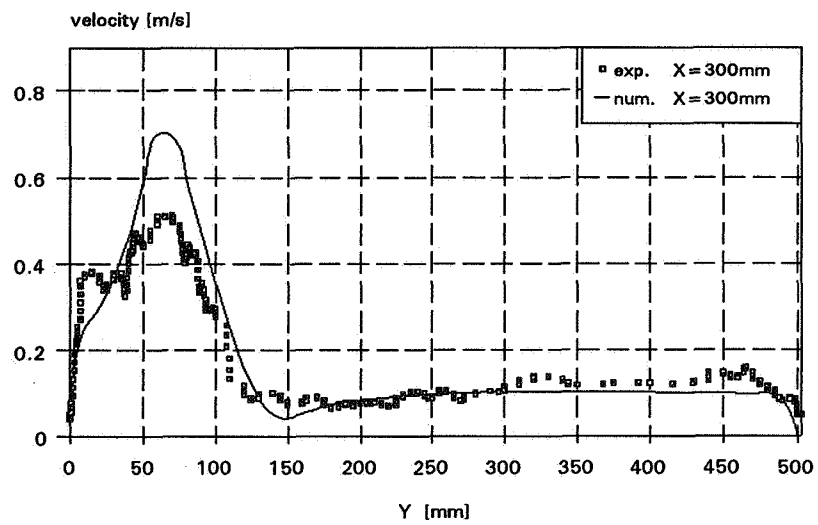
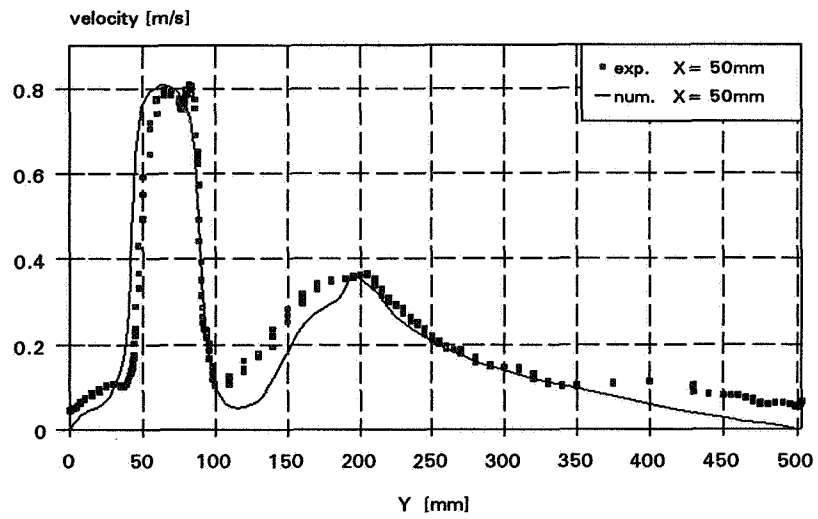


Figure 5: Comparison of experimental and numerical results of the absolute velocities at different Y-Z-planes in the symmetry plane

7. References

- /1/ Leitl, B. :
"Erfahrungen bei der Nutzung verschiedener Raucherzeuger bei der Strömungsvisualisierung". Forschungsbericht,
Institut für Strömungsmechanik, Technische Universität Dresden, 1992

- /2/ Vogel, P. :
"Entwurf eines Modells zur Messung von Raumluftrömungen".
Diplomarbeit;
Institut für Strömungsmechanik, Technische Universität Dresden, 1992

- /3/ Hanel, B. :
"Methoden zur Vorausbestimmung von Strömungsvorgängen in klimatisierten Räumen". Habilitation,
Technische Universität Dresden, Fakultät für Maschinenwesen, 1987

- /4/ Whittle, G.E. :
"Evaluation of Measured and Computed Test Case; Results from ANNEX 20, Subtask 1".
12th AIVC-Convergence, Ottawa, 1991

- /5/ Moser, A. :
"The Message of ANNEX 20 : Air Flow Pattern within Buildings".
12th AIVC-Convergence, Ottawa, 1991

- /6/ Heinrichs, P. and Rosenquist, M. O. :
"Vermessen eines Kalibrierungskanal für Hitzdrahtsonden".
Hermann-Föttinger-Institut, Berlin, 1987

- /7/ Krückels, W. :
"Eine Methode zur photometrischen Bestimmung örtlicher Stoffübergangszahlen mit Hilfe chemischer Nachweisreaktionen". Dissertation,
Technische Hochschule Stuttgart, 1968

- /8/ Richter, E. and Vogel, P. :
"Einsatz eines Bildverarbeitungssystems zur Auswertung von Meßfolien bei der Auswertung von Stoffübergangsmessungen". Institutsbericht, Institut für Strömungsmechanik, Technische Universität Dresden, 1991
- /9/ Rösler, M. :
"Mathematisch-numerische Untersuchungen zur Berechnung von dreidimensionalen inkompressiblen Kanal- und Raumluftrömungen". Dissertation, Technische Universität Dresden, Fakultät Maschinenwesen, 1992
- /10/ Rösler, M. and Hanel, B. :
"Numerical Computation of Flow and Heat Transfer in Air-Conditioned Rooms by a Special Velocity-Pressure Iteration and a Multigrid Method". Will be published in the Proceedings of the international-Conference "ROOMVENT '92", Aalborg/Denmark, Sept. 2.-4. 1992

**Ventilation for Energy Efficiency and Optimum
Indoor Air Quality
13th AIVC Conference, Nice, France
15-18 September 1992**

Poster 26

**A New Method for Determination of Velocity
Pressure Loss-Factors for HVAC System
Components.**

K.W. Cheong, S.B. Riffat

**School of Architecture, University of Nottingham,
University Park, Nottingham, NG7 2RD, United
Kingdom**

SYNOPSIS

This investigation is concerned with the determination of velocity pressure loss-factors for HVAC system components using tracer-gas techniques. Experimental work was carried out using an HVAC system and k-factors for various components such as bends, branches, contractions, expansions and orifice were determined. Results were compared with measurements made using a pitot tube and values given in the CIBSE Guide and ASHRAE Handbook.

The performance of different types of filters used in HVAC systems was also examined. The constant-injection tracer gas technique was used to develop correlations between the pressure drop and face velocity of a synthetic-fibre filter, bag filter and glass-fibre filter. Results were compared with data obtained using traditional instrumentation.

LIST OF SYMBOLS

A	Cross-sectional area of the duct fittings (m^2)
C	Concentration of tracer gas (ppm)
F	Volumetric flow rate (m^3/s)
q	Injection rate of the tracer gas (m^3/s)
k	Velocity pressure loss-factor, dimensionless
V	Bulk velocity (m/s)
t	Air temperature ($^{\circ}C$)
P_v	Velocity pressure (N/m^2)
P_s	Static pressure (N/m^2)
P_T	Total pressure (N/m^2)
ΔP_T	Total pressure loss (N/m^2)
V_f	Face velocity, filter (m/s)
ΔP_f	Pressure drop, filter (N/m^2)
ΔP_t	Pressure drop based on tracer gas measurement, (N/m^2)
ΔP_p	Pressure drop based on pitot tube measurement, (N/m^2)
β	Barometric pressure (N/m^2)
ρ	air density (kg/m^3)

1. INTRODUCTION

Accurate determination of duct pressure losses is a necessary prerequisite for design of energy-efficient heating, ventilation and air conditioning (HVAC) systems. The pressure loss of ductwork supplying air to various zones can be calculated using friction charts and tables of pressure loss-factors (i.e. k-factors) for duct fittings. Pressure loss-factors are usually obtained using values given in the CIBSE Guide "Reference Data"¹. and ASHRAE Handbook "Fundamentals"². These values have been determined experimentally using traditional instrumentation such as pitot tube and orifice meters.

Tracer-gas techniques such as constant-injection and pulse-injection allow accurate measurement of airflow in ducts and duct fittings. Unlike traditional instrumentation, tracer-gas techniques do not require a long measuring duct for establishment of fully developed flow and can be used to measure airflow over wide range of velocities in ducts and fittings of various sizes and shapes. Furthermore, tracer-gas techniques can be used to measure airflow directly and do not require determination of the cross-sectional area of the duct and ducts fittings. Experimental work was carried out in a small-scale HVAC system and k-factors for various components such as a bend, a branch and a contraction were determined and results were compared with measurements made using a pitot tube and values obtained from CIBSE and ASHRAE data. The performance for different types of filters used in the HVAC systems was also examined.

2. THEORY

2.1 Constant-Injection Tracer-Gas Technique

The constant-injection technique was used to measure airflow in an HVAC system. SF₆ tracer gas was injected into the duct fittings at a constant rate and the resulting concentration response was measured. Assuming that the air and tracer gas are perfectly mixed within the duct, and the concentration of tracer gas in the outside air is zero, the following equation can be used for steady-state conditions³:

$$F = (q/C) \times 10^6 \quad (1)$$

The average air velocity is:

$$V = (q/CA) \times 10^6 \quad (2)$$

2.2 Velocity Pressure Loss-Factors For Duct Fittings

Whenever a change in area or direction occurs in a duct or when the flow is divided and diverted into a branch, losses in total pressure occur. These losses are usually greater than losses in a straight duct and are referred to as separation losses; they can be calculated from:

$$\Delta P_T = k P_v = k \rho V^2/2 \quad (3)$$

Substituting equation (2) into equation (3) we have:

$$\Delta P_T = 0.5k \rho (q/CA)^2 \times 10^{12} \quad (4)$$

For standard air (i.e. air at 20°C and 101.325 kPa) ρ is 1.2 kg/m³. For air at other conditions, the loss in total pressure must be corrected using the following equation:

$$\Delta P_T = 0.6(\beta/101.325)[293/(273 + t)] (q/CA)^2 \times 10^{12} \quad (5)$$

The loss factor, k , for various duct fittings can be found using the CIBSE Guide "Reference Data" and ASHRAE Handbook "Fundamentals".

3. EXPERIMENTAL

Measurement of airflow and pressure distribution were carried out in a small-scale HVAC system, Figure 1. This consisted of a fan control and instrumentation console. The fan unit had a volumetric flow rate in the range 0.1 to 0.3 m³/s, dependent upon the ductwork resistance and supply voltage. The console contained a variable transformer for fan speed control and a voltmeter and ammeter for measurement of supply voltage and current respectively. A square-to-round fan intake transition also accepted a standard 600 x 600mm filter. The rectangular-to-round fan discharge transition connected to 200mm diameter ductwork using standard push fittings; the duct was manufactured from galvanised mild steel. The HVAC system was fitted with various types of fittings such as bends, branches, expansions and diffusers. Two types of air supply diffusers were used and the discharge was controlled by means of dampers.

The concentration of tracer gas was measured by an infrared gas analyser, type Binos 1000, made by Rosemount GMGH, Hanau, Germany. The velocity was measured using a pitot-static tube. The velocity and static pressure at the inlet and outlet of duct fittings were measured using an electronic micromanometer, type EDM 2500, made by Airflow Development Ltd, High Wycombe, UK.

SF₆ tracer gas was injected into the duct at a constant rate using mass flow controller, type F100/200, made by Bronkhorst High-Tech BV, Ruulo, Holland. The mass flow controller had a maximum flow capability of 3.9 L/min and a measurement accuracy of $\pm 1\%$.

3.1. Determination of k -factors

A typical arrangement for measuring the pressure loss and airflow rate in a duct fitting is shown in Figure 2. The experimental procedure for determining the k -factor was as follows:

- i) Start the fan and adjust the flow (e.g. 20% of main voltage).
- ii) Connect the micromanometer across the measuring unit as shown in Figure 2 and measure the differential static pressure (i.e. P_s at the inlet - P_s at the outlet of the fitting).
- iii) Inject tracer gas into the duct upstream of the fitting at a constant rate q , using the mass-flow controller. To achieve a good distribution of tracer gas in the duct, a mutli-injection probe should be used.
- iv) Use a mutli-point probe to collect tracer-gas samples downstream of the fitting. Measure the concentration of tracer gas using the gas analyser.

- v) Measure the velocity pressure at the inlet and outlet of the duct fitting using a pitot-static tube.
- vi) Increase or decrease the fan speed in order to alter the airflow rate through the duct fitting and repeat the measurements.

3.2. Development Of Correlation Between Pressure Drop and Face Velocity of Filters

The experimental procedure for determining the correlation between the pressure drop and face velocity of filters are as follows:

- i) Insert a filter into the filter holder on the fan intake.
- ii) Start the fan and adjust the flow (e.g. 20% of main voltage).
- iii) Connect the micromanometer to the tappings on the square filter holder as shown in Figure 3 and measure the pressure drop of the filter, ΔP_s .
- iv) Inject tracer gas into the duct inlet at a constant rate q , using a mass-flow controller.
- v) Measure the concentration of tracer gas at downstream of the duct using the gas analyser.
- vi) Measure the velocity pressure at the downstream of the duct using a pitot-static tube.
- vii) Increase or decrease the fan speed in order to alter the airflow rate through the filter and repeat the measurements.

4. RESULTS AND DISCUSSION

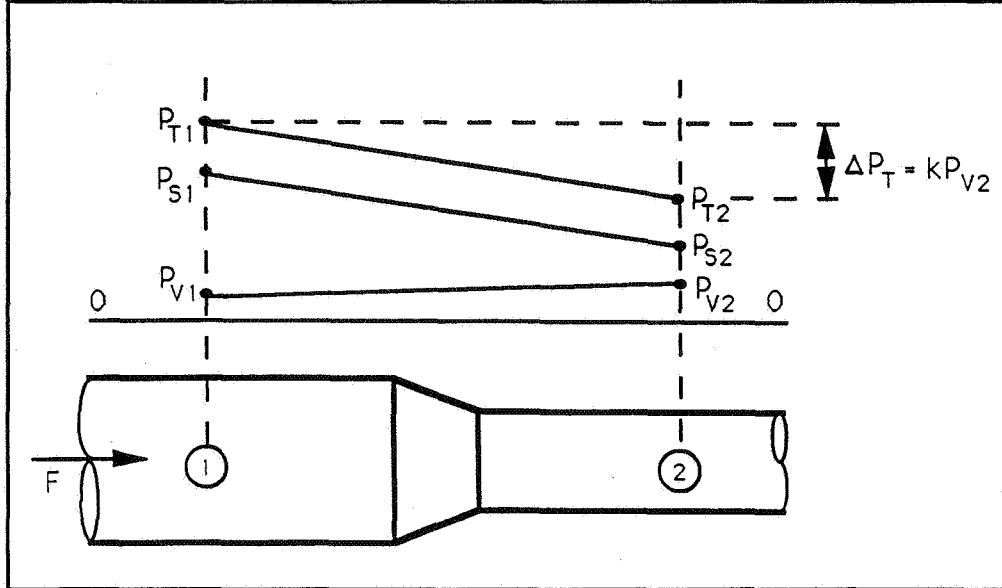
4.1 k-factors For Duct Fittings

k-factors of duct fittings were determined using the constant-injection technique and pitot static traverse method. Fittings tested included a branch, a bend, a contraction, duct exits, an orifice and a perforated plate. The total pressure loss for each fitting was measured and was plotted against the velocity pressure ($P_v = 0.5\rho V^2$) for a range of air velocities. The k-factor was then determined by measuring the gradient.

Table 1 shows typical experimental results, based on tracer-gas measurements, for a contraction. These results are plotted in Figure 4a. The slope, k-factor, of the contraction was found to be 0.14 based on tracer-gas measurements compared with 0.18 based on pitot static traverse measurements. The k-factors of the contraction are 0.13 and 0.09 according to data in the CIBSE Guide and ASHRAE Handbook, respectively.

Table 1 Experimental results, based on tracer gas measurements, for determination of the k-factor for a contraction

Reynolds No.	1.94×10^5	1.90×10^5	1.82×10^5	1.65×10^5	1.38×10^5
F	0.42	0.41	0.39	0.35	0.29
V_1	13.26	12.94	12.34	11.29	9.31
P_{V1}	104.64	100.05	91.08	75.91	51.93
V_2	20.73	20.22	19.28	17.64	14.54
P_{V2}	255.46	244.25	222.35	185.34	126.79
ΔP_{V1}	-150.82	-144.21	-131.28	-109.42	-74.86
P_{S1}	169.00	160.00	147.00	124.00	82.00
P_{S2}	53.00	50.00	45.50	38.50	27.00
ΔP_S	116.00	110.00	101.50	85.50	55.00
ΔP_T	-34.82	-34.21	-29.78	-23.92	-19.86



Similar experiments were carried out to determine the k-factors for other components of HVAC system. Figures 4a, 4b, 4c, 4d, 4e and 4f show variation of total pressure loss versus velocity pressure for various duct fittings. The estimated k-factors from the experimental results and standard data quoted in the CIBSE Guide and ASHRAE Handbook are given in Table 2. The values of k-factors for the branch, a contraction and duct exits given in the CIBSE Guide and ASHRAE Handbook were similar. However significant differences in k-factors for the bend and perforated plate were apparent. Although it is not obvious why there is a difference in k-factors quoted for the perforated plate could be explained by the fact that the CIBSE Guide has not included the effect of plate thickness on k-factor.

Table 2 Velocity pressure loss-factors for duct fittings

Type of Duct Fittings	Velocity Pressure Loss-factors (k)			
	CIBSE	ASHRAE	Pitot Tube	Tracer Gas
90° Branch	1.64	1.62	1.99	1.56
90° Bend	0.67	0.24	0.63	0.49
Contraction	0.13	0.09	0.18	0.14
Duct Exit Without Bellmouth	1.00	1.00	1.19	1.15
Duct Exit With Bellmouth	1.09	1.00	1.03	1.02
Orifice	1.04	Not Given	1.00	0.78
Perforated Plate	7.76	6.77	5.91	5.00

The k-factors estimated from tracer-gas measurements were lower than values estimated from pitot tube measurements and in most cases were in closer agreement with the average values of CIBSE and ASHRAE data. Small differences between our data and CIBSE and ASHRAE data may have resulted from variations in quality, construction and testing of the duct fittings.

In order to estimate pressure losses accurately, it is desirable that the designer uses data for k-factor provided by the manufacturers of the HVAC system in question. There is also a need for research work to provide data for k-factors for a wide range of duct fittings not at present given in the CIBSE Guide and ASHRAE Handbook. Parameters such as thickness and angle of obstruction should be included in these tables.

4.2. Correlations Between Pressure Drop And Face Velocity Of Filters

The correlations between the pressure drop and face velocity of a synthetic-fibre filter, glass-fibre filter and bag filter were developed using the constant-injection technique and pitot-static traverse method. The results indicated that the correlations obtained by these techniques are in close agreement. Tables 3 and 4 show the correlations between pressure drop and face velocity for clean and dirty filters respectively.

Table 3 Correlation between pressure drop and face velocity for clean filters

Types of Filter	Pitot Tube	Tracer Gas
Glass Fibre	$\Delta P_f = -5.698 + 17.791 V_f$	$\Delta P_f = -5.483 + 19.683 V_f$
Synthetic Fibre	$\Delta P_f = -7.239 + 25.847 V_f$	$\Delta P_f = -6.123 + 28.094 V_f$
Bag	$\Delta P_f = -6.492 + 45.206 V_f$	$\Delta P_f = -6.149 + 48.401 V_f$

Table 4 Correlation between pressure drop and face velocity for dirty filters

Types of Filter	Pitot Tube	Tracer Gas
Glass Fibre	$\Delta P_f = -7.399 + 22.998 V_f$	$\Delta P_f = -5.576 + 22.307 V_f$
Synthetic Fibre	$\Delta P_f = -24.991 + 76.715 V_f$	$\Delta P_f = -20.129 + 72.917 V_f$
Bag	$\Delta P_f = -23.609 + 89.326 V_f$	$\Delta P_f = -19.920 + 91.301 V_f$

The pressure drops across the filter varies with the types (see Figure 6) and conditions of the filter used. For example, the pressure drops across the clean-glass fibre filter for a face velocity of 10 m/s were found to be 191.35 Pa (based on tracer gas measurements) and 172.21 Pa (based on pitot tube measurements). For the clean bag filter, the pressure drops measured using the same techniques and face velocity were found to be 477.86 and 445.57 Pa. The difference between pressure drop $[(\Delta P_t - \Delta P_p)/\Delta P_p]$ obtained using constant-injection technique and pitot-static traverse method for the glass fibre, synthetic fibre and bag filters were 7.2%, 9.4% and 11.1% respectively.

5. CONCLUSIONS

- i) The values of k-factors estimated from the tracer technique were lower than those estimated using pitot static traverse method.
- ii) The estimated k-factors from tracer gas measurements for the branch, bend, contraction, exits and orifice were similar to those values given in the CIBSE Guide.
- iii) The k-factors estimated from tracer gas and pitot tube measurements for the perforated plate were smaller than values given by CIBSE and ASHRAE data.
- iv) The k-factor for the bend given in the ASHRAE Handbook was significantly lower than values estimated from tracer gas and pitot tube measurements and the value quoted by the CIBSE Guide.
- v) More experimental work is required to estimate the k-factors for a wide range of duct fittings. The effect on the k-factor of a number of parameters, such as the thickness and angle of obstruction should be investigated.

REFERENCES

1. CIBSE Guides "Reference Data", The Chartered Institution of Building Services Engineers, London, United Kingdom, 1986.
2. ASHRAE Handbook "Fundamentals", American Society of Heating, Refrigerating and Air Conditioning Engineers, Atlanta, USA, 1989.
3. Riffat, S.B. and Lee, S.F., "Turbulent flow in a duct: measurement by a tracer gas technique", Building Services Engineering Research and Technology, 11(1), 1990, pp. 21-26.

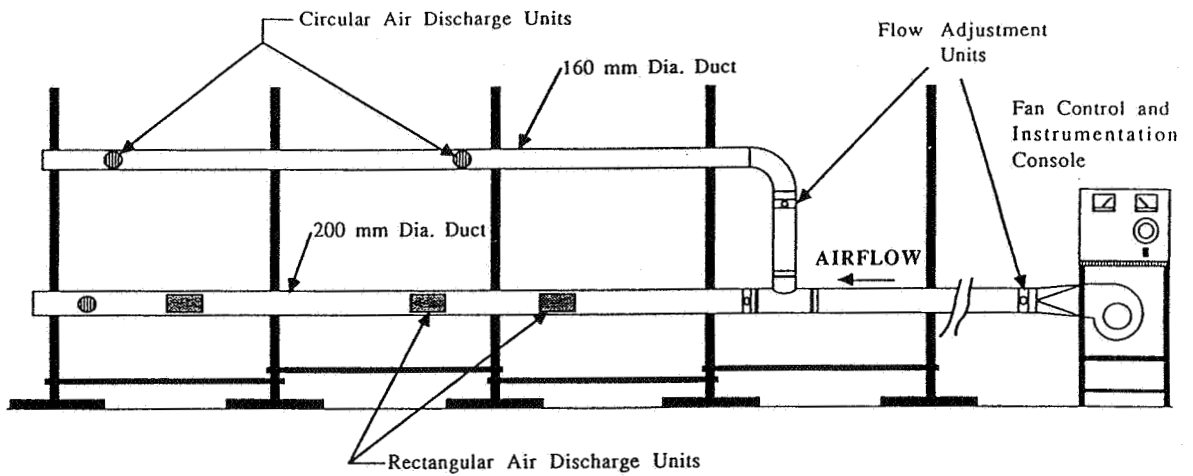


Figure 1 Schematic diagram of the small-scale HVAC system

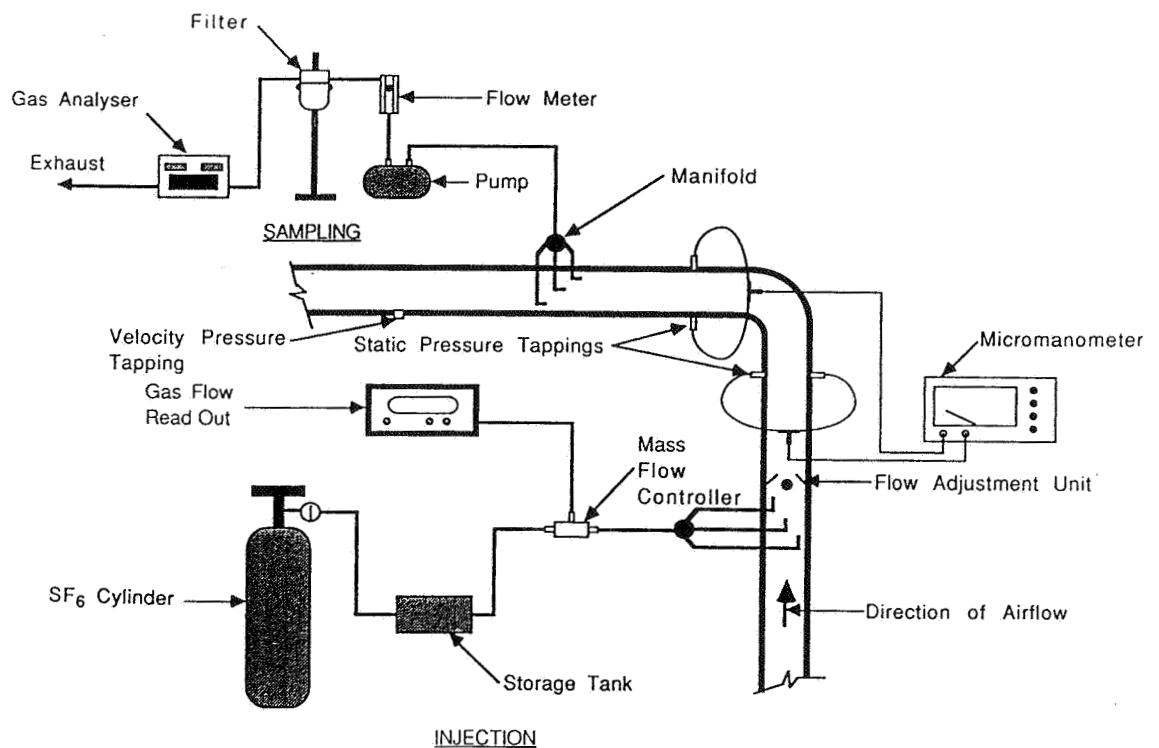


Figure 2 Instrumentation for the constant-injection tracer-gas technique applied to a duct fitting

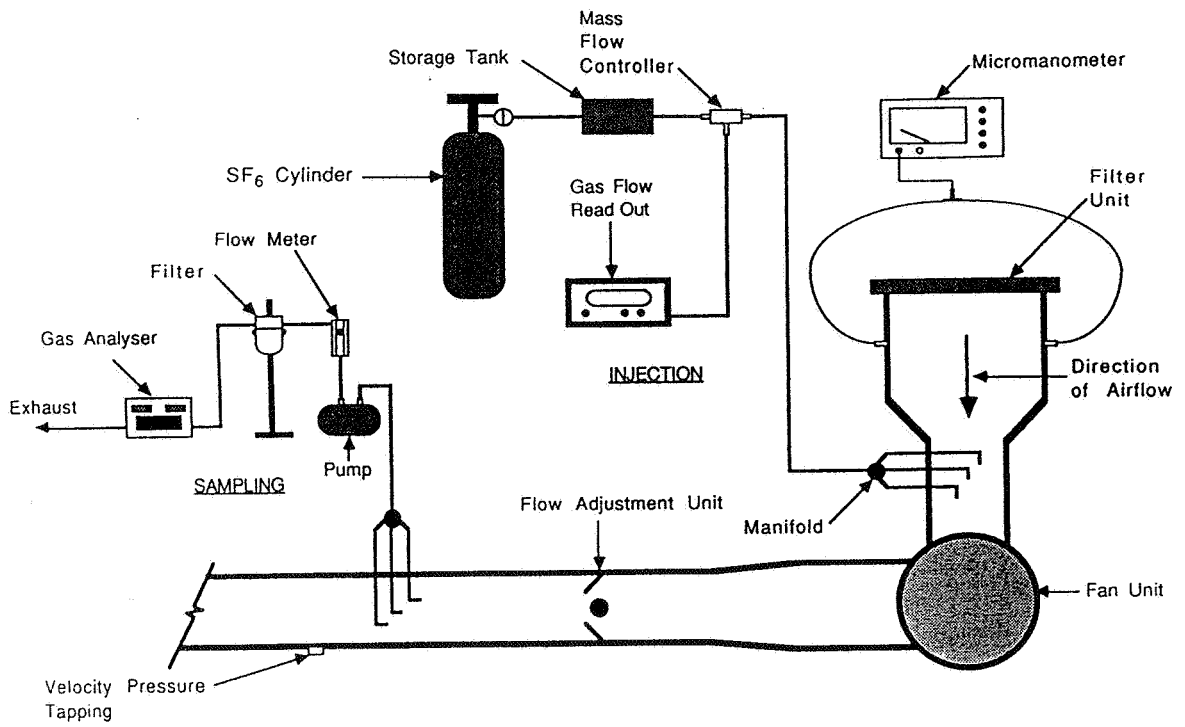


Figure 3 Instrumentation for the constant-injection tracer-gas technique applied to a filter

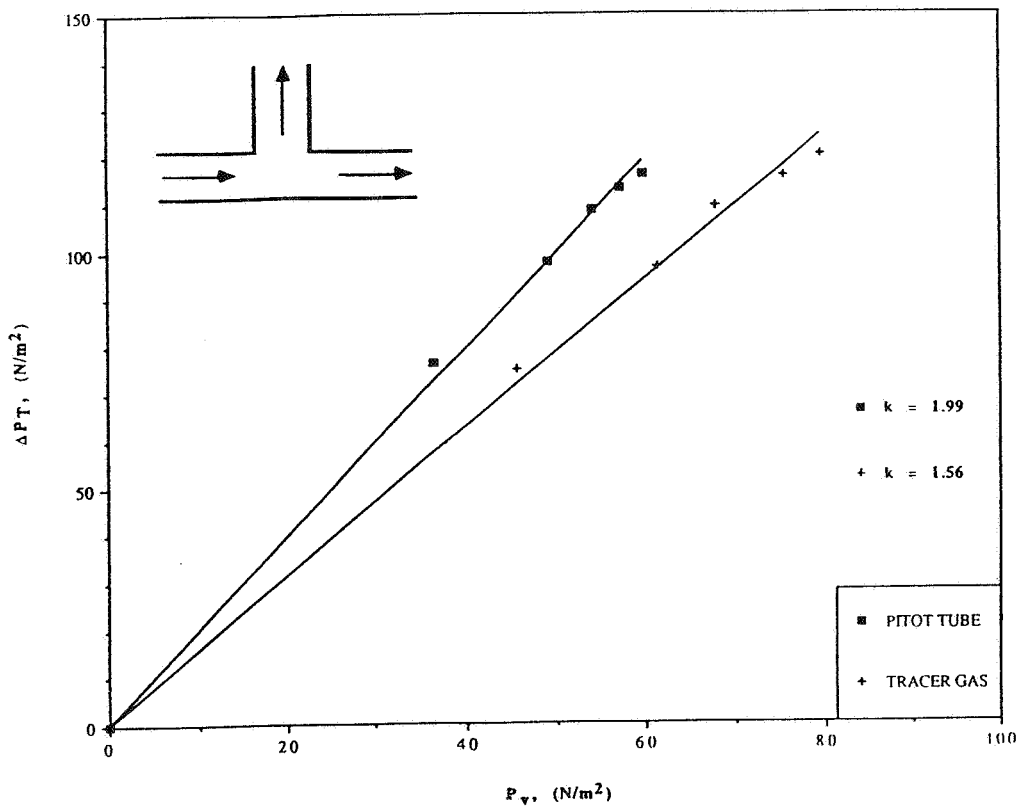


Figure 4a Variation of total pressure loss with velocity pressure, branch

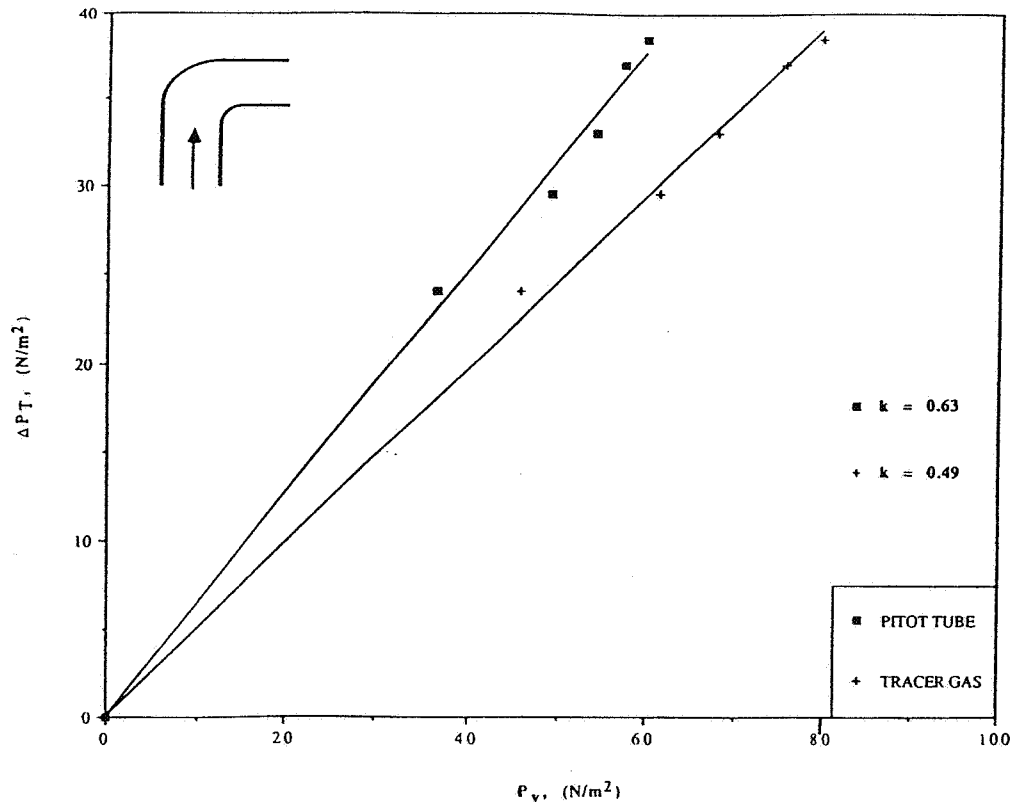


Figure 4b Variation of total pressure loss with velocity pressure, bend

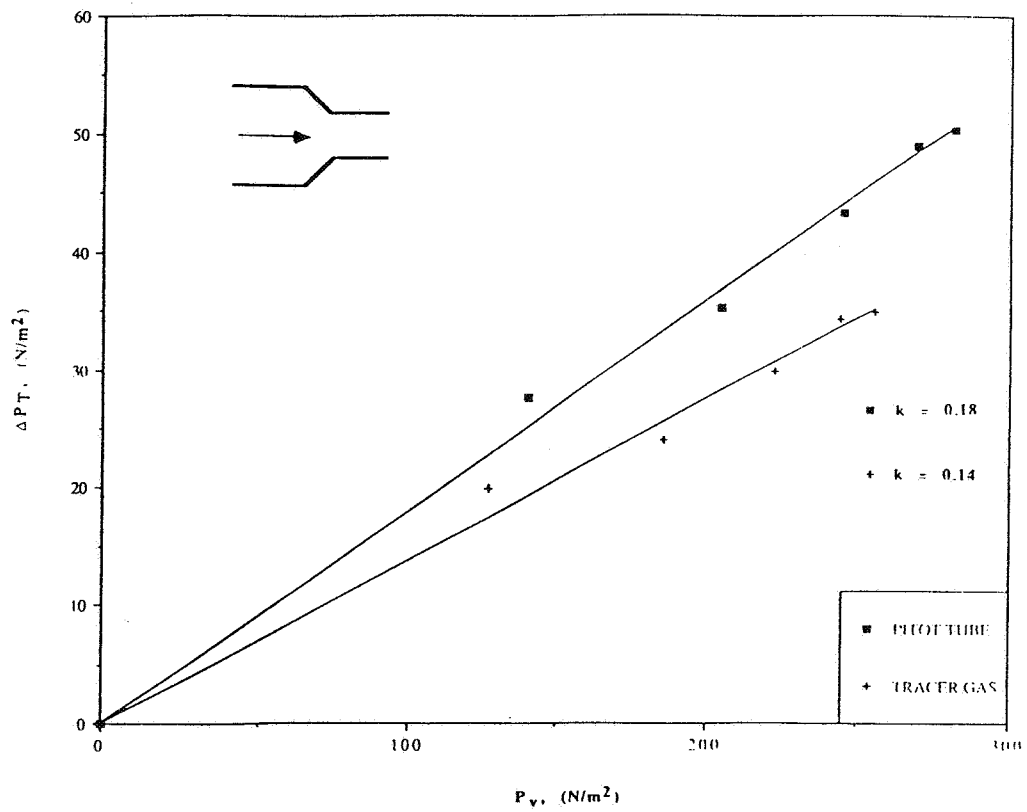


Figure 4c Variation of total pressure loss with velocity pressure, contraction

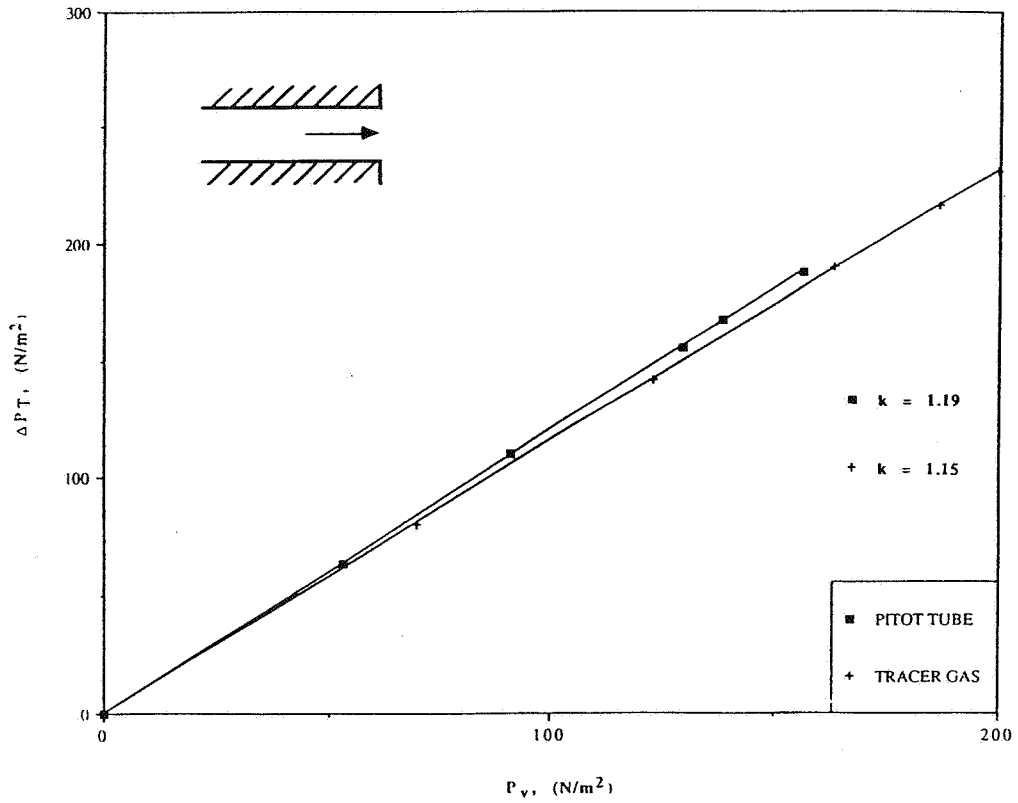


Figure 4d Variation of total pressure loss with velocity pressure, duct exit without bellmouth

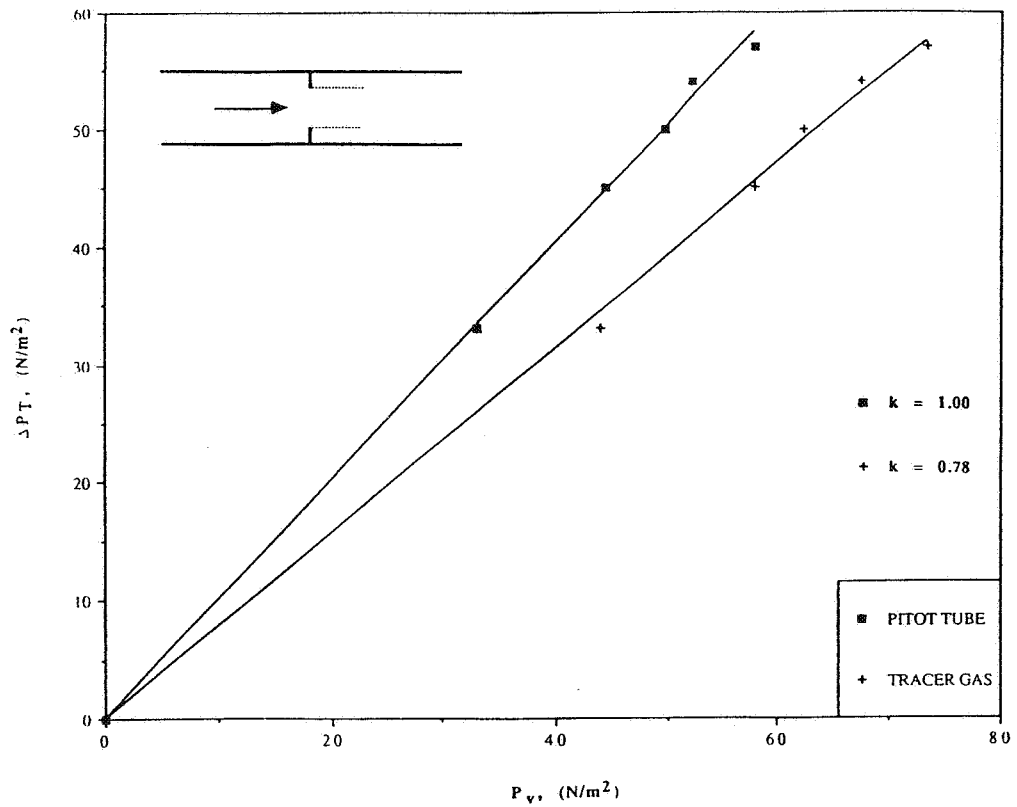


Figure 4e Variation of total pressure loss with velocity pressure, orifice

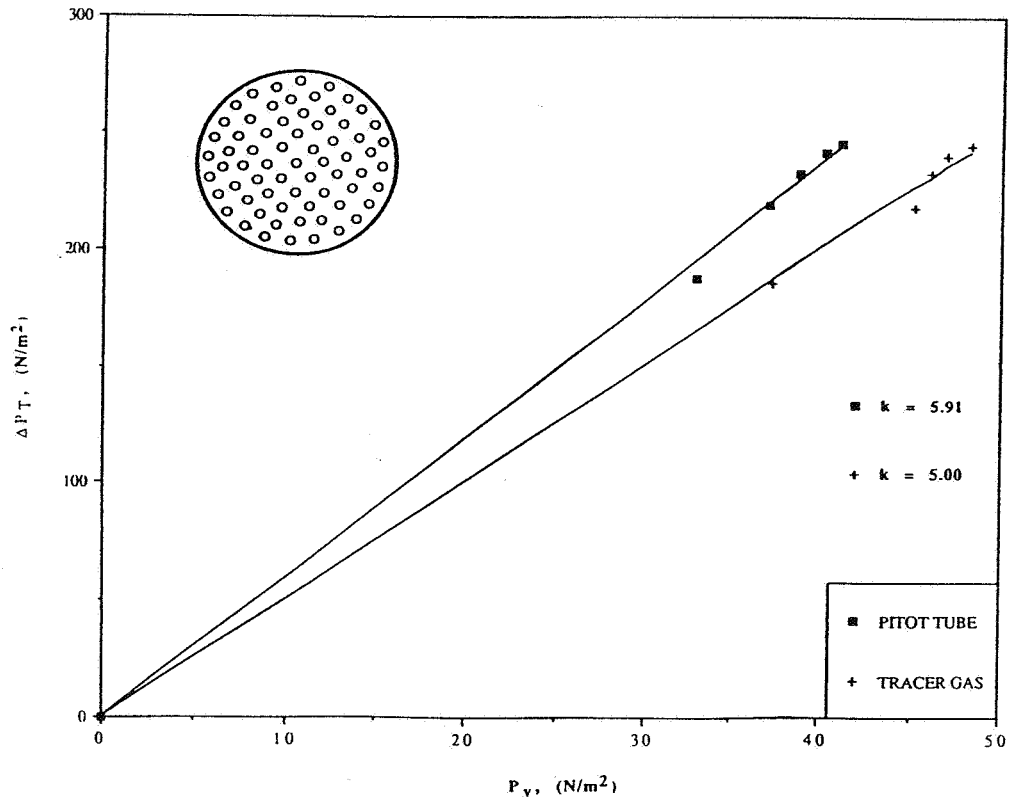


Figure 4f Variation of total pressure loss with velocity pressure, perforated plate

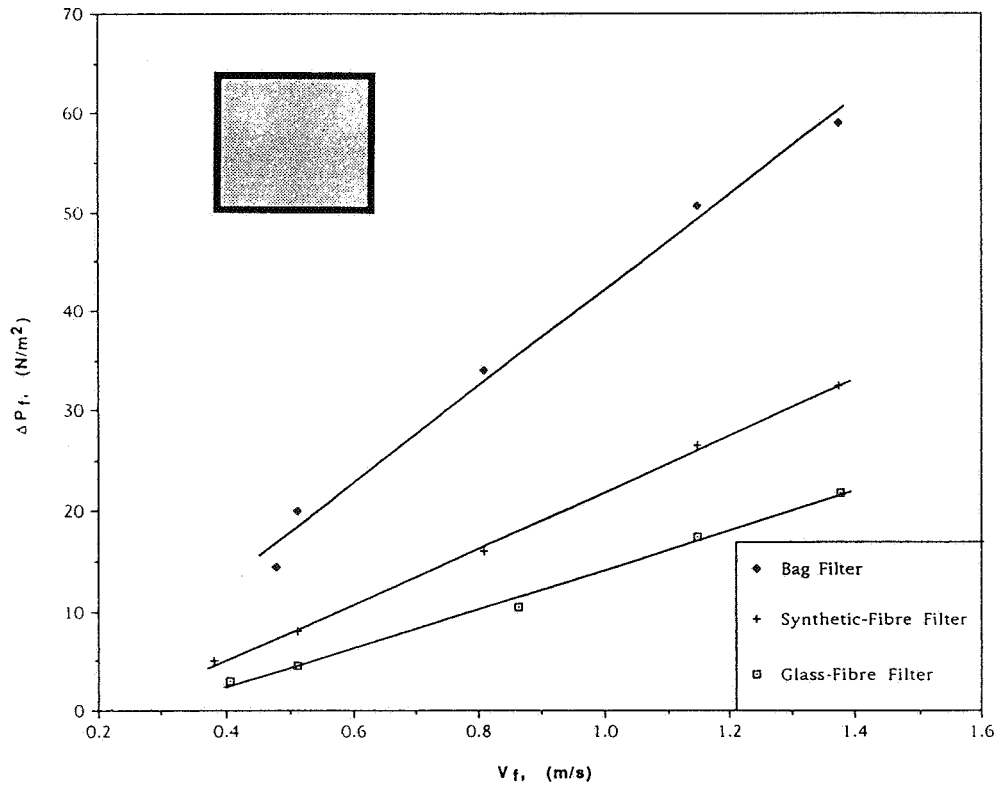


Figure 5 Variation of pressure drop with face velocity, filters



**Ventilation for Energy Efficiency and Optimum
Indoor Air Quality
13th AIVC Conference, Nice, France
15-18 September 1992**

Poster 25

**An Analytical Study of Branched Connections: Its
Implications to Multizone Air Flow Measurements.**

L. Shao, S. Sharples, I. C. Ward, H-G. R. Kula

**Building Science Unit, School of Architectural
Studies, University of Sheffield, P O Box 595, The
Arts Tower, Western Bank, Sheffield, S10 2UJ,
United Kingdom**

SYNOPSIS A branched connection is a single air flow passage connecting more than two zones. Its existence in a building has not been a critical issue for the measurement of air flows of single zones, as far as the validity or accuracy of the measurement techniques is concerned. However, with the ever increasing sophistication of building air flow measurement techniques --- which include tracer gas and multifan pressurisation techniques --- and the ever increasing use of them in multizones, it becomes increasingly desirable to examine the effect of branched connections. This paper presents an analytical study of the validity of the multizone air flow measurement techniques, as they are applied to buildings containing branched connections. It is found that the multifan pressurisation techniques have embedded inadequacies, which could lead to large flow rate measurement errors, if the techniques are applied to buildings containing branched connections. It is also found that all tracer gas techniques are valid regardless of the types of connections present. However, the interpretation of their results is much more restricted than in the case where only direct connections exist in the tested building.

List of Symbols

C	tracer concentration	a,b	tracer species
P	pressure	C	point C in Fig. 1
ΔP	pressure difference	D1	pressurisation fan for zone r
δP	ΔP across air flow passage section	e,0	outside
Q	flow rate	m	pressure ring defined by [1]
Q _i	flow rate; i=2,3,4,e; (Fig. 2)	meas	measured flow rate
Q _{ij}	flow rate from zone i to zone j	o	beginning of test
q	flow rate through a passage section	true	actual flow rate
R	flow resistance of a passage section	superscript	
subscripts		'	a condition at which $\Delta P = \Delta P'$
1,2,3,4,r	zone number as seen in Fig. 1 & 2		

1. Introduction

A connection is here defined as an air flow passage linking otherwise air tight zones --- rooms, corridors and staircases. Connection can be well defined as for an open door or window or they can be poorly defined as for background leakage cracks. The connection can also be classified into the direct connection if it connects only two zones or the branched connection if it connects three or more zones. Branched connections are common in buildings. Under floor or behind-wall wiring, gas supply tubing, central heating tubing and general plumbing all create branched connections between zones. Branched connections may also be found at prefabricated panel joints and room partitioning board joints. Cavity walls plus cracks between building bricks, too, helps creating branched connections.

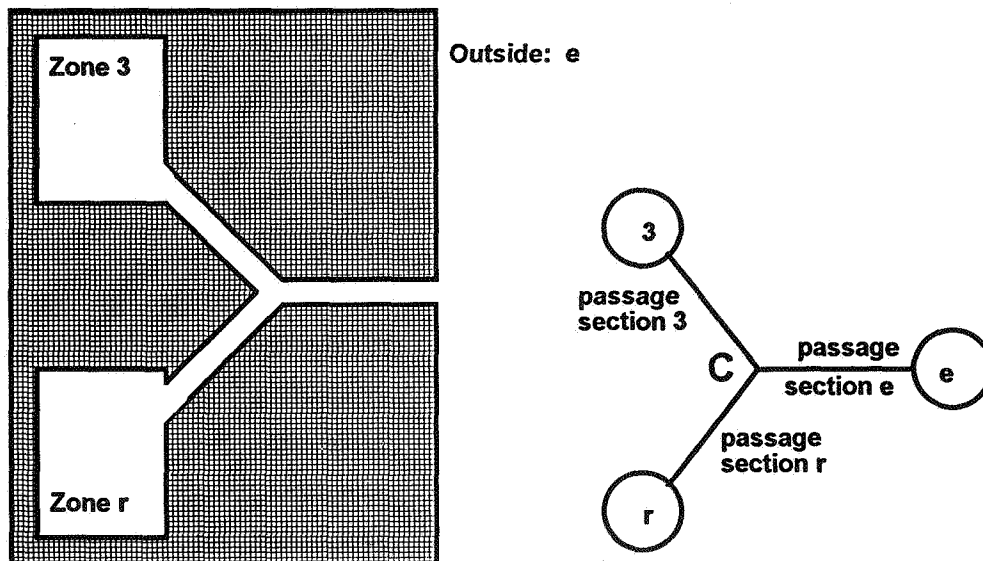


Fig. 1. Schematic of a branched connection linking two zones and the outside.

An example of the simplest branched connections is shown in Fig. 1. The branched connection with three arms links zone r with zone 3 and the outside which is denoted as "e". This arrangement was also depicted using a "circle-bar" diagram, also in Fig. 1, to simplify its graphical presentation and to facilitate the concentration of attention on the essential features of the connection. In this diagram a zone or the outside is represented by a circle and an above mentioned "arm" by a bar. The latter is referred to as a passage section defined as a section of a connection in which there is no branches.

Building air flows has been measured using, predominantly, the pressurisation and the tracer gas techniques. Both methods were first developed for air flow measurements in single zones. They were applied either to single zones or multizones transformed into single zones by, for example, opening the doors of the zones. For these types of applications the validity or accuracy of the two techniques was not in any way related to the presence of branched connections.

In the past few years both the above techniques have become increasingly sophisticated. Multi-tracer gas and multi-fan pressurisation techniques have appeared and have been applied increasingly widely to multizone air flow measurements. However, there has been little research into whether these techniques are valid or accurate when applied to multizone buildings containing branched connections, the answer to which is not as obvious as in the case of single zone air flow measurements.

In the following an analytical work is presented, which was carried out as a step towards answering the above question. One version of the multifan pressurisation method, the deduction technique, and one version of the multi-tracer method, the tracer concentration decay method, is to be examined in the following in terms of their accuracy when the branched connections are present. The other versions of both methods were also examined, details of which will not be discussed in this paper since both the examination method and the conclusions are the same as those presented below. However, more information can be found in Ref. [2].

2. The examination of the multifan pressurisation method

There are two versions of this method, i.e., the deduction technique and the guarding zone technique. As explained in the introduction, the following discussion will be confined to the deduction technique. In addition, the nomenclature used in the original paper[1] on this technique has been adopted for clarity and consistency.

2.1 Brief description of the technique

The multifan pressurisation method was devised for and has been applied to measurements of leakage distributions in multizone buildings. Referring to Fig. 2,

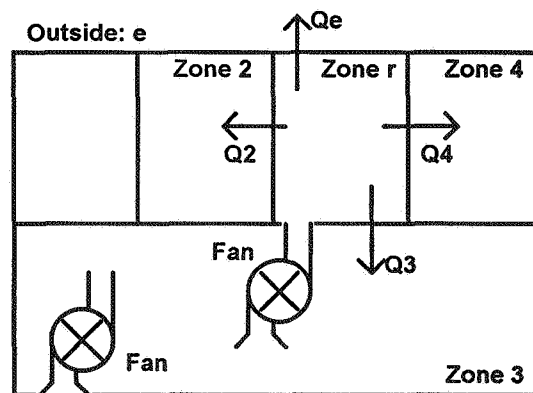


Fig. 2. Schematic of a multi-fan test arrangement.

to measure the leakage distribution for zone r is to obtain the $Q - \Delta P$ curve or the function $Q(\Delta P)$ for all the flows Q_e , Q_2 , Q_3 and Q_4 over a ΔP range of 0 to a practically likely maximum, typically 50Pa. Also, the zone flow to which is to be measured is referred to as the flow recipient zone. E.g., if $Q_2(\Delta P)$ is to be measured then zone 2 is called the flow recipient zone for that measurement.

In applying the deduction technique, the pressure in zone r (P_r) is kept constant while the pressure in the air flow recipient zone, which is also the pressure ring in this technique, P_m , is varied in descending steps from P_r to 0. The flow rates Q_e , Q_2 , Q_3 and Q_4 are measure at each of the steps of pressure differences ΔP , ($\Delta P = P_r - P_m$), thereby obtaining the $Q(\Delta P)$ functions. Some of the above flow rates can be obtained directly, while others are found by subtracting one flow rate from another. e.g. to obtain $Q_3(\Delta P)$ zone r is pressurised to P_r , the pressure in zone 3 (the now pressure ring) reduced in steps and the pressure in all other zones kept at 0 by opening windows or doors. The zone r pressurisation fan flow rate Q_{D1} is measured at each step. One then has $Q_3(\Delta P) = Q_{D1}(P_r - P_m) - Q_{D1}(P_r - P_{m0})$. Note $P_{m0} = P_r$, so

$$Q_3(\Delta P) = Q_{D1}(\Delta P) - Q_{D1}(0). \quad (1)$$

The other $Q(\Delta P)$ functions are obtained in a similar manner. Details can be found in Ref. [1].

2.2 The examination

Consider the simplest multizone configuration, a building of two zones, linked to each other and the outside via a branched connection as shown in Fig. 1. It is assumed that there are no other connections between zone 1 and 2, for the sake of analytical simplicity and clarity, although there must be other, direct connections between each of the two zones and the outside, because otherwise there can not be flows to or from the zones, on a sustained basis. The three passage sections of the connection are assumed in this section 2.2 to be identical and each being a long narrow type crack. These passage sections are assumed to have such large length to height ratios that the entrance effect becomes negligible and the relationship between the flow rate through such a passage section (q) and the pressure difference across it ΔP is linear:

$$\Delta P/q = R = \text{constant}$$

where the ratio R is referred to as the resistance of the passage section. The above assumption was made primarily to give the following analysis a greater degree of clarity and simplicity. As shown later, the conclusions thereby obtained by no means only apply to connections consisting of the above type of passage sections. In fact, it holds true for all practical existing types.

The resistances of the three passages in Fig. 1, leading to zones r, zone 3 and the outside are assumed to be, respectively, $R_r = R_3 = R_e = R$, and the pressure in zone r assumed to be P . The place where the passage sections meet is denoted as node C.

Apply the deduction technique to the building and measure $Q_3(\Delta P)$. At the point of $\Delta P = 0.5P$ (i.e. $P_r = P$; $P_3 = P_m = 0.5P$; $P_e = 0$), according to Eq. 1

$$Q_3(0.5P) = Q_{D1}(0.5P) - Q_{D1}(0) \quad (2)$$

First, consider $Q_{D1}(0)$. It is known at that moment, $P_r = P$; $P_3 = P$ and $P_e = 0$ and according to mass conservation,

$$\begin{aligned} Q_{D1} &= q_r \\ q_r + q_3 &= q_e \end{aligned} \quad (3)$$

where q_r , q_3 and q_e are the rates of flow through the passage sections against the corresponding resistance R_r , R_3 and R_e , respectively. Eq. 3 can be transformed into

$$\frac{P_r - P_c}{R_r} + \frac{P_3 - P_c}{R_3} = \frac{P_c - P_e}{R_e} \quad (4)$$

substituting the resistances and the pressures in Eq. 4 with their values, one has $P_c = 2P/3$ and thus

$$Q_{D1}(0) = q_r(0) = \frac{P_r - P_c}{R_r} = \frac{1}{3} \frac{P}{R}$$

$Q_{D1}(0.5P)$ can be obtained in a similar manner:

$$Q_{D1}(0.5P) = \frac{1}{2} \frac{P}{R}$$

and thus from Eq. 2 one obtains

$$Q_3(0.5P) = \frac{1}{2} \frac{P}{R} - \frac{1}{3} \frac{P}{R} = \frac{1}{6} \frac{P}{R}$$

In other words, if the meter readings for Q_{D1} are absolutely accurate, the measured flow rate for Q_3 is $P/6R$. The true value for Q_3 can be calculated using again Eq. 4. Remembering $P_r = P$; $P_3 = 0.5P$; $P_e = 0$; one obtains $q_r = P/2R$; $q_e = P/2R$; as well as

$$q_3 = 0 \quad (5)$$

Eq. 5 shows that there is no air flow going from zone r to zone 3. The true or practical value of Q_3 is zero. At this particular pressure difference, the relative error of measurement is infinite.

Apply the above analysis method to every point in the ΔP range to obtain the $Q_3(\Delta P)$ function, it is found that the $Q_3(\Delta P)$ measured using the deduction technique, assuming all readings are absolutely correct, is

$$Q_3(\Delta P)_{meas} = \frac{\Delta P}{3R} \quad (6)$$

while the true or practical function is

$$Q_3(\Delta P)_{true} = \begin{cases} \frac{2\Delta P - P}{3R}; & \Delta P > 0.5P \\ 0; & \Delta P \leq 0.5P \end{cases} \quad (7)$$

therefore, the relative error caused by the inadequacy of the deduction technique for this particular case is

$$error = \frac{Q_3(\Delta P)_{meas} - Q_3(\Delta P)_{true}}{Q_3(\Delta P)_{true}} = \begin{cases} \frac{P - \Delta P}{2\Delta P - P}; & \Delta P > 0.5P \\ \infty; & \Delta P \leq 0.5P \end{cases} \quad (8)$$

As seen above, the relative error increases with decreasing ΔP and approaches infinity as ΔP approaches $0.5P$. The large errors are solely due to the inadequacy of the deduction technique in dealing with branched connections, since instrument and operator errors were excluded from the above analysis. Therefore, the deduction technique cannot be relied upon in testing multizone buildings, if they consist of branched connections or the type of connection in them is not known.

2.3 Discussion

The type of sufficiently "long and narrow" passage sections were used in the above examination. This is purely for clarity and simplicity purposes, since their $Q(\Delta P)$ functions are in the simple linear form. However, the use of such a type of passages is not a necessary condition for the above analysis. The conclusions from the above analysis holds true when the common types of passage sections, whose $Q(\Delta P)$ functions are in the power law or quadratic forms[3], i.e., $Q = K \Delta P^n$ or $\Delta P = K_1 Q^2 + K_2 Q$, are used to replace the linear type passage sections. However, there are still some types of passage sections, which are not even described by the above two equations [3]. Their $Q(\Delta P)$ functions can be represented, in most cases, by the following type of equation:

$$q = f(\delta P) \quad (12)$$

where f is a monotonously increasing function. In other words, the flow rate through the passage section in question, q , increases with the pressure difference across it (δP). The conclusion from the above analysis holds true also for this quite general type of passage. This point can be illustrated by the example of further examining the application of the deduction technique to the two zone building in Fig. 1. The only difference between the building used here and that in the above analysis is that the identical linear passage sections are replaced by three identical passages of the general type described by Eq. 12. Again, we focus on a particular point ($\Delta P'$) in the ΔP range, at which $P_3=P_c$ and therefore $q_3=0$ and $Q_3=0$. (The existence of this point is obvious and easily proven.) According to the deduction technique (Eq. 1), there is

$$Q_3(\Delta P') = Q_{D1}(\Delta P') - Q_{D1}(0) \quad (13)$$

Since $Q_3(\Delta P') = 0$, if the deduction technique is correct or valid, then there is $Q_{D1}(\Delta P') = Q_{D1}(0)$ or, noting $Q_{D1} = q_r$

$$q_r(\Delta P') = q_r(0). \quad (14)$$

Denote the condition at which $\Delta P = \Delta P'$ by superscript ' and $\Delta P = 0$ by subscript "o". Eq. 14 is then written as

$$q'_r = q_{ro} \quad (15)$$

From Eq. 15 and Eq. 12, it can be obtained that $\delta P'_r = \delta P_{ro}$. In addition, P_r is kept constant and $P'_r = \delta P'_r + \delta P'_e$; $P_{ro} = \delta P_{ro} + \delta P_{eo}$. So, one has

$$\delta P'_e = \delta P_{eo} \quad (16)$$

From Eq 16 and 12

$$q'_e = q_{eo} \quad (17)$$

Because $q_3 = 0$, then from the law of mass conservation, it can be obtained

$$q'_r = q'_e \quad (18)$$

Combining Eq. 15, 17 and 18, one has

$$q_{eo} = q_{ro} \quad (19)$$

However, in reality, the relation between the two flow rates is

$$q_{eo} = 2q_{ro} \quad (20)$$

because $q_{3o} = q_{ro}$ due to passages being identical and, $q_{3o} + q_{ro} = q_{eo}$.

The contradiction between Eq. 19 and 20 is due to the assumption that the deduction technique represented by Eq. 13 is valid or correct. Therefore it is demonstrated again, in more general terms, that the above named technique is not reliable for testing buildings containing branched connections.

The same has been found true for the guarding zone method. The analysis method was only slightly different to that above and the details can be found in Ref. [2].

The multifan pressurisation technique in general can only be applied to directly linked multizone buildings. It breaks down when air passages to three or more zones cross each other. This is not too surprising since the technique was devised assuming, implicitly, that there are only direct connections. This assumption must be upheld, if they are to be successfully applied to buildings with branched connections. This practically means that each place at which the air passages cross each other should be treated as a zone, included or excluded from the controlled pressure ring or guarding zone, just like the well defined zones like rooms and corridors. This is not the case in the current multifan pressurisation techniques, and consequently they are not valid. Treating a passage junction as a zone and controlling its pressure is not easy in practical terms, unless it is, e.g. a wall cavity with a fairly large internal space. There is also the practical difficulty of identifying branched connections and locating the junctions, which will be discussed later. The tremendous difficulty in improving the multifan pressurisation techniques to cope with branched connections is obvious.

3. The examination of the multi-tracer gas method

The basic principle for the tracer gas method is that the rate of tracer consumption, either in the form of concentration decay or injection rate, in a zone is directly linked to the airflow rate there. For multizone air flow measurements, more than one tracer has to be used, hence the multi-tracer method. There are several versions of the method including the decay technique, the constant concentration technique and the constant injection technique. The first technique was used more often because less monitoring/controlling equipment are required. As explained in the introduction, the following discussion will be confined to the decay technique.

3.1 Brief description of the technique

The description will be given in the context of a two zone, zone 1 and zone 2, building. That for a N zone building can be found in Ref. [2]. Normally the procedure begins with injecting two different species of tracer gases, species "a" and "b", into zone 1 and 2, respectively. The tracer gases are then uniformly mixed with the air in their corresponding zones. Subsequently the tracer concentration decays due to the dilution effect of the interzonal air flows and those between the zones and the outside are measured. The rate of these air flows can then be calculated based on the following equations.

$$V_1 \frac{dC_{a1}}{dt} = -C_{a1}Q_{10} - C_{a1}Q_{12} + C_{a2}Q_{21} \quad (26)$$

$$V_1 \frac{dC_{b1}}{dt} = -C_{b1}Q_{10} - C_{b1}Q_{12} + C_{b2}Q_{21} \quad (27)$$

$$V_2 \frac{dC_{a2}}{dt} = C_{a1}Q_{12} - C_{a2}Q_{21} - C_{a2}Q_{20} \quad (28)$$

$$V_2 \frac{dC_{b2}}{dt} = C_{b1}Q_{12} - C_{b2}Q_{21} - C_{b2}Q_{20} \quad (29)$$

$$Q_{01} - Q_{10} + Q_{21} - Q_{12} = 0 \quad (30)$$

$$Q_{02} - Q_{20} + Q_{12} - Q_{21} = 0 \quad (31)$$

where for $m \in (0, 1, 2)$, $n \in (0, 1, 2)$, V_m is the internal volume of zone m ; C_{am} or C_{bm} are the tracer concentrations in zone m for species a and b respectively; Q_{mn} is the air flow rate from zone m to zone n . Note the outside is here conveniently referred to as zone 0.

3.2 The examination

Consider again the building used in section 2.3 and illustrated in Fig. 1. The three passage section comprising the connection are assumed identical and of the general type described by Eq. 12. In order to conform to the normal nomenclature of tracer techniques, the subscripts 0, 1 and 2 will be used for denoting the outside and the zones, replacing subscripts e, 3 and r respectively. Zone 1 and 2 are both assumed to have an internal spatial volume of V .

Suppose that air is blown, e.g. by using a fan, into zone 2 at a flow rate of "q". Consequently, the flow rates through the passage sections are $q_0 = q/2$, $q_1 = q/2$ and $q_2 = q$. So the true rates of the flow between the zones and between the zones and the outside are $Q_{01} = 0$, $Q_{10} = q/2$, $Q_{02} = q$, $Q_{20} = q/2$, $Q_{12} = 0$ and $Q_{21} = q/2$.

The above six flow rates can also be obtained by applying the tracer decay technique, which in this case utilises two tracers (a and b). At the beginning of the test, tracer a is only present in zone 1 and tracer b in zone 2 and their initial concentrations are C_{a10} and C_{b20} . The validity of the tracer decay technique is then assessed by comparing the measured data with the true data.

As described in the last section in the decay technique, the following are to be measured: V_1 , V_2 , C_{a1} , C_{a2} , C_{b1} and C_{b2} . If the measurement instrument readings are absolutely accurate, then

$$V_1 = V_2 = V \quad (32)$$

$$C_{a2} = 0 \quad (33)$$

The absolute accurate measurement of the other three concentration decay history can be worked out as follows.

For zone 2, based on the mass conservation of tracer b , there is

$$V_2 \frac{dC_{b2}}{dt} = -q_2 C_{b2} \quad (34)$$

Integrating the above equation, noting $V_2 = V$, $q_2 = q$ and the initial condition of $C_{b2} = C_{b20}$ at $t=0$, one obtains the C_{b2} history

$$C_{b2} = C_{b2o} e^{-\frac{qt}{V}} \quad (35)$$

For zone 1, the mass conservation of tracer a requires

$$V_1 \frac{dC_{a1}}{dt} = -q_1 C_{a1} \quad (36)$$

and the mass reservation for tracer b requires

$$V_1 \frac{dC_{b1}}{dt} = -q_1 C_{b1} + q_1 C_{b2} \quad (37)$$

Eq. 36 is solved in the same was as for Eq. 34, to obtain

$$C_{a1} = C_{a1o} e^{-\frac{qt}{2V}} \quad (38)$$

Eq. 37 can be transformed into the form below

$$\frac{dC_{b1}}{dt} + \frac{q}{2V} C_{b1} = \frac{q}{2V} C_{b2o} e^{-\frac{qt}{V}} \quad (39)$$

with the initial condition of $C_{b1} = 0$ at $t=0$. The solution for this equation is

$$C_{b1} = C_{b2o} e^{-\frac{qt}{2V}} - C_{b2o} e^{-\frac{qt}{V}} \quad (40)$$

Substituting Eq. 32, 33, 35, 38 and 40 into the two zone tracer decay equations Eq. 26-31, solving them simultaneously, one obtains the measured flow rates: $Q_{01} = 0$, $Q_{10} = q/2$, $Q_{02} = q$, $Q_{20} = q/2$, $Q_{12} = 0$ and $Q_{21} = q/2$, which are exactly the same as the true flow rates obtained at the beginning of this section. Therefore, the tracer decay technique is perfectly valid in this application.

3.3 Discussion

That the tracer decay technique is successful in the above test case is not at all accidental. The technique is represented, in the above case, by Eq.26-31. They are based on the principle of mass conservation for the tracer gases and the air, which is a universal principle. For example, Eq. 26 interpreted in physical terms means that in zone 1 the rate of tracer a increase (represented by the term on the left side) equals the rate of influx of tracer a (represented by the third term on the right) minus the rate of out flux of tracer a (represented by the first and second terms on the right). In addition, the representation of tracer increase rate by the left side term and the representation of influx and out-flux rates by the right side terms are always correct, for direct or branched connection alike. The former is obvious enough. The latter is principally because the definition of interzonal flow rates Q_{ij} , $i, j \in (0, 1, 2)$, is independent of the path through which Q_{ij} arrives, thus the influx rate of tracer a will be $C_{a2}Q_{21}$ whether Q_{21} comes through a branched connection or direct connection and the same is true for the out-flux terms. The same reasoning can be applied to the other five equations Eq. 27-31. Thus the equations representing the two zone tracer decay technique are always correct regardless of the connection types present. Therefore if V_1 , V_2 , C_{a1} , C_{a2} , C_{b1} , C_{b2} are accurately measured, then by solving Eq. 26-31, the interzonal flow rates will be accurately obtained. The validity of the technique observed previously is guaranteed from here.

The analysis and the conclusions presented so far in this section 3 has been extended to the other two multizone tracer gas techniques --- the constant concentration and the constant injection techniques -- and to buildings containing more than two zones. Details of this work can be found in Ref. [2].

It has been shown above that the tracer techniques are valid for measuring interzonal flow rates Q_{ij} in buildings with branched connections . However, when interpreting the tracer gas results, one must be aware of the possibility and the implication of the fact that Q_{ij} might have come through a branched connection linking others zones as well as zone i and j . In such a situation Q_{ij} not only depends on conditions in zone i and zone j , but also on those of the other zones that the branched connection links. Consequently, Q_{ij} measured under a certain set of zone conditions may not be the same as that from another measurement, even if the conditions in zone i and j are exactly reproduced in the latter test. Indeed, since there is currently no method for knowing which and how zones are linked by branched

connections, it cannot be guaranteed that Q_{ij} measured now can be repeated later, unless the conditions in each and every zone in the building are reproduced. In other words, information on interzonal flow rates obtained using tracer techniques are safely used only under a set of zone conditions identical to those under which the information were obtained.

The restriction brought in by the branched connection in terms of tracer measurement interpretation is much too great, for, in addition to "flow from zone i to zone j is Q_{ij} when they pressure difference between them is ΔP_{ij} " one now has the attached string of "and the pressure differences among the other eight zones in the buildings are.....". This is particularly serious for the setting up of databases for interzonal flows. One has to carry out a set of tests under each and every likely combination of conditions in the zones. The alternative would be to devise a method for detecting branched connections so as to reduce the number of combinations of zone conditions to be tested. A piece of research work on this can be found in Ref. [2]

4 Conclusions

An analytical study of the validity of the multizone air flow measurement techniques, in the presence of branched connections, has been carried out.

It is found that the multifan pressurisation method which includes the deduction technique and the guarding zone technique has embedded inadequacies, which could lead to large measurement errors, if the techniques are applied to buildings containing branched connections.

All versions of the tracer gas method are found to be valid regardless of the types of connections present. However, the interpretation of their of their results is much more restricted than in the case where only direct connections exist in the tested building.

The importance of branched connections is apparent. A survey of their presence in buildings and their likely forms and dimensions would be most useful. For that purpose, a method for detecting branched connections is clearly needed, and it is in this area that research by the authors is proceeding.

Acknowledgement

This study was part of an air infiltration research project funded by the UK Science and Engineering Research Council (Grant No. GR/F28397).

References

1. Furbringer, J.-M. and Roulet, C.-A. "Study of the errors occurring in measurement of leakage distribution in buildings by multifan pressurization." *Building and Environment*, Vol. 26, No.2, pp111-120, 1991.
2. Shao, L., Sharples, S. and Ward, I.C. "Branched connections: its implications to multizone air flow measurements and its detection." Internal report, Building air infiltration research group, Building Science Unit, University of Sheffield, UK, Nov., 1991.
3. Baker, P.H., Sharples, S. and Ward, I.C. "Air flow through cracks." *Building and Environment*, Vol. 22, No. 4, 1987, pp293-304.

**Ventilation for Energy Efficiency and Optimum
Indoor Air Quality
13th AIVC Conference, Nice, France
15-18 September 1992**

Poster 24

**A Combined Pressurisation and Tracer Gas
Technique for Air Flow Measurements.**

L. Shao, H-G. R. Kula, S. Sharples, I.C. Ward

**Building Science Unit, School of Architectural
Studies, University of Sheffield, P O Box 595, The
Arts Tower, Western Bank, Sheffield, S10 2UJ,
United Kingdom**

SYNOPSIS Building air flow is directly related to the building energy consumption and indoor air quality. As buildings become increasingly air tight, air flow through building background cracks becomes more important, and can account for up to half of the total building air infiltration. However, background leakage is not well understood, due to the lack of appropriate measurement methods. The multi-fan guarding zone or deduction technique provides a means for testing background leakage distributions, an important parameter for characterising the background leakage. However, its reliable application in buildings is limited either due to practical constraints or due to the presence of certain types of air leakage paths, namely the branched paths. In this paper an alternative method, for measuring background leakage distributions, which does not have such problems, has been examined. This method is based on the simultaneous use of the pressurisation and tracer gas technique and termed in short the combined technique. It potentially suffers from all the accuracy problems associated with the tracer gas technique, which could be made more serious by the high pressurisation flows. To counter this problem, mixing fans, among other measures, were utilised. The validity of this measure was examined and its effectiveness tested by applying the combined technique to one single and several multi-zone set-ups. Results showed that the technique is of good accuracy with relative errors consistently below 10%.

1. Introduction

The information on building air flows is of great importance to building service engineers. The air flow can occur through well defined openings and less well defined background cracks. As the buildings become increasingly air-tight to reduce energy consumption, the latter become significant, accounting for up to half of the total air infiltration. There are generally two approaches to the measurement of background crack flows. The first one is to measure the flow through individual cracks using, for example, a portable pressurisation facility of the type developed by Baker et al [1]. While this is useful for trouble-shooting and detailed fundamental studies, it is time-consuming and probably impossible for surveying the background leakage cracks in a building or a building zone. The second method is to measure bulk flows from one building zone to the other zones and the outside due to background cracks. In other words, instead of measuring each individual cracks, this method measures the integral effects of the cracks connecting one zone to each of the other zones in the building. The information thus obtained is termed building background leakage distribution which, although not as detailed as that from the first method, is an improvement over the information of overall leakage obtained using the single fan pressurisation technique. The formal definition of the background leakage distribution is the combination of the flow rates through background leakage paths from one zone to the outside and each of the other zones in the building when measured at equal pressure differences between the former and each of the latter. Obviously, each zone in the building has its own leakage distribution.

Building air flow measurements have been relying on either tracer gas techniques or pressurisation techniques. However, the former can not yield the leakage distribution information which requires a controlled pressure environment. In comparison, the pressurisation technique in the form of multi-fan guarding zone or deduction method is more capable in this area [2]. Nevertheless, as pointed out by Wouters et al [3], there are situations in which it is not practical to perform the pressurisation measurements. Moreover, it has been shown that the pressurisation techniques break down as they are

applied to buildings containing branched leakage paths --- those linking three or more zones together[4]. Therefore, neither of the above techniques can be totally relied upon to provide leakage distribution information.

Since the initial work of Wouters et al [3] a technique based on the combination of the above two has emerged, referred to in the following as the combined technique. As for the multi-fan guarding zone technique, pressurisation fans were also used in the combined technique to provide the equal pressure differences mentioned above. However, different to the multi-fan technique, whereby leakage flow is measured indirectly by analysing the flow rates through the pressurisation fans, it does the measurement directly using the tracer gas method. Since the tracer gas method is not affected by the presence of branched paths [4], the combined technique can be applied to any type of building to measure leakage distributions, without having to find out first whether branched paths are present.

The combined technique, while having promising capabilities, potentially suffers from the low measurement accuracy associated with poor tracer mixing. It is well known that for the tracer gas measurement to be accurate, the tracer gas must be reasonably uniformly mixed with the air. This requires that the leakage rate be limited to low values, below 0.5ACH according to Alevantis and Hayward [5]. However, this is highly likely to be exceeded when applying the combined technique, the pressurisation element of which generates strong air flows. The objective of this work, therefore, was to improve the accuracy of the technique, principally by means of enhancing tracer mixing. It was found that using mixing fans led to satisfactory mixing and was acceptable in the combined technique. In the following, experimental work is presented in which the effectiveness of the mixing fan was tested by examining the tracer distribution uniformity (indirectly), the accuracy of the combined technique in measuring high flow rates as well as its accuracy in measuring background leakage distributions. Results showed that the combined technique is consistently accurate, with relative errors smaller than 10%.

2 Test Facility

The experiments were carried out a laboratory, where test conditions can be more easily tailored to suite the many requirements, so that the accuracy of the combined technique can be examined more accurately and under a wider range of situations. Five multi-zone set-ups and one single zone set-up were used in the study. The maximum number of zones in a set-up is five and the zones vary in size from 0.182 to 10.35m³. Summary information, including total number of zones, sizes of the zones and positions of calibrated cracks, on these set-ups can be found in Table 1.

Table 1. Summary information on the various set-ups

	Number of Zones	Zone sizes					Zone Pairs with Connecting Cracks
		1	2	3	4	5	
Set-up 1	1	1.027					
Set-up 2	2	1.027	0.530				1-2
Set-up 3	4	1.027	0.530	0.292	0.182		1-2 2-3 2-4
Set-up 4	5	1.027	0.530	0.292	0.182	0.233	1-2 2-3 2-4 2-5
Set-up 5	2	10.35	10.35				1-2
Set-up 6	3	10.35	5.47	4.88			1-2 1-3

Note that the zone numbering for one set-up bears no automatic relation to that of another. A more detailed description of one of the set-ups, No. 3, will be given in the following. As the experimental arrangements for the all the set-ups are quite similar, this description will not be repeat for the other ones.

The test facility for set-up 3 is schematically shown in Fig. 1. It consists of four zones, the pressurisation equipments and the flow rate measurement equipments.

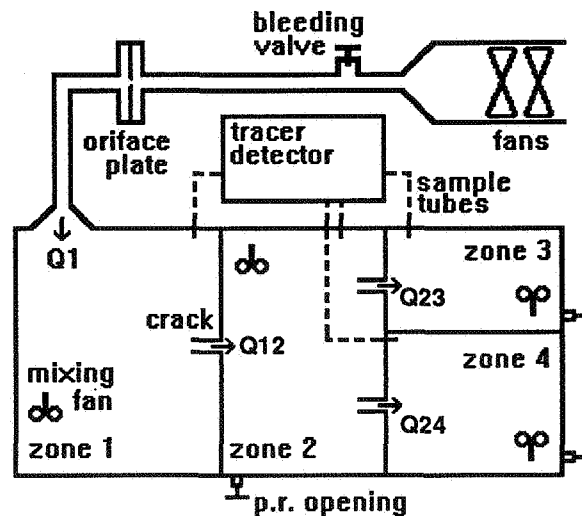


Fig. 1 Schematic of the test facility

The four zones are arranged and numbered as shown in Fig. 1. The zones are wooden structures and have internal volumes of 1.027, 0.530, 0.292 and 0.182 m³, respectively. Wooden panel joints were air-tight sealed, using for example silicon plastic. Manufactured cracks, marked "crack" in Fig. 1, were mounted on the partitions between the zones. The fact that there is a crack connecting zone 2 and zone 4 is described in Table 1 in its last column by means of a number pair 2-4. Likewise, the position of the other two cracks in Fig. 1 or set-up 3, is indicated by the number pairs 1-2 and 2-3. The same system was used for indicating crack positions in other set-ups described in table 1. The above partitions were so designed or so well sealed that the flow between any two zones was solely through the manufactured crack between them. The cracks were pre-calibrated so that the flow rate through a crack at various pressure differences across it was known. This information were then used to judge the accuracy of the measurement data from the combined technique. Details of the calibration is presented later.

The pressurisation was provided by two axial fans linked serially and connected to zone 1. The same arrangement was made for the other set-ups, with only one slight variation for set-up 5 and 6 where the two fans were replaced with a single, more powerful centrifugal fan to cope with the larger volumes. In the experiment, the pressure in each of the four zones frequently needed to be changed or regulated, either for selecting another test condition or for maintaining the equal pressure difference required for the leakage distribution measurement. This was effected by taking one or a combination of the following three measures: adjusting the bleeding valve opening, blocking part of the fan air inlet and adjusting the pressure regulating openings (marked

"p.r. opening" in Fig. 1) in the walls of the zones, the equivalent of which in a real building could be either windows or doors. Pressure tappings were installed in each of the four zones. The pressures there were measured using digital micromanometers and collected using a micro based data acquisition system.

Interzonal flows such as Q_{12} , Q_{23} and Q_{24} in Fig. 1 are usually measured using multi- rather than single tracer techniques. This is because in a multizone situation one zone can receive air flows from two or more other zones but the single tracer method can only measure the sum of these flows, unable to tell one of them from another. However, if the pressure condition is such that a zone receives air flow from only one other zone, then the single tracer method can be used to measure that interzonal flow. A close examination of Fig. 1 shows that the above condition is always the case for zone 2 and if, for example, a zero pressure difference is maintained between zone 3 and 4, then all interzonal flows in Fig. 1 or set-up 3 can be measured using a single tracer gas method. This method was used for all six set-ups, in preference to the multi-tracer version, which is less robust, less portable, more expensive and more difficult to operate. The equipment arrangement was as that described in Ref. [6]. Samples of the tracer (SF_6)/air mixture were periodically taken from the zones to be analysed using an electron capturing detector. The decay of the tracer concentrations were then analysed to provide the flow rates. In this experiment, samples were returned to where they were taken after each analysis to avoid the sample flow being counted towards the interzonal flow.

As said in the introduction the objective of this work was to improve the accuracy of the combined technique by enhancing tracer air mixing. Among the mixing enhancement measures tested, that of using mixing fans was found to be the most effective. The following discussion will be confined to the tests on this method.

Although strict sealing procedures were applied to the construction of the zones, the flow rates through the pressurisation fans --- typically 10ACH --- were still much higher than what is acceptable --- 0.5ACH [5] --- for the reasonable tracer air mixing uniformity. The high flow rate and thus the short flow residence period in a zone means that the flow does not mix well with the mixture in the zone during its stay. The resulting highly non-uniform tracer distribution in a zone contradicts the pre-condition for tracer gas method application and thus can lead to a large flow rate measurement error. To counter this problem, a mixing fan was installed in each of the four zones to improve the mixing. These fans were so positioned that the flows from them are not directed at the manufactured cracks. The use of mixing fans should normally be avoided for conventional tracer gas tests, since the fan may alter the characteristics of the original flow which is to be measured. However, the use of the fan is acceptable for measuring flows driven by given pressure differences as in this case. Calibration tests showed that the crack flow was solely determined by the pressure difference. In other words, turning on the fan did not affect the rate of the flow to be measured, but it helped to measure the flow rate more accurately.

3 Procedures and Results

The above mentioned crack flow calibration was carried out using the same facility as that show in Fig. 1, but with zone 2, 3, 4 and the tracer detecting equipment removed. The calibration procedure was as described in Ref. [1].

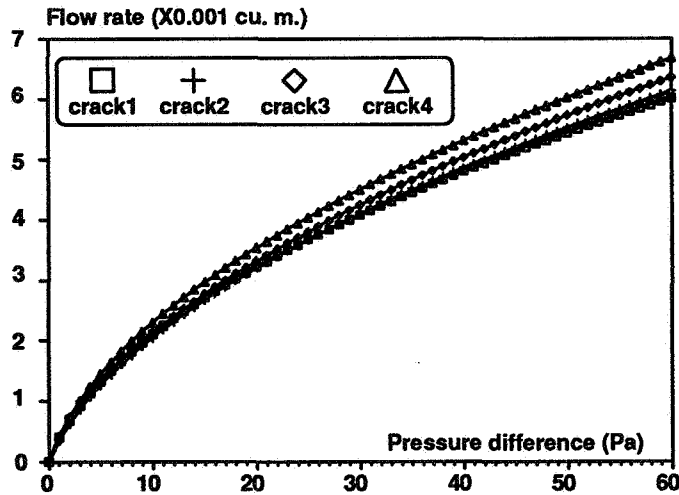


Fig. 2. The flow characteristics of four calibrated cracks

A typical set of calibration results --- the Q - ΔP relation curves for four manufactured cracks --- is shown in Fig. 2. The range of pressure difference was sufficiently wide to cover those likely to be encountered in the combined technique tests. It was found that the calibration curves conformed well to quadratic curves, with deviations about 3%.

The combined technique was first applied to the measurement of high flow rates generated by the pressurisation fans, during which its accuracy and the tracer mixing uniformity were examined. It was then tested on leakage distribution measurements. While the latter must be carried out in set-ups consisting of at least three zones and under strict pressure arrangements, the former can be performed in a single zone and with much relaxed pressure controls, thereby simplifying the procedures and facilitating the concentration of efforts on the essential problem of tracer mixing in large pressurisation flows. Set-up 1, 2, 3 and 5 were used in the above "former" tests, with No. 3 having the most number of zones. As can be seen from Fig. 1, in such a test using set-up 3, air is blown by the fans into zone 1, building up pressure in that zone. The pressure, ΔP_{12} drives air, Q_{12} , into zone 2, building up the pressure there, $\Delta P_{23}, \Delta P_{24}$, which in turn drives air, Q_{23} and Q_{24} , into zone 3 and 4, respectively. These flow rates were measured using the tracer gas method described above and compared with the calibrated flow rates through the cracks under the pressure differences $\Delta P_{23}, \Delta P_{24}$ and ΔP_{12} , respectively. The agreement in the above comparison was then used to evaluate the accuracy of the combined technique in the high flow rate measurement. In addition, the tracer mixing uniformity was evaluated by examining the agreement between the measured tracer concentration decay curve and the theoretical one, which is based on the assumption of absolute tracer concentration uniformity. This information is important as it may add confidence in the technique and the effectiveness of the mixing fan.

The procedure for applying the combined technique to the "latter" tests mentioned above --- measuring leakage distributions --- is similar to that outlined above, except that by definition the equal pressure difference condition must be maintained. For example, suppose flow rates from zone 1 to the neighbouring three zones 2, 3 and 4, Q_{12}, Q_{13} and Q_{14} , form the leakage distribution for zone 1, which is to be measured, then the corresponding pressure difference between zone 1 and 2, 3 and 4, $\Delta P_{12}, \Delta P_{13}$ and ΔP_{14} must be kept equal during the test.

The mixing fan effect on tracer uniformity can be demonstrated by the following results. Refer to the set-up shown in Fig. 1. Fig. 3(a) shows the tracer concentration decay history in zone 1. The theoretical decay curve between the start and the end of the test was obtained with the assumption of perfect tracer air mixing. The good fit between the measured and the theoretical curve indicates that by installing the mixing fan, the mixing problem associated with high pressurisation flows has been solved. Fig. 3 (b) to (d) shows that the same is true for the other zones. Data for the above were then analysed to obtain the measured interzonal flow rates, using the method of Ref. [6].

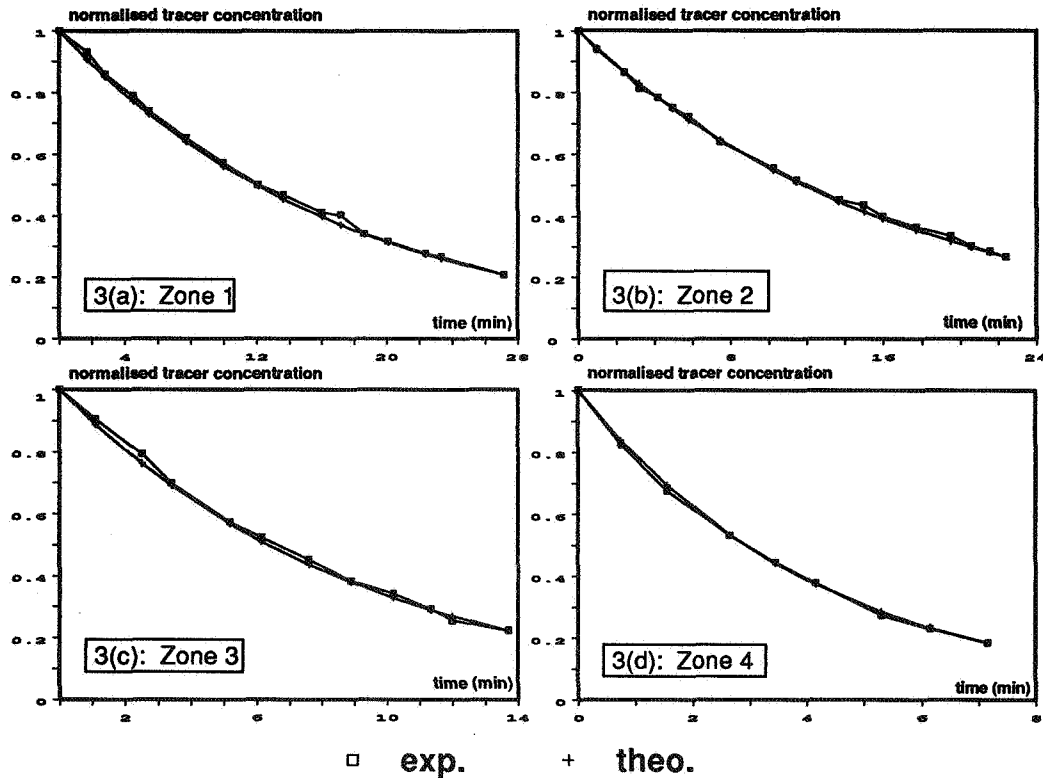


Fig. 3 (a)-(d). Tracer concentration decay in the zones of Fig.1.

The accuracy of the combined technique in dealing with large pressurisation flows was tested in set-ups 1, 2, 3 and 5. The measured inter-zonal flow rate data for each of these set-ups are listed against the corresponding calibration data, in Table 2, which also shows the corresponding relative errors. The subscripts for the flow rates were used to indicate the two zones between which the flow occurs. They correspond to those used in the last column of table 1. For example, Q_{12} of set-up 2 in Table 2 is the flow rate through the crack 1-2 of set-up 2 indicated in table 1.

Table 2 Combined technique measurements as subjected to large pressurisation flows.

	Set-up 1	Set-up 2	Set-up 3		Set-up 5
	Q_1	Q_{12}	Q_{23}	Q_{24}	Q_{12}
Combined Method (m ³ /h)	3.47	1.84	1.77	2.22	28.7
Calibration (m ³ /h)	3.78	1.91	1.61	2.42	29.5
Relative Error (%)	8.2	3.7	9.9	8.3	2.8

As can be seen from Table 2, the combined technique copes well with large flows with relative measurement errors ranging from 3.7% to 9.9% for several small sized set-ups (1, 2 and 3) and 2.8% for the larger sized set-up 5. The case of set-up 1 is slightly different to the others in that the total air change rate, instead of a crack flow rate, of the single zone was measured and compared with the rate measured using an orifice plate.

The combined technique was then applied to the leakage distribution tests, in set-ups 4 and 6. One set of results (i.e. under one pressure difference condition) for each of the two set-ups were listed, again against the corresponding calibration data, in Table 3. The subscripts were used in the same way as in Table 2. The resulting relative errors were all below 10%, showing that combined technique is of good accuracy.

Table 3. Leakage distribution results obtained using the combined technique.

	Set-up 4			Set-up 6	
	Q ₂₃	Q ₂₄	Q ₂₅	Q ₁₂	Q ₁₃
Combined Method (m ³ /h)	2.09	2.24	1.94	35.25	33.8
Calibration (m ³ /h)	2.00	2.46	1.90	37.1	36.9
Relative Error (%)	4.5	8.9	2.1	5.1	9.2

4 Conclusions

Experimental work on a combined pressurisation-tracer gas technique has been carried out. The technique is based on the simultaneous use of the pressurisation and tracer gas methods. It can be used to measure background leakage distributions, which are important building air flow parameters. This technique avoids the problem of a currently available technique, the multi-fan guarding zone or deduction technique, which is ineffective in buildings containing branched leakage paths.

The accuracy of the combined technique has been significantly improved by the use of mixing fans. The test results showed that the technique is now consistently accurate, with a relative error smaller than 10%.

It is felt that a multi-tracer version of the technique should be developed as its application in practice could be more flexible in certain situations than utilising the single tracer method.

Acknowledgement

This study was part of an air infiltration research project funded by the UK Science and Engineering Research Council (Grant No. GR/F28397).

References

- [1] Baker, P.H., Sharples, S. and Ward, I.C. "The validation and application of a portable pressurisation test facility for the measurement of the flow characteristics of background leakage areas." Proc. Int. Congress on Building Energy Management, Lausanne, 28 Sep. - 2 Oct. 1987.
- [2] Furbringer, J.-M., Roecker, C. and Roulet, C.-A. "The use of a guarded zone pressurisation technique to measure airflow permeabilities of a multizone building." Proc. 9th AIVC Conf., Gent, Belgium, 1988, pp233-250.

- [3] Wouters, P., l'Heureux, D. and Voordecker, P. "The determination of leakages by simultaneous use of tracer gas and pressurisation equipment." *Air Infiltration Review*, Vol. 8, No. 1, 1986, pp4.
- [4] Shao, L., Sharples, S., Ward, Ian C. and Kula, H.-G. "An analytical study of branched connections: its implications to multizone air flow measurements." *Proc. 13th AIVC Conf., Nice, France, 14 -18 Sep. 1992.*
- [5] Alevantis, M.S. and Hayward, S.B. "The feasibility of achieving necessary initial mixing when using tracer gas decay for ventilation measurement." *Proc. 5th Int. Conf. on Indoor Air Quality and Climate, Toronto, Canada, 29 Jul. - 3 Aug. 1990, pp349-354.*
- [6] Shao, L. and Howarth, A.T. "Air infiltration through background cracks due to temperature difference." *Building Serv. Eng. Res. Technol.*, Vol. 13, No. 1, pp25-30, 1992.

**Ventilation for Energy Efficiency and Optimum
Indoor Air Quality
13th AIVC Conference, Nice, France
15-18 September 1992**

Poster 22

Spillage Test Results From Gas & Oil Fired Boilers.

T. Shepherd

**Building Research Establishment, Garston,
Watford, WD2 7JR, United Kingdom**

SPILLAGE TEST RESULTS FROM GAS & OIL FIRED BOILERS

Summary

Spillage of combustion products from open flued combustion appliances represents a source of indoor air pollutants which can cause danger to health. Air extract fans are installed in kitchens in order to remove moisture and cooking smells, but the room depressurisation which they create is a potential cause of spillage.

A series of experiments was therefore set up to determine the fan flow rate and internal/external pressure difference at which spillage first occurred in different open flued gas and oil boilers. The effect of room air-tightness, size of air brick, air brick position, internal/external temperature difference and weather conditions were tested. It was found that domestic extract fans of standard size could cause spillage under a variety of conditions and at different room air-tightnesses.

The results indicate that in order to prevent products of combustion spilling into the living space, air extract fans should not be installed if they can depressurise the room or space in which an open flued combustion appliance is installed.

1. Introduction

The problems of condensation and mould growth in kitchens and bathrooms have led to recommendations for extract ventilation being included in the 1990 U.K. Building Regulations (amended 1992). The recommended standard air extract rates for kitchens are a minimum mechanical extract rate of 60 l/s or a minimum extract rate of 30 l/s if incorporated in a cooker hood¹. The aim of the mechanical ventilation is to remove the moisture and smells at source and prevent them travelling around the house.

Combustion appliances require air in order to support combustion of fuel and to ensure correct operation of the flue. An open flued combustion appliance draws this air from the space in which it is sited. If this space is depressurised, the air available to the appliance is limited and it may have difficulty in drawing in adequate fresh air. When the level of depressurisation exceeds a critical value, the exhaust gases will spill into the space in which the appliance is sited. Higher levels of depressurisation will cause total reversal of flow of gases in the flue. Spillage is potentially hazardous since the space surrounding the appliance, which is generally living space, begins to fill with products of combustion.

Extract ventilation tends to create depressurisation in the room in which it is installed and to a lesser extent in the rest of

the dwelling and therefore may have the potential to cause spillage of combustion products.

An investigation and literature search on the subject suggested that domestic air extract fans could, under certain circumstances, create a level of depressurisation high enough to cause spillage, and full flow reversal in the flue. An experiment to determine these circumstances was therefore designed and set up.

One test in particular was used to test the likelihood of flue gases spilling into the room instead of flowing safely up the flue. This test originated in Canada where the Centre for Building Science at the University of Toronto tested about 40 houses for boiler venting problems. The Cold Vent Establishment Pressure² (CVEP) test measures the maximum internal negative pressure (relative to outside) which the combustion appliance can overcome and start up correctly.

The maximum level of depressurisation that can be safely maintained in a room should be less than the CVEP by a safe margin. The maximum depressurisation caused by all the depressurising devices in the room or dwelling should be less than the CVEP, otherwise the risk of spillage presents itself.

2. Experimental Procedure

Two tests were carried out which established three critical points.

The lowest level of depressurisation at which spillage will occur is when the flue is cold because with a cold flue the stack effect is less pronounced and the pressure difference across the flue is lower. The first test finds the minimum spillage pressure (the Cold Vent Establishment Pressure CVEP after Timusk et al.²). The extract fan is turned on so that cold air from outside comes into the room down the flue thus cooling its walls. The fan flow rate is increased to a rate at which the combustion appliance will definitely spill. The appliance is then turned on and the fan flow rate slowly decreased until the combustion gases begin to rise up the flue. The internal/external pressure at this point is called the cold vent establishment pressure. As the gas rises up the flue, the flue walls heat up so that the draught in the flue increases and stabilises.

The second test (Hot Vent Reversal Pressure Test HVRP also after Timusk et al.²) establishes the second and third critical points of spillage. This test as its name suggests is done on a hot flue, so the buoyancy of the gases in the flue is greater. The boiler is turned on and left running for a period of time long enough for the flue to reach its maximum operating temperature.

The fan is then turned on and the flow rate slowly increased. The internal/external pressure difference at which gas is first detected spilling from the dilution air inlet is the hot vent reversal pressure. If the fan flow rate is increased still further the third critical point is reached. This is when the flow in the flue begins to reverse and outside air enters the top of the flue. The internal/external pressure difference at which this happens is the Full Reversal Pressure (FRP).

The most serious of these critical points is the CVEP because it occurs at a lower internal/external pressure difference. Not all fans will be powerful enough to cause spillage at the CVEP and of those that are, the conditions necessary for spillage will not be met every time the fan and boiler are turned on. The fan has to have been in operation for a period of time long enough to cool the flue to ambient or near ambient temperature by pulling in outside air down the flue. The open flued combustion appliance then has to cut in while the fan is still in operation. The other two critical points, although achievable in fewer situations because of the larger fan capacities required, are also serious because they will occur every time the combustion appliance and extract fan are operating simultaneously.

Parameters affecting the fan flow rate and pressure difference required to achieve the critical points were explored in a series of experiments.

Parameters varied were:

Air-tightness of room	Air brick size
Air brick position	Boiler size
Boiler fuel	Flue diameter
Flue construction	Wind speed
Wind direction	Internal/external temperature difference

3. Gas Fired Boilers

3.1 Spillage Test Results

305 CVEP tests and 64 HVRP and FRP tests were done. The following three figures show the internal/external pressure differences for the three critical points. The y axis is wind speed. This was the most significant factor affecting the CVEP, but seemed to have no affect on the HVRP or the FRP. The reason for this is that when the flue is at a higher temperature, the stack effect is the most dominant driving force for the hot flue gases.

Figs. 1, 2 and 3 show the minimum levels of room depressurisation which caused spillage for each of the three critical conditions (CVEP, HVRP, and FRP respectively).

Cold Vent Establishment Pressures

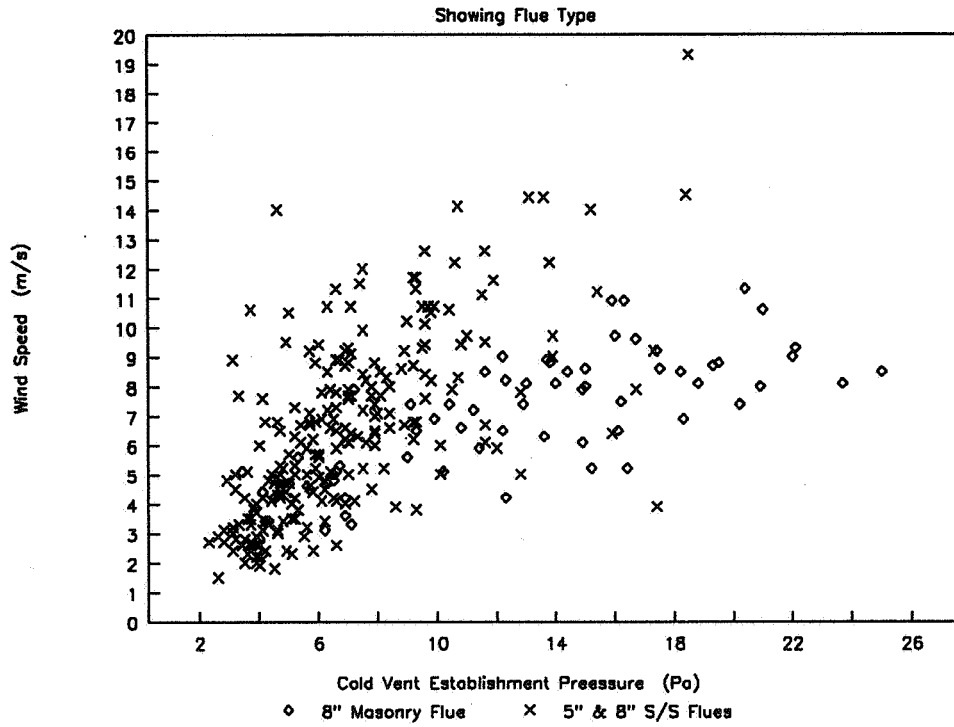


Figure 1

Hot Vent Reversal Pressure

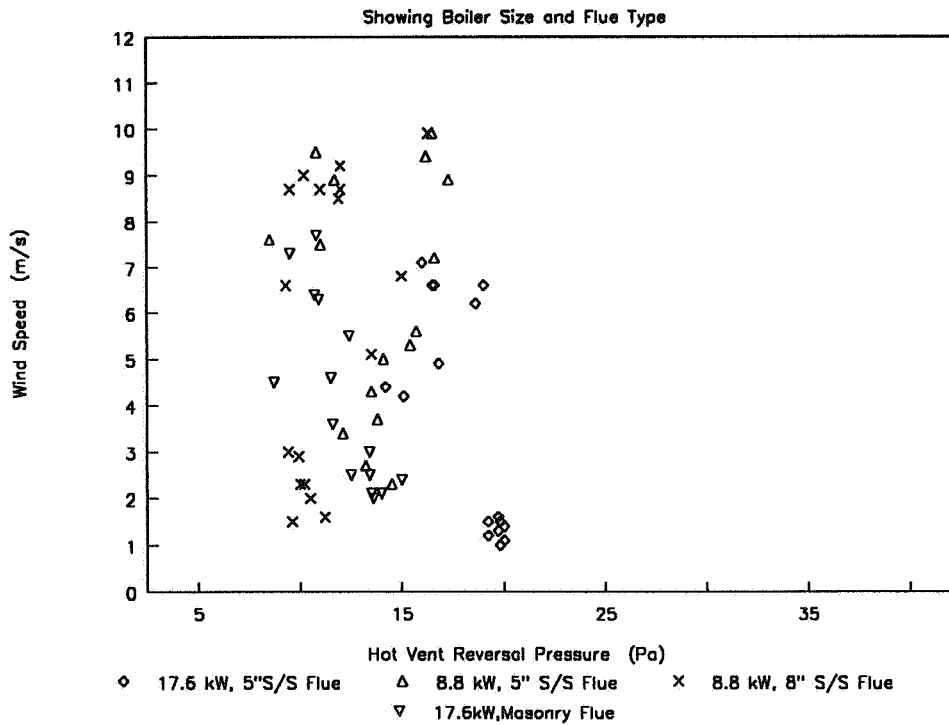


Figure 2

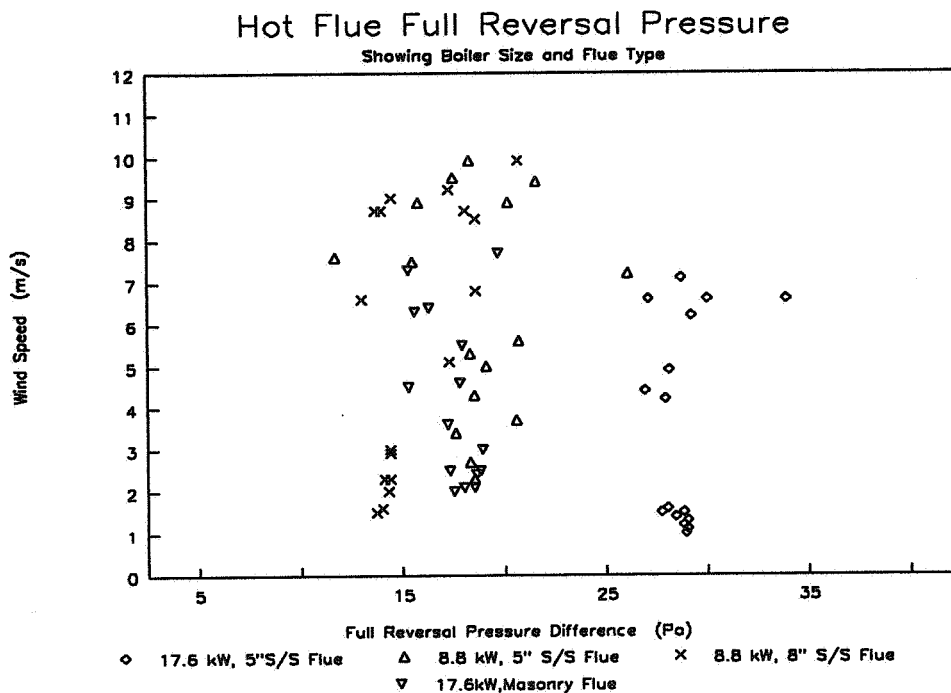


Figure 3

The results were analysed on a computer using a multi-regression package. The dependent variables for the CVEP in order of significance were:

- wind speed;
- type of flue;
- internal/external temperature difference.

Looking at Figs. 2 and 3, the wind speed does not seem to affect the pressure at which spillage occurs since the points are aligned parallel to the wind speed axis. The HVRP and FRP were dependent on:

- flue type;
- flue diameter;
- boiler size.

These are the parameters which determine the temperature of the internal surface of the flue. The internal flue surface temperature being the major driving force of gases up the flue at higher temperatures.

3.2 Indoor Pollution Levels

During all tests, the level of CO₂ and CO was monitored in the kitchen, near to the boiler. At present in the UK domestic indoor air quality criteria are being investigated by the Government but as yet no exposure limits have been set. However, exposure limits for workplaces exist and may be of interest in comparison with the test findings. The Health and Safety Executive 8 hour exposure limits for these gases are: 5 x 10³ ppm for CO₂ and 50 ppm for CO. The 10 minute exposure limits are: 15 x 10³ ppm for CO₂ and 300 ppm for CO. The maximum levels recorded in the kitchen were:

CO: 15.2 ppm CO₂: 8.7 x 10³ ppm = 0.87%

Although the levels recorded do not appear to be dangerous in the short term, they may be harmful over longer periods. It is also worth noting that the boilers tested were new and properly commissioned. Older boilers could well be less efficient in combustion and produce a larger proportion of CO.

The test room at 34 m³ is relatively large for a UK kitchen. In a kitchen of half the volume and with the same boiler installed, spillage would occur at the same internal/external pressure difference. If the cross-sectional area of air leakage paths was reduced proportionately to volume so that the two kitchens had the same air-leakage rate (in air changes per hour), the fan flow rate to cause spillage would be approximately half in the smaller kitchen. At the point of spillage the lower fan flow rate in the smaller kitchen would result in less air being drawn into the room via adventitious ventilation. Spillage results in the same quantity of combustion gases entering the kitchen whatever its volume. The proportion of spilled combustion products to fresh air will therefore be higher in the room of lower volume.

3.3 Air Extract Rates Which Will Cause Spillage

Once it is known at what pressure difference appliances will spill, it has to be ensured that the pressure difference likely to cause spillage is not achievable by mechanical extract ventilation. For this a data base of room air-leakage characteristics is required. This will enable the evaluation of what fan flow rate will create what room depressurisation for a variety of different rooms. The problem with this is the high variation in room air-tightnesses and the unpredictable nature of air-leakage rates.

Air-leakage tests using the fan pressurisation technique were done on a small number of dwellings giving the air change rate of single rooms, combinations of rooms and whole dwellings. These are shown in fig. 4.

The graph shows the fan flow rate which was required to attain a level of depressurisation of 5 Pa. 5 Pa being chosen because that was a pressure at which on a calm day the open flued gas appliances regularly and consistently spilled with a cold flue. Lines have been drawn at 60 l/s and 30 l/s showing the rooms or combinations of rooms which would have produced spillage if fitted with fans or cooker hoods of the minimum recommended size to meet U.K. Building Regulations for kitchens¹. It can be seen that several single rooms and in three cases a combination of more than one room from this small sample come below the 60 l/s line. In the light of this it would be unwise to install an open flued appliance in the same room as an extract fan, or in a neighbouring room, without initially checking that the fan and combustion appliance operate safely by means of a suitable combustion product spillage test. The spillage test should be conducted on a day when the wind speed is less than 4 m/s, so that the effect of the wind assisting the draught up the flue is not too great.

Fan Flow Rates For 5Pa Depressurisation

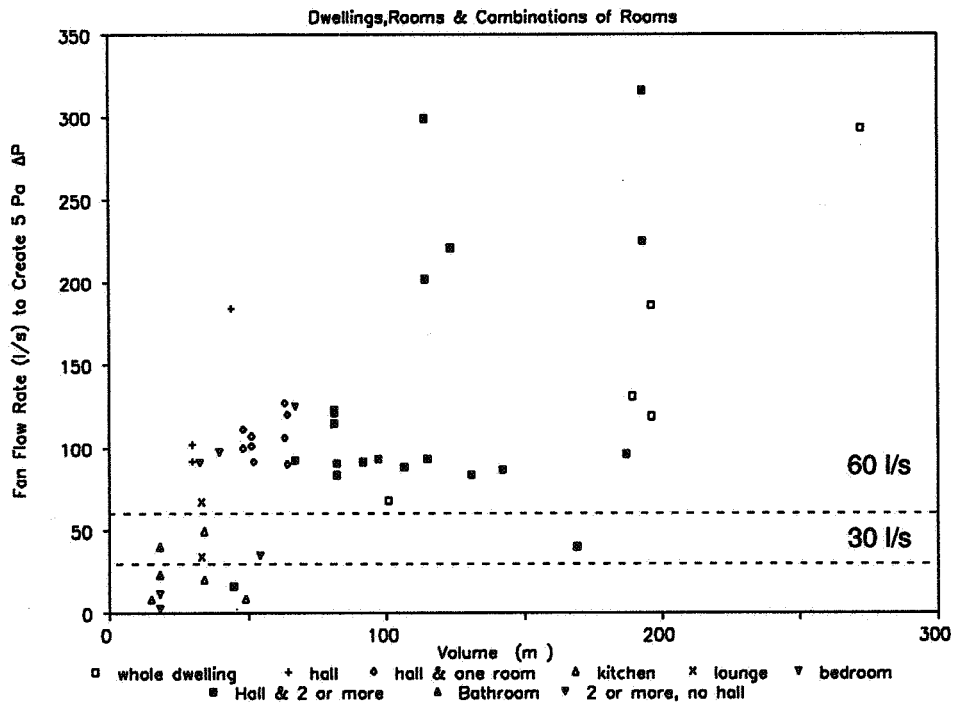


Figure 4

4. Other Gas Fired Combustion Appliances

The experiments reported upon so far have been concerned only with boilers. Other combustion appliances exist which require a flue to vent their burnt gases safely outside. Gas fires and gas solid fuel effect fires fall into this category. They are often installed in old fireplaces when an existing solid fuel fire is removed. The same spillage principles apply to these appliances, i.e. the CVEP should not be exceeded whilst an appliance is likely to be started up.

5. Oil Fired Boiler Results

The oil fired boiler used had a pressure jet burner which is believed to be the only type of burner currently used in new domestic oil boilers in the U.K. The boiler has a fan which takes in the correct quantity of air to allow for complete combustion and adequate dilution. Oil is pressurised and burnt in a firing chamber. The only air inlet to the boiler and flue is through the fan, so for gases to reverse down the flue, the boiler's combustion air fan has to stall or fail somehow. The test was therefore to see if the boiler fan could withstand an adverse pressure applied by a room extract fan.

The oil fired boiler was tested and under no conditions did any combustion gas spill into the kitchen. The room was depressurised up to 200 Pa and the fan supplying combustion air to the boiler still managed to draw in air. The percentage oxygen in the flue gases was seen to decrease with an increase

in pressure difference. An increase in pressure difference of 1 Pa reduced the proportion of oxygen in the flue gases by 0.025 %. The proportion of oxygen in the flue gases recommended by the manufacturers is 4.5 %. Incomplete combustion does not begin to occur until the proportion of oxygen is about 1 %. A pressure difference of 140 Pa would thus be the lowest at which incomplete combustion would occur. The effect of any pressure difference which could be created by a domestic extract fan was of no significance to this boiler.

It should be noted that when installing an oil boiler of the pressure jet burner type. Under room depressurisation it is possible for combustion products to leak out into the room if the boiler casing and flue are not properly sealed.

6. Conclusions

In order to prevent spillage, air extract fans should not be installed such that in isolation or in combination they can significantly depressurise the room or space in which the combustion appliance is installed

A suitable spillage test should always be carried out by the installer of the combustion appliance and/or by the installer of the extract fan. Full account should be taken of the wind conditions at the time of the test and the effect of wind on the performance of the flue. Suitable precautions are now recommended in Approved Documents F and J of the UK Building Regulations. A BRE publication supporting this advice is in preparation.

9. Further Work

Work is currently being carried out on solid fuel open flued combustion appliances. This work will determine the scale of the problem of spillage with solid fuel appliances. Work is also planned to investigate the role and effectiveness of open flued appliances in ventilating the rooms in which they are sited and their ability to remove moisture at source and reduce condensation and mould growth problems. The air-leakage rate of individual rooms and combinations of rooms also warrants further investigation.

8. References

1. Approved Document F: F1 Means of Ventilation. The Building Regulations 1985, 1990 Edition, Amended 1992 (Her Majesty's Stationery Office)
2. Timusk J, Seskus A L, Selby K A, Rinella J. Chimney Venting Performance Study Journal of Testing & Evaluation 16 (2) pp158-177 (March 1988)



**Ventilation for Energy Efficiency and Optimum
Indoor Air Quality
13th AIVC Conference, Nice, France
15-18 September 1992**

Poster 31

**An Investigation of the Potential Use of
Thermography for Building Air Leakage
Measurements.**

J.W. Roberts, S. Sharples, I.C. Ward

**School of Architectural Studies, University of
Sheffield, P O Box 595, The Arts Tower, Western
Bank, Sheffield S10 2UJ, United Kingdom**

An Investigation of the Potential use of Thermography for Building Air Leakage Measurements

J. W. Roberts, S. Sharples and I. C. Ward.
University of Sheffield

Synopsis

The heat loss associated with the external fabric of a building has been greatly reduced by the increased levels of modern insulation, but heating losses associated with cold external air flowing into a building via leakage points in the external facade are still a major problem. Some ventilation is necessary but a detailed knowledge of this leakage would enable the major heat loss routes to be blocked.

A crack has been studied which has hot air of a known temperature and flowrate passing over it. This has been modelled using a finite element analysis enabling the flowrate to be calculated from the measured temperatures. Additional cracks made from various building materials have been studied using infra-red thermography in order to establish the flowrate and therefore quantify the air leakage.

A more extensive mathematical model is now being developed using computational fluid dynamics to predict the airflow based upon a knowledge of surface and air temperatures.

1. Introduction

Heat losses associated with the external fabric of a building have been greatly reduced by the increased levels of modern insulation now required by Building Regulations. This insulation has minimised the heat loss through walls, windows, floors and roofs. The primary source of heat loss is now through leakage points or cracks in the external facade allowing cold external air to flow into the building. A completely sealed building is not desirable due to ventilation requirements to provide fresh air, remove pollutants and control condensation. It would therefore be practical to quantify this air leakage in order to optimize the ventilation.

2. The Preliminary Investigation

Before committing time and money to the study of airflow via temperature measurements it was considered prudent to carry out a preliminary test to verify whether this method would give a reliable answer, or if it would have no correlation whatsoever. To prevent the possible unnecessary building of a test rig this preliminary experiment was carried out using a vent grille in a domestic central heating system. The pumping of hot air to rooms is a popular method of incorporating a central heating system into a newly built house. This method gives a constant flow of hot air of a known temperature over a metal grille. The temperature of the air was set at 42°C, and the temperature of the grille then measured at intervals of 30 seconds. The airflow velocity was measured to be 2.0ms⁻¹.

To try and interpret this data a finite element analysis procedure was adopted. This took into consideration the thermal conductivity of the grille, the velocity and temperature of the airflow, and the dimensions of the grille to calculate the surface heat transfer coefficients. The results of this analysis for various airflow velocities along with the actual measurements are shown in figure 1.

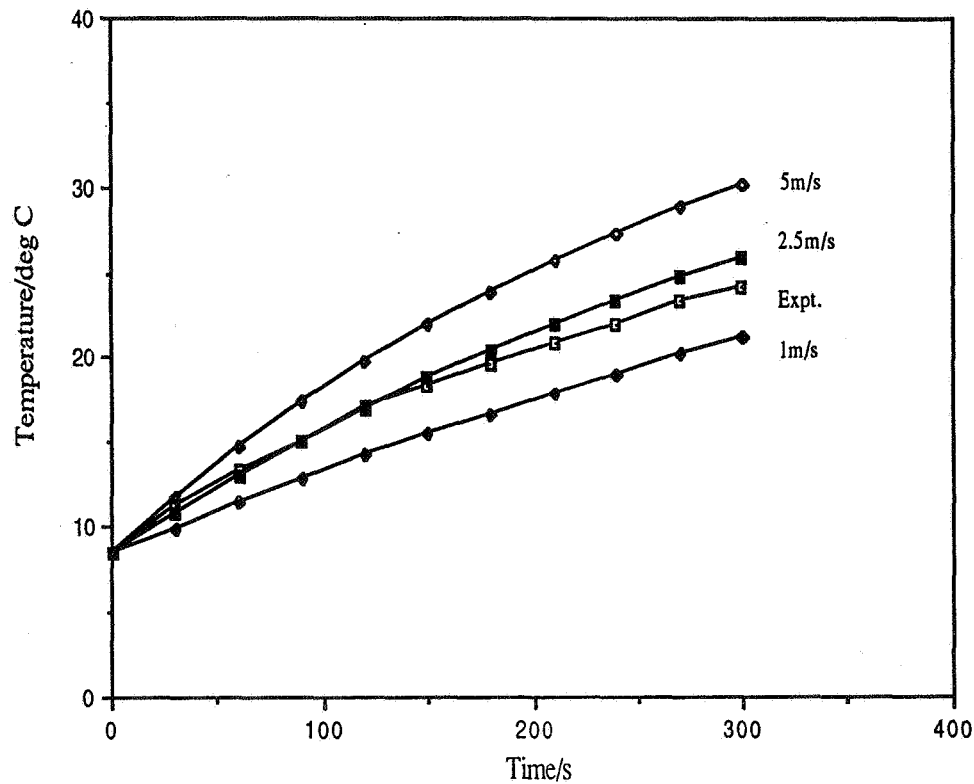


Figure 1: Graph showing preliminary experimental result and finite element calculations.

As can be seen in figure 1 the theoretical predictions are in good agreement with the measured data indicating that calculations of air losses from buildings could be made from a study of temperatures. Obviously when studying the external facade of a large building for heat leakage points the use of a simple temperature probe would be inappropriate. A technique is therefore required that gives quick results and can also be used from a distance so that tall buildings can be studied from ground level. The measurement of the emitted infra-red radiation with a thermography camera would therefore seem to be an ideal method.

3. The Thermographic Method

The initial guidelines for using thermography for air leakage detection were set by Hart [1] in 1986. He stated that the magnitude of the change in temperature depends upon three considerations; the nature and size of the point of leakage, the pressure differential across the construction and the temperature difference between the two sides of the air leakage point which should be at least 5°C.

In this current work these three parameters have all been controlled within the experimental apparatus. Two rooms have been built, each approximately 2m x 2m x 2m, with a partition wall in between allowing the mounting of different cracks at four possible heights. Pre-fabricated cracks have been constructed from typical building materials - hard wood, soft wood and perspex. These cracks all have dimensions of 500 x 50 x 3 mm. In the first stage of the work all the cracks were mounted in turn at a height of 1.75m, with an outlet situated at 1.25m below it to allow the air to circulate.

No pressure differential was set across the crack in this first stage, allowing the only driving force between the two rooms to be the temperature difference. This was achieved by having one room at room temperature, approximately 20°C, and heating the other room to approximately 40°C; thus simulating a building heated to 20°C in winter when the outside temperature is approximately 0°C. The cracks are straight through and constructed to be as smooth [2] as possible on the interior surface.

To use the thermography camera to measure the air temperature, and thus determine the rate of heat loss, the emissivity of the object must be known. The emissivity of a body is defined as the ratio of the spectral radiant power from the body to that from a blackbody at the same temperature and wavelength. The emissivity of the crack material had been measured previously using a known reference and found to be:-

Hard Wood	=	0.90
Soft Wood	=	0.90
Perspex	=	0.96

where a blackbody has emissivity = 1.00.

Thermography utilises the whole of the infra-red spectrum from 0.75 → 100µm and should not be confused with infra-red photography which only utilises 0.75 → 1.2µm - the so-called photographic infra-red spectrum.

The thermography camera was situated 1m from the crack and was connected to a modified video cassette recorder. This enabled a three hour study of the crack to be carried out with time 00:00 defined to be when the crack is opened once the room temperature has reached 40°C. Frozen images were then taken at 10 minute intervals for the whole of the tape using the compatible computer software. This gave 19 images in total. The mean temperature of the crack aperture was then measured and plotted against time, see figure 2.

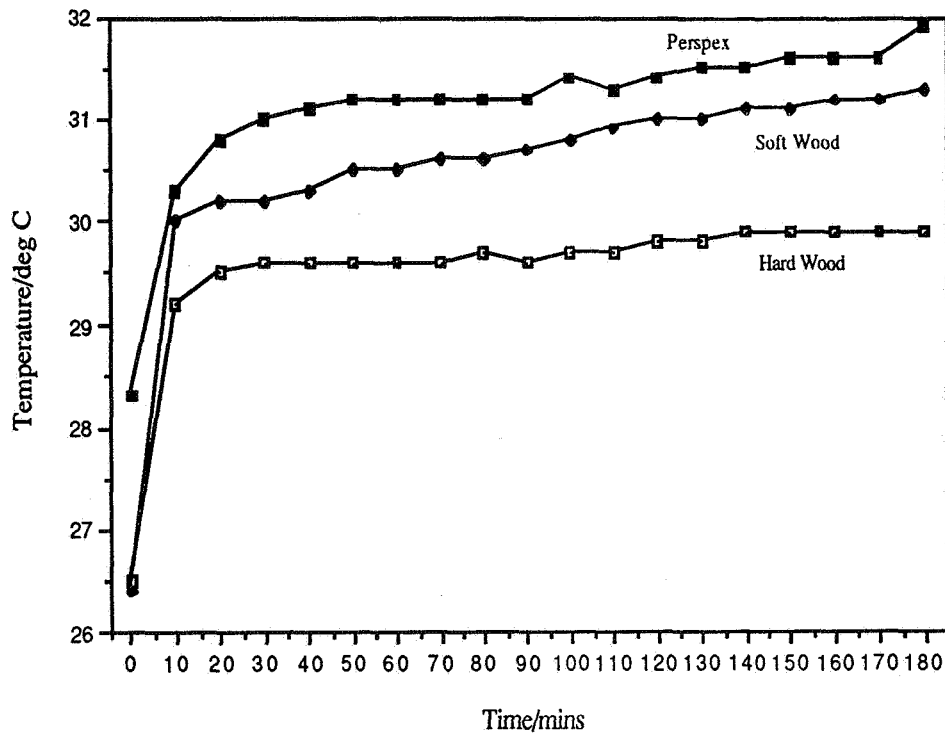


Figure 2: Graph showing temperature change of airflow through various cracks over a three hour period.

4. Results

The heating up curves in figure 2 are similar to those measured with a temperature probe and calculated using the finite element analysis in figure 1. It must be noted that the time scale for the two experiments is different; the temperature of the grille being only measured for 5 minutes whereas the temperature of the pre-fabricated crack is measured over 3 hours. As figure 2 shows, the temperature rises sharply in the first 10 minutes then does not rise by a comparable amount in the next 170 minutes. This tends to suggest that the heat loss is dependant on the dimensions and material of the crack, not on the temperature differential.

To compliment this experimental study and in an attempt to gain a fuller understanding of the air/heat flow a theoretical simulation has been started using the computational fluid dynamics package Fluent®.

5. The CFD Study

Fluent is a complex interactive modelling package that enables various fluid dynamics problems to be studied. The region to be modelled is split into a specified number of cells and then these cells are solved individually according to the initial parameters chosen. An example of the grid of cells for a simple crack is shown in figure 3.

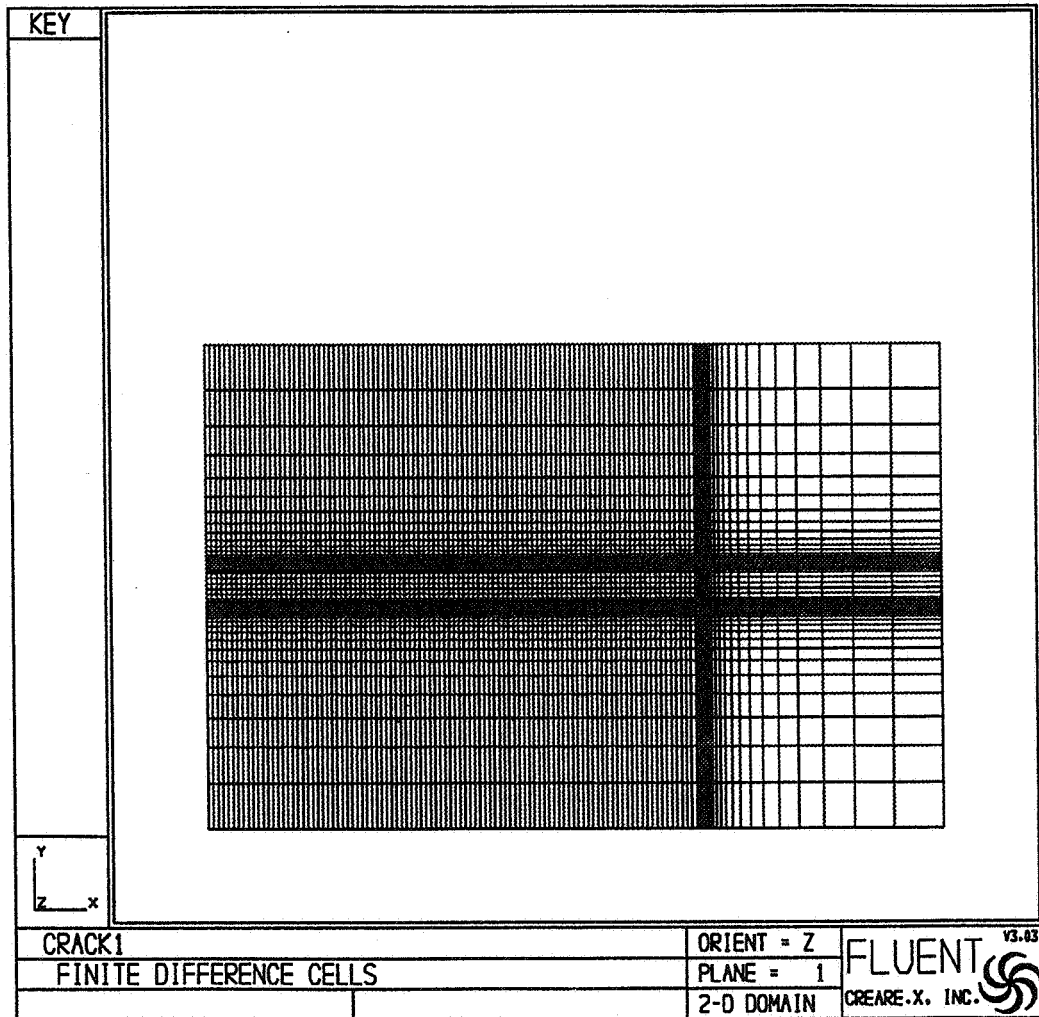


Figure 3: The grid of cells as defined to cover the chosen area .

As a first approximation the grid chosen to study the heatflow through a single crack has dimensions of 150 x 100 cells representing a 50 x 3mm 2-D crack and a 2 x 2m room. To create a temperature differential the room to the right of the crack is set to a temperature of 20°C, and the air entering through the inlet side of the crack set to a temperature of 40°C. Two outlet cells are defined at the top and bottom of the room to satisfy mass conservation. The calculation is performed on a SunC by an iterative process to produce convergent normalised residuals. These residuals may take over a week to reach the required level of convergence. Figure 4 shows a colour-raster plot converted to grayscale of the temperature profile obtained at steady state conditions.

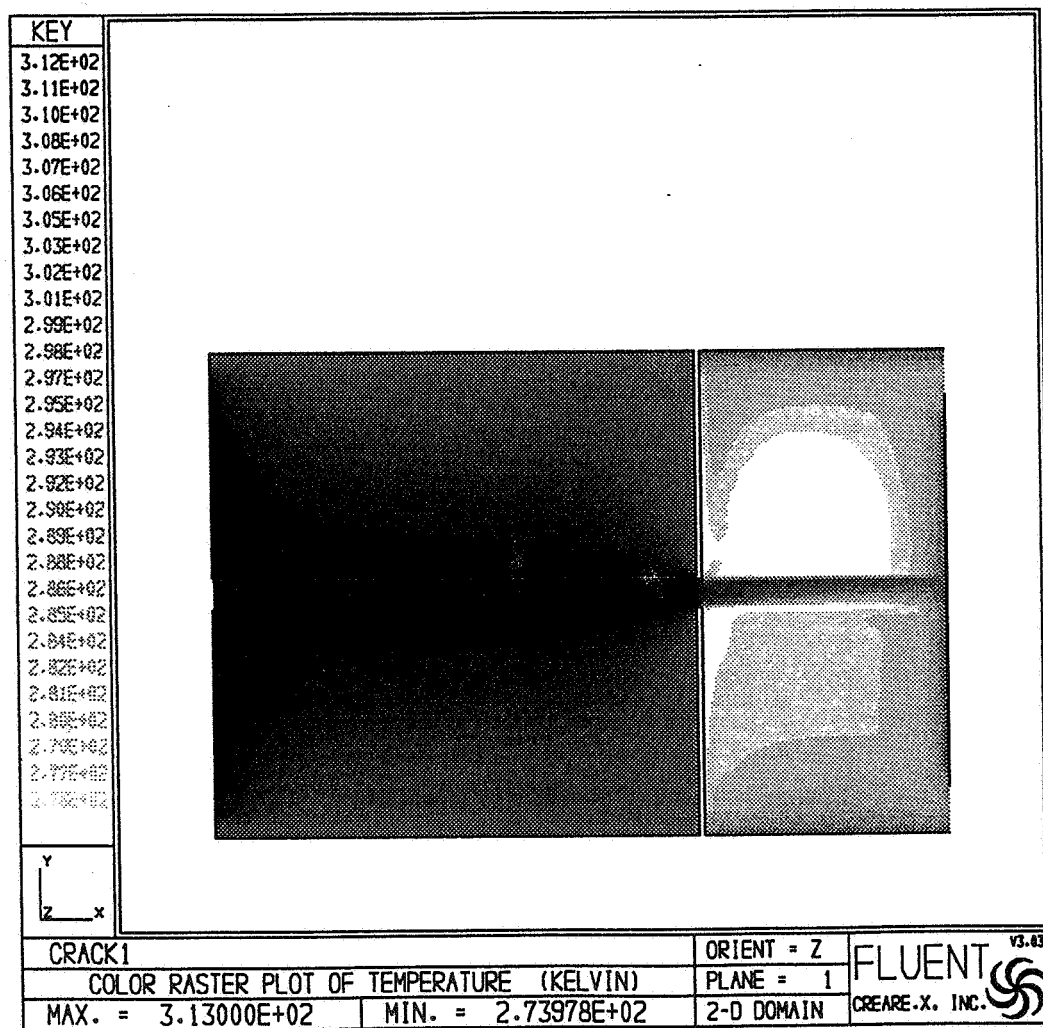


Figure 4: The temperature profile of the crack and room. The key on the left is in Kelvin.

6. Conclusions

Even though this investigation is in its infancy there is enough evidence to suggest that thermography will become an invaluable tool in the study of air leakage measurements. Thermography gives a consistent method of measuring temperatures from a distance, and with our knowledge of how to interpret these as airflow rates it will give a quantitative method of estimating the heat loss via cracks in buildings.

The application of Fluent to this study will give a greater understanding of the airflow through cracks and will give the limiting situations for convective heat flow to occur.

References

1. Hart, J. M., Building Research Establishment publication, ref. no. PD91/86.
2. Kula, H-G. R., Sharples, S. and Ward, I. C., to be published.



**Ventilation for Energy Efficiency and Optimum
Indoor Air Quality
13th AIVC Conference, Nice, France
15-18 September 1992**

Poster 23

**Optibat: A Real Scale Cell in Simulated Climatic
Environment for Multizone Air Flow Pattern in
Building.**

F. Amara^{*}, P. Depecker^{}, F. Allard^{**}**

*** LASH CNRS EP16-ENTPE, Rue M.Audin, 69120
Vaulx en Velin, France**

**** CETHIL-URA CNRS, 1372 INSA, Bât 307, 69121
Villeurbanne, France**

ABSTRACT

One of the main problems about air flows pattern studies remains the experimental validation of numerical codes developed for interzone air flow and pollutant diffusion prediction.

A few years ago, CETHIL developed a real scale experiment made of a 88m² dwelling built in our laboratory hall in a controlled climatic environment. This experimental tool allows a full control of outdoor climatic conditions: air temperature, relative humidity, pressure drop can be controlled on the six faces of the cell: OPTIBAT is thus a reference tool for multizone air flow measurement techniques, and experimental data sets available for validation of numerical models.

The first phase of this experimental projet allowed us to determine air leakage characteristics of indoor and outdoor walls of the cell.

The second element required for the validation of multizone air flow codes is the knowledge of all the interzone air flows. The vast majority of the air flow measurements made to date have involved multiple tracer gas techniques. Using the OPTIBAT facility, we have first used only one tracer gas to determine all the air flows.

The present paper describes the experimental cell and gives the first results about air flows measurements using tracer gas technique. The interzone air flows are computed using two methods. Each method is completed by an error analysis which defines the uncertainty of each result. Both methods give the same results.

NOMENCLATURE

C	Tracer gas concentration matrix	
C _{ik}	Tracer concentration zone i during the k th test	[m ³ /m ³]
q _{ij}	Air flow from the zone j to the zone i	[m ³ / s]
Q	Air flow matrix	
S _{ik}	Tracer source emission rate in the zone i during the k th test	[kg / s]
S	Tracer source emission rate matrix	
T _i	Air temperature of the zone i	[K]
V _i	Volume of the zone i	[m ³]
X _i	Vector containing the six air flows q _{ij} coming to the zone i.	
Y _i	Vector containing the tracer gas rate injected in the zone i.	
σ_x^2	Variance of variable x	
δ_{ij}	Kronecker's symbol	

I. INTRODUCTION

A review of numerical codes about multizone air flow studies has been recently achieved for COMIS project [1]. This review shows that none of multizone codes now developed have been validated .

A few years ago, LASH, CETHIL, CETIAT, three laboratories located in the RHONE ALPES region, have developed together a multizone air flow study project . One of the main supports of this project is the OPTIBAT cell, an experimental tool for multizone air flow measurements to provide experimental data sets needed for validation of numerical codes. These data sets will also be included in Annex 23 of IEA.

We present here OPTIBAT and the first results of interzone air flow measurements obtained using tracer gas techniques.

I.1 Optibat: the experimental tool [2]

A few years ago, CETHIL developed a real scale experiment made of a 88m² dwelling built in our Laboratory hall in a controlled climatic environment [3]. This apartment is in fact a part of a real building built near Lyon at this time

We split the apartment into 6 indoor zones as shown in the Figure 2.

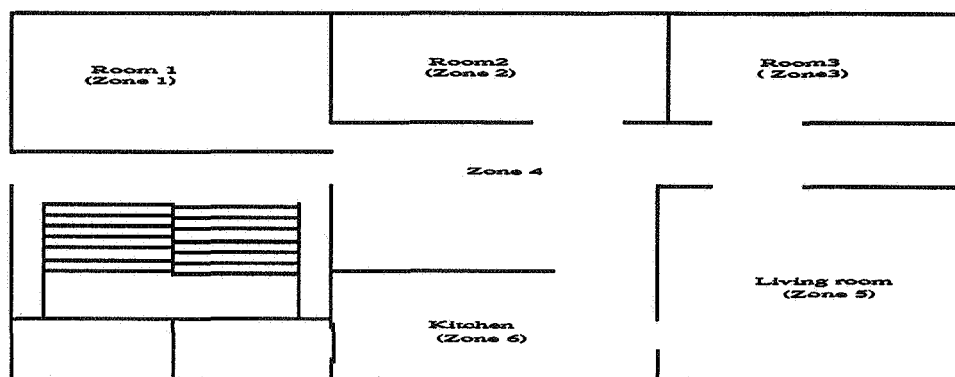


Figure1: The various zones of the experimental cell

To provide measurements under various controlled climatic conditions, climatic housings have been added to each face of the experimental cell (figure 3).

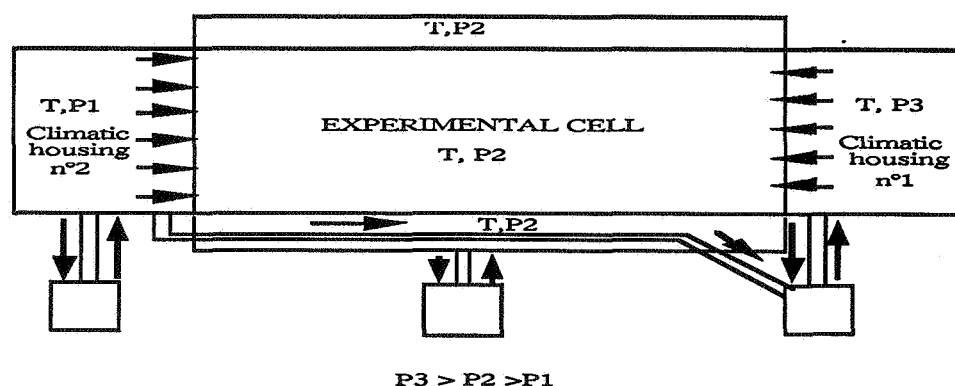


Figure 2: Schematic representation of the climatic conditioning principles
 - On the two main façades, air temperature can vary between -10°C and 30°C, the pressure drop between the two housings can reach 200Pa. Relative humidity varies between 30% and 80%.

- On the other faces, a thermal guard simulates the adjacent apartments. Air temperature and pressure drop are also regulated.

I.2 The experimental project

Since its conception, this experimental facility has been mainly devoted to the validation of various thermal models developed by CETHIL. In order to use it as a reference experiment for multizone air flow studies, we had first to determine the leakage coefficients of all indoor and outdoor walls using two pressurisation methods [3]. Then, we until now, focus our attention on the interzone air flow measurements using tracer gas techniques. The first results of these measurements are presented here.

II. MONOGAS MULTIZONE TECHNIQUE

Most of multizone air flow measurements have involved multiple tracer gases [4, 5, 6]. In each zone a different tracer gas is injected. This needs as many tracers as zones. Whenever in monogas multizone technique, we use only one tracer to determine all the interzone air flows. The SF₆ gas is injected at constant concentration using a PID regulation algorithm. The tracer concentration measurements are provided using a photoacoustic analyser. The measurements are done under steady climatic conditions: outdoor air temperature is controlled at 20°C, the pressure drop between the main façades is equal to 100 Pa.

The principle of this multizone monogas technique is based on the repetition of the same test in each zone under the same climatic conditions. This is possible because all the climatic parameters can be controlled using the OPTIBAT climatic facility.

The six tests required to provide all the interzone airflows are the followings:

-1st test: the SF₆ gas is injected at a constant concentration (10 PPM) in zone 1. A small fan (which air flow rate is 5 m³/h) is installed just front of the injection tube in order to mixed the tracer gas and the volume air. The gas concentration is measured in all the six zones. When we stop the test, the indoor air is purged and taken out far from the hall in which OPTIBAT is built. During the purge the concentration of SF₆ is measured in each zone until it becomes lower than 10⁻² ppm.

-2nd test: After the purge, we injecte the SF₆ at a constant concentration (10 ppm) in zone 2 and we repeat the previous operations under the same climatic conditions.

The test is repeated in each zone. Finally we made six tests under the same climatic conditions. During each test the tracer is injected in a different zone. This technique is equivalent to a multigas test using six tracer gases, each gas being injected in a different zone.

During all the six tests, air temperature is measured in 40 points in the building and in the climatic housings using RTD type PT100 probes. These probes have been calibrated in our laboratory and their accuracy is ± 0.05 C. The pressure drop between each zone and outdoor is also measured.

The results of the measurements of the six tests are reported in Table 1. In upper part of this table, the values represent the mean concentrations of the tracer gas in each zone and in the lower part we represent the source emission rates.

Tracer gas concentration (ppm)						
	Zone 1	Zone 2	Zone 3	Zone 4	Zone 5	Zone 6
Test 1	9.74 ± 0.51	0.08 ± 0.008	0.09 ± 0.008	3.58 ± 0.08	2.85 ± 0.11	3.59 ± 0.10
Test 2	0.1 ± 0.009	9.94 ± 0.34	0.12 ± 0.008	2.89 ± 0.08	2.44 ± 0.054	2.65 ± 0.051
Test 3	0.09 ± 0.01	0.11 ± 0.01	9.97 ± 0.23	3.42 ± 0.11	4.98 ± 0.09	3.54 ± 0.09
Test 4	0.1 ± 0.008	0.13 ± 0.006	0.14 ± 0.006	9.86 ± 0.24	6.96 ± 0.11	10.13 ± 0.15
Test 5	0.06 ± 0.008	0.06 ± 0.008	0.07 ± 0.008	0.11 ± 0.008	10 ± 0.3	1.79 ± 0.11
Test 6	0.06 ± 0.003	0.06 ± 0.006	0.06 ± 0.006	0.18 ± 0.02	0.10 ± 0.0008	9.87 ± 0.35
Tracer gas rate emission (10 ⁴ m ³ /h)						
Test 1	4.6 ± 0.07					
Test 2		3.42 ± 0.07				
Test 3			4.95 ± 0.07			
Test 4				12.41 ± 0.18		
Test 5					6.17 ± 0.09	
Test 6						8.77 ± 0.12

Table 1: Tracer gas concentrations and source emission measured during the six tests.

The confidence intervals shown in Table 1 correspond to the standard deviations.

To describe the interzone air flows, we use both tracer gas mass conservation (equation I) and air mass conservation (equation II) in each zone:

$$\frac{V_i}{T_i} \frac{dC_{ik}}{dt} = \frac{S_{ik}}{T_i} + \sum_j \frac{(C_{jk} - C_{ik})}{T_j} q_{ij} (1 - \delta_{ij}) \quad (\text{I})$$

$$\frac{-V_i}{T_i^2} \frac{dT_i}{dt} = \sum_j \frac{q_{ij} (1 - \delta_{ij})}{T_j} - \sum_j \frac{q_{ji} (1 - \delta_{ji})}{T_i} \quad (\text{II})$$

We used two methods to solve these systems:

II.1 Global approach

In this approach, we consider the complete problem: there are as many tracer gases as zones. Here one test substitutes one tracer.

By writing the matrix form of the equation (I), we obtain under climatic conditions:

$$Q.C = S \quad (III)$$

C_{ik} and S_{ik} represent the values of the k^{th} tracer (test) in the i^{th} zone .

The interpretation of air flow matrix (Q) requires a few explanation [7]: the diagonal elements q_{ii} represent the total air flow incoming or outgoing of zone i and coming from all the zones including outside. The non-diagonal elements represent air flows beetwen zones and should have a negative sign. Thus $-q_{ij}$ represents air flow from the zone j to the zone i. The air flow from the zone j to the zone i can be different from the flow from the zone i to the zone j. This matrix does not need to be symmetric .

For each zone i, we have also determined the infiltration flows q_{i0} by writing:

$$q_{ii} = \sum_{j=0}^6 q_{ij} \quad (IV)$$

$$q_{i0} = q_{ii} - \sum_{j=1}^6 q_{ij} \quad (V)$$

In the same way, the exfiltration flows q_{0i} is determined by writing:

$$q_{ii} = \sum_{j=0}^6 q_{ji} \quad (VI)$$

$$q_{0i} = q_{ii} - \sum_{j=1}^6 q_{ji} \quad (VII)$$

The total infiltration or exfiltration flows for the optibat cell is:

$$q_0 = \sum_{i=1}^6 q_{i0} = \sum_{i=1}^6 q_{0i} \quad (VIII)$$

The second approach we have used to describe the same air flows is the disconnected approach. This approach consists in studiing each zone independently and determining all the flows . [4,8].

II.2 Disconnected approach

As shown in Figure 2, OPTIBAT cell is divided into 6 indoor zones and 1 outdoor zone, there are thus 42 interzone airflows which may theoretically exist.

Nevertheless we suppose that two non-adjacent zones do not exchange air directly without mixing in the intermediate zones [4].

Therefore, among the 42 air flows theoretically possible only 29 air flows do really exist. The other ones are equal to zero.

For each zone we use the conservation mass of each tracer (equation I). The matrix form of this sytem is:

$$C_i X_i = Y_i \quad (IX)$$

$$\text{where } c_i(j, k) = \frac{c(j, k) - c(i, k)}{T_j} \quad (i \neq j) \quad (\text{X})$$

To solve system (IX), we have used two methods:

The first one considers only the tests made in the adjacent zones of zone i . By inverting the square system extracted from the system (IX), we obtain the solution vector X_i

The second method considers all the six tests and using the mean square method, we also identify X_i . The results of this mean square method are in bold characters in Table 3

The results of these two approaches are reported in Tables 2 and 3

$\begin{matrix} i \\ j \end{matrix}$	Outside	Zone 1	Zone 2	Zone 3	Zone 4	Zone 5	Zone 6
Outside	130.5±3.3	46.4±6.3	33.75±1.8	48.6±1.8	2.28±12.1	-1.9±1.5	1.4±3.3
Zone 1	0.27±2.22	47.4±6.6	0.1±0.0	0.2±0.0	46.1±8.7	-2.0±0.8	-1.3±2.1
Zone 2	-1.2±1.2	0.3±0.0	34.5±1.9	0.4±0.0	36.10±3.7	2.36±0.4	-3.50±1.2
Zone 3	-5.6±2.2	0.2±0.0	0.2±0.0	50.0±1.9	42.8±4.7	16.1±1.2	-3.7±2.3
Zone 4	2.8±17.20	0.0±0.0	0.1±0.0	-0.2±0.0	129.3±14.0	43.9±3.9	82.1±16.9
Zone 5	45.9±4.0	0.2±0.0	0.2±0.0	0.3±0.0	0.3±0.0	62.3±4.3	15.3±1.6
Zone 6	88.4±11.7	0.3±0.0	0.2±0.0	0.3±0.0	1.53±0.1	-0.3±0.0	90.4±12.21

Table 2: Interzone air flows q_{ij} (m^3/h) calculated using global approach

$\begin{matrix} i \\ j \end{matrix}$	Outside	Zone 1	Zone 2	Zone 3	Zone 4	Zone 5	Zone 6
Outside	140.1 138.2	46.6 46.6	33.75 33.74	48.8 50.3	0	18.2 12.2	-6.98 -4.69
Zone 1	0.5 0.5	47.4 47.5	0.1 0.1	0	46.9 46.9	0	0
Zone 2	-2.3 -3.3	0.34 0.32	34.5 34.5	0.4 1.2	36.9 36.9	0	0
Zone 3	6.3 8.5	0	0.2 0.2	49.9 52.3	43.6 43.6	0	0
Zone 4	0	0.5 0.6	0.4 0.5	0.7 0.8	129.2 129.2	44.0 47.2	82.2 80.5
Zone 5	46.5 43.8	0	0	0	0.3 0.3	62.2 58.5	15.3 14.4
Zone 6	89.1 89.6	0	0	0	1.53 1.53	-0.1 -0.9	90.5 90.2

Table 3: Interzone air flows q_{ij} (m^3/h) calculated using the disconnected approach. The values in bold characters are obtained using a mean square method.

The confidence intervals in these two tables are obtained by calculating the uncertainty about air flows rates:

III. ERROR ANALYSIS

Several methods are available for estimating the errors made in computing air flow rates. These methods are based on estimates of the precision of the measured tracer concentrations and source emission rates. The knowledge of the covariances of the measured data allows to compute the error about air flows rates. Each method depends on the numerical method used to identify the air flow rates.

III.1 Global approach

We have shown that:

$$Q.C=S \quad (XI)$$

using the matrix indices explicitly:

$$q_{ij} = \sum_{k=1}^6 S_{ik} C_{kj}^{-1} \quad (XII)$$

The emission source rates and concentration are physically independent and, therefore their errors can be assumed to be uncorrelated. The formula for the variance becomes

$$\sigma_{q_{ij}}^2 = \sum_{p,k}^6 \sum_{p,k}^6 \left(\frac{\partial q_{ij}}{\partial S_{pk}} \right)^2 \sigma_{S_{pk}}^2 + \sum_{p,k}^6 \sum_{p,k}^6 \left(\frac{\partial q_{ij}}{\partial C_{pk}} \right)^2 \sigma_{C_{pk}}^2 \quad (XIII)$$

Using equation (XII), we can show that:

$$\frac{\partial q_{ij}}{\partial S_{pk}} = \delta_{ip} C_{kj}^{-1} \quad (XIV)$$

$$\frac{\partial q_{ij}}{\partial C_{pk}} = -q_{ip} C_{kj}^{-1} \quad (XV)$$

The formula for the variance becomes:

$$\sigma_{q_{ij}}^2 = \sum_{p,k}^6 \sum_{p,k}^6 (\delta_{ip} C_{kj}^{-1})^2 \sigma_{S_{pk}}^2 + \sum_{p,k}^6 \sum_{p,k}^6 (q_{ip} C_{kj}^{-1})^2 \sigma_{C_{pk}}^2 \quad (XVI)$$

In the same way, we calculate the variance of q_{i0} , q_{0i} and q_0 using their formulae.

The values of the uncertainties are reported in The tables 2.

IV CONCLUSIONS: Using OPTIBAT facility, it has been possible to use only one tracer gas injected at constant concentration to determine all the interzone air flow rates.

All the measurements have been done under the same steady climatic conditions. The air flows have been computed for the complete problem which assumes that there are as many tracers as zones (one test substitutes one tracer). We have also used the disconnected method by studying all the zones independently.

For the complete problem, an error analysis enables us to give the uncertainties of air flows rates

These first results obtained by the two methods agree well. In order to complete the comparison, we will carry out a more detailed error analysis using a perturbation method..

PERSPECTIVES: although the use of only one tracer gas allows us to describe all the interzone flows, we are now using three tracers gases to determine the same air flows under various climatic conditions.

ACKNOWLEDGEMENT: We thank the French Environment and Energy Management Agency (ADEME) and the Rhône Alpes Region for their support to this study.

REFERENCES

[1] E.A.RODRIGUEZ, F. ALLARD, Coupling Comis airflow model with other transfer phenomena, Energy and Buildings, Vol. 18 N°2, 1992, P147-158

[2] F.ALLARD, J.BRAU, C.INARD, Thermal experiments of full-scale dwelling cells in artificial climatic conditions, Energy and buildings, n°10, 1987.

[3] F.AMARA, P.DEPECKER, G.GUARRACINO , Expérimentation de laboratoire pour l'étude et la mesure des transferts aérauliques dans le bâtiment: phase 1 détermination des perméabilités interzones, Seminaire du GEVRA Mars 1991 Lyon France

[4] C.-A.ROULET, R. COMPAGNON, J.-M.FÜRBRINGER,M.JAKOB, Mesure d'échanges d'air entre les locaux et avec l'extérieur, Rapport final Projet NEFF 339.2 Laboratoire d'Energie Solaire et de Physique du Bâtiment, E.P.F.L Lausanne

[5] F'ANSON S.J., IRVIN C., HOWART T., Air flow measurement using 3 tracer gases, Building and environment Vol 17, n°4, 1982

[6] M.H.SHERMAN , On the estimation of multizone ventilation rates from tracer gas measurements, Buildings and environment Vol. 24 N° 4 1989,P355-P362

[7] M.H.SHERMAN , Uncertainty in air flows calculations using tracer gas measurements, Buildings and environment Vol. 24 N° 4 , 1989, P347-P355

[8] T.W.D'OTTAVIO, G. I. SENUM, R. N DIETZ, Error analysis techniques for perfluorocarbon tracer derived multizone ventilation rates, Buildings and environment Vol 23 N° 3 1988, P187-P194



**Ventilation for Energy Efficiency and Optimum
Indoor Air Quality
13th AIVC Conference, Nice, France
15-18 September 1992**

Poster 15

Energy Saving and CO₂ Reduction.

G. Mertz^{*}, and J. Röben^{}**

*** Fachinstitut Gebäude-Klima e.V., Danziger
Str.20, W-7120 Bietigheim-Bissingen, Germany**

**** Universität Essen, Institut Angewandte
Thermodynamik und Klimatechnik, W-4300 Essen
1, Germany**

Synopsis

The greenhouse effect is one of those topics in environmental politics which are currently worldwide at stake. There are several national concepts aiming at the diminution of CO₂-emission in order to lessen the greenhouse effect. One of these concepts is the CO₂-reduction programme of the Federal Republic of Germany.

With this resolution, passed on November 7th, 1990, Germany's Federal Government aims high: national carbondioxide emission is to be cut back by 25 per cent by the year 2005. The programme contains new requirements to be met by the building equipment technologies, where mainly modifications of residential heating and ventilation systems are to be considered.

This lecture presents the Federal Government's suggestions and discusses them critically in view of the lack of capacity among the building equipment and construction companies. Besides, it gives the amount of CO₂ that can be prevented from emitting into the atmosphere through the installation of ventilation systems with heat recovery.

Contents

1. Introduction	page 3
2. CO ₂ reduction in the building and construction industry	page 3
3. Energy conservation and CO ₂ reduction through mechanical ventilation combined with heat recovery	page 4
4. CO ₂ reduction and investment costs	page 6
5. International aspects	page 7
6. References	page 7

1. Introduction

With the resolution on CO₂-reduction, passed on November 7th, 1990, Germany's Federal Government aims high: as a step towards the protection of the global atmosphere, an extensive national CO₂-reduction programme is supposed to cut back the carbondioxide emissions in Germany by 25 per cent by the year 2005. These values are based on the 1987 figures so that 25 per cent are the equivalent of 300 million tons of CO₂. The following industries are directly concerned: agriculture and forestry, traffic, new technologies and building and construction. As for the latter, an even higher percentage is to be achieved.

2. CO₂ reduction in the building and construction industry

In 1987 – the basic year of the programme in case – carbondioxide emission resulting from heating systems in housing was roughly 130 tons. Hot-water supply caused an additional 20 tons. These figures show that heating and hot-water supply of residential buildings cause 30 per cent (5 per cent respectively) of the total CO₂ emission load (716 t) originating from the consumption of fossile energy sources. The reason for this relatively high percentage are chiefly the average heating load requirements of residential buildings being higher than 220 kWh/m²a. Peak values of 350 kWh/m²a are not unusual.

Given the environmental problems as well as the energy problems known so far or still to become apparent, this fact is definitely unjustifiable and requires, therefore, efficient and immediate measures.

The implementation of the „heat transfer barrier act“, an energy conservation code, was – no doubt – a good and important decision in so far as single family dwellings which were built in accordance with this new resolution produce heating load requirements between 130 and 180 kWh/m²a only. Thanks to this considerable improvement it seems feasible to limit additional CO₂ emission from those residential buildings which are to be built before the end of 2005 to 50 per cent at around 10 million tons CO₂. It is much more difficult, however, to achieve similar results with older buildings. In this area, a potential diminution by 60 up to 65 per cent can only be realized through compre-

ensive measures aiming at the efficient use of energy as well as at the substitution of energy sources.

The heating load requirements of so-called *Niedrigenergiehäuser* („low-energy houses“) are again much lower: single- and two-family dwellings of that type require only between 50 and 90 kWh/m²a, apartment buildings even less. The typical features of such buildings are clearly improved heat transfer barriers on the one hand and highly heat insulated windows on the other hand. The constant diminution of heat transmission losses comes along with important hygienic problems yet: these airtight windows can function properly only if they are kept closed during the heating season. Since this is hardly practicable, it is indispensable to equip the building with a ventilation system in combination with heat recovery in order to prevent high ventilation heat losses.

Qualified calculations showed that CO₂ emission from such highly thermal insulated buildings, which are equipped with that kind of ventilation system, has decreased by 1 to 2 tons per year. In this context further positive effects can be achieved through small heat pumps. These are capable of substituting fossile energy sources in room air-conditioning systems by means of heat recovery.

3. Energy conservation and CO₂ reduction through mechanical ventilation combined with heat recovery

Since, as described above, the building sector has an enormous share in the total CO₂ emissions, as a consequence, many decisive reduction measures will focus on this sector. Here, heat insulation and corresponding insulating measures are of high importance. However, any further steps towards the reduction of the transmission heat losses alone will not lead to the desired result (see figure 1). Hence, in future calculations, the ventilation heat requirements will have to be taken into account more systematically.

Several studies proved that the ventilation heat requirements of an average 70 - 90 m² apartment lies around 5000 kWh/a, depending considerably on the occupant behaviour with respect to ventilating, of course. Yet already for construction and hygienic reasons, this value (5000 kWh/a) can hardly be de-

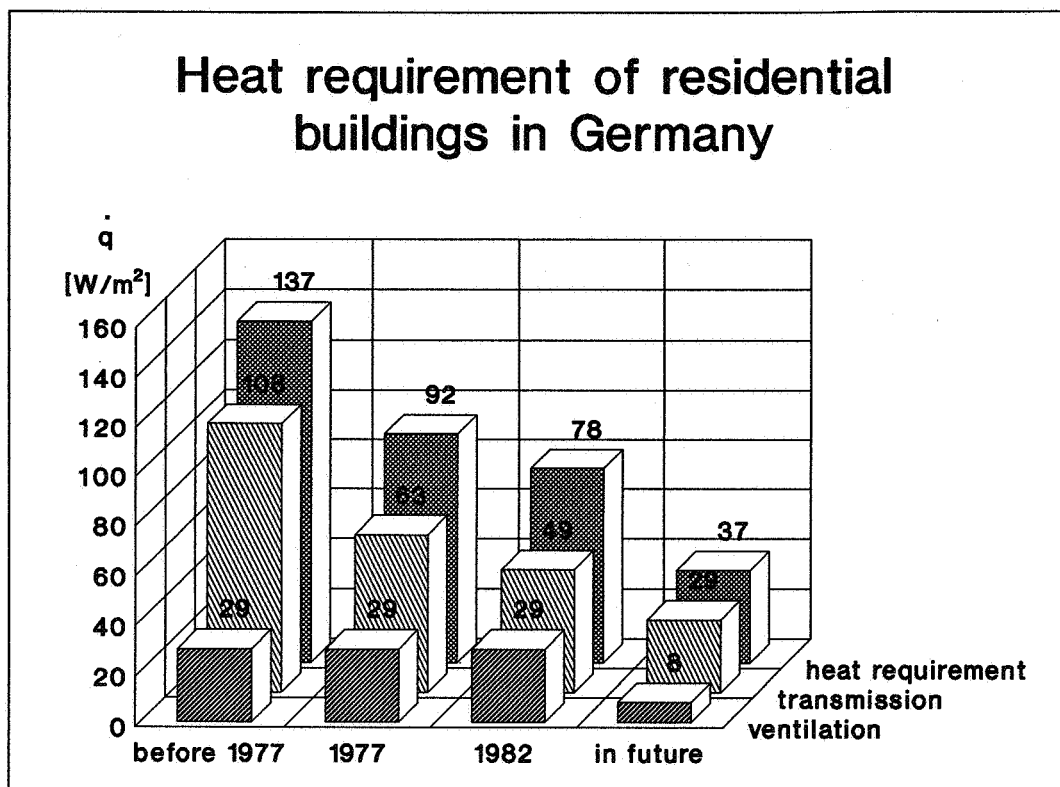


Fig. 1

creased. Such apartments and buildings, however, which are equipped with mechanical ventilation combined with heat recovery and whose heat insulation values correspond to the standard of low energy houses, allow energy saving potentials up to 50 per cent.

Calculations of the HEA* work group „Wohnungslüftung mit Wärmerückgewinnung“ (building ventilation with heat recovery) show how much CO₂ can be saved with these new standards. (* HEA = *Hauptberatungsstelle für Elektrizitätsanwendung* = Advice Centre for Electricity Application)

The HEA calculations suppose that a 70 - 90 m² apartment shows heat requirements around 15,000 kWh/a including ventilation heat requirements around 5,000 kWh/a. Furthermore they distinguish between

- (1) heating systems with natural ventilation
- (2) ventilation systems combined with heat recovery through heat exchangers
- (3) ventilation systems combined with heat recovery through heat exchangers and heat pump devices.

Oil-fired apartments produce 6094 kg/a CO₂ emissions with system (1), 5243 kg/a with system (2) and 4396 kg/a with system (3), whereas gas-fired apartments show the following numbers: 3854 kg/a (1), 3377 kg/a (2) and 2550 kg/a (3).

The calculations take into account the varying CO₂ emissions of different power stations and imply the amount of CO₂ caused by the ventilator.

As can be seen from these numbers, it is possible to reduce CO₂ emission by 46 per cent with oil-fired apartments and by 34 per cent with gas-fired apartments.

4. CO₂ reduction and investment costs

The Federal Building Ministry starts from the assumption that two thirds of all existing residential buildings dispose of – at least partly – considerable energy saving potentials. With the help of intensified measures to save energy, CO₂ emission from housing could be reduced by approximately 50 million tons per year by 2005.

By substituting oil by gas and replacing the heat generator, CO₂ emission could be reduced by an extra load of 10 to 15 million tons per year.

According to estimations of several Federal Ministries, this saving potential is confronted with investments ranking between 250,000 to 350,000 million marks (US: 250 to 350 billion) though. Suppose out of this volume of investment 90,000 million marks can be covered by the saving of energy costs, 160,000 to 210,000 million marks will still be remaining, i. e. roughly 11,000 to 15,000 million marks per year. The specific investment cost to carry through the reduction programme is estimated to be between 3 and 4 marks/kg CO₂. This means that the houseowner has to be offered considerable incentives to make him invest in the renovation of his heating system.

Here, it should be stressed that the amount to be raised is a one-off investment whereas the CO₂ reduction effect will occur every year.

But not only financing represents a problem on the way to realization of the CO₂ reduction programme. A basic question is whether or not the building and construction industry as well as technical building equipment companies are capable at all to satisfy the immense demand potential resulting from the programme. This branch of industry is already booming as an acute shortage in

housing led to the promotion of corresponding aid programmes. At the same time this branch of industry faces a significant shortage of construction workers, so that at the short term an increase in construction capacity seems out of question.

5. International aspects

In view of the current and future environmental dangers resulting from the greenhouse effect, any effort to reduce CO₂ emission must be supported. The concentration on national programmes seems to be little promising nonetheless. Even if the CO₂ reduction programme of the Federal Government turns out successful in 2005, the 25%-reduction of CO₂ emission in Germany represents a worldwide diminution of 1,25 per cent only. And if – as is supposed – CO₂ contributes only 50 per cent to the greenhouse effect, this figure is reduced to 0.675 per cent even.

The sole possible and obvious consequence out of these numbers is that only joint international efforts can combat the greenhouse effect efficiently – sooner or later all nations will be concerned.

6. References

1. RECKNAGEL - SPRENGER - HÖNMMANN
„Taschenbuch für Heizung und Klimatechnik“
Oldenbourg Verlag, Ausgabe 90/91
2. KLAUS, H.
„Entlastung der Umwelt durch CO₂-Reduktion“
In: Strompraxis - spezial '91, pp 18-20.
3. MERTZ, G.
The Carbon Dioxide Reduction Programme of the Federal Republic of Germany
In: Air Infiltration Review, Vol. 13, No 2, March 1992, pp 6-7.

**Ventilation for Energy Efficiency and Optimum
Indoor Air Quality
13th AIVC Conference, Nice, France
15-18 September 1992**

Poster 21

**The Control of House Dust Mites by Ventilation: A
Pilot Study.**

D.A. McIntyre

**EA Technology, Capenhurst, Chester CH1 6ES,
United Kingdom**

1 Synopsis

The house dust mite inhabits bedding and soft furnishings in homes. It is implicated as a major cause of allergic asthma. Maintenance of indoor humidity below a level of 7 g/kg inhibits the growth of the mite population. A pilot survey was carried out by EA Technology in cooperation with the Building Research Establishment to investigate the effect of mechanical ventilation with heat recovery (MVHR) both on indoor humidity and mite abundances.

The temperature and humidity in the main bedroom of 11 dwellings were measured over a period of 1 month in February 1992, and dust samples taken from living and bedroom carpets and mattresses. Bedrooms in houses with continuously operating MVHR showed significantly lower humidities and significantly lower levels of mite concentration in dust taken from the bedroom carpet, when compared with similar houses where the MVHR was not continuously operated.

The results of the survey support the proposition that the use of MVHR in the British climate can act as an effective means of control of house dust mites. In view of the small sample size, confirmation using a larger sample is desirable.

2 House dust mites and asthma

The incidence of asthma is widespread in many parts of the world. In the UK more than two million people are diagnosed as asthmatic, with 1 in 10 children suffering at one time from the disease. The incidence of asthma show a steady increase. The commonest allergen causing asthma in the UK is the house dust mite. The main problem of allergy is caused not by the mites themselves, but by their faecal pellets. Because of the need to preserve water, mites produce no urine, and their excreta are produced in a dry form. The prime allergen contained in the pellets is termed Der p1. Experimental methods of assessing level of mite population in household dust are described by Colloff [1]. A WHO working party [2] recommended provisional standards for mite concentration in household dust:

	Sensitisation	Acute risk
Allergen (ug Der p1/100 mg dust)	0.2	1.0
Mites (mites/100 mg dust)	10	50

Exposure to a level of less than 10 mites/100 mg dust means that an individual has a low risk of sensitisation and development of asthma. Exposure to the higher level of 50 mites/100 mg dust means that an already sensitised individual has a risk of developing acute asthma.

3 Ecology of the house dust mite

The term house dust mite is applied to several related species of the family pyroglyphidae. The predominant species in the UK is *Dermatophagoides Pteronyssinus*, and this is normally implied when the term house dust mite is used [3]. The mite is about 0.35 mm long, and is invisible to the naked eye. It is widely, if not universally distributed in the UK, where it inhabits soft furnishings, carpets, cushions and soft toys. Above all, it is to be found in mattresses and bedding, where the combination of warmth, humidity and a ready supply of food provide an ideal environment.

The primary source of food for the mite is human skin. Human skin scale forms the primary constituent of house dust, giving its characteristic grey colour. The mite lives in an environment where there is no liquid water available and moisture balance is critical to its survival. Laboratory studies show that the optimum conditions for mites are 25°C and 80% RH. Lowering the humidity has an adverse effect on mite population.

Many surveys have demonstrated a general relation between humidity and mite population. Houses in low lying areas near rivers have more mites, while houses at high altitudes, where the humidity is low, are virtually mite free. There is also a seasonal variation in mite population, which is lowest in late winter and spring ie at the end of the period when indoor humidities are at their lowest. Korsgaard [4] investigated the relation between humidity and mites in 50 Danish apartments over one year. Those apartments with low winter indoor humidities had low mite counts; these low concentrations were maintained throughout the summer and autumn, even though the indoor humidity inevitably rose. Hart and Whitehead [5] surveyed dust mites in 30 homes in Oxfordshire and found bedroom humidity to be the most important variable affecting mite numbers. Schober [6] surveyed 11 living rooms in the Netherlands and concluded that mite levels stayed below the hygienic level if the absolute indoor humidity did not exceed 7.1 g/kg. Recent work in France [7] concluded that few mites can develop if the internal humidity is below the value of 7 g/kg. There are thus several studies linking dust mite abundances with humidity in climates similar to that of the UK; the studies support the WHO finding that indoor humidities below 7 g/kg will inhibit the growth of mite populations.

4 Control by Ventilation

The humidity in a room is determined by the dynamic equilibrium between moisture production and loss by ventilation. In winter the outdoor temperature, and hence outdoor moisture content, is low. However, many people restrict ventilation during cold weather, allowing the indoor humidity to increase, thus favouring an increase in house dust mites. The use of mechanical ventilation with heat recovery allows ventilation to be maintained with comfort and economy and offers a practical means of dust mite control.

There are as yet few studies relating the use of mechanical ventilation directly to indoor humidity and dust mite populations. Korsgaard [8] reports an experiment in which mechanical ventilation with heat recovery units were installed in eight houses and compared with a control group. Mite concentrations fell in the experimental houses following the installation of MVHR; concentrations in mattress dust were reduced by two thirds. An investigation was carried out in Denmark as part of a healthy building project [9]. Relatively high air exchange rates of 1.3 air changes per hour were used. Humidities fell significantly, and 11 out of 16 families registered total disappearance of

mites from old mattresses. Significant improvements in health were found, both in subjective feelings and in objective clinical measures. The improvement was highly correlated with changes in house dust mite counts. The study concluded that the high ventilation rate due to mechanical ventilation was the major cause of low indoor humidity and thus to the disappearance of the house dust mites in 11 of 16 families.

5 Objectives of Pilot Survey

A pilot survey was set up during the 1991/92 winter to test the hypothesis that MVHR during cold weather would reduce indoor humidities by an amount sufficient to inhibit the mite population; a secondary objective was to gain experience in measurements techniques, since it was anticipated that a larger survey would subsequently be required. The survey was carried out in association with the Timber Division of the Building Research Establishment. EA Technology organised the houses to be studied and provided the temperature recording apparatus. BRE carried out the house visits and dust sampling and arranged for the dust samples to be analysed.

6 The survey

6.1 Organisation

The Electricity Industry in the UK promotes all-electric housing under the specifications Medallion and Medallion 2000. Medallion 2000 houses are required to be fitted with Mechanical Ventilation with Heat recovery (MVHR). Regional Electricity Companies were asked to cooperate by providing addresses of suitable houses, and houses in South Wales Electricity area were selected. Occupants were contacted by letter and asked if they were willing to take part in the survey; the purpose of the survey was explained to them. Usable results were obtained from 8 houses fitted with MVHR and 3 houses without.

Each house was visited twice, with approximately four weeks between visits. On the first occasion a simple questionnaire established basic details about the house. Dust samples were taken from three sites: living room floor, bedroom floor and main bedroom mattress. A small data logger was left in the main bedroom to record temperature and humidity. On the second visit, further dust samples were taken from the same sites, the data logger removed and a second questionnaire administered.

6.2 Measurements

Temperature and humidity were recorded in the main (occupied) bedroom using a Squirrel logger, set to record a pair of measurements every 30 minutes. Air temperature and RH were measured by a Vaisala transmitter HMW 30 YB. Temperature and humidity records were obtained from the Met Office weather station at Cardiff, some 20 miles from the houses. Dust samples were collected using a small vacuum cleaner fitted with a special sampling head, dimension 14 x 3 cm. Dust was collected on a cellulose filter and kept in a polyethylene bag before sending for analysis. The sampling technique was to continuously vacuum an area of 100 x 100 cm of the carpet, or 60 x 60 cm of the mattress over a period of two minutes. The identical area was sampled on the second visit. Sampling was carried out by an experienced worker from BRE, who had carried out previous dust mite surveys in homes.

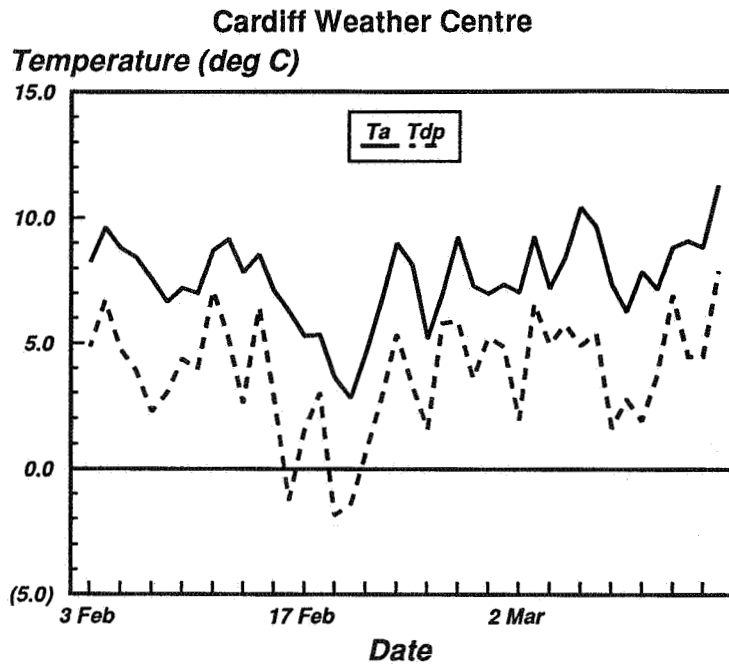


Figure 1. Variation of daily mean air temperature and dew point measured at the Cardiff weather centre during the period of the survey.

Table 1. Mean Air and Dew Point Temperatures

Group	Code	Means over month		
		Ta	Tdp	g/kg
A	1	17.8	6.6	6.0
	2	17.6	6.6	6.0
	10	18.9	5.8	5.7
	11	19.9	7.	
	Mean over group	18.6	6.5	5.9
B	3	19.8	9.9	7.5
	4	17.4	6.4	5.9
	5	20.2	7.8	6.5
	9	17.4	8.1	6.6
	Mean over group	18.7	8.1	6.6
C	6	16.6	7.4	6.3
	7	18.4	7.9	6.5
	8	19.5	9.5	7.3
	Mean over group	18.2	8.3	6.7

Measurement intervals were 26 or 29 days, within period 1 February to 10 March 1992.

Humidities differ significantly between Groups A and B. $P < 0.05$ on a one tailed t test. one tailed t test.

The dust samples were sent to the Scottish Agriculture Science Agency at East Craigs, Edinburgh for analysis. Analysis of the dust was carried out by flotation and staining of the mites [9]. Results are quoted in mites per 100 mg of dust. Mite species were identified and mites were classified as alive or dead at the time of sampling on the basis of the intactness of the body.

7 Results

7.1 Questionnaires

Two questionnaires were administered. The first asked for general information about house type and occupancy; the second questionnaire was administered during the second visit and asked about conditions in the house during the experimental period. House type varied from 4 bedroom house to 2 bedroom flat. The MVHR systems fitted are designed to be used 24 h per day. It was found that use was varied. The respondents were classified into three groups:

A	MVHR used continuously	4 dwellings
B	MVHR fitted, not used continuously	4 dwellings
C	No MVHR	3 flats

Respondents were asked to score the atmosphere in their house on two seven point scales marked "Stuffy/Fresh" and "Dry/Humid". Statistical tests found no significant difference between the groups. The flats in Group C were all about one year old, while those in Groups A and B were about 3 years old.

7.2 Temperature and Humidity

The water vapour content of air may be expressed as relative humidity (RH) or as the absolute water content. It is the absolute water content which is the parameter which is the primary influence on house dust mite viability. It may be expressed as the dew point Tdp or as the moisture content in g/kg. Figure 1 shows the daily external air temperatures and humidities for the duration of the measurement period.

Table 1 summarises the mean bedroom air temperatures and humidities averaged over the experimental period. The mean temperatures ranged from 17.4 to 20.2°C. The mean temperatures for the three groups were similar. The humidity for group A was lower than the two unventilated groups B and C. Humidity in Group A tested significantly lower than in Group B using a one tailed t test ($P < 0.05$).

7.3 Dust mites

Table 2 shows the sample analysis received from SAS at Edinburgh. The overwhelming majority of mites were *Dermatophagoides Pteronyssimus*, which is the species implicated in the production of allergens. A $\log(1+x)$ transformation has been used for analysis. In effect it produces a geometric mean of the values; the addition of 1 is to cope with samples with zero counts. Values of mite concentrations in the tables are given as

Table 2. Results of Mite Analysis

Counts expressed as mites per 100 mg of dust.
Counts transformed as log (1 + x)

	Code	First round			Second round		
		LR1	BR1	MAT1	LR2	BR2	MAT2
Group A	1	0.681	0.531	0.000	0.342	0.342	1.164
	2	1.736	0.756	0.491	2.119	1.086	2.425
	10	1.068	1.164	2.448	1.571	1.567	1.555
	11	0.886	1.182	1.447	0.613	1.522	0.708
	Mean	1.093	0.908	1.097	1.161	1.130	1.463
Group B	3	0.716	2.103	1.489	1.199	miss	1.301
	4	1.238	1.787	0.000	0.633	1.344	2.022
	5	2.343	2.691	3.116	2.312	2.915	2.774
	9	1.369	2.390	1.220	0.806	1.996	1.504
	Mean	1.417	2.243	1.456	1.237	2.085	1.900
Group C	6	0.663	0.892	0.591	1.623	1.233	2.108
	7	0.000	0.851	0.447	0.079	0.279	1.164
	8	0.982	1.898	1.061	1.623	1.470	0.000
	Mean	0.548	1.214	0.700	1.109	0.994	1.091

LR Living room; BR Bedroom; MAT mattress.

Mite concentrations in bedroom dust samples were significantly lower in Group A than in Group B ($P < 0.01$, 1 tail t test)

Geometric mean concentrations:

Group A bedrooms 9.4 mites/100 mg dust
Group B bedrooms 144 mites/100 mg dust

Table 3. Correlation between first and second samples

Living room carpet	$c_2 = 0.27 + 0.85 c_1$ $r^2 = 0.51$. $n = 11$
Bedroom carpet	$c_2 = 0.12 + 0.89 c_1$ $r^2 = 0.74$. $n = 11$
Mattress	$c_2 = 0.42 + 0.56 c_1$ $r^2 = 0.44$. $n = 7$

c_1 and c_2 are the mite concentrations in the first and second samples, log (1 + x) transform used. Turned mattresses excluded from analysis.

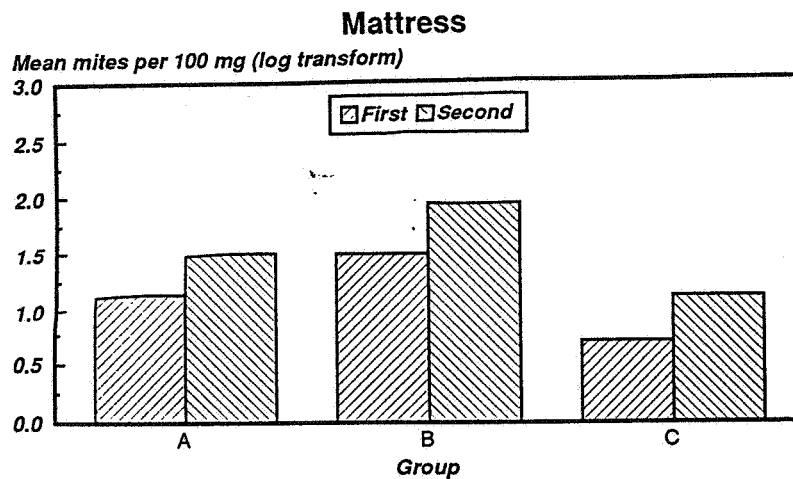
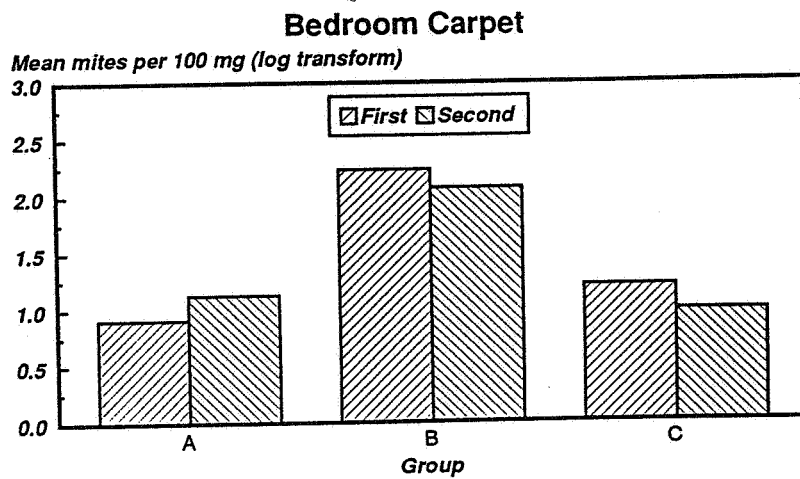
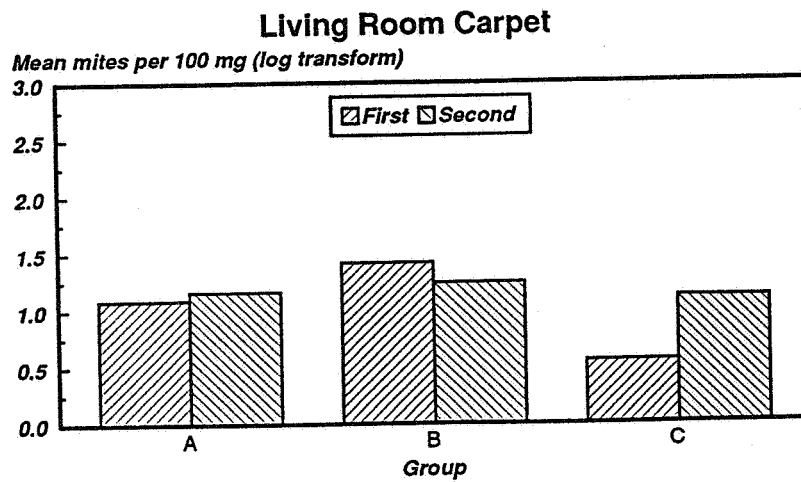


Figure 2. Mean mite counts shown by experimental group. The mite counts for the bedroom carpet in Group B (MVHR not used) are significantly higher than the counts in Group A (continuous MVHR). Group C houses had new carpets with a consequent low mite count.



transformed values. The transformed value of 0 corresponds to 0 mites per 100 mg of dust, 1 to 9, 2 to 99 and 3 to 999.

The repetition of sampling within a four week period served as a check of the sampling and analysis techniques. No changes were made to the environment of the mites during the experimental period so there was no reason to expect any systematic change in abundance. Table 3 shows the correlation within sample site between the first and second dust analysis. The agreement between measurement at the two carpet sites shows reasonably good agreement, which is typical of the reliability found with this technique. Comparison of first and second samples for the mattresses showed initially no correlation at all. The householders were asked if the mattress had been turned between visits. When turned mattresses were eliminated, the correlation improved, though still worse than the carpet sites.

Figure 2 shows the mean log concentration of mites for the different sites, by experimental group and divided by first and second measurements. The mattress measurements have been included for completeness, though as observed above the variation in results makes it impossible to draw reliable conclusions. The results for the living room carpet show that the samples from Groups A and B have similar abundances, while the samples from Group C showed lower counts; the carpets in Group C were under 1 year old. The mite counts in the bedroom carpets were found to be significantly higher in Group B than in Group A, using a one tail t test ($P < 0.01$, 6 df). Again, the counts in Group C with new carpets were lower than in B, even though the dew points were comparable.

7.4 Analysis

The mean absolute humidity in Group A bedrooms over the measured period was 5.9 g/kg, which is lower than the 7.0 k/kg suggested by the WHO working party as the critical value above which mites will proliferate. The control group B had a mean humidity of 6.7 g/kg, close to the critical value. The geometric mean mite concentrations in the bedroom carpets were 9.5 in Group A, and 147 mites/100 mg of dust in Group B. The houses with MVHR thus had a mite concentration in the bedroom carpet dust of below the 10 mites/100 mg level recommended by the WHO as below the level at which sensitisation occurs. The Group B level was above the 100 mites/100 mg dust suggested by the WHO as significantly increasing the likelihood of acute asthma. The low levels of mites in Group C has been considered as of little consequence, notwithstanding the higher humidity levels. The carpets in these houses were all less than one year old, and we would not expect to find high levels of mites.

The relation between bedroom humidity and the dust mite abundance in the bedroom carpet dust are thus in agreement with the hypothesis that MVHR will reduce internal humidity levels, and that dust mite abundance will be reduced by a humidity level below 7 g/kg. Both these findings were statistically significant.

8 Discussion

This study confirmed the expectation that the use of MVHR would reduce house dust mite abundance. It did this for the population in the bedroom carpet, which was the room in which the humidity was measured. The mites in the living room carpet did not show a significant difference between groups; humidity was not measured in this room.

Bedrooms are normally considered the more sensitive site, because of the more favourable conditions for mite growth, of temperature humidity and food supply. The measurements of mites in mattresses proved unreliable. Work is required to establish satisfactory experimental methods before moving on to a larger survey.

The study was designed as a pilot survey and has successfully fulfilled its objectives in giving lessons for a larger survey. The eight houses included in the analysis, although showing significant differences in mite populations, can not be considered a large enough sample to prove an unarguable case for MVHR. It is clear that many variables affect dust mite populations; either these variables must be controlled in an experiment, or the sample must be large enough to ensure randomisation of confounding variables. The intended comparison between MVHR and non-MVHR houses was rendered void by the fact that all the Group C (non MVHR) houses had new carpets.

More work is now needed to confirm the results with a larger sample and to include the effect of ventilation rates, which were not measured in this study. The findings also need to be related to local climatic conditions to establish the geographic applicability of this technique of mite control.

9 Conclusions

The use of mechanical ventilation with heat recovery, used continuously, reduced humidity measured in the bedroom below that in a similar group of houses where the MVHR was not used continuously.

The abundance of house dust mites in the bedroom carpets of the houses with continuous MVHR was significantly lower than the houses with non-continuous MVHR. In the first case the level was below that considered to present a risk of sensitisation to the mite allergen.

The sampling and analysis technique employed did not give reproducible results on mattresses.

Over 85% of the mites were *Dermatophagoides Pteronyssimus*, which is the species implicated in the causation of allergic asthma.

Additional work, using improved sampling techniques and a larger sample of houses, is necessary to consolidate these findings.

10 Acknowledgements

This project was carried out in association with Dr C A Hunter of the Timber Division, Building Research Establishment, who was responsible for the collection and analysis of the dust samples.

The mite analysis was carried out by Mr I G Jeffrey of the Scottish Agricultural Science Agency, East Craigs, Edinburgh. Additional analysis was done by Dr J Korsgaard of Aarhus, Denmark.

11 References

- 1 COLLOFF, M J
Practical and theoretical aspects of the ecology of house dust mites in relation to the study of mite-mediated allergy.
Rev Med Vet Entomol, 79: 611-30, 1991.
- 2 PLATTS-MILLS, T A E and DE WECK, A L
Dust mite allergens and asthma - a world wide problem.
Report on International Workshop, Bad Kreuznach.
J Allergy Clin Immunol, 83: 416-27, 1987.
- 3 BLYTHE, M E
Some aspects of the ecological study of the house dust mites.
Brit J Dis Chest 70: 3-31, 1976.
- 4 KORSGAARD, J
House dust mites and absolute indoor humidity.
Allergy 38: 85-92, 1983.
- 5 HART, B J and WHITEHEAD, L
Ecology of dust mites in Oxfordshire.
Clinical and Experimental Allergy, 20: 203-9, 1990.
- 6 SCHOBER, G
Absolute indoor humidity and the abundance of allergen producing house dust mites and fungi in the Netherlands.
Brussels conference ICS 860. ed C J Bieva et al. pp 395-99, 1989.
- 7 VERVLOET, D, PRADAL, M, PORRI, F and CHARPIN, D.
The epidemiology of allergy to the house dust mite.
Revue des Maladies Respiratoires, 8: 59-65, 1991.
- 8 KORSGAARD, J
Ventilation and House Dust Mites,
Der Allergiker 1: 16-18, 1988.
- 9 HARVING, H, HANSEN, L G, KORSGAARD, J, NIELSEN, P A and OLSEN, O F
House dust allergy and antimite measures in the indoor environment.
Allergy 46 Suppl 11: 33-38, 1991.
- 10 THIND, B B and WALLACE, D J
Modified flotation technique for quantitative determination of mite population in feedstuffs.
J Assoc Anal Chem 67, 866-8, 1984.



**Ventilation for Energy Efficiency and Optimum
Indoor Air Quality
13th AIVC Conference, Nice, France
15-18 September 1992**

Poster 20

**The Penetration of Gaseous Pollutants Into
Buildings in the Case of a Sudden Contamination
of the Outdoor Air.**

K.E. Sirén

**Helsinki University of Technology, Sähkömiehentie
4, 02150 Espoo, Finland**

SYNOPSIS

A sudden contamination of the outdoor air by some toxic gas can have several causes. The primary goal of the investigation was to determine the protection afforded by sheltering indoors. The object of a computational approach was a single family house with two floors. Three different models were utilized as computing tools : MOVECOMP to calculate the infiltration air flows, MULTIC to calculate the contaminant transport inside the building and TDYN to calculate the temperature decay of the building. The variation of the weather parameters was treated using the two-dimensional distribution of the outdoor air temperature and wind speed and a statistical approach. The results show the cumulative distribution functions of the relative doses inside the building for different tightness levels, exposure times and other relevant parameters.

1. INTRODUCTION

A sudden contamination of the outdoor air can be caused by a transportation accident, a sudden emission from an industrial plant, a disaster in a nuclear power plant or even by traffic. The envelope of a building can be utilized as a shelter against the contaminated outdoor air. The protection afforded by sheltering indoors depends primarily on the tightness of the building envelope, the outdoor air temperature and the wind speed. Other parameters, like the leakage distribution, the pressure coefficients, the wind direction and the local environment around the building, have some influence, too. However, the problems involved in sheltering have not been investigated very much [1..3] and there is shortage of useful quantitative knowledge.

The most reliable way to look into the penetration of contaminated air into a building would be to use tracer gas measurements. This would, however, be a very laborious, time consuming and expensive way, and if the effect of the building tightness and the weather statistics were also to be investigated, the amount of work would be enormous. A better way, not as reliable but much more flexible, is to approach the problem using computer models.

2. THE BUILDING

The object of the computational examination is a single family house with two floors and a steep ridge roof. It is not a real, existing building, rather an imaginary one to be used as input data for the calculations. It does, however, represent a common type of house and its leakage characteristics can be fixed on certain levels for calculation purposes. Both floors have five rooms and the floors are connected by stairs. The total floor area of the living space is 140 m². No description of the ventila-

tion ductwork is included because it is assumed that in an emergency situation the ventilation is cut off and the ducts are sealed.

For the air infiltration calculations 80% of the envelope leakage area was distributed proportional to the length of the joints. The remaining 20% was placed in the floor and the ceiling to represent pipe and duct passages. The cracks in the building shell had a flow exponent value of 0.65 [4,5,6]. Four different airtightness levels were used for the whole building. The n_{50} value varied from 1 1/h to 15 1/h, while the distribution of the leakage area and the flow coefficients remained unchanged. The flow coefficients for each level were adjusted using a computational 50 Pa pressurization. The pressure coefficients of the building facades were in situ measured values [7].

For the contaminant transport calculations the building was divided into ten zones. Each room was one zone. The indoor air temperatures of the zones were simply chosen according to the experience gained from measurements in similar situations [8,9]. The temperature difference between adjacent zones, which is the crucial parameter from the viewpoint of the circulating air flows through the open doors and thus the contaminant transport, was chosen to be 0.1 °C. The mean indoor air temperature was 21.0 °C.

3. COMPUTING TOOLS

To calculate the infiltration, exfiltration and internal net air flows, the multizone simulation program MOVECOMP [10] was used. The input data contains a description of the leakage characteristics of the building, the pressure coefficients, the indoor and outdoor air temperatures and the wind speed. The mass balance equations of the system nodes is the basis of the solution. As an output the mass flow rates through the flow paths and the pressures of the nodes are given.

The concentration histories and doses in various zones inside the building were calculated using a computer code MULTIC [11] developed especially for this purpose. The calculation is based on the conservation of mass of the contaminant in the zones. The mixing of the contaminant in each zone is assumed to be complete and instantaneous. The circulating air flows between adjacent zones are calculated using a simple analytical procedure [12]. Some validation of the code has been done [8,9] and it shows that generally the results are satisfactory and the performance of the program can be considered sufficient for the purpose.

4. WEATHER DATA

The most important weather parameters affecting the pressure distribu-

tion and the infiltration and exfiltration flows of a building are the outdoor air temperature and the wind speed and direction. The mean two-dimensional frequency distributions of the temperature and the speed values measured in Finland during the years 1961-1980 [13] were used as input data for the calculations. The wind speed was reduced with a coefficient of 0.5 [4,14] to take the effect of the terrain into account.

5. CONCEPTS

The relevant quantity from the health point of view is the dose, which is the integral of concentration over time. The concentrations and the doses in different zones grow at different speeds. The mean dose in the building is defined as the arithmetic mean of the doses in all zones. Further, the concentrations and doses depend on the concentration level outside. Dividing the indoor dose by the outdoor dose gives the relative dose, which does not depend on the outdoor concentration level. Performing both the operations gives the relative mean dose at the moment t :

$$\langle D^*(t) \rangle = \frac{\frac{1}{N} \sum_{i=1}^N \left[\int_0^t C_i(t') dt' \right]}{\int_0^t C_{out}(t') dt'} \quad (1)$$

where N is the number of zones in the building, $C_i(t)$ is the concentration in zone i at moment t , t' is a dummy variable of integration and $C_{out}(t)$ is the outdoor concentration. This relative mean dose is a very central quantity in the presentation of the computed results.

The two-dimensional frequency distribution of the outdoor temperature and wind speed, which was used as input data, contains approximately 200 pairs of values for a one-year period. To be able to present the results of the calculations in a compact form, a statistical approach has to be utilized. The cumulative frequency of the computed relative mean dose values $F(\langle D^*(t) \rangle)$ is the quantity used in this context.

6. RESULTS

An example of the cumulative frequencies of the relative mean dose is presented in Fig.1. Here the location by which the weather data is determined is Helsinki, Finland. The period for the weather data is one year. All inner doors are wide open. Four different levels of air tightness and five different exposure times $t=1h, 3h, 6h, 12h$ and $24h$ were

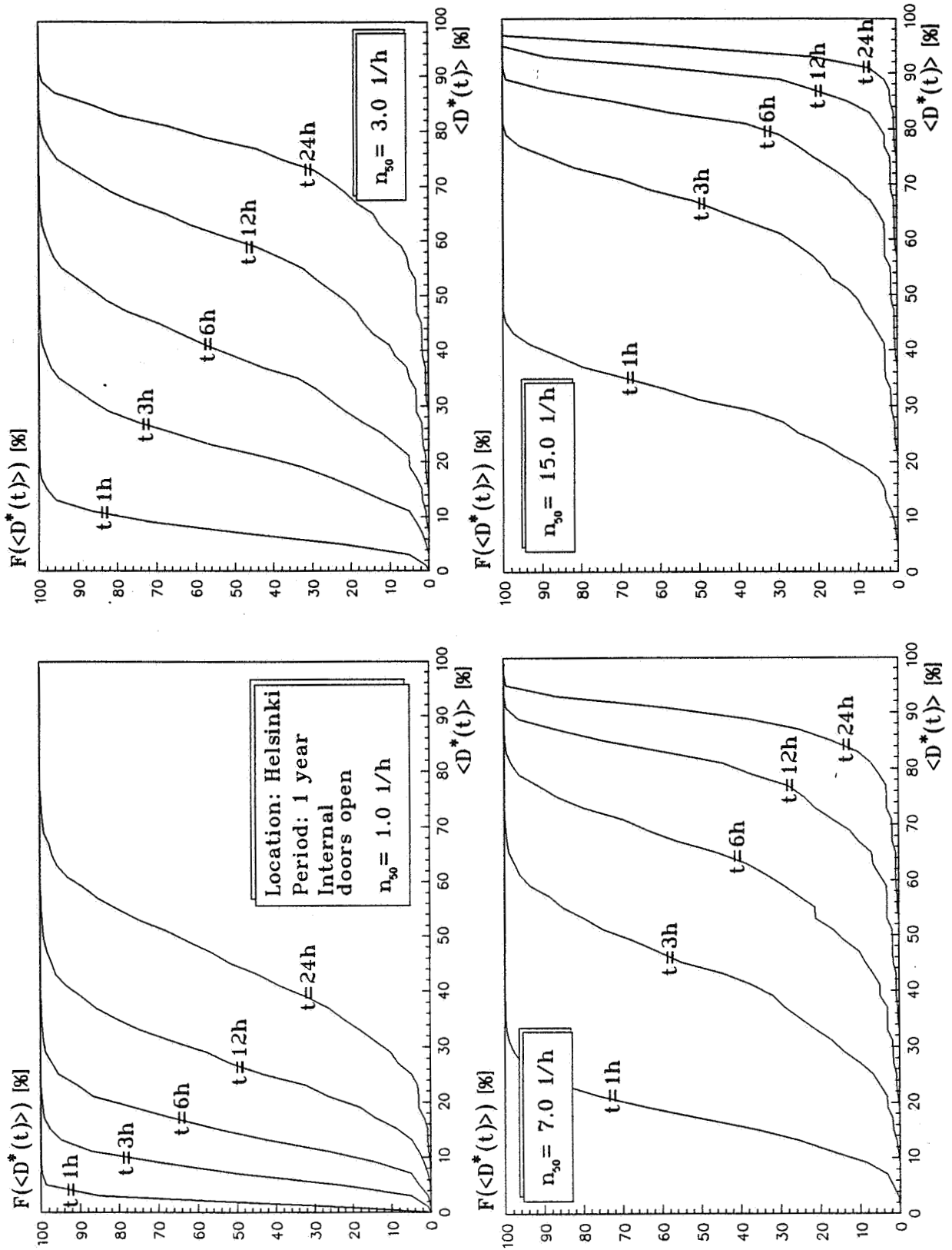


Fig.1 The cumulative frequencies of the relative mean dose.

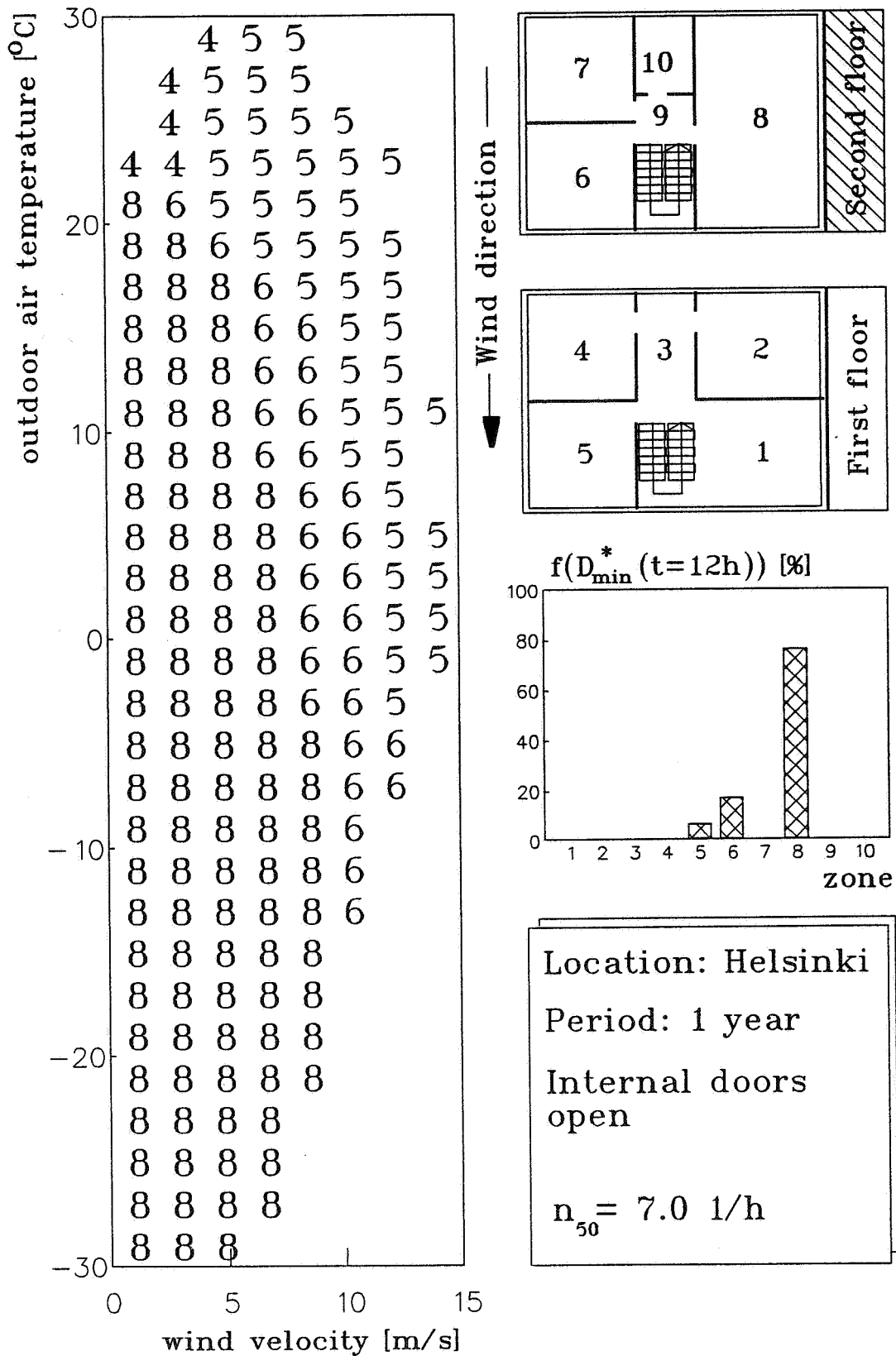


Fig.2 The location of the minimum dose, an example.

used. The cumulative frequency can be interpreted as the probability when the relative mean dose does not exceed the value on the abscissa. If the period is not one year but e.g. January, the frequency curves shift to the right because the temperature difference between indoors and outdoors is larger.

The occupants, when sheltering indoors, should try to minimize the dose by moving into the zone where the lowest concentration occurs. Here, besides the outdoor air temperature and wind speed, the direction of the wind and the status of the inner doors are also of importance. The tightness of the building, on the other hand, does not play an important role in this context. Fig.2 gives an example of the location of the minimum dose values after 12 hours' exposure. A more thorough presentation of the results is given in the reference [15].

7. CONCLUSIONS

From the viewpoint of sheltering, the tightness of the building holds a key position. In a leaky building, depending on the exposure time, the doses are from two to fifteen times as much as in a tight building. By closing the inner doors and choosing the correct location inside the building, the occupant can decrease the dose in favourable conditions by 50% compared with the mean value. This does, however, require knowledge of the local wind direction.

REFERENCES

- 1 Nylund P.O., Spread of gas in buildings exposed to poisonous outdoor air. ASHRAE Transactions **93**, Part 1, 1394-1407, 1987.
- 2 Trepte L., Ventilation strategies in the case of polluted outdoor situations. The Proceedings of the 9th AIVC Conference, Gent, Belgium, 63-79, 1988.
- 3 Wilson D.J., Zelt B.W., The influence of non-linear human response to toxic gases on the protection afforded by sheltering-in-place. OECD/UNEP Workshop on Emergency Preparedness and Response, Boston, Massachusetts, May 7-10, 1990.
- 4 Liddament M., W., Air infiltration calculation techniques - An applications guide. Air Infiltration and Ventilation Centre, 1986.
- 5 Gustén J., Wind pressures on low-rise buildings. Chalmers

University of Technology, Division of Structural Design, Publication 1989:2, Gothenburg 1989.

- 6 Blomsterberg Å., Ventilation and airtightness in low-rise residential buildings. Swedish Council for Building Research, Document D10:1990, Stockholm 1990.
- 7 Luoma M., Marjamäki P., The pressure coefficients of the test houses. Technical Research Centre of Finland, Research report 691, Espoo 1987. (In Finnish with English abstract)
- 8 Sirén K.E., A procedure for calculating concentration histories in dwellings. *Building and Environment* **23**, No.2, 103-114, 1988.
- 9 Sirén K.E., The estimation of concentration histories in dwellings in unsteady conditions. Roomvent'90, International Conference in Oslo, June 13.-15. 1990.
- 10 Herrlin M., A multizone infiltration and ventilation simulation program. *Air Infiltration Review* **9**, No.3, 3-5, 1988.
- 11 Sirén K., A computer program to calculate the concentration histories and some air quality related quantities in a multi-chamber system. Helsinki University of Technology, Institute of Energy Engineering, Report 18, Espoo 1986.
- 12 Sirén K., The mixing of air between adjacent rooms in dwellings. Papers of Room Vent-87, Session 4b, Stockholm, Sweden, 10.-12. June 1987.
- 13 Heino R., Hellsten E., Climatological statistics in Finland 1961-1980. The Finnish Meteorological Institute, Supplement to the meteorological yearbook of Finland **80**, part 1a, 1980.
- 14 ASHRAE Handbook of Fundamentals 1989, Chapter 14, Airflow around buildings.
- 15 Sirén K., A computational approach to the penetration of gaseous pollutants into buildings, part I: Single family house. Helsinki University of Technology, Institute of Energy Engineering, Report 45, Espoo 1992.

**Ventilation for Energy Efficiency and Optimum
Indoor Air Quality
13th AIVC Conference, Nice, France
15-18 September 1992**

Poster 19

**The Composition and Location of Dust Settled in
Supply Air Ducts.**

P. Pasanen^{*}, A. Nevalainen^{}, J. Ruuskanen^{*}, P.
Kalliokoski^{*}**

*** University of Kuopio, Department of
Environmental Sciences, P O Box 1627, SF-70211
Kuopio, Finland**

**** National Public Health Institute, Division of
Environmental Health, P O Box 95, SF-70701
Kuopio, Finland**

ABSTRACT

The amounts, quality and factors affecting of dust accumulation in supply air ducts of eight nonindustrial buildings were studied. The average of surface density of dust settled in supply air ducts was 10.6 g/m^2 and the average of yearly accumulation rate was $3.5 \text{ g/m}^2\cdot\text{year}$. The dust contained 82% of inorganic material, which agrees well with the composition of outdoor air dust in down town areas. In straight air duct the surface density of settled dust decreased as a function of distance from the air handling unit (AHU). The dust was mainly settled on the bottom of the duct and captured by the residues of lubricant oil used in manufacturing of ducts. In some cases soil debris was settled during the building construction period. The floor of the building did not affect the amount of settled dust. Fungal genera was similar to found in outdoor air and microbial growth in the air ducts was not observed in this study. The proportion of pollen grains was 70 mg/g of dust and it varied widely according to plants in surrounding environment. The results show that leakages between filter cassette and assembly frame were common in AHU of nonindustrial buildings.

1 INTRODUCTION

Outdoor air consists always suspended particles of which concentration varies widely even locally. Particulate impurities shall be removed from outdoor air before leading the air to the other parts of air handling unit (AHU). Filtration efficiency of air filters used in nonindustrial buildings is not good enough to prevent all the particles to pass through to heat exchangers, heat recovery unit and other components. This allows dust accumulation to inner surfaces of ventilation ducts. However, the production of high quality supply air provides a clean and odourless ventilation system. Impurities in the ventilation system decrease quality of supply air leading to dissatisfaction to indoor air quality or even health symptoms of the occupants. In several studies the building related illness is connected to the microbial growth in dirty ventilation system (1,2,3). If ventilation system is unclean and stuffy, maintenance of high indoor air quality demands higher ventilation rates that increase energy costs. On the other hand, the saving in filtration and maintenance costs will increase the costs of purifying the ventilation system.

The first purpose of our work was to determine amounts of dust accumulated in different parts of supply air ductwork in nonindustrial building. The other purpose also was to clarify the composition of the dust for evaluation the origin of dust.

2 MATERIAL AND METHODS

2.1 Research objects

Eight supply air duct systems in six mechanically ventilated office buildings were chosen for the study. Four of the ventilation systems were provided with recirculation air (objects 1-4). The maximum proportions of the recirculated air were from 39 to 68% of the total air flow and usually recirculation was used when temperature of the ambient air decreased below -10°C . The age of the ventilation systems varied from 4 to 31 years. In the object number 5 (Table 1) the supply air ducts were partly cleaned with dry brush method three months before the sampling. Two of the objects, three and four, were equipped with humidifiers; during the heating season it was used yearly in object 3 and only in the first year of building in the object 4.

Table 1. Descriptions of the ventilation systems studied.

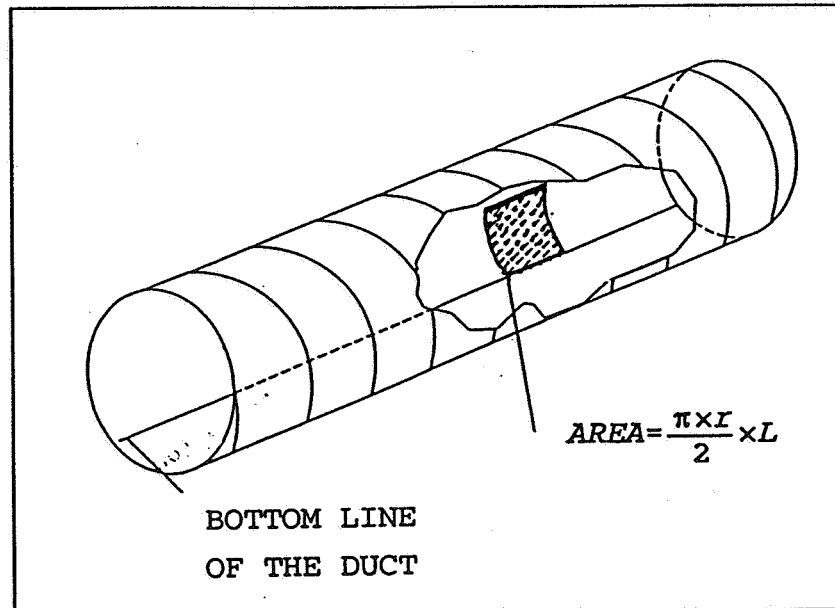
No	Age of building years	Age of duct years	Air flow capacity (m^3/s)	Filter change interval (months)	Filter efficiency (EU)
1	7	7	2.8	6	7
2	7	7	2.7	6	7
3	4	4	2.7	12	5
4	14	14	0.9	6	5
5	67	4	1.7	4	6
6	31	31	2.7	6	6
7	31	31	2.6	6	6
8	51	4	2.3	7	5

2.2 Sampling

A small amount of particles in supply air stream are settled on the bottom of an air duct. In a spherical duct, particles are mainly settled down on the surface which is rejected below the horizontal cross section. In a rectangular duct almost all of settled dust is settled on the bottom of a duct. For standardization of the sampling area to ducts with various diameters of spherical ducts dust samples were collected from an area which is rejected between the bottom line and the line on the widest level of the duct. The length (L) of sample area depended upon the limited space or on the amount of dust (Figure 1).

In rectangular duct the sample was collected from the bottom of the duct. The dust settled on the surface of the duct was loosened by crosswise movements of plastic nozzle as long as the galvanized steel seemed to be clean. The ventilation was turned off during the sampling.

Figure 1.
A schematic picture of the standardized sampling area in a spherical duct. L is the length of the sampling area.



For studying the behaviour of the dust in air ducts the samples were collected at the identical sites in different floors of the building. Both the vertical and horizontal distances were measured. The air flow rate in the sampling point was calculated from the information of the measuring data.

2.3 Analysis

Surface density (g/m^2) and yearly accumulation rate ($\text{g}/\text{m}^2 \cdot \text{year}$) of dust accumulated on the inner surface of supply air duct were determined. For comparison outdoor air dust sample was collected on EU7 classified ventilation filter during nine months. The proportion of the inorganic material of dust was determined as annealing lost by annealing the dried (105°C) sample at 550°C . The material loss indicates the proportion of organic and inorganic carbon (soot) particles.

The amount of different types of pollen were determined by using Bürker's method (4): A homogenized dust sample was divided to two parallel 20 mg portions which were mixed with 1 ml 20% Gelvatol mounting liquid (5). The pollen grains were counted by light microscope. Different types of pollen were divided to four classes according their mass: *Picea* 111 ng, *Pinus* 37 ng, *Betula* 1.4 ng and *Poaceae* c. 20 ng (6).

Viable fungal spore counts and bacteria in the dust were determined by cultivation method on malt extract agar and on trypton-glucose-yeast extract agar, respectively.

3 RESULTS AND DISCUSSION

The average of surface density was 10.6 g/m² (n=44, ranged 1.2 to 58.3 g/m²). The yearly accumulation rate of dust was 3.5 g/m²*year (1.2-8.3 g/m²*year). The yearly accumulation had a slight negative correlation with both horizontal and vertical distances between sampling site and air handling unit. The decrease in the amount of settled dust was observed especially in the main air duct on the top, at the same floor with AHU. This was observed also in our previous study when surface densities along the main air duct were measured and the AHU consisted coarse (EU2) filters. Any single factor, as horizontal or vertical distances from AHU, the height of the air intake from ground level or air flow rate measured in the sampling site had no statistically significant influence on the dust accumulation rate on the duct surface. The average of surface density of dust was about twice and the yearly accumulation rate five times higher than observed in the Danish study, respectively (7).

The proportion of inorganic material in dust was 82%. This agrees well with the result of our previous study, where the proportion was 80% (8). The corresponding proportion of dust sample was 81% collected in the down town area. The results showed that the dust accumulated in ventilation systems was originated from outdoor air which may indicate frame leakages between the filter cassette and assembly frame. The frame leakages of air conditioning filters is observed to be common particularly AHU with coarse filters (9). Soil debris during building construction period was observed in ducts of few objects.

In all randomly selected objects were EU5 classified or more efficient air filters therefore the effect of filter efficiency to dustiness of air ducts could not be examined regard to filtering efficiency. In our previous studies we found that filtration efficiency affected dirtiness of ducts; the coarser the filter more dust accumulated. The differences in accumulated dust are more clearly seen between the coarse filters (EU2-EU4) because of the higher differences in filtering efficiency (by weighting test). The relative dust accumulation into straight air duct by using filters with different efficiencies is presented in Figure 2. The results were calculated to the atmospheric aerosols and both the sedimentation and diffusion losses are taken account of calculation. Filtration efficiency has a significant effect on dust accumulation in supply air ducts. For example, dust accumulation rate into ventilation ducts equipped with EU7 classified filters is about three times slower than into ducts which are equipped with EU3 filters.

The average proportion of total pollen was 71 mg/g, of which about 90% was originated from coniferous trees (*Pinus*, *Picea*). Plants in the surrounding environment of the building affect the composition of pollen found in the ventilation ducts. The objects studied were equipped with fine filters, filter classification EU5 or better, which should be able to separate particles sized as large as analyzed pollen grains were, over 10 μ m. It is obvious that in the systems studied there have been or had been frame leakages or ventilation was used periodically without filters.

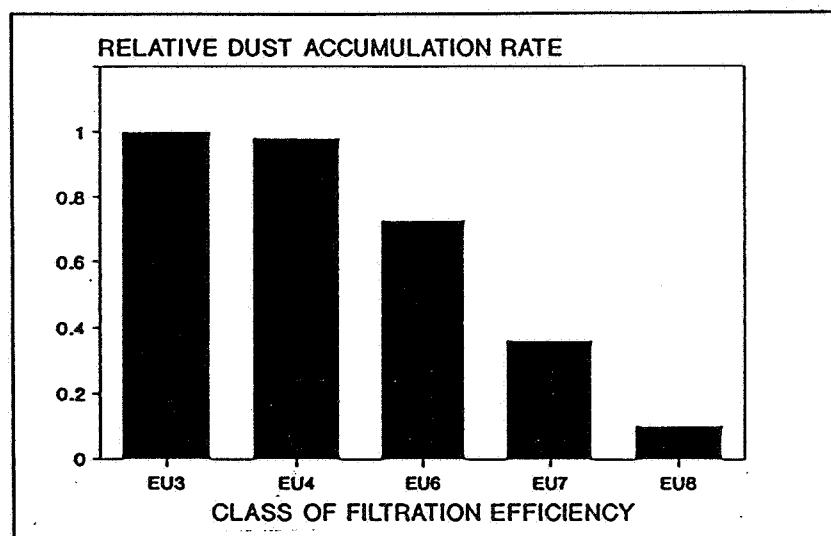


Figure 2.
Relative rate
of dust
accumulation
in supply air
ducts by using
filters with
different
filtration
efficiency.

The average counts of viable fungal spores in the dust of air ducts was moderate low, 990 CFU/g (range 180-2340 CFU/g). That means about one spore per square centimetre. The result agree well with spore counts, obtained with similar method, in Danish study, 1100-1200 cfu/g (7). The fungal genera found in the dust was similar to outdoor air genera in Finland (10). This indicates that fungal growth has not occurred inside the ventilation system. The average counts of viable bacteria in the dust was 1980 CFU/g (from detection limit to 10000 CFU/g). For the sake of comparison the bacteria count levels found in house dust has ranged from 10⁴ to 10¹⁰ CFU/g. Occupants and pets are the major bacterial sources in house dust (11).

4 CONCLUSIONS

The amounts of settled dust on supply air ducts were low. Thus the dust has no significant effects on air flow rates in supply air ducts. The dust found in the ducts had comparable composition with outdoor air dust. Relatively large amounts of pollen grains in the air ducts indicate that frame

leakages between filter cassette and assembly frame is obvious. Both the fungal spore and bacteria count levels were moderate low compared with the levels in other indoor dust samples. The genera of fungal spores were similar those to found in outdoor air. It supports the conclusion about the frame leakages. In properly maintained HVAC system the settled dust on supply air ducts has an unremarkable significance to indoor air quality. If surfaces are moistened due to water condensation or by other reason the dust accumulated inside HVAC system offers an opportunity to microbial growth, and, thus, indoor air problems will arise.

No significant differences was observed between the dust accumulation levels in supply air ducts in different floors of the building. The quality of a particulate air filter had a significant effect on an accumulation rate of debris inside HVAC system. The coarser the filter is the more debris is accumulated in main air ducts.

ACKNOWLEDGEMENTS

This work was funded by a grant by of Ministry of Environment of Finland. We thank Jussi Teijonsalo from Helsinki University of Technology, HVAC-Laboratory for his flow rate measurements in the field. We tank The Finnish Aerobiology Group for the counting of pollen grains.

REFERENCES

1. MOREY, P. and SHATTUCK, D.
"Role of ventilation in the causation of building-associated illness"
Problem buildings: Building Associated Illness and Sick Building Syndrome. 1989, Philadelphia, USA, Hanley and Belfus Inc. pp625-643.
2. MOREY, P. and WILLIAMS, C.
"Is porous insulation inside an HVAC system compatible with a healthy building"
Proceedings of Healthy Buildings, ASHRAE, USA, 1991, pp128-135.
3. TAMBLYN, R. et al.
"A comparison of two methods of evaluating the relationship between fungal spores and respiratory symptoms among office workers in mechanically ventilated buildings"
Proceedings of Healthy Buildings, ASHRAE, USA, 1991, pp136-141.
4. BAKER, F.J., SILVERTON, R.E. and LUCKCOCK E.D.
"Introduction to Medical Laboratory Technology"
1955, London. Butterworth & Co. p330.

5. KÄPYLÄ, M.
"Adhesives and mounting media aerobiological sampling"
Grana, 28, 1989, pp215-218.
6. STANLEY, R.G. AND LINSKENS, H.F.
"Pollen: biology, biochemistry, and management"
1974, Berlin, Heidelberg, Germany. Springer-Verlag.
p307.
7. VALBJØRN, O., NIELSEN, J.B., GRAVESEN S. and MØLHAVE, L.
"Dust in ventilation ducts"
Proceedings of the fifth Indoor Air Quality and Climate,
3, 1990, pp361-364.
8. LAATIKAINEN, T., PASANEN, P., KORHONEN, L., NEVALAINEN
A. and RUUSKANEN, J.
"Methods for Evaluating Dust Accumulation in Ventilation
Ducts"
Proceedings of Healthy Buildings, ASHRAE, USA, 1991,
pp379-382.
9. PASANEN, P. et al.
"Criteria for changing ventilation filters"
Proceedings of Healthy Buildings, ASHRAE, USA, 1991,
pp383-385.
10. PASANEN, A-L., REPONEN, T., KALLIOKOSKI, P. and
NEVALAINEN, A.
"Seasonal variation of fungal spore levels in indoor and
outdoor air in the subarctic climate"
Proceedings of the fifth Indoor Air Quality and Climate,
2, 1990, pp39-44.
11. van BRONSWIJK, J.E.M.H.
"House dust biology for allergists, acarologists and
mycologists"
1981, Zoelmond, The Netherlands. NIB Publishers, p316.

**Ventilation for Energy Efficiency and Optimum
Indoor Air Quality
13th AIVC Conference, Nice, France
15-18 September 1992**

Poster 18

**Odour Threshold of Kitchen Exhaust Air During
Typical Cooking Situations In A Dwelling.**

M. Luoma and K. Kovanen

**Technical Research Centre of Finland (VTT),
Laboratory of Heating & Ventilation, P O Box 206
(Lämpömiehenkuja 3), SF-02151 Espoo, Finland.**

ABSTRACT

The odour threshold value of kitchen exhaust air was experimentally determined during typical cooking situations and tobacco smoking in a dwelling. During cooking, air from the exhaust duct was taken into a sample bag. The odour threshold concentrations of the samples were determined by sensory evaluation using olfactometer and untrained odour panel. Experiments were made both in laboratory and field settings.

The largest odour threshold concentration of 168 o.u./m³ was determined during the frying of herring. In accordance with the definition, here 50 % of the panellists do not observe any odour when the sample gas is diluted 168 times. Thus, the highest permitted exhaust air proportion in supply air would be 0.6 %. The results of the odour tests are used in a study, where the prerequisites for the extraction of exhaust air through the outer wall of multi-storey residential buildings are examined.

1. INTRODUCTION

Within the framework of the LVIS 2000 research programme, in the project "Ventilation systems for the dwellings of the future", the alternatives for ducting away the exhaust air of ventilation systems for individual dwellings in apartment buildings were examined /1/. It was noted that by extracting air directly to an outer wall many of the problems at present occurring are avoided, like disturbances in pressure differences and air flows caused by thermal forces. The space requirement for ducting is reduced as the exhaust ducts do not need to lead to the roof from within the building. The drawback with extraction through an outer wall is the possible migration of exhaust air odours to the open windows or supply air terminal devices in the wall, and via these into the apartment.

A project has been initiated with funding from the Technology Development Centre (TEKES) where the extraction of exhaust air through the outer wall is examined with calculations, as well as wind-tunnel and full-scale testing. Knowledge of the odour threshold for exhaust air is necessary in assessing the exhaust air dilution ratios at the building's outer wall and thus in the supply air based on theory and measurement. As the fumes produced in cooking generally create the odour found in the exhaust air of apartments, it was decided to examine the odour threshold values of exhaust air during the cooking of common foods when strong odours are produced.

2. LITERATURE SURVEY

The literature survey looked for research projects where common or permitted exhaust air concentrations in supply air were presented. Table 1 shows the literature references found.

Permitted leakage values from the outlet side to the supply side for heat recovery equipment were found in the literature. The permitted proportions were 3-10 %.

The re-entry of exhaust air into supply air in an apartment-based ventilation system has been investigated using tracer gas in test houses in Kuopio, Finland. The proportions measured ranged from 0 to 2.3 %. On occasions, the amount of re-entry rose to almost 6 per cent.

However, no fully comparable material concerning odour threshold values nor target values for exhaust air proportions were found from the literature.

3. SUBJECTS OF RESEARCH

The cooking situations examined were boiling cabbage, frying onion, making pancakes and frying herring, in addition to smoking. The rate of extraction of the exhaust air flow from the kitchen was 20 dm³/s, which corresponds to present official regulations /2/. Experiments were carried out both with test equipment constructed in the laboratory (Figure 1) and under field conditions. The construction of the test equipment is such that it efficiently draws in fumes from food being prepared.

4. RESEARCH METHODS

In the performance of the tests, the aim was to simulate the cooking situations so that they corresponded to reality as closely as possible. In frying, the food was put into a hot frying-pan containing cooking oil. In boiling, the food was placed in boiling water.

During cooking, air from the exhaust duct was taken into a sample bag. Five samples were taken in each food-preparation situation. The first sample was taken from the exhaust duct before the start of cooking to determine the background concentration. The next sample was taken immediately after the addition of food. The last sample was taken after the food had been prepared. The sample bags were delivered to the Chemical Laboratory of the Technical Research Centre of Finland for the determination of the odour concentrations. The volume of the sample bag was around 20 dm³, while the filling of the sample bag took around one minute.

During the smoking test, the test person smoked continuously. To ensure the flow of cigarette fumes into the kitchen hood, a sheet of plastic film was placed above the smoker.

The odour threshold concentrations of the samples were determined by sensory evaluation using the Ströhlein olfactometer according to the German standard VDI 3881 /3/. The olfactometer creates increasing concentrations from neutral air and the sample gas until the test person acting as the detector can distinguish an odour in the sample gas flow. On the basis of the test persons' findings, the olfactometer calculates the odour concentration of the sample in the form of odour units/m³ (o.u./m³). The odour concentration refers to the number of times the sample gas flow must be diluted for 50 % of the odour panel members not to observe odour in the sample gas flow.

The acceptability of an odour was determined by asking members of the odour panel how they perceived the odour at the moment it was detected. The odour panel comprised 6-8 persons, all members of staff at the VTT Chemical Laboratory.

5. RESULTS AND EXAMINATION OF RESULTS

5.1 Odour threshold values of exhaust air

The odour threshold values determined from the air samples taken during various cooking situations are presented in Figure 2. The temperature of the exhaust air was 24-29 °C.

The panel members' assessments of odour acceptability are shown in Table 2. Some of the panellists considered the strong odour values found during the frying of onion to be acceptable, while the strong odour values found during the cooking of pancakes and herring were generally considered unacceptable. Acceptability is a subjective assessment.

The largest odour threshold concentration of 168 o.u./m³ was determined during the frying of herring. In accordance with the definition, here 50 % of the panellists do not observe any odour when the sample gas is diluted 168 times. Correspondingly, 84 % of panellists did not note any odour when the same sample gas flow was diluted 219 times.

The herring frying test was repeated in the kitchen of a single-family house. The air sample was taken from the kitchen's exhaust duct. The odour threshold concentration of the air sample was smaller than that found during the corresponding laboratory test (Table 3). This difference was due to the kitchen hood in the single-family house kitchen not efficiently extracting the food fumes, part of these fumes migrating to elsewhere in the kitchen.

The test in the single-family house indicated that increasing the exhaust air flow to 45 dm³/s did not have a significant effect on the odour concentration of the exhaust air.

5.2 Permissible proportion of exhaust air in supply air

For each food preparation situation, the largest odour threshold concentration was chosen from the results to represent the situation in question. From these results, the largest permitted proportion of exhaust air in supply air was calculated from these values so that no odour was discernable in the supply air. The exhaust-air proportion is the reciprocal of the odour threshold concentration. The results are shown in Table 4.

The largest permitted exhaust air proportions in the supply air according to Table 4 are between 0.6 and 2.3 % depending on the quality of the exhaust air. Here it has been assumed that the exhaust air of the apartment does not contain any odour other than that caused by cooking.

5.3 Dilution of exhaust air on the outer wall of the building

The dilution of exhaust air on the outer wall of a building was investigated initially with full-scale tests in one office building. Tracer gas was fed from one point at the building's facade, and tracer concentrations were measured at eight points in the same facade to determine the dilution ratio. An aim was to locate the measurement points at the worst places according to smoke observations. A total of five situations were investigated.

The highest instantaneous value for the exhaust air proportions measured in different wind conditions was 1.6 %. According to the measurements, the local exhaust air concentration fluctuated rapidly and over a wide range according to the nature of the wind. Thus the concentration peaks were short-lived and from these the quality of the supply air cannot be considered measurable. The 2-minute mean values obtained for the exhaust air proportions were lower than the highest permitted exhaust air proportion found in the worst case of the odour tests (frying herring) of 0.6 % (the highest 2-minute mean was 0.5 %).

6. CONCLUSIONS

On the basis of the cooking tests performed, up to 0.6 % exhaust air can be permitted in supply air without food odour being observed in the supply air. The exhaust air proportions determined from full-scale tests in the wall of a building were generally lower (the highest instantaneous value being 1.6 % and the highest 2-minute mean value being 0.5 %). No fully comparable material on odour threshold concentrations nor on target values for exhaust air proportions were found from the literature.

REFERENCES

- /1/ Luoma, M. & Kohonen, R., Demand controlled ventilation systems for dwelling houses of the future. Technical Research Centre of Finland. LVIS-2000 Research Programme. Report 8. Espoo 1990. 103 s.
- /2/ National building code of Finland, Indoor climate and ventilation in buildings. Regulations and guidelines 1987. The Ministry of the Environment.
- /3/ Olfaktometrie, Geruchsschwellenbestimmung, Verein Deutscher Ingenieure, VDI 3881, May 1986.

TABLES

Table 1. Permissible proportion of exhaust air in supply air. Literature survey.

Proportion	Explanation	Reference
5 %	Leakage between supply and exhaust air streams in heat recovery not more than 5 %.	Canadian Standards Association, Residential Mechanical Ventilation Requirements.
3 %	If the carry-over exceeds 3 %, the pressure difference shall be determined before carrying out the efficiency tests.	CEN ENV 308:1991, Heat exchangers.
10 %	Leakage between supply and exhaust air streams may not exceed 10 %, when the pressure difference between exhaust and supply is 200 Pa.	Guidelines for type approval tests for heat recovery devices. 6.5.1983. Finland.
12...36 %	Infiltration between apartments at the pressure difference of 50 Pa, 3 apartments measured.	Levin, P. Air leakage between apartments, 9th AIVC Conference, Gent, 12-15.9.1988.
0...2,3 %	Re-entry from exhaust to supply air, short-term measurements in a test house.	Savolainen, T. etc., Neulamäki test houses: Ventilation and indoor air quality. University of Kuopio, Department of Environmental Sciences. Report 4/1988.

Table 2. Panel members' assessments of odour acceptability.

Frying onion	Odour concentration o.u./m ³	Acceptability		
		Yes	Do not know	No
1. Background	2	2	2	2
2. 0 min	28	2	2	2
3. 2 min	31	1	2	3
4. 5 min	34	2		4
5. 10 min	56	3		3

Making pancakes	Odour concentration o.u./m ³	Acceptability		
		Yes	Do not know	No
1. Background	0			
2. 0 min	28	3		3
3. 3 min	48	1	1	4
4. 6 min	107	2		4
5. 12 min	41	1		5

Frying herring	Odour concentration o.u./m ³	Acceptability		
		Yes	Do not know	No
1. Background	3		2	4
2. 0 min	48	1	1	4
3. 3 min	73	1	1	4
4. 6 min	72	2		4
5. 10 min	168			6

Table 3. Permissible proportion of exhaust air in supply air (frying herring).

Exhaust air flow	Test site	Odour concentration o.u./m ³	Permissible proportion %
20	Laboratory	168	0,6
20	Single-family home	54	1,9
45	Single-family home	43	2,3

Table 4. Permissible proportion of exhaust air in supply air (laboratory tests).

Cooking situation	Odour concentration (P50) max o.u./m ³	Permissible proportion $\frac{1}{(P50)_{max}} \cdot 100 \%$
Boiling cabbage	43	2,3
Frying onion	56	1,8
Making pancakes	107	0,9
Frying herring	168	0,6
Smoking	48	2,1

FIGURES

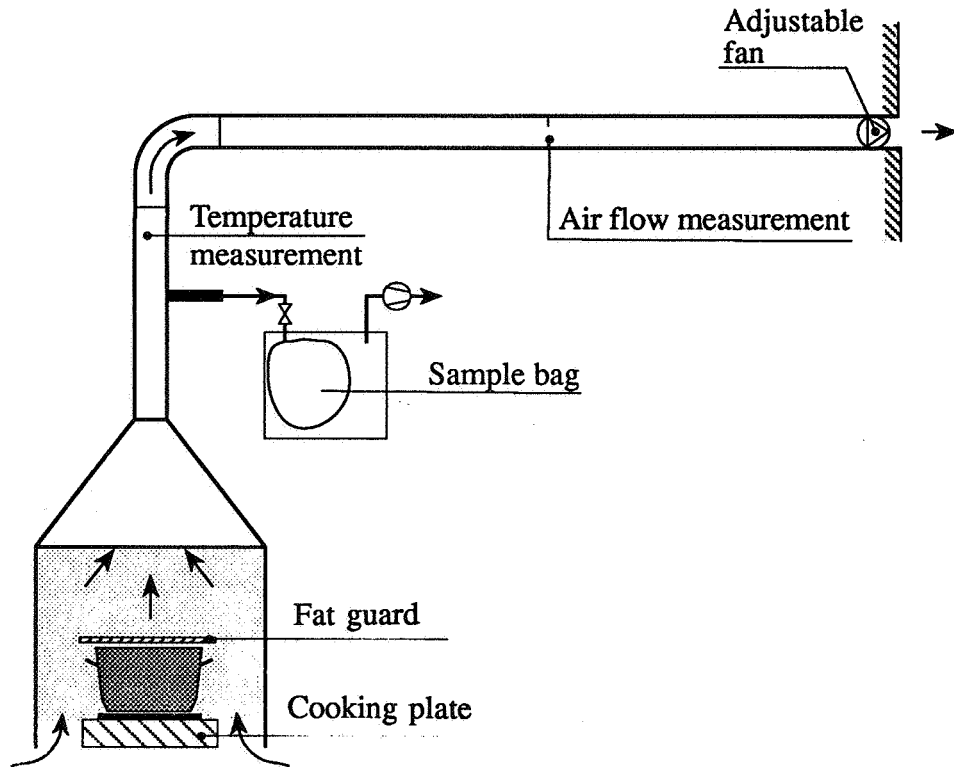


Figure 1. Arrangement for the laboratory tests.

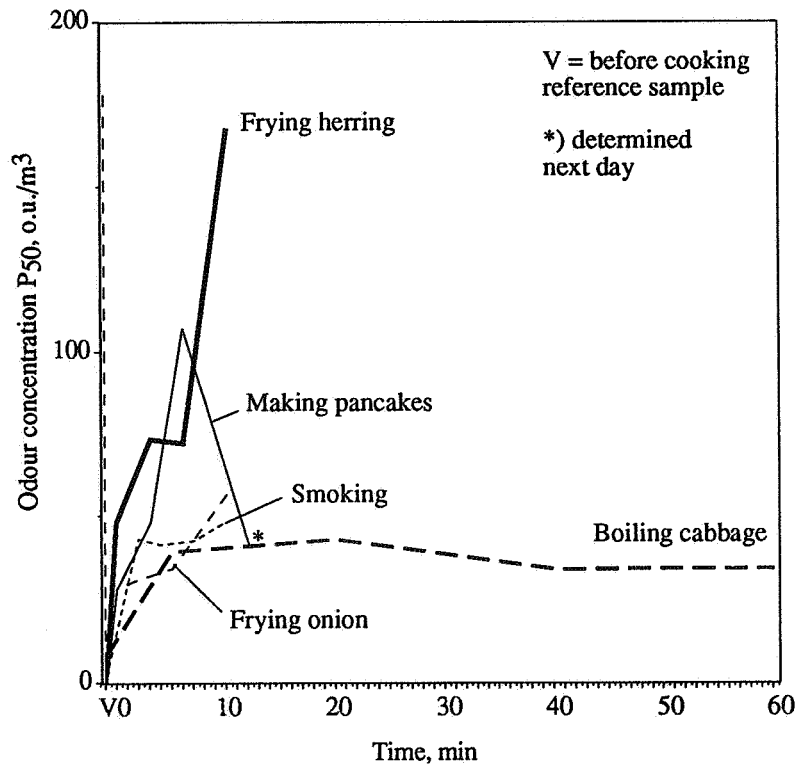


Figure 2. Odour threshold values of exhaust air during the cooking of common foods.

**Ventilation for Energy Efficiency and Optimum
Indoor Air Quality
13th AIVC Conference, Nice, France
15-18 September 1992**

Poster 17

**Humidity Controlled Exhaust Fan in a Natural
Ventilated Single Family House.**

L-G. Månsson^{*}, C-A. Boman^{}, B-M. Jonsson^{**}**

*** LGM Consult AB, Adler Salvius väg 87, S-146 53
Tullinge, Sweden**

**** National Swedish Institute for Building
Research, P O Box 785, S-801 29 Gävle, Sweden.**

Synopsis

A humidity controlled exhaust fan have been tested during the winter season 1991/92. The test have been carried out in a detached one storey house with a flat roof. The relative humidity (RH) have been measured in the following modes:

- * natural ventilation only
- * wall mounted fan, setpoint 70 % RH, and natural ventilation
- * fan in the exhaust duct, setpoint 70 % RH.

The relative humidity levels have been monitored in the shower room and in the other part of the dwelling. The temperatures have been measured in the exhaust duct and in four places in the dwelling.

It is concluded that a wall mounted fan can keep the relative humidity close to 50% RH, causes backdraught in the exhaust duct, and usually has to be switched off manually. A fan mounted in the exhaust duct gives a higher average RH than natural ventilation only.

Background

In Sweden as well as in many other countries attention has been paid to a too high indoor relative humidity (RH). The risks are:

- * House dust mites can grow if the RH is kept on a level over 55 % RH during longer periods, more than a month.
- * Mould groth in the shower-room or bathroom (wet rooms) if the RH is kept above 75 % RH. This gives a "safety factor" not to exceed 80 - 90 % RH at the surface in colder corners in the wet rooms.
- * Condensation on double glazed windows during wintertime causing higher maintenance cost and inconveniences.
- * The risk for interstitial condensation because of imperfectness in the water vapour barrier.

The moisture production in a dwelling is very much dependent on the occupants' activities. The number of people and their age may give an indication of the probability of having a high RH indoors. About 3/4 of all single family houses in Sweden have natural ventilation. Local exhaust is normally installed in the kitchen as a kitchen hood above the stove and only used when preparing food.

the shower-room. No bath in the tub takes place and there is a separate laundry-room.

As the air supply through leakage was not sufficient extra supply air devices were installed in the bedrooms and the living room. The devices are closable.

The fan installed starts or stops at the setpoints, which is said to be either at 55 or 70 % RH. The power is 15 W and with a capacity of 22.2 l/s (80 m³/h). The sensing element is a 1 mm thin triangular piece of wood (beech, *Fagus Silvatica*) glued on a copperplate. The water vapour absorbed in the wood gives a mechanical action and at the setpoint the fan is switched on.

From the beginning the intention was to test at both setpoints, but at the setpoint of 55 % RH the fan never stopped and caused too much noise. This mode was then excluded from the test. Even at 70 % RH the running time tended to be very long. To give the occupants the possibility to have a silent home a manual switch also was installed.

The tests have been carried out in the following modes:

1. Natural ventilation, as constructed from the beginning
2. The fan mounted in the exhaust duct, setpoint 70 % RH
3. The fan mounted on the inside of the external wall, setpoint 70 % RH, and the original natural ventilation.

Monitoring

An automatic monitoring system has been used in the house. The sampled values have been collected as hourly mean values. The indoor temperature is the mean value of four thermistor sensors located in four rooms, see Figure 1. The outdoor temperature is measured at a house 200 m away. The data collected is sent by the telephone net every working day to a central computer. The hourly values are the basis of the analysis.

The RH is monitored by capacitive sensors (Lee-Integer CH 15) located in the shower-room and in the kitchen, see Figure 1. The sensor located in the kitchen represents the average value of the house as it is central in the house, not directly affected by opened entrance doors, and not too close to the stove.

The measuring faults according to the manufacturers are estimated to be:

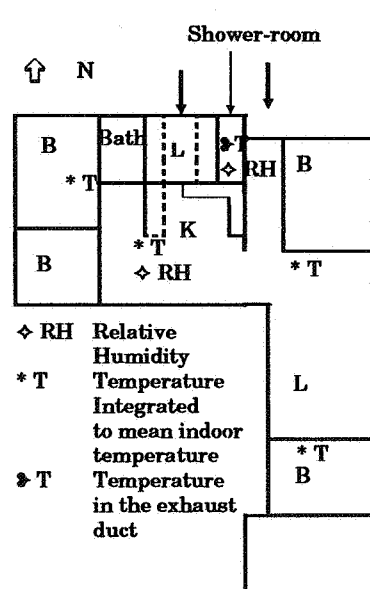
- * for measuring RH - ± 2 %
- * for measuring temperature - ± 0.2 %

The overall purpose with the project was to use electricity more efficient in single family houses heated with electrical radiant panels. About 1/4 of all the electricity used in Sweden is consumed in the 1.8 million single family houses. Saving electricity should not lead to indoor air quality problems. An acceptable level have to be maintained.

Test set up

The objective with this test of a RH controlled fan was to exhaust the air from the shower-room in order not to allow the warm moisture air to go back into the other parts of the dwelling.

The test house is situated in a suburb to Stockholm and selected in a group of 90 similar houses constructed 1972. In Figure 1 is given a short description of the studied house. In the main project this house together with five others were inspected and the insulation quality checked by thermography method, the air tightness and air change rate [h^{-1}] measured according to Swedish standard. The measured air change rate was 0.19 h^{-1} giving an air flow rate of about 17 l/s.



Living space 129 m²
 1-storey woodframe
 Flat roof
 Double glazed windows
 Natural ventilation with kitchen hood fan
 Air tightness n50 6.9 ach/h
 Air change rate:
 Test House 0.19 h^{-1}
 Mean for 6 houses 0.24 h^{-1}
 Range $0.19 - 0.30 \text{ h}^{-1}$
 The family has lived in the house since 1978.
 A 4 person - family
 Children: 2 girls 10 and 15 years old

Figure 1. Short description of the test house.

The family chosen were an ordinary with both parents working outside the home and two children in school 5 days a week. The husband is an engineer and the wife a teacher. All the body cleaning takes place in

Results

As the main interest was to keep the RH close to 50 % on a long term perspective and to avoid condensation on windows the results are given in mean values for weeks. In Table 1 can be seen that the RH in the kitchen always is higher than in the shower-room.

Table 1 Weekly mean RH

Mode	Shower-room RH	Kitchen RH %	Outdoors RH %
Natural ventilation	53	57	73
Fan in exhaust duct	59	60	88
Fan on wall + natural ventilation Dec	54	57	82
" Jan w 1	54	56	73
" w 2	49	55	66
" w 3	50	52	77

The winter season 1991/92 was very mild resulting in one of the mildest ever registered. The mean indoor temperature, about 22°C, is slightly above the Swedish single family home average which is 21°C. In Table 2 is given the temperatures as weekly mean values.

Table 2 Weekly mean temperatures (°C)

Mode	Exhaust duct from Shower-room	Mean room temp	Outdoors
Natural ventilation	22.4	22.0	+1.8
Fan in exhaust duct	--	21.4	+5.3
Fan on wall + natural ventilation Dec	21.5	22.4	+0.1
" Jan w 1	21.6	21.8	+0.5
" w 2	22.0	22.0	-0.8
" w 3	22.6	22.0	-1.2

During a period of 3 weeks there were 16 reliable indications on taking showers. If it was one person or more taking a shower is not possible to conclude, as the measurement gives hourly mean values. In addition there were 7 indications that may be a result of a very short shower giving a RH not higher than in the kitchen.

The indoor temperature range during a three week period is 21.5 - 22.3. This gives the opportunity to make the approximation and use the RH difference between the shower-room and the average in the house measured in the kitchen. In Figure 2 is shown the decay of the RH in those cases when only natural ventilation was used. As can be seen the time to reach normal level takes from 6 h to 10 h. It can be observed that when the fan in the duct is not in operation, the decay

period is longer than for the case with solely natural ventilation. From Figure 3 can be seen that if a fan is used the average RH-level in the house is reached within 2 h. With a fan in the duct the time is even less.

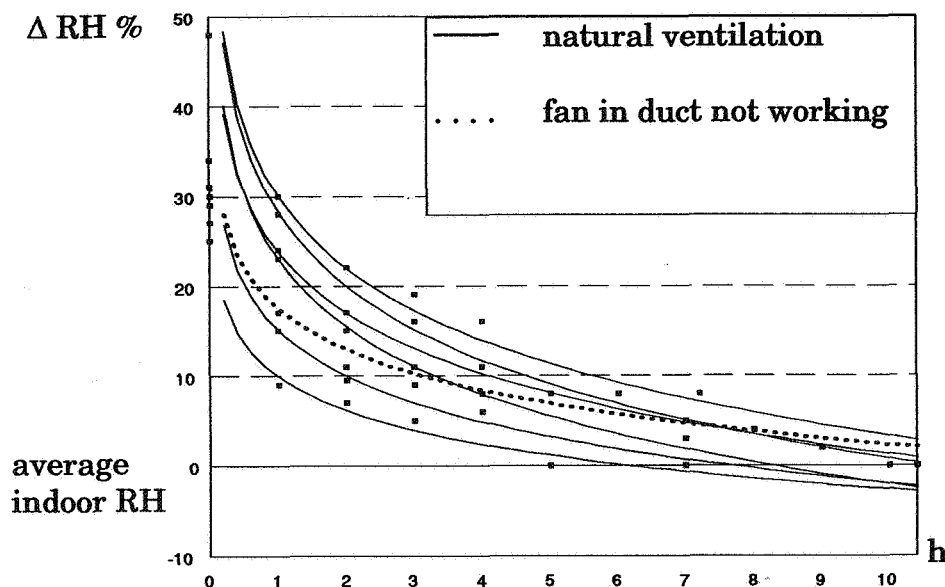


Figure 2. The decay of water vapour with natural ventilation

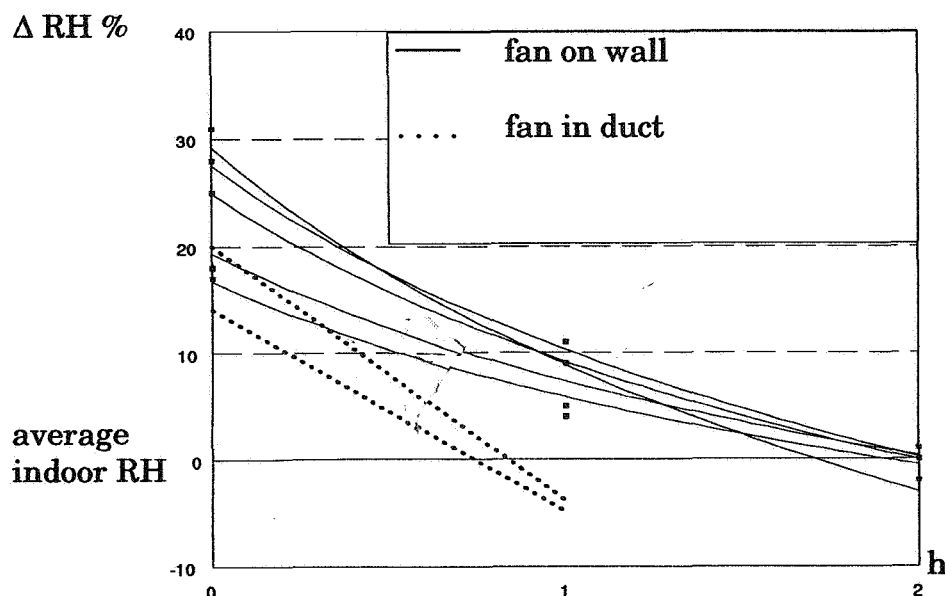


Figure 3. The decay of water vapour with a humidity controlled fan

When the fan is mounted on the wall there is a risk to perceive the cold air as a backdraught from the duct in the shower-room. However, this backdraught was not reported to be of any inconvenience at all to the occupants. The temperature drop measured was from a few °C to 10 °C or more, as can be seen in Table 3. This is of course dependent on the outdoor temperature and the running time.

Table 3. Examples of RH-differences between peak and mean values at different temperature drops in the exhaust duct and running time of the fan.

RH difference peak and mean Shower-Room	Fan operation time h	Temperature drop in exhaust duct °C	Decay from peak to 60 % RH, h	Outdoor temp °C
26	2	4	2	2.4
29	1	4	1	3.6
24	1	7	1	-1.3
36	3	14	3	-1.1
29	1	2	1	0.6
35	3	1	2	5.5
31	1	12	1	-0.3
24	1.5	11	2	1.5

In Figure 4 is given the water vapour content of the air in the kitchen, the shower-room, and outdoors during a period of three weeks. As can be seen the kitchen has the higher level during most of the time, but at the end of the period it is the same. This coincides with less use of the fan in the shower-room.

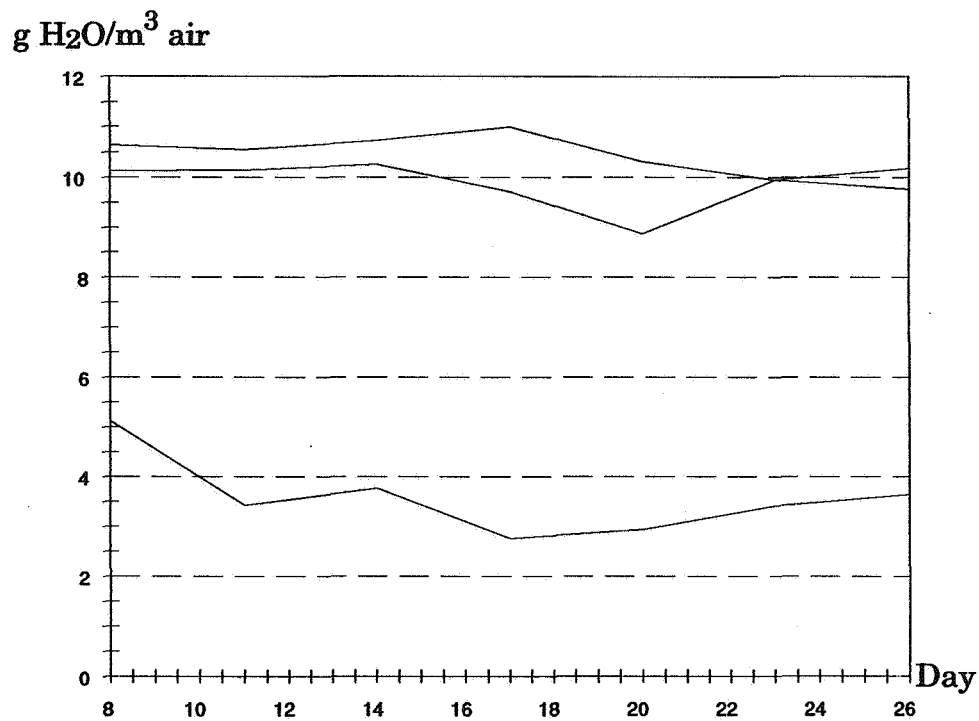
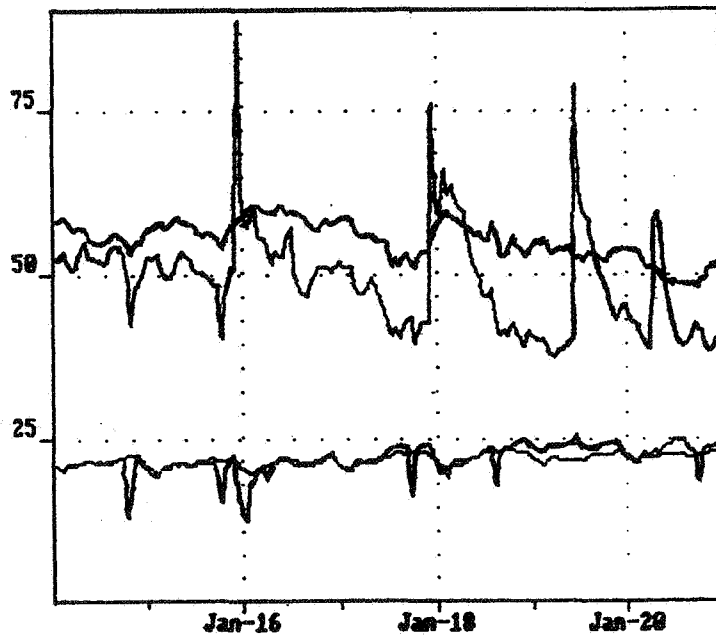


Figure 4. Water vapour content during a three week period with the fan mounted on the wall

In Figure 5 is given an example of the measured values during a week. It can be observed that there are shower-periods with and without the use off the fan in the wall.

RH %



Temperatures [°C]	
Indoors	21.9
Duct	22.0
Outdoors	-0.8
RH[%]	
Kitchen	52
Shower-room	49
Outdoors	77

Figure 5. Fan on wall, one-week-example of measured values on temperatures and RH

Discussion

When comparing the mean room temperature and the temperature in the duct from the shower-room, it is observed that sometimes the temperature is higher in the duct sometimes lower. When counting the peaks and the running times of the fan it can be concluded that the backdraught caused by the fan in operation decreases the temperature to be below the room average. It is also an indication of the use of the fan as it can be manually switched off. At weeks with lower RH-peaks and frequency of showering the use of the fan is lower giving a higher temperature in the duct.

When only natural ventilation is used the temperature in the exhaust duct seems to be slightly higher, less than 0.8 °C, compared to the mean room temperature. This may be caused by the slightly higher temperature in the shower-room and that the house is not airtight enough to get backdraught when using the kitchen hood.

The RH in the shower-room is always slightly lower than in the kitchen as an average during a period of more than a day. It is only with the case of a fan installed in the duct the RH goes up to the same level as for the kitchen. The level is also higher than for other cases during

wintertime. In the case with a fan in the duct the natural ventilation can not work, thus causing more humidity inconveniences than with solely natural ventilation.

When comparing Figures 2 and 3 can be seen that the time with high humidity is considerably cut down when using a fan. Even if the natural ventilation doesn't work when the wall mounted fan is in operation the stack effect begins again after the fan is switched off. This gives a very short decay period, thus making a lower risk for condensation and mould growth.

Even if the water vapour content in the air is higher than is wanted in order to avoid any growth at all of house dust mites, the RH-level is well below the range of 55-85 % RH when a greater population of house dust mites can be expected. To avoid it completely the water vapour content must be lower than 7.0 g water per kg dry air. The margin is not very big but it seems that RH is kept just below the critical level for growing house dust mites especially when it is kept at a dryer level during the two winter months February and March.

The temperature drop in the exhaust duct can be more than 10°C within an hour. This can occur even if the outdoor temperature is around zero. However, this has not caused any draft problem to the occupants.

As the main purpose was to get a better controlled indoor humidity in a longer perspective, a week for mould growth and a month for house dust mites, it was not necessary to have a sensor in the fan well calibrated and excellent accuracy. However, the sensor doesn't seem to have any good accuracy at all as it was impossible to use it at the set point of 55 % RH and that it stopped around 60 % RH at the set point of 70 % RH.

The temperature rises immediately after that the fan on wall has stopped. This implies that the natural ventilation works and that the RH is decreased to an average level of the house. In fact, a set point at the expected average RH may lead to a too low RH, thus wasting energy.

Conclusions

The installed fan mounted on the wall gives the occupants a tool to control the indoor environment with respect to RH. At a level of slightly above 50% RH the family perceive comfort. At this level there is no condensation on windows, rapid decrease of RH in the shower-room, the backdraught is not recognized, and the fan is easy to use.

The accuracy of the sensor in the fan is not very good and is the main reason why the lower set point of 55 % RH could not be used. But if the fan is mounted on wall it is not necessary to have the set point at

55 % RH because the natural ventilation can give this level even if the set point is chosen to be higher, at least at winter conditions. Which set point to be chosen is, however, dependent mainly on the temperature difference.

When the fan is installed in the duct the RH is slightly higher compared to natural ventilation and a fan on wall mounted application. The inconveniences were greater with the fan mounted in the duct than with natural ventilation.

The recommended solution is to have the fan mounted on the wall giving the occupants the best way to control the RH and allowing the natural ventilation to work when the fan is stopped.

Acknowledgments

The work have been funded by The Swedish Council for Building Research.

References

1. G. Hoffmann. House dust mites as vectors for human diseases. Proceedings from Luftqualität in Innenräumen edited by K. Aurand, B. Seifert, J. Wegner. ISBN 3-437-30376-7. (In German).
2. I. Andersen, J. Korsgaard. Asthma and the indoor environment assessment of health implications of high indoor air humidity. Proceedings Indoor Air 1984 Stockholm, Vol. 1. Edited by B. Berglund, T. Lindvall, J. Sundell. ISBN 91-540-4191-0
3. Annex 14 Condensation and energy, Source Book
4. Annex 18 Demand Controlled Ventilating Systems, Source Book.
5. Annex 18 Demand Controlled Ventilating Systems, Case Studies.

**Ventilation for Energy Efficiency and Optimum
Indoor Air Quality
13th AIVC Conference, Nice, France
15-18 September 1992**

Poster 14

**Impact of Subslab Ventilation Technique on
Residential Ventilation Rate and Energy Costs.**

Y.C. Bonnefous^{*}, A.J. Gadgil^{}, W.J. Fisk^{**}**

*** Laboratoire des Sciences de l'Habitat, Ecole
Nationale des Travaux Publics de l'Etat,
Vaulx-en-Velin, France**

**** Indoor Environment Program, Lawrence
Berkeley Laboratory, Berkeley, California, USA**

Summary

Radon is the largest source of risk to human health caused by an indoor pollutant, at least in the industrial countries. Subslab Ventilation (SSV) is one of the most effective and common methods of reducing indoor Rn concentrations in houses with a basement.

In this paper, we first quantify the impact of this technique on the air exchange rate, through numerical modeling of a prototype house with basement for a range of permeabilities of soil and subslab aggregate and various sizes of the cracks in the basement floor. We show that a SSV system can increase the air exchange rate by as much as a factor of 4.5

We then compare the energy and capital costs of a Subslab Depressurisation (SSD) system to those of direct ventilation of the basement as required to lower the indoor radon concentration to an acceptable level, for a Chicago climate. We show that 1) an exhaust ventilation cannot reduce efficiently the indoor radon concentration and may even increase it; 2) a balanced ventilation with heat recovery is only efficient for low premitigation radon concentrations. However, both SSV and balanced ventilation systems are too expensive to be used in low premitigation level houses. A SSD system is the most cost effective technique for reduction of high radon concentrations.

Introduction

Within the United States, exposure to the radioactive decay products of radon (^{222}Rn) in buildings is the most important source of human exposure to environmental radiation and also one of the largest sources of risk to human health caused by an indoor pollutant [1]. In houses with elevated indoor Rn concentrations, the primary source of Rn is usually the surrounding soil where Rn is generated by the radioactive decay of trace amounts of radium. The predominant process of Rn entry into houses with a concrete basement is pressure driven flow of high-Rn soil gas into the basement through small cracks, joints, and holes in its concrete envelope [2].

Subslab ventilation (SSV) is one of the most effective and common methods of reducing indoor Rn concentrations in houses with basements. There are two basic methods of SSV. In subslab depressurisation (SSD), a fan exhausts soil gas from beneath the slab floor to the outside. The fan usually draws air through one or more plastic pipes that penetrate the slab floor. This process decreases the pressure beneath the floor and, therefore, reverses the pressure difference that normally causes soil gas and Rn to flow into the structure. In subslab pressurisation (SSP), outdoor air is forced beneath the slab using a fan (i.e., the direction of air flow is reversed compared to that in a SSD system). SSP ventilates the soil beneath the slab floor, thus reducing radon concentrations within the soil near the slab. Soil gas entry into the structure continues but the concentration of Rn in the entering soil gas is decreased.

Approach

We used a previously tested numerical model [3] to assess the impact of SSV systems on building air exchange rate. The numerical code called Non-Darcy STAR (Non-Darcy Steady State Transport of Air and Radon) is a fully three-dimensional finite difference model, using the Semi Implicit Method for Pressure Linked Equations (SIMPLE) and the Alternate Direction Implicit (ADI) method to solve the Darcy-Forchheimer law (equation 1) together with the continuity equation (2) assuming incompressible gas:

$$\vec{\nabla}p = -\frac{\mu}{k}(1 + c|\vec{V}|)\vec{V} \quad (1)$$

$$\vec{\nabla} \cdot \vec{V} = 0 \quad (2)$$

where p is the disturbance pressure (i.e., pressure change due to the depressurized basement and/or operation of a SSV system), \vec{V} the soil-gas bulk velocity, k the permeability of the porous media, μ the dynamic viscosity of the fluid, and c the Forchheimer term.

Once pressure and velocity fields are computed we use the model "Ra-Trans" (Radon-Transport) to solve the radon mass balance equation :

$$\vec{\nabla} \cdot (D\vec{\nabla}C_{RN}) - \vec{\nabla} \cdot (\vec{V}C_{RN}) + \epsilon(S - \lambda_{RN}) = 0 \quad (3)$$

where D is the bulk diffusivity of radon in bulk soil, C_{RN} is the radon concentration in the soil-gas, S is the production rate of radon into the soil-gas per cubic meter of bulk soil, λ_{RN} is the radon decay constant, and ϵ is the porosity of the media.

Lastly, we compute the radon entry rate and the indoor radon concentration. We assume a typical house geometry consisting of a one story building with a basement and a garage on its side (see figure 1). The pressure, velocity and concentration fields are computed in a soil block of about 27 m x 27 m in an area centered on the basement of the house, and 12.5 m deep below the soil surface. Thanks to a plane of symmetry, only half of this domain is to be modeled. The models assume that 1) each material (i.e. ; soil, backfill and aggregate) is homogeneous and isotropic; 2) the concrete is perfectly impermeable except for cracks; 3) the effect of buoyancy in the soil-gas flow field is negligible; and 4) diffusive transport of radon through concrete and inside the cracks is negligible. The garage is modeled as an impermeable surface. A L-shaped crack is uniformly distributed at all wall/footer/slab joints. The basement is assumed to be depressurized by 10 Pa.

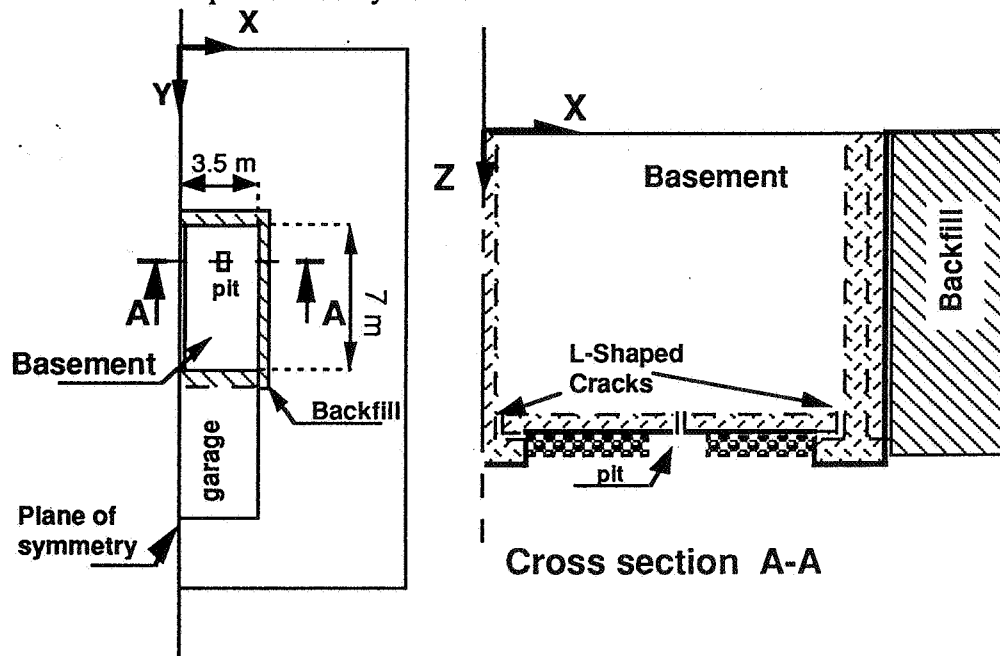


Figure 1: Schematic representation of the typical house as modeled by Non-Darcy STAR .

Impact of SSV systems on building air exchange rate.

We conducted a parametric study on SSV systems. Parameters are soil and gravel permeabilities, mode (SSD or SSP), crack width, and applied pressure. We describe here the effect of SSV systems on the air exchange rate of the building when operating with different parameter values.

The mode of operation, SSD or SSP, has a minor effect on the added air exchange rate. Air is extracted from the basement through the cracks in the slab by a SSD system instead of being blown into the basement through the cracks in the slab by a SSP system. Differences in the flow extracted from and blown into the basement are mainly due to the differences in the pressure gradient between the pit and the basement, e.g.: -60 Pa to -10 Pa for a SSD system versus +60 Pa to -10 Pa for a SSP system. As a consequence, the impact on the building air exchange rate of a SSP system is higher than the one of a SSD system for the same absolute value of applied pressure at the SSV system pit. However, for high values of applied pressure (± 250 Pa) and tight soils (configuration leading to high impacts of the SSV system on the building air exchange rate) flows blown into the basement by a SSP system and flows extracted from the basement by a SSD system differed by less than 10 %. We will only present here results for a SSD system, which is the most common.

Gravel permeabilities and Forchheimer terms used in the numerical simulations were previously measured in a laboratory test [3] and are given in Table 1. Soil permeabilities were chosen in the very top of their reported range. With low permeabilities, the soil acts like a perfectly impermeable media. In addition, models using similar hypothesis than non-Darcy STAR tend to under predict flows in the soil by as much as a factor of eight [4], probably because the effective permeability of soils around houses is greater than the average of several point measurements.

Table 1: Gravel permeabilities and Forchheimer terms.

	Gravel N° 1	Gravel N° 2	Gravel N° 3
Permeability [m ²]	2 10 ⁻⁸	1 10 ⁻⁷	3 10 ⁻⁷
Forchheimer term [s/m]	6	13	20

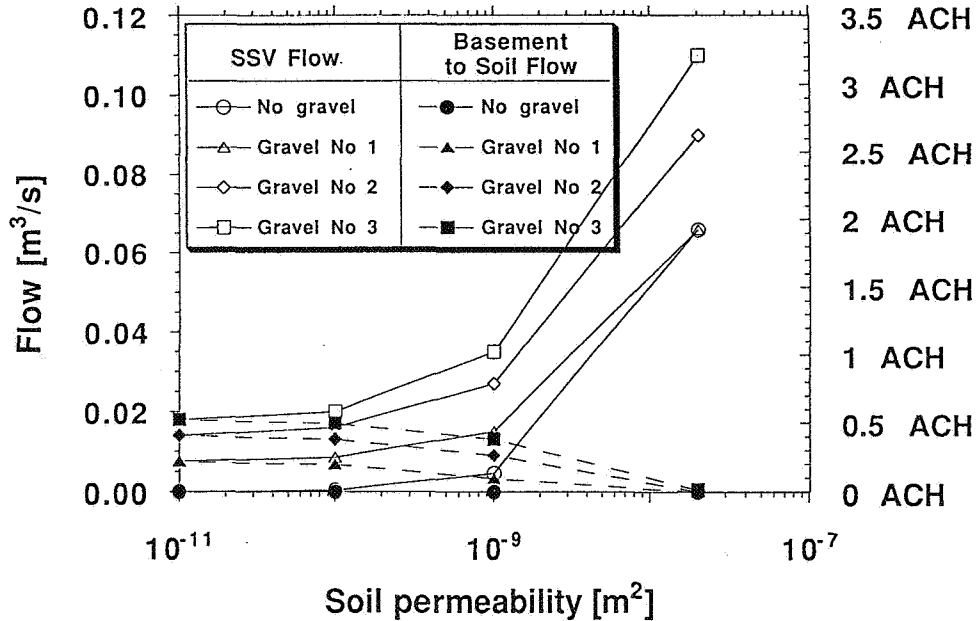


Figure 2: Predicted flows of air in the SSD system and flows of air extracted from the basement through the cracks in the slab. Basement depressurisation is -10 Pa. Applied pressure at the system pit is -60 Pa. A 1 mm L-Shaped crack is uniformly distributed at all wall/footer/slab joints.

We show (Figure 2) that for high soil permeability most of the flow originates from the top soil surface, while for low permeability soils, most of the flow extracted by the SSD system originates from the basement. The flow through the SSD system for a given depressurisation at the pit increases with increasing soil permeabilities and increasing gravel permeabilities. The flow extracted from the basement by the SSD system increases with decreasing soil permeabilities and increasing gravel permeabilities.

Increasing the depressurisation from -60 Pa to -250 Pa at the system pit doesn't affect much the partition of the flows (originating from the top soil surface or from the basement), only their magnitude is increased. The flow extracted from the basement by a SSD system operating at -250 Pa in a 10⁻¹¹ m² permeability soil and a 3 x 10⁻⁷ m² permeability gravel, is 0.06 m³/s (1.8 ACH). The air exchange rate is [5]:

$$R_{tot} = \sqrt{R_{typ.}^2 + R_{add}^2} \quad (4)$$

where R_{tot} is the total building air exchange rate, $R_{typ.}$ is the typical air exchange rate (0.4 ACH [6]) and R_{add} is the additional air exchange rate due to SSD operation (i.e., the flow from the basement to the gravel).

The air exchange rate of the building can be increased by as much as a factor of 4.5. Figure 3 shows that the ratio of air extracted from the basement to total SSD flow increases rapidly with decreasing soil permeabilities: from 0 % to 100 % in 2 orders of magnitude of soil permeability. Sealing the cracks can only modify this ratio for high soil permeabilities. However, by increasing the resistance to flow of the cracks, sealing will lower the SSD system flow.

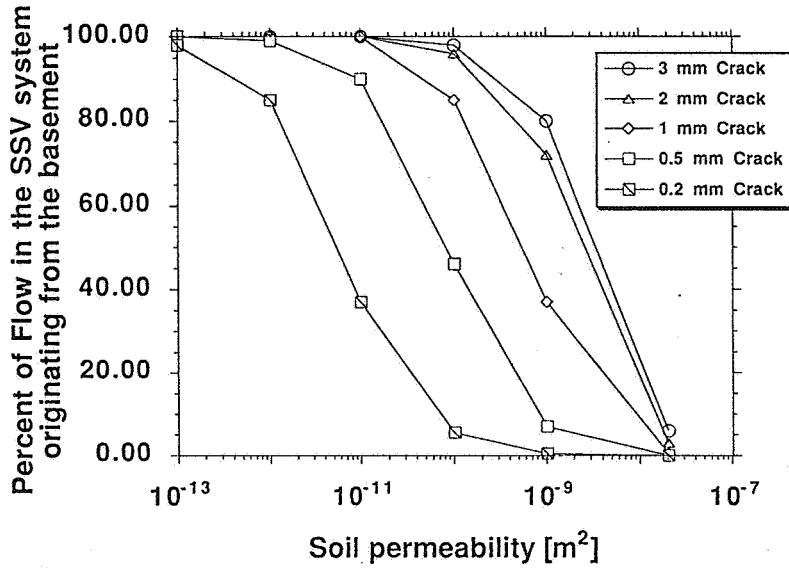


Figure 3: Percent of flow in the SSD system exhaust pipe originating from the basement for various soil permeabilities and crack widths. The gravel permeability is 3.10^{-7} m^2 , and the basement depressurisation is -10 Pa .

Cost effectiveness of a SSD system compared to an exhaust ventilation and to a balanced ventilation with heat recovery as a radon mitigation technique.

We used the previously described geometry with a 1 mm L-Shaped crack, soil permeabilities of 10^{-10} m^2 and 10^{-11} m^2 and gravel n° 2. We computed the indoor radon concentration assuming a single zone well mixed building resulting from combinations of three deep soil radon concentrations ($30,000 \text{ Bq/m}^3$, $90,000 \text{ Bq/m}^3$ and $180,000 \text{ Bq/m}^3$) and three different winter conditions: A) $T_{\text{out}} = -10 \text{ }^\circ\text{C}$; B) $T_{\text{out}} = 0 \text{ }^\circ\text{C}$; C) $T_{\text{out}} = +10 \text{ }^\circ\text{C}$, with a constant wind speed of 3 m/s.

We made this comparison study on the part of the building modeled. Two SSD systems would be used in our typical building, and we assumed that similarly, up to two exhaust fans or two balanced ventilation systems (or twice as expensive) would be installed as each part of the building would be treated separately. The part of the building considered, has an ELA (Effective Leakage Area) of 0.015 m^2 uniformly distributed on its sides. Its volume is 122.5 m^3 .

Case 1: No Mitigation System.

Assuming natural ventilation and no mitigation system, the depressurisation at the basement floor level of the building is given by [7]:

$$\Delta p_f = \Delta p_s + \Delta p_w \quad (5)$$

where the depressurisation due to the stack effect is:

$$\Delta p_s = \rho g \Delta T (z_f - z_n) / T_{\text{int}} \quad (6)$$

and $z_f - z_n$, the difference of elevation between the pressure neutral point and the basement floor level is 3.75 m., $\Delta p_w = 0.6 \text{ Pa}$ for a wind speed of 3 m/s.[7], ρ is the density of air, g the acceleration of gravity, ΔT the indoor - outdoor temperature difference and T_{int} the indoor temperature.

The resulting indoor radon concentrations are calculated by:

$$C_{\text{RN,indoor}} = \frac{\text{Entry} * C_{\infty} + Q_{\text{Tot}} * C_{\text{RN,outdoor}}}{Q_{\text{Tot}}} \quad (7)$$

where $C_{\text{RN,indoor}}$ is the indoor radon concentration, $C_{\text{RN,outdoor}}$ is the outdoor radon concentration equal to 9 Bq/m^3 , Entry is the radon entry rate normalised by the deep soil

radon concentration, C_{∞} , and Q_{Tot} is the total flow of air between the building and its surrounding (including the soil).

Table 2 gives the results from this first set of simulations which constitute the base case for the comparison.

Table 2: Radon Entry rate and indoor radon concentration without any mitigation system.

Out. Temp. [°C]	Soil Perm. [m ²]	Air change Rate [ACH]	Basem. Depres. [Pa]	Entry Rate [cm ³ /s]	$C_{RN,int}$ $C_{\infty}=30000$ [Bq/m ³]	$C_{RN,int}$ $C_{\infty}=90000$ [Bq/m ³]	$C_{RN,int}$ $C_{\infty}=180000$ [Bq/m ³]
-10	10 ⁻¹⁰	0.46	-5.1	195	370	1100	2200
0	10 ⁻¹⁰	0.40	-3.6	150	320	950	1900
+10	10 ⁻¹⁰	0.33	-2.1	89	250	740	1500
-10	10 ⁻¹¹	0.46	-5.1	24	55	150	290
0	10 ⁻¹¹	0.40	-3.6	17	46	120	230
+10	10 ⁻¹¹	0.33	-2.1	10	36	92	170

Case 2: With a SSD system

A SSD system is installed and operated with a -150 Pa depressurisation at the system pit. The new depressurisation in the basement is determined by iterating the following process: 1) computation with non-Darcy STAR of the flow exhausted from the basement by the SSD system for a given basement depressurisation, 2) calculation of the depressurisation in the basement integrating the depressurisation associated to the flow extracted from the basement by the SSD system (equations 8 & 9). If the depressurisation is different than the one used in Non-Darcy STAR return to step one with the newly calculated depressurisation.

$$Q_{Tot} = \sqrt{Q_{stack}^2 + Q_{wind}^2 + Q_{ext}^2} \quad (8)$$

$$\Delta p_{ext} = \frac{\rho}{2} \left(\frac{Q_{ext}}{ELA} \right)^2 \quad (9)$$

where: Q_{stack} , Q_{wind} are the flows due to the stack effect and the wind effect, Q_{ext} is the flow extracted by the system from the basement, and Δp_{ext} is the depressurisation induced by the Q_{ext} .

Table 3: Basement depressurisations and building air exchange rates when a SSD system is operated with a -150 Pa. depressurisation at the pit.

Out. Temp. [°C]	Soil Perm. [m ²]	Induced Depres. [Pa]	Total basem. Depres. [Pa]	SSD Flow [m ³ /s]	Flow from basem. [m ³ /s]	Flow entering basem. [m ³ /s]	Indoor Radon Conc. [Bq/m ³]	Air change rate [ACH]
-10	10 ⁻¹⁰	-2.6	-7.7	0.036	0.031	0	9	1.0
0	10 ⁻¹⁰	-2.6	-6.2	0.037	0.031	0	9	1.0
+10	10 ⁻¹⁰	-2.7	-4.8	0.037	0.032	0	9	0.99
-10	10 ⁻¹¹	-2.8	-7.9	0.034	0.033	0	9	1.1
0	10 ⁻¹¹	-2.9	-6.5	0.034	0.033	0	9	1.0
+10	10 ⁻¹¹	-2.9	-5.0	0.034	0.033	0	9	1.0

In each case, the SSD is fully successful : no soil gas is entering the basement as the depressurisation in the gravel is lower than the depressurisation in the basement. As a result the indoor radon concentration is equal to the outdoor radon concentration (Table 3, col. 8). However, we see (Table 3, col. 3) that depressurisation induced in the basement by SSD system operation is substantial. This could cause backdrafting of the exhaust fumes of the furnace or other appliances into the house. The ventilation rate of the house is also increased greatly.

Case 3 : Exhaust ventilation as radon mitigation technique

We computed the required air exchange rate to reduce the indoor radon concentration given in Table 2 to either the EPA action limit guideline of 150 Bq/m³ or either 37 Bq/m³. From equation 7,

$$R_{tot} = \left[\frac{3600}{Vol} \right] \frac{Entry * C_{\infty}}{C_{RN,indoor} - C_{RN,outdoor}} \quad (10)$$

Where: Vol is the volume of the building considered.

Then, we computed the depressurisation induced by the exhaust ventilation at the basement floor level (equation 9) and we used non-Darcy STAR with the new basement depressurisation to compute the actual indoor radon concentration when the exhaust ventilation is operated.

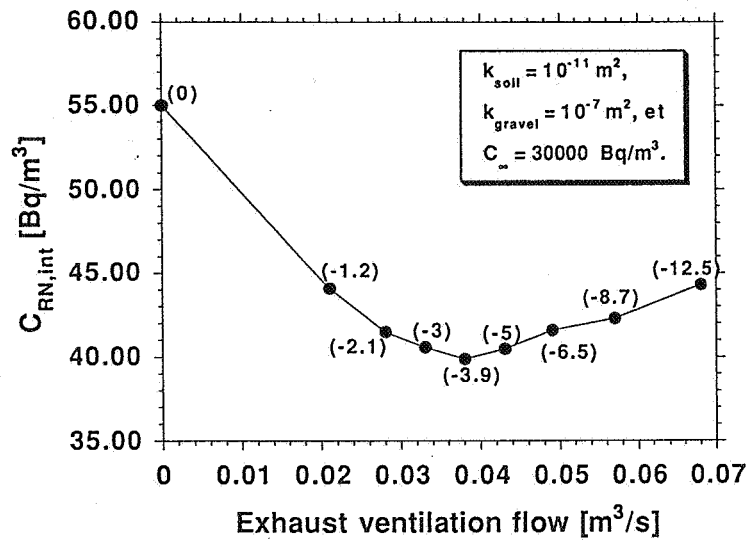


Figure 4: Indoor radon concentration when an exhaust ventilation is operated. The depressurisation in the basement induced by the exhaust ventilation is given in between parenthesis.

For elevated premitigation radon concentration levels, flows required in the exhaust ventilation are unrealistic (up to 6 ACH) When a small reduction of the indoor radon concentration is required, the depressurisation induced by the exhaust ventilation increases the radon entry rate, and the desired indoor radon concentration level is not obtained. We iterated the process : calculation of the required air exchange rate with the latest radon entry rate, calculation of the induced depressurisation and computation of the obtained indoor radon concentration. Figure 4 shows that after a first small decrease in the indoor radon concentration for low exhaust ventilation flows, higher flows may increase the indoor radon concentration. An Exhaust Ventilation shouldn't be used for radon mitigation purposes.

Case 4 : A balanced ventilation system with heat recovery is installed.

A balanced ventilation system doesn't affect the building pressure profile. The building air change rate and then the flow in the balanced ventilation are calculated so that the indoor radon concentration does not exceed 1) 10 Bq/m³ (\approx outdoor radon concentration), 2) 37 Bq/m³, and 3) 150 Bq/m³. (EPA guideline). Air exchange rates are given by equation 11, flows in the balanced ventilation are given by :

$$Q_{bal} = Q_{Tot} - \sqrt{Q_{stack}^2 + Q_{wind}^2} \quad (11)$$

where Q_{bal} is the flow in the balanced ventilation system.

The maximum flow handled by a practical balanced ventilation is around 0.1 m³/s. As a consequence, only premitigation levels lower than 16 Bq/m³ could be reduce to 10 Bq/m³.

Similarly only premitigation levels lower than 210 Bq/m³ and 1030 Bq/m³ could be reduced to 37 Bq/m³ and 150 Bq/m³, respectively.

Attaining an acceptable indoor radon concentration, (but not to the outdoor radon concentration) with a balanced ventilation is only possible if the premitigation concentration is low or moderate. Our simulations show a perfectly working SSD system, however we remind the reader that the geometry of the typical house is design for best performances of a SSD system. Nonetheless, SSD system have shown very good performances in field studies and is the most efficient technique to mitigate houses with high radon concentration premitigation levels.

Cost comparison.

For this cost comparison, we considered the "moderate" climate of Chicago. To compute the heating penalty associated with an additional air change rate, we used the bin method as described in Fisk et al. [9]. We use the weather data from the US-Air Force manual [10]. The indoor temperature is 20°C, the building balanced point is 15.6 °C, and the heating season for Chicago is from October to April. The heating load imposed by ventilation is given by:

$$E = \rho \cdot C_p \cdot Vol \cdot R \sum_j (T_{in} - T_j) \theta_j \quad (12)$$

Where E is the heating load, C_p is the specific heat at constant pressure of air, T_j is the outdoor temperature at the midpoint of the bin j, θ_j is the number of hours the outdoor temperature falls within the temperature bin j.

The electricity cost in 1992 is \$0.0786 KW/h and the projected real escalation rate for the next 10 years is + 0.12 %* . We assumed a 3% real discount rate for money. The net present cost of a system over the next 10 years is then given by:

$$NPC = CC + OPC \sum_{i=1}^{10} \left[\frac{1+f}{1+d} \right]^i \quad (13)$$

where NPC is the net present cost, CC is the capital cost, OPC is the operating cost, f is the real price escalation rate, and d is the real discount rate.

The installation cost of a SSD system is ≈ \$1100. [11]. The SSD operating cost comprises the fan energy consumption : (50 W) \$35 for 1992, and the heating load. The fan energy is lost as the fan is placed in the stream. Maintenance is done by the homeowner at no cost. The building air change rate when the SSD system is operating, is about 1 ACH (Table 3) compared to about 0.4 ACH in absence of the SSD (Table 2). The heating load of a 0.6 ACH added air change rate is 7.9 GJ (from equation 12) which leads to an additional \$172.5 operating cost in 1992. The net present net cost over 10 years of the SSD system is \$2880 .

The installation cost of a balanced ventilation is: \$1700** . Maintenance is done by the homeowner at no cost. The flow in the balanced ventilation is supposed to be fixed over the year at either the value computed for a -10°C outdoor temperature which means that the indoor radon concentration will be lower than the goal concentration 94 % of the time, or either for a 0°C outdoor temperature which means that the indoor radon concentration will be lower than the goal concentration 65 % of the time, but higher 35% of the time.

The effective sensible recovery efficiency of the system is 65 %** . This figure accounts for fan energy consumption and the part of this energy recovered by the building. During the heating season, the operating cost of the balanced ventilation is then equal to the energy cost of the heating load of 35% of the air change rate induced by the balanced ventilation. For the rest of the year, the operating cost of the system is equal to the cost of the fan energy consumption.

* Electricity price and projected real escalation rate from Energy Information Agency, Annual Energy Outlook 1992, p. 66

** Source: Conservation Energy Systems Inc, vanEE, Mineapolis, USA

Table 5 give the net present cost of the balanced ventilation for the different combinations. We see that for small reductions of the indoor radon concentration (≤ 250 Bq/m³), a balanced ventilation system could be cheaper than a SSD system. However the cost of both systems is probably too high for most homeowners to be used for such a purpose. New techniques (passive techniques ?) that do not substantially increase energy use are needed to deal with low premitigation level houses.

Table 5: Net Present Cost of a balanced ventilation with heat recovery over 10 years.

Out. Temp. [°C]	Soil Perm. [m ²]	Indoor Radon Concentration [Bq/m ³]	PNC C _∞ 30000 over 10 years	PNC C _∞ 90000 over 10 years	PNC C _∞ 180000 over 10 years
-10	10 ⁻¹¹	37	2250	3600	NR
0	10 ⁻¹¹	37	2100	3000	4460
-10	10 ⁻¹⁰	150	2600	NR	NR
-10	10 ⁻¹¹	150	NA	NA	2370

Conclusion

Our numerical model shows that with low permeability soils a SSD system can have a great impact on the building air exchange rate, as for tight soil all of the flow in the SSD system comes from the basement. Sealing the cracks in the basement floor will reduce the flow in the SSV system and the amount of increased ventilation in the house.

An exhaust ventilation cannot reduce the indoor radon concentration efficiently and may even increase it. A balanced ventilation with heat recovery could be a cheaper alternative to a SSD system for small required radon concentration reductions (≤ 250 Bq/m³). However, both system are too probably expensive to be recommended at such low premitigation levels.

For elevated premitigation radon levels, a SSD system is the most efficient and cost effective technique.

Acknowledgements

This work was supported at Indoor Program of Lawrence Berkeley Laboratory by the Assistant Secretary for Conservation and Renewable Energy, Office of Building Technologies, Building Systems and Materials Division of the U.S. Department of Energy under Contract DE-AC03-76SF00098

References

- Nero A.V. Sci. Am. 1988, 258 (5), 42-48.
- Nazaroff, W.W.; Nero A.V. Radon and its decay products in indoor air; John Wiley & Sons: New York, 1988.
- Bonnefous, Y.C., Gadgil, A.J., Fisk, W.J., Prill, R.J. and Nematollahi "A. Field Study and Numerical Simulation of Subslab Ventilation Systems". Lawrence Berkeley Laboratory Report LBL-31942, Berkeley, CA, 1992, submitted to E. S. & T.
- Garbesi, K., Sextro, R.G., Fisk, W.J., Modera M.P., and Revzan, K.L. "Soil-Gas Entry into an experimental Basement: Model-Measurement Comparisons and Seasonal Effects", Lawrence Berkeley Laboratory Report, LBL-31873, University of California, Berkeley, CA, submitted to E. S. & T
- Sherman, M. H. (1990) "Superposition in infiltration modelling", Lawrence Berkeley Laboratory Report, LBL - 29116, University of California, Berkeley, CA, submitted to J. Indoor Air.
- Palmiter, L. and Brown, I. (1989) "Northwest residential infiltration survey: analysis and results". Ecotope, 2812 East Madison, Seattle, WA.
- Fisk, W. J. and Mowris, R.J. (1987) "The Impacts of Balanced and Exhaust Mechanical Ventilation on Indoor Radon", Proceedings of the 4th International Conference on Indoor Air Quality and Climate: Indoor Air '87, Berlin, West Germany, 17-21 Août 1987, vol 2 pp 316-320.
- Mowris, R.J. and Fisk, W. J. (1987) "Modeling the effects of exhaust ventilation on radon entry rates and indoor radon concentrations, Lawrence Berkeley Laboratory Report, LBL-22939, University of California, Berkeley, CA.
- Fisk, W. J. and Turriel (1983) "Residential Air-to-Air Heat Exchangers: Performance, Energy Savings, and Economics", Energy and Buildings, (1983) 197-211.
- Facility Design and Planning, Engineering Weather Data, US Air Force Manual 88-29, 1978.
- Henschel, D.B., "Cost Analysis of Soil Depressurisation Techniques for Indoor Radon Reduction" Indoor Air, Vol 1, N° 3, 1992

**Ventilation for Energy Efficiency and Optimum
Indoor Air Quality
13th AIVC Conference, Nice, France
15-18 September 1992**

Poster 16

**Ventilation, Heat and Moisture Conditions in Attic
Spaces.**

J. Kronvall^{*}, H. Kvist^{}, P.I. Sandberg^{***}**

*** Technergo AB, Ideon Research Park, S-223 70
Lund, Sweden**

**** Dept of Building Science, Lund University, P O
Box 118, S-221 00 Lund, Sweden**

*****SP, Swedish National Testing & Research
Institute, P O Box 857, S-501 15, Boras, Sweden**

1 Summary

Due to the complexity in describing the simultaneous effects of a number of factors that influence the climate of an attic space it has proven to be difficult to make simulations of it.

This report deals with the problem of using different computer programs for ventilation, heat and moisture balance in an integrated way so that a proper description of the expected attic climate can be achieved.

A general overview of attic space climate and the factors affecting it will be given and it will be described how the simulation packet works. Results from a simulation will be given and commented upon.

2 Attic space climate

2.1 General

The most important parameters for describing the attic climate as far as the hygro-thermal behaviour of the attic space is concerned are relative humidity values and temperatures for the air in the attic space itself and at the surface of materials exposed to the attic space. Knowing these parameters and their variations quite a lot of conclusions can be drawn regarding the expected durability of the materials, the energy performance etc.

The attic space climate is determined by a number of factors such as ventilation rate, outdoor climate, moisture exchange by convection between the attic space and the heated part of the building, insulation degree of the attic floor, solar radiation on the roof, radiative and convective heat exchange in the attic space, moisture and other properties of materials used etc.

2.2 Ventilation

The purposes of ventilating an attic space is to remove moisture and to decrease the temperature in the attic space. In most cases purpose provided ventilation devices are installed in order to ventilate the attic space naturally, by means of wind and sometimes stack forces. The most simple and perhaps also most common way to provide these vent devices is to leave a slot open (10-30 mm wide) at the eaves of the roof. In this case the ventilation of the attic space is depending on the prevailing wind conditions around the building.

Every attempt to predict the heat and moisture conditions of an attic space must involve a calculation or at least an estimation of the ventilation flow, otherwise calculations cannot be undertaken.

The most severe problem in calculating or estimating the ventilation is to determine what the wind close to the building really is like (speed and direction). Even if the wind is known there is a problem to select reliable pressure coefficients for the intake and outlet openings. Furthermore, you must know the geometry of the flow paths of the ventilation openings.

The wind-driven ventilation of the attic also influences the pressure difference between the attic space and the heated part of the building, thus affecting the convective moisture exchange.

2.3 Heat balance

The heat balance of the attic space is governed by a large number of factors such as the outdoor climate (including solar radiation), the indoor climate and the insulation level of the attic floor, convective heat exchange, radiative heat exchange etc. and again the ventilation. If condensation / evaporation takes place at some surface(s) this will also influence the heat conditions.

2.4 Moisture balance

The moisture conditions of an attic space are governed by the outdoor climate, the convective moisture exchange between the attic and the heated part of the building and the moisture exchange between the attic space and the materials in it, (absorption or desorption). If the relative humidity should be considered, also the temperatures of the air and at surfaces must be taken into account.

3 Simulation package

3.1 General layout

A ventilation program provides the heat balance and the moisture balance programs with an algorithm for the ventilation rate of the attic as a function of wind velocity and direction. There is also an algorithm for the convective moisture and heat exchange between the attic and the heated part of the building.

For the ventilation as well as the other calculations performed a data file of outdoor climatic data is used (Malmö, Sweden, 1971 - a widely used natural reference year for energy calculations in Sweden).

The ventilation algorithms are used in the heat balance program, describing all the convective parts of the heat balance. The heat balance program then performs traditional calculation on heat transfer due to conduction and radiation coming up with a set of temperatures for the attic air and surface temperatures.

The data produced until now is used in the moisture balance program taking into account sorption and desorption in materials, thus producing final data on humidity in the attic space.

3.2 Software

3.2.1 MLNBS

The MLNBS code was originally developed by G Walton at the NBS in US, WALTON (1982), and further developed by M Liddament at the AIVC in UK (unpublished). It is essentially a multi-zone infiltration and ventilation program. In this work a two zone simulation is performed, one zone being the attic space and the other the heated part of the building. As a result of running the program all air flow rates of interest are calculated as a function of the wind velocity and the temperature difference between the attic and the heated part of the building.

The calculations are performed for different levels of airtightness of the walls of the building and the bottom floor in the attic. The calculation results for a building specified in part 4.1 of this report are shown in figures 3.2.1.a - 3.2.1.f. For all the calculations the wind velocity used is the local wind velocity at roof top level.

The pressure coefficients used originate from the AIVC Air Infiltration Calculation Techniques Guide, (Liddament, 1986)

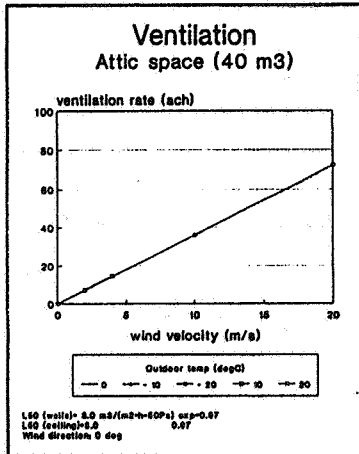


Figure 3.2.1a

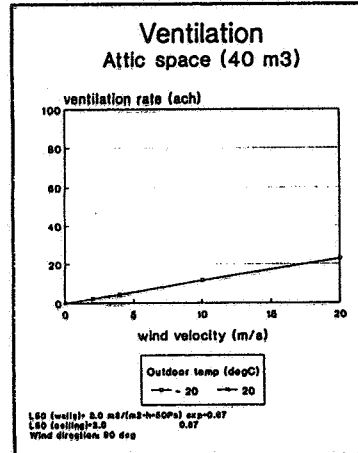


Figure 3.2.1b

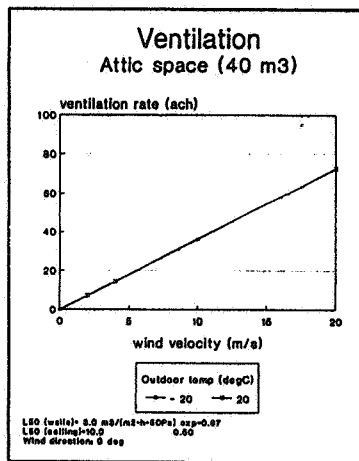


Figure 3.2.1c

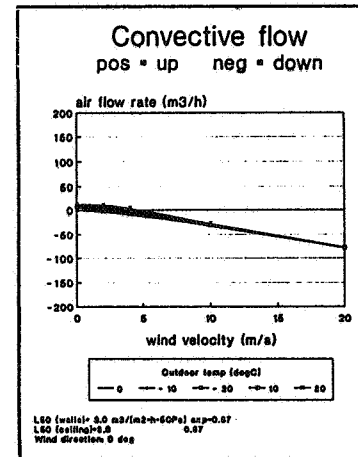


Figure 3.2.1d

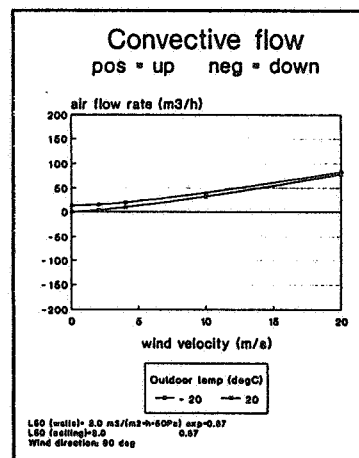


Figure 3.2.1e

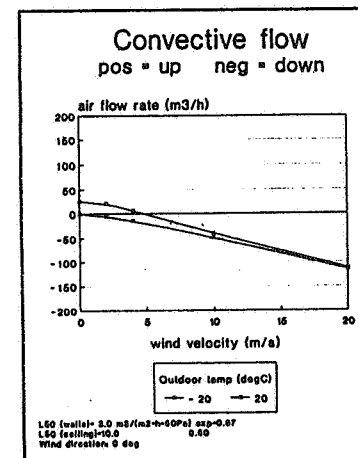


Figure 3.2.1f

3.2.2 DEROB-LTH

DEROB or Dynamic Energy Response of Buildings is a computer program in Standard-Fortran with generalized algorithms for the calculation of temperatures and energy in arbitrarily designed buildings. The program was originally developed by F.N. Arumi at the School of Architecture, University of Texas, Austin, US, (Arumi & Wysocki, 1979 and Arumi, 1979). The work with the development of the program was started in 1971. The program has been further developed at the department of Building Science, Lund University. The version used for the calculations is called DEROB-LTH.

3.2.3 PIVIND

Moisture absorption and desorption at surfaces exposed to the attic atmosphere is calculated by using the moisture transfer equation

$$g = \delta \text{ delta} * \text{grad } v$$

where

g = density of moisture flow rate
 delta = vapour permeability
 v = vapour concentration

and the boundary condition

$$g = \text{beta} * (v_{\text{sur}} \delta v_{\text{attic}})$$

where

beta = surface coefficient of vapour transfer
 v_{sur} = v at material's surface
 v_{attic} = v in the surrounding attic air

The surface temperatures of the various building elements surrounding the attic are taken from the DEROB simulation. The temperature distribution between the surfaces is considered linear, thus disregarding all effects of heat capacity.

To carry out the calculations it is necessary to know the vapour permeability as a function of the moisture content and the hygroscopic sorption curve (relation between moisture content and relative humidity).

A simple forward difference method is used to solve the equations and for each time step the evaporation from the surrounding surfaces (g_{evap}) to the attic is calculated.

For each time step a new attic vapour concentration is then calculated:

$$v_{\text{attic,new}} = v_{\text{attic,old}} + R_{\text{out}} * dt / V * (v_{\text{out}} \delta v_{\text{attic,old}}) + R_{\text{in}} * (v_{\text{in}} \delta v_{\text{attic,old}}) * dt / V + dt / V * g_{\text{evap}}$$

where

$v_{\text{attic,new}}$ = new vapour concentration in the attic air
 $v_{\text{attic,old}}$ = old vapour concentration in the attic air

R_{out}	= air flow to the attic from the outside
R_{in}	= air flow to the attic from the inside
dt	= time step
V	= attic volume
v_{out}	= outdoor air vapour concentration
v_{in}	= indoor air vapour concentration
g_{evap}	= density of evaporation flow rate

4 Simulation application

4.1 General input data

The calculations have been performed for a building by the size of 7.4 m * 7.2 m with a height to the eaves of 2.5 m. The building has a roof with a ridge height of 0.75 m.

The roof of the house consists of a 22 mm thick wooden panel and a roof felt. The roof is supported by trusses (45 mm * 145 mm). The attic floor is insulated with 200 mm of mineral wool ($\lambda = 0.04$ W/mK). The indoor moisture supply (in the heated part of the building) is 0.003 kg/m³.

The wind pressure coefficients used are shown in figure 4.1.a.

Surface	Wind pressure coefficient	
	Wind acting on long side (dir A)	Wind acting on gable side (dir B)
1	0.3	-0.3
2	0.4	-0.3
3	-0.5	-0.3
4	-0.5	-0.3
5	-0.3	0.3
6	-0.3	0.4
7	-0.3	-0.3
8	-0.3	-0.3
9	0.4	-0.4
10	0.4	-0.3
11	-0.5	-0.4
12	-0.5	-0.3

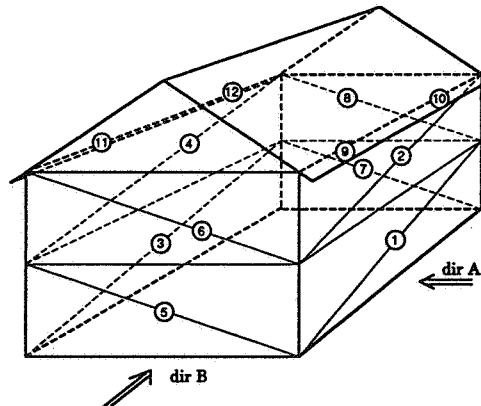


Figure 4.1.a Wind pressure coefficients used in the simulations

The ventilation of the attic space is provided by a 20 mm wide slot at each roof eave along the longer side of the building.

The results of the ventilation and convection calculations performed by means of the MLNBS program were generalised for introduction as algorithms in the DEROB-BKL and the PIVIND programs in the following way

Ventilation of attic space with outdoor air

For wind direction perpendicular to the eaves (0 deg)

$$q = 0.04 u$$

where

q = ventilation flow rate (m³/s)

u = wind velocity at roof top (m/s)

For wind direction perpendicular to the gables (90 deg)

$$q = 0.01 u$$

*Convection from (positive) or to (negative)
the heated part of the building into/from the attic space*

L50 = 3 m³/m²h ('normal' airtightness)

For 0 deg q = 0.0060 - 0.0014 u

For 90 deg q = 0.0014 + 0.0010 u

L50 = 10 m³/m²h (leaky)

For 0 deg q = 0.0060 - 0.0020 u

For 90 deg q = 0.0014 + 0.0020 u

4.2 Output data with comments

In this section results from a simulation will be presented and commented upon. The mere intent of this is to demonstrate the possibilities of the program packet rather than giving a detailed description of the results for a longer period. The month chosen is October and the reason behind the choice is that empirically we know that this may be a month with an outdoor climate giving rise to rather severe impact on the moisture levels in the attic space.

The simulation is performed for wind perpendicular to the eaves during the whole period and with 'normal' airtightness of the attic floor (see above in section 4.1). The outdoor conditions are determined by the climatic conditions in Malmö, Sweden in 1971.

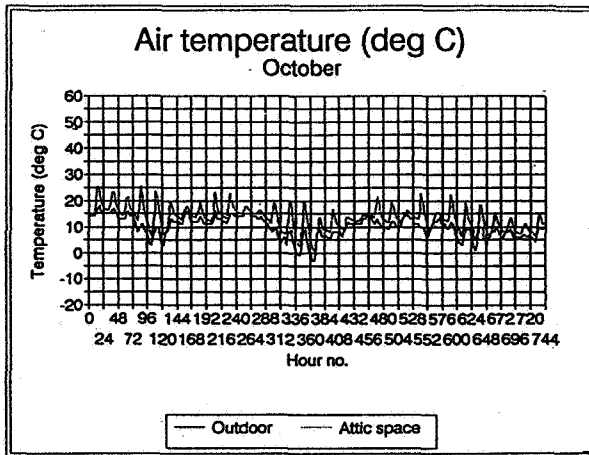


Figure 4.2.a

The figure shows the air temperatures outdoors and in the attic space. It can be seen that the attic air temperature always exceeds the outdoor air temperature. The difference can be up to around 10 deg C, probably on sunny days.

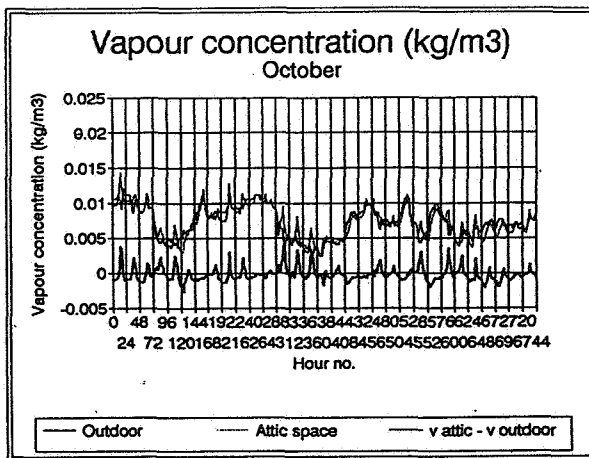


Figure 4.2.b

The figure shows the vapour concentration outdoors and in the attic space, as well as the difference between them. For a number of days a periodical behaviour of the vapour concentration in the attic space can be traced, while in most cases this is not seen for the outdoor condition. This is more easily seen in the graph for the difference in vapour concentration. The main reason for these variations is probably the moisture exchange between the materials in the attic and the attic air. This could be studied more specifically in figure 4.2.d.

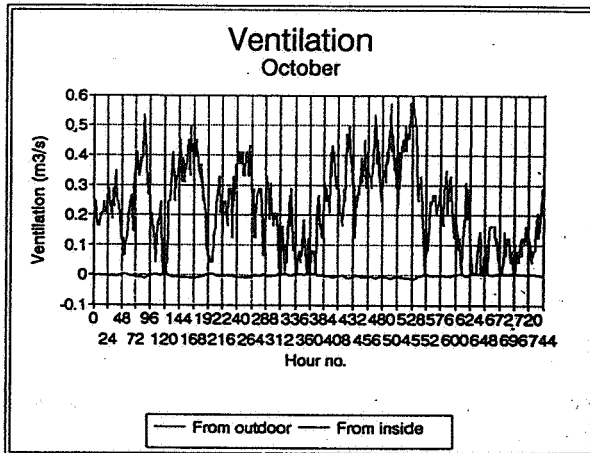


Figure 4.2.c

The figure shows the ventilation with outdoor air of the attic space as well as the convective exchange between the attic and the heated part of the building. First of all it can be seen that, compared to the ventilation, the convective exchange is small. This is probably due to the fact that the simulated case is the most 'favourable' (normal airtightness of the attic floor and wind hitting the long-facade of the house; see section 4.1 for details!). The ventilation rate however varies considerably due to different wind velocities during the period. For the period studied there seems to be a peak in ventilation during daytime. The attic has a volume of 40 m³ so the ventilation rate of 0.2 m³/s e.g. corresponds to $0.2 \times 3600 / 40 = 18$ ach. This seems to be a proper estimation of the average during the period.

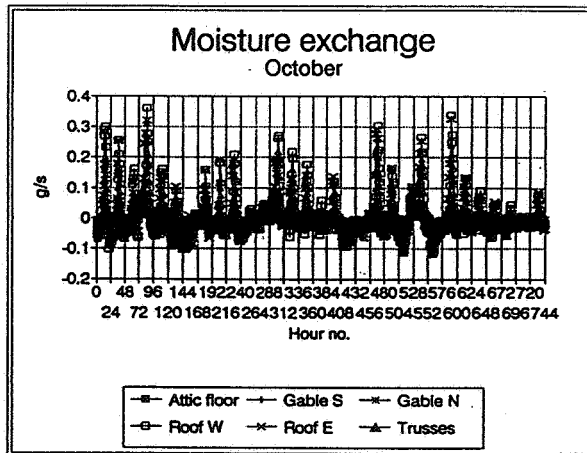


Figure 4.2.d

The figure shows the moisture exchange between the different parts of the envelope of the attic and the attic air. Most surfaces seem to have a relatively modest exchange (close to 0 g/s) while others give relatively large contributions (Roof W, roof E and the trusses especially). By comparing this figure with figure 4.2.a it can be seen that large desorption of moisture is closely connected to sunny days, while, on the opposite, sorption takes place on cold nights.

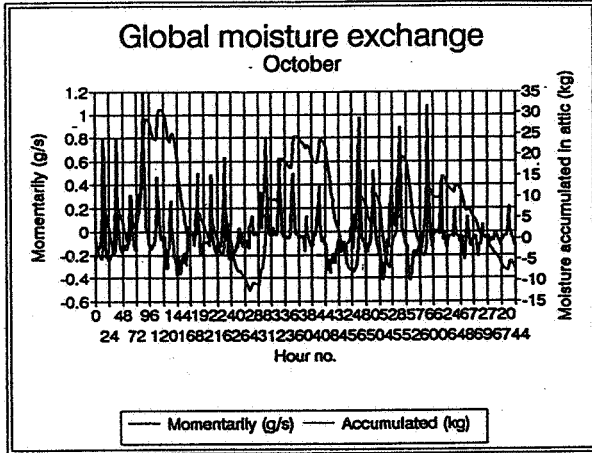


Figure 4.2.e

The figure shows the global moisture exchange for the attic space as a whole, both momentarily and accumulated for the whole month. The peaks for the momentarily case, also seen in the last picture, are still there. The accumulation graph shows that during this month there is a drying out of the attic with appr. 7 kg water, with variations in accumulation between 30 kg and - 15 kg.

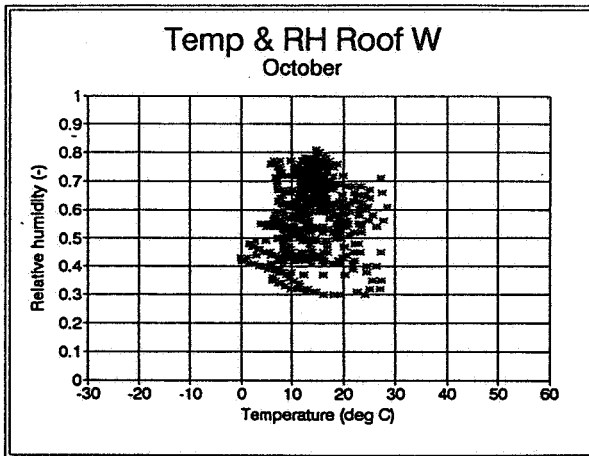


Figure 4.2.f

The figure is a XY-plot of relative humidity at a surface (roof W) against surface temperature. As can be seen there seems to be a concentration of dots around appr 15 degC and RH around 60 per cent. The variations are however large. There is a potential with this kind of plots for predicting the risk for mould growth on surfaces in an attic space since certain combinations of temperature and RH represent different risk levels for mould growth (Nevander & Elmarsson, 1991).

5 Literature

Arumi, F.N. & Wysocki, M. (1979). *The DEROB System Volume I, User's manual for the DEROB System*. Numerical Simulation Laboratory, School of Architecture, University of Texas, Austin, Texas, US.

Arumi, F.N. (1979). *The DEROB System Volume II, Explanatory Notes and Theory*. Numerical Simulation Laboratory, School of Architecture, University of Texas, Austin, Texas, US.

Fredlund, B. & Källblad, K. (1985). *KBKL*DRBBKL-1-FK*. (Internal document). Department of Building Science, Lund Institute of Technology/Lund University, Lund, Sweden.

Liddament, M.W. (1986). *Air Infiltration Calculation Techniques - An Applications Guide*. Air Infiltration and Ventilation Centre, Warwick, UK.

Nevander, L.E. & Elmarsson, B. (1991). *Moisture Design for Wooden Constructions, A Risk Analysis Scheme*, (In Swedish). (Report R38:1991). Svensk Byggtjänst, Solna, Sweden.

Walton, G.N. (1982). *A Computer Program for Estimating Infiltration and Inter Room Air Flows*. (NBS Report NBSIR 83-2635). National Bureau of Standards, US.



5992

**Ventilation for Energy Efficiency and Optimum
Indoor Air Quality
13th AIVC Conference, Nice, France
15-18 September 1992**

Poster 12

Ventilation Requirements in Modern Buildings.

F. Steimle and J. Röben

**Universität Essen, Angewandte Thermodynamik
und Klimatechnik, Universitätsstr.15, W-4300
Essen 1, Germany**

Ventilation requirements in modern buildings

Synopsis

Besides the hygienic aspect, also the aspect of energy saving of heating residential buildings is very important. This is only possible by mechanical ventilation with heat recovery. This paper describes a part of the large variety of systems, which are nowadays available on the market. The main difference of these systems are:

- single room unit/decentral unit and
- central unit for one dwelling or a single family building

For the heat recovery are used:

- only a plate heat exchanger (return air/supply air)
- only a heat pump (return air/supply air or return air/heating water) or
- a plate heat exchanger combined with a heat pump (return air/supply air)

As heat source for the heat recovery are used:

- only the return air
- the return air mixed with the flue gas by using a gas heating system.

List of symbols

k	overall heat transfer coefficient [$\text{W}/\text{m}^2\text{K}$]
k_m	average of the overall heat transfer coefficient [$\text{W}/\text{m}^2\text{K}$]
\dot{Q}_{tot}	total heat requirement [$\text{kWh}/\text{m}^2\text{a}$]
\dot{Q}_V	ventilation heat requirement [$\text{kWh}/\text{m}^2\text{a}$]
\dot{Q}_T	transmission heat requirement [$\text{kWh}/\text{m}^2\text{a}$]
t	temperature [$^{\circ}\text{C}$]

1. Introduction

Due to the energy savings the buildings are more tightly joined today and the basic ventilation is not longer guaranteed. A simple solution to extract the pollutants and moisture is the ventilation through the windows. The comfort for the inhabitants is very often impaired and the heat loss is not irrelevant.

However, if in the future the new regulations of energy demand for buildings is given by law, the buildings must be changed in their construction (walls, windows, insulation) and their ventilation. The demand to save the greatest possible part of energy is justifies a mechanical ventilation system. This kind of system allows a controlled ventilation and in combination with a heat recovery system is it possible to reduce the expenditure of energy. The following paper describes ventilation systems recently introduced in Germany to reach a maximum of comfort with low energy demand.

2. Ventilation of residential buildings

As everyone knows, the function of the ventilation of residential buildings is to create comfortable indoor air quality. As far as "comfort" is concerned, we always talk about the thermal comfort, the temperature and the air velocity, and forget that there are also other important parameters. The heat transfer from the occupants is radiation, convection, and also evaporation of moisture. The latter is mainly due to breathing, but occasionally also occurs through the skin. Approximately 20 - 22% of heat loss from a person doing regular activity is evaporation of moisture. We produce water vapour and this inevitably leads to uncomfortable indoor air quality.

3. Improvement in the window areas

Frequently, there are discussions to improve the insulation of the buildings by increasing the layers of insulation material on the walls. In the next few years it is necessary to improve the thermal quality of windows. There are already many different kinds of windows on the market and research will help to improve the particular window constructions currently available.

An easy way to improve the windows is to use multiple glass with thermal insulated roller shutters. Radiopacity or radiopaque foils can be partitioned

between the glass of the window to trap the energy of the sunlight during the day and the long-wave thermal energy of the building during the night. This idea is, at the moment, in development and prototypes are on the market and currently being tested.

As for the indoor surface temperature in which we are interested at the moment, we can reach a k-value of less than $1.0 \text{ W/m}^2\text{K}$ in the window area. We should not insulate the walls repeatedly but rather do something in the window area in order to get a symmetrical indoor surface temperature to meet the demand of comfort and humidity. It should be clear where the thermal insulation has to be placed because the k-value is only one parameter and the storage the other. An old rule of thermodynamics is that we have to install the thermal insulation always on the cold face, but that means in buildings, in winter on the outside and in summer on the inside.

4. Ventilation heat requirements

Figure 4.1 illustrates the percentage of the ventilation heat requirements to the total heat requirements –according to the kind of insulation against loss of heat of the building– compared to the transmission heat requirements.

It is possible to decrease the transmission heat requirements with certain insulation measures on all parts of the building covering, but the ventilation heat requirements as a rule does not change. There is, regardless of the way of ventilation, a certain amount of energy necessary to heat the supply air from the outdoor temperature up to room temperature. As better the insulation of a building, as higher is the percentage of the ventilation heat requirements to the total heat requirements.

The left beam in figure 4.1 shows the annual expenditure of energy of a single family dwelling. This building, built before 1978, needed approximately $290 \text{ kWh/m}^2\text{a}$, which means nearly a fuel consumption of 28 l fuel oil $/\text{m}^2\text{a}$. The right beam illustrate the expenditure of energy by using a mechanical ventilation system with heat recovery.

Since 1982 a regulations of energy demand for buildings is given by law. The second beam shows the conditions of the present situation in Germany. The result shows the reduction of the transmission heat requirements clearly. That means, that the losses, due to the uncontrolled ventilation

have a main share in the total expenditure of energy. The inset of a heat recovery system leads to improvements by nearly 15% related to the total expenditure of energy.

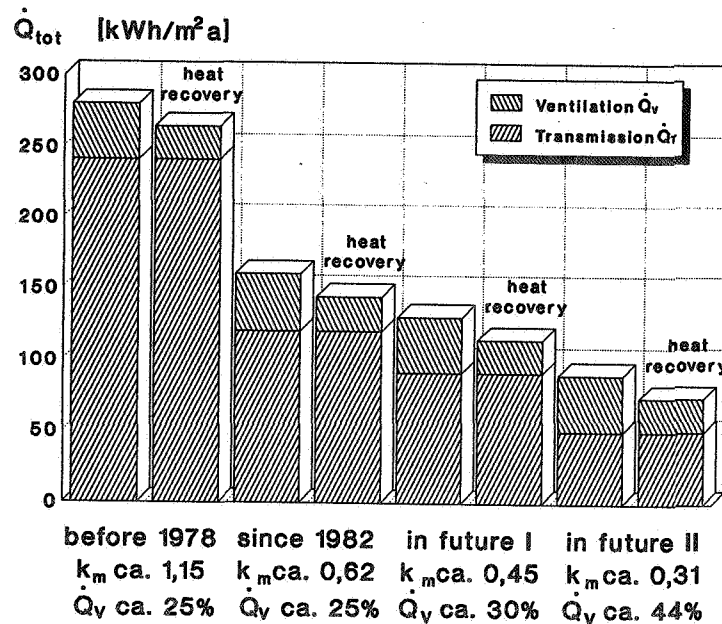


Figure 4.1: Relationship ventilation-/transmission heat requirements

By intensifying the regulations of energy demand in buildings (k-value reduced to 30%), only a slight increase of energy saving is possible. To obtain values of about 60 to 70 kWh/m²a is only possible with a heat recovery system. Without using the heat of the return air -without the inset of a heat recovery system-, the k-values must be minimized. In this case we have to ask for the cost effectiveness.

By using a ventilation system with heat recovery it is possible to save 35% of the total filament energy demand for one single-family dwelling. Furthermore, the CO₂-emission of for example a fuel heating system goes down to 1/3 approximately.

5. Heat recovery in residential buildings

We have different ways to use a heat recovery system in residential buildings. The best way is to extract the air from the kitchen, the bathroom and the toilet, because these are the rooms with the highest pollution. The

supply air is coming into the bedrooms and the living rooms. It is also possible to change it over during the night to have more supply air in the bedroom and during daytime more in the living room. All air is going through a heat exchanger.

The following describes ventilation systems with heat recovery, which are most common in Germany at the moment. Table 5.1 explains the components and the symbols for the skeleton sketch of the ventilation system in figures 5.1 - 5.4.






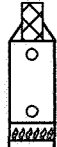


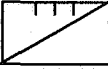



	heat exchanger		fan
	air heater		heater
	evaporator		gas heating system
	compressor		outdoor air
	condensator		supply air
	exhaust air		return air

Table 5.1: Components and symbols for a ventilation system

Figure 5.1 shows a mechanical ventilation system for single rooms with a plate heat exchanger. This system is used for single rooms if there are moisture problems (decentral unit). The supply air temperature is lower than the room air temperature, therefore a special installation is necessary to avoid draughts. It is also possible to install an extra heater before the supply air gets into the room. The supply- and the exhaust air fan are both on the same shaft with one driving motor. This system is independent from the heating system and it saves a part of the energy by a plate heat exchanger.

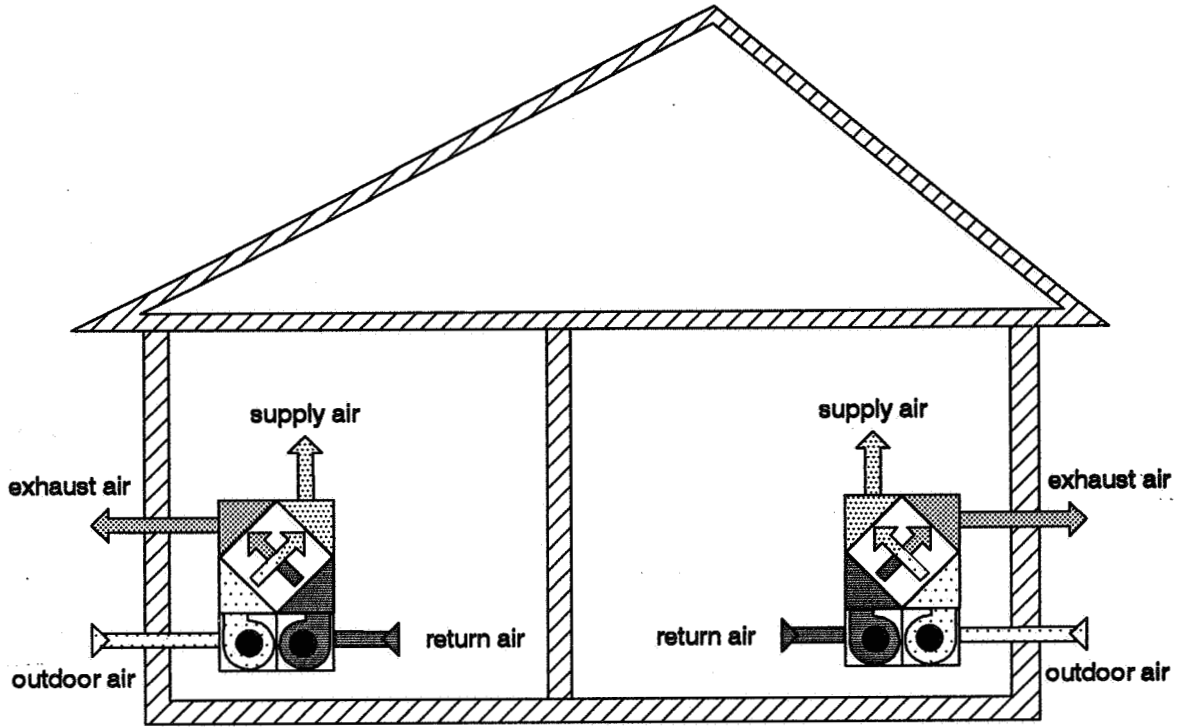


Figure 5.1: Ventilation system for single rooms

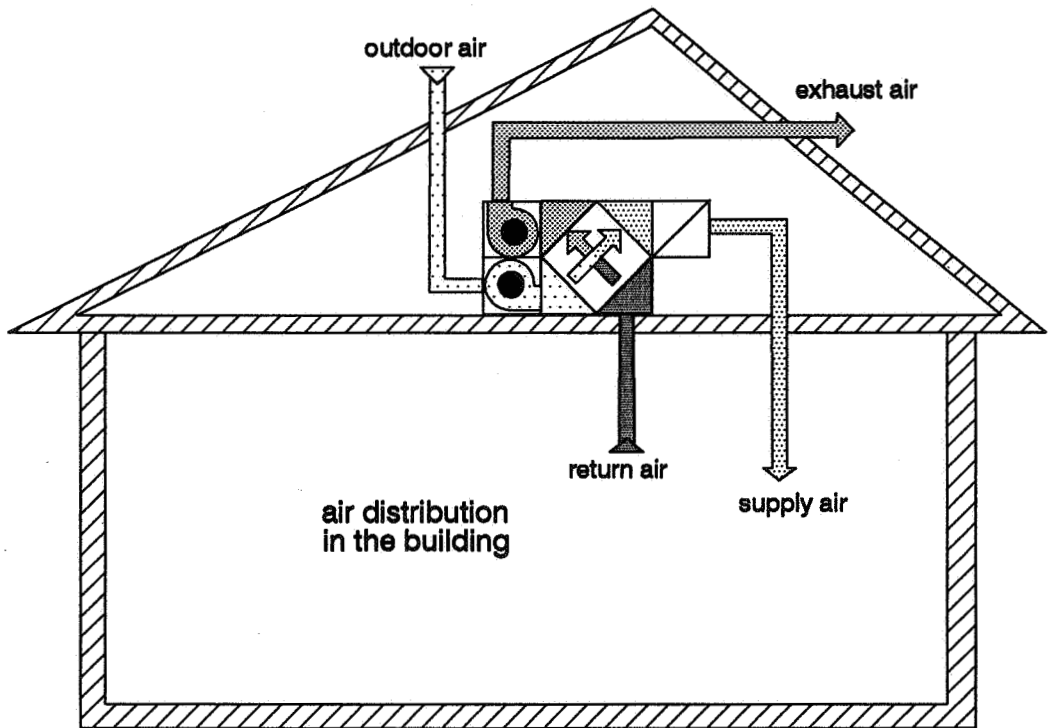


Figure 5.2: Ventilation system for one dwelling or one single family building

A simple system for dwellings or single family buildings is illustrated in figure 5.2. It concerns a central unit with a heat exchanger, and a reheater for the supply air. The position and the type of construction of this ventilation unit can be done for the dwelling in different ways. For example, horizontal in the loft, vertical in the dwelling or hanging combined with a hood in the kitchen or from the ceiling in the area of the hall. This system is independent from the heating system and the reheating of the supply air is made by an electrical heater or by an air/water heat exchanger, which is combined with the heating system.

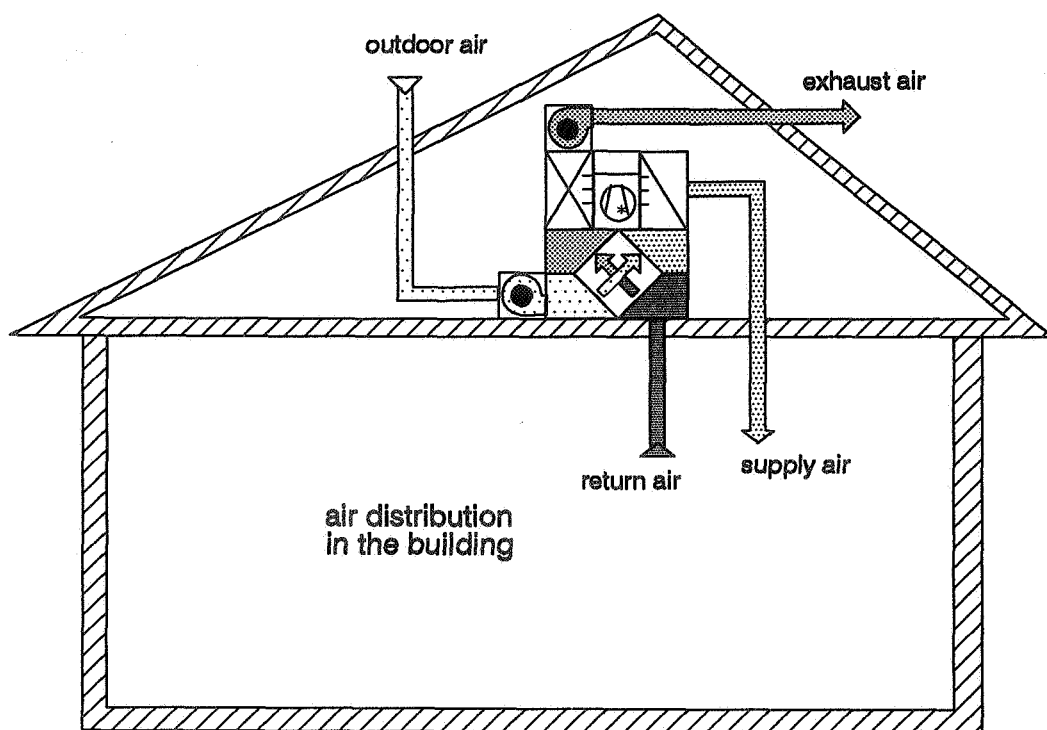


Figure 5.3: Ventilation system with heat exchanger and heat pump

Figure 5.3 shows a ventilation system with heat exchanger and heat pump. The application of this system is also in dwellings or single family buildings and the position and the type of construction is the same as in the system in figure 5.2. The heat recovery is made by a plate heat exchanger and a heat pump, which is added. The heating capacity is larger than the ventilation heat requirements, that the transmission heat requirements can be covered partly. Additional heat capacity is in a high insulated building only necessary if the outdoor temperature t is lower than $0 - 5^{\circ}\text{C}$.

If there is a gas heating system in the dwelling or single family building it is possible to use a ventilation system, which is illustrated in figure 5.4. The central ventilation unit should be installed near the rotate water heater. When the flue gas is mixed with the exhaust air the regulations of chimneys for the exhaust air ducts has to be considered. In this part of the ductnetwork negative pressure must be guaranteed. For this reason the exhaust air fan must be installed near the external covering of the building. The reheating of the supply air by a heat exchanger is integrated in the heating system. The control device is installed separately in the supply air with a thermostat valve. In this system, the heating capacity is larger than the ventilation heat requirements, that the transmission heat requirements is covered partly.

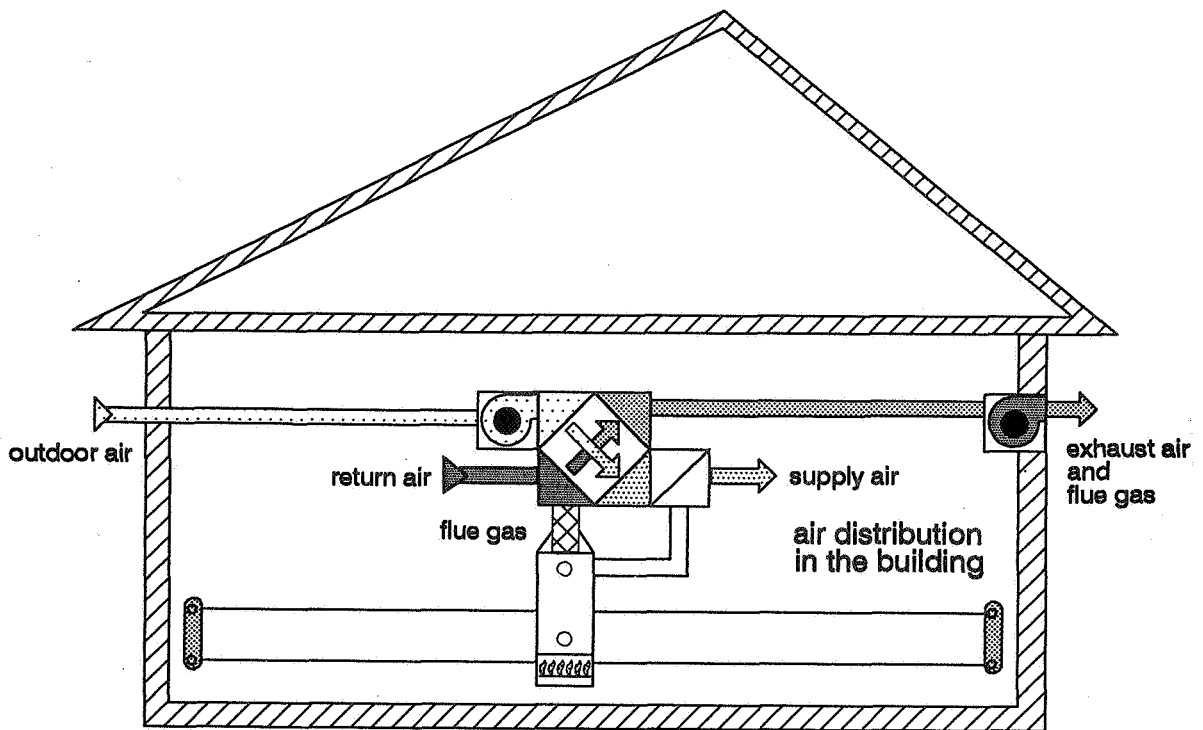


Figure 5.4: Ventilation system combined with the heating system

**Ventilation for Energy Efficiency and Optimum
Indoor Air Quality
13th AIVC Conference, Nice, France
15-18 September 1992**

Poster 11

**Interaction of Heat Load and Air Supply in CAV
Systems.**

J.L.M. Hensen

**Eindhoven University of Technology, Group FAGO,
HG 11.77, P O Box 513, 5600 MB Eindhoven, The
Netherlands**

SYNOPSIS

By means of parametric analyses, the paper describes how the "constantness" of a Constant Air Volume system is affected by temperature differences resulting from heat load variations or otherwise. Several design related parameters are considered.

The paper starts with the background, then an outline of the (simulation based) approach, and how calculations were performed. Results are shown with respect to consequences for volume flow rates and for energy consumption.

The paper finishes with some conclusions, indicating there is a "flaw" in current ventilation standards, that it is hard to make real constant volume system, some preliminary conclusions with respect to energy consumption consequences, and that this type of problem really needs an integral (simulation) approach of building and systems.

1 INTRODUCTION

To minimize the energy consumption related to the distribution of air, a HVAC system could be dimensioned based on constant (and preferably as low as possible) air flows. In such a Constant Air Volume (CAV) design the fresh air flows to the various building zones are supposed to match the fresh air demands. In practice the latter is dictated by governing ventilation standards.

When designing a CAV system, it is common practice to assume constant air temperatures (ie fluid densities). In reality this is not so since the outdoor temperature varies and because the heating or cooling power of a CAV system is controlled by changing the supply air temperatures. Due to buoyancy forces and other density related effects, the air distribution to the various spaces will therefore vary with time.

In order to give some qualitative and quantitative information of the consequences - for flow rates and energy consumption - due to this "constant air temperatures" assumption, parametric studies were carried out based on simulations for a reference CAV HVAC system. These simulations were performed with a modelling environment, which supports analysis of coupled heat and fluid flow.

This paper now continues with a brief outline of the calculation method, a description of the reference CAV system and the results of the parametric studies. It finishes with some conclusions in terms of ventilation standards, flows, energy consumption, design decisions and future work.

2 CALCULATION METHOD

In earlier publications a full account has been given of the internal workings of the *ESP^R* simulation environment both with respect to energy simulation in general (Clarke 1985) and with respect to simultaneous heat and mass flow simulation (Clarke and Hensen 1991, Hensen 1991). An outline of the approach which is used could be: during each simulation time step, the mass transfer problem is constrained to the steady flow (possibly bi-directional) of an incompressible fluid along the connections which represent the building/ plant mass flow paths network when subjected to certain boundary conditions regarding (wind) pressures and/ or flows. The problem reduces therefore to the calculation of fluid flow through these connections with the internal nodes of the network representing certain unknown pressures. A solution is achieved by an iterative

mass balance technique in which the unknown nodal pressures are adjusted until the mass residual of each internal node satisfies some user-specified criterion.

Each node is assigned a node reference height and a temperature (corresponding to a boundary condition, building zone temperature or plant component temperature). These are then used for the calculation of buoyancy driven flows (or stack effect) which are obviously of importance in the current context. Since the approach for buoyancy calculations has already been described in an earlier paper (Clarke and Hensen 1991), this will not be repeated here.

The in ESP^R incorporated flow simulation module *mfs* offers many different flow component types. In the current context, only the flow conduit (duct), flow inducer (fan) and common orifice flow (opening) types were employed. What follows is a brief description of these specific component types, in order to show how fluid densities are taken into account. For a full description of all available flow component types, the reader is referred elsewhere (Hensen 1991).

For fluid flow through a conduit (ie. a duct or a pipe) with (a) uniform cross-sectional area, (b) no pressure gain due to fan or pump, and (c) steady-state conditions, the sum of all friction and dynamic losses ΔP is found from:

$$\Delta P = fL\rho\bar{v}^2/2D_h + \Sigma C_i\rho\bar{v}^2/2 \quad (Pa) \quad (1)$$

where f is the friction factor (-), L is the conduit length (m), D_h is the hydraulic diameter (m), \bar{v} is the average velocity (m/s), and C_i is the local loss factor due to fitting i (-).

The local loss factors represent dynamic losses resulting from flow disturbances caused by for example: entries, exits, elbows, bends, obstructions, etc. Numerical values for the local loss factors can be found in literature.

The friction factor depends on the type of flow, which can be characterized by the Reynolds-number: $Re = \bar{v} D_h/\nu$ (-) where ν is the kinematic viscosity (m^2/s). In ESP^R distinction is made between three regions: for $Re \leq 2300$ laminar flow is assumed, for $2300 < Re < 3500$ a transition region is assumed, and for $Re > 3500$ the flow is assumed to be turbulent. In the current context we only deal with the latter case. For turbulent flow the friction factor is calculated from an explicit approximation of the implicit Colebrook-White equation, which is sufficient accurate for most technical purposes:

$$f = 1/[2 \cdot \log(5.74/Re^{0.901} + 0.27 \cdot k/D_h)]^2 \quad (-) \quad (2)$$

where k is the absolute wall material roughness (m).

The mass flow rate through eg a duct can now be calculated from a "known" pressure difference by:

$$\dot{m} = A \sqrt{\frac{2\rho\Delta P}{fL/D + \Sigma C_i}} \quad (kg/s) \quad (3)$$

where A is the cross-sectional area (m^2). Because, effectively, we have an implicit formulation for \bar{v} , calculation of \dot{m} involves an iterative solution method (fixed point in this case).

Due to practical reasons (ie. lack of detailed data) fan performance modelling is usually based on an empirical approach. According to Wright and Hanby (1988), for system simulation studies an empirical model of fan performance is most appropriate. Fan performance is usually characterized by a curve such as shown in Figure 1, which relates the total pressure rise to the volume flow rate for a given fan/pump speed and fluid

density.

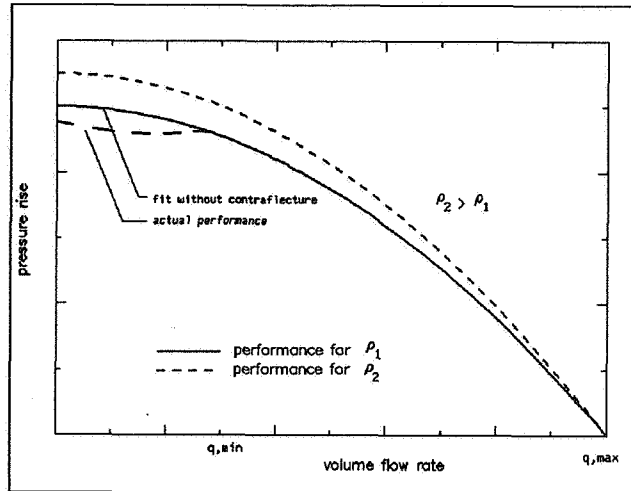


Figure 1 Schematic fan performance curve

As suggested by Figure 1, it is not uncommon for a performance curve to contain points of contraflow, with up to three different flow rates possible at certain values of fan pressure. This causes difficulty in solving for the flow rate. In practice however, it is usually recommended that the fan operates in the region away from the contraflow points. Therefore, the flow characteristic may be modeled with a performance curve that does not include the contraflow as long as it is checked that the fan does indeed operate inside the valid region (if during the simulation the flow rate is outside this region, a warning is issued).

In ESP^R, fan performance is represented by a cubic polynomial:

$$\Delta P_{act} = \frac{\rho_{act}}{\rho_{norm}} \left\{ a_0 + a_1 \left[\frac{\dot{m}}{\rho_{act}} \right] + a_2 \left[\frac{\dot{m}}{\rho_{act}} \right]^2 + a_3 \left[\frac{\dot{m}}{\rho_{act}} \right]^3 \right\} \quad (Pa) \quad (4)$$

and

$$\dot{q}_{min} \leq \frac{\dot{m}}{\rho_{act}} \leq \dot{q}_{max} \quad (m^3/s) \quad (4a)$$

where ΔP is the total pressure rise across the component (Pa), act denotes the actual conditions, $norm$ denotes normalized conditions for which the a_i fit coefficients ($Pa/(m^3/s)^i$), the \dot{q}_{min} lower validity, and the \dot{q}_{max} upper validity limit of the polynomial (m^3/s) have been derived.

The term ρ_{act}/ρ_{norm} follows from the so-called fan law (stating $\Delta P_{act} = \rho_{act}/\rho_{norm} \Delta P_{norm}$) and corrects for air densities which differ from "standard air" conditions (usually dry air, 101.325 kPa and 20 °C; ie $\rho_{norm} = 1.20 \text{ kg/m}^3$). The equation above requires an iterative approach to determine the mass flow rate for a given pressure difference. In this case, a fail-safe combination is used of bisection method (slow but safe) and Newton-Raphson method (simple and fast).

A basic expression for turbulent flow through relatively large openings (e.g. a purposely provided vent or a restriction in a duct), is the common orifice flow equation. If expressed as mass flow rate this is given by:

$$\dot{m} = C_d A \sqrt{2\rho\Delta P} \quad (kg/s) \quad (5)$$

where C_d is the discharge factor (-), and A is the opening area (m^2).

In the equations above the fluid density and the fluid viscosity depend on the direction of flow, ie. the temperature of the sending node.

3 RESULTS

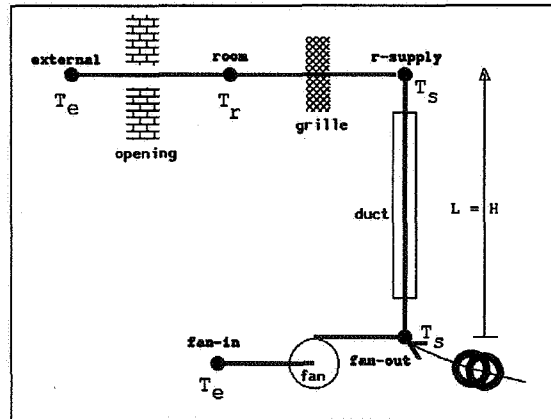


Figure 2 Schematic system lay-out

The present study started from a simplified - part of a - CAV system as schematically shown in Figure 2. The system may be used for fresh air supply and heating or cooling,[†] and comprises a fan (backward-curved blades) - with a performance characteristic quite like Figure 1 - operating at a fixed rotational speed, delivering maximum $360 \text{ m}^3/\text{h}$ at zero pressure rise, respectively maximum 125 Pa pressure rise at zero flow (ie coefficients a_0 to a_3 in equation 3: $125.0, 0., -12500., 0.$); a $.125 \text{ m}$ circular duct (wall roughness $.15 \text{ mm}$) with a local loss factors sum of 5 (-); an inlet grille specified as an opening of $.006 \text{ m}^2$, and an opening from the room to outside of $.02 \text{ m}^2$. At the fan outlet, heat is injected or extracted - resulting in a certain supply air temperature - in order to heat or cool the room. There is no heat loss or gain in the duct. The windspeed is assumed to be zero; ie only system and stack effects are considered. Variables of interest here are height H , duct length L , outdoor air temperature T_e , and supply air temperature T_s . Obviously the latter is related to the building heat load; ie. in a CAV system the supply air temperature will have to increase when the heat load becomes larger.

3.1 Air Flow Rates

For this CAV system, simulations were performed in order to predict the influence of the various variables. The results with respect to flow rates are presented in the following. For clarity, only one variable is varied at a time; all other variables are kept at "base case" values, ie: $H = L = 6 \text{ m}$; $T_e = 6 \text{ }^\circ\text{C}$ (close to average Dutch heating

†

In heating or cooling mode the air flows would probably be larger than those employed in the present examples. However since these additional flows consist of recirculated air (entering the system at a "constant" temperature) these would only introduce a constant offset in the present calculations and are therefore left out of consideration.

season value); and $T_s = 50\text{ }^\circ\text{C}$.

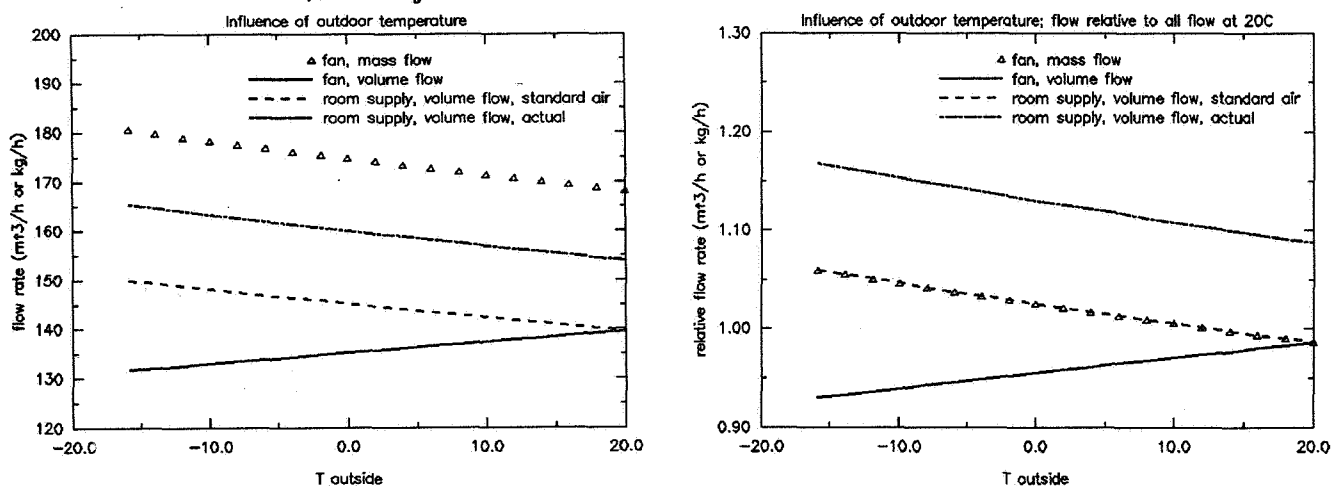


Figure 3 Absolute and relative influence of outdoor temperature; for $H = L = 6\text{ m}$ and $T_s = 50\text{ }^\circ\text{C}$

Figure 3 shows the influence of outdoor temperature variations on mass and volume flow through the fan, and on both the actual and normalized (ie standard air) room supply flow rate. The right hand side figure also shows the flows but now relative to those in case all air temperatures would be $20\text{ }^\circ\text{C}$; ie resulting when density differences would not be taken into account.

It is clear that the flow through this system is affected, although the fan law states that volume flow rate through a fan is independent of density. The latter holds only if the density is constant. The fan volume flow rate variations in the current system are caused by density differences throughout the system. The heat input to the air supply (resulting in $T_s = 50\text{ }^\circ\text{C}$) has two opposite effects: (1) a stack effect which has a positive influence on the fan volume flow which increases linear with increasing $T_s - T_e$; and (2) results in a higher volume flow in the duct (and thus velocity and pressure loss ΔP according to equation 1) relative to the situation where the air temperature and densities are constant. This has a negative influence on the fan volume flow rate, but this effect increases quadratic with increasing $T_s - T_e$. As shown in Figure 3 the net result for the current configuration is that fan volume flow decreases when the outside temperature drops.

In terms of room air supply this still results in higher flow rates when the outside temperature decreases (7% higher when $T_e = -16\text{ }^\circ\text{C}$ instead of $20\text{ }^\circ\text{C}$). Not surprisingly the room supply flow is $\approx 10\%$ higher in reality (ie at $50\text{ }^\circ\text{C}$) than when expressed in terms of standard air ($20\text{ }^\circ\text{C}$). It is surprising however that in most ventilation standards (eg ASHRAE 1989) there is no mentioning whatsoever that required flows are (not ?) expressed in terms of standardized conditions.

Figure 4 shows the absolute and relative (again to the all $20\text{ }^\circ\text{C}$ case) influence of supply air temperature on the normalized room supply flow rate for various outdoor temperatures (ranging from heating to cooling conditions). Also shown is the case where $T_s = T_e$, ie as in mechanical ventilation. In that case the fan flow rate will be independent of outdoor temperature, which is obviously not true for the normalized supply flows (which are $\approx 293 / T_e * \text{fan volume flow}$).

For a given outdoor temperature, the room supply flow decreases with increasing supply temperature. When the system is designed such that the flow rates match flow demands

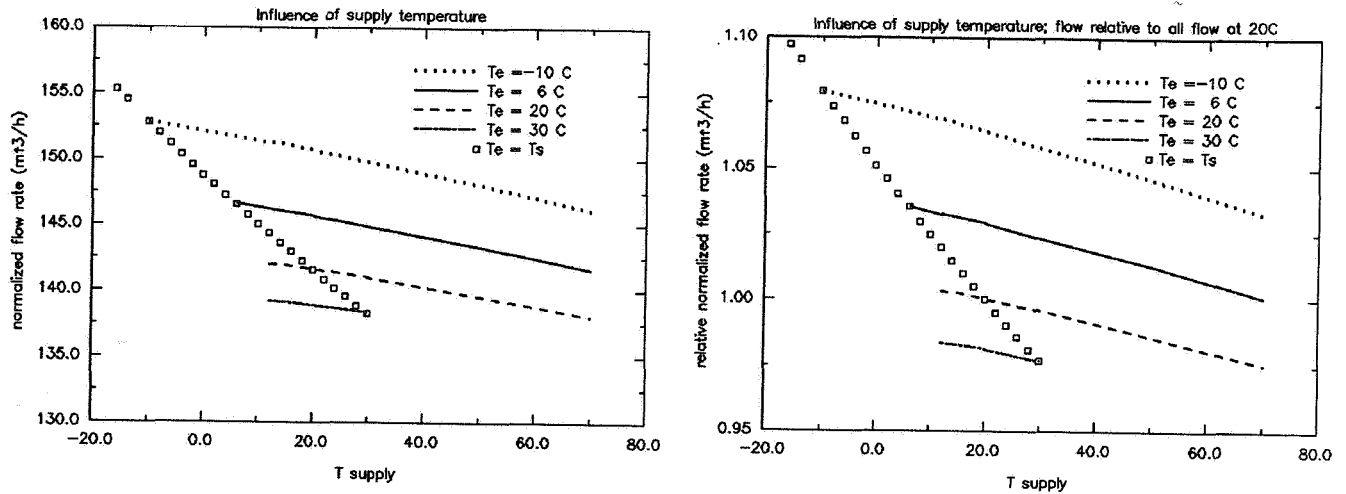


Figure 4 Absolute and relative influence of supply temperature; for $H = L = 6\text{ m}$ and various outdoor temperatures T_e

- assuming all air temperatures are $20\text{ }^\circ\text{C}$ say - the actual flows will be up to $\approx 8\%$ too high depending on outdoor and supply temperatures. ‡ In heating conditions the situation "improves" (ie flows closer to design values) when the supply temperature increases; in cooling conditions when the supply temperature decreases.

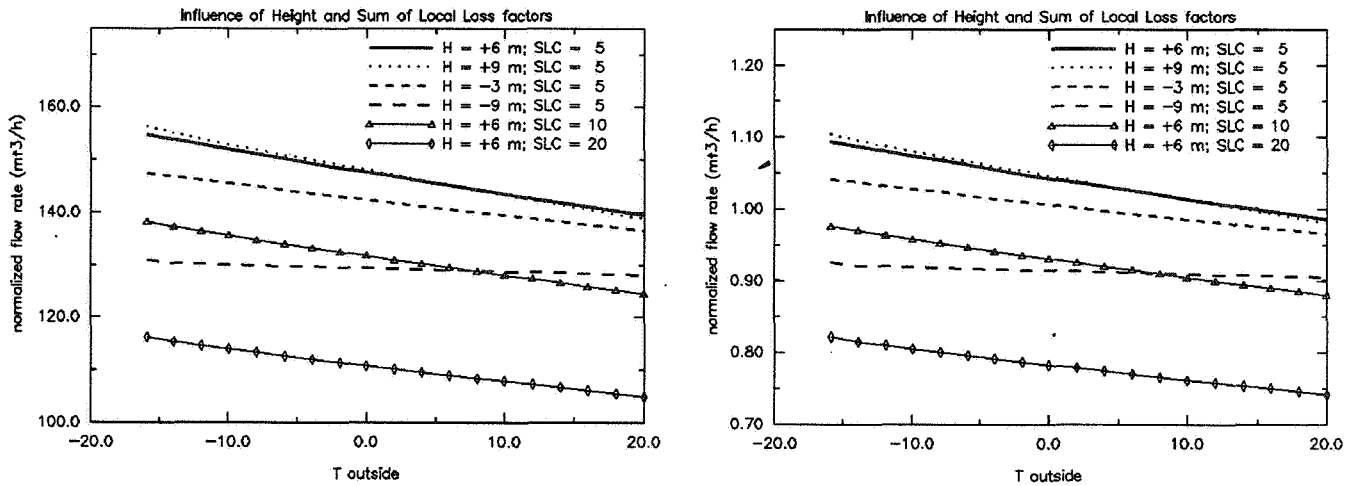


Figure 5 Absolute and relative influence of outdoor temperature for $T_s = 50\text{ }^\circ\text{C}$, various heights H ($L = \text{abs}(H)$) and various sums of local factors (denoted SLC)

Obviously the influence of density differences in the system, is affected by system parameters like height, duct length and dynamic losses due to fittings etc. Some indications are given in Figure 5 which shows the absolute and relative (to all $20\text{ }^\circ\text{C}$ case) influence of outdoor temperature assuming a fixed supply temperature and various

‡

Note that outdoor and supply temperature do not necessarily correlate. High temporary heat loads (and thus high supply temperatures) may also occur after a thermostat set back period. Also, if the heat input is on/off controlled (as opposed to modulating control), the total heat input period - and not the supply temperature - will correlate with outdoor temperature.

values for the parameters above. Note that the duct length is equal to the height difference. When plotted against changing supply temperature, comparable results would be found since the density difference is the governing parameter. A positive increase of height H has two opposite effects: (1) both duct length and pressure loss increase, but (2) stack pressure (negative for +ve height) decreases. For the given configuration and supply temperature, these two effects almost balance out. Since for negative heights (fan above the room) stack pressure increases, these two effects enhance each other in that case. This is clear from Figure 5, which also shows that the relative influence of outdoor temperature variation (ie the slope of the line) becomes smaller as height becomes more negative. This suggests that in the current configuration it is better to locate the fan and heat supply above the room. We may expect the opposite for cooling conditions (ie locate fan and heat "extractor" below the room). Obviously in case of system location on an intermediate level (servicing spaces above and below; as is common in high rise buildings) at least some of the serviced spaces will be affected all the time (depending on whether in cooling or heating mode the rooms below or above).

Figure 5 also shows the influence of local loss factors. Apart from the obvious decreasing flow rate, an increase in local losses also results in a lesser dependency on outside temperature. But of course, this also results in additional energy consumption of the fan for an equal flow.

3.2 Energy Consumption

In terms of energy consumption, it is obvious that fresh air supply in excess of demand will result in increased energy consumption in case of heating conditions and in case cooling is needed and outdoor temperature is above room temperature. Only when cooling is needed and with outdoor temperature below room temperature, fresh air supply in excess of demand is favourable.

As elaborated in the previous paragraph the actual supply flow rate at any time during the heating / cooling season depends on a number of inter-related factors like: outside temperature, supply temperature, system flow characteristics, system lay-out, etc. The supply temperature depends on the heat load which in turn depends on outside temperature, occupancy pattern, and system control.

It may be clear that in the current context, a detailed performance evaluation of a particular building and HVAC system configuration in terms of energy consumption can only be achieved through an integral building / systems (simulation) approach. At present, work is in progress to evaluate energy consumption related aspects of various CAV HVAC systems when used in domestic or small commercial buildings. Due to time and space constraints this work is not further described in the current paper.

To give some quantitative indication of the additional energy consumption due to excessive fresh air supply: in Dutch low-energy houses and small commercial buildings, approximately 50% of the fuel consumption for space heating is due to ventilation. So if the ventilation would be on average 10% higher than actual demands, the total fuel consumption would be $\approx 5\%$ higher than strictly necessary. This may not seem much, but starting from a low-energy building it is very hard to make some additional savings and a feasible saving will usually be of the same order of magnitude (ie a few percent).

4 CONCLUSIONS

Since the volume flow of air is strongly affected by temperature it is at least surprising that in many ventilation standards there is no mentioning whatsoever that required flows are (not ?) - supposed to be - expressed in terms of standardized conditions. Here it was assumed that in fact "standard air conditions" are implied.

By parametric analyses, it was demonstrated that a real Constant Air Volume system is almost impossible to achieve in practice. During the majority of time, a CAV system will either provide too much fresh air which implies waist of energy, or too little fresh air which may have consequences for the indoor air quality.

The relative influence of temperature variations becomes less when the system is above the serviced rooms in case of heating mode. The opposite is true for a system in cooling mode. The relative influence of temperature variations also becomes less when the pressure loss in the (duct) system increases. This will increase fan power consumption however.

Energy conservation by eliminating excessive (ie sup-standard) fresh air supply caused by temperature effects in CAV heating and ventilating systems, may be expected to be in the order of 5% annually in case of low-energy domestic and small commercial buildings in The Netherlands.

Although the results are for an imaginary (but realistic) system the trends are expected to be valid for many CAV systems. The actual air supply rates and energy consumption consequences for a particular building configuration will be the result of many complicated interactions with opposite effects. This makes it extremely difficult - if not impossible - to create simplified design-aids for this purpose. Detailed building performance evaluation can only be achieved through an integral building / systems (simulation) approach.

References

- ASHRAE 1989. "Ventilation for acceptable indoor air quality," ASHRAE Standard 62-1989, American Society of Heating, Refrigerating and Air-Conditioning Engineers, Atlanta, GA.
- Clarke, J.A. 1985. *Energy simulation in building design*, Adam Hilger Ltd, Bristol (UK).
- Clarke, J.A. and J.L.M. Hensen 1991. "An approach to the simulation of coupled heat and mass flow in buildings," in *Proc. 11th AIVC Conf. Ventilation System Performance held at Belgirate (I) 1990*, vol. 2, pp. 339-354, IEA Air Infiltration and Ventilation Centre, Coventry (UK).
- Hensen, J.L.M. 1991. "On the thermal interaction of building structure and heating and ventilating system," PhD dissertation Eindhoven University of Technology (FAGO).
- Wright, J.A. and V.I. Hanby 1988. "HVAC component specification: fans," Energy conservation in buildings & community systems programme. Annex X : system simulation (S12), International Energy Agency. Operating agent: University of Liège



**Ventilation for Energy Efficiency and Optimum
Indoor Air Quality
13th AIVC Conference, Nice, France
15-18 September 1992**

Poster 10

Operation of Passive Stack Systems in Summer.

A.J. Cripps^{*}, J-R. Millet^{}, J-G. Villenave^{**}, D.
Bienfait^{***}**

*** Building Research Establishment, Garston,
Watford, England**

**** Centre Scientifique et Technique du Bâtiment,
Marne La Vallée, France**

***** formerly of CSTB**

OPERATION OF PASSIVE STACK SYSTEMS IN SUMMER

SUMMARY

The ventilation rate in a building depends on many things, one of which is the air temperature. The air temperature in turn depends in part on the ventilation rate. The effects of this relationship are generally overlooked in both thermal and ventilation models.

To study this effect a model has been developed which integrates the models GAINÉ and SILONA developed at CSTB. This allows the prediction of the natural ventilation rates caused by the actual temperatures in the building.

It has been used for predicting summertime temperatures and ventilation rates for a range of different ventilation and thermal parameters. In particular the difference between night and daytime ventilation rates and pollutant levels has been examined. The extract flow is found to be more stable at night than in the day.

1) INTRODUCTION

There has been a lot of work done on the ventilation of dwellings in winter. In those conditions there is a need to balance air quality against the desire to minimise heat losses.

In the summer the problems are different. The need for good air quality in all rooms remains, but there is often a problem of overheating. Problems to be overcome include the failure of wind dependent systems in calm weather and occupants concerns about leaving windows open.

For these reasons a study of the effectiveness of natural ventilation in summer was necessary. A system based on a vertical duct or passive stack from the living space was investigated using a computer code. This type of ventilation works by the stack effect which drives ventilation because of the difference in temperature between the air inside and outside the building. It can help to serve rooms which are otherwise hard to ventilate.

The model was produced by linking two existing models developed at CSTB. These were models of the ventilation and thermal performance of a building in isolation from each other. Results are presented for a range of building parameters, to give the significance of each one. The analysis concentrates on the value of extract flow predicted.

2) THE COMPUTER MODEL

MTV is a computer model which combines a ventilation model, GAINÉ, with a thermal model, SILONA. These two models are representations of different aspects of a building, and both were written at CSTB.

2.1) Description of GAINÉ

GAINÉ is a model of ventilation in multi-storey dwellings. Each level is treated as a separate zone, but each is linked to a common ventilation shaft. The model calculates the pressure in every level of the building and the duct, using iterative methods to balance the mass flows in and out of each level.

The equations used in the model are described elsewhere [1], but the model will be described briefly here. It is a normal 'mass balance' model, which assumes the following:

- (a) A homogeneous air temperature in each room, perfect mixing
- (b) That air is incompressible
- (c) Steady state conditions
- (d) The air inlet and extract opening are at the same level
- (e) Infiltration can be represented by a single opening

Since GAINÉ did not include open windows I have introduced the equations for flow through a large opening from the model SIREN [1], which are the same as those used in the Building Research Establishment's model BREVENT [2].

2.2) Description of SILONA

SILONA [3] calculates the changes in temperature of a building with time, assuming a simple, fixed ventilation rate. It is a tool for studying heat transfer, but it is incomplete if there is much variation in ventilation rate with temperature.

It models the heat exchange between a single zone house and the outside world, using an electrical analogue to represent walls and windows by resistances and capacitances. Temperatures in the system are represented by voltages in the electrical model.

Heat exchange between inside and out by conduction, radiation and convection are included. The external temperature, solar gain and internal heat gains are needed for each hour. The model steps through time, recalculating the resultant and air temperatures each hour, using the Crank Nicholson scheme to approximate the governing differential equation. Because the thermal mass is represented by a capacitance, the model includes the delay in the temperature change of the building as compared to the air in it.

2.3) Description of MTV

Because of the interaction between ventilation rate and air temperature both of the above models are seen to be inadequate under some conditions. This is most clear when the ventilation rate is dominated by the stack effect, when there is a direct relationship between the air temperature and the flow produced.

The basic modelling method used is the following, known as the 'ping-pong' method. Each model is called in turn for each hour of each day. GAINÉ calculates the ventilation rate for the current temperatures, wind speed and direction. Then SILONA is called with the current ventilation rate and solar gain information, to predict the internal temperature. Then GAINÉ is called again with

this newly calculated temperature, and recalculates the ventilation rate. This is then used as input for another call to SILONA and so on until the results are consistent.

For this study both models were called three times for each timestep, to ensure that a consistent pair of air temperature and ventilation rate had been calculated. It will be necessary to add a check on convergence to the model for future work. No problems with convergence were observed in this study. In using this method it is assumed that changes in the system, will be small for any period of one hour modelled.

Using Meteorological Data

There are data available for a number of sites in France [4], which allow modelling to be done with real rather than assumed data. From the full data set, data have been extracted, for every hour of the test year, for external temperature, wind speed and direction, and solar radiation on a horizontal surface. While the temperature and wind speed are fed directly to the models the other data require some manipulation to be used in the model.

The wind direction affects the pressures on the surfaces of a building. Data from wind tunnel tests [5, 6] are used to set pressure coefficients on the surfaces, according to the wind direction. For values between those actually measured the model interpolates linearly on the known data.

The solar input data is given for a horizontal surface and must be converted to give the input to the walls of the house. This depends on the orientation of the wall, the date, time, and latitude of the site. The equations used for this were found in, for example, [7].

Calculating a pollutant level

For low ventilation rates it is not meaningful to compare arithmetic average values of the ventilation rate. This is because a large value for one hour may distort the result. A better idea of the effectiveness of a ventilation system can be seen from the calculation of a pollutant level.

In this model a constant rate of production of pollutant, R (gh^{-1}), is assumed. Assuming perfect mixing, and knowing the air change rate, A (h^{-1}), the total mass, m (g), of pollutant in the room is defined by:

$$dm/dt = R - A.m$$

If A and R are constant for one hour, and M_0 is the mass at the start of the hour, then at a time t (hours):

$$m = (M_0 - R/A).exp(-A.t) + R.t/A$$

This model is used in MTV to calculate a total mass of pollutant in the room for each hour, assuming a constant production rate.

3) RESULTS FROM THE MODEL

3.1) The standard data

for a one storey, three room building, of floor area 60 m².

Data for GAINÉ

- 2.5, Height of ceiling (m)
- 4, Length of duct (m)
- 90, Flow through air inlet under 10 Pa (m³h⁻¹)
- 150, Flow into air outlet under 10 Pa (m³h⁻¹)
- 30, Envelope leakage flow under 1 Pa (m³h⁻¹)
- 0.12, Diameter of duct (m)
- 0.2, Cowl suction coefficient ()

Data for SILONA

- 120, Inertia of the room (kgm⁻³)
- 150.0, Volume of room (m³)
- 12.0, 3.0 Area of North wall, window respectively (m²)
- 10.0, 5.0 Area of South wall, window (m²)
- 0.5, 5.8 K value for wall, window (Wm⁻²K⁻¹)
- 0.1, 0.2 Solar factor for wall, window, ()

The K (or U) value is the normal insulation factor for a building component. The solar factor is the proportion of heat from the sun getting through to the room. It is set low for the windows, 0.2, assuming that shutters or blinds would be closed in the day if the windows are left closed. Only the North and South faces of the building are considered in this model.

As well as the solar gains there are additional gains due to the activity of the people in the house. These have peaks at 13 and 20 hours, which correspond to typical peak cooking times.

3.2) Results for the standard data

The standard data as above was used to describe a dwelling, taken to be in Carpentras, in the south of France. The model was run for five months, May-September, to predict whole summer averages. These are shown below, with results predicted from GAINÉ assuming a constant internal temperature. The average external temperature was 22.8 °C for the day, and 15.0 °C for the night.

	T _{in} (°C)	AC (ach)	Extract Flow (m ³ h ⁻¹)	Pollutant Level (g)
Day	28.2	0.30	31.8	39.2
Night	27.7	0.27	36.0	38.3
Day	20.0	0.24	17.9	57.6
Night	20.0	0.21	24.7	56.9
Day	28.0	0.30	31.0	40.0
Night	28.0	0.28	36.2	39.1

} Fixed
Internal
Temperature

Table 1: Results for the standard case

The considerable differences between the results for an assumed temperature of 20 °C and the full calculation show the value of the model. The average values predicted for a fixed 28 °C are close to the MTV results, but day by day results would be wrong.

The night pollutant level is slightly better than the day value, although the average air change rate is slightly less at night. This shows there is a difference between the averaging methods, and that night ventilation is more stable than day ventilation.

Figure 1 gives the distribution of the predicted extract flows. It shows that the day has a wider spread of values than the night. This is due to the wind speed having both greater variation and higher average values during the day.

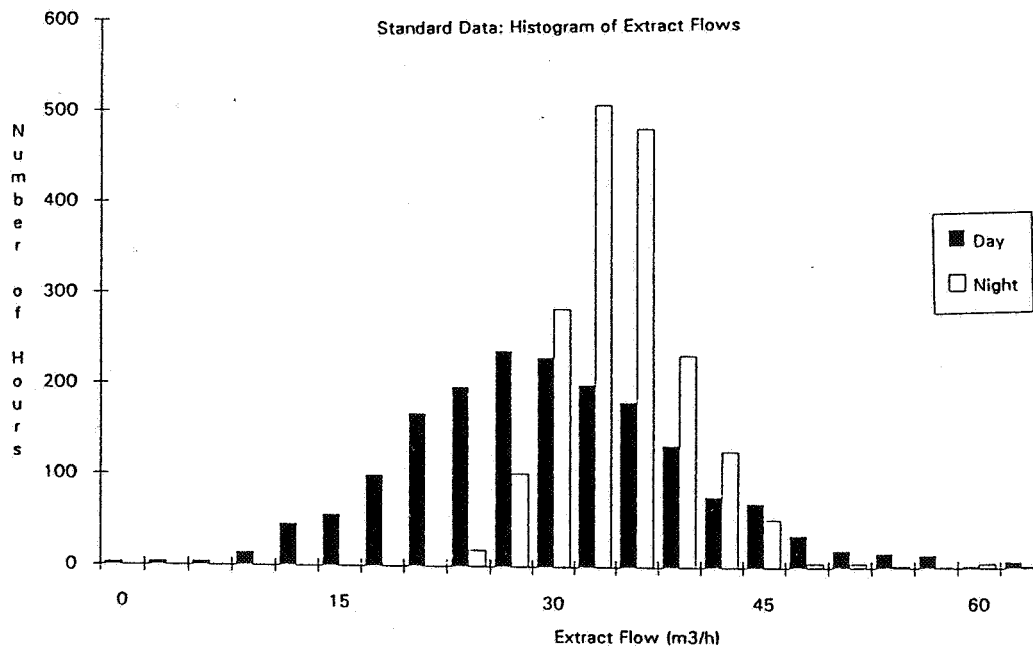


FIGURE 1

However the average of the night extract flows values is higher. This is because the stack effect occurring at night is larger than during the day, due to the lower external temperature. In this case the difference in stack effects is greater than the effect due to the higher daytime wind speeds.

3.3) Sensitivity analysis

The model was run a number of times, changing one parameter at a time to investigate the effect of each. The results are given in table 2. Night is defined as hours 21 to 08, day as 9 to 20.

(a) Inertia

By halving the building's inertia (using 60 (Kgm-3) instead of 120) and hence the thermal mass, the response time of the building temperature is reduced. This results in bigger swings in the internal temperature, but little change in the average temperatures and ventilation rates. In spite of this it is

important for thermal comfort because of its effect on peak temperatures. The inertia would have a bigger effect on the average results in cases where the ventilation rate was better controlled, as for example in g) below.

	T _{in} (°C) Day/Night	AC (ach) Day/Night	Extract Flow (m ³ h ⁻¹) Day/Night	Pollutant Level (g) Day/Night
Standard	28.2/27.7	0.30/0.27	32/36	39/38
(a) Inertia	28.4/27.5	0.31/0.27	32/36	39/38
(b) Solar Factor	33.5/32.2	0.33/0.30	38/41	34/34
(c) Cowl Coeff	28.3/27.3	0.36/0.29	42/40	36/36
(d) AIVC pc's	28.2/27.6	0.31/0.28	40/39	39/39
(e) Wind Shield	28.6/28.1	0.19/0.24	24/34	52/46
(f) Geographical Location of building				
La Rochelle, Average External temperature 19.2/15.4 °C				
Standard	25.6/25.3	0.42/0.37	47/42	27/29
Trappes, Average External temperature 18.0/13.0 °C				
Standard	24.1/23.8	0.33/0.29	38/38	35/38
(g) Results for windows open part of the time				
Open Day	26.8/26.6	5.82/0.27	42/35	4/29
Open Night	23.4/21.8	0.27/3.26	24/37	33/ 6
Occupant control	24.5/23.2	3.24/1.90	31/36	16/15

Table 2: Results for the sensitivity analysis

(b) Solar factor

Increasing the solar factor for the windows from 0.2 to 0.6 causes a large increase in the predicted internal temperature (of order 5°C). The solar factor is the proportion of solar energy getting into the building. The use of blinds, shutters or other protection reduces this factor and the temperature considerably.

(c) Effect of different cowls

By modelling a cowl with a coefficient of 0.7, instead of the value of 0.2 taken as standard, the effect of a better cowl design can be assessed. As expected the extract rate is increased by this change. The effect of this is larger for daytime, (+30%), than at night, (+10%), because of the higher average wind speeds during the day.

(d) Choice of pressure coefficient data

The standard run used pressure coefficient data from CSTB tests. A comparison was made with data from the AIVC for a similar building [6]. The only significant difference is in the predicted extract flows, which are higher for the AIVC data. The overall ventilation rate is nearly the same, so differences in other flows must balance these increases in extract flow.

(e) Location of house 1: Wind Shielding

The wind speeds used come from exposed sites, so to describe a different site the speed used is multiplied by a wind shield factor. Using a value of 0.5 halves the wind speeds and results in much lower daytime extract flows and ventilation rates. This effect is smaller at night, when the stack effect dominates.

(f) Location of house 2: Geographical

To show the effect of different weather types the standard results were compared with those predicted from data for two other sites. These were La Rochelle, on the Atlantic coast, and Trappes, near Paris [4]. For La Rochelle the wind speeds are higher than for the other sites further inland. As a result the extract flows and ventilation rates are higher and the wind effect dominates the stack effect, with the day extract rate higher than the night value. The results for Trappes show little difference between day and night, suggesting a near balance between wind and stack effects. As the location is less windy than La Rochelle and cooler than Carpentras, the result would be expected to fall between those two.

(g) Open Windows

Because of the high internal temperatures being predicted it is necessary to consider the effect on the ventilation caused by different window opening patterns.

(i) Windows open during the day

Opening windows for the day only results in more ventilation but only slightly lower temperatures, so is not ideal.

(ii) Windows open at night

In hot climates it is not unusual to maximise the ventilation at night, and then minimise it in the day, to keep the internal temperature down. This works because the cooler night air removes heat from the thermal mass, which retains this coolness the following day. This is seen to work well, giving a reduction of 5 to 6 °C, as compared to the standard case.

(iii) Occupant controlled window opening

In an attempt to model window opening behaviour, the following system was used; open for $T_{in} > 25$ °C, close for $T_{in} < 20$ °C. This method results in a reduction in temperature, but is not as effective as simple night time opening.

4) CONCLUSION

A model has been produced which provides a link between a thermal and a ventilation model. It introduces into each of these models the effect of the other, producing a tool for studying natural ventilation in summer.

The importance of introducing a thermal model into a ventilation model has been shown by the better information given by the new model, as compared to a model with a fixed indoor temperature.

A sensitivity analysis for the model has shown that:

- . The inertia of the building and the choice of the source of pressure coefficient data does not greatly affect the results.
- . The solar factor is a key parameter for the internal temperature, and must therefore be chosen carefully.
- . The choice of cowl coefficient and the level of wind shielding used have a significant effect on the ventilation rate when it is dominated by the wind.
- . The geographical location of the building is important.

Day flow rates have been seen to vary more than night flows, reflecting the larger variation and average size of wind speeds occurring. Apart from at La Rochelle, where the wind speeds are high, the night time ventilation rate is dominated by the stack effect. As a result, ventilation by vertical duct is seen to be more effective at night than during the day.

REFERENCES

- [1] M.R. Mounajed, "La modélisation des transferts d'air dans les bâtiments: application à l'étude de la ventilation". Thèse de doctorat de l'Ecole Nationale des Ponts et Chaussées. Noisy-le-Grand, October 1989.
- [2] P.R. Warren and B.C. Webb, "The relationship between tracer gas and pressurisation techniques in dwellings". Proceedings of First Indoor Air Infiltration Centre Conference, "Infiltration measurement techniques", Windsor, UK. October 1980.
- [3] J.-R. Millet, "Definition d'un modèle simplifié pour l'étude du confort d'été en climatisation naturelle". CSTB, GEC/DAC-91.26R, March 1991.
- [4] "Conventions unifiées pour le calcul du coefficient B". Cahier du CSTB no 2000, Mai 1985
- [5] J. Riberon, R. Mounajed, "Dimensionnement des Installations de Ventilation Naturelle en Maison Individuelle". CSTB, GEC 88-4457, 1988.
- [6] Table 6.2.2, "Calculation Techniques Guide". Air Infiltration and Ventilation Centre, Great Britain, 1991.
- [7] R. Bernard, G. Menguy, M. Schwarz, "Le Rayonnement Solaire. Conversion Thermique et Applications". Technique & Documentation, 2nd edition, 1980.

**Ventilation for Energy Efficiency and Optimum
Indoor Air Quality
13th AIVC Conference, Nice, France
15-18 September 1992**

Poster 9

**A New Ventilation Strategy for Humidity Control in
Dwellings.**

J.B. Nielsen

**Danish Building Research Institute, Dr. Neergaads
Vej 15, 2970 Hoersholm, Denmark**

Synopsis

This report presents the results from the registration throughout a month of relative humidity, temperature and outdoor air exchange as well as the concentration of carbon dioxide in each room of an inhabited single family house, in which all rooms are ventilated by a mechanical balanced ventilation system with variable air volume. The outdoor air rate is controlled by the relative humidity, which is kept on a value adequate to reduce the living conditions for house dust mites and prevent condensation on the indoor surfaces of the building.

Due to the demand controlled ventilation of each individual room a higher efficiency for reducing water vapors in the dwelling as a whole is likely to be achieved. The results show that it was possible in the context of Danish outdoor climate to maintain humidity conditions that is anticipated to reduce the number of house dust mites in all rooms of a dwelling during more than five months of the year. In all the months the mean daily mechanical ventilation rate is estimated to be 39 % below the level recommended by the Nordic Committee on Building Regulations and in the Danish Building Code. At the same time indoor condensation was avoided on poorly insulated surfaces of the building. The concentration of carbon dioxide was below the level recommended in national ventilation standards.

Synopsis

Ce rapport présente les résultats de l'enregistrement pendant un mois de l'humidité relative de l'air, des températures, du renouvellement d'air de l'extérieur ainsi que de la concentration de dioxyde de carbonique dans chaque chambre d'une maison individuelle habitée, les chambres étant ventilées par un système d'aération mécanique et balancé avec un volume d'air varié. Le volume d'air de renouvellement est réglé par l'humidité relative, qui est maintenue à un niveau suffisant à réduire les conditions d'existence des mites de poussière de maison et à éviter la condensation aux surfaces intérieures de la maison.

Grâce à la ventilation réglée selon les besoins dans chaque chambre de la maison, une meilleure efficacité de ventilation est prévue quant à la réduction d'humidité dans la maison entière. Les résultats démontraient la possibilité, dans le contexte du climat extérieur danois, de maintenir des conditions d'humidité qui réduisent le nombre de mites de poussière dans toutes les chambres d'une maison individuelle pendant plus que cinq mois de l'année. Pendant toute cette période, le volume moyen d'air de renouvellement a été jugé être 39 % au-dessous du niveau recommandé dans le règlement danois de bâtiment. En même temps la condensation intérieure a été évitée aux surfaces mal isolées de la maison. La concentration de dioxyde de carbonique a été inférieure au niveau recommandé dans les normes nationales de ventilation.

1. Introduction

A high concentration of humidity in the indoor air of a building forms growing conditions for house dust mites and mould. Both house dust mites and mould can cause allergy with human beings. In addition, rot and mould may seriously damage the construction of the building. The criteria in building codes and ventilation standards for mechanical ventilation of dwellings have the primary aim of securing the exhaust of humidity from the indoor air, and thus avoiding the disadvantages of too high humidity concentrations. The use of mechanical ventilation guarantees a minimum level of ventilation in dwellings. However, if the ventilation has the same air volume regardless of the ventilation need, the outdoor air exchange and the use of energy for heating may in certain periods be unnecessarily high. Therefore, it is obvious to attempt to regulate the ventilation rate by humidity and only ventilate *where* and *when* humidity occurs. This can be done through a ventilation system which has individual control of air volumes for each room of a dwelling. For instance, humidity in the indoor air can be kept on a level which is just sufficient to prevent condensation on indoor surfaces of the building and below 45% of relative humidity which is the limit necessary to reduce the growth of house dust mites (1,2).

The research results are further described in (7).

2. Purpose

The purpose of the above project was to examine if demand controlled mechanical ventilation with humidity as a regulator can assure:

- The maintenance of an indoor climate with satisfactory physical health conditions, i.e. conditions that reduce the occurrence of house dust mites and fungus spore to a minimum in all rooms of a dwelling.
- The avoidance of condensation on indoor surfaces of the building.
- A reduction of the ventilation needs throughout the majority of the year compared to those recommended by the Nordic Committee on Building Regulations (2) and in the Danish Building Code (3).
- The elimination of the need to adjust the mechanical ventilation system during and after installation.

3. Method

3.1 The dwelling and its inhabitants

A mechanical ventilation system controlled by humidity was installed in a new, 3 room single-family house with a net area of 68 square metres. The house has two inhabitants who are both retired. Once a week during the registration period both inhabitants filled in a questionnaire concerning their indoor activities susceptible of affecting the amount of indoor air humidity.

3.2 The ventilation system

The ventilation system has variable regulation of the air volume and injects air into all rooms including kitchen and bathroom. The system exhausts air from the bathroom and the scullery. The scullery is connected to the kitchen. A regulating damper in the inlet ventilating duct for each room regulates the air volume. The inlet and exhaust performance of the ventilation system is regulated in accordance with the opening or closing of the

five regulating dampers. The ventilation system and the regulating dampers receive their regulating signal from humidity and temperature sensors placed in each room and in the inlet ventilation duct. In the kitchen there is also a manually controlled cooker hood which is not connected to the ventilation system.

3.3 Principles of regulation

The ventilation need for each room is determined by indoor and outdoor air humidity and temperature. The relative humidity in a room should be kept below 45%. In addition, the outdoor air supply must be sufficient to avoid condensation on indoor surfaces. The ventilation system was preset to a performance that will prevent condensation on windows with 2 layers of glass.

The regulations in building codes also aim at removing indoor air pollution. However, if the sources of pollution do not at the same time emanate humidity, the ventilation rate for the tested ventilation system can be insufficient. That is why a minimum ventilation rate of 10 l/s is maintained regardless of the humidity control indicating a lower acceptable air volume.

To ensure that the ventilation rate is not unnecessarily high in the case that the outdoor air already has a high humidity and thus poor or no dehumidification potential, the ventilation rate is set to a maximum of 35 l/s, as recommended in (2,3). A high outdoor air humidity is defined as when the inlet air at room temperature has a relative humidity of more than 40%.

3.4 Control and registrations

Every one minute the ventilation system controller records the temperature and the relative humidity in each room and in the inlet ventilating duct. On the basis of these humidity registrations, the settings of the regulating dampers and later on the ventilation rates are gradually modified in order to meet the indoor ventilation rate control criteria.

As a basis for estimating the indoor air humidity and indoor air quality as well as the regulation possibilities of the ventilation system, the following registrations have been made every 10 minute during more than one month of winter:

- temperatures and relative humidity in each room and in the inlet of the ventilating duct
- carbon dioxide concentrations in each room
- air supply to each room
- total exhaust air volume

The time constant of the humidity and temperature sensors was less than 10 seconds.

4. Results

4.1 Registration period

Since the winter during which the registrations were made was exceptionally warm, only the six coldest nights and the six coldest days have been used for the analysis of indoor humidity and carbon dioxide conditions. During the above registration days and nights, the mean outdoor temperature was 4.2°C and the mean outdoor air humidity was 3.69 g vapour/kg dry air.

For the analysis of the ventilation rate the registrations for more than one month have been used.

4.2 Activities of the inhabitants

On an average, the inhabitants occupied the house for more than 21 out of 24 hours. They felt no need for airing and never opened the windows. Twice a day pillows and eiderdowns were shaken out of the front door for about five minutes. Clothes was washed in a washing machine and dried by hanging in the bathroom and the scullery. During the test period the average cooker hood exhaust was 0.06 l/s.

4.3 Outdoor air supply

The maximum performance of the ventilation plant is registered to be 58.9 l/s, when all regulating dampers are open. This corresponds to an air exchange of 1.3 h⁻¹. If only one regulating damper is open, the maximum possible air exchange in one room can be from 1.4 h⁻¹ in the living room to 7.7 h⁻¹ in the bathroom.

The infiltration of outdoor air into the building has been registered in a summer period at different wind velocities to be between 0.06 h⁻¹ and 0.12 h⁻¹. During the winter registration period of this project, the infiltration of outdoor air is estimated to be 0.15 - 0.20 h⁻¹.

Because of the ventilation being controlled by individual demands it was not necessary to adjust the ventilation system after installation.

4.4 Humidity and temperature

During the six days and nights for which humidity conditions have been analysed the mean indoor temperature varied between 20.5°C in the bedroom and 23.7°C in the living room. The cumulative relative frequency of relative humidity in the kitchen, the bathroom, and the bedroom is shown in figure 1.

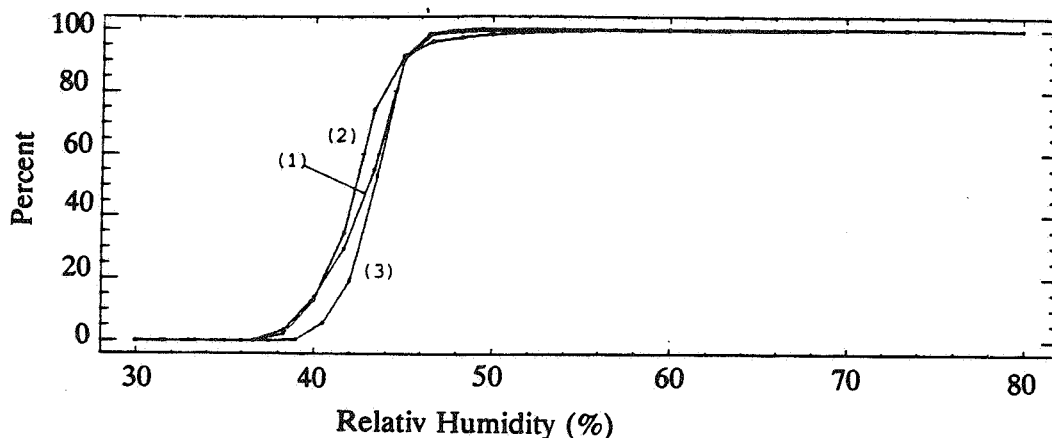


Figure 1. The cumulative relative frequency of relative humidity in the kitchen (1), the bathroom (2), the bedroom (3).

The limit of 45% of relative humidity which is the criterion of preventing the growth of house dust mites has been exceeded in the bedroom and the bathroom for about 10% of the registrations. At a relative humidity of 47% the limit is only exceeded in 1% of the registrations as regards the bathroom and 5% as regards the bedroom.

Condensation on the indoor surfaces of a building occurs first on the surfaces having the lowest temperature. In relatively new Danish buildings these surfaces are the windows and the window frames. Figure 2 shows the limiting cases for the bathroom when condensation is about to occur on thermo windows with two layers of glass having a 12 mm air filled space between the layers.

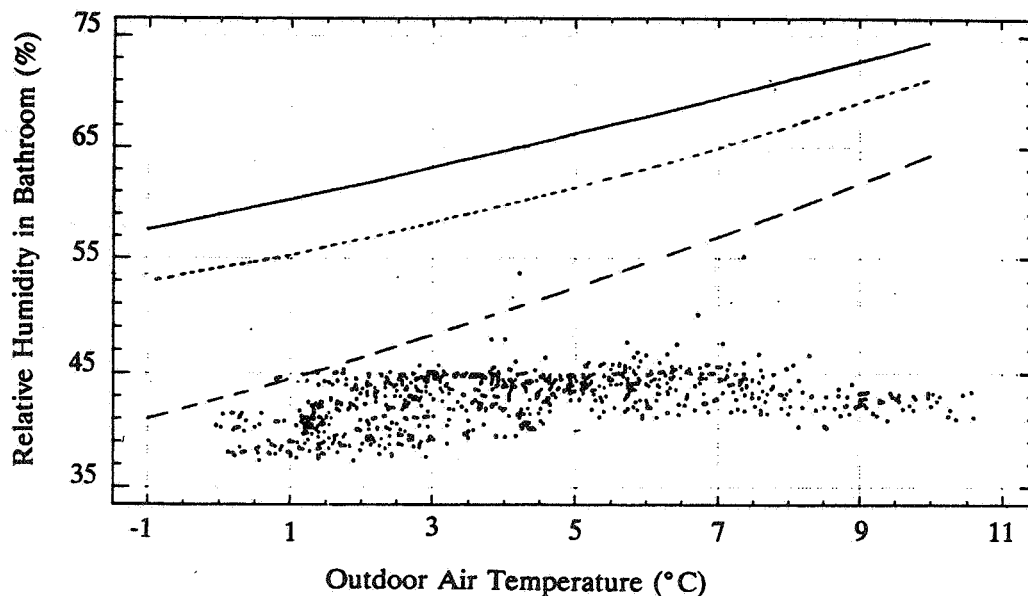


Figure 2. The limit of the occurrence of condensation in the middle of a 1 meter tall window when a curtain has been drawn (--) and when a curtain does not cover the window (---), as well as at the lower edge of the window (---) when a curtain does not cover the window.

The limit of the occurrence of condensation is based on a calculation of the heat transmission of a 1 meter tall window. The heat radiation and the heat convection have been calculated individually and apply for the average glass surface.

Only in a few cases the limits of the occurrence of condensation are exceeded in the middle of the glass surface when the curtain has been drawn, and only two times when the curtain does not cover the window. At an outdoor temperature of about 0°C this curve crosses the ordinate axis of relative humidity at 45%. At an outdoor temperature of less than 0°C the ventilation system must be controlled uniquely by the criterion of condensation, if condensation is to be avoided in the middle of the glass surface with curtains drawn. It was not possible to test the ventilation system controlled by humidity at lower outdoor temperatures than 0°C.

For the other four rooms similar comparisons of limits of the occurrence of condensation and registrations of relative humidity have been made. In these rooms the excesses of the limits of the occurrence of condensation have been even fewer than shown for the bathroom. The inhabitants did not observe condensation on the indoor window surfaces during the test period.

The total amount of humidity developed in the air of the dwelling is calculated to be 12 l of water per 24 hours on an average.

4.5 Carbon dioxide

Interviews with the inhabitants show that they do the same things at approximately the same time every day and night, i.e. they rise, have breakfast, lunch, and dinner, rest, watch television etc. at the same time of day. So it was possible to predict in which room the inhabitants would be at which time. Knowing the concentration of carbon dioxide at different times in each room, it was possible to assess the amount of carbon dioxide that the inhabitants were exposed to during six days and nights. In less than 12% of the time the concentration exceeds 1000 ppm and in less than 2% of the time it exceeds 1200 ppm.

5. Discussion

5.1 Humidity

The criteria that aim at keeping the relative humidity of the indoor air below 45% and at preventing condensation are met in the test building at mean outdoor temperatures below 5.9°C. In Denmark, the mean outdoor temperature is below 5.9°C during 44% of the year. It has not been analysed whether the indoor humidity criteria will be met at mean outdoor temperatures of 5.9°C and above.

In a new study (4), the difference between the absolute outdoor and indoor humidity was registered in 36 single-family houses with constant mechanical exhaust. In 97% of the houses the difference between the absolute outdoor and indoor humidity was below that registered for the present project's test dwelling. In 53% of the houses the total outdoor air volume was below the outdoor air volume of about 30 l/s registered in the test dwelling. At a lower mean inlet air volume more humidity per m³ air was removed from the test dwelling than from the single-family houses on an average. Therefore, the tested ventilation system seems to give a more efficient exhaust of humidity than a ventilation system with a constant ventilation rate.

In (4) the development of humidity per 24 hours was found on the basis of humidity registrations in each of the 36 single-family houses. The indoor humidity was registered in the living room. A similar registration for the test dwelling shows that the total development of humidity is 11.5 litres of water per 24 hours. Only 20% of the houses in (4) are above this level. Therefore, the amount of humidity developed in the test dwelling can be considered sufficient to test the regulation possibilities of the ventilation system.

The analyses in the present test project show that the emanence of humidity from the building construction can be removed through the building infiltration. Therefore, humidity emanating from the building does not affect this project.

The two inhabitants were both retired, but still physically active. However, if the house was inhabited by a family with teenage children, the ventilation need may be higher.

5.2 Carbon dioxide

The registered concentrations of carbon dioxide are generally below the recommendations of 1000 - 1500 ppm found in national ventilation standards (8).

5.3 Outdoor air supply

In dwellings having mechanical ventilation *with a constant ventilation rate*, the exhaust air volume from kitchen and bathroom must be at least a constant of 35 l/s according to the standards in (2, 3).

In (5) and in (6), 38.9 l/s and 33.3 l/s respectively are the recommended values for the mechanical air volume in a dwelling having the size of the test building.

In the present project the possibilities of reducing the mechanical ventilation have been estimated according to the standards and recommendations in (2, 3) and the defined regu-

lation criteria. In (3) an outdoor air exchange of 0.5 h^{-1} is considered to be necessary as a basic ventilation rate in dwellings. This is also part of the estimation. Table 1 shows the estimated reduction of air volumes and air exchange and the period of reduction within the context of Danish outdoor climate.

Standards of comparison	Are reduced to	Reduction in percentage	Period of reduction
35 l/s	21.4 l/s	39%	6 months
0.5 h^{-1}	0.36 h^{-1}	27%	4 months

Table 1. Reduction of air volumes and air exchange

Since an air exchange of 0.5 h^{-1} does not correspond to an air volume of 35 l/s, the two periods differ.

In general, the reduction of air volumes and air exchange in a building will substantially depend of the number of family members and their habits.

5.4 Other pollutions

In the present project the humidity of the air has been used as the parametre of regulation. However, if the pollution for which we are ventilating is for instance gases emanating from furniture and building materials or radon rather than humidity, mechanical ventilation with humidity as the regulation parametre may not be sufficient.

Relatively new results of research indicate that the amount of gases which emanates from furniture and building materials differs considerably. Therefore, a bad choice of furniture and building materials can set the parametre of regulation of air volumes in dwellings with mechanical ventilation. In such cases the ventilation rate obtained by a ventilation system controlled by humidity can be insufficient. This can be avoided by increasing the minimum ventilation rate. Only that means that the reduction obtained of air volumes and air exchange will be less.

5.5 Consumption of electricity

The present project does not involve registrations nor considerations concerning the possibility of saving electricity obtained through the reduction of mechanical ventilation.

6. Conclusion

By the use of a mechanical ventilation system controlled by humidity in all rooms of a dwelling it has been possible to achieve humidity conditions which in the context of Danish outdoor climate can prevent the growth of house dust mites for more than five months of the year. Throughout this period the outdoor air volume supplied by the mechanical ventilation was estimated to be 39% less than stated in the standards and recommendations of (2,3). At the same time, damages to buildings caused by condensation on poorly isolated surfaces are avoided, and the concentration of carbon dioxide in the indoor air is below the maximum level recommended in national ventilation standards.

It has not been taken into consideration whether the demand controlled ventilation system will be profitable and generally applicable.

7. Perspectives of the project

The present project will be followed by an analysis that includes the investigation of mechanical ventilation in 32 flats. Half of the flats will have a ventilation system controlled by humidity, and the other half will have constant ventilation. Comparative studies of the two types of mechanical ventilation will be carried out regarding humidity, outdoor air supply by mechanical ventilation and infiltration, consumption of electricity by the mechanical ventilation system, and the use of energy for heating.

The mechanical ventilation controlled by humidity will only be used in bathrooms and kitchens, and each exhaust ventilator will cover several flats. An internal control of differences in pressure in the ventilation system will regulate the distribution of the exhaust air volume among the flats. In each room there will be a venthole for the supply of outdoor air. The venthole openings and the ventilation rate are regulated simultaneously. The criteria of humidity control will remain the same.

8. Collaboration

The project has been made in collaboration with Danfoss System Controls and with the engineering company Esbensen F.R.I. and is financed by the Danish Ministry of Housing, National Building and Housing Agency.

References:

- (1) Korsgaard, J. The effect of indoor environment on the house dust mite. In P.O. Fanger and O. Valbjørn(eds): *Indoor Climate*, Danish Building Research Institute, Copenhagen 1979.
- (2) Nordic Committee on Building Regulations, NKB, *Indoor Climate - Air Quality*, publication no 61E, June 1991.
- (3) National Building Agency. *Danish Building Regulations for small Buildings*. 1985.
- (4) Bergsoe, N.C. Investigations on air change and air quality in dwellings. CIB W67 Symposium on Energy, Moisture and Climate in Buildings. Rotterdam 1990.
- (5) Ministère Français de la Construction et du Logement. *Code de la construction et de l'habitation*. 1982.
- (6) Verein Deutscher Ingenieure. *Lüftungsanlagen Für Wohnungen*, VDI 2088, Dezember 1976.
- (7) Ministry of Housing, National Building and Housing Agency. *Behovsstyret mekanisk ventilation. Fugt som reguleringsparameter - et pilotprojekt*. Copenhagen, April 1992.
- (8) Raatschen, W., *Demand controlled ventilating System. State of the Art Review. Energy Consumption i Building and Community Systems Programme*, Annex 18, February 1990.



**Ventilation for Energy Efficiency and Optimum
Indoor Air Quality
13th AIVC Conference, Nice, France
15-18 September 1992**

Poster 7

**Draughts Due to Air Inlets: An Experimental
Approach.**

J. Riberon and J.R. Millet

**Centre Scientifique et Technique du Bâtiment, 84
Avenue Jean Jaurès, BP 02, 77421 Marne La Vallée
Cedex 02, France**

ABSTRACT

Draughts due to air inlets are one of the problems to be solved for improving the global performance of mechanical ventilation systems. The CSTB full scale test cell "EREDIS" has been used to quantify draughts risks due to air inlets by measuring air temperatures and velocities with known boundaries of wall temperatures and fresh air. The results allow to improve the design of these inlets and to give advices for a better use in residential buildings. Works are now going on for comparing the experimental results to the ones calculated with a CFD code.

1 - INTRODUCTION

Ventilation systems in residential buildings are primarily intended to insure adequate indoor air quality. They must comply with additional requirements : to limit energy consumptions and to provide a thermally comfortable indoor climate.

In practice, cold draughts due to air inlets may occur in the ventilated rooms. In the rooms where there are draught problems, the occupants often plug up the air inlets or stop the ventilation system and this will decrease the indoor air quality. The occupants too may increase the air temperature to counteract the draught and this will increase the energy consumptions. Therefore cold draughts prevention is a major requirement of air inlets.

Several studies have been conducted in the field of air flow within rooms and a few specific draught studies are available [1 - 5].

The present paper deals with air velocities and temperatures measurements carried out in a testroom at CSTB in order to assess the behaviour of the air jet discharged from a self-regulated air inlet.

2 - EXPERIMENTAL SET-UP

At Marne-la-Vallée, CSTB has a test enclosure, called EREDIS (Enceinte de Recherche sur la Diffusion de l'air et les Interactions Système-enveloppe), devoted to the study and analysis of thermoconvective phenomena inside rooms [6] [7]. EREDIS is a full scale test enclosure with lightweight walls or simulated walls made of water circulation pannels, enabling to bring to steady-state conditions in relatively short delays. It has two original characteristics : variable geometry and monitoring of the walls in temperature or in flux.

The three dimensions of the test enclosure can be modified thanks to the movable suspended ceiling and the three movable inside partitions (see figure 1). The ranges for varying the dimensions of the enclosure enable

the reproduction of a large number of possible room geometries with a single façade, from a small bedroom (L x W x H = 2.7 x 2.7 x 2.5 m) to a large office (L x W x H = 7.2 x 4.5 x 3.0 m).

The inside partitions are adiabatic : they are cavity walls framed with plasterboards insulated outside by 10 cm of polystyrene. The façade consists of chilled water circulation panels, insulated outside. Their inside face can be covered with an appropriate thickness of insulation, simulating the unglazed part of the façade. All glazing geometries can be provided. Outside temperature simulation is by displaying the temperature of the glazing and by supply air at temperature equal to the outside temperature.

In this study, the test enclosure represents a dwelling room with dimensions of 3.6 x 3.6 x 2.5 m equipped with floor heating, uniformly distributed, providing an inside temperature at the centre of the room of 20°C. With a such heating method, the vertical air temperatures differences are minimized. Therefore the air flow patterns due only to the air inlet can more easily be assess. The fresh air is introduced at a temperature of 0°C through a self-regulated air inlet placed above a glazed bay (W x H = 2.0 x 1.4 m), (see figure 2). The surface temperature of the glazed bay is kept at 7°C so that it can simulate an outside temperature of 0°C. The air flow rate of the air inlet is 30 m³/h which corresponds to an air change rate of the room of about 1 ach. Two rectangular exhaust openings are symmetrically located in the sidewalls, at the floor level, far from the air inlet so as not to disturb the air flow in the room.

3 - EXPERIMENTAL PROCEDURE

The fields of air velocities and temperatures were explored by the shifting of a measurement frame in the area of the supply air jet. This exploration method has made it possible to indicate a possible penetration of the cold air stream in the occupied zone. The measurements were carried out in the vertical symmetry plane through the air inlet.

Air temperatures were measured by a platinum resistance sensor. Air velocities were recorded with an constant temperature anemometer DISA 55M01/55M10 provided with an omnidirectional thin-film probe DISA 55R49.

The DISA 55R49 probe using a spherical sensor of small dimensions operated at low sensor temperature it is possible to measure velocities down to 5 cm/s without significant errors from free convection flows created by the sensor itself [8]. Therefore this probe is well suited for measurements air movements in full-scale models of air-conditioned rooms.

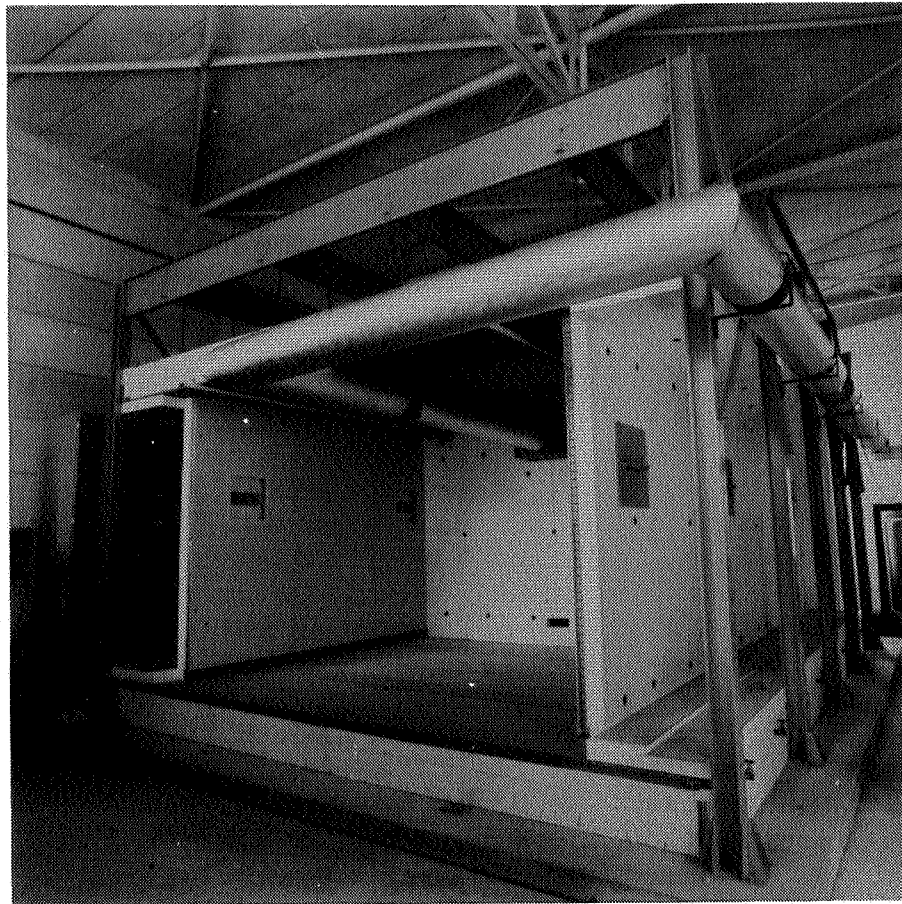


Figure 1 : Outside view of the test enclosure. In this photo, we can make out the lightweight partitions, the suspended ceiling and the supply air network

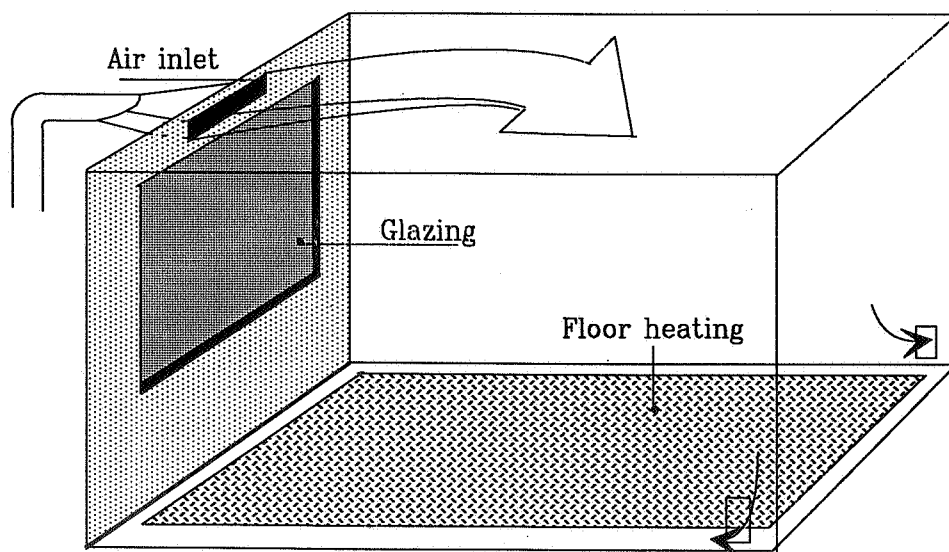


Figure 2 : Sketch of the test enclosure

As the velocity probe is non-temperature compensated and non linearized the real velocity was calculated from the measured temperature and from the measured voltage according to a calibration curve.

The probe was calibrated by using the DISA 55D90 calibration equipment. This equipment produces a variable-velocity low-turbulence free air jet in which the anemometer probe to be calibrated is placed. The relationship between anemometer voltage and air velocity was determined on the basis of twelve calibration points in the range 0 - 1 m/s.

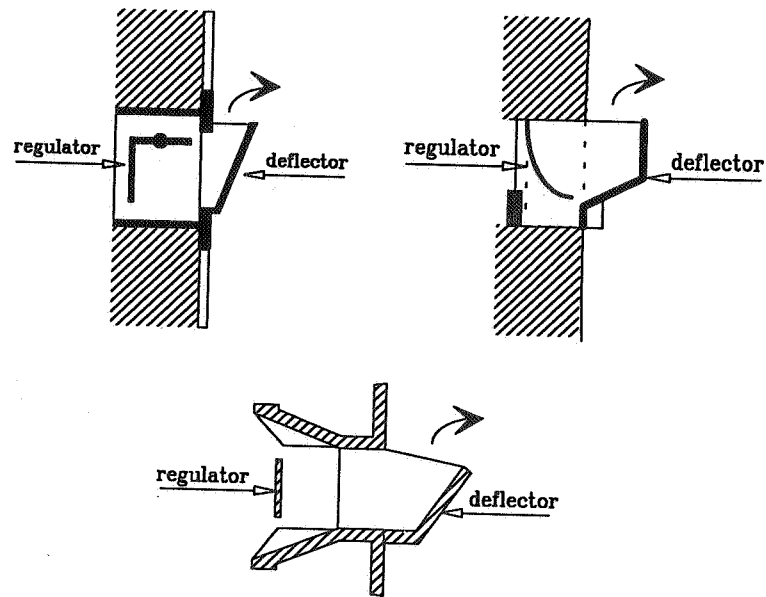
200 velocity measurements were collected at each point, the average of these instantaneous values being used to characterize the velocity at this point. As the temperature change in time was not important, the temperature was not measured at the same rate as air velocity : only one measurement was collected to characterize the temperature at a point. This value was used to accomplish the temperature compensation of the anemometer voltage.

4 - TESTS

In order to assess the risks of cold draughts due to a self-regulated air inlets, tests were performed in the EREDIS enclosure. Various types of self-regulated air inlets marketed in France were tested and the effect of the location of the air inlet on the air flow patterns was analysed.

The way of working of a self-regulated air inlet is the progressive modification of the air passage section of the inlet according to the pressure difference on either side of the inlet. The change in section is as that the air flow rate may be kept constant in a wide range of pressure difference.

The self-regulated air inlets use various air flow control devices : the moving component of the inlet may be either a plastic film shutter or a L profile shutter or a setting stick shutter (see figure 3).



Sketch of various self-regulated air inlet

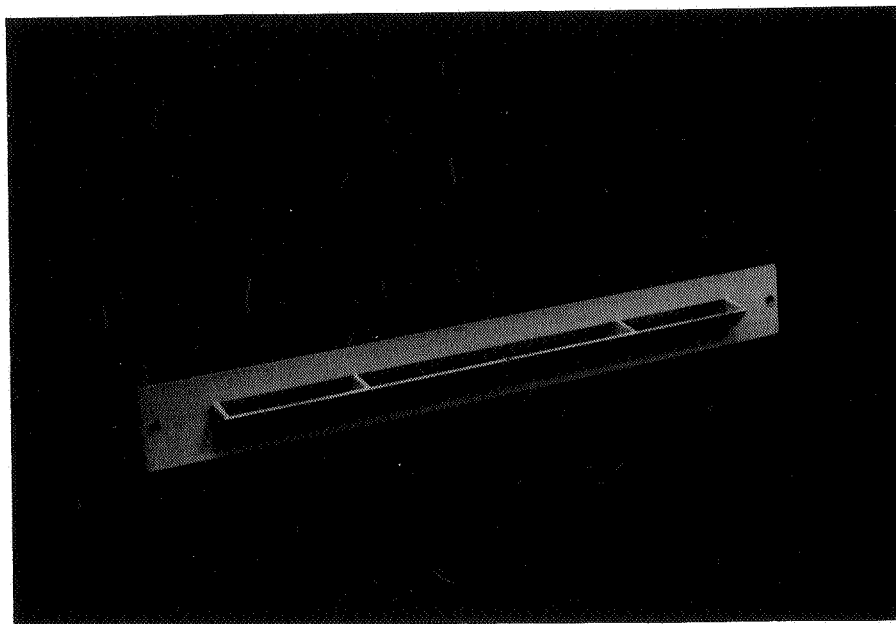


Figure 3 : Self-regulated air inlet devices

Figure 4 depicts a typical flow rate curve of a self-regulated air inlet. These inlets which are in widespread use for more than fifteen years help to prevent uncomfortable draughts when the wind pressure is too high. Also, they contribute to lower heat losses due to cross ventilation.

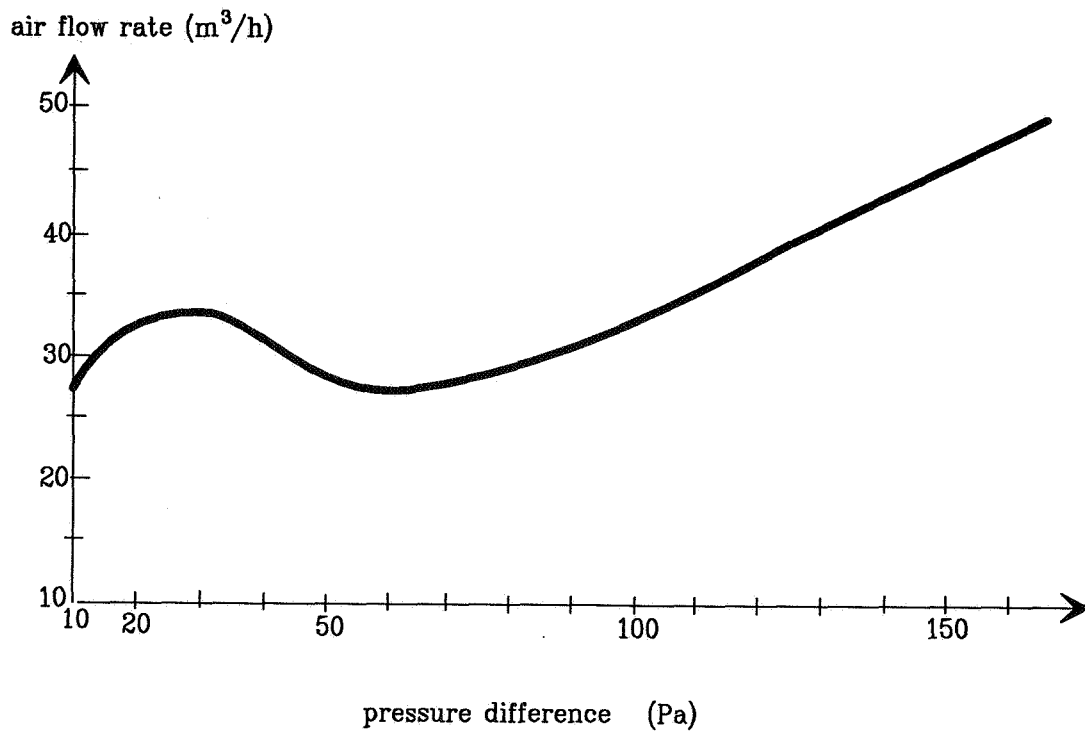


Figure 4 : Self-regulated air inlet characteristic curve

Two sets of tests were performed. In the first, the air inlet was placed in the façade in a vertical position near the ceiling (horizontal air jet). Various distances between the ceiling and the air inlet were chosen : 5 cm, 15 cm, 25 cm. In the second set, the air inlet was installed in the horizontal part of a rolling shutter housing (vertical air jet). The opening is located at 30 cm below the ceiling.

5 - RESULTS

5.1 - Horizontal air jet

The jet issued from the inlet is inclined to stick to the ceiling because the inlet is equipped with a deflector that points the jet upwards.

In addition, since the air inlet is located close to the ceiling there is a tendency for the jet to cling to the ceiling. This effect, called Coanda effect [9], also reduces the influence of temperature differences which normally cause the trajectory of a cold air jet to curve downwards.

The tests have shown that whatever the type of air inlet, when it is located in a vertical wall fairly close to the ceiling, the jet is strongly drawn toward the ceiling and the risk of penetration into the occupied zone is non-existent.

Figure 5 depicts the air jet behaviour issued from a self-regulated air inlet located close to the ceiling. It shows iso-velocity and isothermal maps. The isothermal lines indicates the difference between the air temperature at the centre of the enclosure (20°C) and the local air temperature in the stream.

The air jet behaviour is the result of the combining of the both antagonistic effects :

- thermal forces that incline the jet to curve downwards
- Coanda effect that incline the jet to curve upwards

Figure 5a shows the air jet split up into two parts : the one slightly curves downwards (free jet), the other clings to the ceiling (wall-jet).

5.2 - Vertical air jet

Tests were carried out with a self-regulated air inlet either equipped with a deflector or not. The results have shown the air jet behave like a wall jet running along the cold glazing. When the inlet device is not equipped with a deflector the cross-sectional area of the air jet increases so that the air stream comes into the occupied area (see figure 6).

When the air inlet is intalled in the horizontal part of a rolling shutter housing, it is necessary to deflect the air jet towards the façade ; in all the other cases, the discomfort appears locally near the façade.

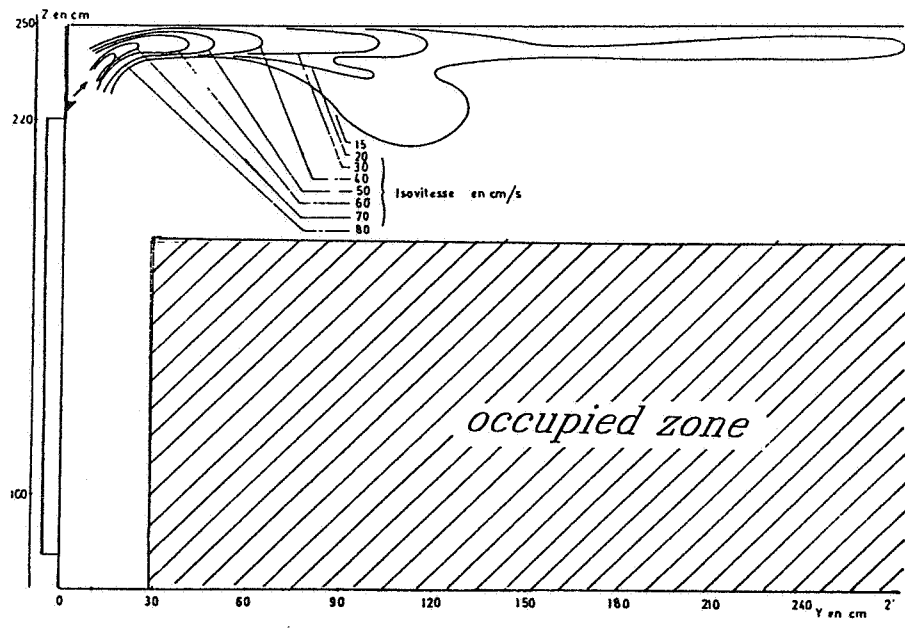


Figure 5a : Iso-velocity map

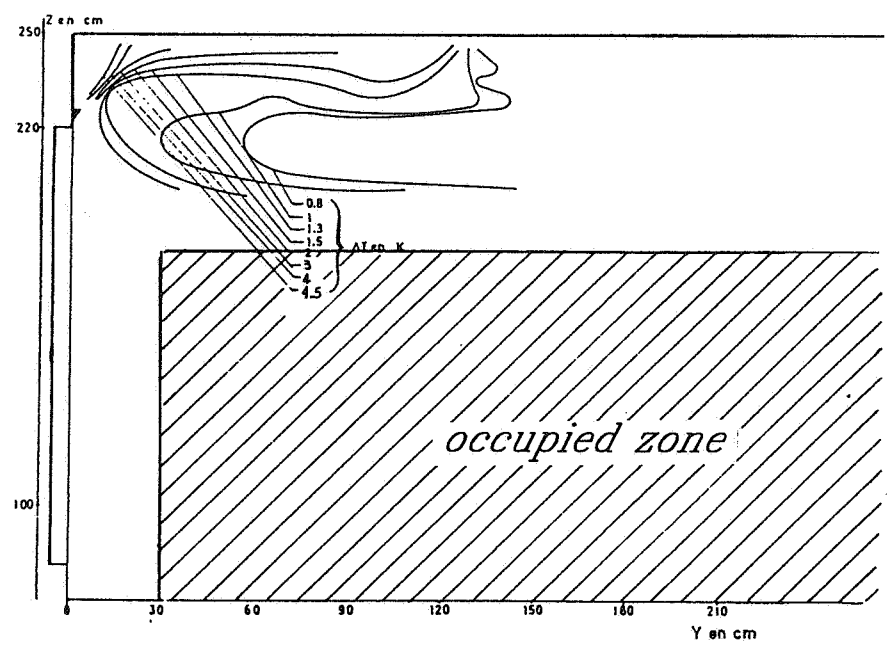


Figure 5b : Isothermal map $\Delta T = t_i - t_x$
 t_i = air temperature at the centre of the room
 t_x = local air temperature

Figure 5 : Air jet behaviour from self-regulated inlet set over a window in vertical position

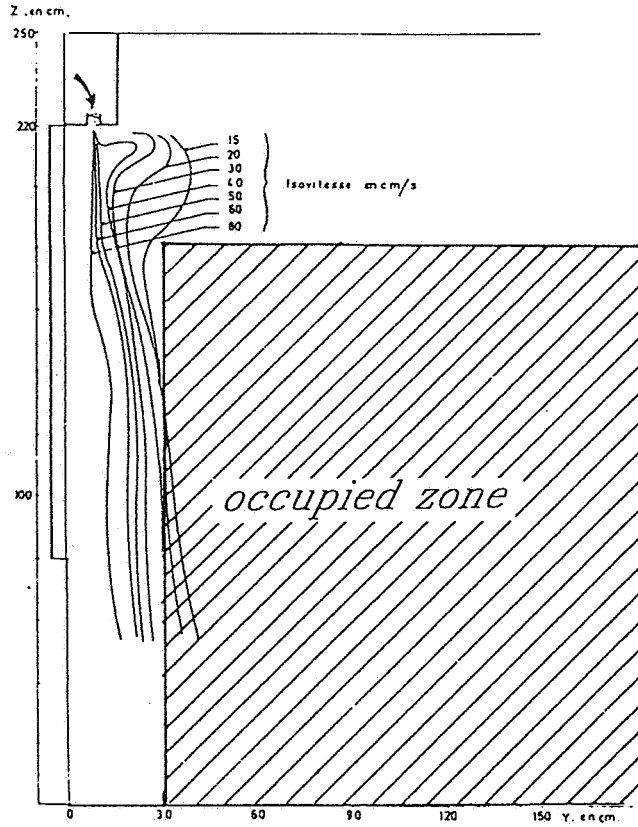


Figure 6a :
Iso-velocity map

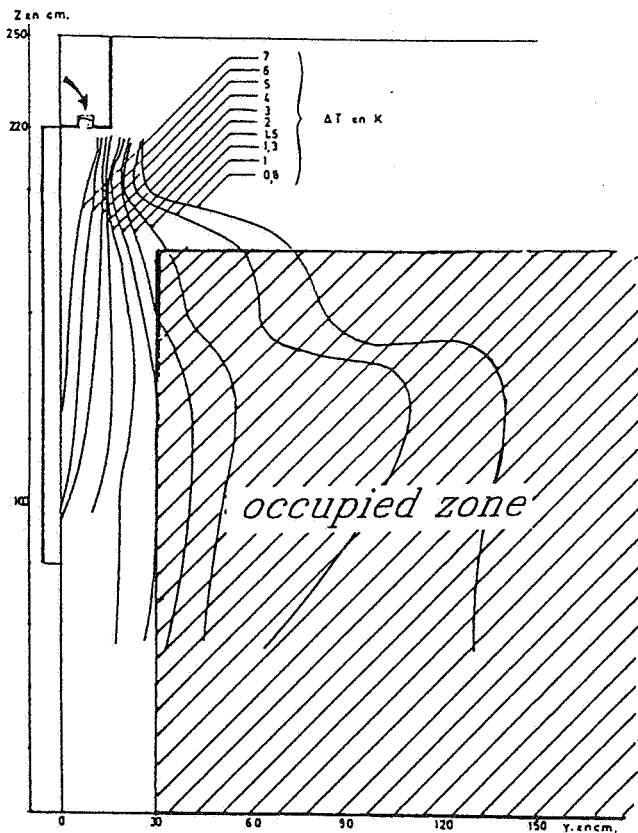


Figure 6b :
Isothermal map
 $\Delta T = t_i - t_x$
 t_i = air temperature
 at the centre of the room
 t_x = local air temperature

Figure 6 : Air jet behaviour from self-regulated inlet set over a window in horizontal position

6 - CONCLUSIONS

In a heated room where the heating provides the thermal comfort of the occupants at the centre of the room, the presence of a ventilation air inlet can affect the comfort conditions at certain points of the occupied area and risk of cold draughts can occur.

Cold draught prevention is based on an adequate air diffusion in order to avoid the penetration of the air jet into the occupied area. The reduction in velocity and temperature difference must be executed outside this area.

When the air inlet is located in the façade so that jet is horizontally discharged, the air jet must be pointed towards the ceiling. The efficient way to avoid draught is the use of a deflector.

When the air inlet is underneath a rolling shutter housing so that jet is vertically discharged, the air jet must be pointed towards the façade ; therefore an air inlet with a deflector must be used. Result without deflector is hardly acceptable.

Thus, this study has shown that experiments in testroom may help to improve the design of air inlet device and their location in room. Also, it has been shown the self-regulated air inlet does not cause uncomfortable draughts if the installation of the inlet device is executed with a few precautions.

Research work is needed to establish correlation between jet characteristics and temperature and velocity field in the room. Nevertheless, the number of experiments to be undertaken to achieve this goal is very high. This is why recourse to numerical approach can enable a faster progress in understanding heat and mass transfer within rooms. Works are now going on for comparing the experimental results to the ones calculated with a Computational Fluid Dynamics code.

REFERENCES

- [1] HOUGHTEN, F.C. GUTBERLET, C. and WITKOWSKI, E.
"draft temperatures and velocities in relation to skin temperature and feeling of warmth"
ASHVE transactions, Vol.44, Paper n°1086, New-York, January 1938.
- [2] RYDBERG, J. and NORBACK, P.
"Air distribution and draft"
ASHVE Transactions, Vol.55, Paper n°1362, Chicago, January 1949.
- [3] CROISET, M. and BIZEBARD, H.
"Ventilation air inlets for dwellings"
NBS Technical Note 710-6, Washington, January 1973.
- [4] FANGER, P.O. and PEDERSEN, C.J.K.
"Discomfort due to air velocities in spaces"
Proceedings of the meeting of commission E1 of the International Institute of Refrigeration, Belgrade, 1977.
- [5] MELIKOV, A.K.
"Quantifying draught risk"
Brüel and Kjaer Technical Review, n°2, 1988.
- [6] RIBERON, J.
"Contribution experimentale à l'étude de la diffusion de l'air dans un local"
Thèse de doctorat de 3ème cycle, Université P. et M. Curie, Paris, Mars 1983.
- [7] RIBERON, J. and HUTTER, E.
"Study of thermoconvective phenomena inside rooms"
Workshop CIB W67, Sophia-Antipolis, April 1989.
- [8] JORGENSEN, F.E.
"An omnidirectionnal thin-film probe for indoor climate research"
Disa Information n°24, May 1979.
- [9] KATZ, P.
"Der Coanda effekt"
Gesundheits Ingenieur n°6, 1973.

**Ventilation for Energy Efficiency and Optimum
Indoor Air Quality
13th AIVC Conference, Nice, France
15-18 September 1992**

Paper 12

**Energy Recovery in Ventilation Systems - A
Worldwide Energy Saving and Environmental
Protection Technology.**

Frank Dehli

**FGK Germany, Marienburger Str.6, D-6900
Heidelberg, Germany**

ENERGY RECOVERY IN VENTILATION SYSTEMS
A WORLDWIDE ENERGY SAVING AND
ENVIRONMENTAL PROTECTION TECHNOLOGY

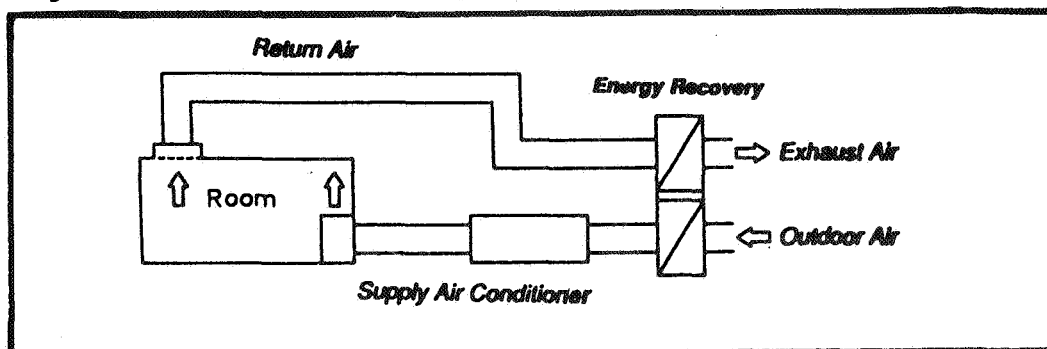
1.0 Energy Recovery

For more than 20 years, energy recovery systems have been operated successfully in European countries in comfort and industrial ventilation systems in order to reduce the heating and cooling capacity as well as to reduce the annual energy consumption for the treatment of supply air. By 1991 the total heating capacity of all installed energy recovery systems in Europe was about 60.000 MW and the equivalent of the annual energy savings was about 10 million tons of oil. This very impressive result of an energy saving technology also includes the annual reduction of emissions of all environmental polluting products: 10 million tons of annual oil savings are corresponding with the reduction of about 50.000 tons of SO₂ and 40 million tons of CO₂. Apart from being an important economic factor both at the private and the national level, energy recovery systems thus also make an important contribution to energy conservation and environmental protection [1].

As shown in Fig. 1, energy recovery in HVAC systems wants the use of sensible as well as latent energy contained in the exhaust air for outdoor air treatment to the greatest possible extent. Therefore the main advantages of energy recovery systems are:

- Reduction of the heating and humidification load demand, which in turn reduces the necessary size and thereby the capital costs of heating plants (boiler, piping, etc.)
- Reduction of the heating energy demand, which reduces operating expenses
- Reduction of the cooling and dehumidification load which reduces the necessary size and thereby the capital costs of the cooling equipment (such as compressor, cooling tower, etc.)
- Reduction of electric energy for refrigeration
- Reduction of air and water pollution due to reduced energy consumption needed for heating and cooling

Fig. 1: Air Conditioning System with Energy Recovery



As the exhaust air conditions hardly change during the annual operation time of a HVAC system it is in general the outdoor air which governs the design, operation and economic efficiency of this energy saving technology. Worldwide there are three different climate regions suitable for the application of energy recovery: moderate climate (wet or semi-dry summers, subpolar), desert climate (dry) and tropical climate (permanent high humidity).

In the past 20 years high energy prices together with high dependence on imported fuel required efficient use of energy, and this in turn resulted in highly developed engineering of ventilation and air-conditioning systems in two parts of the world: Europe - especially in the German-speaking countries and Scandinavia - and the Far East, i.e. Japan [2]. The common feature of these regions is, that these are highly industrialised countries, with their dynamic business-life depending largely on the import of primary energies such as crude oil, natural gas and coal.

As energy prices in the USA and Canada are still comparatively low, the importance of efficient energy utilisation has not yet been fully recognised in these countries, and this is the reason why fewer heat recovery devices are used compared to Europe and Japan.

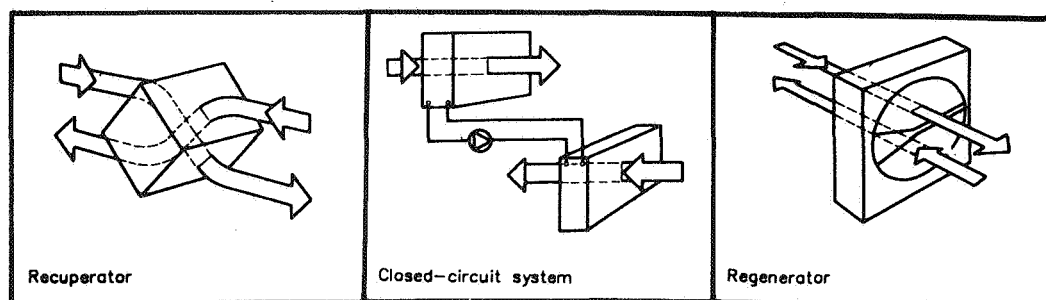
Heat recovery devices can be applied in the following fields [3]:

- High comfort buildings (office buildings, schools, hospitals, hotels, department stores etc.)
- Industrial buildings (production halls and workshops in various industrial branches, e.g. automobile industry, electronic industry, pharmaceutical industry, etc.)
- Process air handling systems (paint-spraying booths, driers and extraction facilities, etc.)

It is necessary for all applications to operate with a high outdoor air rate in order to meet the problems of indoor air quality caused by internally generated pollutions, known as "Sick Building Syndrome" [4].

In accordance with Eurovent 10/1 standard [5] heat recovery devices in Europe are divided into 3 categories (Fig.2):

Fig. 2: Types of Energy Recovery Systems



- Recuperators with plates or tubes, preferably for very small systems and process air handling systems with sensible energy recovery only
- Closed circuit systems with finned heat exchangers connected by pipes, used primarily for modification and retrofit of existing buildings with sensible energy recovery only
- Regenerators with rotary heat storing matrix and combined transfer of heat and humidity, for all fields of application with total energy recovery

The matrix is fabricated in a honeycomb structure of corrugated aluminum or ceramic fiber material with hygroscopic or non-hygroscopic surface.

Based on the experience acquired during many years in regions of moderate climate, and as a result from a growing demand for energy saving HVAC systems, a trend is now noticed towards exporting energy recovery systems from Europe and Japan into countries where different conditions prevail. These are desert countries [6] and the tropics in particular. It has to be mentioned in this context, that the buildings with the lowest specific energy consumption values worldwide are located in Europe and Japan: The office buildings of the NMB Bank in Amsterdam and the Ohbayashi Corporation in Tokyo with a remarkable 110 kWh/m²·a energy consumption for heating, cooling and electric energy supply. In both buildings energy recovery with rotating total energy exchangers, solar energy application and computer control operation are the most important energy saving technologies. The average energy consumption of office buildings today is around 300 to 350 kWh/m²·a [7][8].

2.0 Facts and Figures

In the following, the result of energy recovery in an office building application is calculated for four typical locations worldwide. According to the psychrometric chart and the annual energy consumption diagram, all reduction of capacities, annual energy consumptions, investment costs and the environmental pollutions are derived. As operation time is 8760 hours per year for shorter operation time, equivalent results can be calculated individually. For the environmental pollution the specific figures of a German study on environmental protection [9] are used according to Fig.3

Fig. 3: Specific emissions Kg/MWh final energy

	SO ₂	NO _x	Dust	CO ₂
Oil fired Boiler	0,4	0,31	0,01	370
Gas fired Boiler	0,03	0,16	--	272
Coal fired Boiler	2,82	0,38	0,31	547
Electricity (Oil)	0,6	0,58	--	630
Electricity (Coal)	0,75	0,71	0,09	929

Energy Recovery in Berlin/Germany

Climate Conditions: Moderate Climate

Outdoor Air Rate (50m³/h Person; 10m²/Person) 5 m³/h m²

Energy Supply for Buildings: 60% Oil, 30% Gas, 10% Coal

Energy Recovery (Total Heat Exchanger, 75% Eff.)

Heating Period	5 mths
Cooling Period	2,5 mths
Reduction Boiler Capacity	75%
Reduction Chiller Capacity	30%
Annual Heating Energy Recovery	190 kWh/m ² a
Reduction of Annual Heating Energy	90%
Annual Cooling Energy Recovery	5 kWh/m ² a
Reduction of Annual Cooling Energy	15%

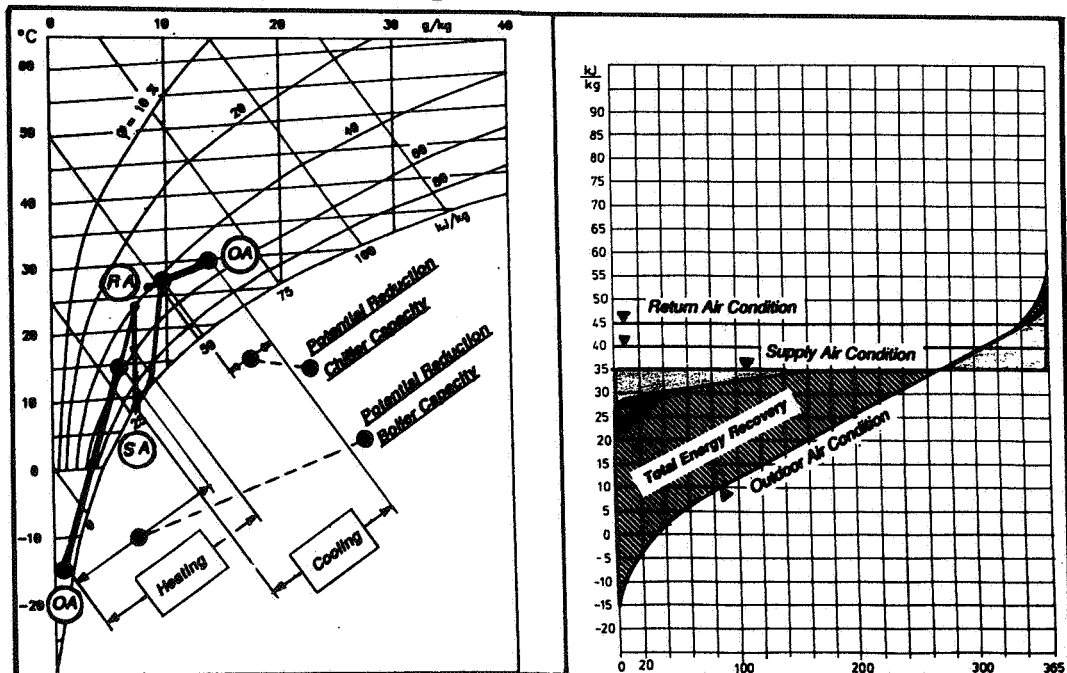
CO₂-Reduction

CO ₂ -Reduction Heating	67 kg/m ² a
CO ₂ -Reduction Cooling	5 kg/m ² a
Total CO ₂ -Reduction	72 kg/m ² a

Reduction Energy Recovery Investment Costs

Red. Boiler Capacity (200,- US\$ per kW)	12,- \$/m ²
Red. Chiller Capacity (400,- US\$ per kW)	7,- \$/m ²
Invest. Energy Recovery (1,40 US\$ per m ³ /h)	7,- \$/m ²
Total Investment Reduction	12,- \$/m ²

Fig. 4: Energy Recovery in Berlin



Energy Recovery in Tokyo/Japan

Climate Conditions: Moderate Climate, wet and humid summer season

Outdoor Air Rate (50m³/h Person; 10m²/Person): 5 m³/h·m²

Energy Supply for Buildings: 70% Oil, 30% Gas

Energy Recovery (Total Heat Exchanger, 75% Eff.)

Heating Period	4 mths
Cooling Period	5 mths
Reduction Boiler Capacity	100%
Reduction Chiller Capacity	50%
Annual Heating Energy Recovery	160 kWh/m ² ·a
Reduction of Annual Heating Energy	90%
Annual Cooling Energy Recovery	25 kWh/m ² ·a
Reduction of Annual Cooling Energy	35%

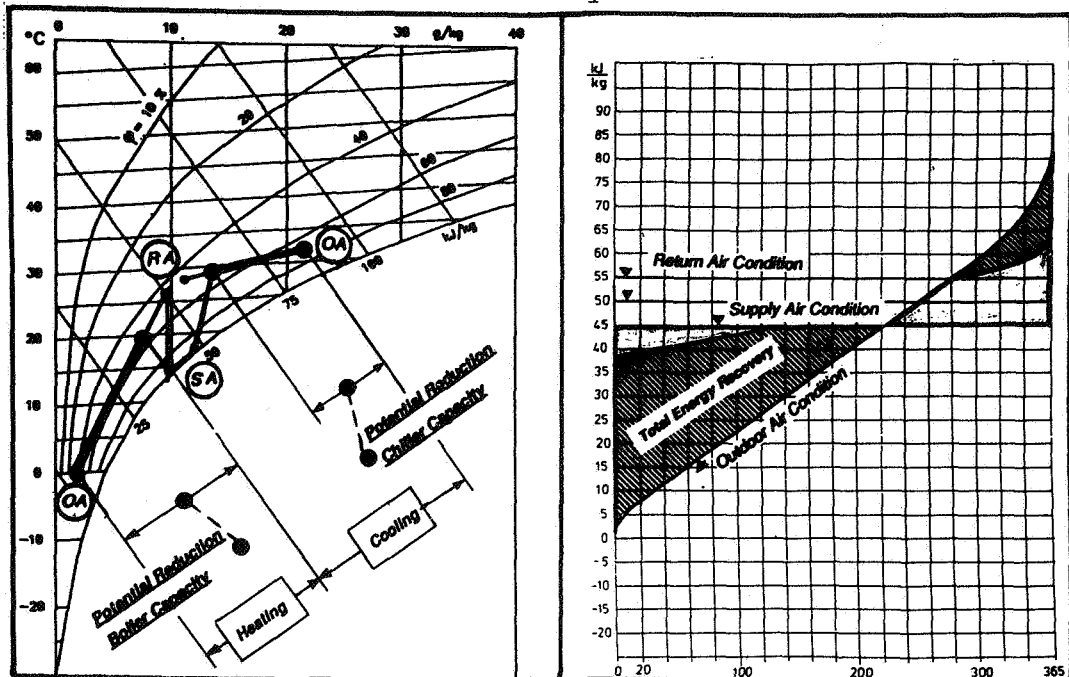
CO₂-Reduction

CO ₂ -Reduction Heating	54 kg/m ² ·a
CO ₂ -Reduction Cooling	9 kg/m ² ·a
Total CO ₂ -Reduction	63 kg/m ² ·a

Reduction Energy Recovery Investment Costs

Red. Boiler Capacity (200,- US\$ per kW)	15,- \$/m ²
Red. Chiller Capacity (400,- US\$ per kW)	13,- \$/m ²
Invest. Energy Recovery (1,40 US\$ per m ³ /h)	7,- \$/m ²
Total Investment Reduction	21,- \$/m ²

Fig. 5: Energy Recovery in Tokyo



Energy Recovery in Riyadh/Saudi Arabia

Climate Conditions: Desert climate, dry and little rain, daily and annual extreme differences of outdoor air temperature

Outdoor Air Rate (50m³/h Person; 10m²/Person): 5 m³/h·m²
Energy Supply for Buildings: 100% Oil

Energy Recovery (Total Heat Exchanger, 75% Eff.)

Heating Period	1,5 mths
Cooling Period	7 mths
Reduction Boiler Capacity	100%
Reduction Chiller Capacity	50%
Annual Heating Energy Recovery	60 kWh/m ² ·a
Reduction of Annual Heating Energy	90%
Annual Cooling Energy Recovery	30 kWh/m ² ·a
Reduction of Annual Cooling Energy	25%

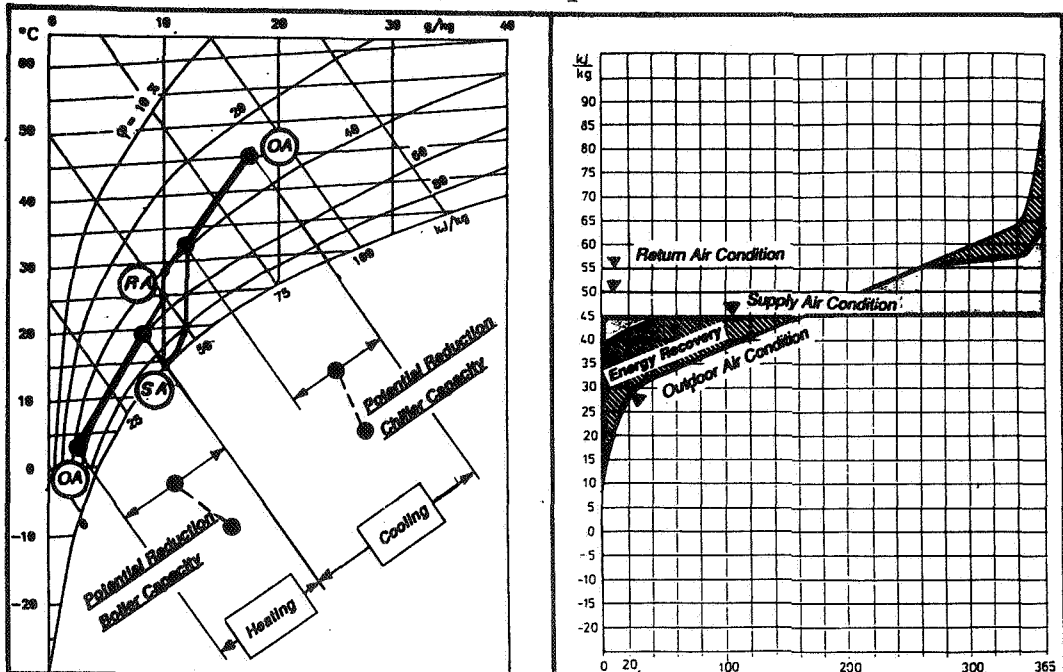
CO₂-Reduction

CO ₂ -Reduction Heating	22 kg/m ² ·a
CO ₂ -Reduction Cooling	8 kg/m ² ·a
Total CO ₂ -Reduction	30 kg/m ² ·a

Reduction Energy Recovery Investment Costs

Red. Boiler Capacity (200,- US\$ per kW)	11,- \$/m ²
Red. Chiller Capacity (400,- US\$ per kW)	15,- \$/m ²
Invest. Energy Recovery (1,40 US\$ per m ³ /h)	7,- \$/m ²
Total Investment Reduction	19,- \$/m ²

Fig. 6: Energy Recovery in Riyadh



Energy Recovery in Singapore

Climate Conditions: Tropic climate, permanent high humidity, only little difference of temperature and humidity

Outdoor Air Rate (50m³/h Person; 10m²/Person): 5 m³/h·m²
Energy Supply for Buildings: 100% Oil

Energy Recovery (Total Heat Exchanger, 75% Eff.)

Heating Period	- mths
Cooling Period	12 mths
Reduction Boiler Capacity	- %
Reduction Chiller Capacity	50%
Annual Heating Energy Recovery	- kWh/m ² ·a
Reduction of Annual Heating Energy	- %
Annual Cooling Energy Recovery	130 kWh/m ² ·a
Reduction of Annual Cooling Energy	35%

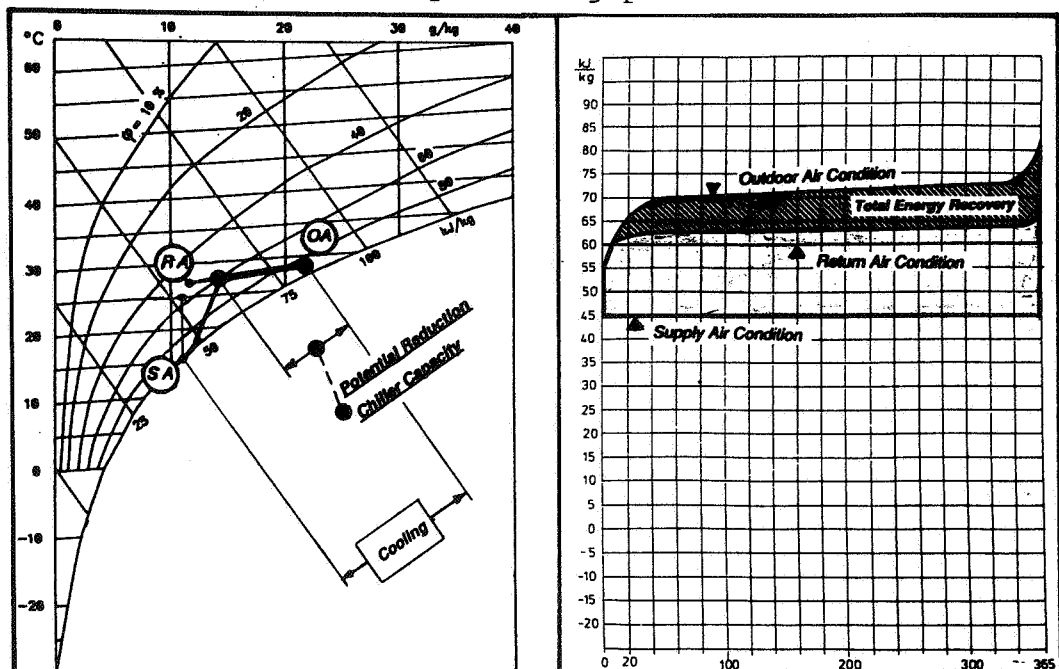
CO₂-Reduction

CO ₂ -Reduction Heating	- kg/m ² ·a
CO ₂ -Reduction Cooling	48 kg/m ² ·a
Total CO ₂ -Reduction	48 kg/m ² ·a

Reduction Energy Recovery Investment Costs

Red. Boiler Capacity (200,- US\$ per kW)	13,- \$/m ²
Red. Chiller Capacity (400,- US\$ per kW)	7,- \$/m ²
Invest. Energy Recovery (1,40 US\$ per m ³ /h)	6,- \$/m ²
Total Investment Reduction	

Fig. 7: Energy Recovery in Singapore



3.0 New Development of Total Heat Recovery Wheel

When using rotating heat exchangers to recover both sensible and latent heat in countries with high relative humidity of outdoor air one has to be aware that those types of heat exchangers are so effective because they adsorb the moisture of outdoor air with high efficiency. The surface of the heat exchanger is therefore made hygroscopic, either by a special treatment of the aluminum material to aluminum oxide or by covering the surface with desiccants like silica gel or zeolite powder. Generally, all these adsorbents have a very good adsorption capacity for moisture, but can also adsorb odorous chemicals of outdoor or indoor air at the same time. This effect can cause cross contamination of odours from return air to supply air, especially when the relative humidity of outdoor air increases rapidly during the rainy seasons or a downpour. The moisture purges out the odorous chemicals which have been adsorbed and accumulated in the pores of the adsorbents by pore condensation. Thus, purged odours would be mixed into the supply air and delivered into the inside of the room. By selecting a special type of silica gel with a defined pore diameter, the pore condensation can be prevented and no odour transfer [10] will happen. This very new type of total heat exchanger has been developed in Japan and is now being applied with very good results without any odour transfer. So all the advantages of the rotating energy recovery systems can be used especially for the reduction of the latent and sensible cooling capacity without any restriction. As shown before in the psychrometric charts of the four locations, only a rotating energy recovery system can meet the requirements of total energy recovery.

4.0 Desiccant Cooling with Energy Recovery Wheels

Due to the threat of an atmospheric ozone depletion leading to a "Greenhouse Effect" mainly caused by CO₂ from burning fossil primary energies and the CFC-based refrigerants used as cooling vapour in compressor chillers [11] new developments of cooling equipment have a realistic chance to enter the HVAC market and may force changes. The main strategy is to replace the standard refrigeration equipment by using the principle of desiccant cooling in order to eliminate the electric power generation in power plants. The desiccant cooling technology as described in Fig. 8 is now available with two rotating energy recovery wheels with extremely high efficiencies for adsorption and heat exchange [12].

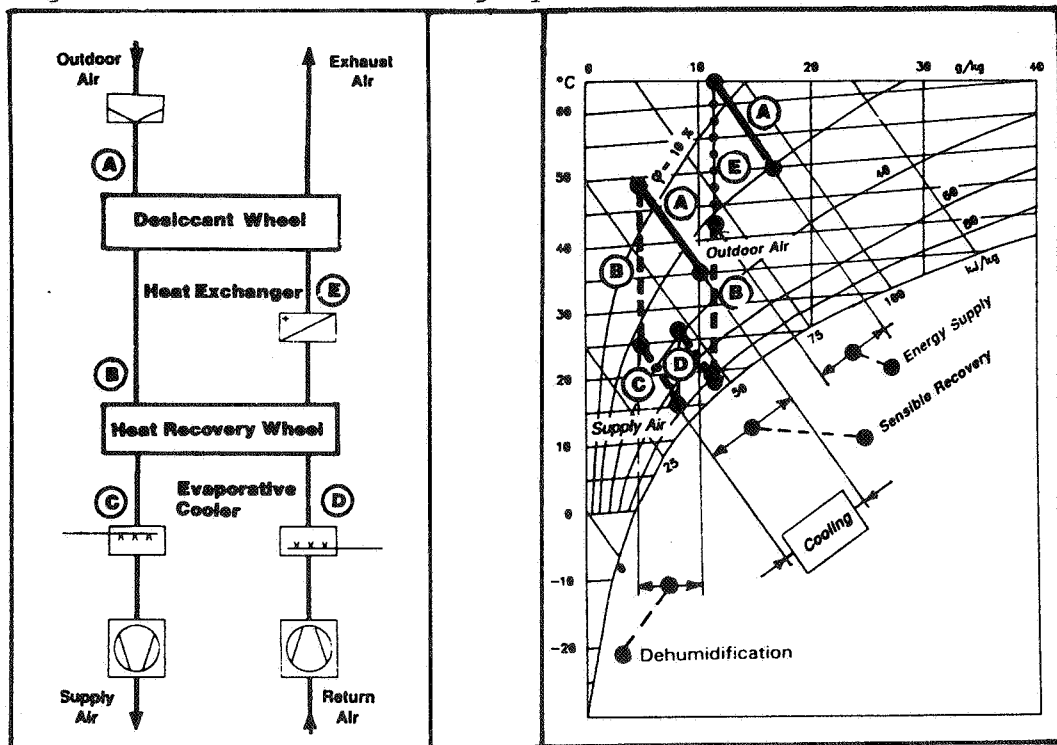
The unit consists of three well-known air processors: a desiccant air dehumidifier, evaporative coolers and a rotating sensible heat exchanger. The individual function of these principal components is as following: the desiccant wheel "A" rotates within the outdoor air

stream and removes the moisture from it. The rotor is fabricated of silica gel reinforced with inorganic fibres and formed into a honeycomb shape. Active silica gel is synthesized and combined in the honeycomb shape by chemical reaction. It has an excellent water adsorbing ability [13][14]. The adsorption of moisture on the silica gel causes the temperature of the air to rise. The heat generated during the drying step is removed from the air by a rotating heat recovery wheel "B" with high efficiency. This heat recovery wheel is non-hygroscopic and fabricated of corrugated aluminum. The evaporative cooler "C" humidifies the dried air to further reduce the dry bulb temperature of the supply air stream.

For the reactivation cycle the return air is used by first reducing the dry bulb temperature in the evaporative cooler "D". The heat originally generated during dehumidification of the supply air is then removed and transferred back into the reactivation cycle by the heat recovery wheel "B". As an additional energy source any kind of solar, waste or fossile energy is used in the heat exchanger "E" to bring the reactivation air to the required temperature for desorbing the desiccant wheel. Due to the new synthesized silica gel this temperature could be set at a minimum of 60° C, which allows to use low level waste heat available from many heat processes especially in summer season.

Numerous installations according to this desiccant cooling principle were realised during the last five years in the USA, Japan and Germany.

Fig. 8: Desiccant Cooling System



5.0 Summary

Energy Recovery is today routinely incorporated into the ventilation systems of office buildings, hospitals, schools, hotels, industrial processes etc. Because of high efficiency for both sensible and latent energy recovery the rotating heat exchangers are superior to the other types of heat exchangers. Therefore they are also very advantageous for the important growing application in the Third World Countries, where the energy consumption in the future is expected to grow dramatically. These countries have mainly desert or tropic climates.

The benefits of energy recovery and related technologies like desiccant cooling are:

- Reduced investment costs due to smaller size of boilers and chillers
- Reduced energy costs for heating energy (90%) and for cooling energy (30%)
- Reduced CO₂ emission due to reduced energy input
- Additional cost reduction if taxes on energy consumption and/or CO₂ emission are introduced
- Higher and more economic outdoor air rate possible to meet the indoor air quality problems
- Reduced dependence on fuel imports
- "Least Cost Planning" technology for public utility services

6.0 References

- [1] DEHLI, F.: "At the Top of Europe", Annual Report 1986 Kraftanlagen AG, Heidelberg/Germany
- [2] ASHRAE JOURNAL: "Heat Exchanger - A Historical Perspective", 2/1989
- [3] HEAT RECOVERY HANDBOOK, Kraftanlagen AG, Heidelberg/Germany
- [4] FANGER, P.O.: "Air Quality and Pollution Sources in Buildings", Int. Congress for Building Services Engineering, Hamburg/Germany, 3/1992
- [5] EUROVENT 10/1: "Heat Recovery Standard", 1985
- [6] BILIC, F.: "Heat Recovery in Desert Countries", HLH 3/1984
- [7] JESBERG, P.: "Human Architecture", ISH Manual, 1991
- [8] OHBAYASHI CORP.: "Super Energy Conservation Building Tokyo/Japan 1986
- [9] MINISTRY: "Energy Systems and Environmental Control", Wiesbaden/Germany 1989
- [10] KUMA, T.: "Total Heat Recovery Wheel", Fukuoka/Japan 1992
- [11] UNCED: United Nation Conference of Environment and Development, Rio de Janeiro 1992 "Declaration"
- [12] BUSWEILER, U.: "Desiccant Cooling", Clima Commerce International, 6/1991
- [13] SEIBU GIKEN: "Active Silica Gel Type Dehumidifier", Fukuoka/Japan 1987
- [14] KUMA, T., HIROSE, T.: "Sheet Adsorbent of Silica Gel/Zeolite with Application to a Honeycomb Rotor Dehumidifier", Int. Symposium on Adsorption, Kyoto/Japan, 1988



**Ventilation for Energy Efficiency and Optimum
Indoor Air Quality
13th AIVC Conference, Nice, France
15-18 September 1992**

Poster 6

EBES - Energy Efficient Residential Building.

J. Laine and M. Saari

**Technical Research Centre of Finland (VTT)
Laboratory of Heating and Ventilation, P O Box 206
(Lampomiehenkuja 3) SF-02151 Espoo, Finland**

SYNOPSIS

The new building and HVAC technology was used when an EBES multistorey residential building was built in Helsinki. In the EBES system the building structures are used as an installation space for the heating, piping, ventilation and electrical systems. Building structures are also used as a storage for heating and cooling energy. The main objectives of the overall EBES system are to improve the indoor air quality and energy economy and at the same time to improve the quality of the construction process and reduce costs.

The ventilation system is a mechanical supply and exhaust air system having efficient heat recovery. It is supported by an intelligent programmable controlling system. The ventilation system is designed so that no adjusting and balancing is required after installation. In the EBES system it is possible to use complex demand-controlled ventilation systems if desired. In this building manual control by residents was used. In each room the indoor temperature is individually controlled and the resident may choose the temperature level desired.

All the HVAC components were tested in the laboratory before installation. All phases of the construction were monitored and filmed by video. The field monitoring of the indoor climate, energy consumption and operation of the system are presently in progress. The project will continue up to the end of 1992.

1. INTRODUCTION

The heating, piping, ventilation and electrical systems and structures of apartment buildings have generally been studied as separate parts independently of each other. A controlled indoor climate, good energy economy, good sound insulation and long service life of the structures can be achieved only through the controlled joint functioning of these parts.

Need for development of an open EBES element building controlling the frame construction in Finnish apartment buildings and the need to develop the indoor climate, energy economy and living standard of apartments without raising the building and operating costs initiated the EBES research project "Energy economic building systems integrated in the heating and ventilation systems of buildings" /1/.

In the EBES system the building structures are used as an installation space for the heating, piping, ventilation and electrical systems. The building structures are also used as a storage for heating and cooling energy (Figure 1).

Advanced EBES building and HVAC technology was used and tested in the experimental building (2-3 storey, building volume 2760 m³, floor area 842 m², eight flats) in Helsinki.

In this paper the results of the field monitoring on the indoor climate, energy consumption and operation of the system are discussed.

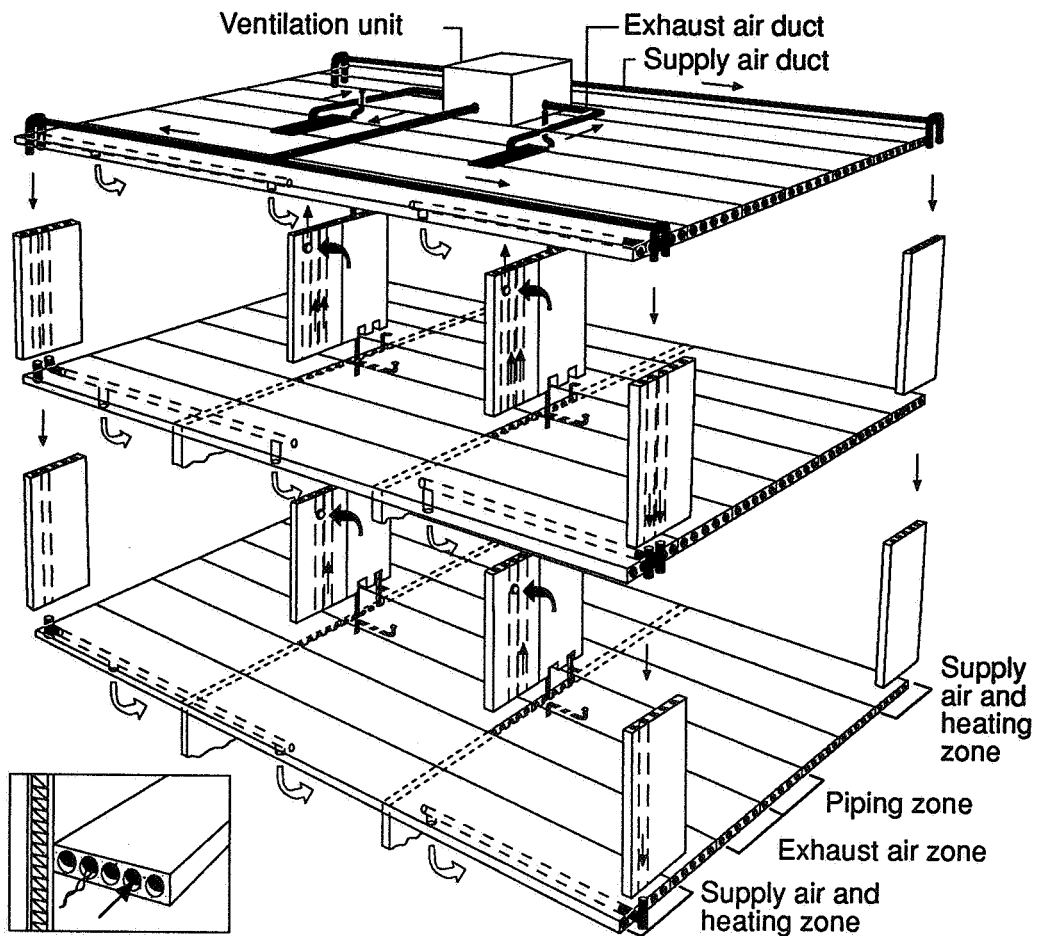


Figure 1. EBES integrated HVAC and building system.

DESCRIPTION OF THE EBES SYSTEM

- Suitable methods for the distribution of air into the rooms.
- A self adjusting air duct system.
- Leading of supply and exhaust air into the hollow spaces of the concrete structures in the load-bearing floor and wall structures.
- Effective heat recovery.
- The use of the building mass as energy storage for cooling and heating.
- The installation of water and sewage pipes into the hollow spaces in the frame structures.
- The installations of the building's electrical equipment, wiring and accessories in the hollow spaces.

2. HEATING SYSTEM

The basic heating system is an accumulating type of electrical heating. At night the heat is stored in the floor and ceiling structures by means of electrical heating cables. In the daytime the heat is transferred to the room spaces. The room temperature control is managed by means of a room-based ventilation heating system that incorporates an accurate electronic thermostat.

Combined radiation and warm air heating was found to be a suitable heating system with regard to the stability of the indoor temperature during heating breaks. Radiation heating feels pleasant even when the temperature drops a bit. During reheating, radiation heating is slow. With warm air heating the indoor temperature can rapidly be raised to the desired level if the design heating effect is sufficient. Although the temperature of the structures (Figure 2) may vary considerably, the room temperature is uniform.

When electricity is used as the heating energy, the heating effect of the building can be controlled according to the loading of the power plant without causing abrupt changes in the indoor temperature during heating breaks.

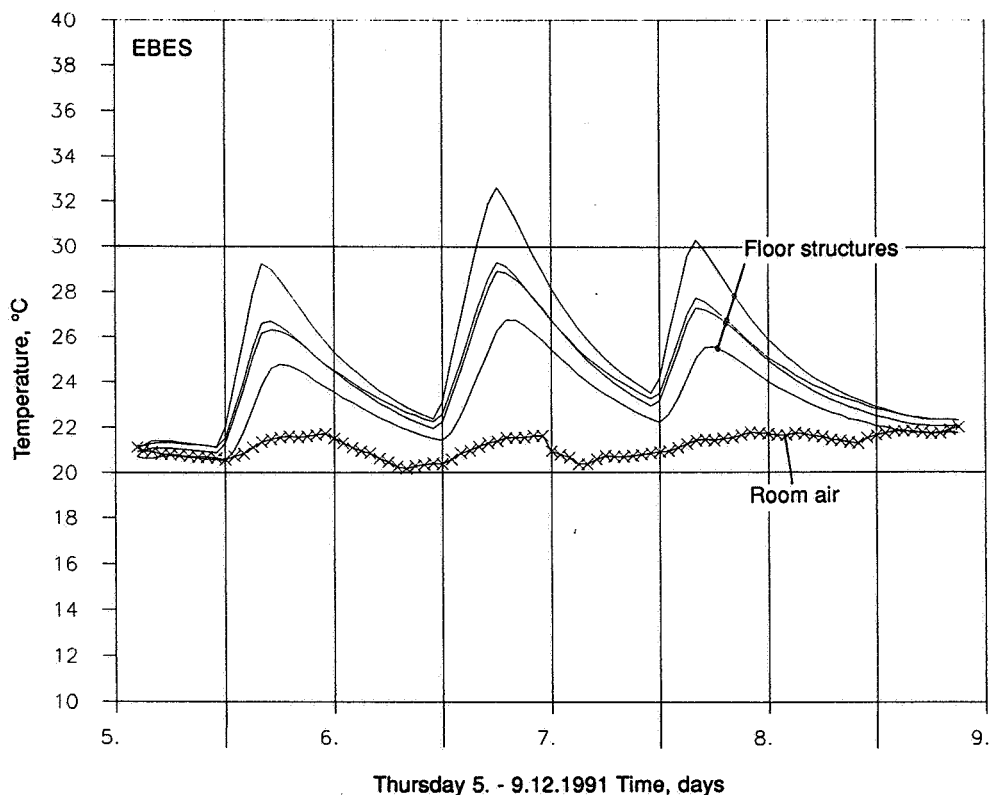


Figure 2. Measured temperatures of floor structures near the heating hollow during heating periods.

The supply air that is led into the hollow core slabs must be preheated to such a high temperature that the surface temperature of the hollow core slab is never below +10 °C. The measured temperatures of supply air in a vertical hollow space during the winter period are shown in Figure 3.

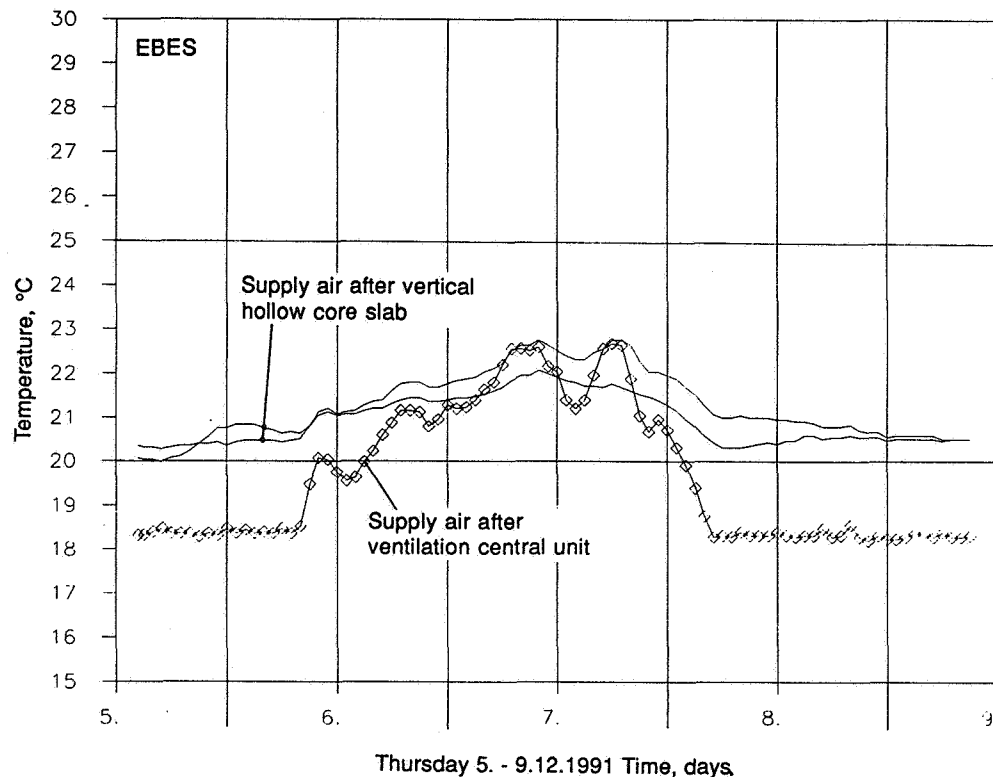


Figure 3. Measured temperatures of supply air after the ventilation central unit and after a vertical hollow (length 6 meters) on the 1st floor.

3. VENTILATION SYSTEM

The ventilation system is a mechanical supply and exhaust air system which embodies heat recovery, efficient filtering and preheating of the supply air. Hollow spaces of hollow core slabs are used as air ducts. Every flat has its own vertical supply and exhaust air hollow spaces. No air flow dampers and no adjusting and balancing of air flows are needed in the EBES system and cleaning of the hollow spaces is easy. Figure 4 shows how the ventilation central unit functions. Total air flows were practically constant.

In each flat the ventilation rates may increased in the kitchen and toilet.

The room-based air flows are preadjusted and measured to the desired values by means of silent and high-quality supply air devices. The resident can control the direction and length of the supply air to accomodate his furnishings so that there is no draught and noise.

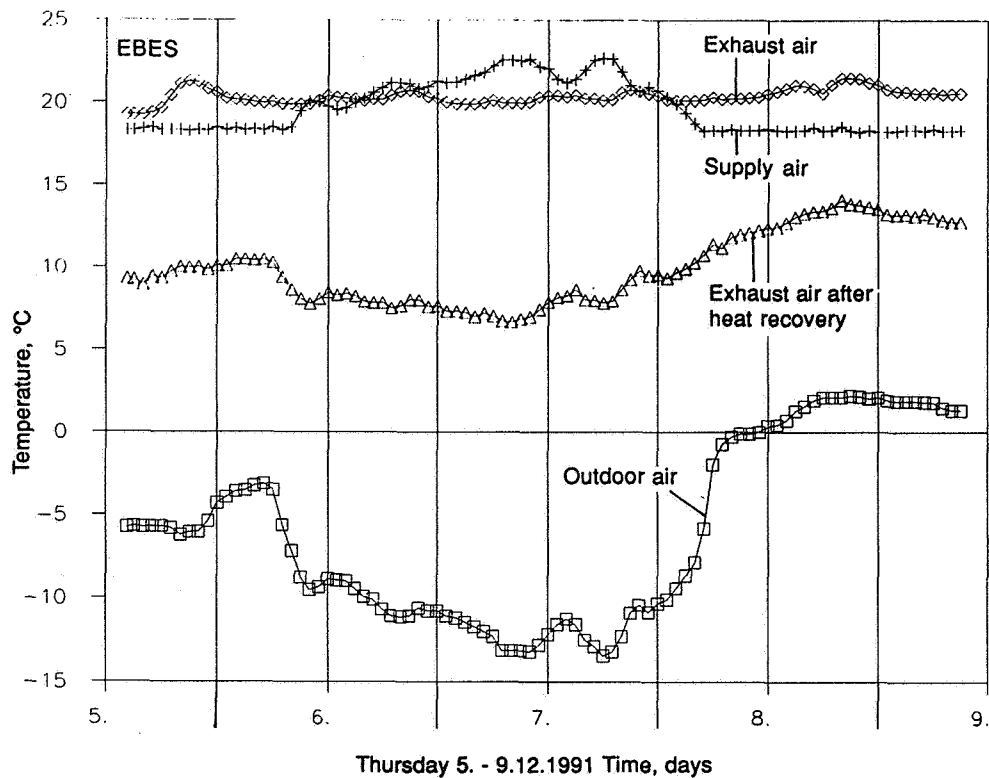


Figure 4. Measured temperatures of air flows in the ventilation central unit.

4. OBJECTIVE VALUES FOR INDOOR CLIMATE AND VENTILATION

The basis of both the heating and ventilation systems of an energy economic EBES block of flats is that the final goals of the indoor climate standard are clearly stated. In addition to thermal comfort and air quality, the noise of the equipment and the sound insulation of the structures must be taken into account.

For residents, the key flexibility requirements of the techniques of controlling the indoor climate in apartment buildings are /4/, /5/, /6/, /7/:

- an ideal and even temperature for each room
- silent demand-controlled ventilation that eliminates draughts
- the prevention of spreading of odours
- good sound insulation.

The objective values of the indoor climate of the EBES block of flats meet the recommended values in the compiled Finnish Building Code. The following values are higher: the indoor air temperature can be controlled to 21 ± 2 °C, the air change is 0.65 - 1.0 l/h and the highest permissible sound level is 25 - 30 dB(A).

5. TECHNICAL PROPERTIES OF THE EBES-BUILDINGS

The functional requirements of a mechanical supply and exhaust air ventilation system that provides sound attenuation and heat recovery - such as that used in the EBES block of flats - is that the outer building envelope ($n_{50} < 0.5$ l/h) and the floors ($n_{50} < 0.1$ dm³/sm²) in particular, are sufficiently airtight. At a test pressure of 200 Pa, the leakage air flow rate of the air ductwork may be a maximum of 0.1 dm³/s per square meter of the envelope surface of the air ductwork. To avoid the disturbances that change the air flows in the ducts and are caused by the thermal forces due to the temperature difference between the outdoor and indoor air as well as by the wind, the static pressure of the duct work must be at least 100 Pa when the building does not have more than seven storeys. The mechanical supply air flow is about 80 % of the exhaust air flow. Air change is continuous.

Air ductwork according to the EBES system is simple to design and easy to adjust. Its features furthermore include technically stable air flow, sound control and the possibility of making changes in the air flows when the flow rates in the main ducts of sheet metal are a maximum of 4 m/s. The air flows in the mutual ducts (vertical hollows) are 3 m/s and those in the room ducts (vertical or horizontal hollows) are 2 m/s /2/, /3/.

MEASURED TECHNICAL PROPERTIES OF EBES BUILDING		
-	Leakage air flow rate of the building envelope (test pressure 50 Pa)	0.7 l/h
-	Normal ventilation rates of the flats	0.77-0.87 l/h
-	Temperature efficiency of the heat recovery	60 %
-	Accuracy of the preadjusted air flows	5 %
-	Leakage air flow rate of the air ductwork (test pressure 250 Pa)	1.0 dm³/sm²
-	Average sound levels	
	bedrooms	24 dB(A)
	living rooms	21 dB(A)
	kitchens	24 dB(A)
	normal ventilation	24 dB(A)
	increased ventilation	29 dB(A)
	toilet	
	normal ventilation	29 dB(A)
	increased ventilation	35 dB(A)
	bathrooms	31 dB(A)
	saunas	28 dB(A)
-	Sound insulation between flats	55-62 dB

NEW PRODUCTS OF THE EBES SYSTEM

- **Sound attenuated, draughtless and air heating supply air devices.**
- **A silent cooker hood capable of effective vapour collection and able to increase the air flow.**
- **An exhaust air device capable of increasing the air flow.**
- **A new type of ventilation central unit equipped with heat recovery.**
- **A connection piece system for the hollow spaces of the hollow core slabs that are used as air ducts.**
- **A control technique for the room-based heating effects of the heat accumulating building frame.**

The measured energy consumption of the EBES building is in Figure 5. Supply air heating energy is very small because the heat recovery is efficient (60 %). About 70 - 85 % of the electricity was low cost night electricity.

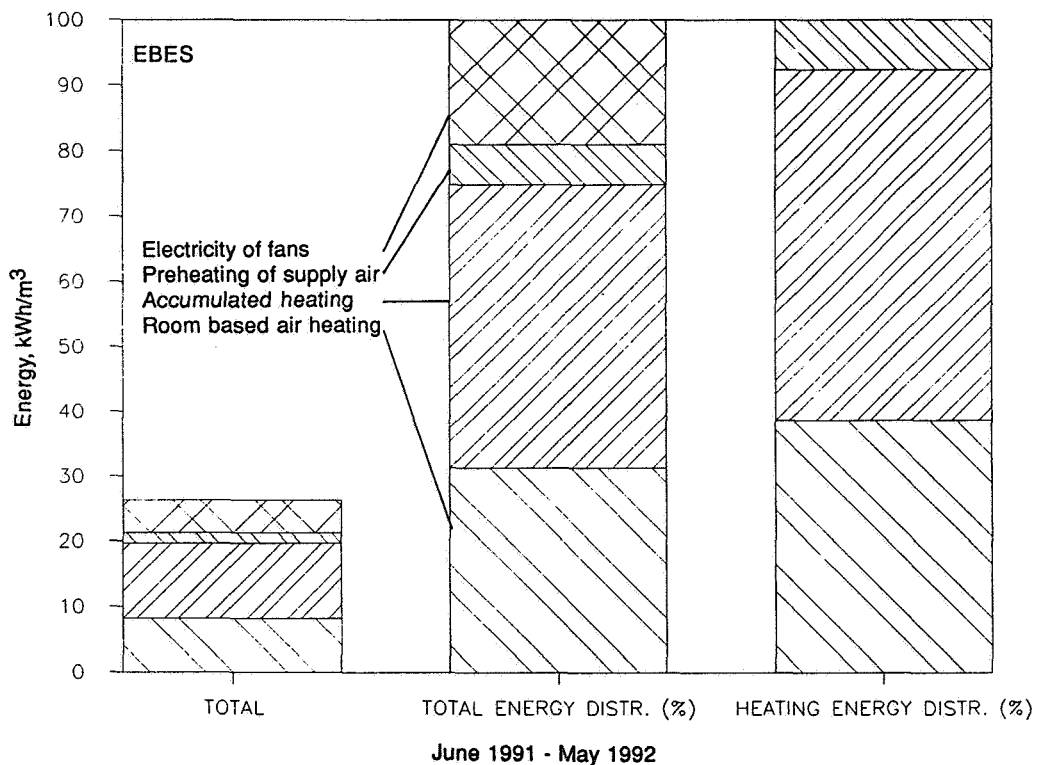


Figure 5. Energy consumption of the EBES building (1 year). Energy: kWh per building volume m^3 . The mean outdoor temperature was $6.5\text{ }^\circ\text{C}$, which was $2\text{ }^\circ\text{C}$ higher than the normal level in Helsinki.

6. CONCLUSIONS

The development of a heating, piping, ventilation, electrical and building system within the EBES research project has increased the possibilities of using an open EBES element building system to improve the standard of living and form a bases for the development of new integrated element building systems that offer all-round economy.

In the EBES building the residents were very satisfied with the thermal indoor climate, the freshness of the indoor air and the controlled ventilation. All technical systems functioned well. Thanks to heat recovery and the use of hollow core slabs, the energy consumption of the supply air heating was only 5 % of the total energy.

ACKNOWLEDGEMENTS

The EBES research was conducted in co-operation with construction companies, precast element manufacturers, consulting engineers, manufacturers of heating, piping, ventilation and electrical equipment and the Technical Research Centre of Finland (VTT). The authors wish to acknowledge the support of the Ministry of Trade and Industry (KTM) and the Ministry of the Environment (YM) in Finland.

References

- /1/ Korhonen, P., Laine, J., Muro, O. & Virtanen, M., EBES-integroitu LVIS- ja rakennejärjestelmä [EBES - integrated HVAC, piping, electrical and building system]. Espoo 1988. Technical Research Centre of Finland, Research Reports 537. 83 p. + app. 2 s. Finnish, English abstract.
- /2/ Laine, J., Toimivaksi mitoitettu ilmakehanavisto. [Well-dimensioned air ductwork]. Espoo 1989. Technical Research Centre of Finland, Laboratory of Heating and Ventilation, Technical Note 3/1989. 2 p. Finnish.
- /3/ Laine, J., Demand controlled ductwork. 10th AIVC Conference, Finland, 25-28.9.1989, Proceedings, Vol. 2, p. 397-411.
- /4/ Luoma, M., Demand controlled ventilation systems for dwelling houses, Indoor air '90-Conference, 29.7.-3.8.1990, Toronto.
- /5/ Luoma, M., Laine, J., Kohonen, R., Demand controlled ventilation in three Finnish demonstration dwelling houses. International CIB W67 Symposium on Energy, Moisture and Climate in Buildings, 3.-6.9.1990, Rotterdam.
- /6/ Luoma, M., Kohonen, R., A Ventilation concept for future dwelling houses. 9th AIVC Conference, Belgium, 12.-15.9.1988. Proceedings, Vol. 1, p. 329-342.
- /7/ Saari, M., Determination of air exchange rates for demand controlled ventilation. 11th AIVC Conference in Italy, 18.-21.9.1990. Proceedings, Vol. 2, p. 167-175.

**Ventilation for Energy Efficiency and Optimum
Indoor Air Quality
13th AIVC Conference, Nice, France
15-18 September 1992**

Poster 5

Efficiency Measurements of Kitchen Hoods.

B. Geerinckx, P. Wouters, P. Voordecker

**Belgian Building Research Institute (WTCB/CSTC),
Aarlenstraat 53, Bus 10, 1040 Brussels, Belgium**

Synopsis

Air extraction in the kitchen is an essential element in all ventilation strategies for dwellings. This can be done by natural ventilation or mechanical extraction. In practice, the use of mechanical kitchen hoods is very common in Belgium.

As part of a research carried out for the Belgian IWONL/IRSIA, the laboratory for Hygrothermics and Indoor Climate of BBRI carried out measurements to evaluate the efficiency of kitchen hoods.

The test procedure applied at BBRI is a mix-up of two existing standards. The major difference between the two standards is the use of an interference device to simulate occupants behaviour. Just this interference device seems to have a crucial influence on the collection efficiency of a kitchen hood.

Besides the determination of the collection efficiency, a definition is given of a pollution index. This index evaluates the pollution level in the room when using a kitchen hood.

Also a method is explained to design and to evaluate a kitchen hood installation taking into account air flow characteristics and collection efficiencies.

List of Symbols

- E : Collection efficiency index
- P_i : Pollution index
- C : Measured concentration of tracer gas [ppm]
- q : Tracer gas injection rate [m^3/h]
- Q : Extraction air flow rate [m^3/h]
- V : Volume of test chamber [m^3]
- t : Time [h]

1. Efficiency measurements

1.1. Introduction

The main function of a kitchen hood is to extract the pollution from cooking. Standards NF E 51-704 and SS433 05 01 describe a method to measure the collection efficiency of a kitchen hood. Based on both standards BBRI constructed in 1991 a test chamber for such kind of evaluations. For a technical description of the test chamber and the method, a reference is made to [1] and [2].

The produced pollution during a cooking process is simulated by a tracer gas. A known quantity is injected in a saucepan at a hot plate while the kitchen hood is working. After stopping the kitchen hood and the injection of tracer gas, the remaining concentration of tracer gas is measured in the test chamber. The collection efficiency index is determined based on this measured concentration.

Figure 1 shows the BBRI test chamber.

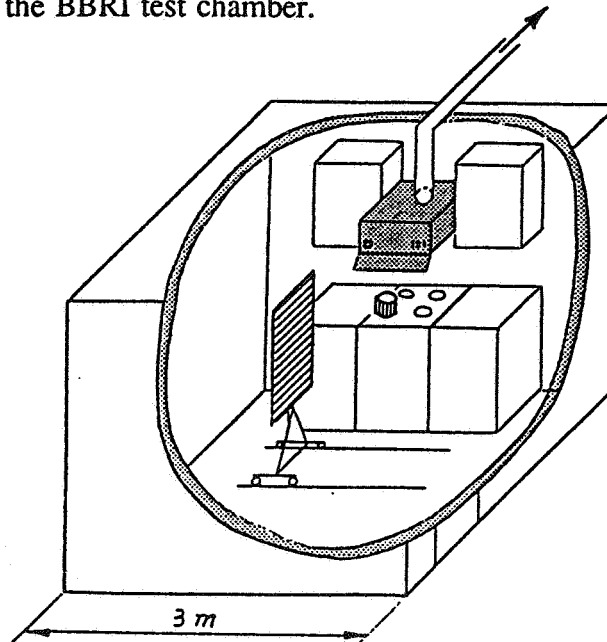


Figure 1 : Schematic view of the BBRI test chamber

1.2. Evaluation indices

Both above mentioned standards express the collection efficiency using the following formula:

$$E = 1 - \frac{C \cdot 10^{-6}}{\frac{q}{Q} \left(1 - e^{-\frac{Q}{V} \cdot t}\right)}$$

The expression in the denominator of this equation is the concentration which should be found in case of perfect mixing, using the same injection and air flow rate as during the test. Perfect mixing means that the tracer gas is completely mixed with the room air before extraction. An efficiency of 0.00 is found if the concentration inside the test chamber is the same as in the case of perfect mixing.

An efficiency of 80 % may be interpreted that 20 % of the pollution is coming into the kitchen before being extracted. The collection efficiency index expresses the effectiveness of the catching of pollutants by a kitchen hood.

A drawback of the definition of the collection efficiency is that no information is obtained about the resulting pollution in the kitchen. The collection efficiency is calculated comparing a measured concentration and a concentration in case of perfect mixing for the same air flow rate.

The effect of the air flow rate on the pollution in the occupied zone is eliminated. The collection efficiency index focuses on the indoor air quality for a given air flow and is an energy related performance index.

It would be interesting to define another index which gives more information about the air quality in the occupied zone. Therefore, "the pollution index P_i " is defined at BBRI.

The pollution index P_i is defined as the relative concentration in the occupied zone for a certain kitchen hood at a certain air flow by taking the situation of $100 \text{ m}^3/\text{h}$ extraction with perfect mixing as a reference. This reference situation corresponds with a pollution index 1.00 .

This corresponds with the following formula :

$$P_i = \frac{C \cdot 10^{-6}}{\frac{q}{100} \left(1 - e^{-\frac{100}{V} \cdot t}\right)}$$

The pollution index focusses more on the indoor air quality level in the room and is a quality performance index. One can probably come to other performance indices.

2. Results

2.1. Results

For the moment, as well Belgian as Dutch kitchen hoods have been tested.

All kitchen hoods are installed at a height of 650 mm above the level of the hot plate and tested at different air flows.

Figure 3 to 4 illustrate the above defined performance indices of the tested hoods as function of the extraction air flows. Besides the results obtained for the kitchen hoods, the figures also give results of the performances of a ventilation grill. This is a ceiling extraction grill, mounted at the ceiling in the left corner of the test room at 50 cm from the rear and side wall. As expected the performances of this ceiling grille are much lower than for the kitchen hoods.

Collection efficiency

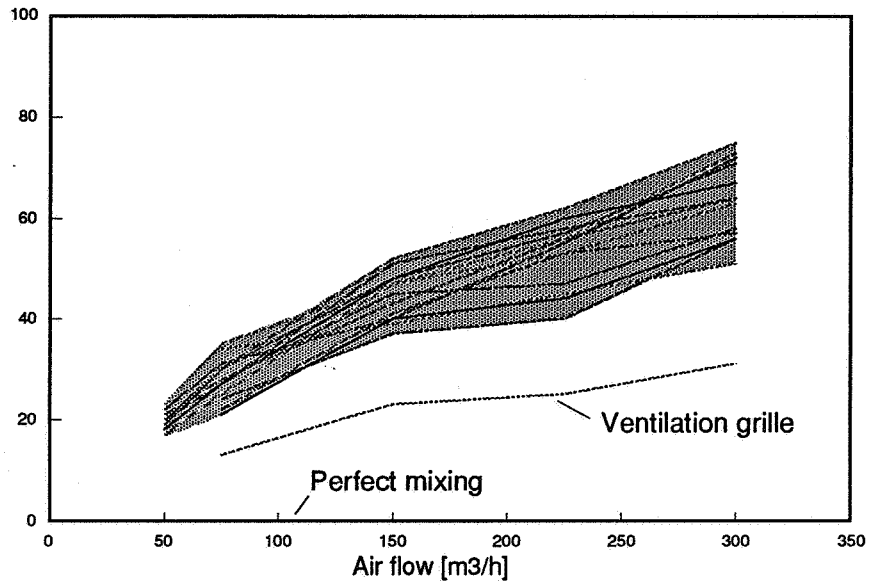


Figure 2 : Collection efficiency indices.

Pollution index

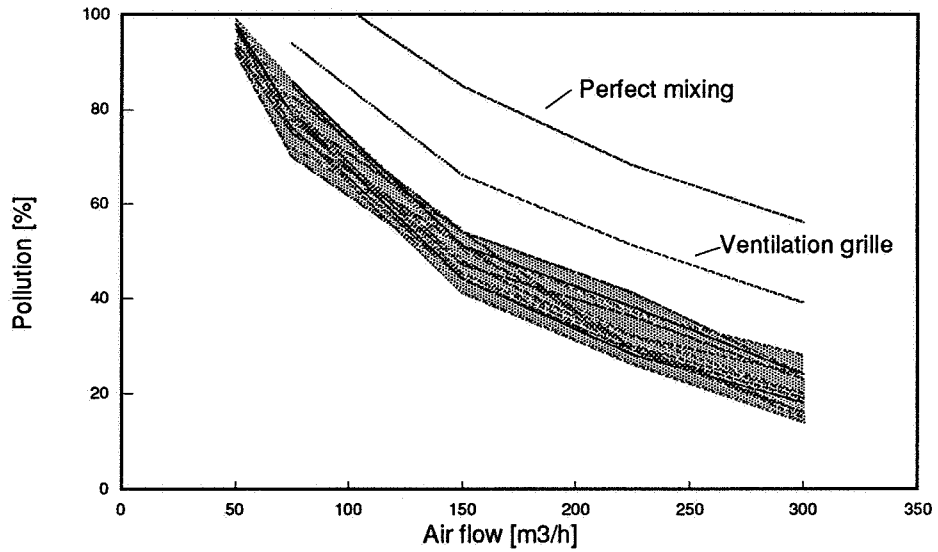


Figure 3 : Pollution indices.

2.2. Interpretation

- 1) It is clear that the collection efficiency increases (and the pollution index decreases) as the air flow increases. Therefore, it is not possible to give one collection efficiency index for an extraction device. It is an air flow related index.
- 2) Above figures shows that the behaviour of the efficiency index as function of the air flow is rather unpredictable. The curves of all hoods have different shapes. This can also be an indication of a rather large measurement error.
- 3) The collection efficiency of an air extraction device is related to the air flow as well with the shape as with the distance between the pollution and the extraction device. When using an air extraction grille with a low air flow (eg. 25 m³/h in a toilet as mentioned in the Belgian standard NBN D 50-001), the assumption of perfect mixing seems to be realistic. When using such a device with an important air flow (> 150 m³/h), the efficiency increases a lot and the assumption of perfect mixing is not longer valid.
- 4) The pollution index gives more information about the pollution level in the space. The pollution index decreases more then the efficiency index increases as function of the air flow. This can be explained by the difference in definition between the two indices. Even by an efficiency of 0.0, a certain amount of pollution is evacuated.
The calculated pollution indices also illustrate that all kitchen hoods evacuate more efficient by 50 m³/h than in case of perfect mixing and 100 m³/h. This is an important remark with respect to energy consumption.
- 5) All tests are carried out using the interference device. As will be explained in §3.3. this interference device has an not neglectible influence on the determination of the collection efficiency index.
- 6) The kitchen hoods have other performances than the extraction grille with respect to efficiency. Table 1 and 2 give an overview of the most important results. A reference is made to figure 2 and 3.

Collection efficiency indices					
Air flow	Perfect mixing	Tested kitchen hoods			Ceiling grille
		MIN	AVG	MAX	
50	0	17	20	23	-
75	0	21	28	35	13
150	0	37	44	52	23
225	0	40	53	62	25
300	0	51	64	75	31

Table 1 : Summary of collection efficiency indices.

Pollution indices					
Air flow	Perfect mixing	Tested kitchen hoods			Ceiling grille
		MIN	AVG	MAX	
50	119	92	96	99	-
75	109	70	78	86	94
150	85	41	48	54	66
225	68	26	32	41	51
300	56	14	20	28	39

Table 2 : Summary of pollution indices.

- 7) One must remember that the test procedure at BBRI is not conform with the French or Swedish standard but a mix up of both standards. The test procedure, especially the starting up of the experiment, seems to be more logical than the one described in both standards.

3. Sensitivity analyses

3.1. Repeatability of tests

As also mentioned above, the results are rather unpredictable. This can include a rather large uncertainty in the measurements. Table 3 represents the results of 4 measurements on the same installation evacuating an air flow of 300 m³/h.

Test nr.	Collection efficiency [%]
1	72
2	72
3	73
4	71

Table 3 : Repeatability of efficiency tests

From these first results, one can conclude that the measurements are reliable. But due to the low number of comparative tests, following 95% confidence interval is obtained for the efficiency: $\hat{E} = 72 \pm 2.6$ [%]

3.2. Influence of height of installation of the hood

The influence of the height of the kitchen hood above the cooking plate doesn't seem to be neglectible. The following table gives the results of a kitchen hood installed at different heights. The test is done using an extraction device installed in a hood (width: 0.6 m, depth: 0.55 m, height: 0.08 m). The mentioned height of installation is the distance between the hot plate and the hood.

Figure 4 illustrates the effect of the placing of the kitchen hood on the collection efficiency.

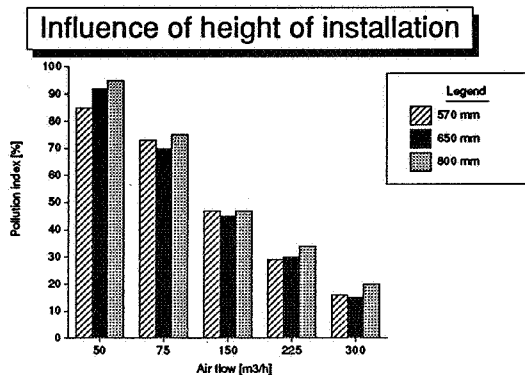


Figure 4 : Influence of installation height

For the investigated height of this kitchen hood, the height has little effect on the pollution in the kitchen. The influence of the air flow on the pollution is much bigger. This conclusion can only be taken for the tested configuration : the hood installed between cupboards and a wall behind it. The influence of the height can be more important in other configurations e.g. cooking isles and if cross ventilation occurs in the kitchen.

3.3. Influence of interference device

As also reported in [2], the interference device has a non neglectible influence on the extraction performances of a kitchen hood. This is in contradiction with the results reported in [5]. As mentioned in the Swedish Standard SS433 05 01 (May 81) a wooden plate (height: 1m, width: 0.5 m) is used to simulate the occupants behaviour. The interference device is moving from one side wall to another with a speed of 0.5 m/s and a frequency of 0.125 Hz. The purpose of the interference device is to simulate occupants behaviour.

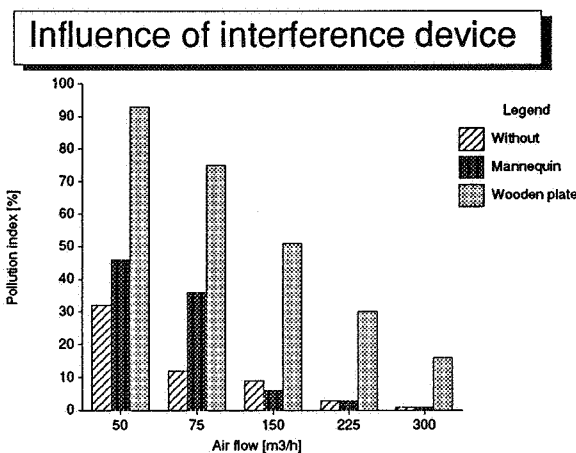


Figure 5 : Influence of interference device

Figure 5 illustrates the performances of a kitchen hood without interference device, with a wooden plate as interference device and a non-dressed female mannequin as device. The interference device has a crucial influence on the pollution in the kitchen. The most important difference between above mentioned standards is the use of the interference device. With respect to standardisation, the choice of this interference device seems to be important.

4. Evaluation and dimensioning of a kitchen hood installation.

The main purpose of a kitchen hood is to evacuate pollution during cooking. The capability to perform this job depends mainly on :

- the extracted air flow
- the collection efficiency of the kitchen hood.

Figure 6 illustrates a procedure to design a kitchen hood installation and to evaluate its performances taking into account both above mentioned parameters.

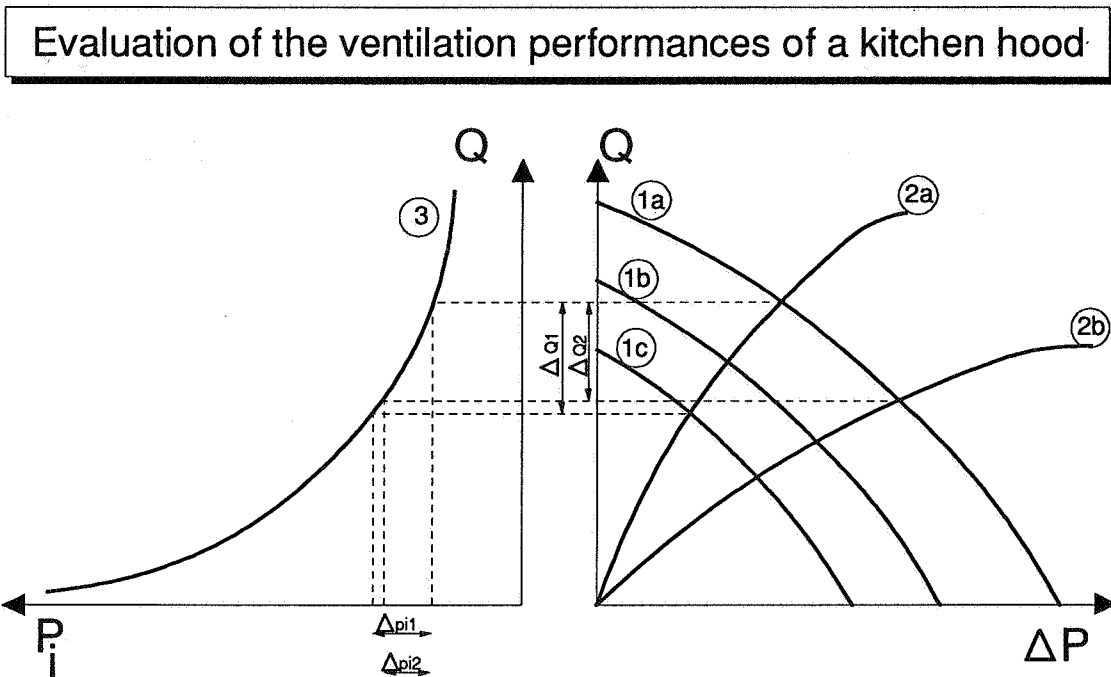


Figure 6 : Evaluation of the ventilation performances of a kitchen hood

The six curves on the figure are :

- 1a) relation 'pressure difference across kitchen hood-air flow rate' for a kitchen hood and operating in stand max.
- 1b) relation 'pressure difference across kitchen hood-air flow rate' for a kitchen hood and operating in stand medium.
- 1c) relation 'pressure difference across kitchen hood-air flow rate' for a kitchen hood and operating in stand minimum.
- 2a) relation 'pressure difference across ductwork-air flow through ducts' for a certain ductwork.
- 2b) relation 'pressure difference across ductwork-air flow through ducts' for a another possible ductwork.
- 3) relation 'air flow rate-kitchen hood pollution index' corresponding to the kitchen hood of curve 1 to 3.

Curves 1x) can be provided by the manufacturers of kitchen hoods, curves 2x) can be calculated when the flow characteristics of the used ducts are known. Curve 3 can be one general curve (see figure 3) representing the pollution index for kitchen hoods.

Some examples :

- 1) ΔQ_1 at the figure gives an idea of the difference in air flow rate that will be extracted by the kitchen hood connected to a ductwork if different stands (max \leftrightarrow min) will be used.
- 2) Δp_{i1} gives an idea of the difference in pollution index obtained by the same kitchen hood connected at a ductwork but using different stands.
- 3) ΔQ_2 gives an idea of the difference in extracted air flow rate by a kitchen hood operating in the same stand but connected at different ductworks.
- 4) Δp_{i2} illustrates the difference in pollution index obtained by a kitchen hood operating in the same stand but connected to different ductworks.

Above graphs allow to design an appropriate ductwork for a certain kitchen hood, to evaluate its evacuation performances and to investigate the performance differences using different fan speeds.

Remark :

Above approximations don't take into account the pressure drop in the kitchen due to airtightness. But this does not influence the idea behind this manner of designing and evaluating because the effect of airtightness can be included in the curve expressing the pressure drop in the ductwork. Therefore the philosophy remains the same.

4. Conclusions

- 1) Instead of only defining the collection efficiency index it seems to be interesting to define another performance index, more specific the pollution index, to evaluate the air quality performances of an extraction device.
- 2) As proven in previous experiments the interference device has a big influence in the determination of the performance indices. Therefore, it is important to link the obtained results with the interference device.
- 3) One must remember that the test procedure at BBRI is not conform with the French or Swedish standard but a mix up of both standards. The test procedure, especially the starting up of the experiment, seems to be more logical then the one described in both standards.
- 4) When air flow characteristics are known of the used apparatus and also collection efficiencies, a theoretical evaluation of the system can be done.

5. Acknowledgements

The research as described in this paper was partly granted by the Belgian Institute for Encouragement of Scientific Research in Industry and Agriculture (IWONL/IRSIA) and the IEA ANNEX 23 - project. The programme is followed up by a Working Group consisting of Belgian representatives of kitchen hood manufacturers and distributors.

Many thanks to all, especially to Didier L'Heureux and Richard Bossicard who prepared the experiments and built the required equipment.

6. References

- [1] WOUTERS, P., GEERINCKX, B. and VANDAELE, L.
"Performance Evaluation of Kitchen Hoods"
12th AIVC Conference, Ottawa, Canada, Air Movement & Ventilation Control within Buildings, Warwick, 1991.

- [2] GEERINCKX, B., WOUTERS, P. and VANDAELE, L.
"Efficiency Measurements of Kitchen Hoods"
AIR-review of AIVC Vol. 13, No.1, p. 15-17, December 1991.

- [3] NF E 51-704
"Code d'essais aérauliques et acoustiques des hottes de cuisine raccordées à un circuit VMC"
French standard, 1986.

- [4] SS 433 05 01
"Cooker fans and cooker hoods - performance testing"
Swedish standard, 1981.

- [5] SIMON, J.
"Etude sur la détermination de l'efficacité de captation des hottes de cuisine"
document technique de CETIAT, 1984.

**Ventilation for Energy Efficiency and Optimum
Indoor Air Quality
13th AIVC Conference, Nice, France
15-18 September 1992**

Poster 4

Demand Controlled Ventilation: A Case Study

B Fleury

Vimaeroplast, BP 120, 79400 Azayle Brule, France

1.0 Synopsis

Good indoor air quality in buildings becomes such a major concern that new design recommendations emerge in many countries (USA, Nordic Countries, ...) Improvement of the interior environment should not be at the expense of higher energy consumption. Heat recovery systems are one appropriate answer to this challenge. However, additional energy savings could be achieved by applying demand controlled ventilation when the internal loads vary significantly.

A CO₂ controlled ventilation system has been installed in a conference room with high variable occupancy in mid 91. In this paper, we present the survey of 6 months of use, the limits and the benefits of such a system. We focus on the practical aspects to offer the optimum air quality and to integrate the occupants and building owner's requirements.

2.0 Description of the building and its ventilation system

The two story building is located in the suburb of a small town. Offices and exhibition hall benefit of a conventional exhaust ventilation system with a fixed flow rate. CO₂ controlled ventilation system has been installed in a 200 M² room used for conferences, training courses, business meetings, reception ceremony as well as parties. Internal loads can vary from an occupancy of 2 to 50 persons. This room has an independent VAV ventilation system.

Figure 1 represents a sketch of the installation. A CO₂ meter is located on the main internal partition at a 1.4 meters height above the floor level. It analyses continuously the CO₂ concentration. The measurement is based on the infrared photoacoustic principle. The sensor delivers a linear output signal (0-10 Volts) proportional to the carbon dioxide concentration in the 0 -2000 PPM range. A frequency inverter integrates the sensor signal over a two minute period. Diagram 1 shows its programmed answer in response to the input signal. The motor adjusts its rotation speed according to the frequency and the exhaust flow rate of the fan varies linearly with the input between 350 and 1100 M³/H. Six low pressure exhaust valves are uniformly distributed over the room ceiling. Fresh air is supplied through air inlet grilles evenly located on the facade.

3.0 Experimental set-up

The CO₂ concentration and the total flow rate have been recorded during 6 months every 5 minutes. Occupants filled up questionnaires. An agent visited the installation every other months to check any potential problems.

3.1 Results

The occupancy of the room varies greatly and exceeds sometimes the maximum expected number. It reflects the various uses of this room. The CO₂ concentration fluctuates between 350 ppm to 850 ppm with a peak at 1100 ppm when the internal load was extreme. The sensibility of the system can be appreciated with the detection of events such as aperitifs. When the room is used after a period of absence, the dilution time is noticed. During a meeting, any variation in the internal load is perceived by the sensor and consequently the flow rate is adjusted. As already noticed in other experiments [1], the CO₂ sensor can adjust the air flow much more quickly than a temperature or enthalpy sensor.

During the survey, the room was less used than expected. Therefore, the minimum ventilation rate was often encountered. Keeping the ventilation to a minimum seems to guaranty the quality of the air, even at 8 a.m. the day after a high occupancy. The room is correctly purged of pollutants.

Integration time of the frequency inverter should be long enough in order to avoid any pumping and acoustic effect in the ductwork. The absence of integration time induces a contineous variation of frequency and an erratic input to the fan motor.

The CO₂ sensor does not integrate all the pollutions. For exemple, after a party, the odor of wine and food is persistent. Even if some people may appreciate, it is not acceptable. Therefore, new systems integrate a boost position within the room. Occupants or managers can interfere on the functioning of the ventilation when special events occur.

Different means of variable air volume exists but frequency inverters act proportionnally on the speed of the motor and therefore, the functioning point of the fan moves along a network curve. When the CO₂ concentration decreases, the flow rate decreases proportionally and the pressure also but to the square. No noise is generated whatever the working point is situated.

In the design stage of any buiding, the profiles of occupancy as well as the density are key parameters which are rarely well apprehended. An on/off or a two level ventilation system can induce a high energy consumption and a poor indoor air quality because the the exhaust or supply air flow is not adapted to the needs. CO₂ ventilation partly solves this problem.

3.2 Occupants'perception

Six questions were asked to the occupants:

1. Are you satisfied of the air quality ?
2. Do you notice a difference with the others spaces?
3. How do you judge the acoustic environment?
4. Do you encounter a difference in the air quality over the space and the time?
5. Do you notice a better indoor environment in the presence of smokers in comparison with the other spaces?
6. Do you know the type of ventilation system if any?

The occupants were unanimous in their answers to questions 1,3,4. The air quality is qualified from good to excellent within the entiere space and over the time. Special mentions and positive comments were related to the high quality of the acoustic environment. For questions 2 and 5, occupants were either without opinion or noticed an improvment with other spaces. Interwieved occupants did not know always the existence of a ventilation system and even less the type.

4.0 Conclusions

In this building, occupants and managers were delighted by the quality of air and specially the acoustic environment, the ease of operation and the energy benefit. CO₂ controlled ventilation with frequency variation explains this satisfaction. The cost reduction of these two essential components: the sensor and the inverter should lead to a larger use of this ventilation process.

5.0 Reference

1 L. NORELL
Demand-controlled Ventilation
Flakt Review n°74, Energy Conservation

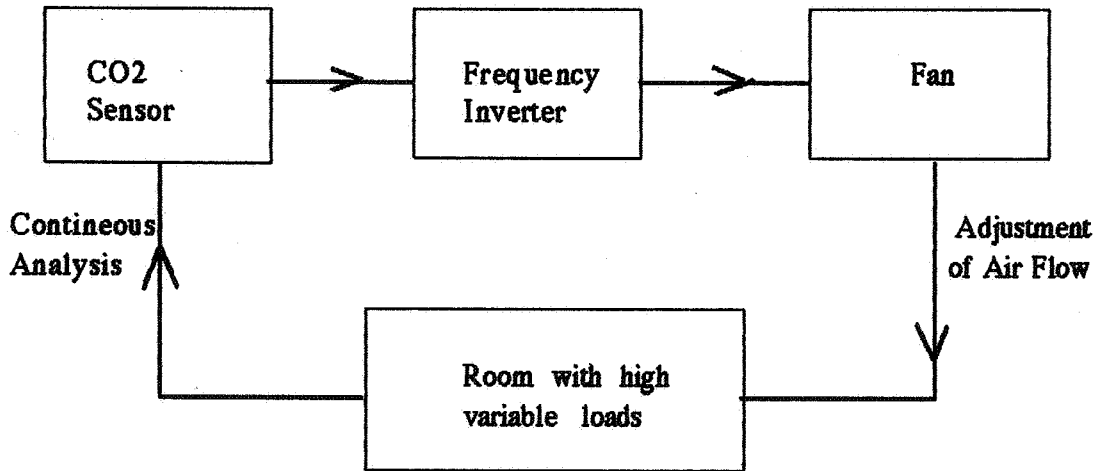


Figure 1: Principle of the system

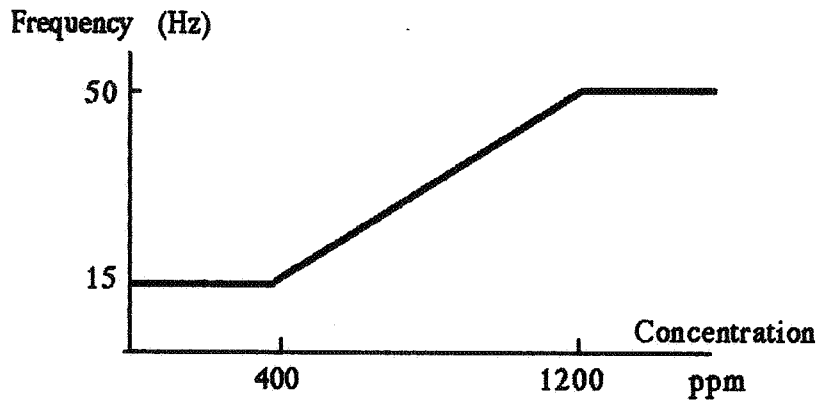


Diagram 1 : Response of the frequency inverter

**Ventilation for Energy Efficiency and Optimum
Indoor Air Quality
13th AIVC Conference, Nice, France
15-18 September 1992**

Poster 3

**Field Evaluation of the Indoor Environment of
Naturally Ventilated Offices.**

D.J. Croome, G. Gan, H.B. Awbi

**Department of Construction Management &
Engineering, University of Reading, Reading,
United Kingdom**

SYNOPSIS

Experiments were carried out in four naturally ventilated offices to measure the indoor environmental parameters such as air velocity, turbulence intensity and air temperature at three vertical levels. Air change rates for various indoor and outdoor climates were determined. The concentration of carbon dioxide in the room was monitored. Subjective assessment was made to evaluate the thermal comfort and indoor air quality in the offices. The effect of opening windows and doors on the indoor comfort conditions was also investigated.

Models were developed for assessing the indoor environment based on the field measurements. It was found that in real situations the occupants were more sensitive to the deviation of air temperature from neutrality than predicted using Fanger's comfort model. The indoor environment in the offices was found to be unsatisfactory and recommendations are given for its improvement.

1. INTRODUCTION

Thermal comfort is an important factor that influences occupants' satisfaction with the room environment. Fanger¹ developed models for the prediction of indoor thermal comfort based on laboratory testing. However, a number of field studies have shown that these models could not accurately predict the occupants' thermal responses under working surroundings. For example, Schiller, et al.² found that optimum satisfaction with the thermal environment in office buildings was achieved at a lower temperature than that found under laboratory conditions. Moreover, these laboratory based models are derived from measured data which give an overall state of room environment but not the sensitivity of different parts of the body to the surroundings. A more reasonable model for comfort should be able to reflect these differences.

Air quality in offices has been a major concern in recent years. Odour intensity is one of the indicators of indoor air quality and is often associated with the level of carbon dioxide. The results of indoor CO₂ measurements have been used to specify minimum ventilation rate requirements. However, Fanger, et al.³ found that more than 30% of the subjects were dissatisfied with the indoor air quality in randomly selected office buildings and assembly halls even though the average ventilation rate was up to 25 l/s per occupant, which is far higher than the recommended value of 7-8 l/s per person referred to in the CIBSE Guide⁴ and based on the maximum allowable CO₂ level of about 1000 ppm. This could have been attributed to the presence of other sources of pollution indoors as well as poor air distribution to the occupied zone.

The objective of the present work is to evaluate the indoor environment in naturally ventilated offices using detailed field measurements of the environmental parameters and thence to develop models for assessing indoor thermal comfort and air quality based on the field measurements.

2. METHOD

This investigation has been carried out by means of physical measurements combined with a subjective assessment of the indoor environment in four naturally ventilated office rooms (denoted as room A, room B, room C and room D). The offices are situated in the FURS building at the University of Reading. Rooms A and B are built of one concrete external wall and three concrete brick walls connected to other rooms, situated in the north wing of the building. They are both connected to the north corridor via hinged wooden doors. There are two small weatherstripped double-hung aluminium frame windows in the north face of room A and one large window in the north face of room B. Room C is located between the two corridors which connect the south and north wings. The walls separating the room and the corridors are glazed while the other walls are made of concrete bricks. There is a small axial fan in the north face near the ceiling for supplying air into the room. Room D has a similar structure to room A but is situated in the south wing and connected to the south corridor. All the offices are heated by hot water radiators in cold seasons. During hot days a portable propeller fan was used in some of the tests. The investigation lasted for eight months in the year 1991/92. In terms of seasons, tests were conducted in winter in room A, early spring in room B, late spring in room C and early summer in room D.

2.1 Physical measurements

During an experimental test the air velocity, turbulence intensity and air temperature were measured using thermal anemometers (DANTEC Multi-channel Flow Analyser type 54N10). Measurements were taken at points 0.1 m (foot/ankle level), 0.6 m (centre of gravity of a seated person) and 1.1 m (neck/head level of a seated person) above the floor. The plane radiant temperature and indoor air humidity were measured using an indoor climate analyser (Bruel & Kjaer type 1213). Thermal comfort indices (PMV and PPD) were measured using a comfort meter (Bruel & Kjaer type 1212). A CO₂ gas analyser was used for the measurement of indoor CO₂ concentrations.

The air change rate was determined using the concentration decay method with an infra-red gas analyser. A portable fan was employed to ensure a good mixing of tracer gas (isobutane) and air in the room for

a few minutes after injecting the gas. The wind speed was measured with three vane cup anemometers and the wind direction with a wind anemometer mounted on the top of the building (about 5 m above the roof). The outdoor air temperature and humidity were measured using a copper-constantan thermocouple (radiation shielded) and a hand-held humidity meter respectively.

2.2 Subjective assessment

A subjective assessment was made simultaneously with the physical measurements. The assessment of the thermal environment was based on the occupants' vote on the thermal sensation and air movement in the offices under various outdoor and indoor conditions and different arrangements of window and door openings. This assessment was based on judgements at head and foot levels as well as for overall comfort. The indoor air quality was assessed according to the impressions of odour and freshness of air. A seven-point thermal sensation scale was used to evaluate thermal sensation and a five-point scale to rate the impressions of comfort with regard to air movement, odour intensity and air freshness. These rating scales are given in Table 1.

Table 1. Rating scales for thermal sensation (TS), air movement (AM), odour intensity (OI) and air freshness (AF)

Rating	TS	AM	OI	AF
-3	cold			
-2	cool	too draughty	not detectable	very fresh
-1	slightly cool	draughty	slight	fresh
0	neutral	acceptable	moderate	neutral
1	slightly warm	stagnant	strong	slightly stuffy
2	warm	very stagnant	very strong	stuffy
3	hot			

3. RESULTS AND DISCUSSION

A summary of the results for physical measurements of the environment in the four rooms is shown in Table 2. These results are discussed and compared with those obtained from subjective evaluation.

3.1 Thermal sensation

The mean thermal sensation was found to be on the warm side of the neutral point defined in Table 1. However, the measured PMV values, which were obtained using Fanger's comfort equation, were close to the neutral point for most of the test conditions. This suggests that Fanger's equation under-estimates the thermal impressions and is less sensitive to changes in the environmental and personal parameters. This may be

Table 2. Physical properties of room environment

Item	Room No.	A	B	C	D	ABCD*
Dimension (m)						
Length		5.4	11.6	4.2	4.4	
Width		2.3	2.9	3.5	2.3	
Height		2.6	3.4	2.6	2.6	
Effective volume ⁺ (m ³)		29.3	108.2	37.5	25.0	
Normal occupants		1	3	2	1	
Average air change rate (h ⁻¹)		0.86	0.86	7.60	3.03	
Average air supply rate (l/s per person)		7.0	8.6	36.9	21.0	
Mean air velocity (m/s)						
Head level		0.059	0.071	0.098	0.063	0.072
Foot level		0.064	0.100	0.111	0.086	0.081
Overall		0.060	0.082	0.099	0.067	0.076
Turbulence intensity (%)						
Head level		39.4	59.2	43.8	38.6	43.8
Foot level		28.7	44.4	34.0	33.0	34.0
Overall		34.7	54.3	41.2	37.1	40.4
Mean air temperature (°C)						
Head level		23.1	23.8	25.7	27.1	24.8
Foot level		21.4	21.7	24.5	25.0	23.1
Overall		22.4	22.9	25.1	26.2	24.0
Difference between air temperature and radiant temperature (K)		0.6	0.7	-0.7	0.6	0.4
Relative humidity (%)		45.8	45.7	42.9	47.6	45.5
Calculated neutral temperature (°C)						
Head level		22.4	22.4	23.2	22.8	22.2
Foot level		21.4	20.4	21.1	22.1	21.0
Overall		22.0	21.7	22.5	22.7	21.8
Neutral temperature predicted from Fanger's equation (°C)		22.8	22.8	22.3	22.9	22.7
Difference in neutral temperature between measured and predicted (K)						
Head level		0.4	0.4	-0.9	0.1	0.5
Foot level		1.4	2.4	1.2	0.8	1.7
Overall		0.8	1.1	-0.2	0.2	0.9

Notes: * average of the data for rooms A, B, C and D;

+ excluding the space occupied by obstacles.

due to three main reasons. One is the assumption of steady state laboratory conditions used in the derivation of Fanger's equation. Another is the approximation of the metabolic rates of the occupants (1.2 met). The third

reason is the sensitivity of PMV to clo values (thermal resistance of clothing). In a laboratory test the clo values are consistent whereas in field tests the clothing levels vary with occupants and time.

From the data for the four rooms it was found that the thermal sensation is linearly related to the air temperature. The regression equations for the thermal sensation judgement at head level, foot level and overall against mean air temperature (T , °C) (involving 133 data points) are as follows:

$$\text{head} \quad TS = 0.3915 T - 8.66 \quad (r = 0.70) \quad (1)$$

$$\text{foot} \quad TS = 0.4655 T - 9.78 \quad (r = 0.72) \quad (2)$$

$$\text{overall} \quad TS = 0.4586 T - 10.01 \quad (r = 0.73) \quad (3)$$

where r is the correlation coefficient. The correlations have confidence levels of 99.5%.

Figure 1 shows the relationship between the occupant's thermal sensation response and mean air temperature. The PMV line predicted from Fanger's equation is also presented for comparison (assuming a metabolic rate of 1.2 met and a clo value of 0.8 and using the average values of the measured air velocity and radiant temperature for the four rooms). From such equations or the corresponding plots in Figure 1 the neutral temperatures T_n corresponding to $TS = 0$ can be obtained. The neutral temperature predicted using Fanger's equation is the air temperature corresponding to $PMV = 0$. The calculated neutral temperatures from the correlated equations and from Fanger's equation together with the difference in neutral temperature between them are shown in Table 2.

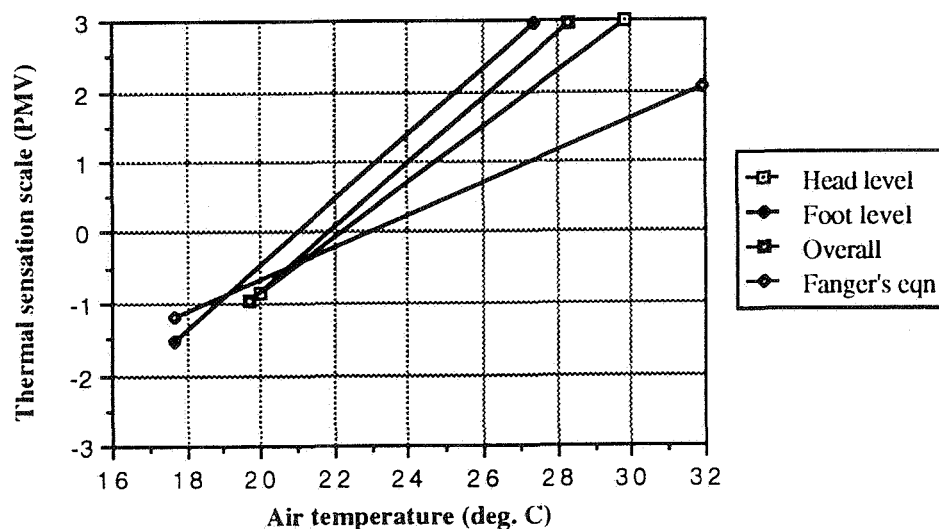


Fig. 1 Effect of air temperature on thermal sensation responses

It can be seen from Table 2 that Fanger's equation generally overpredicts the neutrality, which confirms the findings by Schiller, et al.² and Brager⁵. They found that the predicted neutral temperature was on average 2.4K higher than that measured for 304 workers in 10 buildings. Kahkonen⁶ also found that workers in offices estimated the thermal environment warmer than that calculated using Fanger's equation. Another important feature from the present investigation is that the correlated curves in Figure 1 are steeper than that given by Fanger's equation, suggesting the occupants are more sensitive to changes in air temperature. This fact was also observed by Fishman and Pimbert⁷ whose field study showed that the gradient of the curve from the observations deviated from Fanger's equation particularly at temperatures above 24°C. In addition they found that Fanger's comfort equation over-predicted the neutral temperature by 0.6K compared with that from the field survey. This was attributed to the incorrect estimation of the subjects clothing.

Fanger¹ defined the central three categories of the thermal sensation scale as an indication of an acceptable state for thermal comfort whereas the votes outside these central categories as dissatisfaction with the thermal state. According to this definition, the results suggest that one quarter to one half of the responses were dissatisfied with the thermal environment. Most of the dissatisfaction that occurred in rooms A and B when the windows and door were closed in cold seasons was caused by overheating, which could be avoided by controlling the heat output from the emitters if a thermostat was available or by window opening. For room C however these measures are not sufficient because the heater was turned off in the test period. One way to decrease the indoor temperature is to introduce air directly from the outside of the building rather than from the corridor (as it was the case during the tests) using the existing ventilating fan. Due to its location a comfortable thermal environment for room D is difficult to achieve in hot sunny days during the summer unless it is air conditioned.

3.2 Air movement

The overall impression of the air movement in the rooms was on the side of being stagnant. Although the measured air velocity and turbulence intensity in rooms C and D were generally higher than those in room A, the proportion of votes on being stagnant or very stagnant was higher in these two rooms. This may be attributed to the higher air temperature in the rooms. For room A when a window and/or the door were partly opened, the impression of air movement shifted to being slightly draughty⁸. The main cause of the draught was attributed to the low temperature as the air velocity and turbulence intensity were not high.

The correlations between the ratings for air movement (AM) and the indoor environmental parameters are as follows:

$$\begin{aligned} \text{head} \quad \text{AM} &= 0.1258 T - 4.28 V - 2.35 \\ &\quad (r = 0.42) \end{aligned} \quad (4)$$

$$\begin{aligned} \text{foot} \quad \text{AM} &= 0.1579 T - 3.13 \\ &\quad (r = 0.42) \end{aligned} \quad (5)$$

$$\begin{aligned} \text{Overall} \quad \text{AM} &= 0.1401 T - 4.65 V - 0.0060 Tu - 2.31 \\ &\quad (r = 0.45) \end{aligned} \quad (6)$$

where T is the air temperature ($^{\circ}\text{C}$), V is the air velocity (m/s) and Tu is the turbulence intensity (%).

Defining a "comfortable" temperature for air movement as the air temperature corresponding to an acceptable air movement, such a temperature can be derived from Equations (4) to (6) for specified values of air velocity and turbulence intensity. Using the average values of air velocity and turbulence intensity for the four rooms, the calculated comfortable temperatures are 21.1°C , 19.8°C and 20.7°C for the head level, foot level and overall judgement respectively, which are about 1K lower than the corresponding neutral temperatures. It seems that the preferred indoor temperature for air movement is lower than that for thermal sensation. Therefore a compromise between the requirements for warmth and air movement may have to be made sometimes to achieve an acceptable thermal condition.

3.3 Odour intensity

In room A odour was detectable in most cases. The measurement of CO_2 levels during occupancy indicated that its concentration was normally well above the criterion of 1000 ppm at low air change rates when the windows and door were closed⁸. Even when the air change rate was higher than 10 l/s, the CO_2 level was not much lower, suggesting that some of the air infiltrated from the corridor was not fresh at all but rather contaminated air exhausted from other rooms.

Although the air flow rate in room B was higher than in room A and the CO_2 level was usually below 1000 ppm, there was a higher proportion of complaints on the odour intensity than those experienced in other rooms. The following two causes may be attributed to the complaints. One is the occasional smoking by one of the occupants and the other is the old furnishings in the room. In contrast, a large proportion of votes in room C showed that odour was not detectable and there was no evidence of strong odour. This is consistent with the measured low CO_2 concentrations in the room because of the provision of the ventilating fan which maintained the indoor CO_2 at a

similar level to that in the corridor of around 700 ppm (during the Easter vacation period). In room D there was an even distribution of odour intensity between undetectable and moderate except for a small fraction of votes for strong odour. The CO₂ level in this room with occupancy was normally above 1000 ppm and odour was detectable when the windows were shut and the odour level decreased when a window was partly open.

In this investigation, no satisfactory correlation between odour intensity, CO₂ level and air change rate could be established. In some cases when the CO₂ level was low, or the air change rate was high, the odour was still perceivable while in other cases where the CO₂ level was higher than 1000 ppm the odour intensity was rated as not detectable. This seems to suggest that there were other pollution sources such as building materials or furnishings which could have been more significant than the CO₂ emission from the occupants. Also, the judgement could have been affected by a fatigue of the olfactory sense of the occupants.

3.4 Air freshness

In rooms A, B and D the rating of air freshness was in general slightly stuffy and occasionally the air was rated as fresh when the air temperature was lower than the neutral temperature. In room C however there was no impression of very fresh air due to the predominantly high air temperature.

Air freshness may be related to the air temperature, velocity and turbulence intensity in the following form:

$$AF = 0.0474 T - 3.02 V - 0.0107 Tu \quad (r = 0.48) \quad (7)$$

Thus, air freshness increases when the air temperature decreases; or when the air velocity or turbulence intensity increases.

5 CONCLUSIONS

Models for evaluating the thermal sensation, air movement and air freshness have been developed. These parameters are dependent on the air temperature, velocity and turbulence intensity under normal office conditions. When the indoor air temperature is substantially higher than that for neutrality, temperature is the predominant factor that decides the occupants' response to thermal comfort and air freshness.

From the present investigation, it can be postulated that thermal models based on laboratory tests at steady state conditions can not accurately predict the real thermal environment where the climatic conditions are transient and where the occupants invariably change their

activities or clothing especially beyond the comfort zone. For the cases investigated Fanger's equation for thermal comfort generally overpredicts the neutral temperature and under-predicts the comfort requirement when air temperature deviates from neutrality.

To achieve a good indoor climate and air quality, fresh air should be introduced into rooms either by opening windows or by installing a suitable vent. The size of the vent opening should ideally be controllable, either manually or by an odour sensor so that the indoor air will be invigorated, the odour reduced or eliminated and the air freshness enhanced. Also, the heating costs in cold seasons can be reduced by adjusting the heat emission from radiators using, for example, a thermostatic valve or by a weather compensated room heating system.

REFERENCES

1. FANGER, P.O.: "Thermal Comfort — Analysis and Applications in Environmental Engineering", 1982, Robert E. Krieger Publishing Company, Florida.
2. SCHILLER, G.E., ARENS, E.A., BAUMAN, F.S., BENTON, C., FOUNTAIN, M. and DOHERTY, T.: "A field study of thermal environments and comfort in office buildings", ASHRAE Trans., 1988, 94(2), pp280-308.
3. FANGER, P.O., LAURIDSEN, J, BLUYSSSEN, P. and CLAUSEN, G.: "Air pollution sources in offices and assembly halls, quantified by the olf unit", Energy and Buildings, 1988, 12, pp7-19.
4. CIBSE: "Environmental criteria for design", CIBSE Guide (Section A1), 1986, Chartered Institution of Building Services Engineering, London.
5. BRAGER, G.S.: "Using laboratory-based models to predict comfort in office buildings", ASHRAE Journal, April, 1992, pp44-49.
6. KAHKONEN, E.: "Draught, radiant temperature asymmetry and air temperature — a comparison between measured and estimated thermal parameters", Indoor Air, 1991, 4, pp439-447.
7. FISHMAN, D.S. and PIMBERT, S.L.: "Responses to the thermal environment in offices", Building Services and Environmental Engineer, January, 1979, pp10-11.
8. CROOME, D.J., GAN, G. and AWBI, H.B.: "Air flow and thermal comfort in naturally ventilated offices", Roomvent '92, Aalborg, Denmark, September 2-4, 1992.

**Ventilation for Energy Efficiency and Optimum
Indoor Air Quality
13th AIVC Conference, Nice, France
15-18 September 1992**

Poster 1

**Improved Indoor Environment and Ventilation in
Schools. A Case Study in Växjö, Sweden.**

R. Larsson^{*}, S. Olsson^{}**

*** Swedish National Testing & Research Institute,
Box 857, S-501 15 Borås, Sweden**

**** FLK Consulting Engineers, Box 43, S-351 04
Vaxjo, Sweden**

SYNOPSIS

During the last decade several surveys in Sweden have indicated that the indoor climate in existing schools is unsatisfactory, therefore a thorough project was carried out in Växjö.

The indoor climate was investigated in three schools during 1989. Detailed measurements were made of ventilation (e.g. rates, air exchange efficiency), indoor air quality (e.g. CO₂) and thermal comfort (e.g. air velocity). The main results were: high indoor temperatures, low air velocities and high concentration of CO₂. Improvements were made in all three schools during 1990. One of the classrooms was rebuilt to have its own separate ventilation system with the possibility to use either ceiling diffusers or floor supply air terminal devices.

After the improvements the measurements were repeated. The CO₂ concentration and the air temperature were measured at different locations within the classroom, at different air flow rates and at different supply air temperatures. The air exchange efficiency was determined for different air flow rates and different air supply systems.

The following recommendations were made for the schools in order to obtain

- an optimum indoor air quality: air flow rate 8 l/s and person, supply air temperature 18 °C and four ceiling diffusers
- a satisfactory thermal comfort: automatic exterior shading, circulation fan in the classroom, night cooling with outdoor air during fall and spring.

The results of this project will be used to produce a manual "Indoor Climate in Schools".

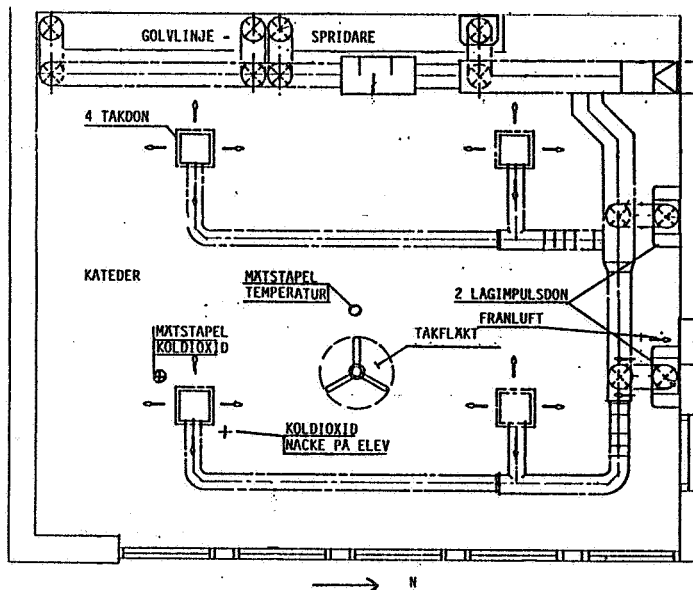
1. INTRODUCTION

In Sweden there are many schools today which need to be rebuilt and replanned. The reason is changing demands regarding education, the age of the buildings, and problems with the indoor climate and the air quality.

In Växjö a project has been carried out, partly financed by the Swedish Council for Building Research. The project concerns the indoor climate in schools, and three schools of various types have been chosen. During the school year 89/90 measurements were made to clarify the situation. During the summer and autumn -90 certain reconstructions were made. Measurements and evaluations were concluded in the summer 1992.

The aim of this project is to clarify the influence of the HVAC systems on the indoor climate in the classrooms before and after the measures were taken. The purpose is to be able to come up with explicit proposals for systems and design guidelines for classrooms with principles for air flows, temperatures etc.

The three schools are Bokelund (primary and middle school), built in 1968, Fagrabäck (high school), built in 1966, and Katedral (senior high school), built during 1958/1977. The schools have different building constructions and HVAC systems.



Plan of classroom in Fagrabäck showing location and type of air terminal device, and location of measuring point for CO₂ and air temperature.

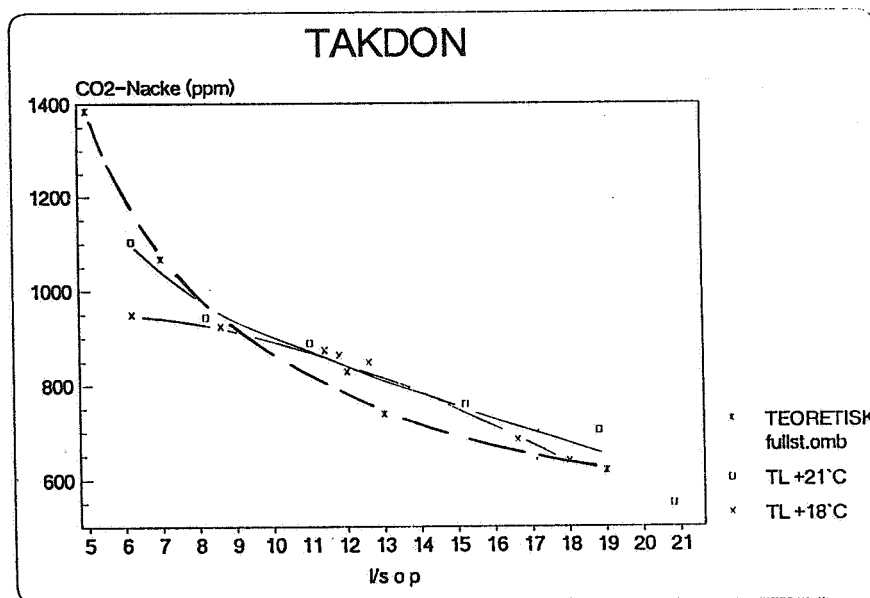


Figure 1. CO₂-content at the neck of the pupil as a function of air flow (l/s and person) at different supply air temperatures. Each point corresponds to one set of measurements, i.e. one lesson. The dotted line is a theoretical calculation. Takdon = ceiling air terminal device.

The figure shows very clearly the reduction of the CO₂ content at an increasing flow. Furthermore, you can see that the supply air temperature has a noticeable influence on the CO₂ content at flows lower than appr. 8-9 l/s per person.

2. RESULTS BEFORE MEASURES

The most important results from the preliminary measurements (during the school year 1989/90) are the following:

- High indoor temperatures (winter +24 °C, summer +30 °C)
- Low air velocities in the room (<0.1 m/s)
- Low contents of chemical substances in the air (tot. voc < 100 µg/m³)
- High contents of carbon dioxide (only at Bokelund lower than 1000 ppm)
- Low contents of formaldehyde (<40 µg/m³)
- Low contents of radon
- No unnormal presence of mould
- High contents of cat's hair in dust

The measurements proved that the most obvious problem is the high indoor temperatures. In order to reduce this problem the strategy was to install sun shading like sun-blinds and Venetian blinds, and cool night-air to cool the building.

At Katedralskolan a questionnaire was added to the investigations. This questionnaire showed low values as to well-being and social status and. The conclusion was that improvements on the visual surroundings like colouring etc were motivated.

3. MEASURES OF REBUILDING CARRIED OUT

The following measures have been taken during the autumn of 1990 in the school buildings:

Bokelund

A sun-blind has been installed as well as control equipment for night cooling.

Fagrabäck

In one class-room three different systems for supplying air have been installed. The class room has also been equipped with a fan and a sun-blind, and possibilities of increasing the airflow. Most of the measurements will take place here. There are possibilities of varying a great number of parameters making comparisons.

Katedral

Three classrooms have been redecorated and the old windows have been changed to new, tighter windows with blinds. The ventilation system has been cleaned and equipped with a control function for night cooling.

4. MEASUREMENTS OF CARBON DIOXIDE AND TEMPERATURES

Measurements were made during winter conditions in 1991. Figure 1 shows the contents of CO₂ by one pupil's neck in the classroom (at the end of the lesson) as a function of the specific flow (l/s and person) when ceiling supply air terminal devices are being used. The ceiling supply air terminal devices consisted of four symmetrically located perforated supply air terminal devices.

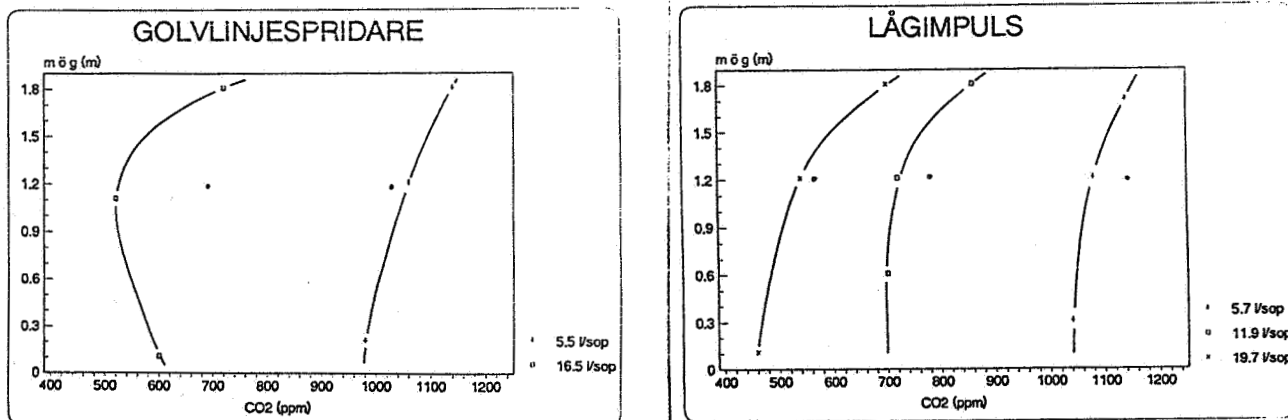


Figure 4. CO₂-content at different heights for different air flows. Supply air temperature +18 °C. The dot at 1.2 m above floor level represents the C₂-content at the neck. Lågimpuls = low velocity. Golvlinjespridare = line floor supply.

For the measurements shown in figure 3 and 4, the corresponding temperature gradients are shown in figure 5 and 6. Figure 5 and 6 show that the ceiling air terminal devices with greater flows (12 and 16.5 l/s per person respectively) give an insignificant temperature gradient (<0.5 °C). Other alternatives (including ceiling air terminal devices with small flows) give a temperature gradient which is 1 - 2 °C, i. e. no temperature gradient of importance.

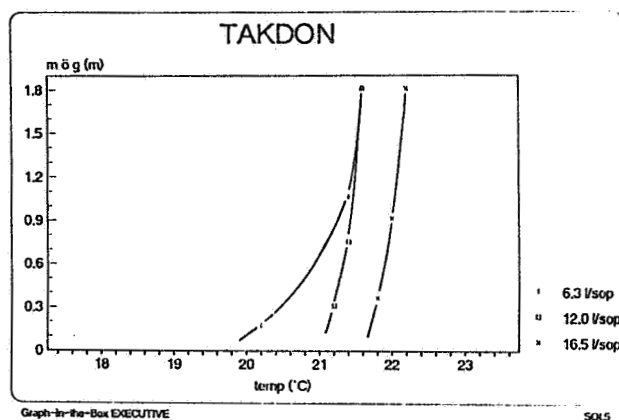


Figure 5. Temperature gradient for different air flows with ceiling air terminal devices. Supply air temperature +18 °C.

The measurements show that you can meet the requirement on 1 000 ppm CO₂ by the neck with the four supply air terminal devices with a supply air temperature of 18 °C and flows of 6 - 7 l/s per person. The calculated content of CO₂ for complete mixing at these flows is about 1100 ppm. The results from the measurements with low velocity air terminal devices (two behind pupils) throwing the air in a bow and with a line low velocity air terminal device (appr. 6 m long) show at the lower flows somewhat higher (100 - 200 ppm) contents of CO₂ than the ceiling air terminal devices (see figure 2)

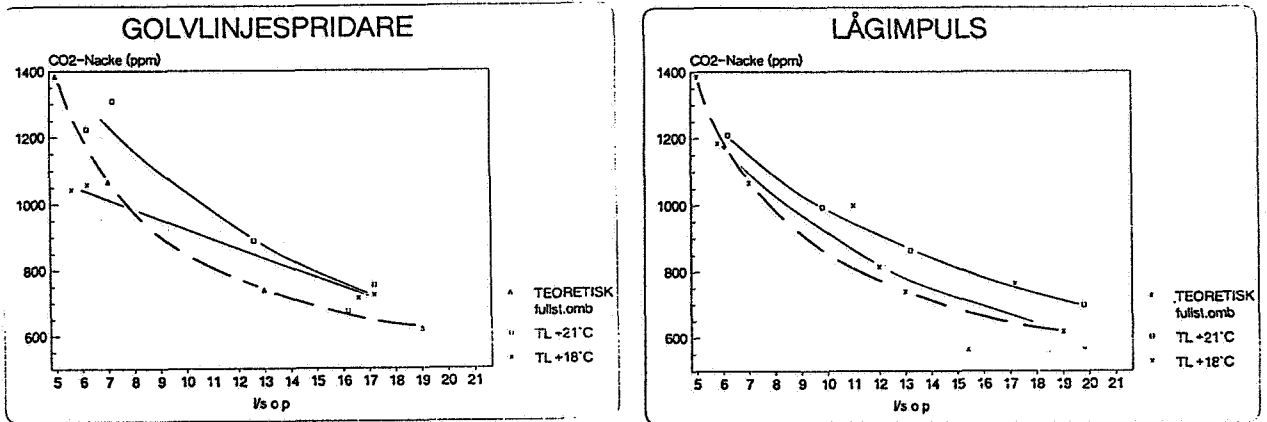


Figure 2. CO₂-content at the neck of a pupil as a function of air flow (l/s and person) at different supply air temperatures. The dotted line = theoretical calculation with complete mixing. TL = supply air. Lågimpuls = low velocity. Golvlinjespridare = line floor supply

Figure 3 and 4 show the vertical gradient of the CO₂ content with different air terminal devices and flows at 18 °C supply air temperature. It appears very clearly that ceiling air terminal devices give a lower gradient (a negligible divergence vertically) than the low velocity air terminal devices and the line floor supply air terminal device. It is also interesting to observe that the CO₂ content at the neck is somewhat higher when using low velocity air terminal devices than at points measured in the aisle between the desks (the gradient).

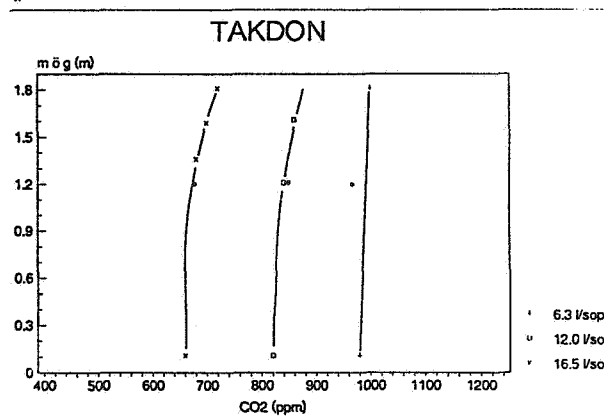


Figure 3. CO₂-content at different heights for different ceiling air terminal devices. Supply air temperature + 18 °C. The dot at 1.2 m above floor level represents the CO₂-content at the neck.

Furthermore, using night cooling is a simple and cheap way to cool the classroom during the night. It is well known that the surface temperature is as important as the air temperature for the experienced temperature, and with night cooling you can lower the surface temperature of the room.

Another circumstance effecting the experienced temperature is the air speed. When the speed increases, the experienced temperature is reduced. A ceiling fan, managed by teachers and pupils with a thyristor in the class-room, will get the air circulating, which leads to a feeling of the temperature being lower. The ceiling fan has been very much appreciated by the teachers and pupils, who have accepted astonishingly high air speeds (0.25 - 0.30 m/s).

7. AIR EXCHANGE EFFICIENCY BEFORE MEASURES

During August 1989 to March 1990 a series of different measurements was carried out regarding the air exchange efficiency in the different class-rooms. The measurements were made both with and without pupils. The results show that in most cases, regardless of the type of ventilation system, you will get close to a complete mixing ventilation when the class-rooms are being used (see figure 7). On the contrary, the result may be very varying when the class-rooms are empty, depending on the kind of ventilating system. During the measurements the airflow and supply temperatures have been kept constant. The reason for the mixing effect when pupils are present is the air movements caused by free convection from the pupils.

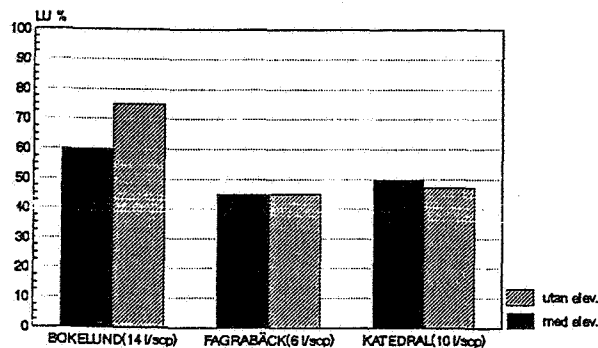


Figure 7. Air exchange efficiency before measures. Supply air temperature 2-3 °C lower than room temperature.

8. THREE DIFFERENT SYSTEMS

During the summer and autumn 1990 three different systems were installed in a class-room at Fagrabäck. Several measurements were made during January and February 1991, always with pupils in the class-room.

There were some difficulties in achieving identical conditions during the different measurements, e.g. the same number of pupils, the same activity by the pupils. The difference between measurements with identical boundary conditions is caused by small disturbances due to normal activity in the classroom, like opening and closing doors. The measurements show that there are big differences in air exchange efficiency mainly due to the supply air temperatures and flows being used, but also to some extent due to the ventilation system.

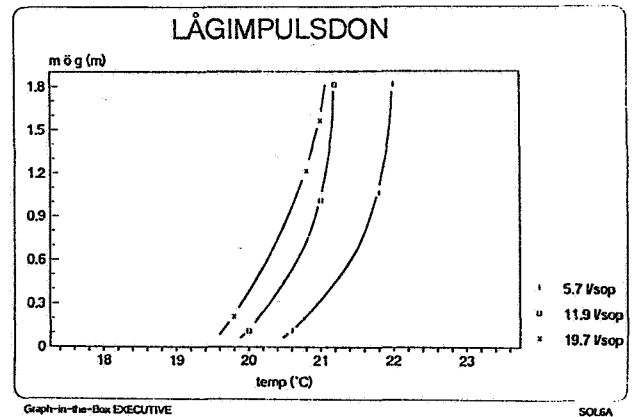
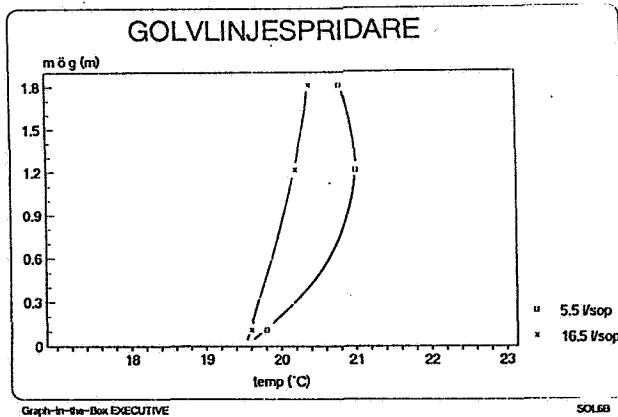


Figure 6. Temperature gradient for different air flows with low velocity supply air terminal devices and line supply air terminal devices. Lågimpuls = low velocity. Golvlinjespridare = line floor supply.

The low velocity air terminal devices and the floor line supply air terminal device are rather large for the lower flows, which results in a low temperature gradient. The measurements described above were made during the winter season.

5. CORRELATION BETWEEN VENTILATION AND CO₂

The measurements during May have proved that both the low velocity air terminal devices and the floor line supply air terminal device give a lower content of CO₂ by the neck than the ceiling air terminal devices do. The level is between 100 to 200 ppm lower compared to ceiling air terminal devices at the flow 6 - 7 l/s per person. The explanation why the low impulse/floor line supply air terminal device does not give better values than ceiling air terminal devices during winter may be that the temperature on the inside of the two-glass windows was low (appr. 10 °C lower than the indoor temperature) and also that the surface temperature of the walls is somewhat lower than the indoor temperature. These low surface temperatures cause free convection (the thermostatic valve on the radiator closed) which gives an airflow causing a stirring of the air around the room, thus disturbing the displacing effect. This airflow, caused by free convection has been estimated to around 50 - 100 % of the ventilation flow.

The measurements during May further showed that while the low velocity air terminal device/floor line supply air terminal device gave a better result by the pupil 's neck, the CO₂ content was considerably higher by the teacher standing up. This also caused complaints.

6. HIGH TEMPERATURES

We can conclude that an exterior sun shading (like a blind) is necessary in order to lower the indoor temperature. The blind should be automatically controlled by a solar radiation sensor so that it also goes down early in the morning and later when no people are in school. Our measurements showed that a classroom with windows facing east already is warmed up (to 25 - 27 °C) at 8 o'clock in the morning when the teachers and pupils arrive. After that it does not help to air the room all day long.

A big airflow into the class-room makes the air whirl around, causing a mixing ventilation. This happens irrespective of what kind of ventilation system is being used. The supply temperature versus room temperature is not of any greater importance in this case (within the temperature range considered to be reasonable, i.e. somewhat below room temperature).

A low flow into the class-room can give a tendency to short circuit. In this case however, the type of ventilation system and supply temperature are of great importance.

In figure 8 you can see a tendency to piston flow for low air flows. This tendency appears both with ceiling air terminal devices and line floor supply air devices, at flows between 6 and 10 l/s per person. For low velocity air terminal devices there is a tendency towards piston flow at low air flows and loads. The inaccuracy in the measurement of the air exchange efficiency is estimated to be $\pm 10\%$. The local mean age of air was measured at nine different locations. The difference in local mean age between different locations was negligible.

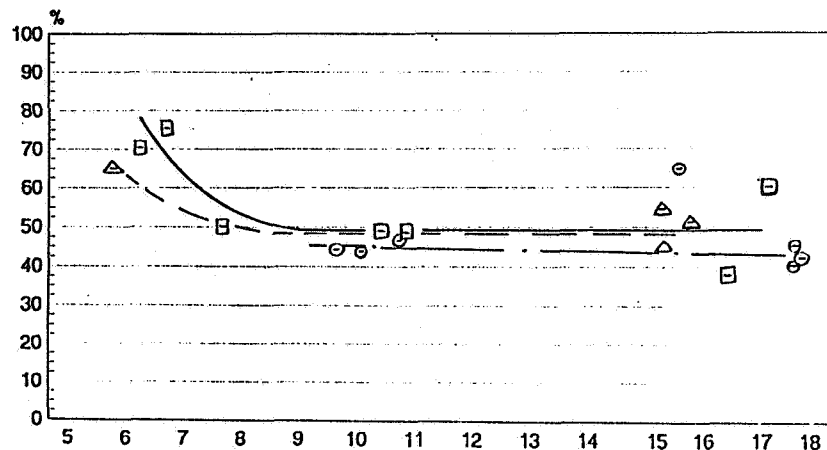


Figure 8. Air exchange efficiency as a function of air flow and supply air system. Measured after measures were taken in Fagrabäck.

- ☐ = ceiling air terminal device with a supply air temperature lower than room temperature (1 - 3 °C)
- ⊙ = low velocity air terminal device with a supply air temperature lower than room temperature (1 - 3 °C)
- △ = line flow air terminal device with a supply air temperature lower than room temperature (0 - 1.5 °C)

9. CONCLUSIONS

Ceiling air terminal devices, correctly designed as to number and location, will meet the requirement within the breathing zone 1000 ppm carbon dioxide content, with low air speeds and a small temperature gradient at a flow of 6 to 8 l/s per person. To obtain 800 ppm you will have to double the flow.

The measurements show that during the winter (with warm radiators and cold double-pane windows) the low impulse devices and line floor supply air terminal devices will give a somewhat higher content of CO₂ by the neck than the ceiling air terminal devices would at flows of 6 to 8 l/s per person. At spring conditions (with the radiator and window temperature about the same as the room temperature) the low impulse device and line floor supply air terminal will obtain 800 ppm CO₂ content within the breathing zone, with the flow 6 to 8 l/s per person.

The air speed at the feet of the pupils (close to the air terminal device) was appr. 0.2 m/s. In spite of this there has not been a single complaint of draught! The measurements also show that a teacher standing up will get a higher content of CO₂ (>1000 ppm) within the breathing zone with this solution, compared to ceiling air terminal devices.

Exterior sun shading, tyristor controlled ceiling fan and night cooling together are an effective way of reducing the indoor temperature without using comfort cooling.

The measurements of the air exchange efficiency and the mean age of air in the room show that even at relatively low flows you can achieve a moderate mean age compared to a higher airspeed. By a more effective airchange the flow can be kept down maintaining a low mean age. Relatively low flows (6 - 8 l/s per person) give a good air exchange efficiency and an acceptable mean age, and there is no reason for using higher flows (>10 l/s per person).

There is also no reason for rebuilding ventilation systems with ceiling air terminal devices to low impulse devices. It is more important to see to that the ventilation system has the correct supply air flow compared to the number of persons, the correct supply air temperature, and that the flow is distributed from a sufficient number of ceiling air terminal devices. It is also important that thermostatic valves on the radiators are set to a maximum temperature, to avoid an unnecessary increase of the indoor temperature.

Our recommendations are:

Airflow: 8 l/s per person. Supply air: 18 °C (preferably lower in spring and autumn).
Number of ceiling air terminal devices: 4 pcs. Max-reduction of thermostatic valve: closed at 20 °C. An automatic exterior shading, ceiling fan, and night cooling to reduce the indoor temperature.

10. REFERENCES

1. LARSSON, R. and OLSSON, S.
"Indoor Climate in Schools".
Swedish Council for Building Research RXX:1992

**Ventilation for Energy Efficiency and Optimum
Indoor Air Quality
13th AIVC Conference, Nice, France
15-18 September 1992**

Paper 24

Simulation of Gas Leaks in Ventilated Rooms

E. Cafaro^{*}, N. Cardinale^{}, G.V. Fracastoro^{*}, E.
Nino^{**}, R.M. Di Tommaso^{**}**

*** Dipartimento di Energetica del Politecnico di
Torino, Corso Duca degli Abruzzi 24, 10129 Torino,
Italy**

**** Dipartimento di Ingegneria e Fisica
dell'Ambiente, Universita della Basilicata, Via
N.Sauro, 85 - 85100 Potenza, Italy**

SIMULATION OF GAS LEAKS IN VENTILATED ROOMS

E. Cafaro (*), N. Cardinale (**), G.V. Fracastoro (*), E. Nino (**), and R.M. Di Tommaso (**)

(*) Dipartimento di Energetica del Politecnico di Torino, Corso Duca degli Abruzzi, 24 - 10129 TORINO (Italy).

(**) Dipartimento di Ingegneria e Fisica dell'Ambiente, Università della Basilicata, Via N. Sauro, 85 - 85100 POTENZA (Italy).

SYNOPSIS

The study deals with the theoretical and experimental simulation of gas leaks in buildings. Such simulations may provide helpful information about the flow characteristics and dangerous concentrations as a function of the ventilation system (if any), the geometrical features and the thermal constraints on the room, and eventually about the positioning of gas monitoring devices.

Theoretical simulations are performed using a three-dimensional, finite volume CFD package in order to provide the velocity, temperature and concentration fields in a room. Experimental simulations have been performed in the full-scale ventilation test room at the University of Basilicata.

1. Introduction

The paper is concerned with a particular case of contaminant diffusion indoors, related with natural gas leaks, the consequences of which may be dramatic if concentrations above 5-6 % are reached [1]. The correct positioning of gas leak detectors is of paramount importance, and requires a detailed knowledge of gas diffusion within the building. The influence on gas diffusion paths of ventilation systems, rooms geometry and thermal conditions on one side, and gas leak flow characteristics on the other side has to be thoroughly investigated.

The philosophy of this study was to carry on both a theoretical and an experimental evaluation of the phenomenon. The experimental part of the study was performed using a full-scale test room, the so-called CVC (Controlled Ventilation Chamber) of the University of Basilicata. In the CVC the experiments were performed using N_2O and SF_6 , while CH_4 is being used only recently.

The theoretical simulations were carried on at Turin Polytechnic: among the growing number of computer codes existing in this research field [2], the Create Inc. FLUENT package has been chosen, because of its reliability in predicting contaminant diffusion indoors and outdoors. A validation of FLUENT package has already been performed recently, with fair results [3].

In a first phase of the work the code was used to simulate the non-uniform decay of concentration of a tracer gas, while more recently the concentration increase with time has been investigated. In both cases, the main parameter was assumed to be the ventilation strategy, in terms of number of air changes and positioning of inlets/outlets.

Results were obtained in terms of both concentration and velocity fields, but particular attention has here been devoted to concentrations.

2. The experimental apparatus

The description of CVC was the aim of previous papers [4], [5], to which the reader is sent back for more information.

The CVC has a volume of 17 m³ and allows balanced, immission or extraction ventilation, with air entering or being extracted from up to four grilles, located on two opposite vertical walls, and ventilation rate ranging between 0 and 10 ach. Instrumentation includes a three-cell Gas Analyzer (SF₆, NO₂, and CH₄), six non-directional hot film anemometers working in the range from 0 to 0.5 m/s, a flowmeter for the measurement of air flow rate to the CVC, and two computer driven, automatic systems, one for establishing the air sampling sequence across six ducts, and the second for moving the air sampling ducts and the velocity sensors around the test room.

3. The main features of the CFD package

A turbulent flow in isothermal conditions and in the presence of a pollutant source, as in this set of tests, can be modelled by the Reynolds-averaged equations for mass, momentum (Navier-Stokes equation), and concentration, and the state equation for the fluid.

The above set of equations do not represent a closed system because the viscous stresses depend in their turn on the fluctuating components of the velocity vectors, which are unknown.

The "closure" of the system requires the introduction of a suitable turbulence model, i e, to express the components of the Reynolds stress tensor as a function of known, equivalent time-averaged quantities.

Different options exist for turbulence modelling: FLUENT package offers a two-equation k-ε Model for high Reynolds number and an Algebraic Stress Model.

The k-ε Model is generally, but not universally believed to be the appropriate level of turbulence model for air flow in buildings. However, for certain situations the limitations due to assuming isotropic turbulence may prove to be inadequate: an Algebraic Stress Model may be adopted although the increased computing time may prove prohibitive. The computational overload of an Algebraic Stress Model is found to be approximately 100 %.

The set of seven non-linear partial differential equations involved in the CFD model may be represented by the single prototype equation:

$$\frac{\partial(\rho \phi)}{\partial t} + \frac{\partial}{\partial x_i} (\bar{\rho} \bar{u}_i \phi - \Gamma_\phi \frac{\partial \phi}{\partial x_i}) - S_\phi = 0$$

where

- ϕ = main variable
- Γ_ϕ = exchange coefficient
- S_ϕ = source term for the main variable

The meaning of the generalized symbols for each equation is given in Table I.

The values of the coefficients in the k-ε model are standardized for most engineering flows, but are not universal constants for any turbulent flow. The present calculations are performed using the standard values

which may be found in the literature [6].

The airflow model field equations in the FLUENT package are expressed in time-implicit and conservative finite difference form on a staggered grid, and solved using the SIMPLE pressure correction algorithm: two variants, namely the SIMPLEC and the PISO algorithms are also available. The variants are claimed to improve the rate of convergence. Selecting the PISO algorithm a slight increase in the size of the used computer memory appears. Underrelaxation is used to promote stability and convergence: the right selection of the underrelaxation parameters is of paramount importance for a correct solution.

The SIMPLE scheme is strongly elliptic with unitary ellipticity measure, which characterizes the amplification of errors in the high wave number modes: energy cannot accumulate in the grid scale wave number component and the occurrence of the grid scale pressure oscillation is prevented. Additionally, the use of a finite volume discretization ensures the integrability of the SIMPLE scheme.

Two differencing schemes are available, namely, a "hybrid" scheme and the Quadratic Up-Stream Interpolation for Convective Kinematics (QUICK).

The mathematical model has to be completed with suitable initial and boundary conditions. For this specific problem the following conditions were assumed:

- at the inlet cells: the distribution of air velocity, of turbulent kinetic energy, and of turbulent kinetic energy dissipation rate for the ventilation air and the leaking gas;
- at the outlet cells: the longitudinal component of the velocity vector, calculated making use of the equation of continuity;
- at the walls: the gradients of the main variable are assumed zero; suitable "wall functions" are used for the determination of the parallel components of velocity vectors.

The initial turbulent kinetic energy has been calculated by means of the relation:

$$k_0 = (3/2) \cdot I^2 \cdot U_0^2$$

where

I = non-dimensional turbulence intensity, assumed equal to 0.15

U_0 = mean value of the velocity vector at the inlet

The initial dissipation rate has been calculated by the following equation:

$$\epsilon_0 = k_0^{1.5} / (\alpha H)$$

where

H = characteristic dimension of the system

α = suitable numerical coefficient

To the domain of calculation a non-uniform cartesian grid including 22x44x8 cells has been superposed. The simulation has been performed in a three-dimensional domain and adopting a symmetry plane in longitudinal direction. It should be stressed that the solution is not grid-independent, while the adoption of different values of k_0 and ϵ_0 does not seem to produce relevant variations in the calculations.

Simulations have been performed on two PC IBM compatible 80386 and 80486, and a workstation HP 720 Apollo. The running time ranged from about 48 hours for the 80386 to 8 hours for the Apollo.

4. Comparison of theoretical and experimental results

A complete scheme of the experimental tests performed both for the concentration decay and for the concentration growth with time is shown in Table II.

Theoretical simulations were mainly dealing with decay analysis using SF_6 and N_2O , and growth analysis using SF_6 and CH_4 .

The main problem in comparing the results is that the outputs are not homogeneous, that is:

- while the numerical results are known at fixed time steps (usually of five minutes), the experimental results are continuous

- while the numerical results are known at a number of locations varying between 15,500 and 50,000, the experimental data are collected only at five locations simultaneously, along a vertical rod, plus the exhaust. In order to multiply the number of points, measurements were repeated, trying to reproduce exactly the same experimental conditions, and moving the vertical rod around the CVC. Fig. 1 illustrates the position of measurement points on the CVC plan.

In order to verify the repeatability of experiments, the concentration at the exhaust was adopted as primary key. For example, for case B1, shown in Fig. 2, concentrations at the exhaust were confined within a band of 10 - 20 ppm, corresponding to 5 - 10 %. On the same graph the computed value is shown: this appears underestimated during the first 15', then falls beneath the band of measured values and appears slightly overestimated at the end of the 30' period.

Fig. 3 reports the volume of tracer gas removed from the CVC with time, given by the integral of the concentration-volume air flow product. In this case the theoretical and experimental results are very close one to the other (3-4 %). This parameter seems more reliable than instantaneous values, which are subject to random errors.

The comparisons are carried on for the decay cases B1, B3, C3, and for the growth case B1, and will be shown in terms of concentration fields.

The results are shown for some of the points on the plan of CVC shown in Fig. 1, adopting the height above the floor as a parameter. Fig. 4 and 5 illustrate respectively the measured and computed values for case B1 at the room centre (point 0), as an example. Errors keep in a 10 % range at any time below 0.80 m and at the exhaust, but may rise to 80-90 % at points above 1.50 m, after the first 20'.

Fig. 6 shows the ventilation efficiency for case B1, defined as the ratio between concentrations at the exhaust and at the considered point, calculated and measured at three different heights at point 1.

Figs. 7 and 8 show the concentration fields after 10' for cases B3 and C3. It should be observed that case C3 provides a much better result, without stagnancy situations as for case B3.

Figs. 9 and 10 show the velocity fields for cases B3 and B1. They present an interesting phenomenon, which could not be easily predicted: in the first case the air creeps along the floor until it reaches the opposite wall, while in case B1, due to the low horizontal component of velocity and the density difference between clean air and air with tracer gas (SF_6), it climbs along the wall where the outlet grille is positioned under the action of a sort of "stack effect".

Finally, Figs. 11 and 12 show the measured and calculated "concentration growth" for case B1. It appears evident, from the comparison, that the actual distribution of concentration is, at least in the first 30', much more uniform than the calculated one. However, the concentrations at the exhaust - termed "sc" in both Figures - are quite similar and end with

exactly the same value (120 ppm). After the first 30' the expected SF₆ stratification appears also in the experimental results.

5. Conclusions and future developments

Although the comparisons are limited to a small number of cases and the experimental procedure still needs some adjustment, some conclusions may already be drawn for the "decay" tests:

- in general there is a fair qualitative agreement between measured and calculated concentration values both for space and time variations;
- for the decay tests, the difference between measured and calculated data tends to increase with time, as could be expected, due to the uniformity of initial concentration. It also systematically increases with height.

For the "growth" cases, the concentration time trends show a fair agreement, while the calculated space variations appear overestimated.

Future developments include, in the experimental part of the work, the completion of measurement campaigns using CH₄, and the execution of visualization tests by means of a reduced-scale physical model, already realized at the Department of Energetics.

Future developments of the theoretical part of the work include the use of Algebraic Stress Models, and the adoption of Body Fitted Coordinate system in order to improve the meshing of the region at the supply opening.

6. Acknowledgements

The research was funded by the Italian Ministry for University and Scientific Research MURST 60 %, under the program "Controlled ventilation within confined spaces", coordinated by G.V. Fracastoro. The authors wish to express their gratitude to C. Cima and M. Perino for their skillful and patient assistance in the calculation phase, and to F. Mariniello for his assistance in the measurement campaigns.

7. References

[1] Harris, R.J., *The investigation and control of gas explosions in buildings and heating plant*, British Gas, E & FN Spon, London, New York.

[2] Liddament, M.W., *A Review of Building Air flow Simulation*. AIVC, Technical Note 33, March 1991.

[3] Cafaro, E., Fracastoro, G.V., Nino, E., Perino, M., *Analisi teorico-sperimentale della diffusione degli inquinanti negli ambienti confinati*, Atti del 46° Congresso nazionale A.T.I., Cassino-Gaeta, 25-27 settembre 1991.

[4] Fracastoro, G.V., Nino, E., and Coretti, G., *The Ventilation Chamber of the University of Basilicata*, Proc. 11th AIVC Conference, Belgirate (Italy), 1990.

[5] Fracastoro, G.V., Nino E., *La Camera a Ventilazione Controllata*

[6] Patankar, S.V., *Numerical Heat Transfer and Fluid Flow*, Hemisphere Publishing Co., 1980.

Table I
Meaning of the symbols in the prototype equation.

Equation	Principal variable ϕ	Exchange coefficient Γ_ϕ	'Source' term S_ϕ
Momentum	\bar{u}_i	μ_{eff}	$\bar{\rho} \bar{X}_i + \frac{\partial}{\partial x_j} \left[\mu_{eff} \left(\frac{\partial \bar{u}_j}{\partial x_i} - \frac{2}{3} \frac{\partial \bar{u}_k}{\partial x_k} \delta_{ij} \right) \right] - \frac{\partial \bar{p}}{\partial x_i}$
Continuity	1	0	0
Turbulence energy	k	$\frac{\mu_t}{\sigma_k}$	$\mu_t C_1 - \rho \epsilon$
Energy dissipation	ϵ	$\frac{\mu_t}{\sigma_\epsilon}$	$\frac{\epsilon}{k} (C_1 \mu_t G - C_2 \rho \epsilon)$

Table II
List and features of experimental tests.

Test	Air changes	Vent. strategy	Conc./No.pnts.	Vel./No.pnts.
(1)				
Decay				
A1	1	A	5x1+exhaust	No
B1	1	B	5x12+exhaust	No
C1	1	C	5x1+exhaust	No
D1	1	D	5x1+exhaust	No
E1	1	E	5x1+exhaust	No
A1.5	1.5	A	5x1+exhaust	No
B1.5	1.5	B	5x1+exhaust	No
C1.5	1.5	C	5x1+exhaust	No
D1.5	1.5	D	5x1+exhaust	No
E1.5	1.5	E	5x1+exhaust	No
A2	2	A	5x1+exhaust	No
B2	2	B	5x1+exhaust	No
C2	2	C	5x1+exhaust	No
D2	2	D	5x1+exhaust	No
E2	2	E	5x1+exhaust	No
B3	3	B	5x9+exhaust	6x30
C3	3	C	5x1+exhaust	6x30
Growth				
A1	1	A	5x3	No
B1	1	B	5x3	No
C1	1	C	5x3	No
D1	1	D	5x3	No
E1	1	E	5x3	No

- (1) A = inlet down(D)/right(R), outlet D/left(L)
 B = inlet D/R, outlet up(U)/L
 C = inlet D/R, outlet U/R
 D = inlets D/R, outlets U/R + U/L
 E = inlets D/R + U/L, outlets D/L + U/R

Fig. 1 – CVC Plan

Measurement points

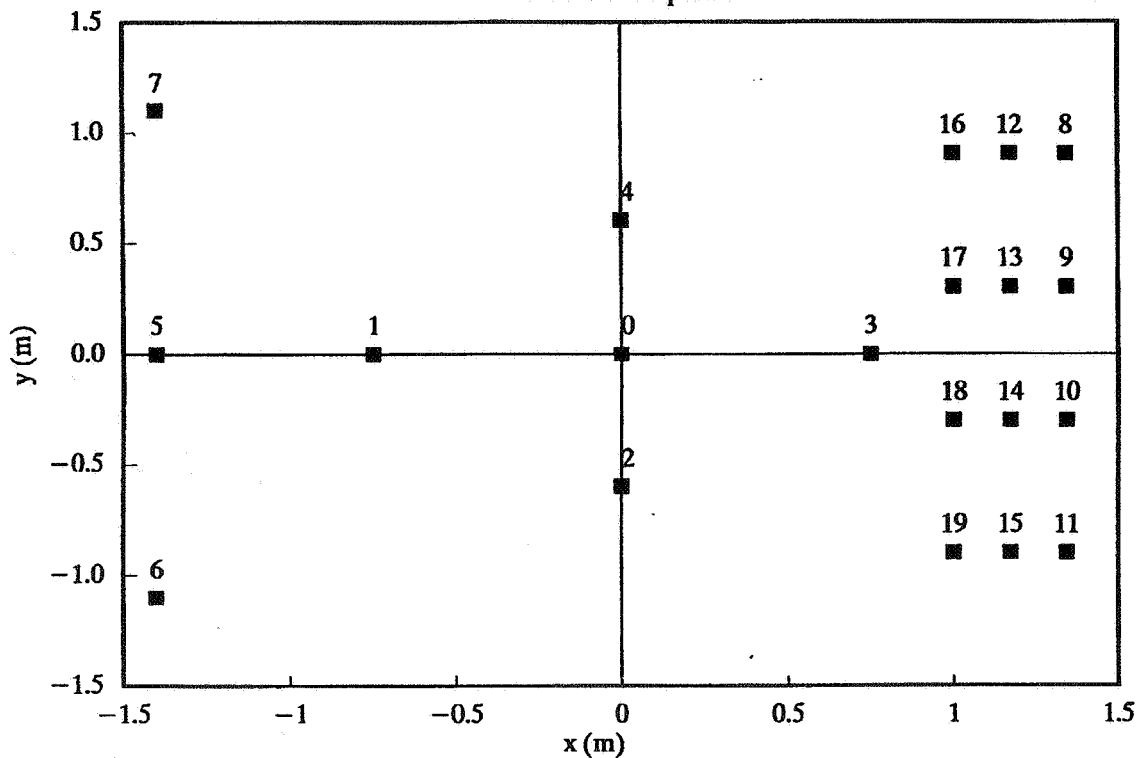
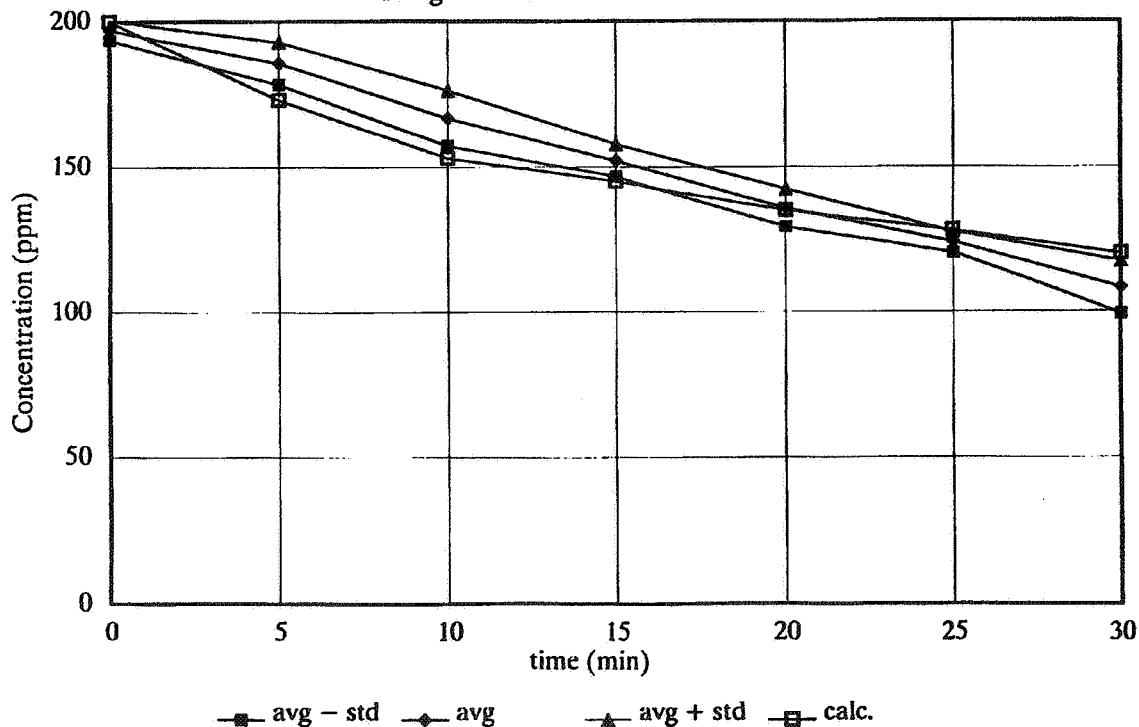


Fig. 2 – Concentration at the exhaust

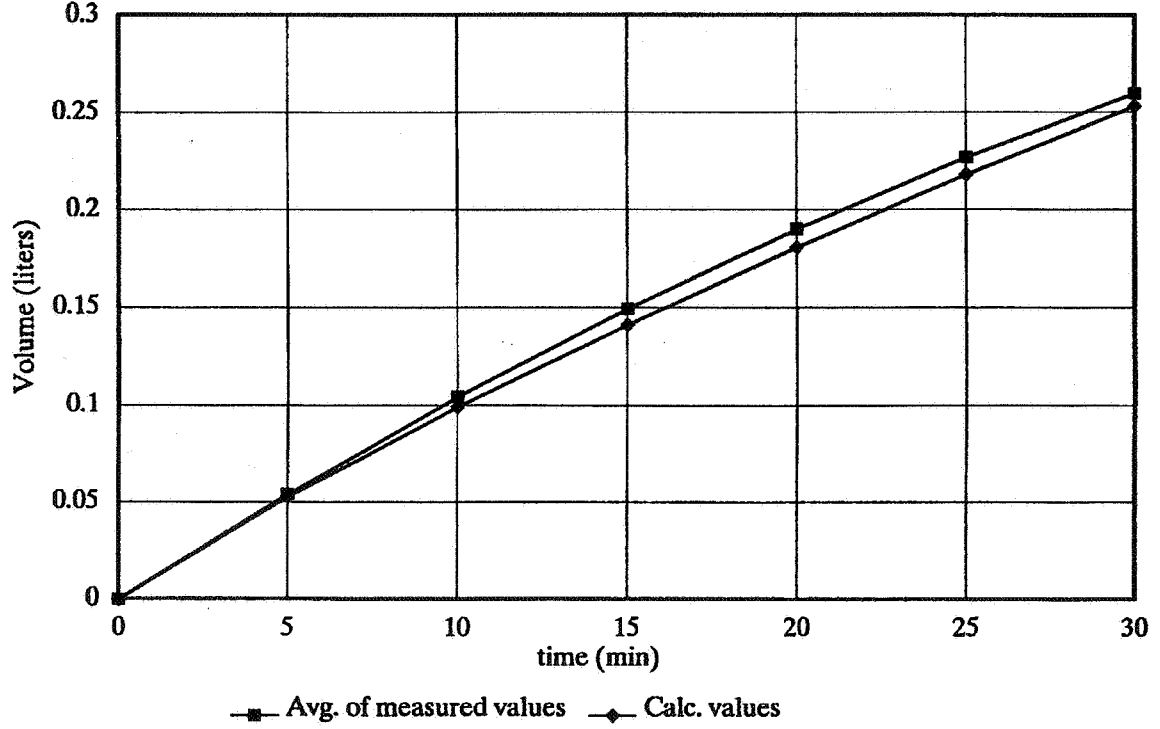
Range of measured and calculated values



Case B1

Fig. 3 – Volume of removed tracer gas

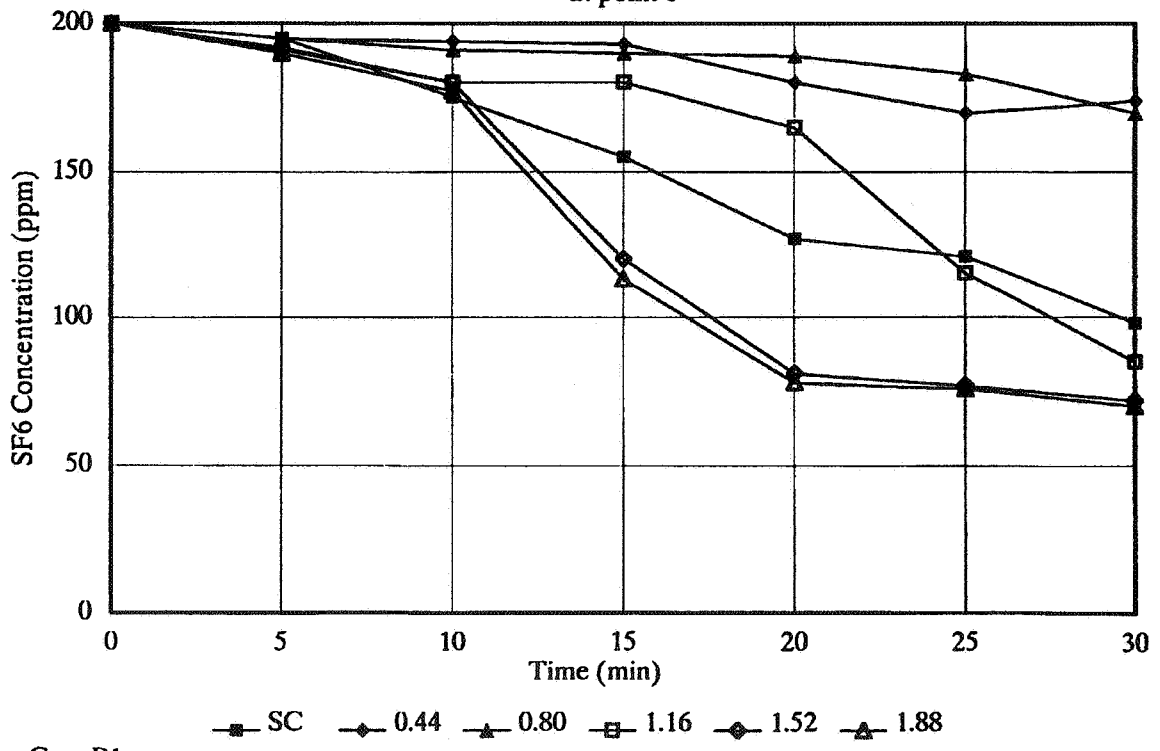
Calculated and measured values



Case B1

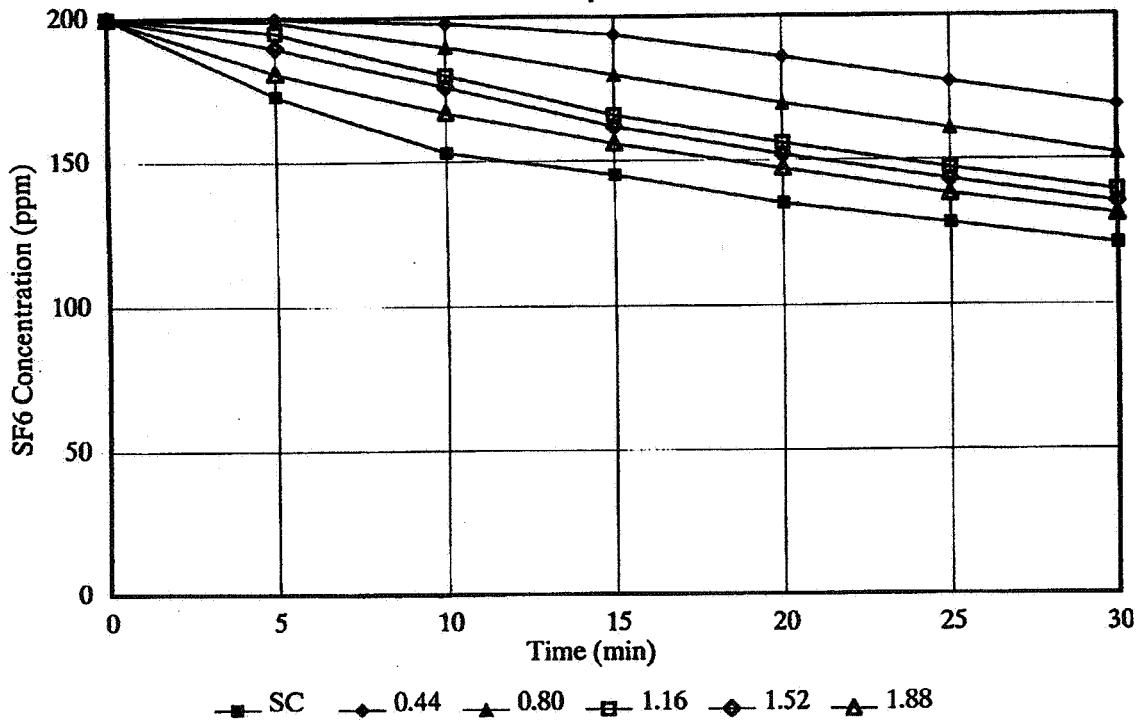
Fig. 4 – Measured Concentration decay

at point 0



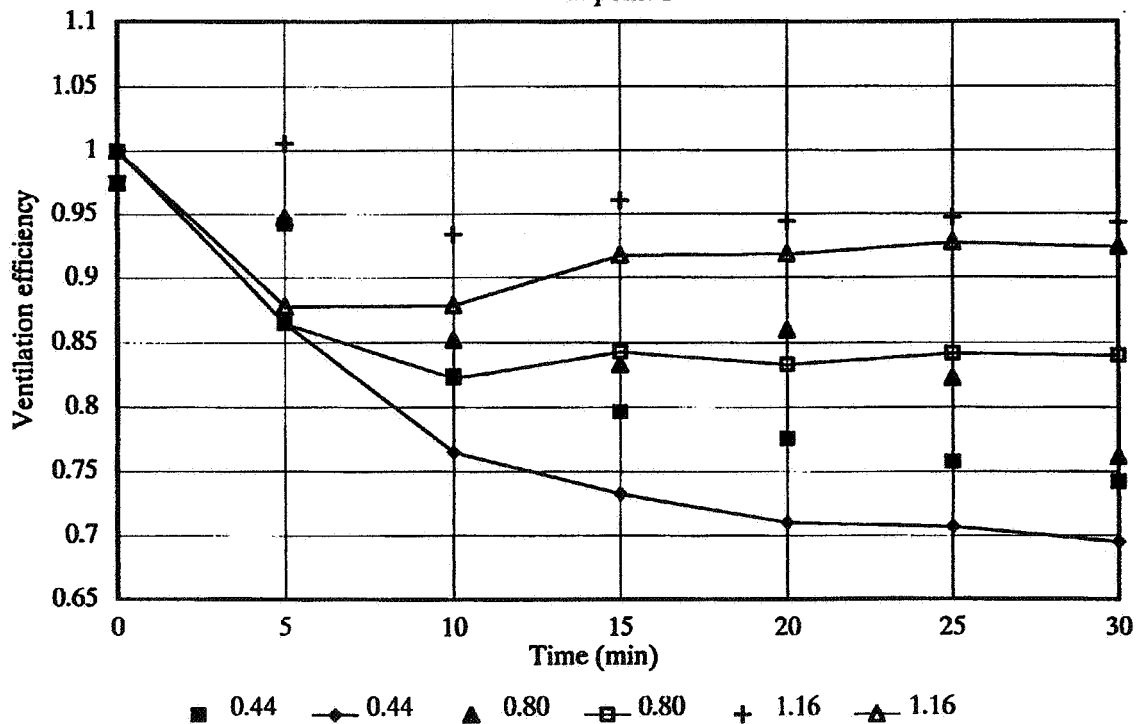
Case B1

Fig. 5 – Calculated Concentration decay
at point 0



Case B1

Fig. 6 – Meas. vs. calc. ventilation efficiency
at point 1



Case B1

Fig. 7 – Calculated concentration field

At time $t = 10'$ – Case B3

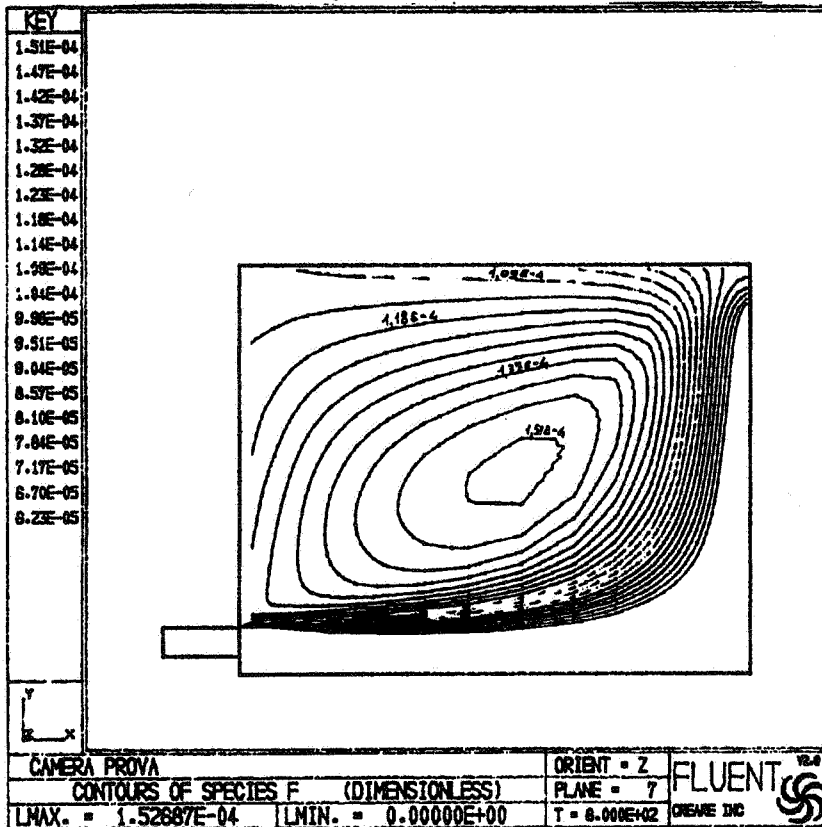


Fig. 8 – Calculated concentration field

At time $t = 10'$ – Case C3

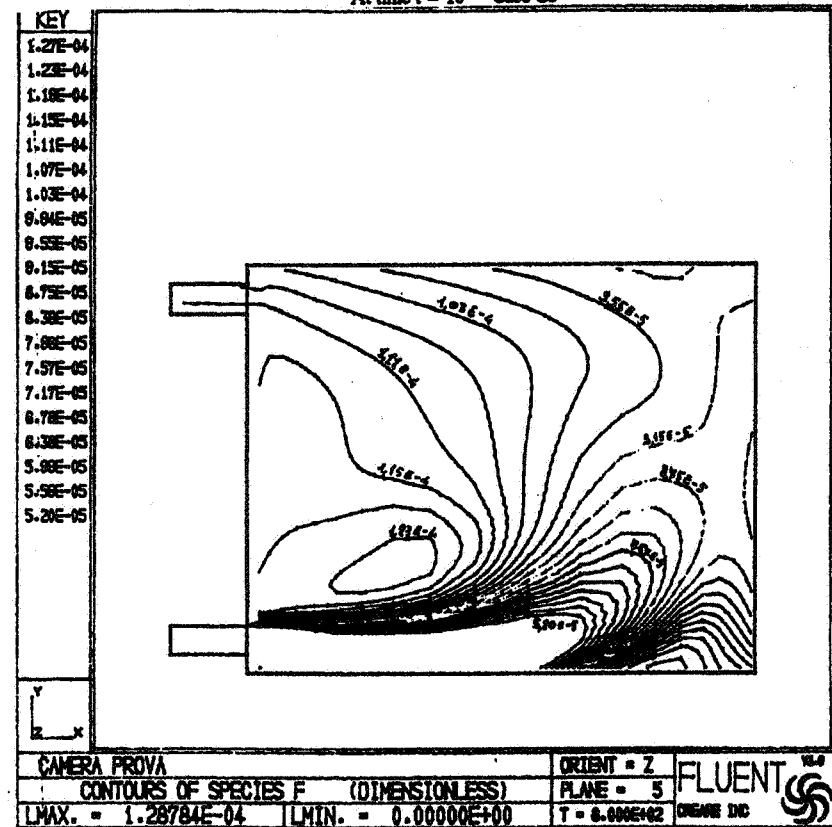


Fig. 9 – Calculated velocity field

At time $t = 10^7$ – Case B3

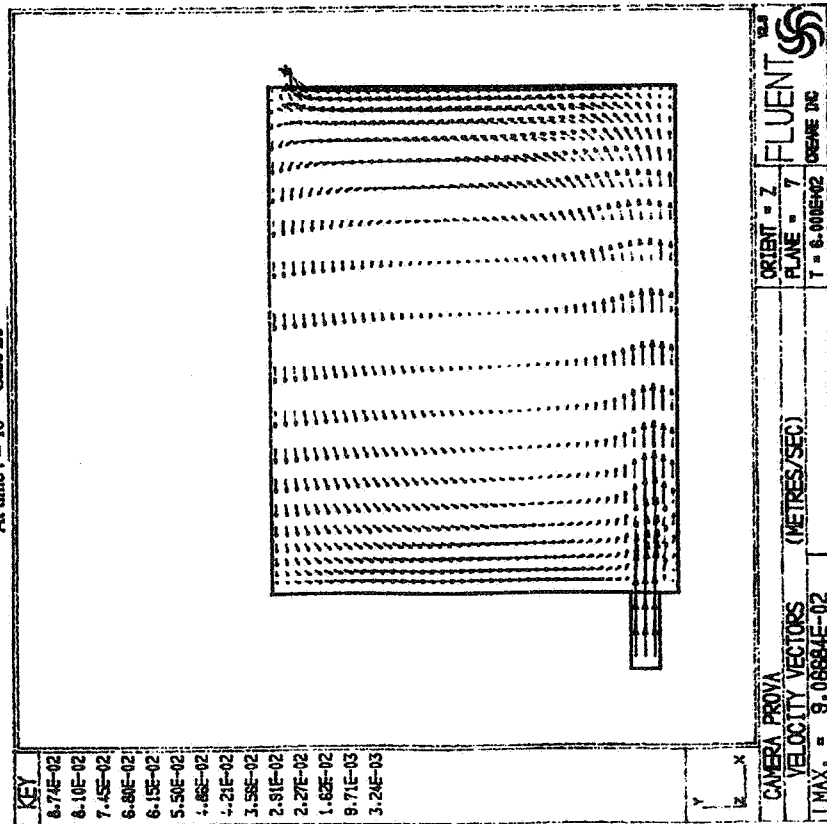


Fig. 10 – Calculated velocity field

At time $t = 10^7$ – Case B1

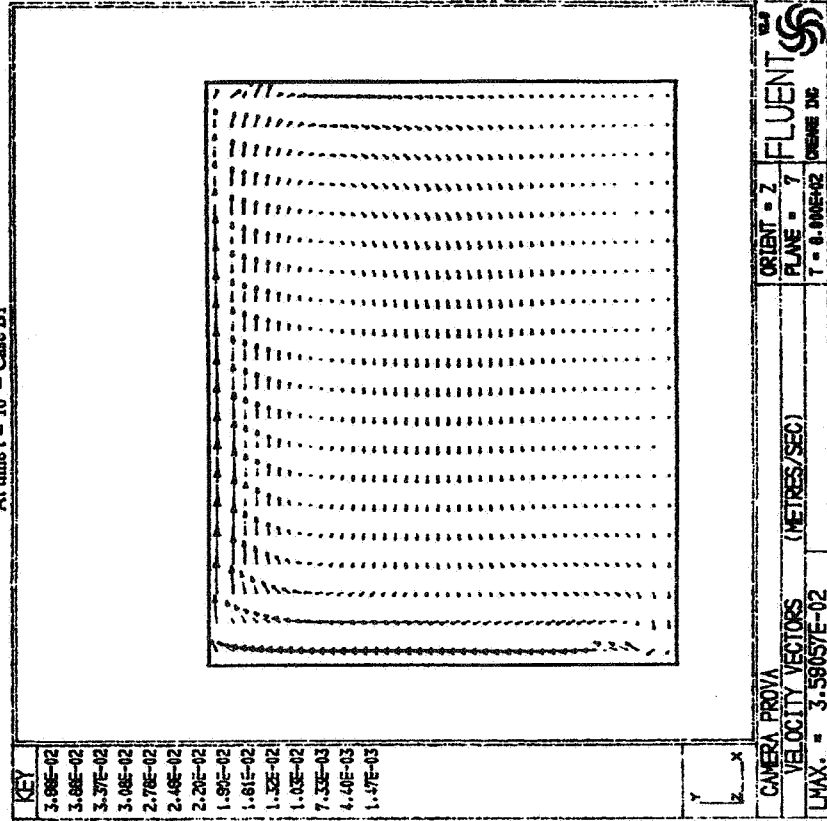


Fig. 11 – Measured concentration growth
at point 7

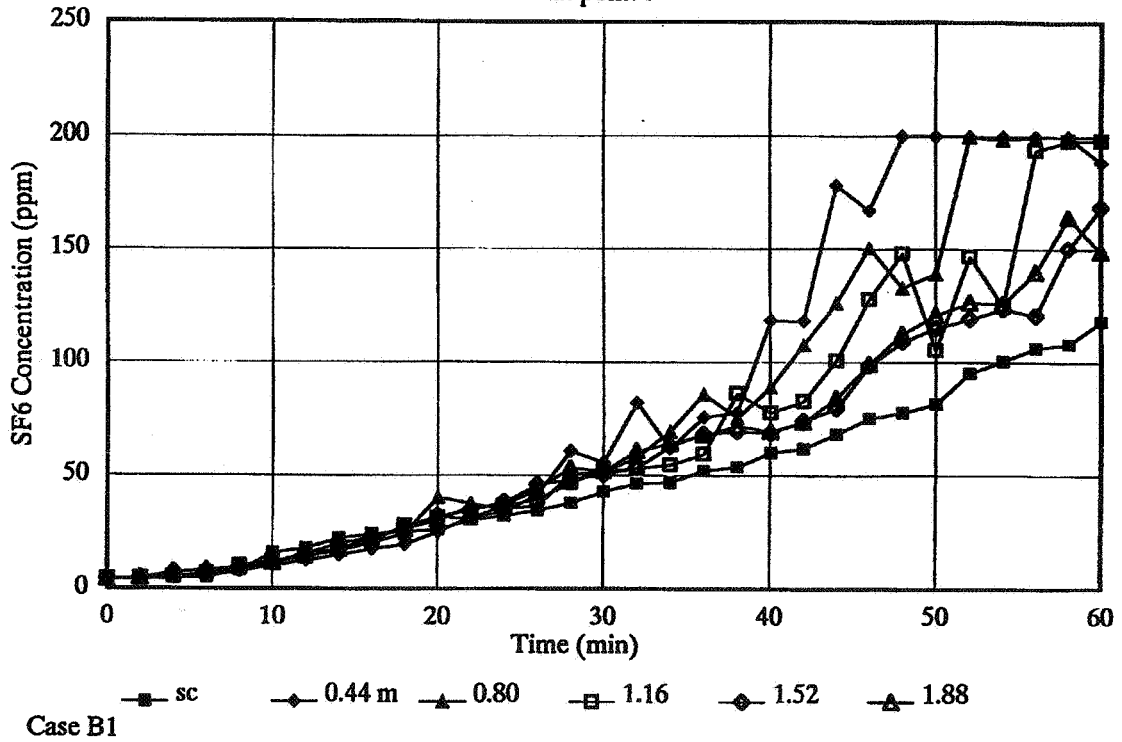
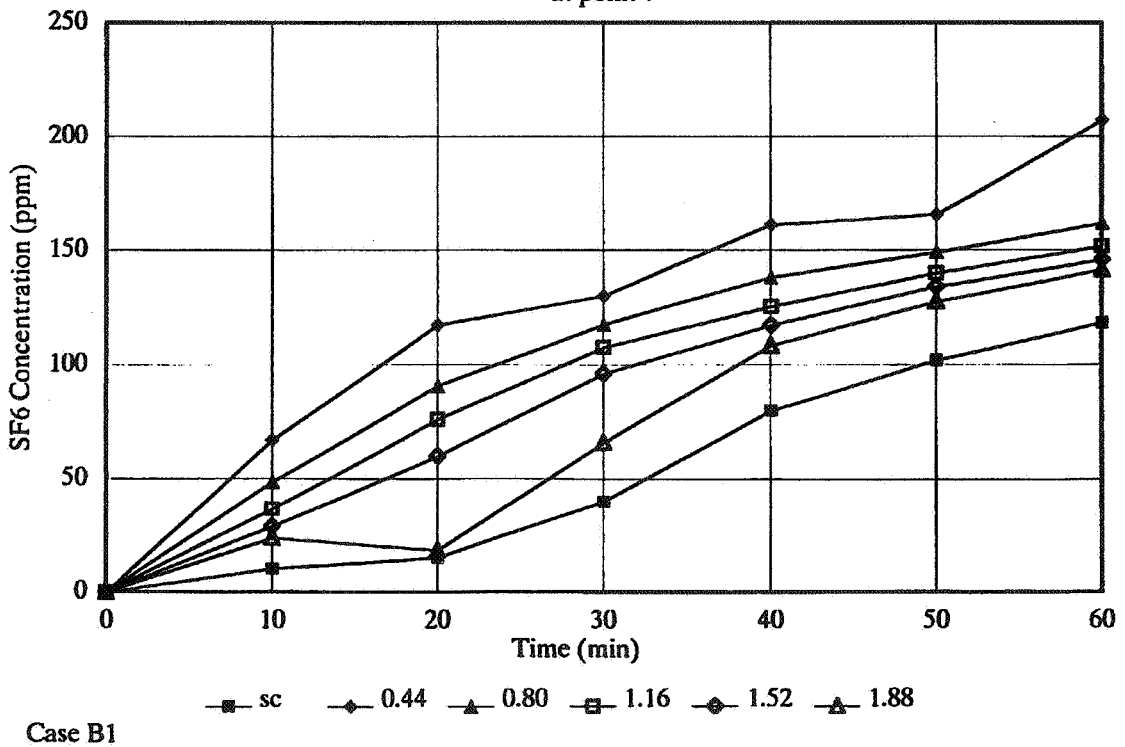


Fig. 12 – Calculated concentration growth
at point 7



**Ventilation for Energy Efficiency and Optimum
Indoor Air Quality
13th AIVC Conference, Nice, France
15-18 September 1992**

Paper 23

**Field Measurements of Air Change Effectiveness
Using Tracer Gas Techniques.**

B.W. Olesen and J. Seelen

**Indoor Environment Program, College of
Architecture & Urban Studies, Virginia Tech.,
Blacksburg, Virginia, USA.**

ABSTRACT

The present paper reports on tracer gas measurements performed in five large buildings during normal operating conditions. In all buildings air was supplied through ceiling diffusers and returned through a ceiling plenum. The measurements were taken during summer with the systems in cooling mode, i.e. the supply temperature was lower than the room temperature.

The global air change effectiveness and the occupied zone average air change effectiveness were calculated based on the age-of-air concept. The local air change effectiveness i.e., for one point in the space, was calculated in two ways: (1) Age-of-air in the return duct divided by local age-of-air at breathing level, and (2) Age-of-air at return grille in ceiling divided by local age-of-air at breathing level. To measure age-of-air the tracer gas step-up method was used.

The global air change effectiveness as well as the average air change effectiveness in the occupied zone for all systems indicated complete mixing. The local air change effectiveness showed, however, larger differences, indicating that the air in the occupied zone was not uniform mixed in all buildings.

INTRODUCTION

The cause for many cases of Sick Building Syndrome is often poor ventilation: either a low level of outdoor air coming into the building or poor distribution of the air in the system or in the occupied space. The distribution of the air influences both the thermal conditions and the indoor air quality in the space. Therefore, it is important to know how efficient the air is being distributed in the space. Also, from an indoor air quality standpoint, it is important to know how efficient contaminants are being removed from the occupied zone. These two factors are often described as air change effectiveness (efficiency of the air distribution) and contaminant removal effectiveness (Brouns 1991) (efficiency of contaminant removal).

This paper presents measurements of air change effectiveness performed in several large buildings. The intention is to contribute to the knowledge about air change effectiveness in typical buildings during typical summer conditions, and not to study the influence of the type of building or system. Other studies that report data on the efficiency of the ventilation systems are, based on controlled laboratory measurements: Sandberg 1986, Mathisen and Skaaret 1983, Qingyan 1988; or, based on field measurements: Fisk et al. 1988, 1989, 1991, Persily et al. 1985, 1986, 1990, 1991.

AIR CHANGE EFFECTIVENESS AND CONTAMINANT REMOVAL EFFECTIVENESS

The outdoor air requirements or the air change rates listed in existing standards and codes (e.g. ASHRAE 62-89, Table 2) assume perfect mixing of the air in the ventilated space. This assumption does not always apply. It is necessary, therefore to take into account how efficient the air is distributed in the occupied zone. If there are zones of stagnant air and/or short circuiting, it may be necessary to increase the amount of outdoor air. If, on the other hand, there is a displacement flow, the amount of outdoor air may be reduced. To properly assess the ventilation in the breathing zone, one must determine:

- The air renewal/air distribution process: How quickly "old" contaminated air is placed with "new" outdoor air in the occupied zone.
- The contaminant removal process: How quickly generated contaminants are removed, and how effectively the contaminants are prevented from spreading to critical areas, like the occupied zone.

These two processes are related but generally not identical and therefore need to be treated separately. For both air renewal and contaminant removal it is important to make clear if the results are based on room average, occupied zone average or local conditions. To assess the indoor air quality, the occupied zone average and local conditions must be determined.

The effectiveness of air renewal and contaminant removal are referred to as "air change effectiveness" and "contaminant removal effectiveness" respectively. In the literature there is some confusion regarding these terms. Some publications use air change efficiency or air exchange efficiency to characterize the air renewal/air distribution process. In these publications complete mixing is being referred to as 50% efficiency and complete displacement flow to 100%. In recent standards (ASHRAE 62-89; COST-613 1992) however, perfect mixing is referred to as 100% efficiency. Because an efficiency can not exceed 100% it is recommended to use the word effectiveness. The process of removing contaminants from the space is normally referred to as contaminant removal effectiveness or ventilation effectiveness (COST-613 1992). ASHRAE Standard 62-89 is using the term "ventilation effectiveness" to characterize the air renewal/air distribution process.

Air Change Effectiveness

Air change effectiveness is based on the age-of-air concept (Sandberg 1983; Skaaret 1982; Sutcliffe 1990). The age-of-air in a room is a measure of the time it takes the supply air to reach a given location in the room. Age-of-air can be considered as the local age-of-air, the room or global average age-of-air, and the occupied zone average age-of-air.

The *local age-of-air* is measured at individual points within a room and used if the ventilation at individual work stations, or the distribution of air in naturally ventilated buildings, is to be assessed. It can also be used to map airflows through rooms. The local age-of-air can be determined taking the area between the concentration curve and the final concentration and divide this by the final concentration (equation 1, Table 1). The *room average age-of-air*, measured in the room return air, or *global average age-of-air*, measured in the section return air, quantifies the performance of a ventilation system and can be calculated using equation 2 in Table 1 (Sandberg 1983; Sutcliffe 1990). It takes into account both the amount of ventilation air supplied to the room and the efficiency with which this air is distributed in the room. The *occupied zone average age-of-air*, is the mean value of the local age-of-air measured at breathing level at different points in the occupied zone. The air change effectiveness of the ventilation system can be calculated by dividing the local age-of-air in the return by the room average age-of-air.

The air diffusion effectiveness (Fisk et al. 1991) is calculated by dividing the age-of-air at a return grille by the age-of-air at breathing level, measured at a location close to that return grille in the occupied zone. The air diffusion effectiveness is a better indicator of the airflow in the room because it is not influenced by the residence time of air in the plenum and/or the leakage of supply air into the return plenum. The method used to determine the age-of-air in the measurements presented here, was the step-up tracer gas method. This method has been described earlier by Sutcliffe, 1990.

Contaminant Removal Effectiveness

Contaminant removal effectiveness is the effectiveness of the ventilation system to remove contaminants generated in the room. It can be calculated by dividing the contaminant concentration in the extract air (return air from the room) by the average contaminant concentration in the breathing zone. If the contaminant sources are evenly distributed in the room (i.e. building materials, carpet, people) the contaminant removal effectiveness will be

similar to the air change effectiveness. This paper only reports measurements of air change effectiveness.

FIELD MEASUREMENTS

The following data were collected from a series of independent field tests. The measurements were part of a general characterization of the indoor climate and the performance of the HVAC systems in the studied buildings. The tracer gas technique was used to measure air flow in ducts, outside air supply, outside short circuiting, infiltration air, and age-of-air. All measurements were done during summer conditions.

The buildings were multi-story served by one or more air handling units. Typically the outdoor air was 10% to 20% of the total supply. All spaces had supply diffusers in the ceiling and returned the air through a ceiling plenum. A short characterization of the test spaces is shown in Table 2 and 3. Each test involved only one section of a building. A section is defined as the total of all spaces covered by one air handling unit and one outdoor air supply. In some of the sections studied the supply duct from the air handling unit branched out to cover different zones. A zone could either be one room (classroom, single office, open plan office floor) or a group of rooms connected to the same return duct. The age-of-air measurement in the return duct after all branches are reconnected, represents the room or global average age-of-air for a section. A schematic of a section in a building is shown in Figure 1.

Test Procedure

A multi point doser and sampler unit (6 points) was used together with a gas monitor. The detection limit for the tracer gas used (SF_6) was 0.005 ppm. Concentrations were monitored in the occupied space, and in the return ducts. In the occupied zone concentrations were measured at breathing level, 1.1 m for sedentary persons, and in some of the tests also at return grilles in the ceiling. During a test the conditions were stable, i.e., amount of outside air, total air flow, and temperature conditions were constant. During occupancy, measurements may have been influenced by opening and closing doors, increased mixing due to body movements, etc..

RESULTS

The results for all buildings are presented in Table 2 and 3. In buildings A, B, C, and D (Table 2) the age-of-air in the return duct represented an entire section. In building F (Table 3) the age-of-air was measured both for the zone and the section. The results for F2 and F3 are from the same open plan office floor measured on two different days in ten different locations at breathing level and corresponding return grilles in the ceiling. The measurements in the returns from the section and the zone were at the same locations both days. The results for F4 were taken at the same locations as F2, but taken during the night when there were no occupants.

The local age-of-air was calculated using equation 1 and the average age-of-air for the section and/or zone was calculated using equation 2 in Table 1. The global or zone air change effectiveness, ACE_G and ACE_Z , the occupied zone average air change effectiveness, ACE_{BL} , and the local air change effectiveness, ACE_L , were calculated using respectively equation 3, 4, and 5. The air diffusion effectiveness, ADE, was calculated using equation 6 in Table 1.

The air change rate n , can be calculated as the reciprocal of the age-of-air in the return $1/\tau_N$. For the buildings presented here, the air change rates varied between 0.5 and 3.5 h^{-1} .

DISCUSSION

The average air change effectiveness for the section (ACE_G) and zone (ACE_Z) were in all tests between 0.8 and 1.1. Based on studies and evaluations from Fisk et al. (1991) the 95% confidence limit for these types of measurements are $\pm 20\%$. This means that the air distribution in the buildings tested was not significantly different from complete mixing i.e. 1.0. It is generally thought that many systems are unable to distribute the air well and have, therefore, short circuiting of air or zones of stagnant air in the room. The present results on the global air change effectiveness, do not support this, but measurements were only done in the summer season with the systems in the cooling mode, i.e. the supply air temperatures were significant lower than the room temperatures. Other studies have shown (Offermann 1988; Sandberg 1986; Olufsen 1991) that in the winter season, with similar systems in heating mode, i.e. supply temperatures higher than room temperatures, you may find a lower air change effectiveness in the range 0.5 to 0.7.

Although the air change effectiveness for a section/zone shows a value around 1.0, implying complete mixing, this does not necessarily mean that the air distribution in the occupied zone is uniform. To evaluate the distribution of air in the occupied zone, the average age-of-air in the occupied zone $\langle \tau_{BL} \rangle$ is compared to the age-of-air in the return from the section τ_N . Except for building D, the average air change effectiveness of the occupied zone (ACE_{BL}) varies between 0.8 and 1.2, which is not significantly different from complete mixing, 1.0. The corresponding air change effectiveness measured in building D, $ACE_{BL} = 1.4$ could be caused by stagnant/slow moving air in the plenum or displacement flow in the room. Unfortunately no age-of-air measurements were made in the return grilles in the ceiling in this building, which would have given an indication why the air change effectiveness of the occupied zone was higher than in the other buildings.

Even an average age-of-air in the occupied zone (ACE_{BL}) of around 1.0 does not necessarily mean perfect mixing. There may still be variation in the age-of-air at the different locations in the occupied zone. This can be evaluated by comparing the local age-of-air measurements at breathing level in the occupied zone τ_{BL} to the age-of-air in the return from the section τ_N . The local air change effectiveness, ACE_L varies significantly in building A (0.7 to 1.2), D (1.0 to 1.8) and F (0.8 to 1.2), which means the air in these buildings is not uniform mixed. In building B (1.1) and C (1.1 to 1.2) the variations are negligible indicating uniform mixing of the air. Since age-of-air at the return grilles in the ceiling was not measured in building A, C and D, the air diffusion effectiveness could not be determined for these buildings. For building B and F the results for the air diffusion effectiveness varied between 0.9 and 1.2, which is similar to the calculated values for the local air change effectiveness, ACE_L , both indicating uniform mixing.

The presented results agree well with measurements reported elsewhere in large office buildings under similar conditions. Fisk et al. (1991) summarized his results from nine different buildings. In these studies the global air change effectiveness, ACE_G varied between 1.0 and 1.4 and the occupied zone average air change effectiveness, ACE_{BL} varies between 0.8 and 1.4. Persily et al. (1985; 1986; 1990; 1991) reported a global air change effectiveness in the range of 0.9 to 1.1.

Although the majority of studies use the age-of-air concept, the question remains which locations represent best the conditions in the space (room average, occupied zone average, breathing level average) and which locations should be used as the reference (return duct from the entire section, return duct from the zone, nearest return grille in the ceiling). Furthermore, because some data are reported assuming perfect mixing to be an effectiveness of 1 or 100%, while others assume perfect mixing to be 0.5 or 50% and complete displacement flow to be 1 or 100%, there is a definite need for guidance and standardization.

CONCLUSION

This paper reported on the field measurements of the air change effectiveness in large commercial buildings during summer (cooling season). In all measurements the tracer gas step-up technique and the age-of-air concept were used. The data indicate that there is limited short circuiting in large buildings operated under summer conditions when the supply air temperature is lower than the room temperature.

The global air change effectiveness, ACE_G , implied perfect mixing but since ACE_G integrates the flow pattern in the entire test space (building) including flow in ducts, flow in ceiling plenums, flow around and in the occupied zone, this is not a good representative of the effectiveness of the distribution of the air in the occupied zone. A better parameter is the occupied zone average air change effectiveness, ACE_{BL} , which is based on age-of-air measurements at breathing level at several locations. But even if this value indicates perfect mixing, there may be locations with stagnant air (effectiveness lower than 1) or locations with displacement flow (effectiveness greater than 1). Therefore, the local air change effectiveness, ACE_L , and/or the air diffusion effectiveness should be evaluated to assess the ventilation at individual work spaces.

Future research should include field measurements taken for different seasonal conditions especially heating periods, and measurements to determine the contaminant removal effectiveness in order to assess the efficiency of contaminant removal. Furthermore, the way of measuring and reporting air change effectiveness should be standardized.

Acknowledgments: We thank Bruel and Kjaer, Inc. for providing the necessary instrumentation to perform the measurements.

REFERENCES

1. ASHRAE. "ASHRAE Standard 62-1989, Ventilation for acceptable indoor air quality". 1989.
2. Commission of the European Communities. "COST-613, Indoor Air Quality and its impact on man: Ventilation Requirements" 1992. (In press)
3. Brouns, C.; and B. Waters. "A Guide to Contaminant Removal Effectiveness". AIVC, Technical Note no. 28-2, 1991.
4. Fisk, W.J.; R.J. Prill; and O. Seppanen. "Commercial building ventilation measurements using multiple tracer gases". Proceedings of the 9th AIVC Conference, Effective Ventilation, 1988.
5. Fisk, W.J.; R.J. Prill; and O. Seppanen. "A multi-tracer technique for studying rates of ventilation, air distribution patterns, and air exchange efficiencies". ASHRAE, Building Systems: Room Air and Air Contaminant Distribution, 1989.
6. Fisk, W.J.; D. Faulkner; and R. Prill. "Air Exchange Effectiveness of Conventional and Task Ventilation Offices". ASHRAE Proceedings of IAQ'91, Healthy Buildings, 1991.
7. Mathisen, H.M.; and E. Skaaret. "Efficient Ventilation of Small Rooms". IIR, Commission E1, 16th Int. Congress of Refrigeration, Paris, 1983.

8. Offermann, F.J. "Ventilation effectiveness and ADPI measurements of a forced air heating system". ASHRAE Trans. 94 Part 1, 1988, pp694-704.
9. Olufsen, P.L. "Field studies on ventilation efficiency in mechanically ventilated rooms". ASHRAE Trans. 97, Part 2, 1991.
10. Persily, A.K. "Ventilation effectiveness in mechanically ventilated office buildings". National Institute of Standards and Technology, NBSIR 85-3208, 1985.
11. Persily, A.K. "Ventilation effectiveness measurements in an office building". ASHRAE Proceedings of IAQ'86, Managing Indoor Air for Health and Energy Conservation, 1986.
12. Persily, A.K.; and W. S. Dols. "Field measurements of ventilation and ventilation effectiveness in a library building". Proc. of the 11th AIVC Conference, Ventilation System Performances, Vol. 2, 1990.
13. Persily, A. K; and W.S. Dols. "Field Measurements of Ventilation and Ventilation Effectiveness in an Office/Library Building". Indoor Air, Vol 1, No. 3, 1991.
14. Qingyan, C.; J. Van der Kovi; and A. Myers. "Measurements and computation of ventilation efficiency and temperature efficiency in a ventilated room". Energy and Buildings, No. 12, 1988.
15. Sandberg, M.; and M. Sjoberx. "The use of moments for assessing air quality in ventilated rooms". Buildings and Environment Vol 18, 1983, pp. 181-197.
16. Sandberg, M. "Luftutbyteseffektivitet, Ventilations-effektivitet i cellekontor". The National Swedish Institute for Building Research, Meddelande M 85:24, 1986.
17. Skaaret, E.; and H. M. Mathisen. "Ventilation Efficiency". Environment Int., No.8, 1982.
18. Sutcliffe, H. "A guide to air change efficiency". AIVC, Technical Note no. 28,1990.

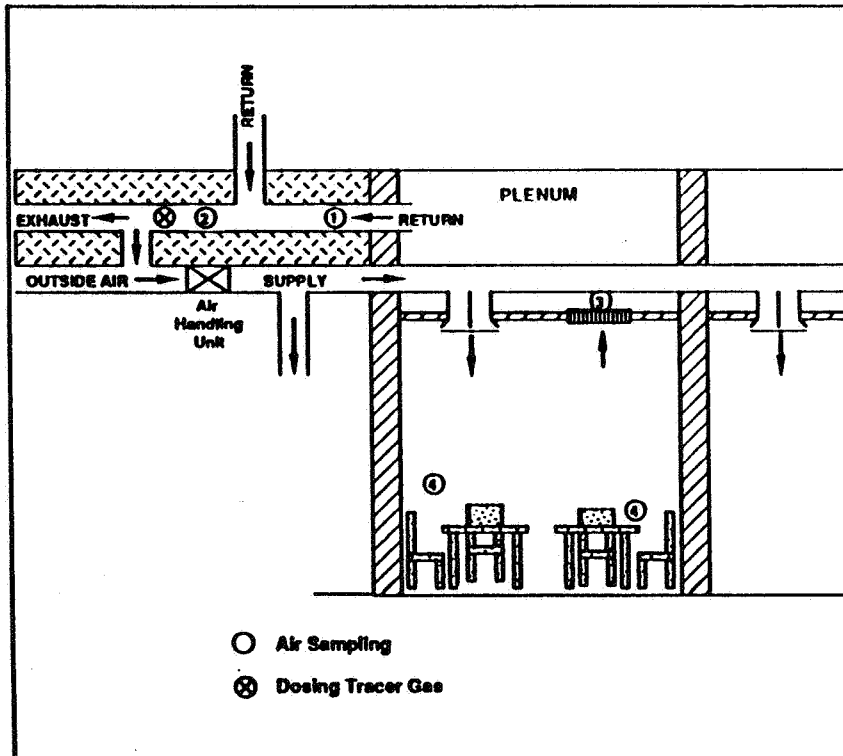


Figure 1. Schematic of a section of a building, showing location of dosing and sampling points in a typical measurement. Sample locations: 1: zone return; 2: section return; 3: grille; 4: breathing level.

#	Parameter	Equation	Unit
1	Local age-of-air	$\tau_p = \int_0^{\infty} (1 - \frac{C(t)}{C_{\infty}}) dt$	h
2	Average age-of-air	$\langle \tau \rangle = \frac{\int_0^{\infty} (1 - \frac{C_{ex}(t)}{C_{\infty}}) t dt}{\int_0^{\infty} (1 - \frac{C_{ex}(t)}{C_{\infty}}) dt}$	h
3	Air Change Effectiveness, global	$ACE_g = \tau_N / \langle \tau \rangle$	
4	Air Change Effectiveness, occ. zone	$ACE_{BL} = \tau_N / \tau_{BL}$	
5	Air Change Effectiveness, local	$ACE_L = \tau_N / \tau_{BL}$	
6	Air Diffusion Effectiveness	$ADE = \tau_{RG} / \tau_{BL}$	
where $C(t)$ = concentration t, ppm C_{∞} = concentration at time $t = \infty$, ppm C_{ex} = concentration in extract, ppm t = time, s (h) τ_N = local age-of-air in section return τ_{BL} = local age-of-air at breathing level τ_{RG} = local age-of-air at return grill			

Table 1. Equations for calculation of age-of-air and air change effectiveness.

Open office with partitions		Age - of - Air (hours)										Air Change Effectiveness														
		Occ. zone					Return					Average					Local					Occup. zone avg.				
		Ch#	τ_{BL}	Breathlevel $\langle \tau_{BL} \rangle$	Sec. τ_N	Zone τ_z	Grill τ_{FG}	Ave. $\langle \tau \rangle$	Sec. ACE _G	Zone ACE _Z	Sec. ACE _L	Zone ACE _{LZ}	Grill ADE	Sec. ACE _{BL}	Zone ACE _{LZ}	Grill ADE	Sec. ACE _{BL}	Zone ACE _{LZ}	Grill ADE							
F2 occupied	1-2	1.75				1.64			0.9	1.0	1.0	0.9														
	3-4	1.51				1.47			1.0	1.2	1.0	1.0														
	5-6	1.34	1.63			1.33			1.2	1.3	1.0	1.0						1.0								
	7-8	1.87				1.88			0.8	1.0	1.0	1.0														
	9-10	1.69				1.70			0.9	1.0	1.0	1.0														
	11			1.56			1.66	1.0		1.0			1.0													
12				1.76		1.72										1.1										
F3 occupied	1-2	1.98				1.92			0.8	0.9	0.9	1.0														
	3-4	1.73				1.64			0.9	1.0	1.0	1.0														
	5-6	1.72	1.83			1.55			0.9	1.0	1.0	0.9						1.0								
	7-8	1.87				1.91			0.8	1.0	1.0	1.0														
	9-10	1.83				1.98			0.8	1.0	1.0	1.1														
	11			1.51			1.59	1.0		1.0			0.8													
12				1.77		1.63					1.1							1.0								
F4 un-occupied	1-2	1.57				1.81			1.0	1.4	1.4	1.2														
	3-4	1.47				1.57			1.0	1.5	1.1	1.1														
	5-6	1.34	1.58			1.22			1.1	1.6	0.9	0.9														
	7-8	1.82				1.81			0.8	1.2	1.0	1.0														
	9-10	1.72				1.91			0.9	1.3	1.1	1.1														
	11			1.52			1.61	0.9					1.0													
12				2.19		2.20					1.0							1.4								

Table 3. Results of age-of-air and air change effectiveness measurements on one floor of an office building.

		Age - of - Air (hours)					Air Change Effectiveness					
Building	Ch#	Occup. zone		Return			Average	Local		Occup. zone avg.		
		τ_{BL}	Breath.level $\langle \tau_{BL} \rangle$	Sec. τ_N	Grill τ_{RG}	Avg. $\langle \tau \rangle$		Sec. ACE_G	Sec. ACE_L	Grill ADE	Sec. $\langle ACE_{BL} \rangle$	Grill $\langle ADE \rangle$
A	Open office with partitions, occupied	2	.39					1.2				
		3	.54					0.8				
		4	.63	.51				0.7			0.9	
		5	.48		.45		.42	1.1				
		6										
B	School classroom, occupied	1	.46					1.1				
		2	.46	.46	.50	.48	1.0	1.1	1.1	1.1	1.1	1.1
		4-3						1.1				
		5-6	.45			.52		1.1			1.2	
C	Single and open office with partitions, occupied	1	.66		.71			1.1				
		2	.65					1.1				
		3	.60	.62			.85	1.2			1.1	
		4	.59					1.2				
		5										
		1	.98		1.12		1.34	0.8				
		2	.91					1.1				
		3	.98	.95				1.2				
		4	.98					1.1				
		5	.94					1.2				
D	Office floor and meeting rooms, occupied	1	.30		.30			1.8				
		3	.17				1.0					
		4	.18					1.7				
		5	.20	.21				1.5			1.4	
		6	.31					1.0				

Table 2. Results of age-of-air and air change effectiveness measurements in four different buildings.

**Ventilation for Energy Efficiency and Optimum
Indoor Air Quality
13th AIVC Conference, Nice, France
15-18 September 1992**

Paper 22

**Measurement of Ventilation Effectiveness
Parameters in an Electronics Factory.**

J.R. Waters and C.E. Brouns

**Coventry University, School of the Built
Environment, Priory Street, Coventry CV1 5FB,
United Kingdom**

ABSTRACT

A very large electronics factory had been completely refurbished, and new mechanical ventilation systems installed. In an area of the factory where the principal activity was the bench assembly of small components, there were persistent complaints of eye nose and throat irritations, and absenteeism among the workforce was excessive. Careful examination of the environment had failed to identify any significant contaminants in the air. The situation was similar to the Sick Building Syndrome in office buildings. The problem was investigated by measurements of Ventilation Parameters, using the theory and techniques described in AIVC Technical Notes 28 and 28.2. Pulse, step-up, and decay measurements were carried out, and the results analysed to give air change efficiency, contaminant removal effectiveness, local air quality index, dosage index and transfer index. The results showed that the principal source of air entering the area was not the mechanical ventilation system. This made it difficult to interpret the values obtained for air change efficiency. However, the results for the contaminant removal parameters were consistent with the problems experienced by the workforce. The paper describes the difficulties of conducting ventilation effectiveness parameters in a complex industrial environment. Results are presented which show consistency in the determination of some parameters, and how these suggested solutions for this particular building.

INTRODUCTION

The electronics factory at New Horizon Park, Coventry was refurbished, and new mechanical ventilation systems were installed approximately two years ago. In an area of the factory where the principal activity is the soldering and bench assembly of small components, there were persistent complaints of eye nose and throat irritations, and absenteeism among the workforce was excessive. These problems began soon after the completion of the new ventilation system. Analysis of air samples taken from the environment did not identify any significant airborne contaminants. The situation appeared to be similar to the Sick Building Syndrome in office buildings.

A preliminary investigation revealed that other areas of the factory where similar production activities took place had also been refurbished at the same time, but there were no complaints in these other areas. Consequently the problem could not be associated with the production process, nor could it be associated with particular employees. The complaints were clearly specific to one particular area of the factory served by one air handling unit. The air handling unit itself and its associated ductwork were identical to those installed in other areas of the factory and seemed to be

functioning normally.

In the absence of any obvious cause of the problem, an environmental survey was carried out. This included measurements of temperature and air velocity, but the main purpose of the survey was to measure the ventilation effectiveness parameters of the space.

DESCRIPTION of the INSTALLATION

Apart from the administration units, the factory is single storey throughout. Figures 1,2 and 3 show the general site layout, the area under investigation, and the layout of the air handling system. The problem area is approximately 50m x 11m, with one long side and one short side bounded by brick walls. The other two sides adjoin identical areas, each served by identical air handling units. The roof is a typical triangular construction with glazed northlights, but an open mesh "eggcrate" style suspended ceiling has been installed at a height of 3m above floor level. The volume of the problem area between floor level and ceiling level (the occupied zone) is 1568 m³, and the volume of the roof void above the ceiling (the unoccupied zone) is 1228 m³.

The air handling unit and the supply ductwork are mounted in the roof trusses above the suspended ceiling, and the sixteen air supply grilles are fitted flush with the ceiling. Return air passes up through the "eggcrate" ceiling, and flows along the roof space back to the air handling unit. The unit has separate supply and extract fans, and adjustable dampers which enable the proportion of recirculated air to be varied between 0% and 100%. The intake and exhaust for the unit are both at roof level. The design air flow capacity of the unit is 2.36 m³.s⁻¹ with the fans at full speed. The unit also included a heating coil downstream of the supply fan, but no cooling coil.

INITIAL ANALYSIS

The expected air change rate with the fans at full speed and the dampers set to 0% recirculation is 5.4 air changes per hour, if it is assumed that the system ventilates only the occupied zone. The rate becomes 3.0 air changes per hour if the volume of the roof void is included. As there was a very low level of contaminant generation in the occupied zone, these air change rates should have been adequate. However, the placing of the ductwork supply terminals flush with the open "eggcrate" ceiling suggested that a proportion of the air flow from the terminals would short-circuit the occupied zone and go directly into the roof void, especially in winter when the supply air was heated. A preliminary analysis of this possibility was carried out by representing the problem as a two zone model, as shown in figure 4. The air flow from

the terminals is assumed to be divided between zone 1 (the occupied zone) and zone 2 (the unoccupied zone) in a proportion, x , which can be varied. General buoyancy effects are included by means of an internal recirculation factor, y , of the fan supply rate. Recirculation within the air handling unit can be included by means of a factor, r . This leads to the following equations for the interzone flows.

$$\begin{aligned}
 F_{01} &= (1-x)(1-r)Q \\
 F_{02} &= x(1-r)Q \\
 F_{10} &= 0 \\
 F_{12} &= (1-x)(1-r)Q + rQ + yQ \\
 F_{20} &= (1-r)Q \\
 F_{21} &= rQ + yQ
 \end{aligned}$$

where F_{ij} is the flow from zone i to zone j , and $i=0$ corresponds to outside air. This model was used to compute Ventilation Effectiveness Parameters for a range of values of x , and for $r=0$ (full fresh air) and $r=0.5$ (50% recirculation). The most useful parameters [1,2] are the Local Mean Age of Air, the Local Air Change Index, and the Local Air Quality Index, the last of these being evaluated for contaminant injected in zone 1 only. Figure 5 shows plots of these parameters against the variable x .

Several matters of interest arise from figure 5. The point of intersection of the lines on the Local Air Change Index graph occurs at approximately $x=0.44$, which is the value of x when the flow rate into the zones is proportional to their volume. There is a similar intersection on the Local Mean Age graph. Both these graphs confirm the expected decline in the fresh air provision in the occupied zone as the proportion of the output from the supply terminals going into the upper zone increases. Additionally they show that below $x=0.44$ recirculation, either via the air handling unit or by buoyancy effects, worsens the provision, whereas above $x=0.44$ it improves it. Paradoxically, therefore, if it happens that $x>0.44$, increasing the fresh air intake into the air handling unit by reducing its recirculation setting will actually make things worse. The Local Air Quality Index graph leads to a similar conclusion, except that the worsening is true for all $x>0$.

MEASUREMENTS

The measurement programme covered the period from the 11th to the 22nd of November 1991 inclusive. For measurement and analysis purposes, the total space was considered as four zones. In the occupied space below the ceiling, three zones of equal volume were defined, and the space above the ceiling was defined as a single zone. Figure 3 shows the layout of the ventilation system and the zones. Tracer gas

sampling points were placed approximately at the centre of each zone, and also in the supply and return ducts of the air handling unit. Step-up tests were carried out by injecting tracer gas (sulphur hexafluoride) into the air immediately upstream of the supply fan. The tracer gas concentrations following switch-off of the tracer were treated as decay measurements. Pulse tests were carried out by injecting a short burst of tracer into one of the zones. This was repeated for each of the three zones in the occupied space. The tracer gas concentration curves were analysed using software based on the usual Ventilation Effectiveness theory [1,2]. The three types of test, step-up, decay and pulse were analysed as follows.

1. Step-up tests

For the first set of step-up tests, the rise in the tracer gas concentration in the return duct followed very closely the rise in the inlet duct, and was ahead of the rise in the four zones. This caused some surprise, and led to a close inspection of the air handling unit. It was discovered that the indicator on the outside of the unit, which was showing 0% recirculation (or full fresh air) was exactly the wrong way round. In other words, the system was set to 100% recirculation, so that contaminated air was being fed back into the ductwork. The rapidity of the rise in the return duct suggested also that there was some short-circuiting of air from the supply side to the return side. The fact that the system was on 100% recirculation was known to the maintenance engineer, who explained this setting as being necessary to both conserve heating energy and to prevent complaints of low temperatures from the operatives. The 100% recirculation setting made the analysis of the step-up tests largely meaningless.

2. Decay tests

These were used to establish the average air change rate of the space. This is valid because the ventilation system maintains stirring of the air throughout the decay process. The time constant over a series of tests ranged from about 28 minutes to about 40 minutes. This represents air change rates of between 1.5 and 2.1 air changes per hour. However, this cannot all be fresh air, and most of it must have come from other areas within the factory. One test with the system set to 100% fresh air yielded an air change rate of between 3.3 and 3.9 air changes per hour. This test also gave values for the Local Mean Age and the Local Air Change Index of the air in the zones.

Table 1 - Local Mean Age and Local Air Change Index

Zone	Local Mean Age (minutes)	Local Air Change Index
1	23	0.79
2	16	1.13
3	9	2.01
4	21	0.86

3. Pulse tests

These were used to derive the local mean age of the contaminant and the total dosage index. The averages and standard deviations derived from several sets of measurements are shown in the following tables.

Table 2 - Local Mean Age of Contaminant, minutes

Zone of Injection	Zone of Measurement			
	1	2	3	4
1	22 ± 5	29 ± 3	43 ± 8	21 ± 2
2	21 ± 2	16 ± 3	40 ± 23	19 ± 3
3	31 ± 4	22 ± 4	14 ± 4	26 ± 6

Table 3 - Total Dosage Index, vpb.hrs/ml

Zone of Injection	Zone of Measurement			
	1	2	3	4
1	0.255±0.072	0.114±0.007	0.111±0.062	0.191±0.022
2	0.165±0.075	0.244±0.137	0.125±0.125	0.157±0.090
3	0.092±0.077	0.090±0.043	0.175±0.088	0.071±0.059

The Local Air Quality Index can be derived from the Total Dosage Index for a pulse test by means of the equation

$$\epsilon_p^c = \frac{V_{cp}}{Q \cdot D_p}$$

where D_p is the Total Dosage Index due to a release of a volume equivalent of contaminant V_{cp} . Using the median of the results of the decay tests gives the effective fresh air supply rate, Q , as $1.4 \text{ m}^3 \cdot \text{s}^{-1}$. The values in Table 3 were used to construct Table 4.

Table 4 - Local Air Quality Index

Zone of Injection	Zone of Measurement			
	1	2	3	4
1	0.78	1.74	1.79	1.04
2	1.20	0.81	1.59	1.26
3	2.16	2.20	1.13	2.79

SIMULATIONS

From the results of the experimental measurements, an intuitive estimate was made of the most likely flow rates between the zones of the four zone model. These flows, which are shown in Figure 6, were entered into the multi-zone air movement model, in order to compute theoretical values of the Local Mean Age of the Contaminant, the Total Dosage Index, and the Local Air Quality Index. Tables 5,6 and 7 show the results.

Table 5 - Local Mean Age of Contaminant, minutes

Zone of Injection	Zone of Measurement			
	1	2	3	4
1	21	41	43	38
2	37	20	38	37
3	44	34	16	34

Table 6 - Total Dosage Index, vpb.hrs/ml

Zone of Injection	Zone of Measurement			
	1	2	3	4
1	0.418	0.122	0.079	0.152
2	0.170	0.330	0.093	0.157
3	0.097	0.116	0.231	0.130

Table 7 - Local Air Quality Index

Zone of Injection	Local Air Quality Index of Zone			
	1	2	3	4
1	0.39	1.34	2.08	1.08
2	0.96	0.50	1.75	1.04
3	1.68	1.41	0.71	1.26

DISCUSSION and CONCLUSIONS

Inspection of the measured results shows that in many cases the standard deviations were large. This was not surprising, as the buoyancy of the air leaving the terminal units would have varied with both the weather conditions and the cycling of the heating coil. In general, the results from individual tracer gas tests within each set tended to produce values in the same rank order, again suggesting that the large standard deviations were due to real changes in the performance of the installation

rather than excessive experimental error.

With the air handling unit on its usual setting of 100% recirculation, the measured air change rate of between 1.5 and 2.1 ach could be entirely accounted for by air exchange with other parts of the factory. This means that the area received no direct fresh air, that is all incoming air was stale air. In practice, some fresh air would have entered the area from the external door at one end, and by leakage through the structure. With the unit on 100% fresh air, a rate of between 3.3 and 3.9 ach is consistent with the fan rating, which taken by itself would have given 3.0 ach. The extra could be due to leakage and exchange with adjacent areas.

When the system was tested on 100% fresh air, the results for the Local Mean Age and the Local Air Quality Index suggest that the distribution of fresh air was poorest to zone 1, where the majority of the complaints occurred.

The results of the pulse tests show that the Dosage Index for each zone due to a contaminant released within itself is highest for zone 1, next highest for zone 2, and lowest for zone 3. The same is true for the Local Mean Age of Contaminant. This is consistent with a high rate of complaint from the occupants of zone 1. The Local Air Quality Index is lowest in zone 1, next lowest in zone 2, and highest in zone 3, which is also consistent a high complaint in zone 1.

The results for the simulations carried out on the four zone model of the installation show that some of the individual values are very close to their measured counterparts, whereas some differ by a substantial factor. Nevertheless the results of the simulations show the same trends as the measurements, and hence confirm the poor ventilation of zone 1.

The overall conclusion is that the measurement of ventilation effectiveness parameters in a complex environment has provided definite evidence to support and explain a problem which had otherwise been evident only from the subjective responses of the occupants. In this particular instance, the contaminant removal effectiveness parameters have been the most helpful in identifying and quantifying the problem. The use of zonal models has also been of benefit in this case. The initial analysis using the two zone representation showed that there was likely to be a potential problem, and the four zone model, assembled from information on the fan rating and from the evidence of the measurement programme, was useful in confirming the conclusions, and also in giving an indication of the probable air flow patterns. The solution for this installation appeared to be relatively simple, namely to reduce the recirculation setting of the air handling unit.

REFERENCES

1. "A Guide to Air CHange Efficiency", AIVC TN28, 1990
2. "A Guide to Contaminant Removal Effectiveness", AIVC TN28.2, 1991

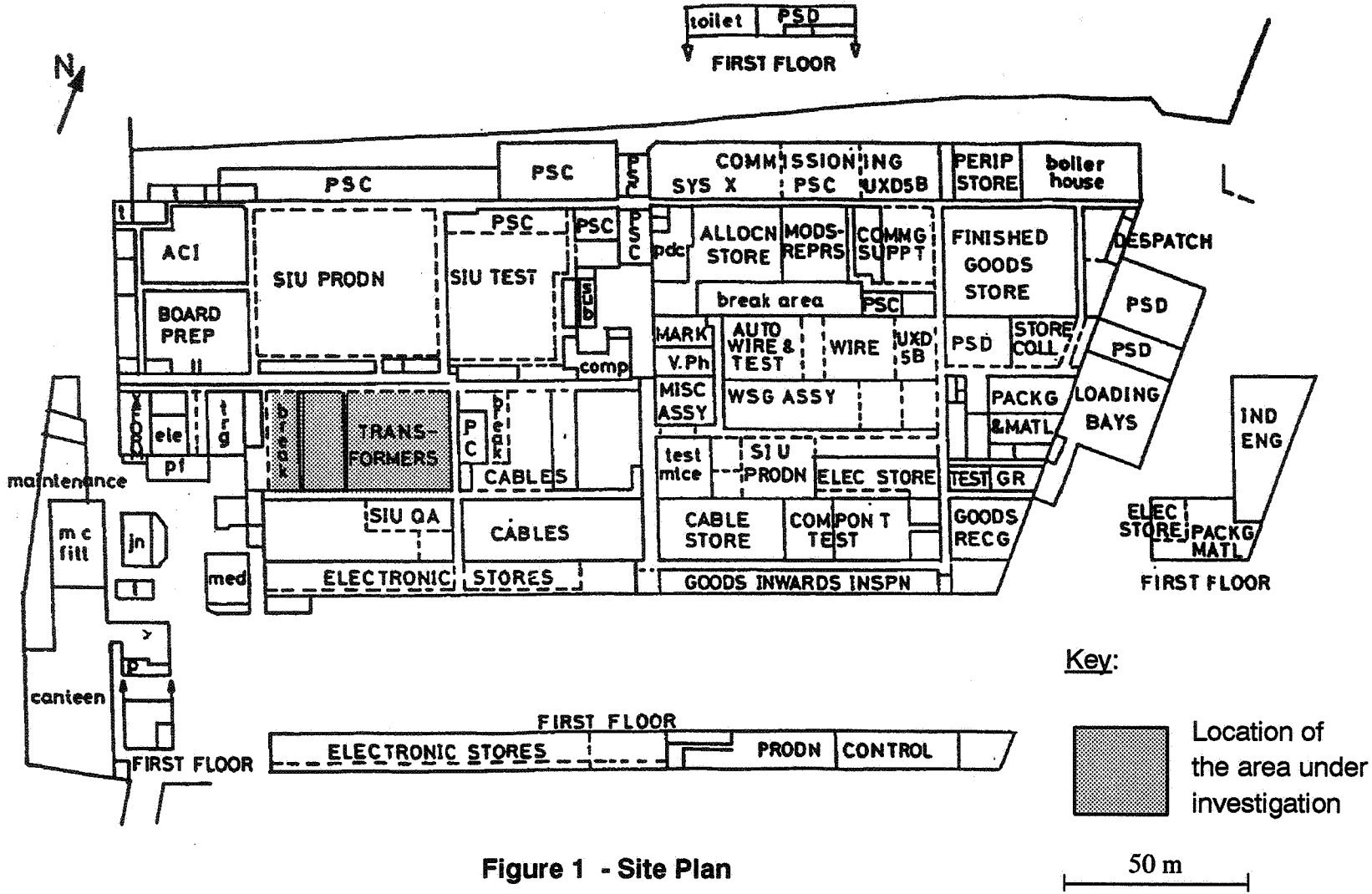


Figure 1 - Site Plan

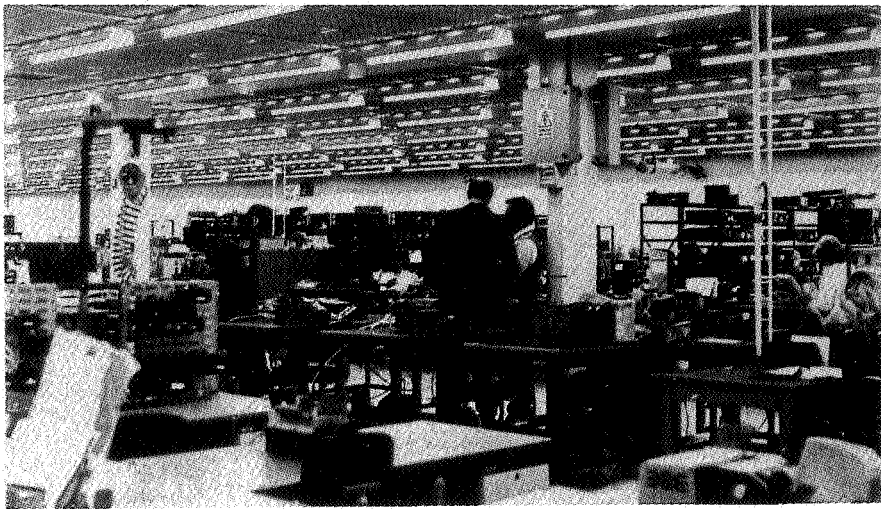


Figure 2 - Area under investigation.

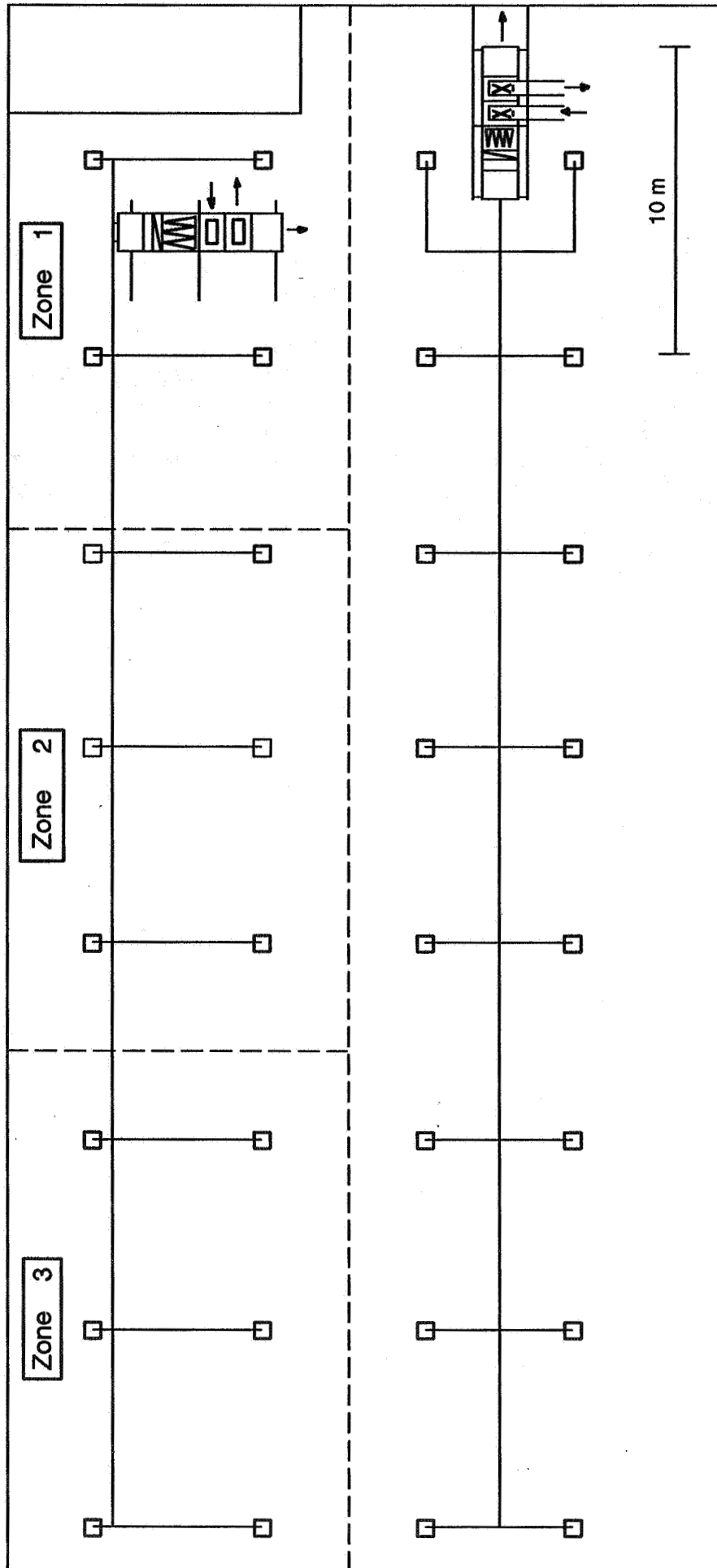


Figure 3 - Layout of the Heating and Ventilation System.

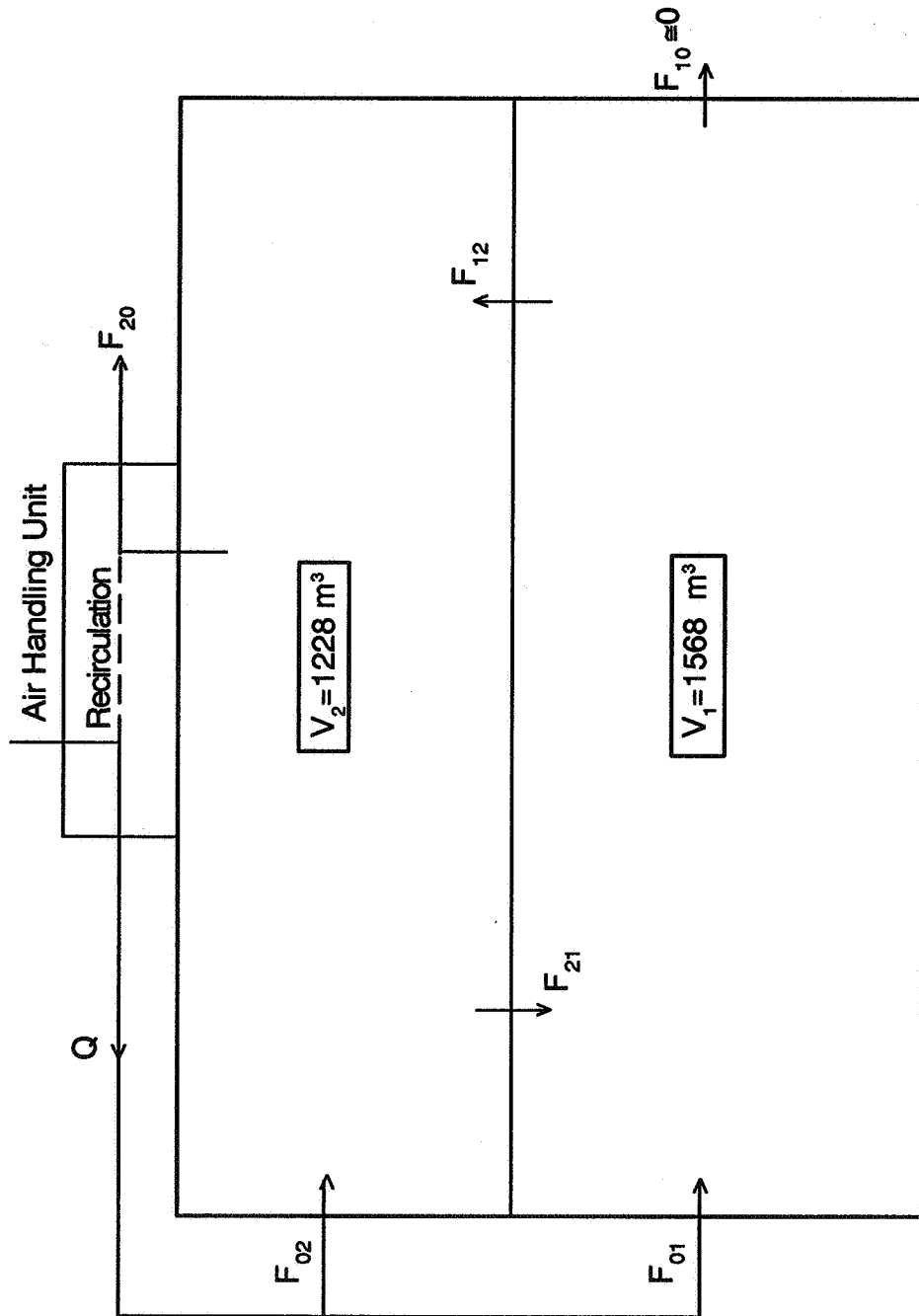


Figure 4 - 2 Zone Model.

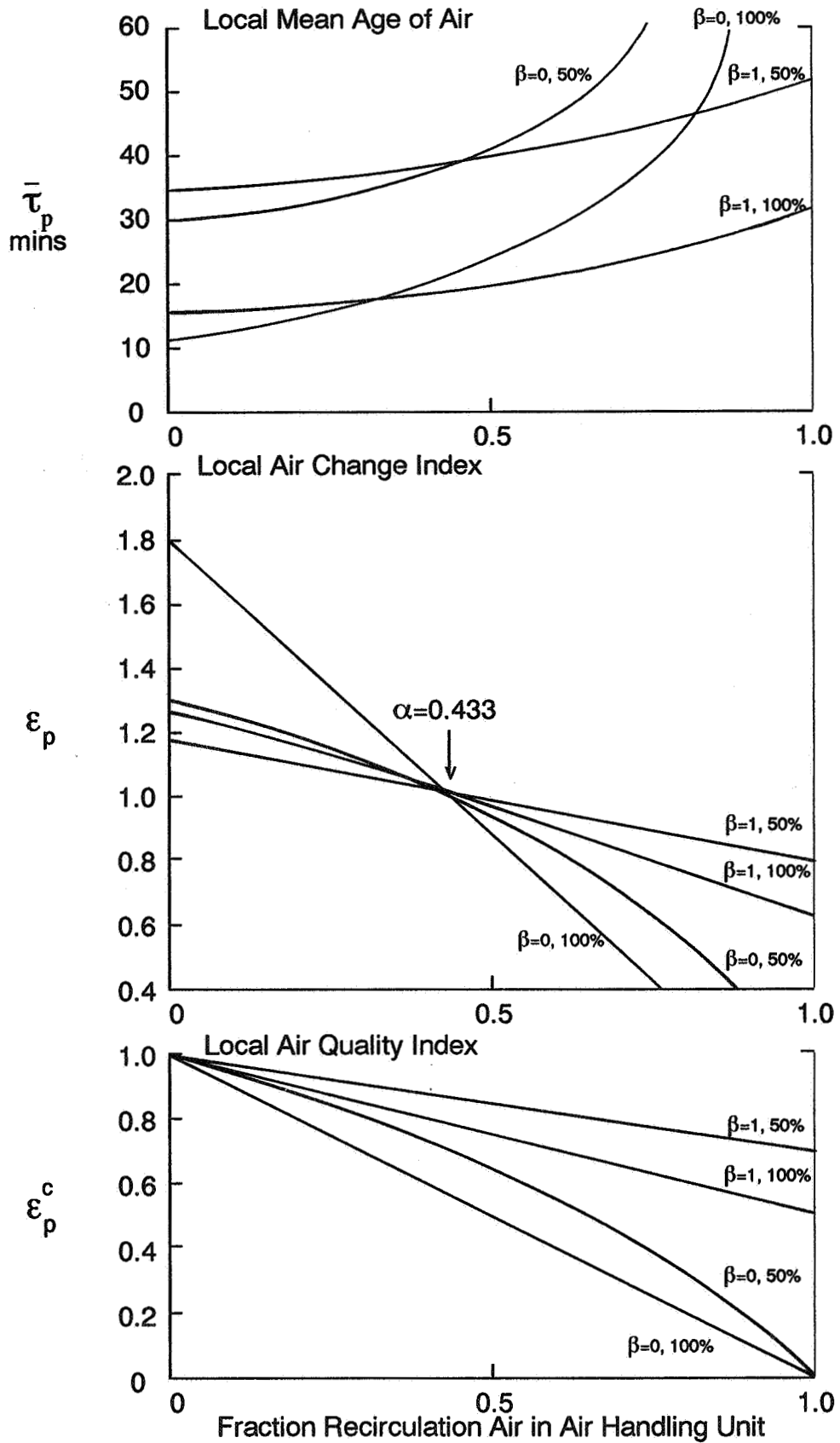
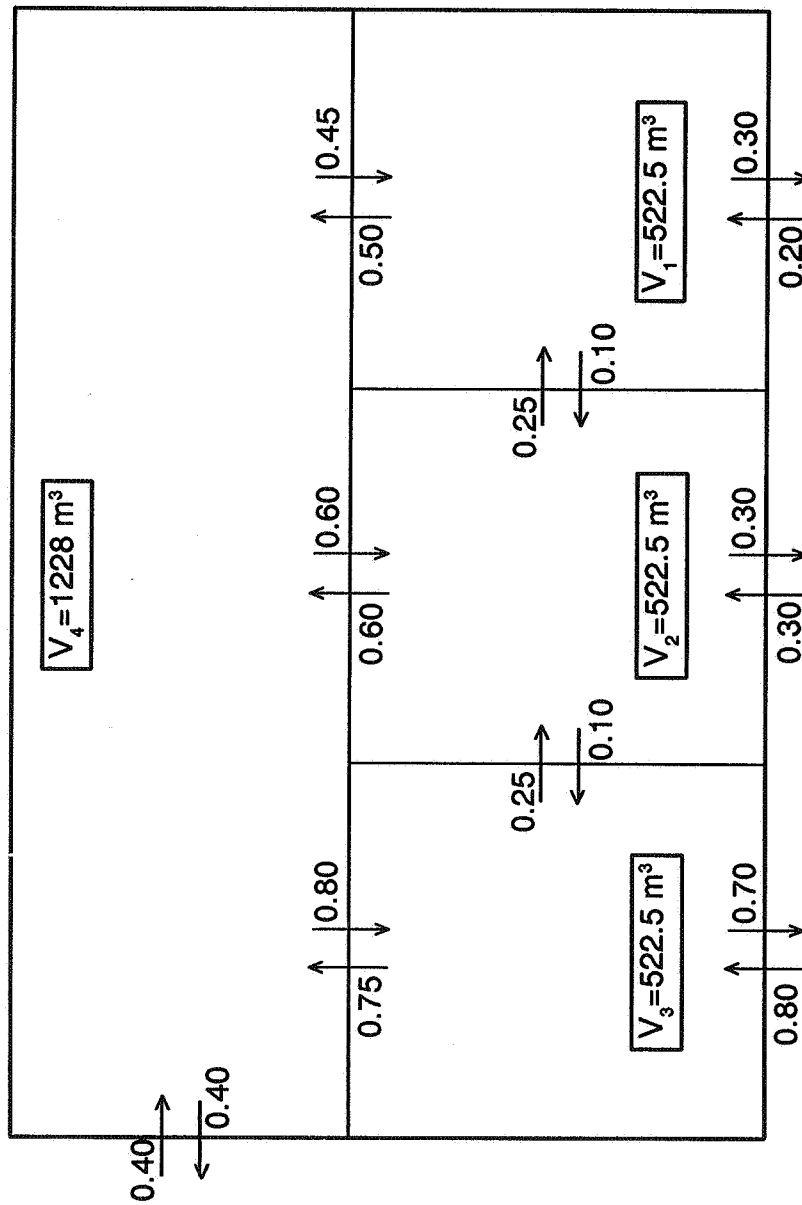


Figure 5 - Results of the 2 zone model.



Please note that all the air flow rates in the above figure are expressed in m^3/s .

Figure 6 - 4 Zone Model.

5978

**Ventilation for Energy Efficiency and Optimum
Indoor Air Quality
13th AIVC Conference, Nice, France
15-18 September 1992**

Paper 21

**Contaminant Dispersal Measurement Using Laser
Light Sheet Illumination and Digital Image
Processing Techniques.**

J.W. Axley and L.K. Norford

**Building Technology Program, Massachusetts
Institute of Technology, 77 Massachusetts Avenue,
Cambridge, MA 02139, USA.**

Synopsis

This paper describes a method for measuring the dispersal of airborne contaminants by light-sheet illumination of aerosol tracers and digital image processing techniques. The goals of the research were two-fold: to use field-portable and safe equipment to make near-instantaneous measurements of tracer aerosol concentrations over arbitrarily positioned two-dimensional planes of near-room dimensions; and to carefully define similarity conditions under which aerosol dispersal can be considered an accurate surrogate for passive molecular dispersal.

The measurement method involves five procedures: tracer generation by condensation of a glycol vapor; light sheet illumination using a projected laser; image capture using a CCD video camera linked to an analog-to-digital converter; point-calibration measurement, via light attenuation, of aerosol concentration; and image processing using a public-domain microcomputer-based program. This paper will briefly review the method and evaluation tests and will emphasize technical and theoretical issues concerning the relationship between captured images and aerosol concentration and the similarity of tracer to molecular dispersal.

List of Symbols

- C is the molecular species concentration, moles/m³.
 \bar{C} is the time-smoothed concentration averaged across the section of the duct.
 c_f is a friction coefficient.
 \vec{c} is the particle migration velocity vector (e.g., settling velocity), m/s.
 D is a characteristic dimension of the flow regime, m.
 \mathcal{D}_α is the molecular diffusivity of a species α , m²/s.
 \mathcal{D}_p is the particle diffusivity of the aerosol particles, m²/s.
 \vec{f} is a rapidly varying stochastic force due to molecular agitation, g-m/s².
 I is the intensity of light, lumens/m² or watts/m².
 m is the effective mass of the particle, g.
 n is the particle concentration, #/m³.
 n^* is a dimensionless concentration equal to the concentration divided by a reference concentration.
 R is the radius of the duct, m.
 r_f is the radius of the particle, μm .
 r_f/D is the interception parameter.
 $Re \equiv DV/\nu$ is the Reynolds number.
 $Sc_p \equiv v/\mathcal{D}_p$ is the aerosol particle Schmidt number.
 $Sc_\alpha \equiv v/\mathcal{D}_\alpha$ is the molecular Schmidt number for species α .
 t^* is a dimensionless time equal to $(V t/\mathcal{D}_p)$ or $(V t/\mathcal{D}_\alpha)$.
 \vec{u} is the particle velocity, m/s.
 \vec{v} is the local fluid velocity vector, m/s.
 \vec{v}^* is a dimensionless velocity equal to the actual velocity divided by a suitable reference velocity V .
 \bar{v} is the time-smoothed mean velocity.
 x is the distance along a duct, m.
 z is the distance along a given optical path, m.
 γ is the extinction coefficient, m⁻¹.
 $\nabla^* \equiv D \nabla$ is a dimensionless del operator, where D is a suitable reference dimension.
 ν is the kinematic viscosity of the fluid (e.g., air), m²/s.

1. Introduction

The growing concern for the quality of air in indoor environments and the economic importance of air contaminant control in clean room design have together focused attention on contaminant dispersal in buildings, in general, and within room in particular. Actual personal exposure to indoor air pollutants [1] and the success or failure of a clean room design both depend critically on the spatial distribution, or mixing, of

contaminants within rooms and the variation of this mixing with time.

Recognizing the critical importance of mixing, researchers in the field have attempted to study the general character of room mixing using both experimental and computational techniques. Airborne contaminant distributions in rooms have been measured using discrete, point-sampling techniques. These techniques, however, (a) provide poor spatial and temporal resolution, (b) tend to be invasive, and (c) tend to be limited to laboratory investigations due to their complexity and expense.

Computational determination of velocity flow fields and the associated computational determination of tracer dispersal driven by these flow fields – *microscopic analysis* – offers a very attractive alternative to the experimental approach because, in principle, the dispersal in space and time may be determined to any degree of resolution [2-5]. Regrettably, however, this analysis must be based on semi-empirical *dispersal turbulence models* that have yet to be thoroughly validated and is presently limited to rooms of simple geometry and stationary flow conditions.

On the one hand, then, experimental evaluation of mixing based on discrete sampling can not provide sufficient data to fully characterize the spatial or temporal nature of mixing in rooms and, on the other, computational determination of dispersal can not be considered reliable until experimental techniques are developed that can provide the detail needed for their validation. Laser light sheet illumination techniques have the potential to provide an answer to this dilemma.

Building on light slit illumination techniques, several investigators have illuminated reflective aerosol tracers in various flow fields by laser light sheets to effectively reveal the qualitative structure of the flow field and its variation with time [6, 7]. Saunders and Albright described the preliminary development and feasibility testing of a method to quantitatively investigate pollutant mixing by illuminating glycol aerosol tracers and processing captured images [8]. They assumed (a) tracer concentration was proportional to scattered light intensity, (b) tracer aerosol dispersal would be similar to passive molecular dispersal, and (c) only scattered light was received by the image acquisition system. The work described in this paper addresses these assumptions explicitly in an effort to establish the limitations of quantitative measurement of sheet-illuminated aerosol tracer distributions in room airflow.

2. Development of the Proposed Method

The measurement method reported herein evolved over a two-year period through review of the literature and a series of trial and error investigations relating primarily to (a) the selection of an appropriate aerosol tracer, (b) the selection of system components from those that were commercially available, (c) the development of experimental protocol, and (d) the selection of tests that would aide in the development of the method.

2.1 Measurement Method and System Components

The measurement method investigated involves five procedures supported by the hardware and software components described below and illustrated in Figure 1.

Tracer Generation & Injection: A glycol-based condensation generator was used to generate an aerosol tracer. This *theatrical fog generator* provides an aerosol tracer that scatters light efficiently yet is harmless and what little residue it leaves can be easily cleaned. Detailed particle size distribution measurements indicate that initially the generated aerosol is practically monodisperse with a mean particle diameter of approximately 0.5 μm . It then undergoes agglomeration, the mean diameter grows with time, the particle size distribution spreads to become polydisperse, and eventually settling of the larger particles becomes significant. To allow the initial rapid agglomeration to pass before injection and to better control tracer injection, generated fog was temporarily stored in an accordion-like collapsible storage cylinder approximately 2 m by 0.3 m in diameter. Subsequent tracer injection was realized by the controlled collapse of the storage cylinder.

Light Sheet Illumination: A *dynamic light sheet*, generated by projecting a laser light beam onto a rapidly oscillating mirror (*scanner*) to scan the beam over a triangular segment of a plane, was used to illuminate the aerosol. Hardware components included a 50 mW Argon ion laser and commercially available optical components, function generator, amplifier, and scanner. The laser was selected from among the highest output power lasers that can operate on standard 120 V, 15 amp supply. This class of lasers is also relatively safe and field portable.

Image Capture & Point Measurement: Images were captured using a CCD video camera linked to a microcomputer-based analog-to-digital converter that together provided a gray level resolution of 256 values (i.e., 8 bit). A simultaneous concentration measurement was made at a single point within the field of view to allow calibration of the captured image.

Image Processing: Digital processing of the acquired images was required to correct for both systematic error (*normalization*) and random error (*noise reduction*) and to transform the recorded gray level data to tracer concentration values (*calibration*). All image processing was realized using the program Image 1.40; a public-domain program distributed through the National Institutes of Health.

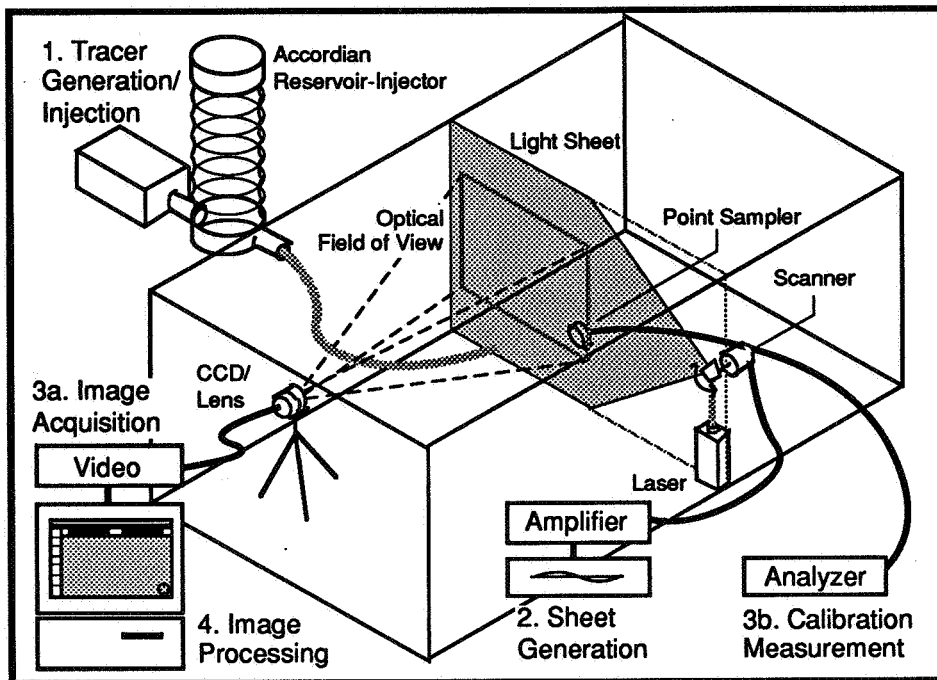


Figure 1. Laser light sheet measurement system components.

2.2 Development Test Series

The development of the method was based on tests that would allow fundamental evaluation of the spatial and temporal resolution, accuracy, and repeatability of the proposed method rather than investigating specific cases of contaminant dispersal in rooms. Four test series were central to the development of image normalization, noise reduction, calibration, and measurement protocol and used to evaluate similarity:

Aerosol Particle Size Distribution Measurements: measurements of the particle size distribution of the freshly generated aerosol and its variation with time to (a) provide data needed to develop a relation between extinction measurement and concentration used for calibration purposes, and (b) to evaluate time-dependent transformations of the aerosol tracer due to agglomeration,

No-Flow Compartment Tests: tracer dispersal studies in a small, sealed, well-mixed chamber to evaluate the reliability of proposed normalization and noise reduction procedures by comparison of measured distribution uniformity with expected uniformity and to assess time-dependent transformations of the aerosol tracer,

Steady-Flow Compartment Tests: tracer dispersal studies in a small, well-mixed chamber under conditions of steady ventilation flows to evaluate the accuracy of the method at moderate rates of data acquisition necessary to capture slowly varying concentration fields and to again evaluate the reliability of proposed normalization and noise reduction procedures, and

Stationary Flow Duct Tests: tracer dispersal studies in a 12 m long circular duct of 0.30 m diameter under stationary turbulent flow conditions to evaluate the accuracy of the method at high rates of data acquisition necessary to capture rapidly varying concentration fields.

3. Relating Scattered Light to Aerosol Concentration

If interest is limited to the dispersal of aerosols similar to the properties of the aerosol tracer used in the proposed measurement method then one need only be concerned with the ability of the image acquisition system to record scattered light from the illuminated field and the relation between recorded scattered light and tracer concentration or density.

3.1 Aerosols Properties and Behavior

The proposed method depends on the efficiency with which the chosen aerosol scatters light from the

light sheet. Broadly speaking, aerosol particles are classified into three groups: particles small relative to the wavelength of the incident light; particles very much larger than the wavelength of the incident light; and those falling in the range in-between. Rayleigh scattering theory predicts, and measurements confirm, that small-particle aerosols scatter light inefficiently; classical optical theory predicts that large-particle aerosols will scatter light more efficiently; and Mie theory predicts that the moderate-sized aerosols will scatter light most efficiently for a given volume of particles. Hence, to maximize light scattering we prefer to use aerosols with particle sizes just above the Rayleigh, small-particle range or, for visible light scattering, above the 0.1 to 0.5 μm particle diameter range.

The intensity of light scattered from a given aerosol may be increased simply by increasing the concentration of the aerosol, but there are practical limitations to this strategy. At very high concentrations the aerosol will tend to obstruct both the view of the illuminated sheet and the ability of the laser to illuminate the sheet evenly - both unacceptable conditions. At moderate concentrations an undesirable and generally unknown nonlinear relation will exist between aerosol concentration and scattered intensity, due to the increased probability of *multiple scattering*, that will complicate the calibration of captured images. Multiple scattering will create so-called *virtual emissions* within the view of the image acquisition system that will tend to veil the light scattered from the illuminated sheet.

Finally, all aerosols tend to agglomerate or suffer deposition as individual particles collide with each other or surfaces and, as a result, the size distribution and, to a lesser extent, the amount of aerosol varies with time. The time variation of particle sizes can result in a variation in scattered light intensity that is unrelated to aerosol concentration and as such must be minimized. As higher concentrations will tend to accelerate the rate at which aerosol particles agglomerate we shall prefer to implement the proposed method using low aerosol tracer concentrations.

3.2 Experimental Protocol

Considering all these factors then, we prefer to inject tracers with particle size distributions just above the Rayleigh scattering size range at concentrations sufficiently low so that the aerosol particle size distribution does not vary significantly during the test time period. Measurements of our condensation-generated glycol aerosol indicate these objectives may be achieved by generating then temporarily storing the aerosol (e.g., for 10 minutes) - to allow an initial stage of rapid agglomeration to pass - before injection. By maintaining peak aerosol concentrations within a concentration range of 10^5 to 10^7 particles/cm³ scattered intensities remain detectable (i.e., with our equipment) yet changes due to agglomeration vary slowly with an effective time constant on the order of tens of minutes.

3.3 Image Processing

Captured images of practically uniform distributions of aerosol proved not to be uniform - they not only contained consistent unstructured nonuniformities (e.g., lighter and darker edges and "smudges") but revealed consistent structured patterns of vertical stripes from image to image. A composite of three images of light scattered from a uniformly distributed aerosol tracer is illustrated in Figure 2 with histogrammic distributions of gray-values shown for each third. The lower third of this image is a pseudo gray-scale representation of the raw image data. To correct for sources of systematic error, captured images were normalized against light scattered from well-mixed distributions of aerosol tracer following the example of Long et al [9, 10]. The result of this normalization is indicated by the middle third of Figure 2. (Details of the normalization algorithms will be included in a forthcoming report.)

The vertical stripes evident in the raw image due, presumably, to electromagnetic interference are visually obvious but also indicated by the bimodal character of the histogram in this case. Less obvious, but indicated by the alternating comb-like appearance of the raw data histogram, is the fact that analog-to-digital board used favored odd gray-values. Finally, a careful examination of the series of images taken during this particular test reveals consistently brighter conditions along the lower and left edges of the images.

Normalized images revealed a *salt and pepper* distribution of gray values that is characteristic of random error due to electromagnetic noise, the *dark current* produced by CCD devices, or to the natural stochastic distribution of the aerosol itself. Two standard schemes to remove this source of error were considered - *mean* and *median filtering* - wherein each pixel value of an image is replaced by the either the mean or median of the pixel values in the 3×3 array of pixels centered on the chosen pixel. Both strategies appeared to be equally effective, although, given the expected stochastic distribution of the aerosol particle sizes, the mean filtering should be more appropriate. The result of this noise reduction is indicated by the upper third of Figure 2.

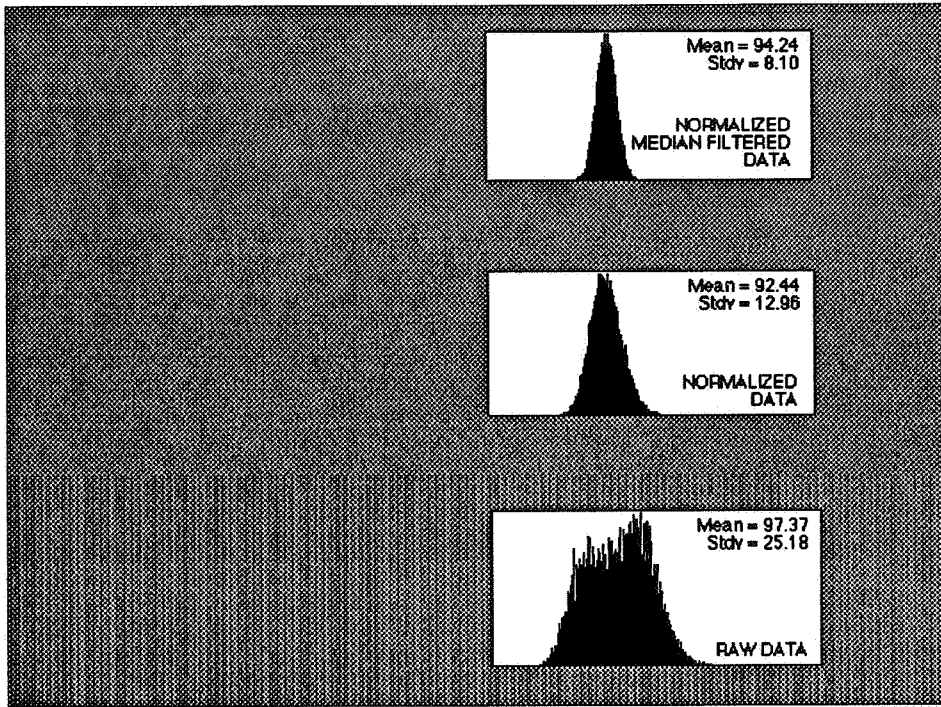


Figure 2. Representative results of normalization and noise reduction of images captured from a uniform distribution of aerosol tracer.

3.4 Calibration

The aerosol tracer concentration was calibrated by relating the intensity of scattered light at a single point in the captured image to a particle concentration estimated on the basis of a light extinction measurement. The extinction coefficient, defined as fraction of light scattered and/or absorbed within a media per unit length of optical path:

$$\gamma \equiv -\frac{dI}{I dz} \quad (1)$$

can be linearly related to the particle number concentration, using Mie scattering theory, when the number distribution of particles as a function of size is known and conditions of single, independent scattering are realized. These conditions are realized when the optical depth, the integral of the extinction coefficient over the path from the sheet to the acquisition system, is less than approximately 0.1.

4. Similarity of Aerosol and Molecular Dispersal

Strictly speaking, the dispersal of the chosen aerosol tracer may be expected to be similar only to other aerosols with the same particle size distributions and densities. Practically, however, we may identify conditions under which the aerosol dispersal will be similar to other contaminants and, specifically, to molecular species. A *first similarity condition* relates to agglomeration. By maintaining conditions of low aerosol concentrations, as discussed above, the effects of agglomeration may be mitigated.

4.1 Miscible Two-Phase Continuum Transport

To identify additional similarity conditions it is useful to compare continuum two-phase convection-diffusion transport theory for molecular and aerosol transport (e.g., see [11, 12]):

$$\text{Molecular Transport} \quad \frac{\partial C}{\partial t} + \vec{v} \cdot \nabla C = D_a \nabla^2 C \quad (2)$$

$$\text{Aerosol Transport} \quad \frac{\partial n}{\partial t} + \vec{v} \cdot \nabla n = D_p \nabla^2 n - \nabla \cdot \vec{c} n \quad (3)$$

These two equations will have the same form if the last term of Equation 3, the settling velocity term, becomes negligible. This establishes a *second similarity condition* that particle sizes must be small enough so that settling is insignificant. Practically, this limits particles to diameters smaller than about 10 μm .

Equations 2 and 3, with the settling term removed, may be recast in dimensionless form as:

$$\frac{\partial n^*}{\partial t^*} + \vec{v}^* \cdot \nabla^* n^* = \frac{1}{Re Sc} \nabla^{*2} n^* \quad (4)$$

Consequently, molecular dispersal will be similar to aerosol dispersal when the product $Re Sc$ is of similar magnitude for each case; $Re Sc_a = Re Sc_p$. For full-scale or field measurements the Reynolds numbers will be identical so we may assert a *third similarity condition* that Schmidt number similarity is needed to achieve our objective.

Regrettably, aerosol particle diffusivities, for the particle size range of use here (0.5 to 10.0 μm), are on the order 10^{-7} cm^2/s while molecular diffusivities are some six orders of magnitude larger. Kinematic viscosities for both aerosol-air and molecular-air systems will be of similar magnitude – in the range of 1 to 2×10^{-1} cm^2/s . Consequently, molecular Schmidt numbers may be expected to be close to 1 while particle Schmidt numbers will be near 10^6 and, as a result, it will be practically impossible to satisfy this third condition. If, however, the diffusion term of Equation 4 is negligibly small (i.e., transport is dominated by convective processes) then this third condition becomes irrelevant. For turbulent flow, this becomes the case as, from one perspective, molecular or particle diffusivities become overwhelmed by *eddy diffusivity* (i.e., due to small scale turbulence) that is expected to be (nearly) identical for both cases. (Consideration of the time-smoothed formulations of Equations 2 and 3 using the eddy diffusivity turbulence model, leads to this last conclusion.)

The *third similarity condition*, therefore, establishes two limiting conditions. At one extreme, for fully developed turbulent flow the dispersal of aerosol particles and molecular species may be expected to be practically identical as eddy diffusion will dominate. At the other extreme, for very low flow the dispersal of aerosol particles can not be expected to be similar to that of molecular species. Between these limiting cases one may encounter situations where convective, yet nonturbulent, transport dominates the flow (e.g., laminar flow in clean rooms) and thus the diffusion term becomes negligible and similarity is realized or, alternatively, where particle/molecular diffusion transport is significant and, hence, similarity can not be expected.

The particle/molecular-diffusion limit may not be critical in room studies as room air is invariably in motion due to ventilation, infiltration, and natural convection and, as a result, true stagnant conditions are practically never achieved. Rodes reviews measurements of air velocity and turbulence intensity (i.e., the relative standard deviation of velocity) in rooms that indicate average velocities on the order of 5 cm/s with HVAC systems off and 15 cm/s with HVAC systems on, with turbulence intensities ranging from 20-120% [1]. Most airflows in rooms may, therefore, be expected to exceed 2 cm/s. From kinetic theory, the net velocity of a single particle, due to Brownian motion, or a single molecule, due to kinetic motion, is on the order of $\sqrt{2 D_p}$ or $\sqrt{2 D_a}$ respectively [13]. For the representative diffusivities discussed above, then, the net kinetic velocity of a single molecule will be approximately 0.3 cm/s and that of a tracer aerosol particle 0.0003 cm/s, both substantially less than expected minimum air velocities in rooms. From this discussion we may establish a *fourth similarity condition*: if minimum flow velocities are well above the net kinetic velocity of the molecular species being considered, $\sqrt{2 D_a}$, then one may assume that diffusion transport mechanisms are negligible and, consequently, the dispersal of molecular and tracer particle species will be similar. Regrettably, in laminar flow situations this condition may not be satisfied in directions orthogonal to the flow streamlines.

The boundary conditions for aerosol particle transport are necessarily different from those used for molecular transport because of the finite size of aerosol particles [12]. As particles will intercept the boundary upon surface contact, one may define a boundary condition that the aerosol particle concentration becomes zero at a distance equal to the radius of the particle r_f from the surface rather than directly at the surface. As a consequence, an added dimensionless variable, the interception parameter r_f/D , may be introduced. Effectively, for molecular flow the interception parameter is zero. A *fifth similarity condition* may then be stated that aerosol particle dispersal will be similar to molecular dispersal when the interception parameter is practically negligible. That is to say, we can not expect to resolve dispersal detail approaching the tracer particle size close to surfaces. This condition presents no practical problem in room distribution measurements for the tracers used.

4.2 Non-Continuum Transport

From a microscopic point of view aerosol particles are discrete, finite objects submerged in a fluid flow field and no longer appear to be a continuous phase. As discrete, finite objects, particles will tend to lag behind fluid motion in regions of accelerating flow.

This case may be analyzed following the argument presented by Long et al. [9]. An equation of motion may be formulated for an individual particle as:

$$m \frac{d\vec{u}}{dt} = c_f(\vec{v} - \vec{u}) + \vec{f} \quad (5)$$

where it is normally assumed that \vec{f} is independent of the velocities, fluctuates more rapidly than the velocities, and has a mean value that vanishes over time [12].

Equation 5 clearly indicates that particles lag behind fluid velocity – *slip* – when accelerated. Furthermore, the frictional force acting on the particle $c_f(\vec{v} - \vec{u})$ tending to correct the slip is directly related to the *slip velocity* (i.e., the relative particle velocity $(\vec{v} - \vec{u})$). Given the independence of \vec{f} , Equation 5 and, hence, the slip velocity may be characterized by a relaxation time constant:

$$\tau_{relax} = \frac{m}{c_f} \quad (6)$$

that provides an order-of-magnitude estimate of the time required for a particle to “catch-up” with the airflow.

Using published correlations for the friction coefficient [12] and the physical properties of the aerosol system used in the current investigation the relaxation time constant, τ_{relax} , will range from 7×10^{-5} s to 5×10^{-6} s for particle Reynolds numbers ranging from 0 to 1000. Within occupied regions of rooms airflows are normally limited for comfort reasons to approximately 0.25 m/s and, as the instantaneous slip velocity is bounded by this value, maximum particle displacement lags would be well below the spatial resolution of the proposed measuring method:

$$\tau_{relax} (\vec{v} - \vec{0}) \approx (7 \times 10^{-5} \text{ s})(0.25 \text{ m/s}) = 17.5 \mu\text{m}$$

Air velocities at diffusers may be as much as two orders of magnitude greater so displacement lags may conceivably approach 2000 μm or 2 mm – still within the spatial resolution of the measurement method.

From this analysis we may assert a *sixth similarity condition* that aerosol dispersal will be similar to molecular dispersal if the slip relaxation time of the particles is small. For room airflow dispersal studies the Rosco fog should satisfy this condition. That is, we should expect the lag of Rosco fog particles in regions of accelerating flow to be negligible.

4.3 Immiscible Two-Phase Continuum Transport

A sufficiently dense aerosol cloud having well-defined boundaries will tend to act, at least initially, as a single body of immiscible fluid. The motion of such a cloud will be determined not by the motion of individual particles but by the bulk mechanics of the cloud as a whole, consequently, the cloud may settle at a faster rate than individual particles in the cloud. For the present application, *cloud settling* may prove to be a problem when injecting an aerosol tracer into a flow regime under study.

Hinds provides an introductory discussion of the bulk motion of aerosols [13] although the descriptive theory presented is limited to the settling of a spherical aerosol cloud. To gain some sense of the importance of cloud settling the table below (abridged from a similar table in Hinds [13]) shows the number concentration that will result in a cloud settling velocity of 1 cm/s for various values of particle diameter and cloud diameter for particles of specific gravity 1.0 at standard conditions.

Particle Diameter (μm)	Number Concentration (cm^{-3}) for a Cloud Settling Velocity of 1 cm/s	
	Cloud Diameter = 1 cm	Cloud Diameter = 10 cm
0.1 μm	8.5×10^9	2.0×10^8
0.4 μm	1.3×10^8	3.1×10^6
1.0 μm	8.5×10^6	2.0×10^5

Table 1 Number concentration to produce a cloud settling velocity of 1 cm/s for a spherical cloud of 1 μm particles of unit specific gravity in air at standard conditions.

From this discussion we made establish a *sixth similarity condition* that aerosol tracers must be injected at sufficiently low concentrations to avoid significant cloud settling. For injection plumes on the order of centimeters or less this will limit injected tracer concentrations to values less than 10^6 to 10^8 particles/ cm^3 .

5. Stationary-Flow Duct Test Results

The test setup for the stationary flow duct test is illustrated below in Figure 3. In these tests aerosol

tracer was injected as a pulse upstream in a 12 m long circular duct of 0.30 m diameter under conditions of stationary turbulent flow, a plane was illuminated with the laser sheet 6 m downstream, and images of the resulting scattered light were recorded at rapid intervals as the aerosol pulse passed through the laser light sheet. These tests were devised to challenge the data acquisition rate of the system.

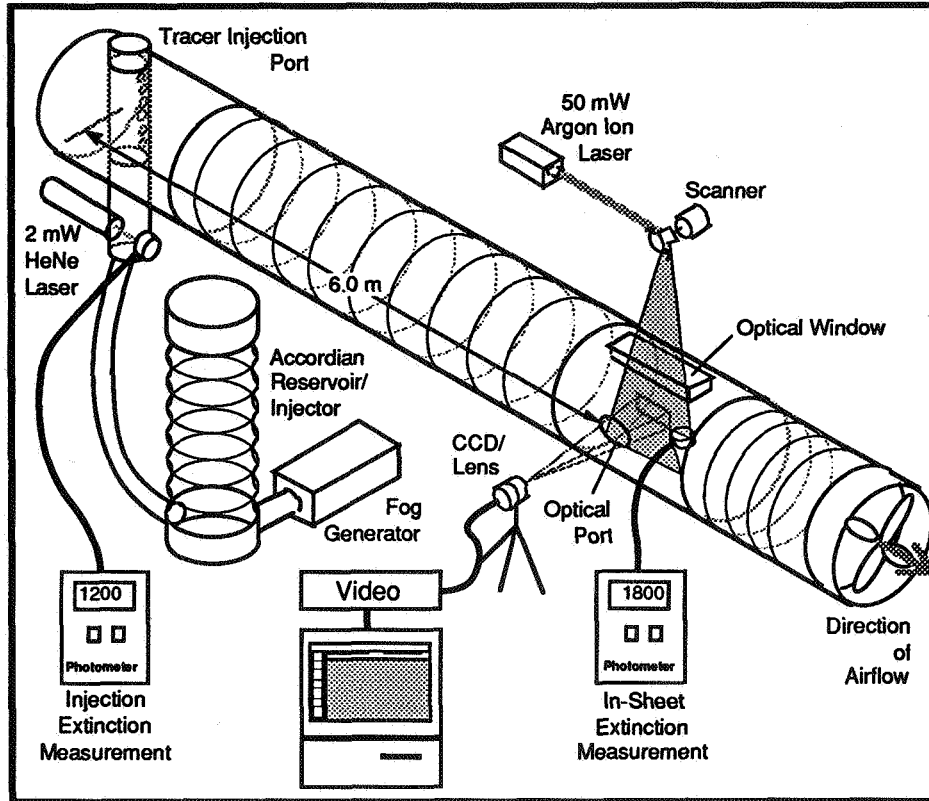


Figure 3 Configuration of the duct test systems.

Several pulse injection tests were conducted at a range of flow Reynolds numbers from 3,220 to 35,400 and measured results were compared to predicted results obtained from finite-element solutions of the 1D axial-dispersion equation:

$$\frac{\partial \bar{C}}{\partial t} + \bar{v} \frac{\partial \bar{C}}{\partial x} = D_{eff} \frac{\partial^2 \bar{C}}{\partial x^2} \quad (7)$$

The *effective* or *axial* dispersal coefficient, D_{eff} , is well correlated to the flow Reynolds number alone for fully developed turbulent flow (i.e., $Re > 10,000$) [14, 15]:

$$D_{eff} \approx 2\bar{v}R \left(\frac{3.0 \times 10^7}{Re^{2.1}} + \frac{1.35}{Re^{0.125}} \right) \quad (8)$$

All predicted results were based on this equation that may be expected to yield accurate results for $Re > 2,500$ and $Sc \approx 1$ – that is to say for molecular dispersal.

In the laminar flow regime (i.e., $Re < 2,500$) the nature of axial dispersion changes considerably as radial transport becomes more dependent on the diffusivity of the phase being transported. Transported phases having a high Schmidt number (low diffusivity), such as the Rosco fog, will tend to experience more rapid transport in the core flow as radial transport will be inhibited and flow velocities in the core are greater than in the perimeter. Effective dispersal coefficients are, consequently, greater in laminar flow than in fully turbulent flow (Levenspiel 1962). The nature of dispersal for phases with particularly high Schmidt numbers like the Rosco fog in the transition region (i.e., $2,500 \leq Re \leq 10,000$) has not been well studied.

Representative comparisons of measured and predicted results are illustrated in Figures 4, 5 and 6. Each of these figures illustrates the predicted results for the estimated Reynolds number (solid line) and for Reynolds number 10% smaller and greater (gray lines), corresponding to the uncertainty in mean air flow velocity measurement. Error bars corresponding to the standard deviation of the (spatial) mean gray value of each captured image along with the mean gray value itself (solid markers) are also illustrated.

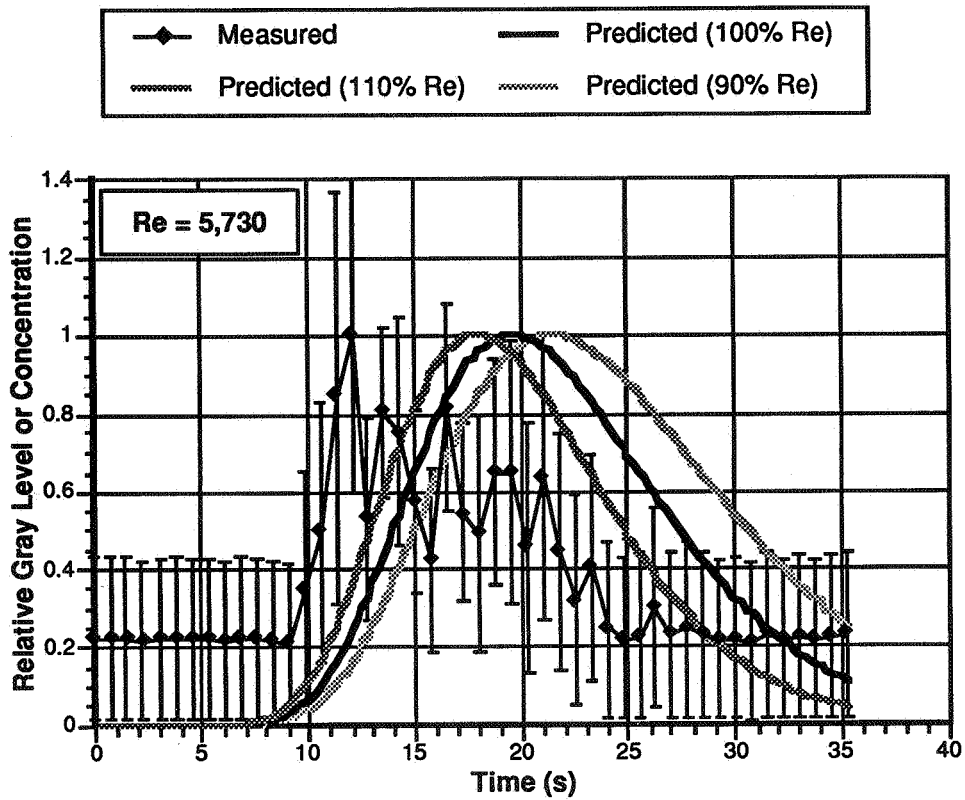


Figure 4 Comparison of measured mean gray level and predicted aerosol concentration time histories of a passing tracer pulse in a 0.30m diameter duct under conditions of transitional flow with a Reynolds number of 5,730.

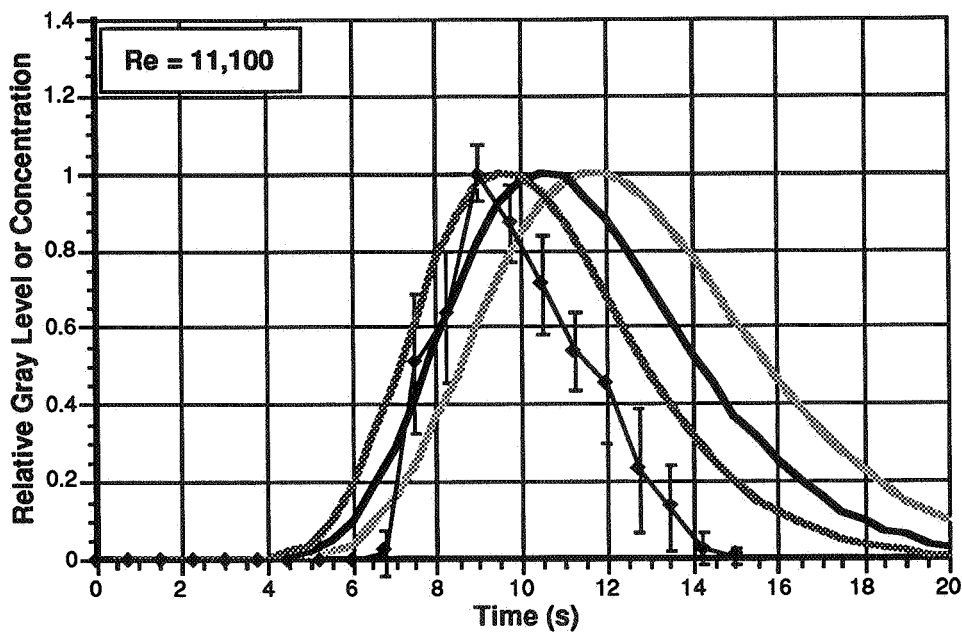


Figure 5 Comparison of measured mean gray level and predicted aerosol concentration time histories of a passing tracer pulse in a 0.30m diameter duct under conditions of transitional flow with a Reynolds number of 11,100.

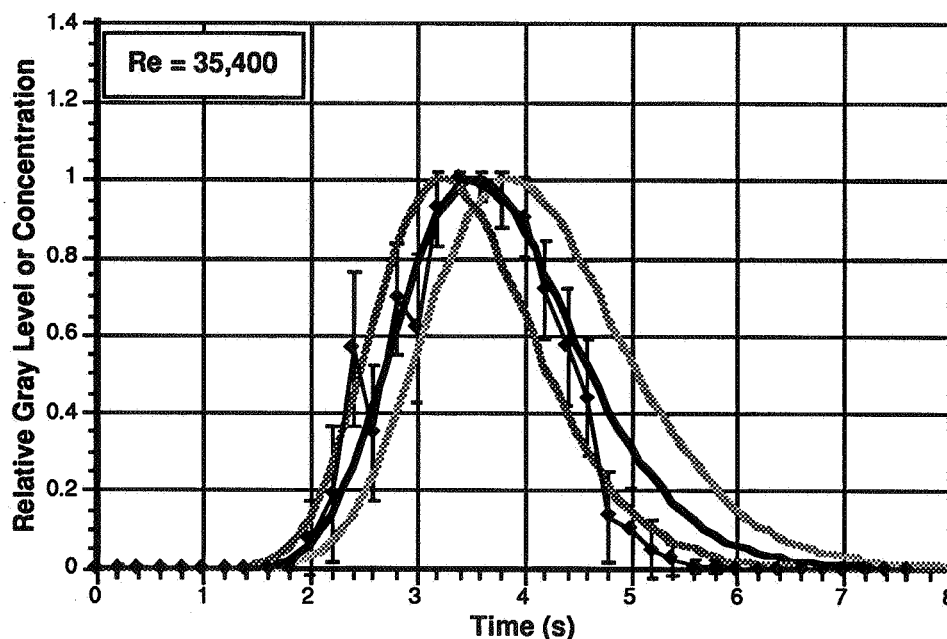


Figure 6 Comparison of measured mean gray level and predicted aerosol concentration time histories of a passing tracer pulse in a 0.30m diameter duct under conditions of turbulent flow with a Reynolds number of 35,400.

The high flow test, Figure 6 with $Re = 35,400$, was anticipated to present the greatest challenge to the proposed measurement system yet the results show a closer correspondence between predicted and measured dispersal than the lower flow tests even though images were captured at the rate of five per second – a data acquisition rate that should be more than sufficient for most room air distribution studies. These results are, however, consistent with theoretical expectations. That is to say, the correspondence between predicted (molecular) dispersal and measured (particle) dispersal is greatest for fully developed turbulent conditions (i.e., $Re > 10,000$) while at lower flow rates the axial dispersal of the Rosco fog, having a large Schmidt number, is greater than that of molecular species, hence the tracer pulses measured at the duct centerline arrived earlier than the predicted (molecular) pulses. Captured images revealed the presence of mixed laminar and medium scale turbulence providing a direct indication of transitional flow.

Somewhat surprisingly, then, these tests provided a means to evaluate the similarity of aerosol and molecular dispersal rather than challenging the acquisition rate of our equipment. The results, while not conclusive, indicate that similarity may not be realized under conditions of laminar or, even, transitional flow.

6. Conclusion

A method to measure airborne concentration distributions of an aerosol tracer over arbitrarily positioned two-dimensional planes of near-room size dimensions using laser light sheet illumination and digital image acquisition and processing techniques has been described. Technical considerations concerning the relationship between captured images and aerosol concentration and the similarity between the dispersal of the chosen aerosol tracer and molecular species dispersal have been reviewed and tests to evaluate the spatial and temporal resolution, accuracy, and repeatability of the method were discussed.

Test results presented in this paper indicate that the proposed method, using field portable, safe, and relatively inexpensive equipment, can resolve the spatial and temporal details of tracer dispersal in rooms, although similarity with molecular dispersal may not be realized for all conditions of flow. Specifically, turbulent conditions will tend to assure similarity providing aerosol settling is avoided and the aerosol tracer is seeded at sufficiently low concentrations to minimize time changes due to agglomeration, and to avoid cloud settling of injected tracer. These provisions may be realized for aerosol tracers with particle size distributions well below $10\ \mu\text{m}$ by maintaining aerosol tracer concentrations below approximately 10^5 to 10^6 particles/cm³. Similarity may not be realized under conditions of laminar or transitional flow.

Aerosol concentration may be expected to be linearly correlated to scattered light if the aerosol tracer is seeded at sufficiently low concentrations to lead to conditions of single, independent scattering and to minimize particle size changes due to agglomeration. Fortunately, these objectives may be realized using the criteria above.

The low concentration levels demanded, however, pushed the acquisition system used in the current study to its practical limits of detectability for relatively small fields of illumination of approximately one meter square. Furthermore, due to the limited, 8-bit, dynamic range of the image acquisition system used it proved difficult to capture images that were not either clipped due to intensity saturation at the upper-end or contained pixel data that fell below the detectable limit of the system at the lower-end of the range. A next generation system should take advantage of video acquisition systems that are now available that provide greater dynamic range (i.e., 12 to 24-bit) and greater low-light sensitivity with reduced noise characteristics (e.g., cooled CCD cameras). Alternative scanning systems and, possibly, light sources will be considered in future investigations to reduce system costs.

Acknowledgment

The research reported in this paper was supported with a generous grant from the Shimizu Corporation of Japan.

References

1. RODES, C.E., R.M. KAMENS, AND R.W. WIENER, The Significance and Characteristics of the Personal Activity Cloud on Exposure Assessment Measurements for Indoor Contaminants. *Indoor Air: International Journal of Indoor Air Quality and Climate*, 1991. Vol. 2: p. pp. 123-145.
2. MURAKAMI, S. AND S. KATO, Numerical and Experimental Study on Flow and Diffusion Field in Room. *Indoor Air - International Journal of Indoor Air Quality and Climate*, 1991. DRAFT.
3. CHEN, Q., P. SUTER, AND A. MOSER, A Data Base for Assessing Indoor Airflow, Air Quality, and Draft Risk. *ASHRAE Transactions*, 1991. Vol. 97(Pt. 2).
4. WHITTLE, G.E. Evaluation of Measured and Computed Test Case Results from Annex 20, Subtask 1. in 12th AIVC Conference: Air Movement and Ventilation Control Within Buildings. 1991. Ottawa, Canada: Air Infiltration and Ventilation Centre, Coventry, Great Britain.
5. LIDDAMENT, M., Technical Note AIVC 33: A Review of Building Air Flow Simulation. 1991, Air Infiltration and Ventilation Centre:
6. PORCAR, R., J.P. PRENEL, AND G. DIEMUNSCH, An Optical Method to the Study of Instabilities in Flows, in *Fluid Control and Measurement*, M. Harada, Editor. 1986, Pergamon Press: Oxford. p. 731-738.
7. MURAKAMI, S., S. KATO, AND S. AKABAYASHI, Visualization with Laser Light Sheet Applied to Internal and External Air Flows in Building Environmental Engineering, in *Fluid Control and Measurement*, M. Harada, Editor. 1986, Pergamon Press: Oxford. p. 731-738.
8. SAUNDERS, D.D. AND L.D. ALBRIGHT. A Quantitative Air-mixing Visualization Technique for Two-Dimensional Flow Using Aerosol Tracers and Digital Image Analysis. in *Building Systems: Room Air and Air Contaminant Distribution*. 1988. University of Illinois at Urbana-Champaign: ASHRAE.
9. LONG, M.B., B.T. CHU, AND R.K. CHANG, Instantaneous Two-Dimensional Gas Concentration Measurements by Light Scattering. *AIAA Journal*, 1981. Vol. 19(No. 9): p. pp. 1151-1157.
10. ESCODA, M.C. AND M.B. LONG, Rayleigh Scattering Measurements of the Gas Field in Turbulent Jets. *AIAA Journal*, 1983. Vol. 21(No. 1): p. pp. 81-84.
11. BIRD, R.B., W.E. STEWART, AND E.N. LIGHTFOOT, *Transport Phenomena*. 1960, New York: John Wiley & Sons, Inc. 779 pages.
12. FRIEDLANDER, S.K., *Smoke, Dust and Haze: Fundamentals of Aerosol Behavior*. 1977, New York: John Wiley & Sons. 317 pages.
13. HINDS, W.C., *Aerosol Technology: Properties, Behavior, and Measurement of Airborne Particles*. 1982, New York: John Wiley & Sons.
14. LEVENSPIEL, O., *Chemical Reaction Engineering*. 1962, New York: John Wiley and Sons, Inc. 501 pages.
15. WEN, C.Y. AND L.T. FAN, *Models for Flow Systems and Chemical Reactors*. 1975, New York: Marcel Dekker, Inc.

**Ventilation for Energy Efficiency and Optimum
Indoor Air Quality
13th AIVC Conference, Nice, France
15-18 September 1992**

Paper 20

**Correction of Tracer Gas Measurement Results for
Climatic Factors.**

K. Adalberth^{*}, C.A. Boman^{}, J. Kronvall^{*}, U.
Norlen^{**}**

*** Technergo AB, Ideon Research Park, S-223 70
Lund, Sweden**

**** National Swedish Institute for Building
Research, P O Box 785, S-801 29 Gävle, Sweden**

1 SYNOPSIS

This paper deals with the problem of the weather influence on ventilation rate for naturally ventilated buildings with purpose provided openings and vertical shafts. Hitherto, it has not been possible to predict the ventilation rate or to extrapolate it for other weather conditions than the measured ones, without performing a heavy calculation exercise by means of running a computer program.

In the paper a prediction as well as an extrapolation procedure is outlined. The procedures are based on generalized output data from a single zone infiltration and ventilation model (AIDA). The generalizations are made up by means of two simple equations in which the n_{50} , difference between indoor and outdoor temperature, wind velocity and a simple description of the purpose provided ventilation devices are input parameters.

Validation work is in progress and the results regarding this will be reported at the end of 1992.

2 BACKGROUND

Measurements of building ventilation performed by means of tracer gas technique are often related to specific occasions with their specific outdoor climatic conditions.

In order to be able to use such measurement data, for estimating the ventilation rate for naturally ventilated buildings during a more extended time base, the heating season or a standard condition e.g., it is necessary to have a calculation or estimation procedure for such an extrapolation.

There are at least two principal approaches possible for the extrapolation. The first one would be purely statistical by frequent experimental studies of the ventilation rate under different prevailing climatic conditions for a set of typical buildings. The second approach would involve use of a theoretical model for the extrapolation, also taking into account the air tightness performance of the house.

The statistical approach is associated with heavy work in performing detailed measurements on different types of buildings. Probably the work needed to be done is far too extensive to be a realistic alternative for practical use.

The theoretical approach would also involve detailed measurements - apart from the theoretical work with a model - on a set of buildings, in order to validate the model used. However the number of measurements could be limited, compared to the pure statistical approach.

A theoretical model for the calculation of the ventilation rate of a building, based on wind data, temperature data and air tightness data for the building was presented by one of the authors in 1980; KRONVALL (1980). It was anticipated that this model, more or less modified, could form the basis for the kind of extrapolation needed.

We distinguish between extrapolation and prediction whereas a prediction model must form the basis for extrapolation.

3 APPROACH

The theoretical model, mentioned above, is based on the use of the following equation (eq. 1). This is taken as a point of departure for the present discussion.

$$n = n_{50} / 50^b * (c_1 * (\Theta_{int} - \Theta_{ext}) + c_2 * u^2)^b \quad (\text{eq. 1})$$

where:

n = ventilation rate due to infiltration (ach) through the building envelope and purpose provided openings in the envelope.

n_{50} = specific air leakage at 50 Pa (ach) including the influence of purpose provided openings and flues

- b** = flow exponent from pressurisation curve (-)
c₁ = model coefficient (Pa/°C)
c₂ = model coefficient (Pa/(m/s)²)
⊕ int = indoor air temperature (°C)
⊕ ext = outdoor air temperature (°C)
u = wind velocity at 10 m above ground (m/s)

The rationale of the model is the "power law" for air flow through a permeable building component e.g. The equation for the "power law" is:

$$Q = a * \Delta p^b * A \quad (\text{eq. 2})$$

where:

- Q** = rate of air flow through the building component (m³/s)
a = flow coefficient (m³/(s*m²*Pa^b)
Δp = pressure difference (Pa)
b = flow exponent (-)
A = area of the building component (m²)

The envelope of the building is considered as permeable and the purpose provided openings are also included in the leaking system. This average leakiness of the building is described in the factor $n_{50} / 50^b$ in the model. The average pressure difference across the envelope of the house is described by the factor $(c_1 * (\oplus_{int} - \oplus_{ext}) + c_2 * u^2)$. The exponent b describes the air leakage characteristic of the envelope.

In order to test the feasibility of the model, a number of calculations were performed with a single zone infiltration simulation model - the AIDA model; LIDDAMENT (1989). A good ability of comprising the results of AIDA calculations for a set of buildings and for a set of different wind and temperature combinations would then be a proof of the feasibility of the model.

If this is shown to be successful it would be possible to predict the ventilation rate of more or less arbitrarily chosen types of buildings once the air tightness behaviour, the ventilation arrangements and the weather conditions (wind and temp diff) were given.

Normally only the air tightness performance of the envelope (i.e. the n50-value) is known or estimated. More seldomly is the value of the exponent in the power-law expression known. Tentatively there is a correlation between the n50-value and the value of this exponent, so that for low n50-values the exponent value would be close to 1.0 and for high n50-values the exponent value would be close to 0.5. Furthermore, the n50-value for the air leakage behaviour of the envelope only is not suitable for eq. 1. In this equation the n50-value should represent the air leakage behavior for the envelope and purpose provided ventilation openings, such as air terminal devices for supply of outdoor air and vertical shafts for weather driven exhaust of air from the building. Thus for prediction use of the model (eq. 1) it is necessary to have a procedure for modifying the "normal" n50 and exponent values to new, modified ones.

So far we have been discussing eq. 1 for prediction use only. For extrapolation use - from one weather condition to another - the following equation is used (indexes: 1 = first weather condition, 2 = new weather condition):

$$n_2 = n_1 * [(c_1 * (\oplus_{int,2} - \oplus_{ext,2}) + c_2 * u_2^2) / (c_1 * (\oplus_{int,1} - \oplus_{out,1}) + c_2 * u_1^2)]^b \quad (\text{eq. 3})$$

4 DATA USED FOR SIMULATIONS

For the simulations with the AIDA program a set of "significant" building types were chosen; a 1 storey detached house, a 1 1/2 storey detached house and three different flats in a 3 storeys multi-family house. These include a non-through flat on the ground floor and on the top floor, and finally a through flat on the top floor.

General data for the simulations were:

Wind: at weather station

Terrain/shielding: urban options were: - open countryside
conditions: - scattered windbreaks
- urban
- city

Floor: solid (airtight)

Wind pressure coefficients: according to the AIVC Calculation Techniques Guide (LIDDAMENT 1986)

Specific data for each type of building are shown in table 1.

The following parameters were given different values in the different calculations:

- n50
- exponent b
- wind direction (perpendicular to or along face wall)

For each set of the parameters above calculations were performed for wind velocities of 0 to 10 m/s and temperature differences between 0 and 40 degC.

Table 1. Specific data for each type of building, used for simulations with the AIDA computer program.

	Detached houses --->		Flats ----->		
	1 storey	1 1/2 st	Non thru Gr floor	Top fl	Through Top fl
Building height (m)	4.8	6.5	9.0	3.0	3.0
Eaves height (m)	2.5	2.5	2.5	2.5	2.5
Roof pitch angle (deg)	30	45	0	0	0
Building length (m)	15	15	9	9	7
Building width (m)	8	8	9	9	12
Building volume (m3)	300	540	203	203	210
Number of airtight comp.	0	0	4	4	3
Number of vent openings	7	7	3	3	4
Vent 1					
Location	front	front	front	front	front
Height (m)	2.0	2.0	2.3	2.3	2.3
Area (cm2)	60	60	90	90	60
Vent 2					
Location	rear	rear	ceiling	ceiling	rear
Height (m)	2.0	2.0	10.0	10.0	2.3
Area (cm2)	60	60	100	100	60

cont...

Vent 3					
Location	left	left	ceiling	ceiling	ceiling
Height (m)	2.0	2.0	10.0	10.0	4.0
Area (cm ²)	30	30	100	100	100
Vent 4					
Location	right	right			ceiling
Height (m)	2.0	2.0			4.0
Area (cm ²)	30	30			70
Vent 5					
Location	ceiling	ceiling			
Height (m)	4.8	6.5			
Area (cm ²)	100	100			
Vent 6					
Location	ceiling	ceiling			
Height (m)	4.8	6.5			
Area (cm ²)	100	100			
Vent 7					
Location	ceiling	ceiling			
Height (m)	4.8	6.5			
Area (cm ²)	100	100			

5 RESULTS

5.1 Generalization of computed ventilation rates by means of the model (equation 1)

A set of significant calculation results obtained by running the AIDA program is shown in figure 1 to 6.

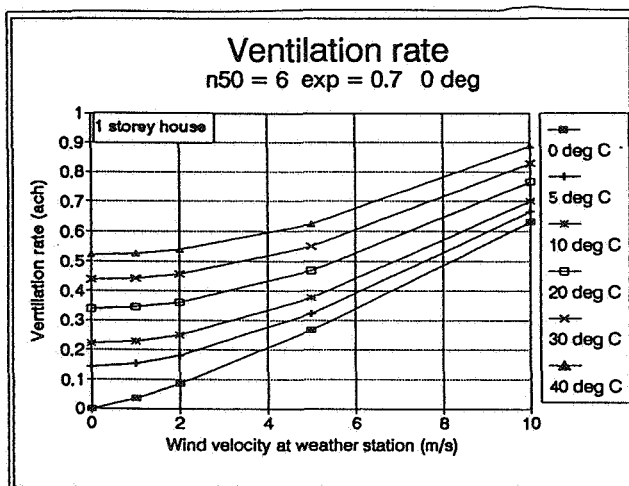


Figure 1

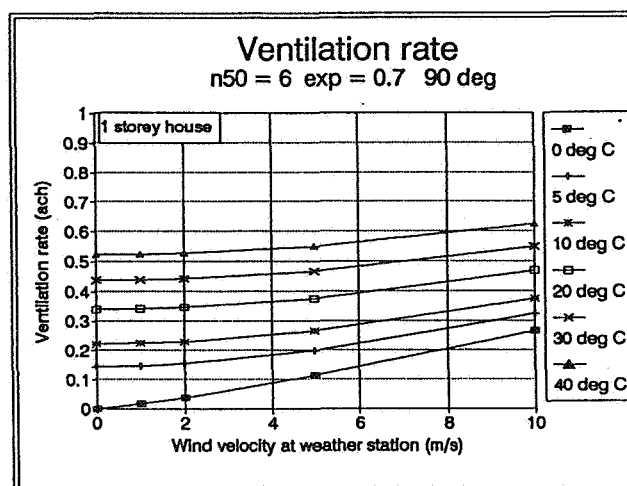


Figure 2

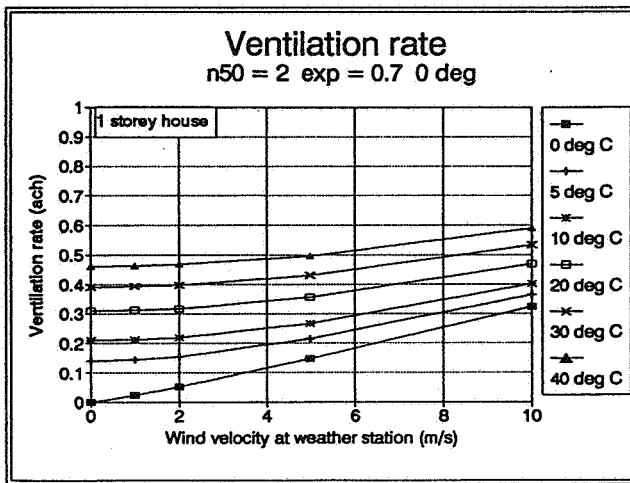


Figure 3

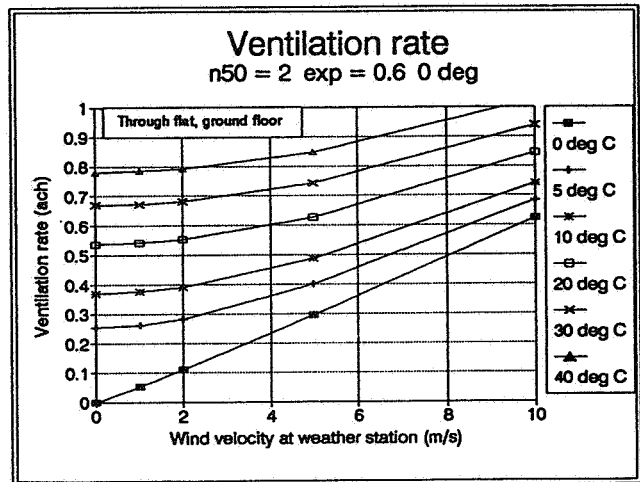


Figure 4

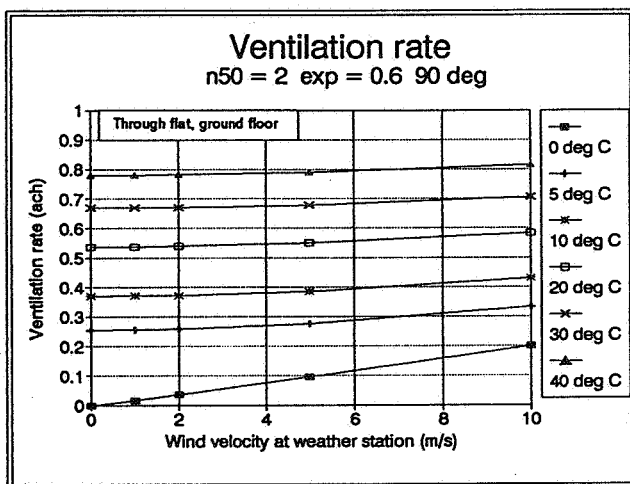


Figure 5

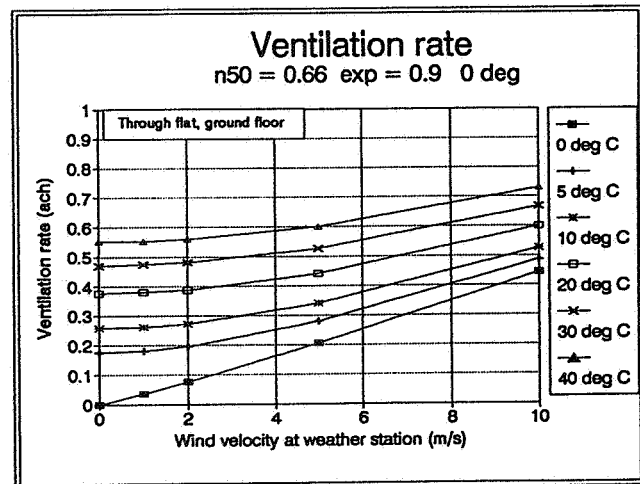


Figure 6

In order to generalize the computation results by means of using equation 1, it is essential to include the impact of the purpose provided ventilation openings on n_{50} and the exponent. The modification was made in such a way that the calculated air flow rates for purpose provided openings for pressure differences between 0 and 50 Pa were added to the flow rate calculated by means of the original n_{50} and b values. Curve fitting using the least-square method finally gave the modified values. (These modified values correspond to those obtained when a pressurization test with open purpose provided openings is performed.)

The calculated values of the ventilation rate for different wind velocities and temperature differences were placed in a spread-sheet (QUATTRO[®] PRO 4.0). This program has an ability of optimization, based on linear-programming technique, which was used in order to settle the values of c_1 and c_2 in the model (equation 1).

First the value of c_1 (the temperature coefficient) was estimated by putting c_2 equal to 0 (fixed) for the case that the wind velocity was 0 m/s. Then the program calculates the value of c_2 that best satisfied the model in the least squares sense. For control purposes the squared residuals (differences between calculated ventilation values acc. to the model and those from the AIDA calculations) were summed up and a mean value was calculated. The square root of this obtained mean square error for a case was in the range of $10^{-2} - 10^{-3}$. Thus, it could be stated that the model (equation 1) describes the outputs of the infiltration and ventilation model AIDA quite well and in a very handy way.

The values of the coefficients c_1 and c_2 for the different cases are shown in table 2.

Table 2. Coefficients c_1 and c_2 for different simulation cases. 0 deg corresponds to the case when the wind direction is perpendicular to the facade and 90 deg to wind along the facade.

Type of building	Temperature		Wind				
	c_1		c_2				
	mean	highest lowest	0 deg mean	0 deg highest lowest	90 deg mean	90 deg highest lowest	mean
Houses							
1 storey	0.018	0.024 0.009	0.005	0.007 0.004	0.002	0.003 0.001	0.004
1 1/2 st	0.022	0.035 0.007	0.010	0.014 0.007	0.006	0.008 0.004	0.008
Flats							
Ground	0.051	0.057 0.040	0.013	0.016 0.011	0.002	0.002 0.001	0.008
Top	0.013	0.016 0.011	0.008	0.009 0.006	0.001	0.001 0	0.005
Top through	0.013	0.015 0.009	0.004	0.005 0.003	0.001	0.001 0.001	0.003

As can be seen in table 2 the mean of the coefficient c_1 takes a value of 0.017 +/- 0.005 for all cases except for the flat on the ground floor where $c_1 = 0.05$. This is reasonable as the ventilation shaft is higher in this case. The c_2 values are around 0.005 with some variation for all cases, which is reasonable also because of the fact that the wind influence was modelled in the same way for all cases.

The wind influenced coefficient c_2 is lower than the temperature influenced coefficient c_1 . Thus, it might be tempting to use the model for prediction without involving the wind effect. In order to see whether this is possible or not a calculation was made of the relative influence of temperature only in the expression for the wind and temperature influence in equation 1. The results are shown in figure 7.

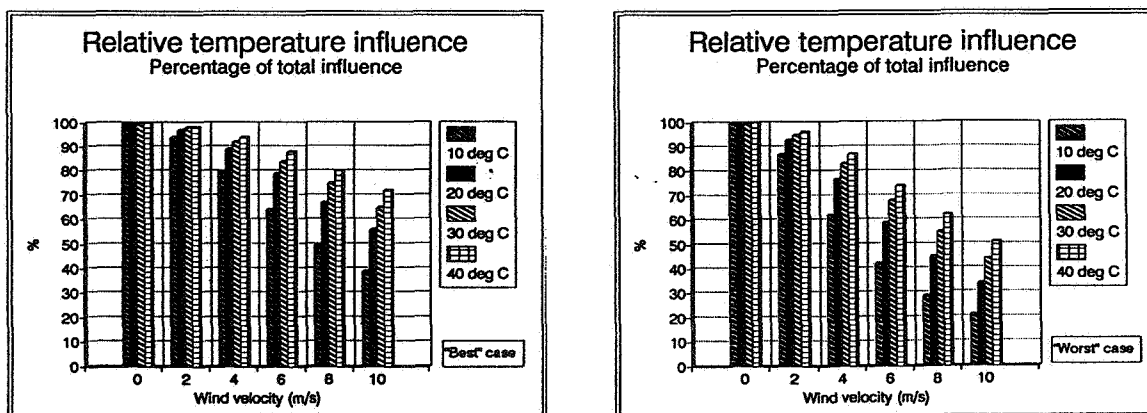


Figure 7. Relative temperature influence.

"Best case" corresponds to the case with the smallest difference between c_1 and c_2 , i.e. the non-through flat on the top floor.

"Worst case" corresponds to the greatest difference, i.e. the flat on the ground floor.

It is obvious for the "best" case, which is significant for buildings on the ground and higher up in a multi-storey building, that the wind-driven ventilation is of relatively low importance compared to the temperature-driven - at least for lower wind velocities ($< \text{appr. } 4 \text{ m/s}$). For the case with a flat on the ground floor this is obviously not valid.

5.2 Outline of a prediction procedure

Using equation 1 for prediction of the ventilation rate in a building involves the following parameters to be settled:

- n50 The air permeability parameter which also should reflect the influence of purpose provided openings.
- b The flow exponent corresponding to n50 above.
- $\Theta_{\text{int}} - \Theta_{\text{ext}}$ The temperature difference between in- and outdoor
- u The wind velocity.

Normally only the n50 value for the building envelope itself (with purpose provided openings sealed) is available or is estimated based on empirical knowledge and/or "help-schemes" (Such ones are under preparation and are going to be included in the AIVC Numerical Database, to be published late 1992).

Originally a hypothesis was that - due to different flow characteristics for large and small (resp.) openings or cracks - there is a correlation between the n50-value and the value of the exponent b, so that for low n50-values the exponent value would be close to 1.0 and for high n50-values the exponent value would be close to 0.5.

This hypothesis was tested by analysing some 30 pressurization test results - more or less arbitrarily chosen. The result is shown in figure 8. From only a quick look at the figure it is obvious that the hypothesis should be rejected.

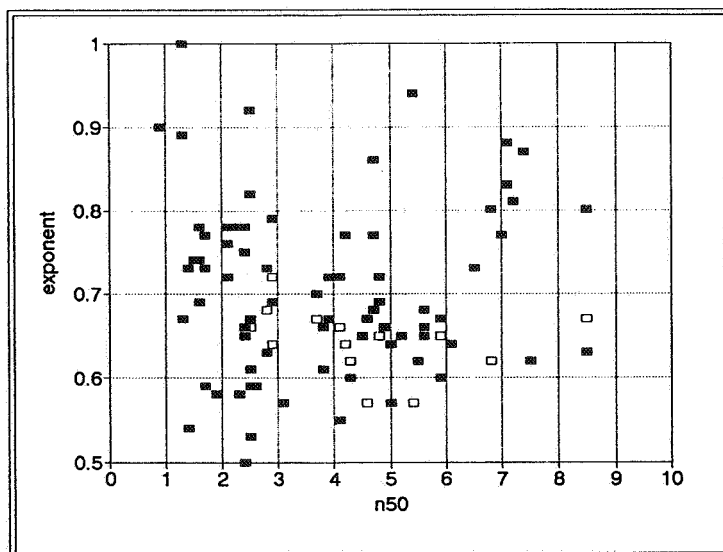


Figure 8. Exponent values plotted versus n50-values.

Apparently, when making predictions, a value for the exponent must be chosen. According to general experience and figure 8, a value of 0.7 would be reasonable. Based on this assumption, a set of diagrams, figures 9 - 12, were made up for the estimation of an n50 value and an exponent value which are modified

for the influence of purpose provided openings. Three different levels were chosen for the total area of purpose provided openings, viz. 100, 200 and 300 cm².

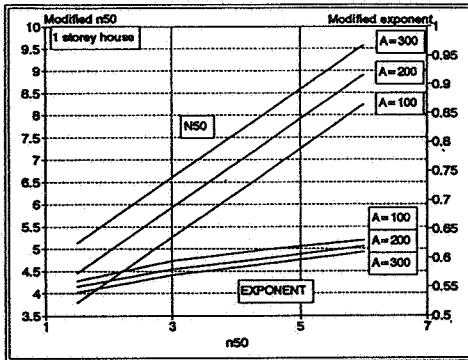


Figure 9

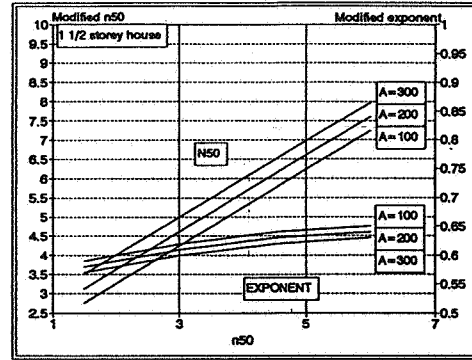


Figure 10

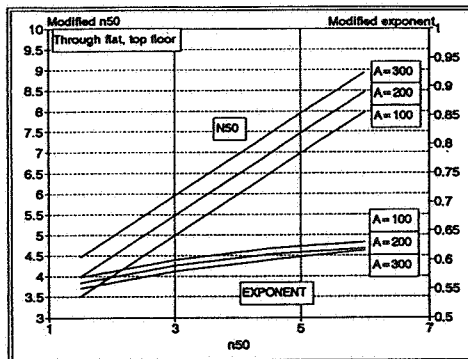


Figure 11

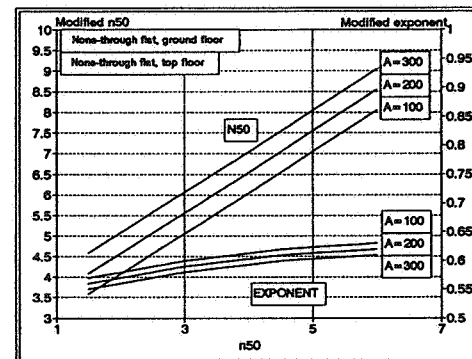


Figure 12

EXAMPLE

Estimate the ventilation rate in a one storey detached house in an urban area with $n50=4.5$ ach at 50 Pa. The wind velocity at a weather station in the vicinity is 4 m/s and the difference between outdoor and indoor temperature is 23.5 degC. The total area of purpose provided openings is 200 cm².

The $n50$ value does not account for purpose provided openings, so it has to be modified for use in equation 1. This is done by means of using the diagram in figure 9. From this it can be seen that the modified $n50$ will be 7.3 ach at 50 Pa and the modified exponent 0.60.

c_1 and c_2 are taken from table 2 ; $c_1=0.02$, $c_2=0.004$.

Now equation 1 gives the solution:

$$n = 7.3/50^{0.60} * (0.02*23.5 + 0.004*4^2)^{0.60} = 0.48 \text{ ach}$$

5.3 Outline of an extrapolation procedure

As outlined in chapter 3, it is possible to get an expression for extrapolation from one weather condition to another simply by dividing equation 1 for the extrapolated condition (2) with the equation for the base case (1), eq. 3.

It can be seen that $n50$ no longer influences the calculations. This is reasonable since the base case (1) gives the relative level of the ventilation rate for the house and the extrapolation only adjusts for the extrapolated condition.

6 FURTHER DEVELOPMENT AND VALIDATION

It is apparent that a validation exercise must be carried out in order to test the feasibility of the models, both the model for prediction (eq. 1) and the model for extrapolation (eq. 3). The purpose of this paper is merely to present an outline of a possible way to make simple predictions and extrapolations on ventilation rates in not too complicated buildings, which can be treated as a single zone.

An excellent opportunity to carry out such a validation (and possibly adjustment) work will be given via a current investigation of the energy performance and indoor climate of Swedish houses, undertaken by the National Swedish Institute for Building Research. 1 600 randomly selected Swedish single and multi family houses have been investigated by inspections and measurements on site, during 1991-92.

NORLÉN et al (1991) & STYMNE et al (1991). Among many other things, the ventilation rate has been measured in each of the houses for 3 - 4 weeks by means of a passive tracer gas technique (PFT) developed at the institute. STYMNE & ELIASSON (1991). Furthermore, a sub sample of some 100 buildings out of the 1600 ones are being studied more extensively regarding ventilation e.g. In this sub sample the ventilation is measured also by means of tracer gas decay method. This will give an opportunity to estimate the occupant's behaviour with regard to ventilation for the houses tested with the passive technique. Finally a small group of 19 buildings out of the total sample, naturally ventilated with vertical shafts, is studied very extensively by means of repeated decay tracer gas and PFT measurements under different weather conditions. These measurements form an excellent basis for validation of the extrapolation model (equation 3).

These validation exercises will take place during late summer and autumn of 1992 and will be reported in the end of 1992.

7 ACKNOWLEDGEMENTS

The authors would like to express their gratitude to Dr. M. Liddament, AIVC, for his help with the AIDA program and his encouraging attitude shown to us in the work with the project. Mr S Skogberg, National Swedish Institute for Building Research, has provided us with building statistics and is performing the field measurements in a very efficient way, which is greatly acknowledged.

8 REFERENCES

KRONVALL, J, Correlating pressurisation and infiltration rate data - tests of an heuristic model. Contribution to the 1st AIC Conference. AIVC, AIC-PROC-1-80. Warwick, UK, 1980.

LIDDAMENT, M, Air infiltration calculation techniques - an applications guide. AIVC, Warwick, UK, 1986.

LIDDAMENT, M, AIDA - Air infiltration development algorithm. Air infiltration review, Vol 11, No. 1, December 1989, AIVC, Warwick, UK, 1989.

NORLÉN, U, HÖGBERG, H and ANDERSSON, K, A survey of the indoor climate in the Swedish housing stock. Proc. ASHRAE/CIB Healthy Buildings - IAQ Conference, Sept 4-8, 1991, Washington, US, 1991.

STYMNE, H, BOMAN, C A, MELANDER, H, NORBERG, P and STRIDH, G, Methods for indoor climate measurements in large scale surveys. Proc. ASHRAE/CIB Healthy Buildings - IAQ Conference, Sept 4-8, 1991, Washington, US, 1991.

STYMNE, H & ELIASSON, A, A new passive tracer gas technique for ventilation measurements. Proc. 12th AIVC Conference, Ottawa, Canada sept 1991, AIVC, Warwick, UK, 1991.

**Ventilation for Energy Efficiency and Optimum
Indoor Air Quality
13th AIVC Conference, Nice, France
15-18 September 1992**

Paper 19

**Measurement of Actual Performances of
Ventilation Systems in Buildings.**

J. Riberon, J.G. Villenave, R. Simeon, J.R. Millet

**Centre Scientifique et Technique du Batiment, 84
Avenue Jean Jaurès, BP 02, 77421 Marne La Vallee
Cedex 02, France.**

ABSTRACT

Airtightness deficiencies of building envelopes and weaknesses in the ventilation systems can disrupt the operation of heating and ventilation systems. This can lead to an insufficient level of air quality and higher energy consumptions. In order to assess the performances of buildings and ventilation systems, CSTB has designed and developed different experimental devices for field testing.

In a first step, an equipment was produced to measure the envelope air leakage. This apparatus is mainly used for research purposes. In order to allow low-cost controls in dwellings, two simplified methods have been developed using either the ventilation system itself or a light and compact device. To measure both air leakage and pressure loss in ventilation ducts, two devices have been produced : the first one applies to single-family dwellings with mechanical ventilation, the second one to multi-family dwellings with passive stack ventilation.

1 - INTRODUCTION

Ventilation of buildings is necessary both to insure adequate air quality and to protect the building itself against condensation and mould growth. On the other hand, ventilation flow rates must not lead to excessive energy consumptions.

To comply with these requirements the airtightness of buildings must be improved. Nevertheless, it is recognised that the improvements in the airtightness can lead to a reduction in the air quality unless the ventilation problem is dealt with. Therein, examination and testing of ventilation systems must be required to ensure that they operate effectively.

A great deal of effort has been devoted to the determination of the relevant parameters of ventilation which should be measured and several measurement techniques for air infiltration and ventilation have been examined by the International Energy Agency [1-3].

In order to assess the performances of buildings and ventilation systems, CSTB has defined measurement methods and designed and developed different experimental apparatus. These apparatus which are used for the building envelope or ventilation duct airtightness measurements have been tested on different types of dwellings.

2 - MEASUREMENT OF BUILDING AIRTIGHTNESS

Attention must be paid to control of the building envelope airtightness. Indeed, air leakage through the building envelope is detrimental to the performance of the building equipped with a ventilation system. Air leakage wastes energy and can disturb the operation of the ventilation system leading to an insufficient air quality. In addition, it can cause draught and noise problems.

This is why research work has been carried out in order to improve the knowledge in the field of air infiltration [4-6]. In many countries, air leakage measurement methods have been developed [7-9] ; and in some countries a specific level of airtightness is required and the new dwellings are checked according to the standardized measurement method [10].

In France, a guide describes how to measure the overall air leakage of a dwelling by using the fan depressurization method [11]. This test method is suitable for research work or field study. In order to extend its field of application to building inspection two simplified methods have been developed.

2.1 - Traditional method

The test procedure involves replacing an external door with a panel door and using a fan to depressurize the dwelling. The air flow rate is measured for different values of the pressure difference between the inside and the outside of the building. This technique was selected because the dwellings usually have a

negative pressure owing to the mechanical exhaust systems with which they are equipped.

The test equipment, so-called "fausse-porte CSTB", was developed in the late seventies. It is composed of a panel door to apply tightly into the grooves of the existing door frame, a fan, a long measuring pipe where the pressure difference over an orifice plate is translated to air flow, a micromanometer (see figure 1). The panel door can be adjusted in height and width to fit a wide variety of existing door sizes. A set of orifice plates makes it possible to accurately measure a wide range of air flow rate.

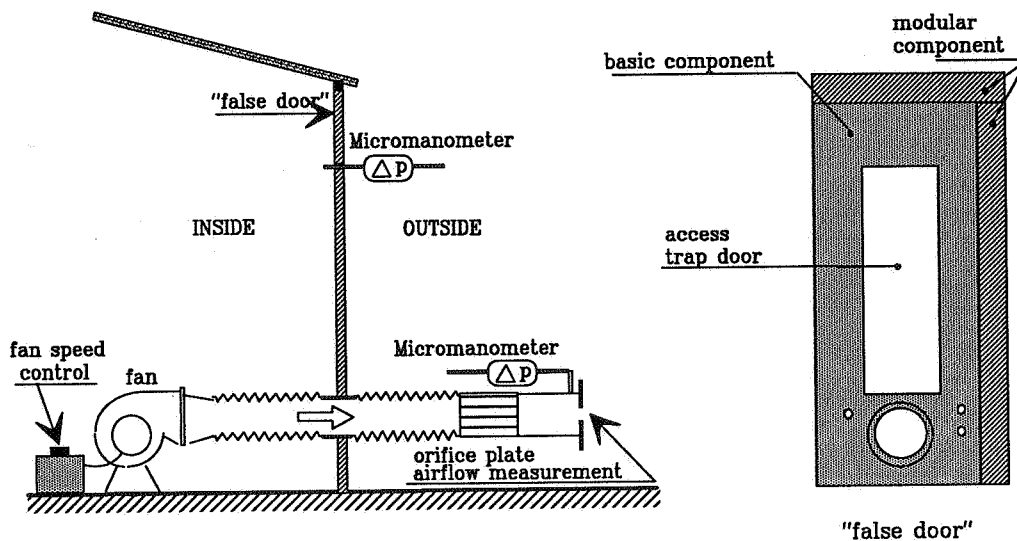


Figure 1 : sketch of dwelling airtightness test equipment "fausse-porte CSTB"

Once the test equipment is set up, all vents are sealed off, then the leakage flow rate is measured for at least ten values of pressure difference in the range 10 - 60 Pa. The measurement data are analysed using the power law fit :

$$Q = k \Delta P^n$$

- where
- Q is the air flow rate (m³/h)
 - k is the air flow coefficient (m³/h at 1 Pa)
 - ΔP is the pressure difference across the building envelope (Pa)
 - n is the flow exponent (0.5 ≤ n ≤ 1)

Values of k et n describe the air leakage characteristics of the tested dwelling.

The guidance about preparing the building and setting up the equipment, the instrumentation required, and the procedure for carrying out the test is laid down in the guide [11] and ensures the accuracy of results.

Numerous measurements were performed according to this method (see section 2.3) and led to get a better understanding of the airtightness deficiencies related to the type of construction. However, this method is mainly intended for research purpose because it needs sophisticated equipment and highly specialised technicians ; that is why it was necessary to develop simplified methods in order to make dwelling check easier.

2.2 - Simplified methods

Two simplified methods for inexpensive checking of dwellings airtightness have been developed [12-13]. The first method involves using existing fan in the block of flats for depressurization. Investigations conducted in Scandinavian countries [1-14] have shown that is a good and sufficient method to show if the dwelling envelope is airtight enough or too leaky. The second method uses a compact and light specific apparatus to depressurize the dwelling.

2.2.1 - Using existing fan

This method is quite suitable for the air leakage measuring of multi-family dwellings having a mechanical exhaust ventilation. The test procedure is quick and easy (see figure 2). The air flow rate across the dwelling envelope is measured by means a flowmeter applied to one exhaust vent (e.g. kitchen vent), all the other ventilation openings are sealed off. The pressure difference across the envelope is measured by means a micromanometer and a capillary tube introduced through one air inlet. Here, a particular attention must be paid to seal up the air inlet opening.

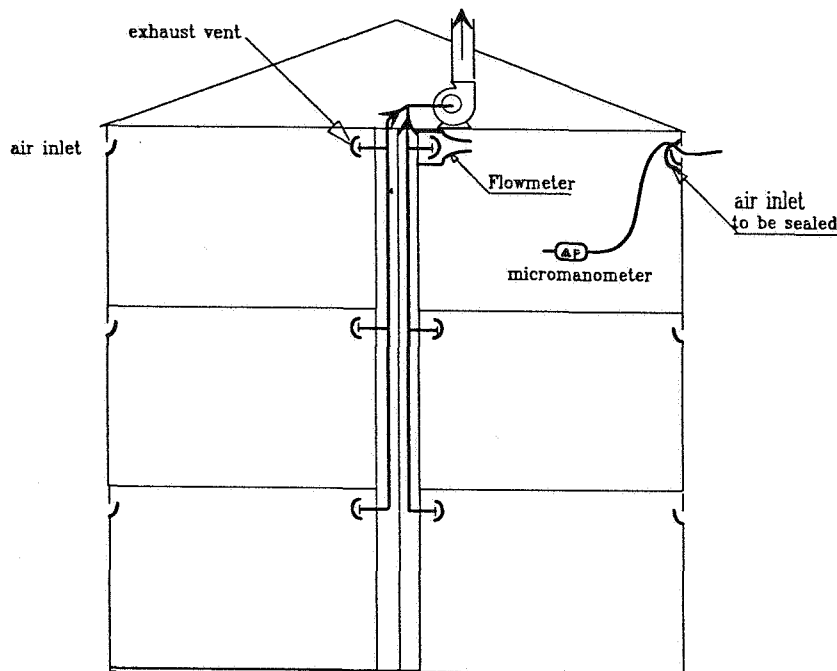


Figure 2 : sketch of airtightness test using the fan of the building

Unsealing several exhaust vents makes it possible to obtain several flow rate and pressure difference measurement points. The method for expressing the measurement result(s) assumes that the exponent flow n is conventionally equal to $2/3$; the final result is the air change rate at 10 Pa i.e. air flowrate at 10 Pa divided by the volume of the dwelling.

This method was tested in a flat located in a six-storeys building. I was possible to create a pressure difference of about 40 Pa. This method was compared with the traditional method i.e. fan-depressurization method involving a panel door. Both measurement results are in close agreement ; difference in air leakage level between simplified and traditional methods is of 11 % which is reasonable since the accuracy is not the same according to the methods.

When the dwelling is tight enough it is possible, according with this method, to depressurize it up to about 30 Pa and thus to assess the airtightness level of the dwelling. When the dwelling is too leaky or large ventilation system is insufficient to create an available pressure difference and it is required another simplified method. Such a method is described below.

2.2.2 - Using a compact specific equipment

When the dwelling is not equipped with a mechanical ventilation or when the ventilation system does not enable to create a sufficient pressure difference (e.g. mechanical exhaust ventilation of single-family dwellings) a specific measurement equipment must be used to perform the airtightness test.

The basic principle of this method is the fan-depressurization. The test procedure is the following : All vents are sealed off. The measurement equipment is connected to an extract duct (e.g. kitchen extract duct), then it creates and measures the air flow rate. Pressure difference across the building envelope is measured by means a micromanometer like in section 2.2.1.

The airtightness measurement equipment is composed of a small fan linked with a flowmeter and a supple jointing duct 2.7 m long with a terminal device to be applied to the exhaust vent (see figure 3). The equipment is light (10 kg) and easy to handle. The flow calibration and flow-pressure curves of this equipment have been derived from laboratory tests.

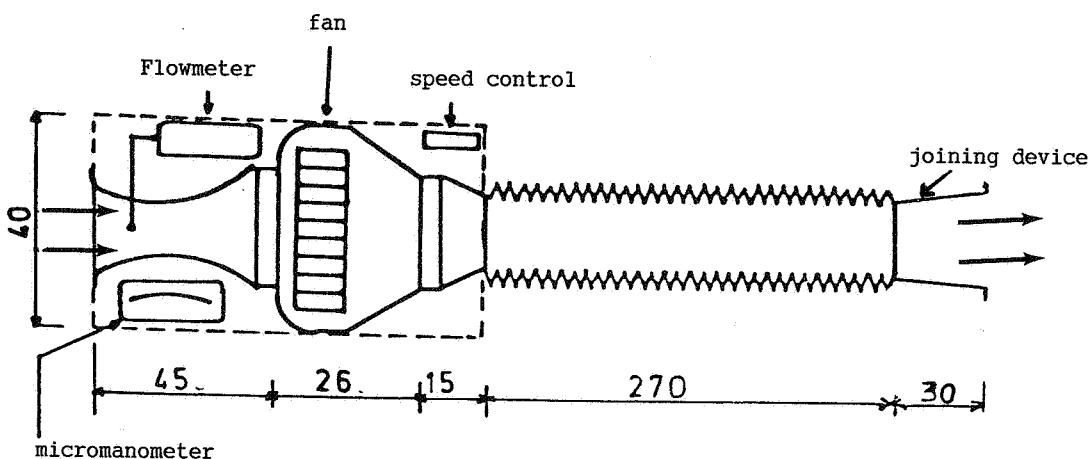


Figure 3 : compact equipment for airtightness measurement

In order to test this equipment for ability, airtightness measurement were carried out on a house by using both simplified equipment and "fausse porte". The results showed the air leakage flow rate measured by the simplified equipment is higher than the flow rate measured by the "fausse-porte". The main explanation for this is that leak of the external door of house is not taken into account with the "fausse-porte" method. After this correction, both methods yielded the same result within approximately 10 %.

2.3 - Results

Numerous campaigns of airtightness measurement were carried out on dwellings by using the "fausse-porte CSTB". Synthesis of measurement results is given in the table 1 relevant to the type of construction.

	type of construction				
	heavy frame				light frame
	exterior insulation		interior insulation		
house	flat	house	flat	house	
average	0.26	0.12	0.36	0.17	0.39
standard deviation	0.07	0.10	0.12	0.14	0.18
number of dwellings	9	39	93	23	16

Table 1 : Air change rate of dwellings (ach at 1 Pa)

The tests have made it possible to identify the most frequently encountered leakage paths.

The airtightness deficiencies are particularly important on walls with interior insulation (plasterboard plus insulation complexes). A route by which air enters is also door and window frames, electrical ducts, gaps around water pipes, attic access trap doors, ...

In France, manufactured windows and doors are built in compliance with standards ; these components are classified in groups according to the air leakage performance. The measurement results have shown that the actual performances are in agreement with the required level. These building components have good airtightness ; on the other hand, the airtightness between the window frame and the wall is generally poor.

3 - AIR LEAKAGE AND PRESSURE LOSS MEASUREMENT IN SUPPLE DUCTS

Measurements were performed on about twenty newly-built single family dwellings having a mechanical exhaust ventilation system, in order to get a better understanding of the actual functioning of the ventilation [15].

3.1 - Method

The test procedure involves using an appropriate apparatus enabling to accurately measure air leakage as well as pressure loss in the supple extract ducts. The apparatus is composed of a portable case housing a centrifugal variable speed fan. The upstream side of this case is connected to a flattened cone-shaped adapter taking the duct to be tested and the downstream side to an air flow measuring pipe which is 1 m in length and 156 mm in diameter and equipped with an orifice plate. The use of the adequate orifice plate among a set of five (from 19 to 76 mm) ensures an accurate measuring of the air flow. The case has a tapping for measuring pressure downstream in the duct.

The test procedure for pressure loss measurement is the following : the apparatus is installed in the attic of the house, close to the extract unit of the ventilation system (see figure 4). The duct to be tested is taken off the extract unit then connected to the adapter of the apparatus ; the related exhaust vent being taken out. The pressure below the duct is measured For a given air flow rate. Usually, three or four measurement points can be obtained thanks to the variable speed fan. for air leakage measurement, the same procedure is used except that the exhaust vent is sealed off and that a smaller orifice plate is necessary.

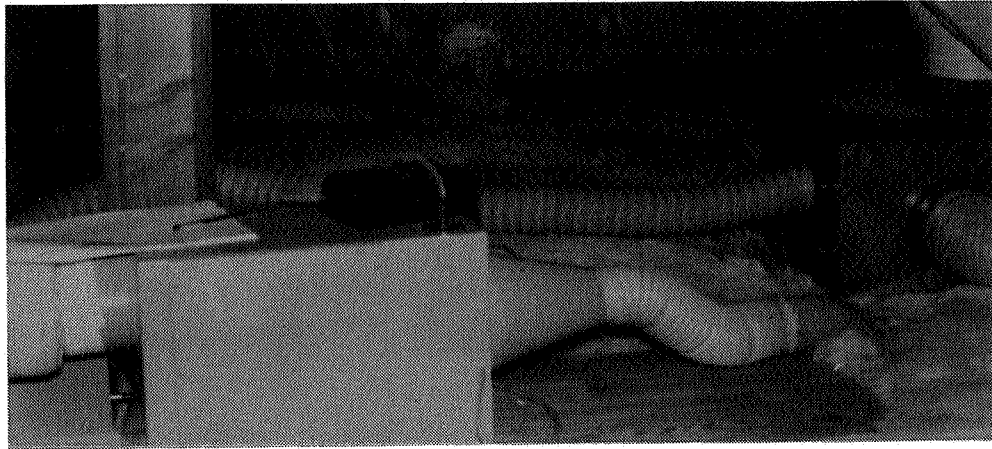


Figure 4: equipment for measuring air leakage and pressure loss in supply extract ducts

3.2 - Results

Figure 5 depicts the distribution of pressure losses measured in the supply ducts. The pressure loss coefficient Λ was derived from the measurement results and the dimensional characteristics of the duct. In 55 % of cases, ducts have an actual Λ value comparable to the theoretical value measured in laboratory (about 0.5), that means installation work is properly achieved. The higher values of Λ may be due to failing in installation work such as sharp bends, insufficient stretch in the supply duct, numerous windings in the ductwork. In a few cases, the pressure loss is very high (Λ value is over 1.8), that indicates the supply air duct is trampled down.

Figure 6 depicts the distribution of air leakage rate in the ducts defined as the ratio of the air leakage flow to the exhaust air flow calculated at the same pressure difference. The results have shown the sample might be divided into three groups :

- . Airtight duct (64 % of the sample)
the range of the leakage flow rate is 0.7 - 3 m³/h at 100 Pa. The leakage rate is contained between 2 % and 12 %.
- . Little leaky duct (24 % of the sample)
the range of the leakage flow rate is 3 - 10 m³/h at 100 Pa. The average value of the leakage rate is approximately 30 %. Leak is usually caused by a bad connection to the extract unit.
- . Very leaky duct (12 % of the sample)
the leakage flow rate is from 30 up to 190 m³/h at 100 Pa. It is so considerable that the exhaust air flow is exceedingly low, indeed non-existent. Miscellaneous reasons cause this poor result, particularly : joining deficiencies with the exhaust vent or with the extract unit, damage in supply duct caused by poor design or installation.

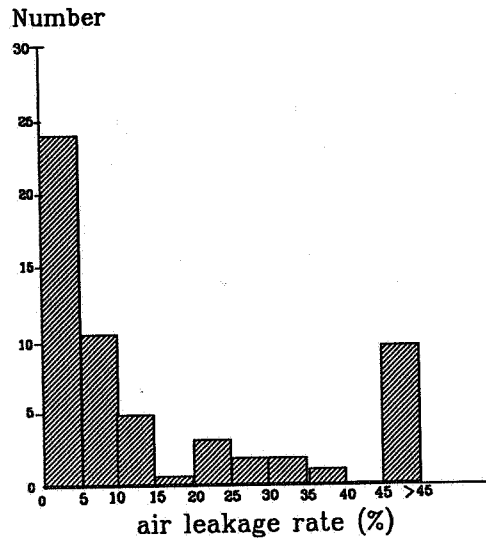


Figure 5 : distribution of air leakage rate in ducts (total number of ducts = 59)

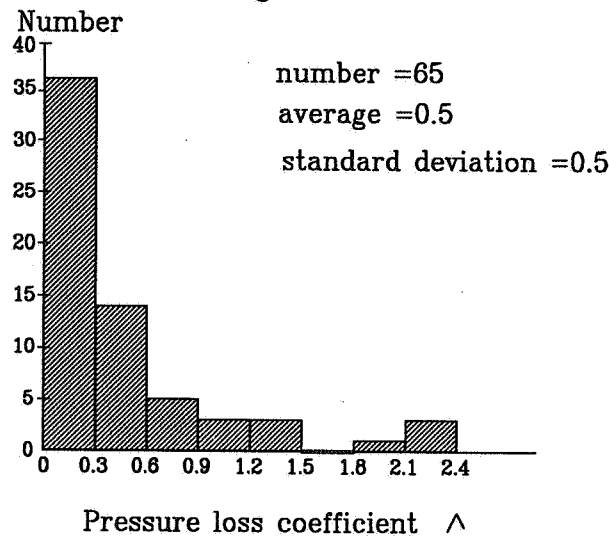


Figure 6 : distribution of pressure loss in ducts for 19 dwellings

4 - MEASUREMENT OF SHUNT DUCT AIRTIGHTNESS

Numerous buildings built in the sixties and before have to be renovated ; in that times, ventilation by building envelope leakages compensate for stack effect ventilation insufficiency.

Façade renovation (thermal and acoustic insulation) reduces the cross ventilation ; the new ventilation system have to make use, if possible, of the existing ventilation and exhaust smoke ducts ; for this use the ducts airtightness has to be measured [16]. In this section a measurement method of shunt ducts airtightness is described and tested on existing buildings.

4.1 Method

After sealing air outlets with bladders or sticky tape, a variable speed fan is connected at the top of the duct and makes it possible to depressurize the shunt duct. The negative pressure in the duct related to the atmospheric pressure is measured with an micromanometer, the air flow rate with a measuring pipe equipped with an orifice plate (see figure 7).

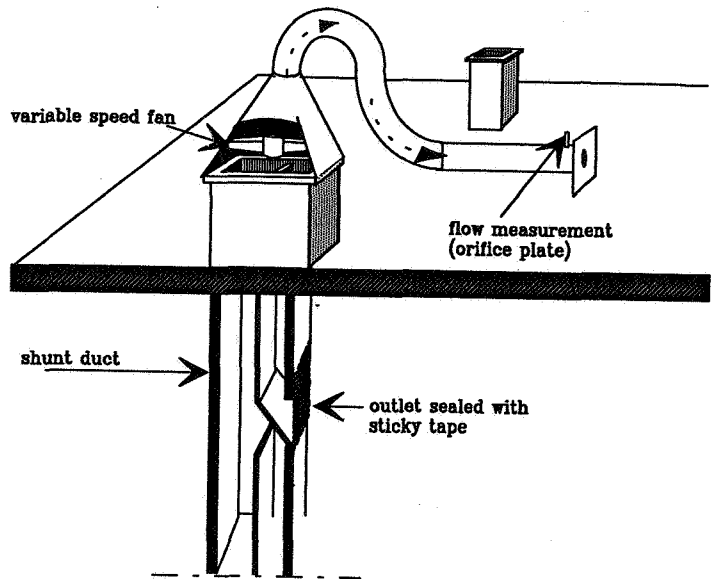


Figure 7 : sketch of shunt duct airtightness test

The equation describing the air leakage in shunt ducts is given in section 2.1. Values of flow exponent n describe the air leakage characteristic of the duct :

- $n \sim 0.5$ holes or thick cracks
- $n \sim 0,66$ little cracks
- $n \sim 1$ duct porosity

The equivalent leakage area (ELA) is a measure of the total area of all cracks in the duct. The ELA value in cm^2 is approximately equal to the air flow rate (in m^3/h) for a pressure difference of 10 Pa.

Several pressure taps are within the duct and measuring the negative pressure all duct long can indicate the location of leakages.

4.2 - Results

Two measurements results given in tables 2 et 3 show how this method makes it possible to assess actual performance of the shunt ducts.

Table 2 shows the change in pressure into a shunt duct 17 m long when air flow rate varies. Pressure difference is measured at the top storey. The values of the flow coefficient K and the flow exponent n are derived from the fit for the air flow equation :

$$K = 2.2 \text{ m}^3/\text{h} \text{ at } 1 \text{ Pa}$$

$$n = 0.98$$

air flow rate (m^3/h)	18	105	270	390
pressure difference (Pa)	7	50	130	190

Table 2 : Airtightness measurements on a shunt duct for six storeys
length : 17 m cross-sectional area : 0.2 m x 0.2 m

These values indicate there is no important leaks, like hole, but only duct porosity. The equivalent leakage area is 21 cm^2 .

Table 3 shows the change in pressure into a eight-storeys duct according to the storey height for an extract flow rate of $1230 \text{ m}^3/\text{h}$. At the sixth floor the pressure difference rises suddenly that indicates an important crack in the shunt duct.

floor	1	2	3	4	5	6	7	8
pressure difference (Pa)	16	22	25	28	30	43	84	115

Table 3 : Airtightness measurement along a eight-storeys duct

5 - CONCLUSION

Tools well suited for on-site measurements have been developed and used to assess the actual performance of ventilation systems in regard to indoor air quality and energy efficiency.

Airtightness measurement carried out on nearly two hundred dwellings using the fan depressurization technique demonstrated the air leakage of envelope was important. The average air change rate at a pressure difference of 1 Pa is about 0.15 ach for a flat and 0.35 ach for a single-family dwelling. The air leakage depends on the type of construction and the quality of workmanship.

The method used is very time consuming ; consequently new simpler methods have been developed. To depressurize the dwelling these simplified techniques utilize either the mechanical ventilation of the building or a light equipment. Comparison tests have shown the simplified and traditional methods yielded the same result within 10 %.

A test equipment was produced to quantify the air leakage and pressure drop in the supple ducts of the mechanical ventilation system. measurement carried out on twenty newly-built single-family dwellings revealed that in most cases leakage was insignificant and pressure loss not to high.

Another technique has been developed for the assessment of the airtightness of shunt duct in tests were usefully performed according to this technique in order to know the actual conditions of the shunt ducts before planning retrofit for existing buildings.

REFERENCES

- [1] ELMROTH, A. and LEVIN, P.
"Air infiltration control in housing : a guide to international practice"
IEA, Air Infiltration Centre, Swedish Council for Building
Research, Stockholm, 1983.
- [2] CHARLESWORTH, P.S.
"Air exchange rate and airtightness measurement techniques -
An applications guide"
IEA, Air Infiltration and Ventilation Centre, August 1988.
- [3] "Air flow rate and airtightness measurement techniques. An application
guide. Part II : Air leakage measurements methods" IEA-ECB Annex 20 :
Air flow patterns in Buildings BBRI.
(Edited by P. Wouters and L. Vandaele), June 1990.
- [4] ETHERIDGE, D.W.
"Crack flow equations and scale effect"
Building and Environment, Vol.12, 1977.

floor	1	2	3	4	5	6	7	8
pressure difference (Pa)	16	22	25	28	30	43	84	115

Table 3 : Airtightness measurement along a eight-storeys duct

5 - CONCLUSION

Tools well suited for on-site measurements have been developed and used to assess the actual performance of ventilation systems in regard to indoor air quality and energy efficiency.

Airtightness measurement carried out on nearly two hundred dwellings using the fan depressurization technique demonstrated the air leakage of envelope was important. The average air change rate at a pressure difference of 1 Pa is about 0.15 ach for a flat and 0.35 ach for a single-family dwelling. The air leakage depends on the type of construction and the quality of workmanship.

The method used is very time consuming ; consequently new simpler methods have been developed. To depressurize the dwelling these simplified techniques utilize either the mechanical ventilation of the building or a light equipment. Comparison tests have shown the simplified and traditional methods yielded the same result within 10 %.

A test equipment was produced to quantify the air leakage and pressure drop in the supple ducts of the mechanical ventilation system. measurement carried out on twenty newly-built single-family dwellings revealed that in most cases leakage was insignificant and pressure loss not to high.

Another technique has been developed for the assessment of the airtightness of shunt duct in tests were usefully performed according to this technique in order to know the actual conditions of the shunt ducts before planning retrofit for existing buildings.

REFERENCES

- [1] ELMROTH, A. and LEVIN, P.
"Air infiltration control in housing : a guide to international practice"
IEA, Air Infiltration Centre, Swedish Council for Building
Research, Stockholm, 1983.
- [2] CHARLESWORTH, P.S.
"Air exchange rate and airtightness measurement techniques -
An applications guide"
IEA, Air Infiltration and Ventilation Centre, August 1988.
- [3] "Air flow rate and airtightness measurement techniques. An application
guide. Part II : Air leakage measurements methods" IEA-ECB Annex 20 :
Air flow patterns in Buildings BBRI.
(Edited by P. Wouters and L. Vandaele), June 1990.
- [4] ETHERIDGE, D.W.
"Crack flow equations and scale effect"
Building and Environment, Vol.12, 1977.

- [5] WARD, I.C. and SHARPLES, S.
"An investigation of the infiltration characteristic of windows and doors in a tall building using pressurisation techniques"
BS68, University of Sheffield, August 1982.
- [6] MOYE, C.
"La perméabilité à l'air des bâtiments d'habitation"
Cahiers du CSTB n°2019, livraison 262, September 1985.
- [7] STEPHEN, R.K. and WEBB, B.C.
"Building Research Establishment recommended standard procedure : determining the airtightness of buildings by the fan pressurization method"
BRE, January 1985.
- [8] ROULET, C.A.
"Etanchéité à l'air"
Groupe de recherche en énergie solaire, Ecole Polytechnique Fédérale de Lausanne, Février 1985.
- [9] WOUTERS, P.
"La ventilation et l'infiltration dans les bâtiments : la situation en Belgique"
CSTC, revue n°314, Juillet-Décembre 1986.
- [10] COLTHORPE, K.
"A review of building airtightness and ventilation standards"
IEA, Air Infiltration and Ventilation Centre, technical note AIVC 30, September 1990.
- [11] RIBERON, J.
"Guide méthodologique pour la mesure de la perméabilité à l'air des enveloppes de bâtiments"
Cahiers du CSTB n° 2493, livraison 319, Mai 1991.
- [12] RIBERON, J. BIENFAIT, D. and CHANDELLIER, J.
"Perméabilité à l'air des bâtiments"
Séminaire ventilation et renouvellement d'air, AFME, INSA de Lyon, Villeurbanne, 21-22 Mars 1991, pp. 37-48.
- [13] RIBERON, J. and SIMEON, R.
"Dispositif de mesure simplifiée de la perméabilité à l'air des logements"
CSTB-GEC/DAC-91.105R, Champs-sur-Marne, Octobre 1991.
- [14] RAILIO, J. and SAARNIO, P.
"Air infiltration problems in ventilation systems"
Proceedings of CIB W67, Third international symposium on Energy Conservation in the Built Environment, Vol VI, Dublin 1982, pp. 6.A.31 - 6.A.41.

- [15] RIBERON, J. and VILLENAVE, J.G.
"Comportement en oeuvre des systèmes de ventilation en maison individuelle"
Séminaire ventilation et renouvellement d'air, AFME,
INSA de Lyon, Villeurbanne, 21-22 mars 1991, pp. 17 - 28.
- [16] VILLENAVE, J.G.
"Influence de la réhabilitation des façades sur la ventilation"
CSTB-GEC/DAC-91.67R, Champs-sur-Marne, Septembre 1991.

**Ventilation for Energy Efficiency and Optimum
Indoor Air Quality
13th AIVC Conference, Nice, France
15-18 September 1992**

Paper 18

**Indoor Ozone Concentrations: Ventilation Rate
Impacts and Mechanisms of Outdoor
Concentration Attenuation.**

J.A. Cano-Ruiz^{*}, M.P. Modera^{}, W.W. Nazaroff^{*}**

*** Dept of Civil Engineering, University of California
at Berkeley, Berkeley, CA 94720, USA**

**** Energy and Environment Division, Lawrence
Berkeley Laboratory, Berkeley, CA 94720, USA**

INDOOR OZONE CONCENTRATIONS: VENTILATION RATE IMPACTS AND MECHANISMS OF OUTDOOR CONCENTRATION ATTENUATION

J. Alejandro Cano-Ruiz*[†], Mark P. Modera* and William W. Nazaroff*[†]

* Energy and Environment Division, Lawrence Berkeley Laboratory, Berkeley, CA 94720

[†] Department of Civil Engineering, University of California at Berkeley, Berkeley, CA 94720

The classification of outdoor (ambient) air as fresh for the purposes of ventilation is not always appropriate, particularly in urban areas. In many cities of the world, urban air frequently violates health-based air quality standards due to high ozone concentrations. The degree of protection from exposure to ozone offered by the indoor environment depends on the relationship between indoor and outdoor ozone levels. Existing concentration data indicates that indoor/outdoor ozone ratios range between 10 and 80%. This paper analyzes several of the key issues influencing indoor ozone concentrations, including: 1) the degree of penetration of outdoor ozone indoors, 2) removal within the indoor environment (removal at surfaces and within air distribution systems), and 3) the correlation in time between outdoor ozone levels and ventilation rates. A model for calculating the degree of ozone removal in typical building leaks and air distribution systems is described and applied to a range of typical cases. This model indicates that the degree of removal is minimal for most wooden building cracks, but could be significant in leaks in concrete or brick structures, and is strongly dependent on the lining material for air distribution systems. Indoor ozone exposure estimates based on hourly outdoor ozone monitoring data and hour-by-hour weather-based simulations of infiltration rates and building operation are reported for a few residential scenarios. These estimates serve as a basis for exploring the impact of energy-efficient ventilation strategies on indoor ozone exposures.

Symbols

A	Cross sectional area (m ²)
$\sum A_j$	Total indoor surface area (m ²)
C	pollutant concentration (moles m ⁻³ , or parts per billion by volume)
d	parallel plate separation distance (m)
\mathcal{D}	pollutant molecular diffusion coefficient (0.182 x 10 ⁻⁴ m ² s ⁻¹ for O ₃)
D_h	hydraulic diameter [4A/P (2d for parallel plates)] (m)
f	friction factor (-)
f	reaction probability (-)
h	heat transfer coefficient (W m ⁻² K ⁻¹)
J	pollutant flux (moles m ⁻² s ⁻¹)
K_m	minor head loss coefficient (-)
k_g	thermal conductivity of fluid (W m ⁻¹ K ⁻¹)
L	length of parallel plates or ducts in the flow direction (m)
Nu	Nusselt number [hD_h/k_g] (-)
n	flow exponent in infiltration power law [$u_m \propto (\Delta p)^n$] (-)
Δp	Pressure difference (Pa)
P	leak or duct perimeter (m)
Pr	Prandtl number [ν/α] (-)
q	volumetric flow rate (m ³ s ⁻¹)
R	pollutant loss rate (moles s ⁻¹)
Re	Reynolds number [$u_m D_h/\nu$] (-)
s	pollutant generation rate (moles s ⁻¹)

Sc	Schmidt number $[v/D]$ (-)
Sh	Sherwood number $[(J/C)D_h/D]$ (-)
u	fluid velocity in the flow direction ($m\ s^{-1}$)
V	volume (m^3)
v	fluid velocity ($m\ s^{-1}$)
$\langle v \rangle$	Boltzmann velocity of pollutant ($362.5\ m\ s^{-1}$ for O_3 molecules at 298 K)
v_d	pollutant deposition velocity ($m\ s^{-1}$)
x	coordinate in the flow direction (m)
y	coordinate in the direction normal to the wall (m)
α	thermal diffusivity of fluid ($0.21 \times 10^{-4}\ m^2\ s^{-1}$ for air at room temperature)
η	pollutant removal efficiency $[(C_{entrance} - C_{exit})/C_{entrance}]$ (-)
μ	dynamic viscosity of fluid ($1.8 \times 10^{-5}\ kg\ m^{-1}\ s^{-1}$ for air at room temperature)
ν	kinematic viscosity of fluid ($0.15 \times 10^{-4}\ m^2\ s^{-1}$ for air at room temperature)
ρ	density of fluid ($1.2\ kg\ m^{-3}$ for air at room temperature)

Subscripts

a	air handling system
app	apparent
c	combined
i	indoors
L	laminar
M	transport limited
m	mean value
o	outdoors
T	turbulent
S	surface-uptake limited
w	wall or fluid at the wall
x	local value

1. INTRODUCTION

Although outdoor (ambient) air is generally considered fresh for the purposes of ventilation, this classification is not always appropriate, particularly in urban areas. Ozone (O_3) is frequently the pollutant responsible for the violation of health-based air quality standards in many cities around the world. For example, in 1988 ozone levels in more than 100 cities in the United States exceeded the federal standard (hourly averaged concentrations not to exceed 120 parts per billion by volume more than once a year, U.S. Environmental Protection Agency, 1989). The air basin in which Los Angeles is located exceeded the 120 ppb level on 196 days of 1989 (California Air Resources Board, 1991). In Mexico City, hourly-averaged ambient ozone concentrations typically exceed 110 ppb on more than 250 days of the year (Bravo *et al.*, 1991), and concentrations twice as high are common. Since ozone is a powerful oxidant, exposure to elevated levels in urban air presents a serious public health problem. Short-term health effects associated with exposure to concentrations in the range 80-200 ppb include irritation to the airways and decrease of respiratory function, while long-term exposure can result in accelerating the aging of the lung (Lippman, 1989).

The prevailing policy for dealing with severe smog episodes is to advise people to decrease their physical activity (to reduce respiration) and remain indoors, since indoor ozone concentrations are lower than those outside. However, indoor/outdoor concentration ratios vary over a wide range, and can be as high as 80% (Weschler *et al.*, 1989). Evidently, the degree of protection afforded by the indoor environment against exposure to ozone depends on the actual

concentrations indoors. The goal of this paper is to examine some of the key issues surrounding the attenuation of ozone from outdoor air to indoor spaces, emphasizing the penetration of outdoor ozone into the living or working environment. Specific aspects of this problem addressed here include: 1) the degree to which ozone is removed in building leaks, 2) removal in ducts and unoccupied spaces through which air is flowing (e.g. the crawlspace in a house), and 3) the coincidence between the times of high outdoor ozone concentrations and high air entry rates into buildings.

2. BACKGROUND

Ozone in the indoor environment has been studied for about 20 years. Mueller *et al.* (1973) investigated the rate of decay of ozone in an office, a bedroom and several tests rooms, and showed that this pollutant decomposes rapidly after it enters living spaces, following first-order decay. Sabersky *et al.* (1973) studied ozone decay in homes and used a test chamber to evaluate the rate of ozone decomposition on several common materials. Further data were obtained by Allen *et al.* (1978) and Selway *et al.* (1980) for the decay of ozone in offices in their study of the emissions from photocopying machines. Thompson *et al.* (1973) conducted measurements of indoor ozone in several types of buildings and compared them to outdoor levels. Shair and Heitner (1974) developed a general single-chamber indoor air quality model that included the effects of ventilation, filtration, and heterogeneous surface losses, and applied it successfully to the prediction of indoor ozone levels in office rooms supplied by a mechanical ventilation system. Based on this model, Shair (1981) designed and operated an activated carbon filter to keep indoor levels below 80 ppb in an office/laboratory building in Pasadena, CA. Researchers at the California Institute of Technology (Shaver *et al.*, 1983; Druzik *et al.*, 1990, Cass *et al.*, 1991) studied indoor ozone concentrations in museums in relation to the deterioration of works of art. Nazaroff and Cass (1986) expanded the model of Shair and Heitner to an arbitrary number of chambers and included explicitly the effect of gas-phase chemical reactions, obtaining good agreement between their model results and measurements in an art gallery in Southern California. Weschler *et al.* (1989) conducted continuous measurements of indoor and outdoor ozone concentrations for a period of 5 months in an office complex in New Jersey, and compiled ozone indoor/outdoor data from the literature. Hayes (1991) used a single-chamber air quality model similar to that of Shair and Heitner to estimate peak concentration indoor/outdoor ratios in various home, office and vehicle microenvironments, and to analyze the sensitivity of these ratios to various parameters.

The mass balance of ozone in a building with a simple mechanical ventilation system can be represented by a model such as the one shown in Fig. 1 (Druzik *et al.*, 1990). The indoor ozone concentration would be governed by the differential equation:

$$V \frac{dC_i}{dt} = (1-\eta_{oa})q_{oa}C_o + q_{oi}C_o - \eta_{ia}q_{ia}C_i - q_{io}C_i + s - R \quad (i)$$

Inherent in this model are the following assumptions: 1) Indoor air can be considered well mixed, 2) ozone is unaffected by its passing through the building envelope into the building, 3) the only components in the ventilation system where O₃ may be destroyed are the filters, 4) buildings can be modeled as single chambers for the purpose of predicting indoor ozone concentrations, and 5) air has constant density throughout the system (no contraction or expansion). Although not explicitly stated in the model, it is frequently assumed that the only indoor sink is the heterogeneous reaction of ozone with surfaces (modelled in terms of an average deposition velocity as $R = v_d(\sum A_j)C_i$), and that indoor ozone sources are nonexistent, except for the case when there are photocopying machines or electrostatic precipitators in operation. This paper focuses on the validity of assumptions 2, 3 and 4. Nazaroff and Cass (1986) found that the treatment of a building as a single chamber is adequate, for the case of a building having high recirculation rates through the mechanical ventilation system, but the question of whether the modeling of a residence as a single chamber is adequate has not been addressed.

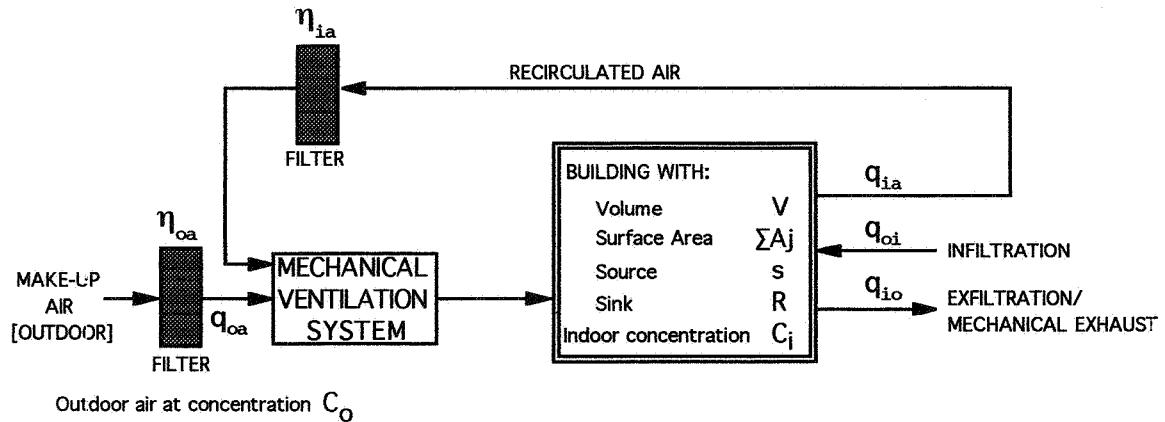


Fig. 1: Representation of a building for modeling indoor ozone concentrations

3. ANALYSIS

The penetration of outdoor ozone indoors depends on the product of three factors: 1) outdoor concentration levels, 2) the rate of infiltration of outdoor air and/or the rate of supply of make-up air by the ventilation system, and 3) the efficiency of removal of ozone in each path through which air flows. Until now researchers have assumed that ozone penetrates without loss along all air flow paths, except through activated carbon filters, which are very efficient in removing ozone (Shair, 1981); however, the question of removal in building leaks or ventilation system ducts merits closer examination. Another important question to be addressed is the relationship among weather, outdoor ozone concentrations, air flows and ventilation rates. Consideration is also given to the decay of ozone in unconditioned spaces that may serve as a significant source of the air infiltrating into the living areas. For example, if air infiltrating into a house passes through the basement or crawlspace first, then the ozone concentration of infiltration air would be that prevailing in the basement/crawlspace instead of the outdoor value.

3.1 MODEL FOR THE REMOVAL OF OZONE IN BUILDING LEAKS

We first address the issue of ozone entry through building leaks, since it is possible that scrubbing of ozone in the building envelope could at least partially account for some of the observed reduction of ozone concentration from outdoor to indoors, especially for cases in which the main mechanism for outdoor air entry is infiltration through cracks. We present results of a theoretical analysis of the potential for ozone scrubbing in typical residential building leaks based on the following simplifications: 1) a building leak can be modelled as a uniform-width gap between parallel plates, 2) flow in the leaks is laminar, but may not be fully developed, 3) the air velocity profile at the leak entrance is uniform, 4) air can be considered to have constant physical properties (ρ , μ) during passage, and 5) pollutant diffusion in the flow direction can be neglected.

The first step in solving this problem is the prediction of the flow rate in a leak based on its geometry and the pressure difference between the living space and outdoors. The solution presented here expands on the work of Baker *et al.* (1987) and Sherman (1990), by explicitly taking into account the effects of developing flow. The total pressure drop resulting from laminar flow between parallel plates is given by:

$$\Delta p = f_L \frac{L}{d} \frac{\rho u_m^2}{2} + (\sum K_m) \frac{\rho u_m^2}{2} \quad (2)$$

The first term accounts for losses due to shear stress at the walls and, in the case of developing flow, for the change in momentum required to accelerate the fluid from a flat velocity profile at the entrance to its exit profile. The second term accounts for pressure drops associated with flow contraction and expansion at the entrance and exit of the leak. The coefficients for minor losses (K_m) at sharp entrances and exits are 1.0 and 0.5, respectively. For fully developed laminar flow between parallel plates, the friction factor in Eq. (2) is the Fanning friction factor (defined as the ratio of wall shear stress to the flow kinetic energy per unit volume) and has the value $f_L = 24/Re$. In the case of developing flow, an apparent friction factor (f_{app}) may be defined so that Eq.(2) still holds. Shah (1978, p.168) gives the following formula for obtaining the value of f_{app} :

$$f_{app} Re = \frac{3.44}{(x^+)^{1/2}} + \frac{24 + 0.1685(x^+)^{-1} - 3.44(x^+)^{-1/2}}{1 + 0.000029(x^+)^{-2}} \quad (3)$$

$$\text{where } x^+ = \frac{\nu L}{4u_m d^2}$$

In order to use Shah's formula for computing the mean air flow velocity in the leak, Eq. (2) may be rewritten as:

$$\Delta p = \left(\frac{f_{app} Re}{2} \right) \frac{\mu L u_m}{d^2} + (\sum K_m) \frac{\rho u_m^2}{2} \quad (4)$$

Solving Eq. (4) for the mean velocity yields:

$$u_m = \left(\frac{f_{app} Re}{2} \right) \frac{\mu L}{(\sum K_m) \rho d^2} \left[\sqrt{1 + \frac{2\Delta p (\sum K_m) \rho d^4}{\left(\frac{f_{app} Re}{2} \right)^2 \mu^2 L^2}} - 1 \right] \quad (5)$$

The mean velocity can then be obtained as a function of the applied pressure and the geometry of the leak, by first assuming $(f_{app} Re) = 24$ and then iterating on Eqs. (5) and (3) until convergence is achieved. It should be noted that u_m depends on L and d in the ratio d^2/L , so that the leak geometry dependence can be captured by plotting the flow variables of interest against this ratio.

It is useful to relate the above results to observed flow exponents from leakage measurements in residences, for which leakage data are normally fit to a power-law relationship between flow and pressure. The relationship is depicted in Fig. 2, which was obtained by computing mean velocities for the range of pressure differentials observed between indoors and outdoors (0 to 10 Pa), and fitting the power-law model to the velocity-pressure data for different d^2/L ratios. The flow exponents measured in the field are typically between 0.55 and 0.75 (Sherman *et al.*, 1984), suggesting that leaks representative of the bulk of the leakage area in a residence should have d^2/L ratios in the range 10^{-4} to 10^{-3} m.

The second step in understanding ozone removal in building-envelope leaks is to examine pollutant transport from air to the leak walls. Under our model assumptions, and at steady state, the advection-diffusion equation describing ozone conservation in air assumes the form:

$$\mathbf{v} \cdot \nabla C = D \frac{\partial^2 C}{\partial x^2} \quad (6)$$

The solution to this equation under developing flow conditions is not trivial. However, the problem has been solved numerically for several sets of boundary conditions in the heat transfer literature (e.g. Hwang and Fan, 1964; Siegel and Sparrow, 1959). As discussed by Nazaroff and Cass (1989), the governing equations for the distribution of temperature and the distribution of concentration of dilute, reactive gaseous pollutants in a forced convection flow are of analogous

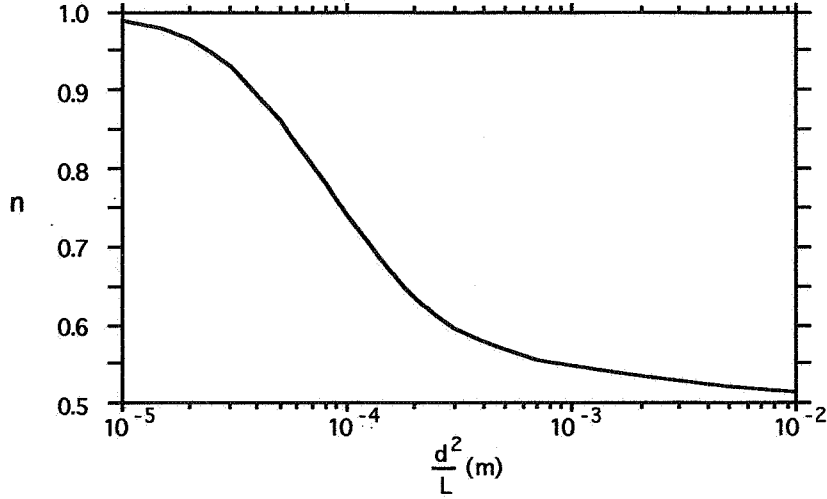


Fig. 2: Flow exponent as a function of parallel plate geometry

form. In order to use the heat transfer results (usually given as Nusselt numbers), we need to relate the boundary conditions for ozone uptake at the wall to the analogous wall boundary conditions in heat transfer. Two possibilities are considered here for the outcome of the interaction of ozone with the leak walls: either ozone is perfectly removed at the walls, or only a fraction f of the collisions between ozone molecules and the walls result in removal. The first case is analogous to the heat transfer boundary condition of constant wall temperature (the concentration at the surface is constant and equal to 0). The second case corresponds to the boundary condition of finite resistance to heat transfer through the wall. At steady state, the flux of ozone towards the wall must be equal to the rate at which ozone is removed by a unit area of wall surface. This rate is given by the rate of collisions of ozone molecules with the wall per unit area, as predicted by the molecular theory of gases, multiplied by the reaction probability f :

$$-D \frac{\partial C_w}{\partial y} = f \frac{\langle v \rangle}{4} C_w \quad (7)$$

The boundary condition in Eq. (7) may be cast in dimensionless form to yield a wall Sherwood number analogous to the heat transfer wall Nusselt number:

$$Sh_w = f \frac{\langle v \rangle 2d}{4D} \quad (8)$$

At steady state, the equation describing pollutant concentration in a leak of arbitrary cross-section with uptake at the walls is:

$$\frac{dC_{m,x}}{dx} = - \frac{J_x P}{u_m A} \quad (9)$$

where $C_{m,x}$ is the flow-averaged pollutant concentration at a distance x from the leak entrance. Expressing Eq. (9) in terms of a local Sherwood number and the hydraulic diameter, we obtain after rearranging:

$$\frac{dC_{m,x}}{C_{m,x}} = -4 \frac{Sh_x D dx}{u_m D_h^2} \quad (10)$$

Integrating Eq. (10) from the entrance ($x=0$) to the exit ($x=L$) of the leak yields:

$$\frac{C_{m,x=L}}{C_{m,x=0}} = \exp\left(-\frac{4D}{u_m D_h^2} \int_{x=0}^L Sh_x dx\right) \quad (11)$$

so that the removal efficiency of the leaks can be expressed as a function of mean Sherwood number and a dimensionless leak length:

$$\eta = 1 - \exp(-4 \text{Sh}_m L^*) \quad (12)$$

$$\text{Sh}_m = \frac{1}{L} \int_{x=0}^L \text{Sh}_x dx \quad (13)$$

$$L^* = \frac{L/D_h}{\text{ReSc}} = \frac{\mathcal{D}L}{4u_m d^2} \quad (14)$$

Shah (1978, p. 190) gives an approximate formula obtained by Stephan (1959) for the values of Nu_m for the case of constant wall temperature. Substituting the Schmidt number for the Prandtl number, the formula becomes:

$$\text{Sh}_{m,M} = 7.55 + \frac{0.024(L^*)^{-1.14}}{1 + 0.0358(L^*)^{-0.64} \text{Sc}^{0.17}} \quad (15)$$

Using appropriate values of L and d , one can obtain ozone removal efficiency values for parallel plate leaks as a function of the leak flow exponent and the pressure difference between the spaces connected by the leak. These values are shown in Fig. 3, and imply that if every collision of ozone molecules with the wall resulted in removal, scrubbing of ozone in typical building leaks ($n=0.66 \pm 0.09$, Sherman *et al.*, 1984) would be significant. However, ozone has been shown not to be removed at the mass-transport limited rate in many settings (e.g. Cox and Penkett, 1972). For the case of finite wall resistance to ozone uptake, the solution to the penetration problem can be given in terms of a combined Sherwood number, analogous to the overall Nusselt number in heat transfer for the case of finite wall thermal resistance:

$$\eta = 1 - \exp(-4 \text{Sh}_{c,m} L^*) \quad (16)$$

$$\frac{1}{\text{Sh}_{c,m}} = \frac{1}{\text{Sh}_{m,S}} + \frac{1}{\text{Sh}_w} \quad (17)$$

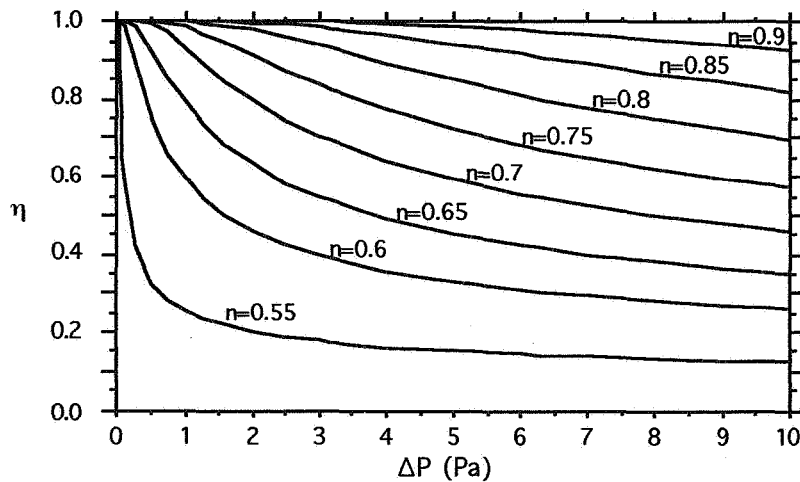


Fig. 3: Ozone removal in parallel-plate leaks for the case of perfect removal at the walls ($f = 1.0$), as a function of applied pressure and flow exponent.

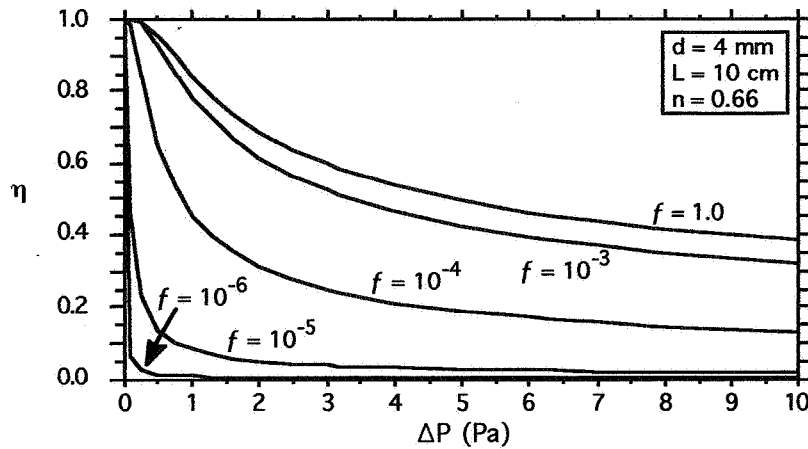


Fig. 4: Ozone removal efficiency of a typical parallel plate leak ($n = 0.66$) as a function of applied pressure and ozone-wall reaction probabilities.

Since no approximate formulas are available that allow an easy determination of $Sh_{m,S}$ (the mean fluid Sherwood number for limited surface-uptake) as a function of L^* , Sc and Sh_w , we will use the values of $Sh_{m,M}$ (the zero wall resistance Sherwood number) instead as a first approximation for the purpose of computing η . This approximation is based on the fact that the analogous Nu for finite wall heat transfer resistance approaches the constant wall temperature Nu asymptotically for small values of $1/Nu_w$; for large values of $1/Sh_w$ (f small), $Sh_{c,m}$ is approximately equal to Sh_w .

Figures 4 and 5 are plots of ozone penetration values in two different parallel plate leaks as a function of pressure difference and reaction probability. Crack dimensions were chosen to yield flow exponents characteristic of a typical ($n=0.66$) and a very tight leak ($n=0.9$). These figures show that if the reaction probability of ozone with wall materials is below 10^{-6} , ozone removal would be minimal even in tight leaks. Table 1 lists f values for various materials calculated on the basis of experimental data for the decay of ozone in test chambers and the penetration of ozone in tubes (Cano-Ruiz *et al.*, 1992). Based on our model and these data, we conclude that ozone removal would be minimal in wooden cracks ($f < 10^{-6}$), and that there is a potential for significant scrubbing of outdoor ozone in leaks present in concrete or brick structures, for which f could be as large as 10^{-4} .

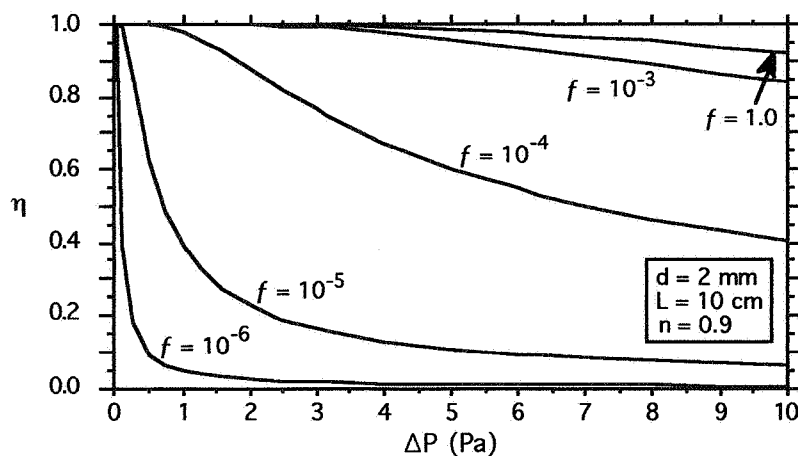


Fig. 5: Ozone penetration in a tight parallel plate leak ($n = 0.9$) as a function of applied pressure and ozone-wall reaction probabilities.

Table 1: Reaction probability of the collision of ozone molecules with various materials (calculated by Cano-Ruiz *et al.*, 1992)

Material	f	Data used to obtain f
Teflon	$7 \cdot 10^{-9}$	Altshuller <i>et al.</i> (1961)
"	$5 \cdot 10^{-7}$	Simmons and Colbeck (1990)
Glass	10^{-9} to $5 \cdot 10^{-7}$	Altshuller <i>et al.</i> (1961)
"	$6 \cdot 10^{-8}$ to 10^{-7}	Sabersky <i>et al.</i> (1973)
"	$3 \cdot 10^{-6}$ to $5 \cdot 10^{-6}$	Simmons and Colbeck (1990)
Aluminum	$6 \cdot 10^{-8}$ to $5 \cdot 10^{-7}$	Altshuller <i>et al.</i> (1961)
"	$6 \cdot 10^{-8}$ to 10^{-7}	Sabersky <i>et al.</i> (1973)
Stainless steel	$5 \cdot 10^{-8}$ to $4 \cdot 10^{-6}$	Altshuller <i>et al.</i> (1961)
Polyethylene	$2 \cdot 10^{-7}$ to 10^{-6}	Altshuller <i>et al.</i> (1961)
"	10^{-6} to $3 \cdot 10^{-6}$	Sabersky <i>et al.</i> (1973)
PVC	$6 \cdot 10^{-7}$ to $4 \cdot 10^{-6}$	Altshuller <i>et al.</i> (1961)
Plywood	$6 \cdot 10^{-7}$ to $4 \cdot 10^{-6}$	Sabersky <i>et al.</i> (1973)
Neoprene	$2 \cdot 10^{-6}$ to $9 \cdot 10^{-5}$	Sabersky <i>et al.</i> (1973)
Concrete	$4 \cdot 10^{-5}$ to 10^{-4}	Simmons and Colbeck (1990)
Bricks	$2 \cdot 10^{-4}$ to $4 \cdot 10^{-4}$	Simmons and Colbeck (1990)

3.2 EXTENSION OF THE MODEL TO ANALYZE REMOVAL IN DUCTS

The model for pollutant removal in leaks may be extended to analyze the removal of ozone in ventilation system ducts. The main difference between the two cases is that flow in ventilation ducts is turbulent. A large number of semiempirical relationships for computing the Nusselt number can be found in the heat transfer literature, and have been compiled by Bhatti and Shah (1987). For the case of fully developed turbulent flow in smooth ducts they recommend using the formula:

$$Nu_m = \frac{(f_T/2)(Re - 1000)Pr}{1 + 12.7(f_T/2)^{1/2}(Pr^{2/3}-1)} \quad 2300 \leq Re \leq 5 \cdot 10^6; 0.5 \leq Pr \leq 2000 \quad (18)$$

$$\text{where } f_T = 0.00128 + 0.1143Re^{-0.311}$$

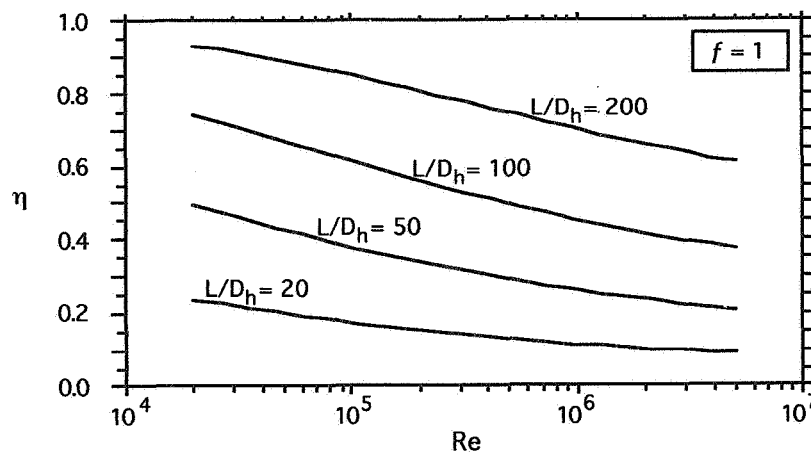


Fig. 6: Ozone removal in ducts with walls acting as perfect sinks, as a function of Reynolds number and duct geometry.

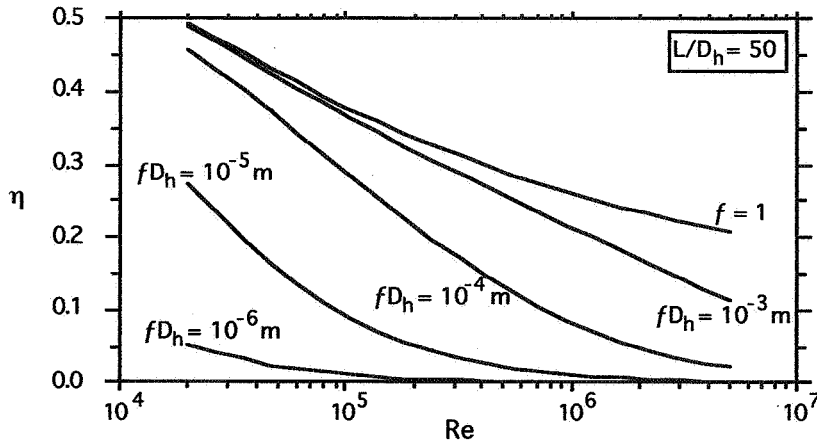


Fig. 7: Effect of ozone-wall reaction probabilities on ozone removal in ducts.

Substituting the ozone Schmidt number (0.82) for the Prandtl number in Eq. (18), the Nusselt numbers obtained can be used as Sh_m in Eq. (12) and $Sh_{m,S}$ in Eq. (17), since the Nusselt numbers for both of the analogous heat transfer boundary conditions are the same when the flow is turbulent. Ozone removal efficiency of ducts as a function of Reynolds number and duct geometry are shown in Fig. 6 for the case of perfect removal at the walls. This shows that in a typical residential ventilation system supply duct ($D_h = 16$ cm, $L = 8$ m, $f_{xi} = 180$ m³/hr), about 50% of the ozone entering the duct would be removed if the walls acted as perfect sinks. However, actual ozone removal is dependent on the reaction probability of the lining material, as is illustrated by Fig. 7. For the duct parameters given in the example, ozone removal would decrease to about 30% for $f = 6 \cdot 10^{-5}$, and would be negligible with a reaction probability of 10^{-7} . Common materials used in the manufacture and lining of ducts include sheet metal (galvanized steel), fiber glass, aluminum, maylar and neoprene, with f values from Table 1 ranging from $6 \cdot 10^{-8}$ to $9 \cdot 10^{-5}$ for some of these materials. These data and our analysis indicate that ozone scrubbing in distribution systems is strongly dependent on the lining material of the ducts, and that it could be significant, especially in the case of commercial buildings, where L/D_h ratios are larger than in residences.

3.3 SIMULATION RUNS

In this section we give the results of a few indoor ozone simulation runs designed to explore the relationship among weather, air conditioning strategies (and the resulting ventilation rates), and indoor exposures to ozone. This effort was motivated by the interest in the impact of energy-conserving measures on indoor air quality. The pollutant transport module of the COMIS airflow network code (Feustel and Raynor-Hoosen, 1990) was modified and used to obtain hour-by-hour indoor ozone concentrations for a period of one year in each run. Inputs to this model included: 1) hourly ambient ozone data for 1989 monitored by the California Air Resources Board, and 2) hourly air flow rates based on heating/cooling loads and on weather data from the CTZ weather tapes, which contain one year of hour-by-hour data for each of the 16 climate zones in California; assembled by the California Energy Commission.

We ran simulations of indoor ozone concentrations in a one-story ranch house with an attic, a crawlspace and a garage. This prototype house has an area of 144 m², and is equipped with a central furnace/air conditioning unit (located in the garage), ten supply ducts and one return duct. Flows among the house, crawlspace, attic, garage, and outdoors were obtained by using the DOE-2 thermal simulation code (Birdsall *et al.*, 1990) in conjunction with the COMIS multizone infiltration model and a the duct-performance simulation model DUCTSIM. A flow chart of the

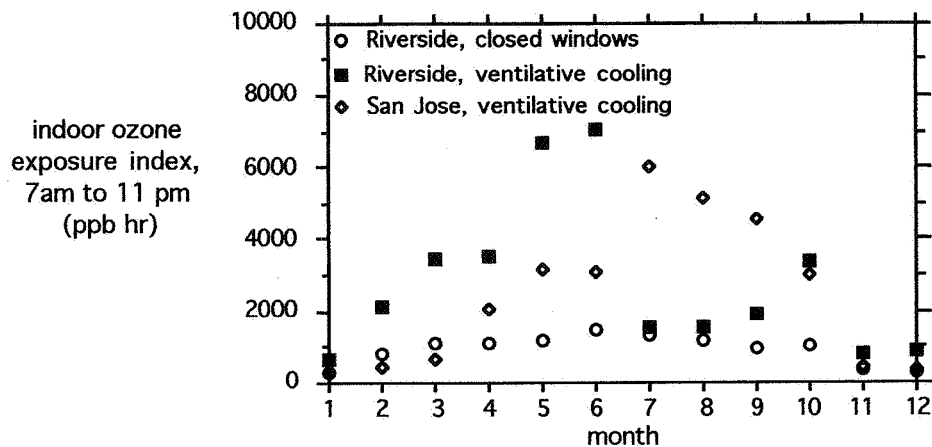


Fig. 8: Predicted monthly indoor ozone exposures for prototype residence in Riverside and San Jose.

use of these three codes and a full description of the house are presented elsewhere (Modera and Jansky, 1992). We present selected results from three simulation runs, corresponding to: 1) a house located in Riverside, CA with windows closed throughout the year, 2) the house in Riverside with windows open to provide natural ventilation cooling whenever the enthalpy of outdoor air is lower than that indoors, and 3) the same house located in San Jose, CA using natural ventilation cooling. The ozone deposition velocity in the house and the unconditioned zones (attic, garage, crawlspace) was assumed to be equal to 0.06 cm/sec in all the simulations (based on the observations of Sabersky *et al.*, 1973), and ozone scrubbing in leaks and ducts was ignored in order to isolate the effects of ventilation.

Figure 8 shows the results from these three runs expressed in terms of a monthly exposure index, defined as the time integral of ozone concentrations (units: ppb hr) throughout each month. We call this measure an exposure index because the true exposure depends on the respiration rate of the exposed individuals. For comparison, the monthly exposure indices based on 1989 outdoor concentrations are shown in Fig. 9 for both Riverside and San Jose. Times between 11 pm and 7 am were not included in the calculations, since O₃ concentrations at those times are very low and people are expected to remain indoors with the windows closed. Examination of both figures reveals that:

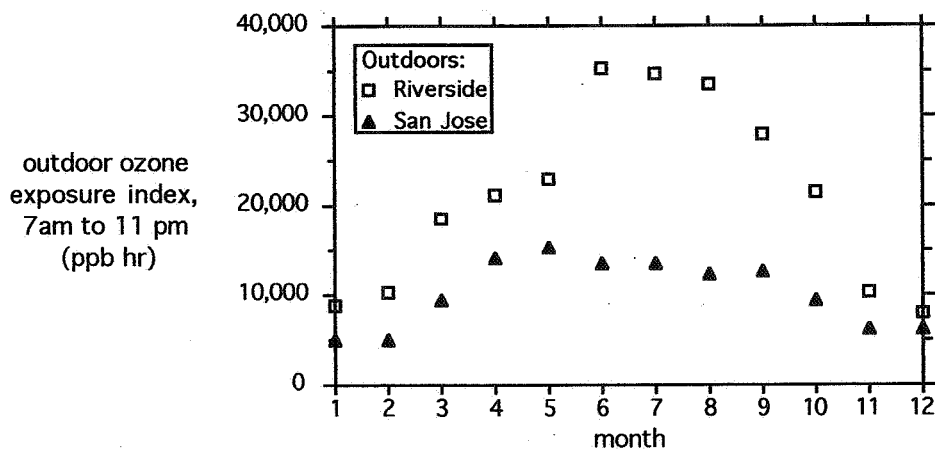


Fig. 9: Monthly outdoor exposure index from monitoring data (1989).

- a) Monthly indoor exposures can be almost 5 times higher if windows are opened than if air conditioning alone is used for cooling (compare both Riverside exposures for June),
- b) Even though the highest outdoor ozone concentrations in Riverside occur from June to September, indoor exposures in July, August and September are very low. This is because during these months outdoor air cannot be used to cool the house during the times of high outdoor ozone concentrations, and the windows are kept closed. As the weather in San Jose is cooler, window opening can be efficiently used there for cooling, and the monthly indoor ozone exposure index can be 2 to 4 times the Riverside value in July-September, even though outdoor ozone concentrations in San Jose are typically about 40% those in Riverside during this period.

With respect to acute exposures, the federal standard of 120 ppb ozone was exceeded outdoors in 1989 on 325 hours in Riverside, while no violations were reported for San Jose. The maximum outdoor ozone concentrations in that year were 290 ppb and 120 ppb, respectively. The maximum indoor ozone concentration predicted for the closed house in Riverside was 35 ppb, well below the health-based standard, but levels higher than 120 ppb occurred in the Riverside house during 7 hours when ventilative cooling was used, with a maximum predicted indoor concentration of 180 ppb.

4. DISCUSSION

Ozone scrubbing in leaks in wood-frame structures appears not to be significant, but could be important in reducing ozone entry into masonry buildings during periods when windows are closed. However, these are the periods when indoor ozone concentrations are likely to be low indoors as a result of low air exchange rates and the rapid decay of ozone on indoor surfaces. The importance of reducing these low concentrations depends upon the health impacts of long-term exposure to ozone at low concentrations, which is an unresolved issue in toxicology. On the other hand, removal of ozone in duct systems could have a significant effect on exposures in buildings with continuous operation systems, or systems with longer residence times (e.g. in commercial buildings). The amount of removal will depend on the lining material: for example, neoprene-lined ducts would be expected to have a more significant effect than sheet-metal ducts. Also related to air distribution systems is their impact on room air motion, which in turn affects the rate of ozone decay. One study (e.g. Sabersky *et al.*, 1973) showed a factor of three increase in the rate of ozone removal in a house when the internal circulation system was operating.

There are very few measurements in the literature of the rate of decay of ozone in residences. Mueller *et al.* (1973) measured decay rates in a bedroom and Sabersky *et al.* (1973) obtained decay rates in one house, but to our knowledge no further data has been gathered since then. There is no information about the decay rates in buffer zones (e.g. attic, basement, crawlspace), or about the effects of furniture, rugs, drapes, etc. on ozone decomposition. We ran a few sensitivity simulations in order to examine the effect of the buffer zones on indoor ozone concentrations. Assuming that no decay took place in these zones resulted in the doubling of average indoor concentrations during periods in which windows were kept closed, as compared to the assumption used in our simulations, that ozone had a deposition velocity in these zones equal to that of the conditioned space of the house. As in the case of removal in leaks, the impact of ozone decay in buffer zones with respect to overall indoor exposure is not likely to be high if ventilative cooling is used.

Our simulations indicate that the correlations in time among weather, cooling loads and outdoor ozone concentrations should be considered when designing alternative cooling strategies, so that energy conservation may be achieved without compromising indoor air quality.

It is important to note that indoor exposure to ozone in our simulations was dominated by the periods of high ventilation rates, that is, when the windows were open. This indicates that during smog episodes it is not enough to advise people to stay indoors, but to advise them to stay

indoors *with the windows closed*. Using an indoor/outdoor concentration ratio is not enough to estimate indoor exposures to ozone in residences, since indoor/outdoor ratios and outdoor concentrations exhibit large variations in time. Knowledge about the window opening behavior of people during periods of likely high outdoor ozone concentrations is probably more useful, in terms of estimating total indoor exposure to ozone, than the determination of isolated indoor/outdoor ratios.

5. CONCLUSIONS AND RECOMMENDATIONS FOR FURTHER WORK.

Based on our analysis we conclude that: 1) the use of ventilative cooling can have dramatic impacts on indoor ozone exposures, 2) temporal variations in venting and outdoor ozone concentrations must be taken into account when evaluating indoor exposures, 3) ozone scrubbing in building leaks and distribution systems depends principally on the reaction probability associated with the collision of ozone molecules with wall and lining materials, and 4) the removal of ozone in the unconditioned spaces of a house is significant on a relative basis during periods when ventilative cooling is not used.

The results of this theoretical analysis need to be confirmed by experiment. A critical variable in the prediction of ozone removal efficiencies in leaks and ducts is the reaction probability of ozone with the wall materials, but there are not enough data to allow reliable extraction of f values for most materials of interest. Another area where experiments can improve our understanding of indoor ozone concentrations is in the measurement of ozone decay rates in the different zones of a residence. As the venting behavior of the occupants of a residence is a critical determinant of indoor ozone exposures, the applicability of our assumptions in regard to window opening need to be examined more carefully. Finally, the challenge of modelling indoor ozone concentrations in residences and confirming hour-by-hour predictions with measurements still remains.

ACKNOWLEDGEMENTS

This work is part of a exploratory research project funded by the California Institute for Energy Efficiency (CIEE), a research unit of the University of California. Publication of research results does not imply CIEE endorsement of or agreement with these findings, nor that of any CIEE sponsor. We express our gratitude to Dwight Oda and Ron Rothacker of the California Air Resources Board for providing us with ozone monitoring data. The assistance of Richard Jansky on the execution of the air flow component of the simulations is greatly appreciated, as is the advice of Helmut Feustel on the pollutant transport module of COMIS.

REFERENCES

1. ALLEN, R.J., R.A. WADDEN, E.D. ROSS, "Characterization of potential indoor sources of ozone," *Am. Ind. Hyg. Assoc. J.* **39**: 466-471 (1978).
2. ALTSHULLER, A.P., A.F. WARTBURG, "The interaction of ozone with plastic and metallic materials in a dynamic flow system," *Int. J. Air and Water Poll.* **4**: 70-78 (1961).
3. BAKER, P.H., S. SHARPLES, I.C. WARD, "Air flow through cracks," *Building and Environment* **22**: 293-304 (1987).
4. BHATTI, M.S., R.K. SHAH, "Turbulent and transition flow convective heat transfer in ducts," in *Handbook of single-phase convective heat transfer*, S. Kakaç, R.K. Shah, W. Aung (eds.), John Wiley & Sons, New York, 1987.
5. BIRDSALL, B., W.F. BUHL, K.L. ELLINGTON, A.E. ERDEM, F.C. WINKELMANN, "Overview of the DOE-2 building energy analysis program, version 2.1D," Lawrence Berkeley Laboratory Report LBL-19735 Rev.1, Berkeley, CA, February 1990.
6. BRAVO, H., G. ROY-OCOTLA, R. SOSA AND R.TORRES, "Report of the historical trends (1986-1990) in the levels of ozone monitored at the suburban monitoring station of the University of Mexico at Mexico City," presented at the 84th annual meeting & exhibition of the Air & Waste Management Association in Vancouver, British Columbia, June 16-21, 1991.
7. CALIFORNIA AIR RESOURCES BOARD, "California air quality: A status report," Sacramento, CA (1991).
8. CANO-RUIZ, J.A., D. KONG, R. BALAS, W.W. NAZAROFF, "Removal of reactive gases at indoor surfaces: combining mass transport with surface kinetics," in preparation, (1992).
9. CASS, G.R., W.W. NAZAROFF, C. TILLER, P.M. WHITMORE, "Protection of works of art from damage due to atmospheric ozone", *Atmos. Environ. Part A* **25**: 441-451 (1991).
10. COX, R.A., S.A. PENKETT, "Effect of relative humidity in the disappearance of ozone and sulphur dioxide in contained systems," *Atmos. Environ.* **6**: 365-368 (1972).
11. DRUZIK, J.R., M.S. ADAMS, C. TILLER, G.R. CASS, "The measurement and model predictions of indoor ozone concentrations in art museums", *Atmos. Environ. Part A* **24**: 1813-1823 (1990).
12. FEUSTEL, H.E., A.R. RAYNOR-HOOSEN, "Fundamentals of the multizone air flow model COMIS," Air Infiltration and Ventilation Center technical note AIVC TN29, University of Warwick Science Park, Coventry, Great Britain.
13. HAYES, S.R., "Use of an indoor air quality model (IAQM) to estimate indoor ozone levels", *J. Air Waste Manage. Assoc.* **41**: 161-170 (1991).
14. HWANG, C.L., L.T. FAN, "Finite difference analysis of forced-convection heat transfer in entrance region of a flat rectangular duct," *Appl. Sci. Res., Sect. A* **13**: 401-422 (1964).
15. LIPPMAN, M., "Health effects of ozone, a critical review," *JAPCA* **39**: 672-695 (1989).
16. MODERA, M.P., R. JANSKY, "Residential air-distribution systems: interaction with the building envelope," submitted to ASHRAE-DOE-BTECC Conference on Thermal Performance of the Exterior Envelopes of Buildings V, December 7-10, 1992. Lawrence Berkeley Laboratory Report LBL-31311, Berkeley, CA (1992).
17. NAZAROFF, W.W., G.R. CASS, "Mathematical modeling of chemically reactive pollutants in indoor air", *Environ. Sci. Technol.* **20**: 924-933 (1986).
18. NAZAROFF, W.W., G.R. CASS, "Mass-transport aspects of pollutant removal at indoor surfaces," *Environment International* **15**: 567-584, (1989).
19. SABERSKY, R.H., D.A. SINEMA, F.H. SHAIR, "Concentrations, decay rates, and removal of ozone and their relation to establishing clean indoor air," *Environ. Sci. Technol.* **7**: 347-353 (1973).

20. SELWAY, M.D., R.J. ALLEN, R.A. WADDEN, "Ozone production from photocopying machines," *Am. Ind. Hyg. Assoc. J.* 41: 455-459 (1980).
21. SHAH, R.K., *Laminar flow forced convection in ducts: A source book for compact heat exchanger analytical data*, Academic Press, New York (1978).
22. SHAIR, F.H., K.L. HEITNER, "Theoretical model for relating indoor pollutant concentrations to those outside," *Environ. Sci. Tech.* 8: 444-451 (1974).
23. SHAIR, F.H., "Relating indoor pollutant concentrations of ozone and sulfur dioxide to those outside: economic reduction of indoor ozone through selective filtration of the make-up air," *ASHRAE Transactions* 87: Part 1 116-139 (1981).
24. SHAVER, C.L., G.R. CASS, "Ozone and the deterioration of works of art," *Environ. Sci. Technol.* 17: 748-752 (1983).
25. SHERMAN, M.H., D.J. WILSON, D.E. KIEL, "Variability in residential air leakage," presented at ASTM Symposium on Measured Air Leakage Performance of Buildings, Philadelphia, PA, April 2-3, 1984. Lawrence Berkeley Laboratory Report LBL-17587, Berkeley, CA (1984)
26. SHERMAN, M.H., "A power-law formulation of laminar flow in short-pipes," Lawrence Berkeley Laboratory Report LBL-29414, Berkeley, CA (1990).
27. SIEGEL, R., E.M. SPARROW, "Simultaneous development of velocity and temperature distributions in a flat duct with uniform wall heating," *AIChE J.* 5: 73-75 (1959).
28. SIMMONS, A., I. COLBECK, "Resistance of various building materials to ozone deposition," *Environ. Technol.* 11: 973-978 (1990).
29. STEPHAN, K., "Wärmeübergang und druckabfall bei nicht ausgebildeter Laminarströmung in Rohren und in ebenen Spalten," *Chem.-Ing.-Tech.* 31: 773-778 (1959).
30. THOMPSON, C.R., E.G. HENSEL, G. KATS, "Outdoor-indoor levels of six air pollutants," *JAPCA* 23: 881-886 (1973).
31. U.S. ENVIRONMENTAL PROTECTION AGENCY, "A preliminary comparison of 1988 ozone concentrations to 1983 and 1987 ozone concentrations," U.S. EPA, Research Triangle Park, NC, February 17, 1989.
32. WESCHLER, C.J., H.C. SHIELDS, D.V. NAIK, "Indoor ozone exposures," *JAPCA* 39: 1562-1568 (1989).

**Ventilation for Energy Efficiency and Optimum
Indoor Air Quality
13th AIVC Conference, Nice, France
15-18 September 1992**

Paper 17

**CMHC Residential Indoor Air Quality - Parametric
Study.**

T. Hamlin^{*} and K. Cooper^{}**

*** Canada Mortgage and Housing Corporation,
Ottawa, Ontario K1A 0P7, Canada**

**** SAR Engineering Ltd, 8884 15th Avenue,
Burnaby, British Columbia, V3N 1Y3, Canada**

SYNOPSIS

The purpose of this study was to carry out a mathematical modelling analysis of the effect of indoor pollutant source strengths and ventilation rates on the concentration of pollutants. These concentrations are then compared to various human exposure limits and targets. The modelling was carried out for a variety of ages of residential detached housing for a range of Canadian climatic conditions.

Although a literature search was performed, pollutant source strength data for housing was not generally available. A few houses had been surveyed for CMHC and had concurrent pollutant concentrations and passive tracer gas air change rate measurements. These were used to establish pollutant source strengths or emission rates. The study was directed at building generated pollutants. Soil gas pollutants and combustion appliance spillage were not modelled in this study.

Air change rates including air leakage and mechanical ventilation were estimated using a computerized model. Pollutant concentrations were calculated and analyzed for periods, system types and house types which were potentially undesirable.

For some pollutants including Volatile Organic Compounds (VOCs), no established residential exposure limits have been established. Industrial limits and proposed guidelines are discussed relative to the concentrations predicted. Formaldehyde was compared to Canada's exposure guidelines. Emission limits and ventilation strategies appropriate for housing can be developed through this kind of research work. Further work is needed.

THE AQ1 MODEL

A high degree of variation was known to exist in the airtightness of houses (1,2), the weather conditions in Canada and the sources strengths of pollutants. A relatively simple, fast model was needed to predict effects of various combinations of inputs and estimate indoor air quality for the general population of houses. Multizone models were avoided due to run time and the need for input data not available especially for a wide variety of houses. A single zone, hourly air infiltration model as per Walker and Wilson (3) was selected and combined with a fan/ air leakage interaction model by Palmiter (4) and a pollutant concentration model.

The pollutant concentration is calculated based on previous concentration, air change rate, and source strength as developed by Palmiter and Bond (5). For air change rates greater than 0.0001,

$$C_1 = C_0 e^{-at} + S (1 - e^{-at}) / f,$$

and the integrated average for each hour,

$$C_{av} = (C_0 - C_1) / a + S / f,$$

otherwise,

$$C_1 = C_0 e^{-at} + S (1 - a(0.5 + a/6)) / V,$$

and,

$$C_{av} = (C_0 + C_1) / 2.$$

where C_1 is the new concentration (ppm),
 C_0 is the original concentration (ppm),
 a is the air change rate (h^{-1}),
 t is one hour,
 S is the emission rate (mL/h),
 f is the flow rate (m^3/h), and
 V is the volume of the house (m^3).

This model avoids problems of blow up in concentration for low air change rates. In addition, a minimum difference in indoor/outdoor temperature is a model input for the heating season. Two degrees was used in the simulations as a minimum temperature difference to be expected as a result of solar and internal gains. Integration of a thermal model would be necessary to more accurately model these periods.

Several other features were also included in the model. There is a capability to simulate control of mechanical ventilation based on sensing of the outdoor/indoor temperature difference. Time constants and schedules for emissions can be modelled. The effect of absorption and reemission was not explicitly modelled but could have an effect similar to a longer emission time constant at a lower rate.

PARAMETRIC STUDY

Information on emission rates and especially time constants for emissions were not found for residential indoor pollutant sources. Some limited information performed in CMHC surveys (6,1) was used to establish emission rates. Because these surveys were small, and not randomly selected, they do not provide a true representation of source strengths in general. Examples of source strengths derived from these concurrent passive air change rate and pollutant concentration measurements are shown in Figures 1 and 2. The 5 houses in British Columbia have source strengths 3 times that of the rest of Canada. This anomaly should be investigated. A larger resample in this region would be appropriate. The average for the rest of Canada was used in the simulation of formaldehyde concentrations. For volatile organic compounds (VOCs), the average pollutant emission rate from 20 two year old houses in Saskatchewan and 28 various aged houses in Ontario were used. Toluene had the highest variability in source strength. For the VOCs, the sampling periods for air change rate were one week while the VOCs samplers were exposed for only one day. Source apportionment to building components and activities was not possible due to a lack of data.

Most existing Canadian houses rely on air leakage to provide ventilation. Due to the highly variable nature of accidental leakage individual houses and weather conditions can result in very low air change rates. Several data sets were obtained from recent airtightness testing surveys. Over 400 tests were available as shown in Figure 3. Three regions were selected for data completeness covering all ages of homes and representation of varying climate and average airtightness. The tightest houses are found in the prairie region. The loosest housing in Canada is found in the Vancouver area. Ontario is typical of most other regions of

Canada. Figure 3 displays the variability in this data. Seventy fifth and 90th percentile air tightness's were calculated from the actual data. Because of the small sample size after stratification by age and region, the 90th percentile is not considered as representative as the 75th. Either one is better than the average or the maximum because they represent a significant portion of houses but are unlikely to be the result of anomalous or erroneous measurements.

Figure 4 displays typical output from the analysis of new houses. Airtightness and volume were assumed to be related. House characteristics and weather were region specific. This reflects the increased airtightness in colder regions. Average pollutant source strengths were used. Source strengths did not show a good correlation to volume. For the simulations, volumes were only varied by less than 15 % which is much smaller than the range of source strengths. Risk of exposure was not estimated in more detail as data on variation in source strengths was not considered sufficient to estimate exposure in more detail. From Figure 4, it is apparent that the predicted hourly concentrations exceed Health and Welfare Canada's guideline for the hourly maximum values in the summer months. Since air conditioning is common in Ontario, this may be a health risk. Monthly average values are also near the Action limit. Residential health limits have not been established for the VOCs but predictions exceed those proposed by Seifert (7). On the other hand concentrations are more than 3 orders of magnitude lower than industrial limits. Also shown on the same figure are values predicted for an indoor to outdoor air temperature controlled ventilation system. A dramatic improvement is seen in the indoor air quality. Similar data for the Prairie and British Columbia regions may not be as critical. The summer values are unlikely to occur due to the low incidence of air conditioning in these areas and high usage of open windows at this time of year. The most critical months are therefore May and October for the Prairies. A temperature controlled set to turn on a 25 L/s ventilator at less than 8 C can maintain average concentration below the action limit. Figure 5 displays hourly output. Although thermal modelling was not performed, very low energy impact is expected to result with this form of ventilation control. Similarly in British Columbia, formaldehyde can be controlled even with a higher formaldehyde source strength.

Since source strengths may be significantly lower for older house, and data was unavailable, maximum emission rates were estimated which could maintain concentrations below the action guidelines for various locations and age groups of housing. If a target of 0.05 ppm is desirable, the emission limit would be proportionately cut in half. Data for British Columbia is shown in Figure 8. Renovations involving flooring, cupboards and furniture would be of most concern. Surveys of materials in typical houses would allow an approximate apportionment of sources and emission targets for each type of material.

CONCLUSIONS

An analysis capability was developed to explore the relationships between various types and rates of pollutant emissions and various rates of air change in detached houses. Rates of air change were modelled from hourly weather data, house airtightness, and mechanical ventilation equipment operation.

As indoor air quality depends on both emissions and ventilation, a balanced approach should be taken. This study has explored possibilities of what emission rates could be tolerated in various housing with air leakage only. For formaldehyde, the maximum tolerable emission rates are achievable. Similarly rates could be determined for other pollutants if health guidelines are available. Ventilation in houses which are not airtight can be controlled by outdoor to indoor air temperature difference. This control strategy significantly reduces the higher concentrations predicted and minimizes the energy cost of ventilation.

Further refinement and calibration of these modelling techniques should be done. More source strength or emission rate data is required including duration of emission and material quantification. Quantification of materials will be necessary to develop emission rates for each type of material in a typical house. Ventilation control by temperature difference has good potential especially in conjunction with retrofit sealing and should be field tested.

REFERENCES

1. Hamlin, Tom, "Ventilation and Airtightness of New Detached Canadian Housing" ASHRAE Symposium paper, Indianapolis, June 1991.
2. Parekh, Anil, Development of a Database on Housing Characteristics Representative of the Canadian Housing Stock CMHC Research Report, May 1992.
3. Walker I.S. and Wilson, D.J. The Alberta Air Infiltration Model Aim-2 University of Alberta, Dept. of Mech. Eng. Report 71, January 1990.
4. Palmiter, Larry and Bond, Tami "Interaction of mechanical Systems and Natural Infiltration", 12th AIVC Conference pp285-295, Ottawa, Sept. 1991.
5. Cooper, Ken, Moffat, Peter, Palmiter, Larry "Indoor Air Quality Analysis", draft CMHC report, July, 1992.
6. Dumont, Rob, Snodgrass, Lawrence, "Volatile Organic Compound Survey and Summarization of Results" CMHC Report, January 1992.
7. Seifert, Bernd, "Regulating Indoor Air", Indoor Air '90, Toronto, pp 35-49 Vol 5. July, 1990.

Figure 1.

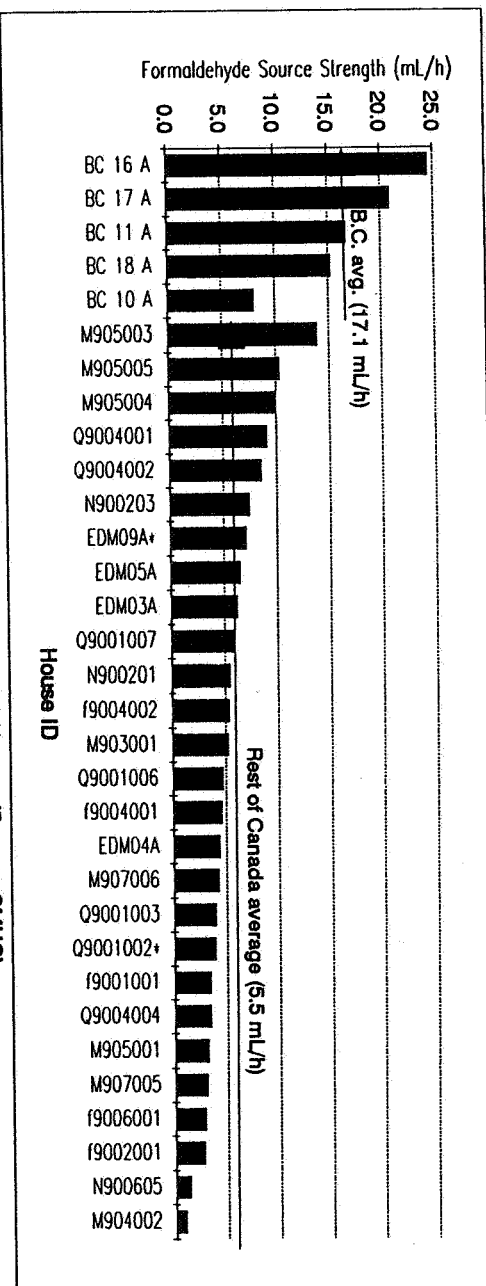
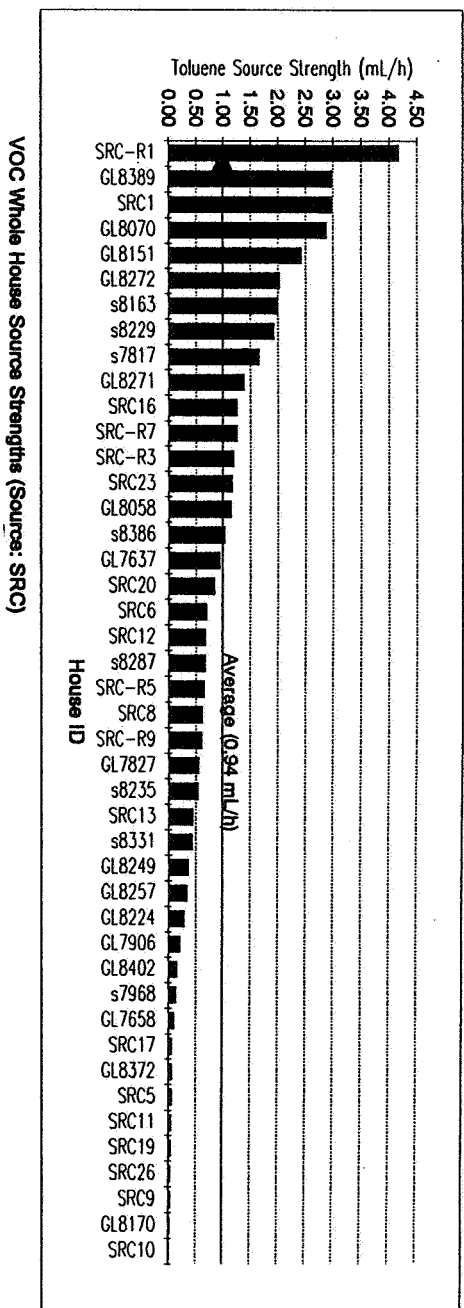


Figure 2.



Air-tightness Summary

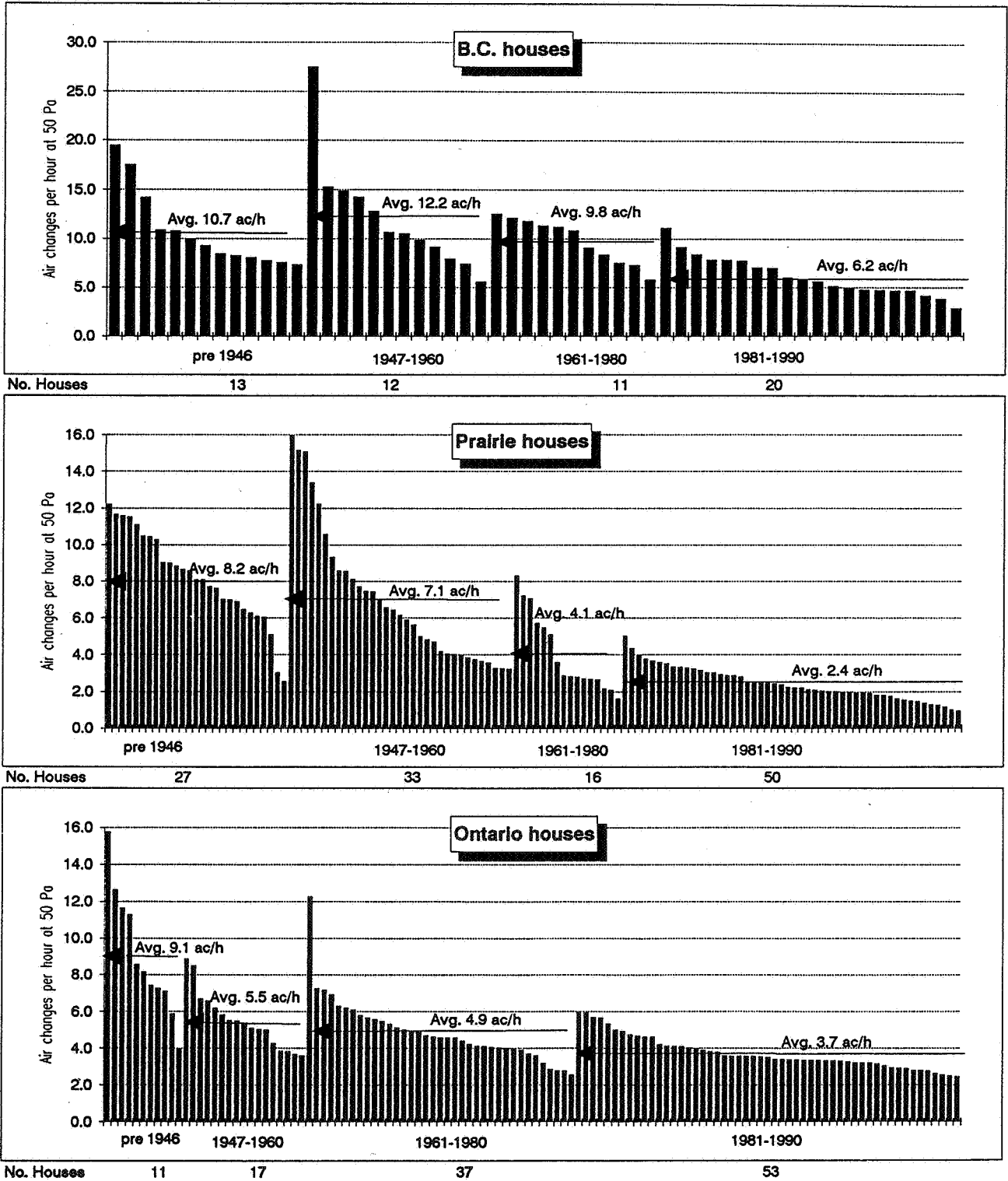


Figure 3.

Indoor Air Quality Profile

Description:

Region: ONT
 Age: 1981 to 1990
 Percentile: 75
 Ventilation Type: Balanced
 Ventilation Flow: 25 L/s
 (Ventilation on if temp. difference to outside <8C, off otherwise)

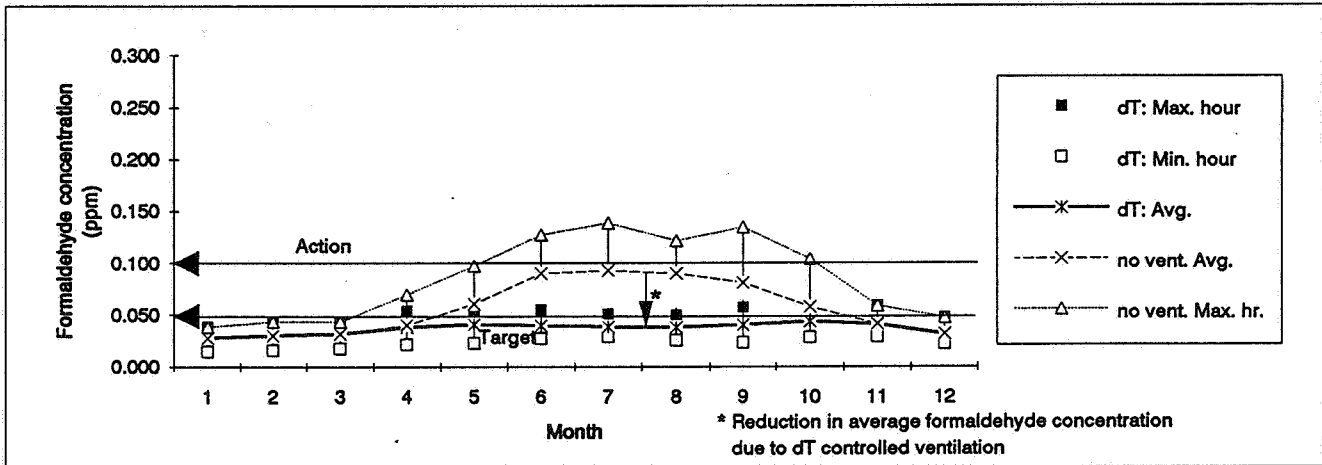
Volume: 725 m³
 Bldg. Ht: 6.5 m
 Flue: none
 Foundation: Bsm't
 C: 169 L/sPaⁿ
 n: 0.69
 ELA: 3,323 cm²

Run ID #	dT control	no vent.
	66303	66331
Infil. Coeff:		
R	0.60	0.60
X	0.00	0.00
Y	0.00	0.00
Shelter:		
Building	0.80	0.80

Pollutant Source Strengths:

Whole house source strengths based on: 22 houses

House	Formaldehyde	Benzene	Toluene	Xylene	Nonane (mL/hr)	Undecane	Limonene	A-pinene	Ethylbenzene	Source strengths:
	5.500	0.985	0.856	1.162	N/A	N/A	0.521	0.805	0.385	SFC avg. meas. (whole house)



Pollutant Health Limits (ppm)

	Formaldehyde	Benzene	Toluene	Xylene	Nonane	Undecane	Limonene	a-Pinene	Ethylbenzene	
Classes:	Aldehyde	Aromatic Hydrocarbons			Alkanes		Terpenes		Ether	Class limits are from Seifert Aldehyde limit is from EHD (Canada) for formaldehyde.
Class Limits:	0.05	0.008	0.007	0.006	0.010	0.008	0.003	0.002	0.002	
ACGIH TLV	1.00	9	100	100	200	N/A	N/A	N/A	100	
Predicted Pollutant Concentrations with dT controlled ventilation (ppm)										
Avg. Year	0.037	0.007	0.008	0.008	not avail.	not avail.	0.003	0.005	0.003	Highest monthly average for each period
Max: Oct-Apr	0.043	0.008	0.009	0.009	not avail.	not avail.	0.004	0.006	0.003	
May-Sep	0.043	0.008	0.009	0.009	not avail.	not avail.	0.004	0.006	0.003	
Max. hour	0.059	0.011	0.012	0.012	not avail.	not avail.	0.006	0.009	0.004	

Infiltration & Ventilation: dT control (ac/h)

	Month											
	1	2	3	4	5	6	7	8	9	10	11	12
Max.	0.581	0.541	0.457	0.434	0.416	0.383	0.321	0.384	0.411	0.326	0.327	0.429
Min.	0.173	0.157	0.151	0.104	0.104	0.102	0.102	0.102	0.104	0.102	0.104	0.145
Avg.	0.285	0.267	0.244	0.206	0.191	0.195	0.201	0.201	0.193	0.178	0.191	0.250

Infiltration with no Ventilation (ac/h)

Avg.	0.285	0.267	0.244	0.196	0.132	0.087	0.085	0.088	0.102	0.141	0.190	0.249
------	-------	-------	-------	-------	-------	-------	-------	-------	-------	-------	-------	-------

Monthly Average Temperatures (C)

Outside	-8.8	-4.7	-3.0	4.2	12.0	18.2	19.4	19.0	15.6	9.6	4.6	-4.8
Inside	20.0	20.0	20.0	20.0	20.5	22.2	22.6	22.6	21.1	20.1	20.0	20.0

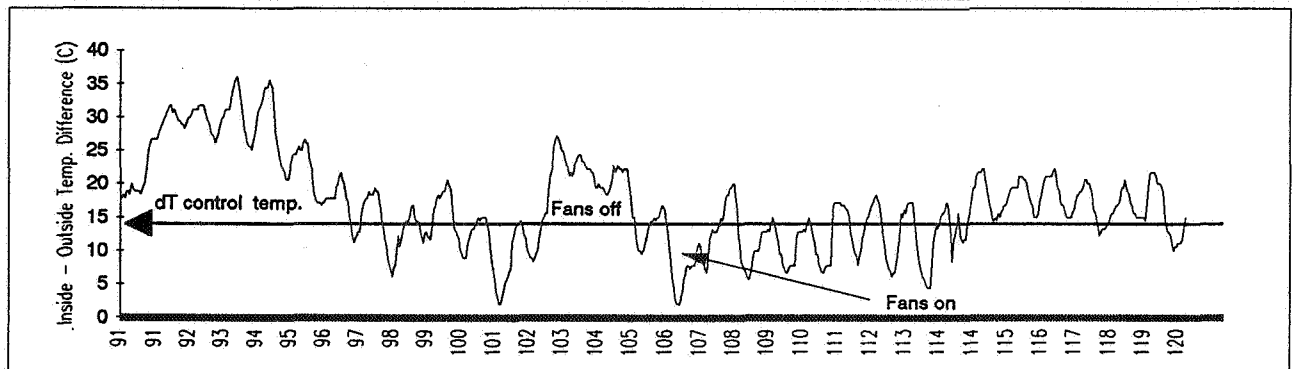
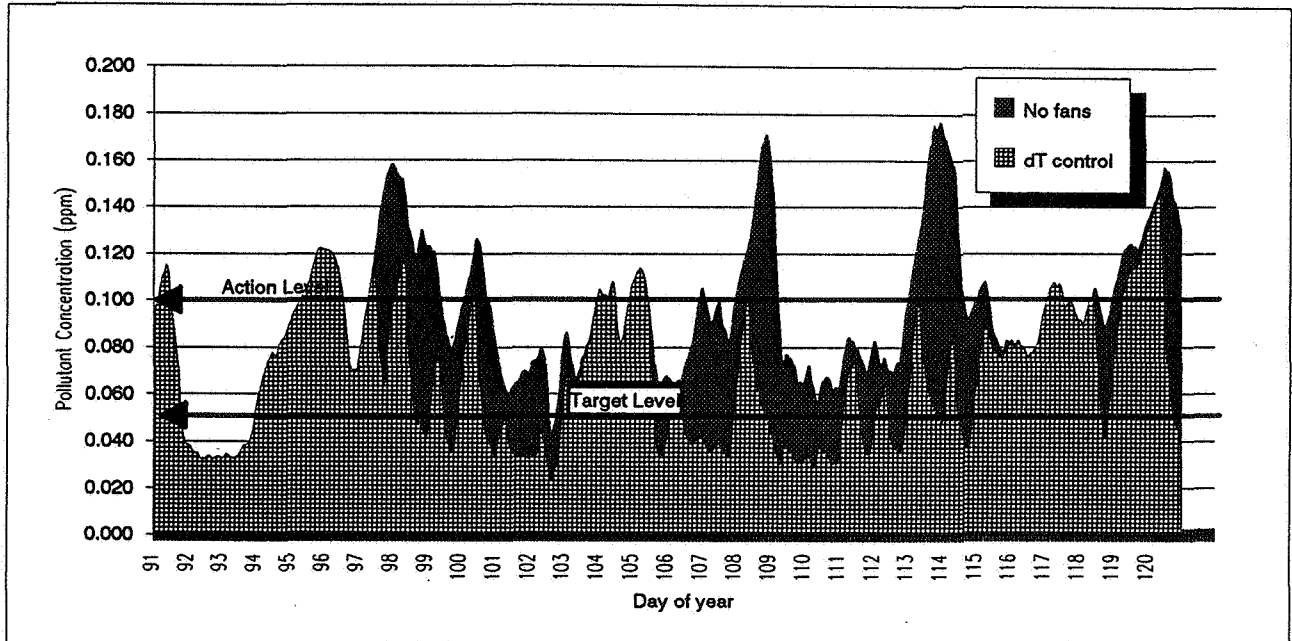
Monthly Average Winds (m/s)

AES Station	5.3	5.8	4.8	4.8	4.0	3.1	3.5	3.5	3.3	3.6	4.8	4.4
Building	2.1	2.3	2.0	1.9	1.7	1.4	1.5	1.5	1.4	1.5	1.9	1.8

Figure 4.

Prairies

April



Formaldehyde concentrations (ppm)

	no Fans	Fans with dT control
Average	0.095	0.068
Minimum	0.033	0.023
Maximum	0.177	0.147

Percentage of hours with concentration greater than limit of 0.1 ppm

	no Fans	Fans with dT control
Percentage	40%	18%

Total Infiltration and ventilation

	no Fans		Fans with dT control	
	(ach)	(L/s)	(ach)	(L/s)
Average	0.13	18	0.20	28
Minimum	0.02	3	0.05	7
Maximum	0.44	60	0.55	75

Fan operation:

	no Fans	Fans with dT control
Hours	0 hours	260 hours

Description:

Source strength: 5.5 mL/h

Fans: balanced, 25L/s
(with dT control, fans are off unless inside to outside temperature difference is less than 14C)

House ID: 3630 (no flue)
1981-1990
75th percentile
Volume: 494 m³
C: 50 L/sPaⁿ
n: 0.71
ELA: 1,030 cm²
Basement foundation

Figure 5.

Figure Maximum formaldehyde source strength: B.C.
 Maximum house emissions to maintain concentration below
 Action level of 0.1 ppm (house closed all year)

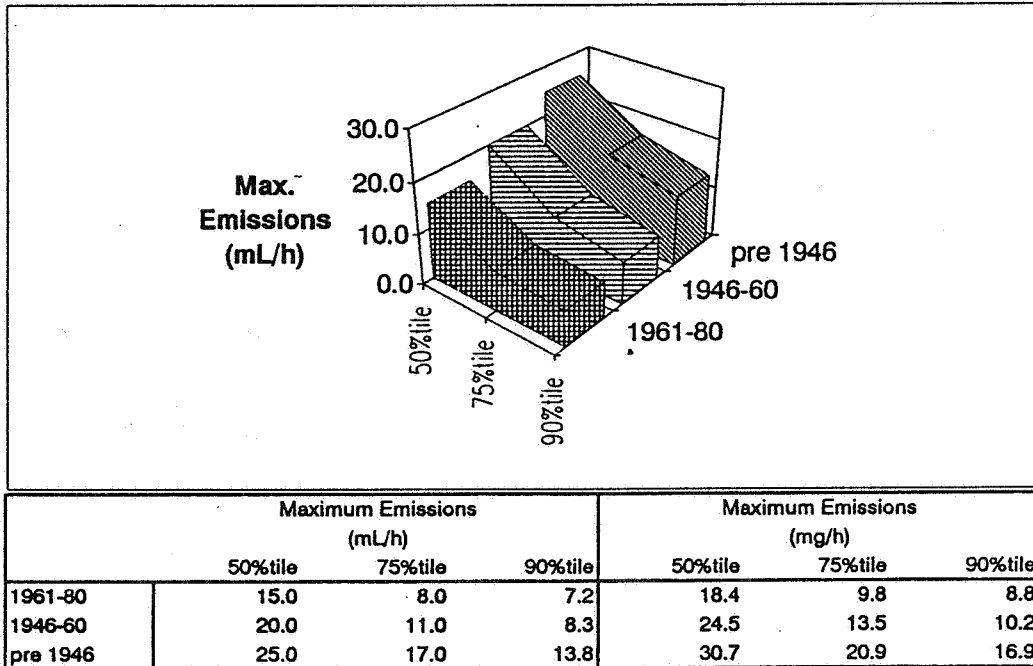


Figure 6.

**Ventilation for Energy Efficiency and Optimum
Indoor Air Quality
13th AIVC Conference, Nice, France
15-18 September 1992**

Paper 16

**Occupants' Behaviour with Respect to Window
Opening: A Technical and Sociological Study.**

B. Fleury and C. Nicolas

**EDF DER DAE, Les Renardières, Route de Sens,
77250 Moret sur Loing, France**

1.0 Synopsis

The occupant's behavior with respect to window opening may greatly affect the ventilation system, the energy consumption or/and the indoor air quality. In order to quantify the magnitude of opening times, many surveys have focused on climatic parameters and concluded to the temporal correlation between the timelength of opening and the outside temperature or the solar irradiation. In this paper, we study the influence of sociological and technical parameters on the average time of opening during the winter. The research is based on a sociological survey and a two year monitoring of thirty houses with recording sensors on every window.

The wife at home or not, the size and age distribution of the family are key variables in the kitchen, bathroom, children's bedroom. The orientation of the living room related to the sun explains the occupant's behavior in this room. For the parent's bedroom, none of the selected parameters emerges, the distribution and frequency of opening time are so erratic. The type of ventilation systems, natural versus mechanical, is not the main explainable variable, as well as the degree of equipment of the family.

2.0 Introduction

In the past years, research has focused on understanding air infiltration and improving ventilation systems. Building construction techniques and ventilation products have now reached a high quality standard. However, we still face some claims for a better indoor environment. Satisfying this demand implies a clear identification of occupants' wishes and behavior. In this paper, we analyse the technical and sociological parameters impacting occupants' behavior with respect to window opening during winters. We will not present the influence of the weather data on their behavior.

3.0 Methods

Given the complexity of understanding the occupants' behavior with respect to window opening, we used different approaches to examine this issue :

- a two year monitoring on 30 individual electrically heated houses, recording duration and number of openings on each window /1/
- a questionnaire survey on 60 households including the 30 monitored one /2/
- 3 household interviews.

3.1 Building group

The studies were conducted in the same geographical area near Lyon (France) with houses built between 1982 et 1985. In the measurement group, 10 dwellings were equipped with humidity controlled ventilation (numbered 1 to 10), 5 with natural ventilation system (numbered 11 to 15) and 15 with mechanical exhaust ventilation systems (numbered 16 to 30).

3.2 Recorded parameters

Instead of an automatic monitoring of the entire house, we decided to develop miniature sensors with an periodical inspection.

Every two or three weeks, the following data were recorded :

- duration of opening of each window
- number of opening of each window
- energy consumption (day and night)
- functioning time of the ventilation.

During the visit, the agent noted :

- temperature and humidity in the living-room
- flow rate in exhaust rooms
- angle of opening of opened windows if any
- cleanliness of exhaust valves
- temperature and humidity in the parents' bedroom.

At the local weather station, the following data were recorded :

- global solar irradiation (MJ/m²)
- diffuse solar irradiation (MJ/m²)
- number of hours of sun (h)
- water precipitation (mm)
- wind speed (m/s).

For analysis, all the previous data were converted to a daily basis.

3.3 Characteristics of the households

For each instrumented houses, we have identified :

- number of persons
- number of children at school
- women at home
- number and type of pets
- equipment of the house (diswasher,microwave,cooker hood,....),
- orientation of the living room window (north or other).
- number of babies (not at school)
- number of smokers,
- men working during nights
- ventilation system,

4.0 Results

4.1 Recorded duration of opening

Table 1 is the synthesis of two winters. Winter in 90 was more severe than in 89, (average temperature 2° C less). Consequently, the durations were slightly different but the same order of magnitude is respected.

If we compared with foreign experiences, the figures are different but the building techniques and HVAC systems also differ significantly. However, the parents' bedroom is also the room where the window is often opened.

	Present Experiment	Netherlands /3/	Belgium /4/
Kitchen	30 mn	1h45	1h
Living room	50 mn	1h	30 mn
Bathroom	45 mn		1h30
Parents' bedroom	2h30	5h	4h
Children's bedroom	1h	1h45	2h30

Table 1 : Duration of opening in every room

4.2 Estimated duration of opening

Table 2 compared the estimated duration of opening in each room with the recorded one. We notice that occupants underestimate this variable, especially in the bedrooms and living-room. At the opposite, the evaluation is quite accurate in the bathroom.

	Kitchen	Living room	Bathroom	Parents' bedroom	Children's bedroom
Overestimation	26	13	10	7	14
Underestimation	43	57	35	73	57
Rigth estimation	30	30	55	20	29

Table 2 : % of people under, over or correctly (+/- 10 mn) estimating the duration of opening

4.3 Multivariable analysis

4.3.1 Method

The sociological survey identified explanatory parameters of the occupants' behavior and a kind of hierarchy. Using the Morgan and Sonquist method, we have tried to identify the main explanatory variables of the recorded duration of window opening.

The segmentation criteria is based on the variable which is going to maximize :

$$W = \sum P_j (M_j - M)$$

Where M is the average of the duration of opening

M_j is the average of the duration of opening of the state of the explanatory variable

P_j is a weighting values.

Repeating the segmentation criteria at different levels, we can build a segmentation tree with a hierarchy for the explanatory variables. This method is really attractive but presents some risks. When no variable

represents a strong segmentation criteria, the segmentation tree can be unrealistic because a bifurcation was not pertinent. This fact should lead to a comparative analysis of W for the various explanatory variable. Because of the limited number in the sample, we will consider only the first levels of the segmentation tree.

4.3.2 Kitchen

The wife working full time, part-time or at home is the main variable for the kitchen. The time available for cooking activities explains the difference between the various households. As we will notice for other rooms, the larger the family is, the less the window is opened. Finally, we notice a shorter duration of opening in a house equipped with a mechanical exhaust ventilation system. In a naturally ventilated house, the wife may need to open the window to exhaust the pollutions.

4.3.3 Living-room

The orientation of the living-room is the key variable: occupants open widely their windows by sunny days. The presence of smokers induces a longer duration of opening, babies within the family lead to the opposite.

4.3.4 Bathroom

The households without children leave the window open for a long time. The presence of babies in the family leads a short duration of opening.

4.3.5 Children's bedroom

When the bedroom is occasionnaly used, the window is opened for large period of time. In fact, this room can be used for other activities and is largely ventilated before the welcome of a guess. When the wife is working full time, this room is rarely opened.

4.3.6 Parents' bedroom

No explanatory variable emerges from the statistical analysis. None of the listed parameters can correlate the opening. In fact, we notice a difference behavior in any class. From a few minutes to hours, the entiere spectrum was recorded.

4.3.7 Conclusions

The wife working or not, the presence and the age of children are the key variables explaining the occupants' behavior. However, usually another specific variable emerges in any room. The type of ventilation systems is not fundamental in the occupants' behavior except in the kitchen where the natural ventilation system is not sufficient to exhaust pollutions. These results are in agreement with the sociological survey and illustrate the major role of the household with respect to the window opening and the ventilation system.

4.4 Energy consumption

This study has identified a large spectrum of behavior with respect to window opening. The act of opening is usually combined with the switch of the electric radiator and we did not point out a correlation between the time of opening and the energy consumption.

5.0 Conclusions

This study illustrates the crucial role of sociological parameters regarding to the occupants' behavior with respect to window opening. Even if the conclusions are limited to this reduced sample, this research points out that the specifications and the operation of a HVAC system should better integrate the occupants' behavior. An excellent system from a theoretical and technical approach can be a failure if it does not include, in the design approach, the occupants.

6.0 References

- /1/ B. Fleury, P. Niard
Comportement des occupants vis à vis de l'ouverture des fenêtres,
Rapport EDF HE 12 W 3065, Nov 90.
- /2/ J. Rivoire
Les habitants et leurs fenêtres, Rapport EDF, Jan 90.
- /3/ J .E.F. Van Dongen
Inhabitants'behavior with respect to ventilation
7th AIVC Conference, Stratford, UK, Oct 86.
- /4/ P. Wouters, D.de Baets
A detailed statistical analysis of window use and its effect on the
ventilation rate in 2400 Belgium social houses, 7th AIVC Conference,
Stratford, UK, Oct 86.

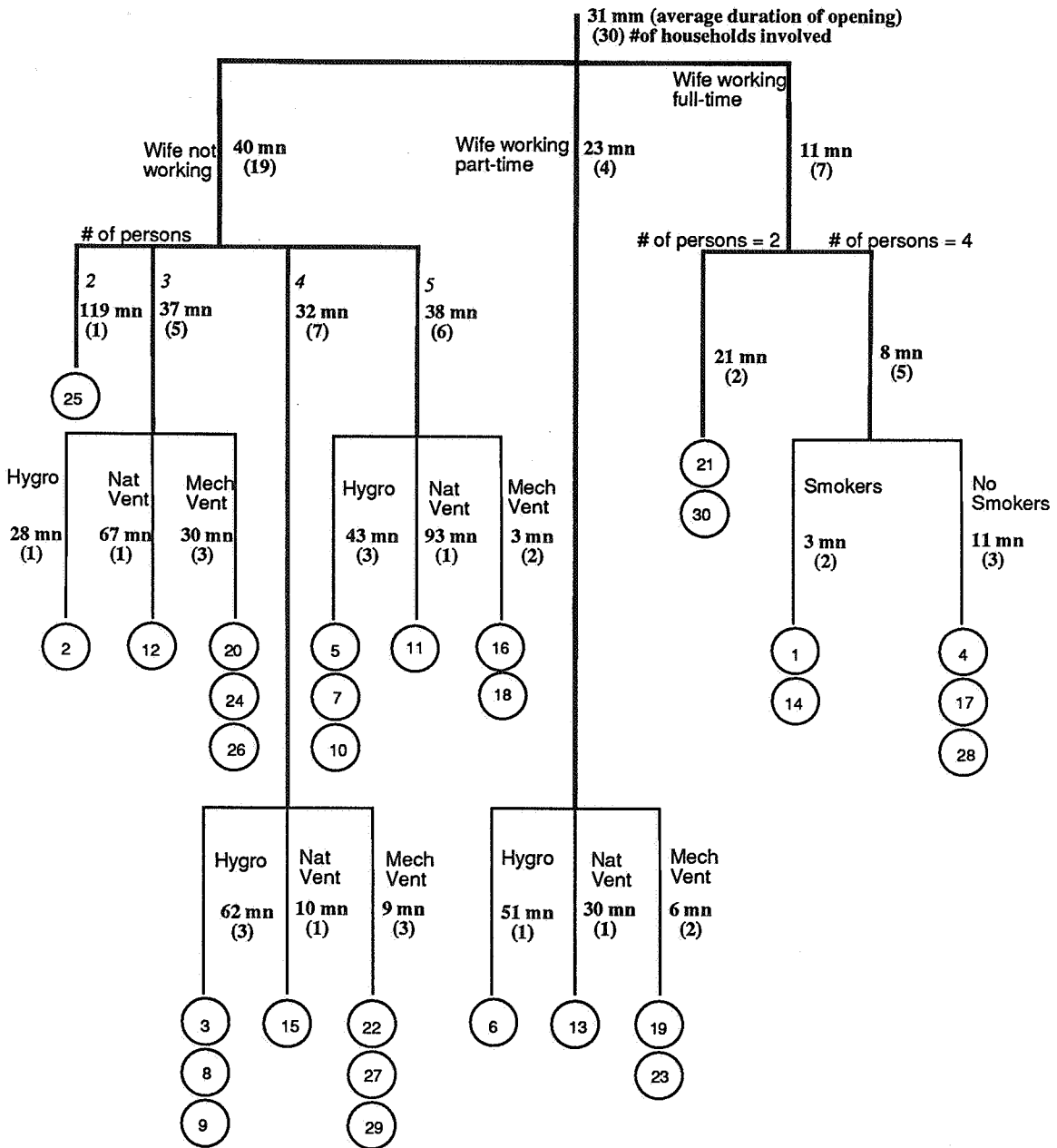


Figure 1 : Duration of opening for the window of the kitchen

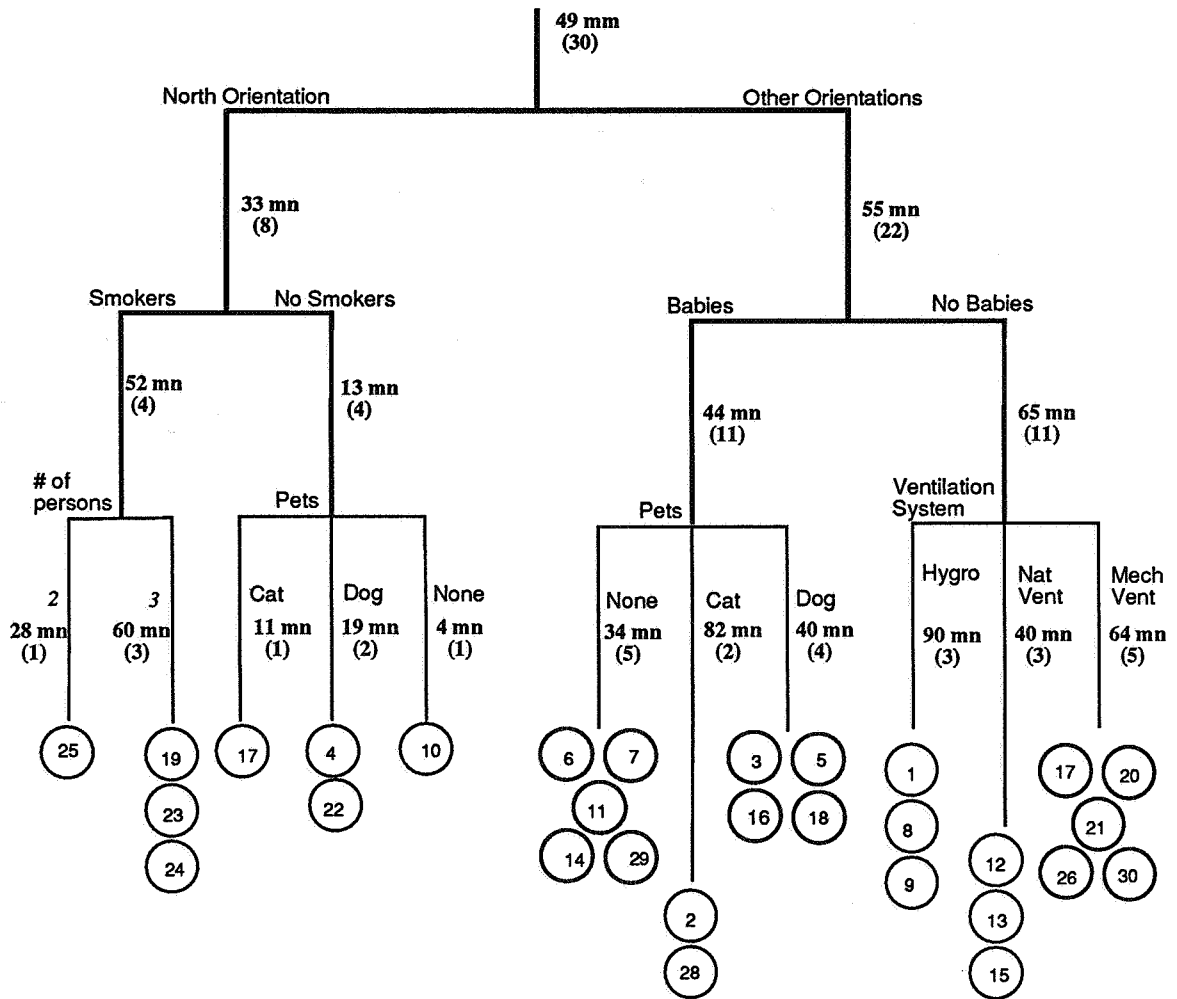


Figure 2 : Duration of opening for the window in the living room

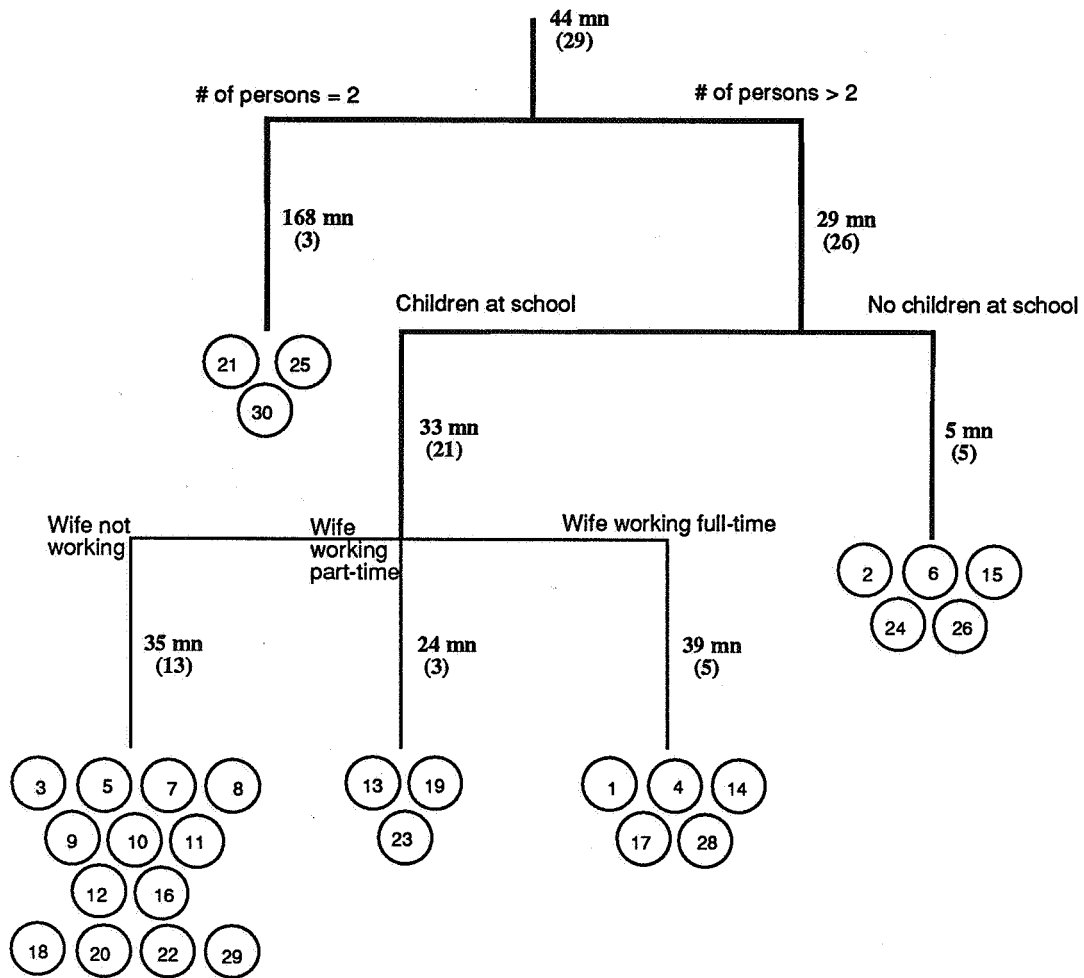


Figure 3 : Duration of opening for the window of the bathroom

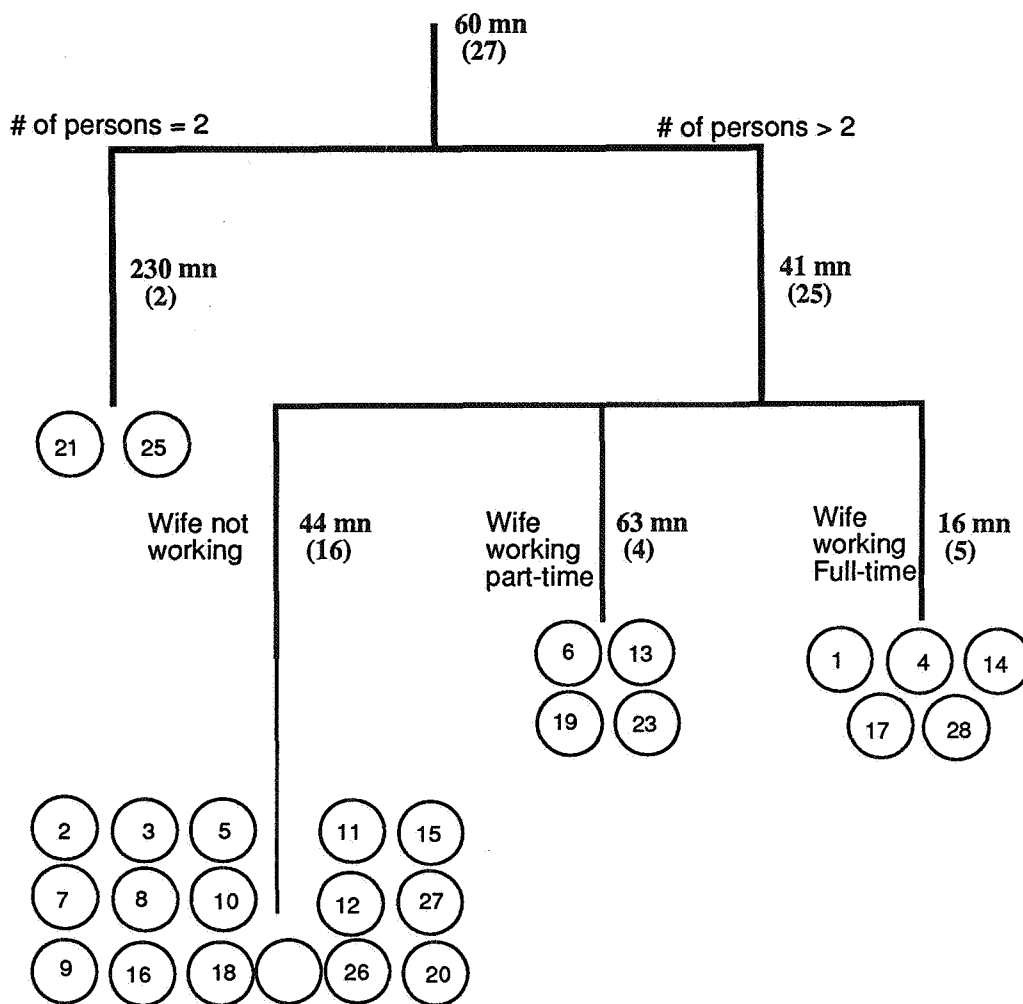


Figure 4 : Duration of opening for the window of the children's bedroom

**Ventilation for Energy Efficiency and Optimum
Indoor Air Quality
13th AIVC Conference, Nice, France
15-18 September 1992**

Paper 15

**Airborne Moisture Movement in Occupied
Dwellings. A Case-Study Approach.**

M. Kolokotroni, N. Saiz, J. Littler

**Research in Building Group, The University of
Westminster, 35 Marylebone Road, London NW1
5LS, United Kingdom**

ABSTRACT

This paper reports the results of humidity and ventilation measurements in occupied residential buildings to study the effect of airborne moisture movement on condensation risks. The dwellings have been fitted with a cooker hood and an extractor fan (both with variable speed control) in the kitchen and an extractor fan in the bathroom. The investigation of each case-study included monitoring the temperature and humidity at four locations in the house for a number of weeks during the heating season in order to examine the water vapour cycles in each room as affected by moisture production in the space and moisture migration from adjacent rooms and outside. Detailed short time measurements have been also taken to study the effect on the humidity in one room of water produced in other rooms, and the efficiency of the variable flow-rate extract devices for the local removal of moisture before it becomes well mixed.

In this way the efficiency of each ventilation device, in isolation and in combination with the others, in removing moisture from the rooms in which it is produced, has been examined as well as its effect in reducing the rate of moisture migration to the rest of the house. It has been possible to find relationships between the moisture loads in the rooms in each case-study, thus describing the effects of interzonal moisture flows in situations typical of those found in dwellings at risk of condensation.

1 INTRODUCTION

Water vapour is one of the internal environmental contaminants which is rarely mentioned when discussing air quality. However, although it might not affect people in the same dramatic manner as CO₂, NO_x, O₃ and HCHO, it is present in a large proportion of buildings, mainly residential, it is transported in a similar manner [1] and it is impossible to eliminate its sources. High relative humidity can cause structural deterioration and is connected to human illness such as asthma and allergies due to dust mites [2-5]. Excessive humidity can create condensation, mould problems and discomfort; but low humidity can cause its own problems. Apart from discomfort due to dehydration of the skin and mucous membranes, some bacteria and viruses like lower humidities [6]. Therefore, humidity extremes need to be avoided, with an optimum zone in the middle of the relative humidity scale.

A high percentage of the residential building stock suffers from the effects of excessive moisture. According to the latest English Housing Survey [7] more than half of UK households are affected with problems ranging from condensation on windows to mould on walls and furniture. The problem is also present in other cold countries such as Canada where results of a survey in 1991 indicated that 39% of the people had at least one moisture or mould indication in their homes [8]. The problem appears to be more acute in new housing where low ventilation levels coupled with cold bridges have increased the problem [9].

It is only the last 30 or so years that there is evidence that air movement is very important in moisture migration in the same way as water vapour diffusion through the fabric of the buildings [10]. Only recently the importance of ventilation in removing moisture at source has been emphasised in the Building Regulations [11] and publications on methods of avoiding condensation and evaluating the risks have appeared [12] including international efforts aimed at providing solutions to the problem [13].

Increased ventilation seem to be the solution in most cases. The effectiveness of extractor fans and cooker hoods in reducing the migration of moisture to other spaces of the dwellings is the subject of this paper. Three small homes were investigated before and after the installation of extract devices and it was found that excess vapour pressure (internal vapour pressure above outside vapour pressure) has been reduced in source rooms (kitchens and bathrooms) and also in sink rooms (living rooms and bedrooms).

2 DESCRIPTION OF THE CASE-STUDIES

The floor plans of the three case studies are presented in Fig. 1.

The first case study is a maisonette in East London, a region of low cost housing with most of the house stock built after World War 2. Two adults live in the flat which comprises a kitchen, living room and bathroom on one floor and a bedroom on another, with a total floor area of approximately 65m². The maisonette is situated on the two upper floors of a five storey block of flats containing 70 housing units. There is no thermal insulation in the brick walls or the roof and the windows are timber framed and singly glazed. Heating is provided by a time-controlled gas boiler (located in the kitchen) and radiators in every room apart from the bathroom which is heated with an electric wall mounted radiant bar. Ventilation is provided by sash windows, window vents (which were all blocked by the occupants) and vents into a bricked-up chimney in the living room.

The second case study is a 60's maisonette in South London in a council owned block of flats. Two adults occupy the flat which comprises a kitchen and living room downstairs and a bathroom and two bedrooms upstairs with a total floor area of 60m². The maisonette occupies the two upper floors of a four storey building containing 55 housing units. The walls are not thermally insulated and the windows are steel framed, singly glazed. However, plastic double glazed windows have been recently installed in the bedroom windows, following complaints about condensation and draughts. Heating is provided by a open gas fire in the living room and an electric heater situated at the top of the staircase. The only ventilation means is through the openable windows.

The last case study is a converted end of terrace ground floor flat also in South London. A single parent with a child lives in the flat which consists of a kitchen, bathroom, living room, bedroom and spare room, all on one floor covering a total area of 70m². The brick walls are uninsulated with single glazed timber framed openable windows for natural ventilation. Heating is provided by a time controlled gas boiler (located in the kitchen) with radiators in every room of the flat.

For the purpose of this study, all three dwellings were fitted with extract devices in the kitchen and bathroom in order to evaluate their effectiveness at removing moisture in source rooms and in preventing moisture migration to sink rooms. In the kitchen a window mounted extractor fan was installed with a maximum flow rate of 78.6l/s equipped with variable speed controller. In addition a cooker hood was installed and ducted outside, with a maximum flow rate of 82l/s. In the bathroom the humidistat controlled extractor fan has a maximum flow rate of 28l/s. In all cases, they comply with the 1990 UK Building Regulations [11].

3 MONITORING THE HUMIDITY AND TEMPERATURE

The temperature and relative humidity were monitored for a minimum period of one week before the installation of the ventilation equipment and at least one week after, by placing thermohygrographs in the main rooms of each house, ie: kitchen, bathroom, living room and one bedroom. The data is used to characterise the basic climate of the houses; that is, temperatures, mixing zones, basic flow paths and occupant use/interference.

The aim is to examine whether there is a reduction in the excess vapour pressure not only in the moisture source rooms (kitchen and bathrooms) but also in the moisture sink rooms (living room and bedroom). The assumption is that the only different parameter (apart from the external conditions) affecting the internal moisture balance before and after the installation of the fans is the way that they are used.

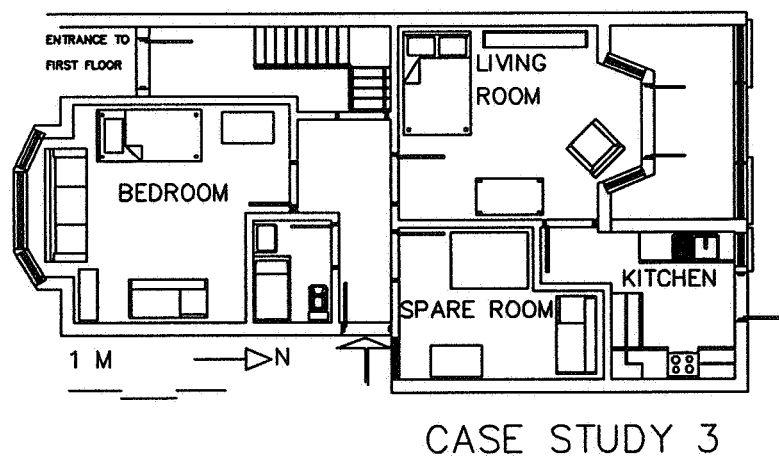
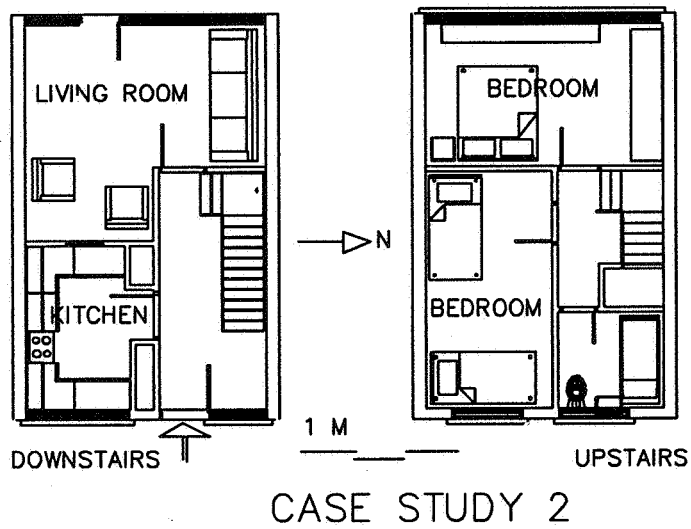
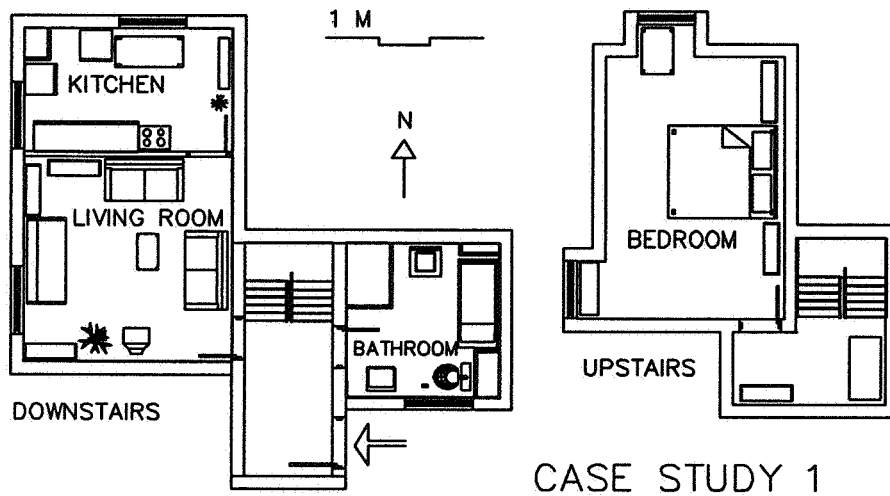


Figure 1: Floor plans of the three case-studies.

An example of the vapour pressure outside and four locations in the first case study under normal occupation and fan operation regime is shown in Fig. 2. Vapour pressure is significantly higher indoors than outdoors indicating the effect of interior moisture production and restricted ventilation as is usually the case in the majority of homes in winter. Vapour pressure is the highest in the unheated bathroom (equipped with a humidistat controlled extractor fan), followed by the kitchen, living room and bedroom. Although, the vapour pressure in the living room and bedroom are similar, temperatures in the bedroom are lower than in the downstairs living room, so that the relative humidity is much higher upstairs, thus creating more condensation problems. As expected, there is a loose correlation with external humidities apart from the times that high and sudden moisture production indoors alters the internal patterns.

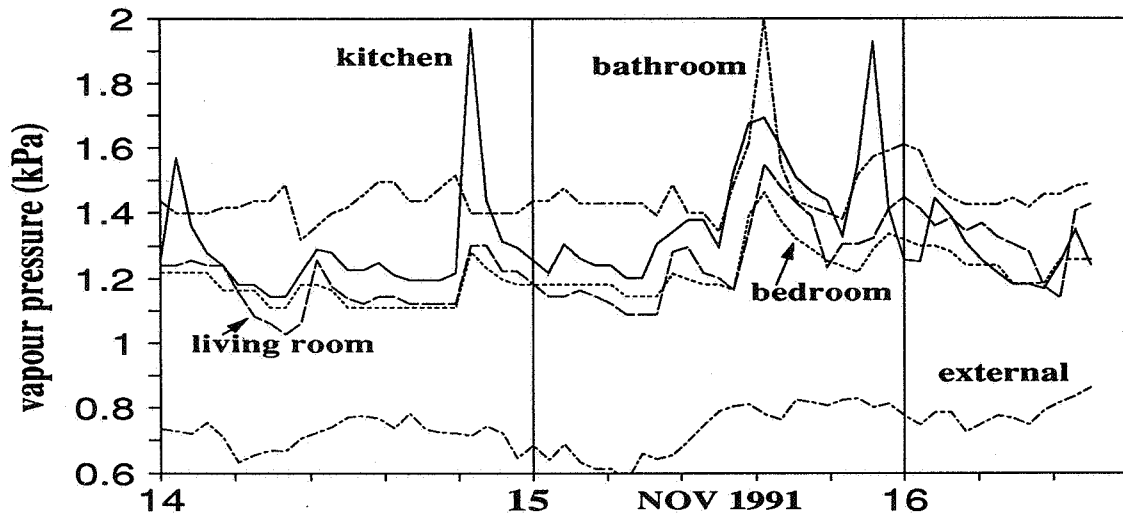


Figure 2: Typical plot of vapour pressure indoors and outdoors.

Figure 2 also presents data for two subsequent days during which the home was used in a different manner. During the first day cooking for dinner was the only source of moisture (apart from metabolic activities) while in the second day, cooking for lunch and dinner, bathing and laundry were performed. This has resulted in elevated vapour pressure in all the rooms for longer time during the second day.

It is evident that moisture produced in the kitchen or the bathroom has an effect on the vapour pressure in the living room and bedroom. It seems that the living room is affected more than the bedroom both from moisture migration from the kitchen and the bathroom for this particular house layout. This is a point requiring closer examination because it determines how much the moisture produced in one room affects the moisture in another, and discussed in section 4.

Considering the humidity status of the dwellings for the weeks before and after the installation of the extract devices, it was obvious that the mean humidity level has been reduced as a consequence of the combined use of the two extractor fans and cooker hood. An example of this, is shown in Fig. 3, where the external and internal relative humidity for the four rooms of case-study 1 have been plotted. Similar temperatures were maintained during the "before" and "after" periods due to the thermostat located in the hallway (there is a difference in the living room and in the bedroom of 1°C but the kitchen and bathroom are almost identical). The relative humidity however has fallen quite considerably in the three rooms (kitchen, living room and bedroom) but not in the bathroom. In this case the low flow rate, humidistat controlled extractor fan, set to 80% RH cut off point, has maintained the RH below 80%. However, it is now apparent that the humidistat was incorrectly set and this has influenced the internal humidity. As a result of less ventilation as the windows are opened

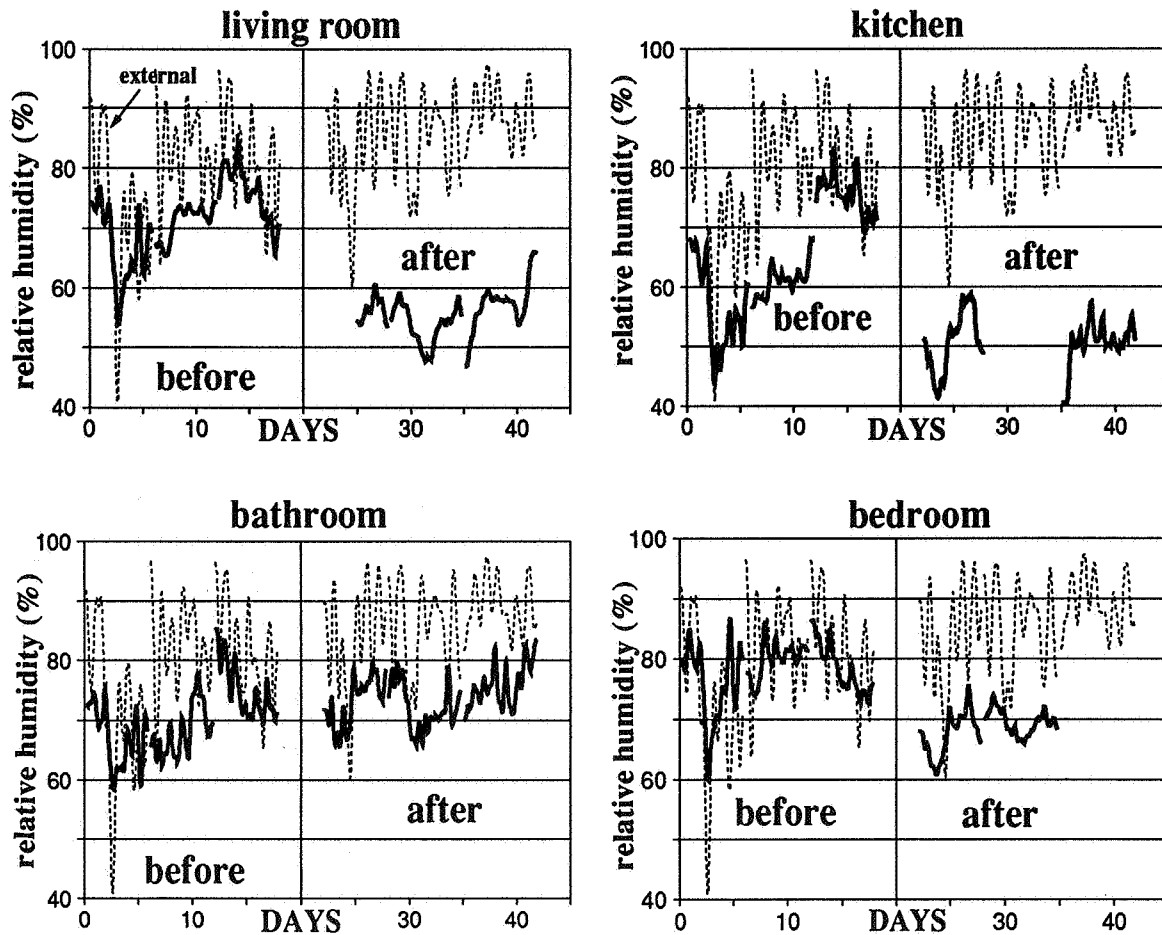


Figure 3: External and internal relative humidity values for the monitored four rooms of case-study 1. The average external temperature is 9.9°C before the installation and 7.4°C after. The internal temperatures are 18.3 , 21.3 , 18.6 and 16.7°C in the living room, kitchen, bathroom and bedroom correspondingly before the installation and 19.2 , 21.0 , 18.3 and 15.4°C after.

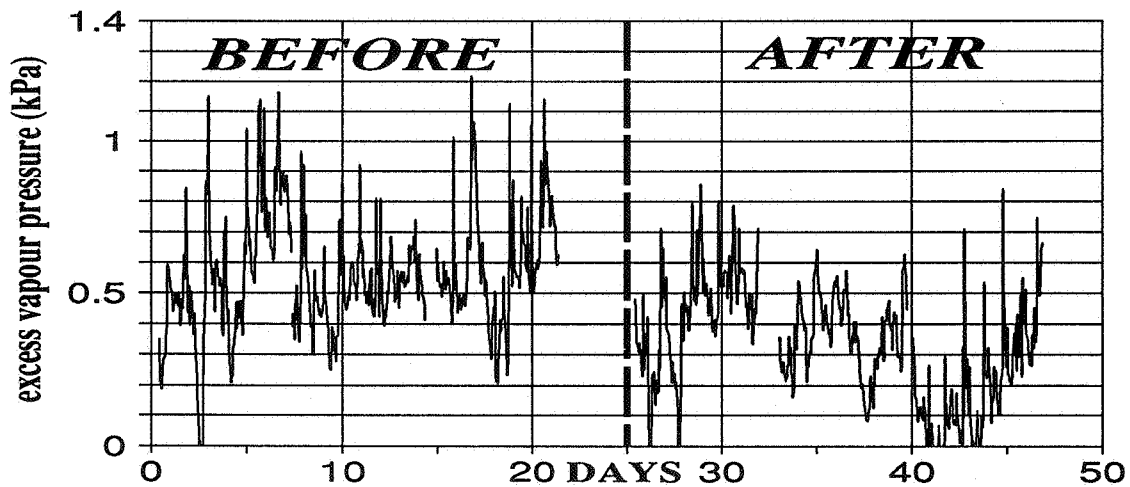


Figure 4: The installation of extract devices in case study 1 in normal use, reduced the mean excess vapour pressure in the three of the four rooms.

less frequently, the excess vapour pressure has increased. The average excess vapour pressure of the three rooms (excluding the bathroom) are presented in Fig. 4. The average reduction of mean excess vapour pressure is over 40%, which for an average temperature of 19°C results in an average RH reduction of more than 10%. The RH in the bathroom has increased by 4% (from an average value of 70% before the installation of the fans to 74% after).

BS5250 [14] classifies households as "dry", "moist" and "wet" occupancy. Dry occupancy (usually a building unoccupied during the day) results in an internal vapour pressure up to 0.3kPa in excess of the external vapour pressure. In moist occupancy water vapour excess is between 0.3kPa and 0.6kPa while in wet occupancy water vapour excess is greater than 0.6kPa. As shown in Table 1, the three households studied although unoccupied during the day fall into the moist category.

In case study 1, excess vapour pressure was reduced by 50% in the kitchen, almost 40% in the living room and 25% in the bedroom, bringing the values near the "dry" occupancy category. The reverse has happened in the bathroom, because of the high setting of the humidistat.

Table 1: Mean values of excess vapour pressure in the three case studies before and after the installation of extract devices.

		Kitchen	Living Room	Bedroom	Bathroom
CASE 1	before	0.68	0.51	0.51	0.52
	after	0.33	0.31	0.38	0.64
	% change	-51	-39	-25	+23
CASE 2	before	0.54	0.22	0.43	0.66
	after	0.51	0.36	0.41	0.45
	% change	-5	+63	-5	-32
CASE 3	before	0.54	0.45	0.53	0.45
	after	0.46	0.34	0.26	0.30
	% change	-15	-24	-51	-33

In case study 2, the results are less dramatic with only 5% reduction in the kitchen and in the bedroom but more than 30% reduction in the bathroom. In this case the volume of the bathroom is smaller than case study 1 and the humidistat was set more reasonably to 70%RH. The operation of the fans has increased the humidity in the living room. This is probably due to the fans in the kitchen and bathroom through which the air is mainly extracted so that infiltration occurs mainly through the living room in the downstairs half of the dwelling. This change of air flow patterns coupled with the higher external vapour pressure during the "fans operating" monitoring period and the low ventilation rate in the living room, has increased the vapour pressure in it.

In case study 3, there is also a reduction in the excess internal vapour pressure after the installation of the fans. In this case, the greatest reduction is observed in the bedroom (more than 50% reduction) which is affected by moisture in the kitchen and the bathroom because of the flat's layout.

As nothing has change in the operation of the households after the installation of the ventilation devices, we can assume that the operation of the fans (higher ventilation rates where and when required) has produced the reduction of the excess internal vapour pressure. Also, because moisture is extracted at source rooms at the time it is produced, the effect should be greater than uniformly increasing the ventilation rate at all times. Intermittent ventilation as and when required also eliminates energy waste.

Let us use case study 1 as an example to demonstrate this point. The ventilation rate of the dwelling was measured using the tracer gas decay method. It was found the average ventilation is 0.53AC/H without any extract devices on, while the ventilation rate becomes 0.85AC/H when the cooker hood is on in the kitchen. The higher ventilation rate happens only for about one hour per day and this has an effect of almost 40% reduction in the average excess vapour pressure of the house. In addition, it may replace opening windows during cooking which would waste more energy without offering the efficiency of a cooker hood.

The discussion of section 3 was concerned with the steady state performance of the three houses and has shown that reduction of the excess vapour pressure is possible by using extractor fans. This finding agrees with findings of a nationwide survey in UK [15] which concluded that *ventilation devices*, air movement, heating and insulation are more important than occupants' behaviour and energy consciousness. However, what it has not shown so far is by how much the moisture production in the kitchen and in the bathroom affects the humidity of other rooms and what is the effectiveness of each fan in isolation. For this reason, experiments on cooking and bathing simulations with simultaneous tracer gas release were performed in two of the case-studies (1 and 3) to examine the effect of air flow on the migration of moisture and the effect of adsorption by surfaces.

4 MEASUREMENTS OF MOISTURE AND AIR FLOW

It has been found [16] that if adsorption and condensation are ignored water vapour behaves very similarly to tracer gases. Therefore, if a way of accounting for absorption and condensation were found, tracer gases, could be used to predict airborne moisture movement in buildings. For this reason, as well as to understand the relation between the layout of a dwelling and the effect of adsorption in the migration of moisture from source to sink rooms, the following experimental procedure was set up.

Periods of cooking and bathing were simulated and the spread of two contaminants (water vapour and sulphur hexafluoride) from a hot source to various rooms was measured. To simulate cooking the contaminants were released for 25mins from the cooker's hot plate. In this experiment 1.46 litres of water was boiled and 2500 ml of tracer gas was released. To simulate bathing the contaminants were released for 11.5 mins, from the middle of the bath (total amounts released 0.62 l of water and 1150 ml tracer gas). The concentrations were measured with a Bruel & Kjaer photo-acoustic effect gas analyser which pumped samples of air from each room via an automated manifold, measuring one room in two minutes. Nineteen experiments were performed in each dwelling to include different settings of the fans.

The Transfer Index (TI) [17] in each room was calculated for the moisture and sulphur hexafluoride. The average Transfer Index of all the rooms in any experiment represents the total contaminant load of the house thus indicating the effectiveness of a specific fan for a specific flow rate for a particular plan configuration. Figures 5 and 6 demonstrate the removal effectiveness of the fans examined in the two flats.

It can be seen from the figures that during the bathroom experiments the air becomes saturated and the fan proved to be underpowered in removing the moisture even at its boost position (29l/s) in both flats. Therefore, no comparison can be easily made with the tracer gas behaviour. However, it can be seen that the flow rate recommended by the Building Regulations for intermittent powered extraction in bathroom (15l/s) is an underestimate.

In the kitchen experiments almost straightforward comparisons between moisture and tracer gas removal are possible. In case study 1 the cooker hood at all settings proved to be more effective than the extractor fan. In case study 3, however, the cooker hood and the fan seem to be almost equally effective. This introduces another dimension into the problem. In case study 3 the fan is situated nearer to the cooking hob than in case study 1. Therefore, the proximity of the source and removal at source appear to be important.

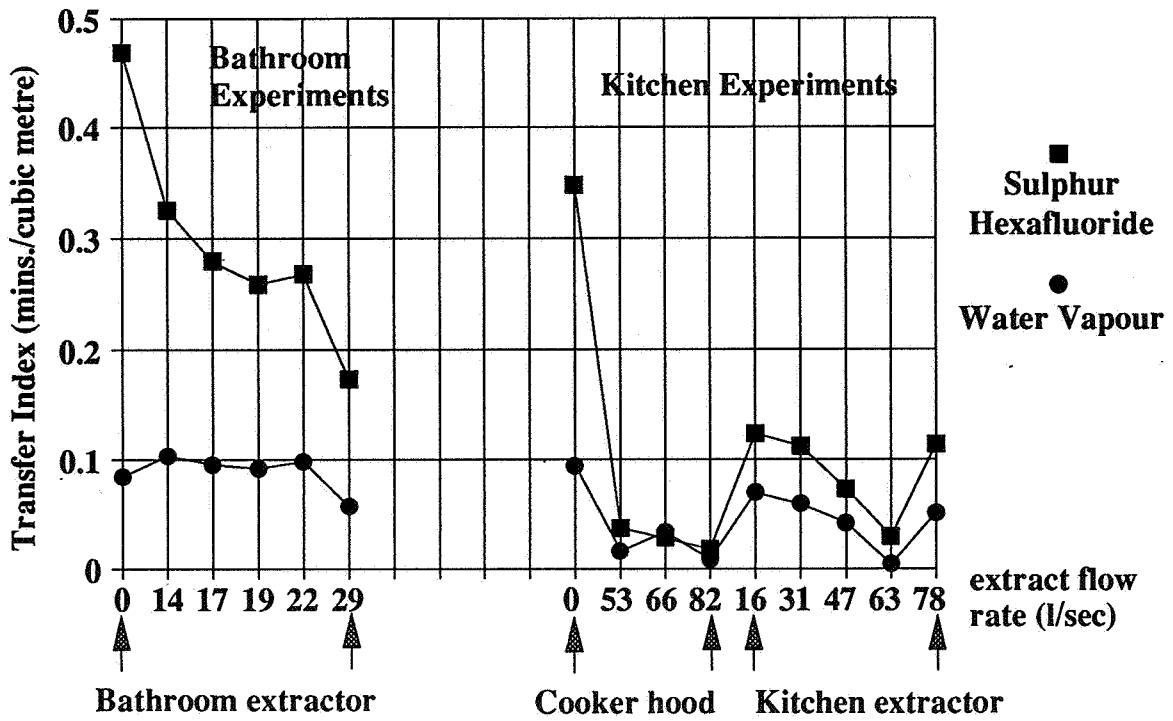


Figure 5: Effectiveness of the extract systems judged by the effect in the whole dwelling of case study 1.

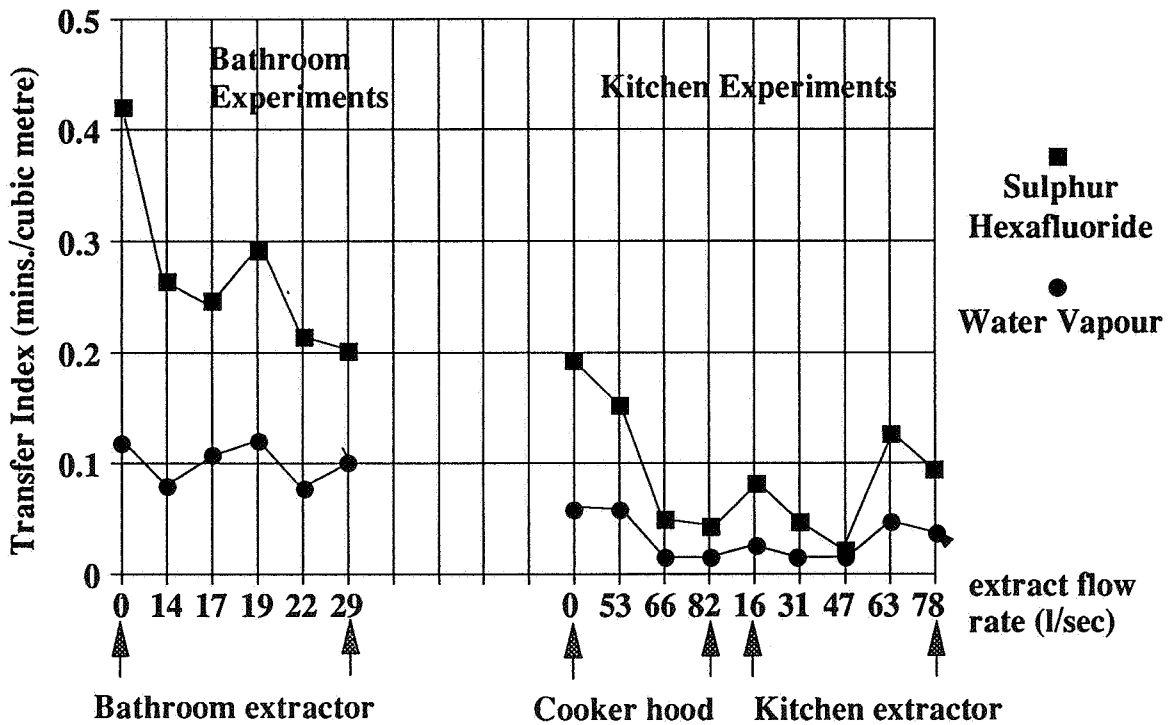


Figure 6: Effectiveness of the extract systems judged by the effect in the whole dwelling of case study 3.

So far the average TI of the dwellings as a whole was considered. By examining the TI of each room separately we can begin to understand the impedance of pathways for the pollutant migration between zones. The degree of linkage reflects the adjacency of the rooms and configuration of the building plan. The linkages for the two case studies are presented in Table 2. It can be seen from Table 2 that moisture absorption by surfaces is considerable, resulting in much lower TI values for moisture than for the tracer gas. However a strong correlation between the TI of tracer gas and moisture exists; $r=0.993$ for case study 1 and $r=0.994$ for case study 3. This indicates the suitability of tracer gas to describe airborne moisture movement between spaces.

In addition, a correlation between the monitored data and short term simulation type experiments of cooking and of bathing was found, indicating that the long term performance of extract devices for each room of a house can be predicted by short term experiments. A correlation of $r=0.949$ was found in case study 1 and $r=0.82$ for case study 3. The correlation with tracer gas measurements is also strong ($r=0.95$ in case study 1 and $r=0.734$ in case study 3). These results indicate that it might be possible to predict the effect of ventilation devices on moisture by performing short term experiments using either water or tracer gas.

The above correlations were calculated as follows; the steady state change of vapour pressure in each room can be expressed by the ratio of the average excess vapour pressure in each room after the installation of the fans to the average excess vapour pressure before the installation. This value can be compared with the ratio of a room's TI calculated from experiments in which some fans were used to the TI for which no fans were used. It was found that the best relationship exists if the steady state values are correlated with the average of the TI calculated from (a cooking experiment without fans) + (a cooking experiment with the cooker hood on) + (a bathing experiment with the bathroom fan on) divided by the average of a cooking and a bathing experiment with no fans.

Table 2: Average linkages between rooms for tracer gas and moisture during cooking and bathing experiments.

		Kitchen	Living Room	Bedroom	Bathroom
CASE 1					
Cooking- Experiment	SF ₆	0.155	0.085	0.055	0.061
	H ₂ O	0.072	0.037	0.019	0.024
Bathing- Experiment	SF ₆	0.080	0.131	0.205	0.668
	H ₂ O	0.030	0.035	0.073	0.226
CASE 3					
Cooking- Experiment	SF ₆	0.183	0.067	0.026	0.048
	H ₂ O	0.059	0.030	0.013	0.019
Bathing- Experiment	SF ₆	0.062	0.109	0.159	0.664
	H ₂ O	0.038	0.035	0.071	0.233

5 CONCLUSIONS

The effectiveness of extract devices and the merits of user control versus humidistat control, have been discussed before [18,19] and reviewed [20]. Also the capture efficiency of cooker hoods has been investigated [21,22]. In this paper the aim was to examine the effect that the installation of "off the shelf" extractor devices has on the humidity in occupied small dwellings.

The use of tracer gas techniques to augment humidity measurements has been investigated before [23,24], and short term measurements have been made of humidity in kitchens and adjacent rooms [25] and in bathrooms [26]. The uniqueness of the present study is in offering monitored data of moisture before the installation and during normal use of extract devices in occupied dwellings coupled with "laboratory" like experimental measurements of tracer gas and water vapour taken in the same dwellings.

From the monitored data it was found that a reduction of the excess vapour pressure was observed in most rooms of the case-studies after the installation of ventilation equipment. The biggest changes were found in the source rooms (kitchen and bathroom) but considerable changes occurred in the sink rooms (living room and bedroom).

From the experiments the average Transfer Index of the house as well as zone Transfer Indices (for individual rooms) were calculated which give useful information for the linkage of sink rooms to source rooms and information on the effectiveness of individual extract devices for the particular house configuration. The linkage values depend on the length and shape of the pathway and determine how easily contaminants can migrate. Finally, by comparing tracer gas and water vapour measurements we can get an impression of the amount of moisture adsorbed by the surfaces and the effect of surface condensation.

It was found that Transfer Indices derived from water vapour measurements describe the steady state performance of the moisture balance in the examined case studies. There is also a strong correlation between the transfer indices calculated from tracer gas and water vapour measurements. The actual values differ considerably. It was found [27] that this is due to adsorption by surfaces and condensation, and not to any other mechanisms of airborne contaminant migration. Therefore, if adsorption and condensation can be accounted for by using some coefficients [28], tracer gas short term experiments in existing houses or even CFD analysis for proposed design can be used to predict the long term steady state moisture balance of a dwelling.

6 ACKNOWLEDGMENTS

Thanks are due to Xpelair and Airflow Developments for supplying the extract devices fitted in the case-studies and to the owners of the dwellings Mr and Mrs Lemmon, Mr McCallum and Mr McKrith for their cooperation. This project is supported by the Science and Engineering Research Council (SERC) of the UK.

7 REFERENCES

- 1 Phaff J C and deGids W F, *Airflow driven Contaminants, Transport through Buildings*, Proc 'Air Movement & Ventilation Control Within Buildings' 12th AIVC Conference, Ottawa, Canada, pp123-140, 1991.
- 2 Seymour J, *Science on your doorstep*, New Scientist, pp50-52, 7 Dec 1991.
- 3 Strachan D P and Sanders C H, *Damp Housing and Childhood Asthma; Respiratory Effects of Indoor Air Temperature and Relative Humidity*, Journal of Epidemiology and Community Health, Vol43, No1, pp 7-14, March 1989.
- 4 Packer C N, Stewart-Brown S and Fowle SE, *Housing and Health in Worcester, Some Associations from a Lifestyle Survey of Residents aged 16-64*, in Conf 'Unhealthy Housing: The Public Health Responses' University of Warwick, Legal Research Institute, 18-20 Dec 1991.
- 5 Svendsen UG, Olsen O T and Pedersen L N (eds), *House dust mites and allergy*, Position papers, Danish Society for Allergology, Allergy, Supplement Vol 46, No 11, Munksgaard Copenhagen, 1991.
- 6 *The role and Control of Humidity in IAQ*, Indoor Air Quality Update, Vol4, No 7, July 1991.

- 7 *English House Condition Survey:1986, Supplementary (Energy) Report*, Chapter 8 Damp and Mould Growth, London, HMSO, 1990.
- 8 White J, *Moisture, Mould and Ventilation*, Solplan Review, pp3-6, April-May 1991.
- 9 Samuelson I, *Mould Problems in New Swedish Building*, AIVC Technical Note 20, Airborne Moisture Transfer, New Zealand Workshop, 1987.
- 10 Trethowen H A, *Air, Earth, Water.... The Sources of Moisture*, AIVC Technical Note 20, Airborne Moisture Transfer: New Zealand Workshop, 1987.
- 11 *The Building Regulations 1985*, Part F, Ventilation, HMSO, 1990 Edition.
- 12 Garrat J and Nowak F, *Tackling Condensation*, BRE Report, 1991.
- 13 International Energy Agency, Annex XIV, *Condensation and Energy*, Vol 1-4, 1991.
- 14 British Standard 5250, *Control of Condensation in Buildings*, British Standards Institution, 1989.
- 15 Raw G and Fox T A, *Condensation, Heating and Ventilation in Small Homes*, Building Research and Information, Vol 19, No 2, 1991.
- 16 Kolokotroni M, Saiz N and Littler J, *Moisture Movement: A Study Using Tracer Gas Techniques and CFD Modelling*, Building Services Engineering Research & Technology, Vol13(2), pp113-117, 1992.
- 17 Brouns C and Waters B, *A Guide to Contaminant Removal Effectiveness*, AIVC Technical Note 28.2, 1991.
- 18 Boyd D and Cooper P, *Domestic Kitchen Extract Fans: Effectiveness in Surface Condensation Prevention*, Building and Environment, Vol 24, pp 335-345, 1989.
- 19 Cornish P, *Condensation & Mould Growth*, Building Services, p75, Sep 1984.
- 20 Parnham P, *The effectiveness of Domestic Extract Fans*, Proc Unhealthy Housing: The Public Health Response, Warwick University, Dec 1991.
- 21 Geenrinckx B, Wouters P and Vandaele L, *Efficiency Measurement of Kitchen Hoods*, Air Infiltration Review, Vol 13, No 1, pp15-17, Dec 1991.
- 22 Yu Y, Narasaki M, Satoh R and Yamanaka T, *Prediction of Capture Efficiency of Kitchen Exhaust System Buoyant Plume From Gas Cooking Stove*, Proc 'Indoor Air '90' Vol4, Building and System Assessments and Solutions, pp497-502, 1990.
- 23 Oldergarm J, Pernot C and deWit M, *Modelling: combined heat, air and moisture transport*, Chapter 5 in 'Condensation and Energy, Sourcebook, Report Annex XIV, Vol1, IEA, 1991.
- 24 Oldengarm J and deGids W F, *Field Experiments on Airborne Moisture Transport*, Air Infiltration Review, Vol 12, No 2, pp8-11, March 1991.
- 25 Poel A, *Vapour Distribution in Dwellings: A Preliminary Study*, NCIV Dutch Institute for Social Housing, Contribution to Annex XIV, IEA, 1988.
- 26 Fransson J, *Ventilation and Humidity in Bathrooms*, in 'Air Movement & Ventilation Control Within Buildings', 12th AIVC Conference, pp 173-185, Sep 1991.
- 27 Kolokotroni M, Saiz N and Littler J, *Effects of Air Movement on the Moisture Distribution Within a Zone*, in 'Quality of the Indoor Environment' Lester J N, Perry R and Reynolds G L (Eds), Selper Ltd, pp 179-196, 1992.
- 28 Jones R H L, *Modelling Water Vapour Pressure Conditions in an Enclosed Space*, BRE/122/2/1, March 1990.

**Ventilation for Energy Efficiency and Optimum
Indoor Air Quality
13th AIVC Conference, Nice, France
15-18 September 1992**

Paper 14

**Correlation Between Carbon Dioxide Concentration
and Condensation in Homes.**

A. Grelat^{*}, M. Cohas^{*}, M-C. Lemaire^{}, R.
Fauconnier^{***}, D. Creuzevault^{****}, J-C.
Loewenstein^{*****}**

*** CEBTP, Domaine de Saint Paul, BP 37, 78470
Saint Remy Les Chevreuse, France**

**** ADEME, 500 Route des Lucioles, Sophia
Antipolis, 06565 Valbonne Cedex, France**

***** FNB, Domaine de Saint Paul, BP 1, 78470
Saint Remy Les Chevreuse, France**

****** GDF-DETN, 361 Avenue du President Wilson,
93211 La Plaine Saint Denis, France**

******* EDF-DER, 6 Quai Wattier, 78401 Chatou,
France**

CORRELATION BETWEEN CO₂ CONCENTRATION AND CONDENSATION IN HOMES

Alain GRELAT, Michel COHAS
CEBTP, Domaine de Saint Paul, BP 37
78470 SAINT REMY LES CHEVREUSE

Marie Claude LEMAIRE
ADEME, 500, Route des Lucioles, Sophia Antipolis
06565 VALBONNE Cedex

Roland FAUCONNIER
FNB, Domaine de Saint Paul, BP 1
78470 SAINT REMY LES CHEVREUSE

Didier CREUZEVAULT
GDF-DETN, 361, Avenue du Président Wilson
93211 LA PLAINE SAINT DENIS

Jean-Claude LOEWENSTEIN
EDF-DER, 6, Quai Wattier
78401 CHATOU

1. INTRODUCTION

Ventilation systems in dwellings should not only maintain the quality of the air, in other words limit pollutant concentration whatever the origin, but protect the structure, that is, limit condensation and the storage of excessive humidity in existing materials.

Domestic ventilation represents a significant element of energy loss. It is a function that should be provided at minimum cost in terms of energy and therefore be directly dependent on fresh air requirements. Hence the introduction on the market of so-called hygro-adjustable ventilation systems. However, these systems do not necessarily meet air quality requirements and, at present, on the French market, there is no existing model of a ventilation system adapted to the residential sector and controlled by gaseous pollution content.

To be able to offer dual heating/ventilation systems which meet air quality requirements, while remaining low on energy costs, the ADEME, GDF, EDF, FNB and CEBTP have combined their skills and capabilities in a research programme involving, first a national survey followed by in-situ measurements and, second, the development of a hygrothermal and ventilation code incorporating pollutant transfers i.e: the BILGA programme (FNB/CEBTP).

One application of the programme was to find out whether there was a correlation between carbon dioxide concentration (present in most pollutive productions) and condensation hazards in dwellings, making it possible to control ventilation on the basis of a single criterion and then examine various ventilation strategies.

This study is currently in progress.

2. THE BILGA PROGRAMME

Developed in 1980 by the CEBTP and the FNB, BILGA is a hygrothermal and multi-zone ventilation simulation tool based on a detailed description of the building shell, the ventilation system, occupancy and environment.

In order to best define indoor atmospheres, the basic version was completed by two modules which allowed for humidity exchanges with the furniture and the walls, as also the transfer of gaseous pollutants, the aim being to determine an overall air quality index for a given dwelling.

2.1 Humidity Exchanges

The general equation of the mass balance of steam in a room may be written as follows:

$$\dot{m}_w = \dot{m}_e - \dot{m}_s + \dot{m}_o + \dot{m}_a - \dot{m}_m - \dot{m}_p \quad [\text{kg/s}]$$

where:

- \dot{m}_e , \dot{m}_s are the mass flowrates of steam entering and leaving the room by convection process,
- \dot{m}_o , \dot{m}_p the internal production due to the metabolism and activities of the occupants,
- \dot{m}_m , \dot{m}_p the flowrates of steam absorbed/desorbed by the furniture and walls.

2.2 Gaseous Pollutant Transfers

The model currently takes into account the evolution of ten gaseous pollutants (CO_2 , CO, NO_2 , HCHO, O_3 , ...).

The overall equation of the mass balance of a pollutant in a given room can be written:

$$V \cdot dC / (E_f \cdot dt) = F_p \quad [\text{g/s}]$$

V being the volume of the zone, C the pollutant concentration, E_f the ventilation system efficiency (as a function of the air renewal rates, the location of the ventilation openings and the source of pollution). F_p being the pollutant flux corresponding to:

- internal productions due to occupancy and appliances,
- productions/absorptions due to materials and chemical reactions,
- pollutant fluxes exchanged with the exterior and with other rooms, by convection, diffusion and gravity.

2.3 Air Quality Index

An air quality index defined by the "Fédération Nationale du Bâtiment" (National Building Federation), postulates occupant exposure to a pollutant and two limit concentration values:

$$AQI(p,ts) = \frac{E(p,ts) - LRV(p,ts)}{SRV(p,ts) - LRV(p,ts)}$$

$E(p,ts)$ [exposure] is the maximum mean concentration level during the life ts of the pollutant p in the room,
 LRV the Limited Risk Value,
 SRV the Significant Risk Value, as defined by the pollutant.

If $AQI < 0$, the pollutant is without effect on the occupants,
if $AQI \geq 1$, the risk due to pollution is deemed "unacceptable".

The air quality index of the least favourable room in a dwelling was assumed to be the overall air quality index for that dwelling.

For this study, the overall air quality index for a dwelling was determined on the basis of carbon dioxide concentrations, considered to be the pollutant the most representative of domestic activity (occupancy, smoking, cooking appliances, the exterior).

Confronted with the diversity of the limit values proposed for carbon dioxide, we have assumed the WHO values (1982):

$$\begin{aligned} LRV \text{ CO}_2 &= 4500 \text{ mg/m}^3 \quad (2300 \text{ ppm}) \\ SRV \text{ CO}_2 &= 12000 \text{ mg/m}^3 \quad (6100 \text{ ppm}). \end{aligned}$$

3. CONDENSATION AND AIR QUALITY INDEX

3.1 Hypotheses

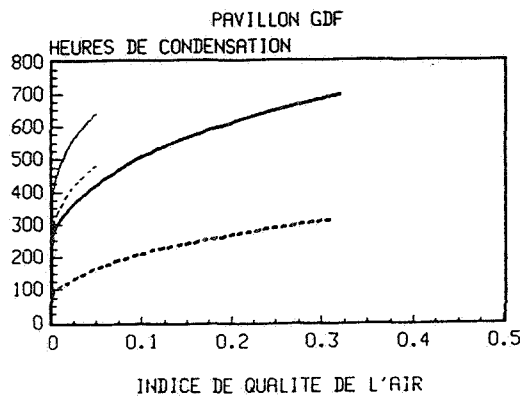
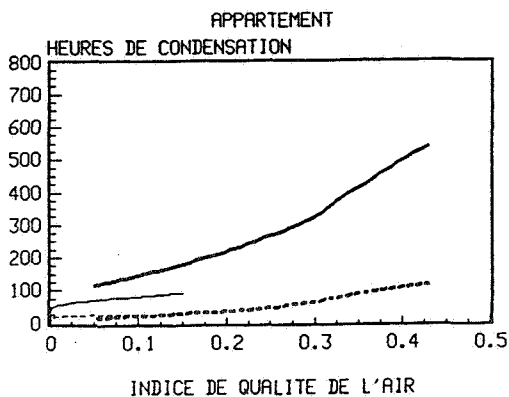
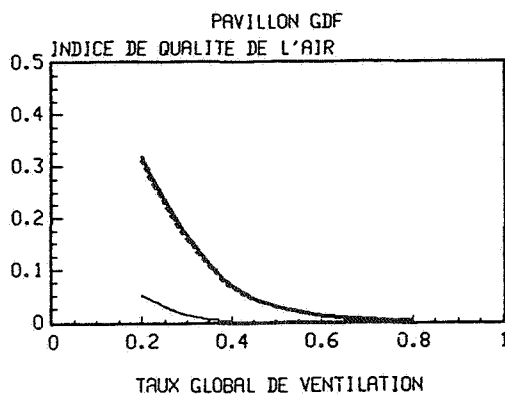
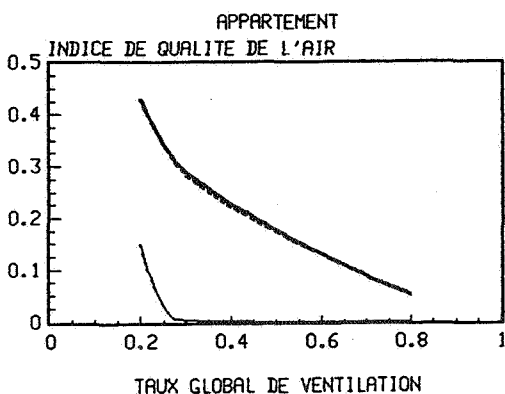
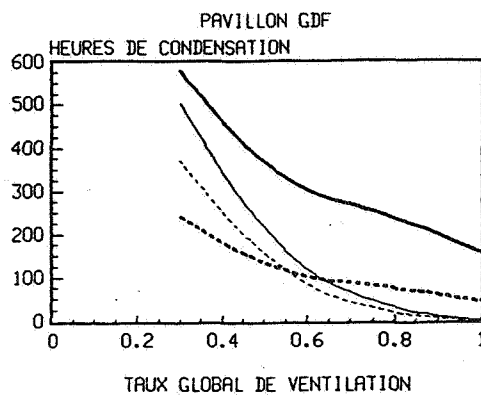
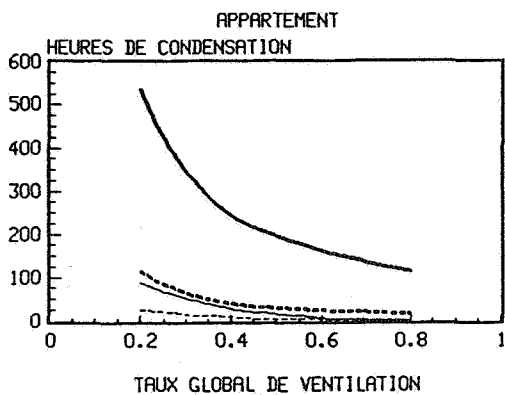
This study covered an eight-month period and involved two types of dwellings (an individual house and an apartment in a multi-family apartment block) in a temperate climate (STRASBOURG and CARPENTRAS).

The global ventilation rate (single status) varied from 0.2 to 0.8 volume/hour. The internal masses were not taken into account. Daily steam production in the kitchen was 3.2 kg. The kitchen was fitted with a 2.3 kW oven (CO_2 emission: 98 mg/s) and with a 3 kW cooker (CO_2 emission: 150 mg/s) operating according to 9 min. sequences.

3.2 Results

The graphs hereinafter show the relations obtained between ventilation rates, condensation hazards and the air quality index in the different situations analysed.

Condensation times and air quality index
as a function of the ventilation rate



— SDB
STRASBOURG
— CUISINE
STRASBOURG

--- SDB
CARPENTRAS
--- CUISINE
CARPENTRAS

Whatever the climate and type of housing, the highest condensation hazards are to be found in the kitchen (production of 3.2 kg/24 h).

By comparison with the individual house, for a same given climate and same global ventilation rate (0.3 vol/h), the apartment exhibited less significant condensation hazards in the kitchen (lower occupancy rate) and in the bathroom (no wall in contact with the exterior).

Although the influence of climate was significant on condensation hazards, it was negligible on the air quality index.

The global air quality index is that of the kitchen (related to the use of cooking appliances).

By comparison with the individual house, for a same given total ventilation rate, the total air quality index was higher in the apartment (the kitchen air renewal rate was lower), but remained acceptable for a low total ventilation rate (0.2 vol/h).

In spite of the existence of Controlled Mechanical Ventilation, steam and carbon dioxide migrations from the kitchen to the main rooms were observed.

Such transfers are the consequence of extensive ventilation recycling caused by a temperature rise in the kitchen when cooking appliances are put to use.

Condensation can occur on windows while the quality of the indoor air is satisfactory and, conversely, in the presence of smokers and with an extremely reduced ventilation rate, an unacceptable pollution level is observed without any concomitant condensation.

There is a predominant occurrence of condensation in bathrooms.

The mildness of the climate increases the degree of independence of condensation hazards in relation to the air quality index.

The correlation between condensation hazards and the overall air quality index being globally slight, the results of the study show that the dependence of domestic ventilation on a single criterion (condensation or pollution), cannot constitute a universal solution for maintaining satisfactory indoor atmospheres.

However, as will be seen later, the situation should be examined differently for each type of room, and allowance made for the type of heating and domestic equipment.

4. STUDY OF DIFFERENT VENTILATION CASES

4.1 Objective

A proposal for a ventilation system can be based on a forecast estimation of efficiency in respect of the three criteria i.e: air quality, hygrometry limitation and energy saving.

By virtue of their different functions, the situations in the rooms of a dwelling show extreme differences:

Kitchen : significant emissions, short and generally correlated of CO₂ and steam.
Bathroom : significant short steam emission, CO₂ emission limited to a single person.
Bedrooms : slight correlated emissions of CO₂ and steam.
Living-room: slight steam emission related to occupancy, occasional emission of pollutants (smokers).

A very slight ventilation rate is required in the absence of any occupancy.

The ventilation system should therefore provide a response adapted to each situation.

The following study proposes an example of a comparison between certain ventilation strategies in order to single out certain trends.

4.2 Study hypotheses

The study was carried out on a standard, multi-family, four-roomed dwelling (210 m³), based on realistic occupancy hypotheses (assumed in order to assess the hygro-adjustable systems), over the course of two five-day periods, typical of winter in the Paris area, one being moderately cold (-5, +1 °C, 70-95 % HR) and the other mild and damp (+5, +10 °C, 75-95 % HR).

The CO₂ emission from appliances was the same as above.

Humidity exchanges with the furniture and walls were taken into account.

Three types of ventilation were considered:

- conventional CMV system : (Type 3)
45 m³/h in kitchens, 60 m³/h in sanitary units.
- hygro-adjustable ventilation: (Type 2)
kitchen : 10 to 45 m³/h for 35 to 65% RH
bath-room : 5 to 45 m³/h for 35 to 65% RH
W-C : 30 m³/h permanent basis.
- reduced ventilation : (Type 1)
10 m³/h in kitchens, 35 m³/h in sanitary units.

With or without, in each case, the utilization of a high flow-rate in kitchens (120 m³/h) for 2 hours a day, when cooking appliances were in use.

4.3 Results

The graphs hereinafter show the different types of results for both periods:

- In-flow, heating consumption on fresh air intake,
- Condensation times (kitchen and bath-rooms),
- Maximum CO₂ concentrations (averaged over an hour).

The minimum ventilation option results in unacceptable condensation times and air quality.

In rooms located on facades that are oriented "under the wind", the effect of the prevailing wind impedes the effect of ventilation, and moreover, the air quality deteriorates in such rooms (not shown).

Hygro-adjustable ventilation is more efficient when climatic conditions are cold and dry. In periods of mild damp weather, efficiency and utilization costs are comparable to those of the conventional CMV.

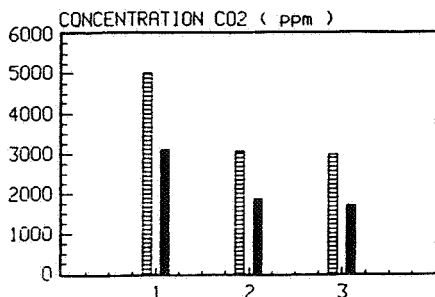
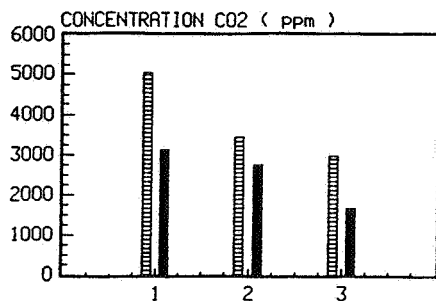
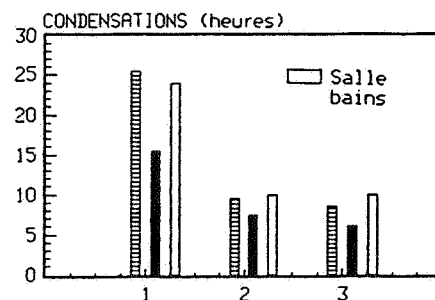
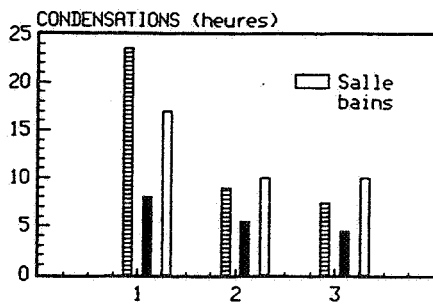
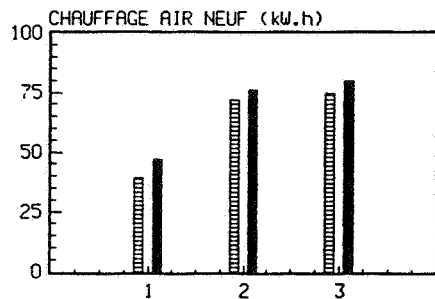
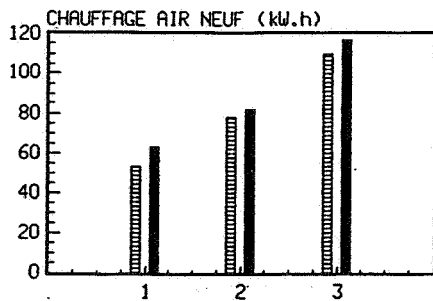
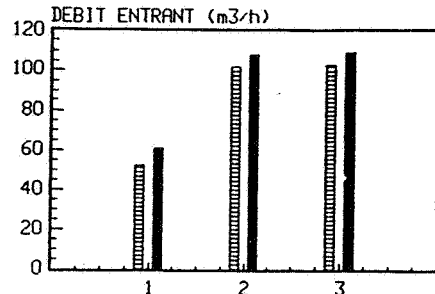
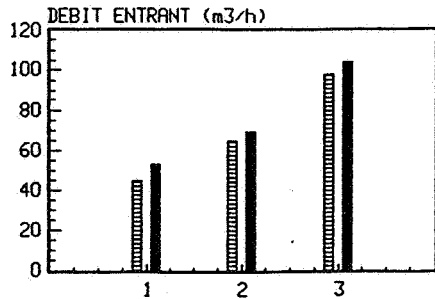
In all cases, the use of accelerated ventilation flow in the kitchen considerably reduces the risk of condensation and maximum CO₂ concentration for only a minor extra cost in terms of energy.

Absence of condensation in the bath-room, when in use, can only be achieved under accelerated operating conditions.

These observations suggest, that for systems of ventilation by extraction, provision should be made for 3 levels of activity:

- reduced operating conditions for periods of non occupation (governed, for instance by CO₂ concentration used as a monitor),
- low occupancy operating conditions, which complement the above,
- forced operating state, governed by the presence of humidity or CO₂ according to the intended purpose of the room in service and the manner in which it is fitted out.

Comparison of Ventilation Scenarios



TYPE DE VENTILATION

TYPE 1 : REDUIT
 TYPE 2 : HYGROREGLABLE
 TYPE 3 : NORMAL

■ STATUT DOUBLE
 ▨ STATUT UNIQUE

TYPE DE VENTILATION

TYPE 1 : REDUIT
 TYPE 2 : HYGROREGLABLE
 TYPE 3 : NORMAL

**Ventilation for Energy Efficiency and Optimum
Indoor Air Quality
13th AIVC Conference, Nice, France
15-18 September 1992**

Paper 13

**Improved Ventilation Combined with Energy
Efficiency in Naturally Ventilated Houses.**

A. Blomsterberg

**Swedish National Testing and Research Institute,
Box 857, S-501 15 Borås, Sweden.**

SYNOPSIS

Modern one-family houses in Scandinavia built before 1980 are often naturally ventilated and heated by electric baseboard heaters. The overall supply of fresh air is often inadequate during the heating season in many of these houses. Long periods of time individual rooms might get too little fresh air. The performance of a natural ventilation system is very much dependant upon the overall airtightness and the distribution of the airtightness of the building and the weather.

This paper examines the performance of six modern one-family houses before and after the ventilation system was improved. Different means of improving ventilation are described. The constant concentration tracer gas technique was used to examine the supply of fresh air. Fan pressurization combined with infrared photography were employed to characterize the air leakage of the building. A simplified theoretical model was used to further evaluate the measurements.

It is obvious from the tested houses that the overall ventilation and the ventilation of individual rooms were improved. The ventilation losses were increased and therefore energy conserving measures had to be taken. The overall costs were high compared with the energy savings obtained.

LIST OF SYMBOLS

ach = air changes per hour

1. INTRODUCTION

In Sweden there are close to 500000 one-family houses heated by electric baseboard heaters. Of them 90 % were built before 1980. In this group the most common ventilation system is natural ventilation. Half of all houses with electric baseboard heaters were built between 1971 and 1980.

The Swedish Council for Building Research has been asked by the Swedish government to carry out a program concerning the efficient use of electricity in buildings. Consequently one-family houses with electric baseboard heaters and with a high consumption of electricity are an area where research and development and demonstration projects are needed.

Making the use of electricity efficient in one-family houses with electric heating includes measures to reduce the consumption and to reduce the power demand. In one project, which is carried out in four different cities (Umeå, Stockholm, Göteborg and Lund), 37 one-family houses have been investigated.

The object of the project is to show how electrically heated one-family houses can use electricity more efficiently employing existing techniques. The indoor climate is to be kept at the same level or improved. An important aspect of indoor climate is ventilation, which was an important part of the investigation in Lund. This paper deals with the investigation in Lund, which included six houses .

2. THE HOUSES TESTED

Two types of houses were studied, a 1½ storey detached one-family house and a one storey detached one-family house. Both types are very common in Sweden. The 1½ storey house is part of a group of 100 identical houses built in 1974. The houses are 140 m², with a kitchen, laundry, bathroom, living room, bedroom downstairs and three bedrooms and a bathroom upstairs. A detached non-heated storage also belongs to the house. The one storey house is part of a group of 120 identical houses built in 1974. The houses are 121 m², with a kitchen, laundry, bathroom, living room and 3 - 4 bedrooms.

The 1½ and the one storey houses are built on a slab on grade. Space heating is provided by electric baseboard heaters and an electric heating cable (1 kW) inside the slab along the perimeter of the house. The exterior walls are of traditional wood frame construction with 120 mm of mineral wool. The attic insulation consists of 150 mm of mineral wool. The windows have double panes. The window area is large, 28 % of the floor area. The houses are naturally ventilated with vertical shafts from bathrooms, kitchen and laundry. There are no supply vents for outdoor air.

3. TEST METHODS

3.1 AIRTIGHTNESS

The standard method for finding the leakage function of a building is fan pressurization. The estimated inaccuracy in the measured air leakage is $\pm 10\%$. According to the Swedish standard for fan pressurization all openings in the exterior envelope intended for ventilation purposes must be sealed before the test is performed. Other openings are kept closed. For the purpose of modelling air infiltration and exfiltration it is advantageous to also make a test with open supply vents part of an exhaust fan ventilation system and with open vertical shafts part of a natural ventilation system.

3.2 VENTILATION

The most straightforward method of measuring the total ventilation rate i.e. the combined effect of mechanical ventilation and natural ventilation is to measure it directly (Blomsterberg 1990). In a mechanical ventilation system the air flow in the ducts can be measured with different techniques for volume and mass flow rate measurements. There are many ways of measuring total ventilation, and almost all of them involve a tracer gas, which permits the indoor air to be labelled so that the outdoor air ventilation can be traced.

The tracer gas is injected into and mixed with the indoor air and its concentration is monitored. The mixing is assumed to be complete, which is probably the largest single source of error in tracer gas measurements. There are three different schemes; decay, constant concentration, and constant flow of a tracer gas. All

measurements are governed by the continuity equation. The single-chamber continuity equation is given here:

$$V \frac{dC}{dt} + Q C = F$$

where V is the effective volume, m^3

$\frac{dC}{dt}$ is the time rate of change of concentration

Q is the outdoor air ventilation rate, m^3/s

C is the concentration and

F is the effective injected tracer gas flow rate, m^3/s

In the two houses tested a constant concentration of tracer gas was maintained in order to measure the ventilation rate. One of the principle advantages with this technique is that it eliminates the problem of estimating the effective volume as the effective volume is eliminated from the continuity equation ($\frac{dC}{dt} = 0$). The outdoor air ventilation is obtained directly. The field of application for the constant concentration technique is to continuously monitor the supply of outdoor air to several individual rooms simultaneously, i.e. outdoor air which enters an individual room directly instead of first passing through an adjacent room. The estimated inaccuracy in the measured outdoor air ventilation rate is $\pm 10\%$.

4. RESULTS AND DISCUSSION - BEFORE RECONSTRUCTION

In all six houses the airtightness has been tested before reconstruction. When these houses were built there was no official requirement on airtightness. All houses were pressurized and depressurized with open and closed vertical shafts (see table 1).

Table 1. Measured airtightness at 50 Pa, ach.

House	closed shafts	open shafts
# 1, 1 storey	2,5	4,4
# 2, 1 storey	2,9	5,3
# 3, 1 storey	2,9	4,5
# 4, 1½ storey	4,1	5,4
# 5, 1½ storey	3,7	5,3
# 6, 1½ storey	4,7	5,8

All houses have a good level of airtightness, the one-storey houses even meet today's requirement. The 1½ storey houses are leakier, generally due to the fact that it is difficult to achieve a good airtightness in the joints between ceiling and wall upstairs and the joint between the intermediate floor and exterior walls. This is in particular valid for a house without a continuous plastic air/vapour barrier.

Tracer gas measurements using the constant concentration technique were performed in two houses, # 1 and # 4. House # 1 had a total outdoor air ventilation rate of 48 m^3/h (0.16 ach) during a measuring period of 6 hours (see table 2 for individual rooms).

Table 2. Measured outdoor air ventilation for individual rooms in house # 1, m³/h. The wind speed at a height of 10 m was 0.7 m/s and the outdoor air temperature was 6 °C.

Bedroom 1	7
Bedroom 2	26
Bedroom 3	3
Kitchen/living room	1
Study	1
Bathroom	10
Laundry	0
Hallway	<u>0</u>
Total	48

House # 4 had a total outdoor air ventilation rate of 71 m³/h (0.21 ach) during a measuring period of 3 hours (see table 3 for individual rooms).

Table 3. Measured outdoor air ventilation for individual rooms in house # 4, m³/h. The wind speed at a height of 10 m was 1.4 m/s and the outdoor air temperature was 9 °C.

Laundry	46
Kitchen	13
Bedroom	2
Living room	6
Bedroom upstairs	0
Bedroom upstairs	0
Living room upstairs	0
Bedroom upstairs	0
Bathroom upstairs	<u>4</u>
Total	71

Both tested houses have an inadequate ventilation. Some individual rooms hardly receive any outdoor air at all. The outdoor air ventilation will probably be higher if it is windier. The wind direction decides which rooms will receive outdoor air in a leaky house. The outdoor air ventilation rate will also be higher if the outdoor air temperature is lower than during the measurements i.e. more representative for a winter.

Low ventilation rates have been reported from many dwellings. Measurements of ventilation rates have been carried out in connection with energy analysis of buildings and with analysis of sick buildings. The Swedish Institute for Building Research has recorded measurements of ventilation rates in 900 dwellings (see table 4) (Lyberg 1989). The houses were not randomly sampled. The results are not statistically relevant. All values are from short term measurements and are not valid for an entire year. Most of the measurements were made with the tracer decay technique and can therefore have an inaccuracy of $\pm 30\%$.

The ventilation rate in naturally ventilated one-family houses tend to be lower the newer the house is. One-family houses built after 1972 have an average ventilation rate of 0.26 ach, which is half of the stipulated value of 0.5 ach. Houses with mechanic ventilation have a satisfying average ventilation. The variation between individual houses is, however, considerable.

Table 4. Measured ventilation rates in 900 dwellings (recorded by the Swedish Institute for Building Research).

Type of dwelling	Ventilation system	ach
<u>Mechanical ventilation</u>		
Apartment	Exhaust fan	0.63 ±0.23
One-family house	Exhaust fan	0.48 ±0.18
Mixed	Balanced	0.64 ±0.17
<u>Natural ventilation</u>		
Apartments		
built before 1940		0.62 ±0.22
built 1940-1960		0.55 ±0.27
built after 1960		0.33 ±0.13
One-family house		
built before 1960		0.45 ±0.29
built 1960-1971		0.38 ±0.20
built after 1971		0.26 ±0.14

Previous investigations carried out by the Swedish National Testing and Research Institute show that the ventilation rate can be low not only for entire one-family houses, but even lower for individual rooms. This is especially true for naturally ventilated houses, but also true for exhaust fan ventilated houses.

In order to determine the ventilation rate during the heating season calculations were made using the LBL-modell (Blomsterberg 1990). The calculations were first made for the tracer gas measuring periods (see table 5). The agreement between modell and measurement is reasonable for a winter day with mild weather.

Table 5. Calculated (LBL-modell) ventilation rates vs measured ventilation rates.

	House # 1	House # 4
Ceiling leakage area, cm ²	80	200
Floor leakage area, cm ²	0	0
Total leakage area, cm ²	170	400
Vertical shaft leakage area, cm ²	80	30
Wind speed, m/s	0.7	1.4
Outdoor temperature, °C	6	9
Calculated ventilation, m ³ /h (ach)	38 (0.12)	80 (0.23)
Measured ventilation, m ³ /h (ach)	48 (0.16)	71 (0.21)

Estimates for a heating season during a reference year give a ventilation rate of 57 m³/h (0.19 ach) for house # 1 and 126 m³/h (0.37 ach) for house # 4.

The houses are not airtight enough for a balanced ventilation system. The installed exhaust air heat pump delivers heat to domestic hot water and to two centrally located radiators.

The main improvement to the building envelope was new windows. The old double-pane windows ($U = 2.5 \text{ W/m}^2 \text{ }^\circ\text{C}$) were exchanged for new quadruple-pane windows ($U = 1.0 \text{ W/m}^2 \text{ }^\circ\text{C}$).

6. RESULTS AND DISCUSSION - AFTER RECONSTRUCTION

After reconstruction all houses were pressurized and depressurized again. This time it was done with open and closed supply vents (see table 6).

Table 6. Measured airtightness at 50 Pa, ach, before and after reconstruction.

House	closed vents		open vents	
	before	after	before	after
# 1, 1 storey	2,5	2,1	4,4	2,9
# 2, 1 storey	2,9	2,4	5,3	3,0
# 3, 1 storey	2,9	2,4	4,5	3,1
# 4, 1½ storey	4,1	5,9	5,4	6,7
# 5, 1½ storey	3,7	3,8	5,3	4,6
# 6, 1½ storey	4,7	4,6	5,8	5,4

The 1-storey houses met today's requirement before and have become even airtighter, mainly due to new windows. Two of the 1½-storey houses have unchanged airtightness and the third has become leakier. The window areas have become airtighter for the same reason as for the 1-storey houses, but more new penetrations for heating and ventilation have worked against this improvement.

Tracer gas measurements using the constant concentration technique were performed in two houses, # 1 and # 4. House # 1 had a total outdoor air ventilation rate of 52 m³/h (0.17 ach) before and 151 m³/h (0.50 ach) after reconstruction (see table 7 for individual rooms).

Table 7. Measured outdoor air ventilation for individual rooms in house # 1 before and after reconstruction, m³/h.

	Before	After
Outdoor temperature, °C	6	6
Wind speed, m/s	0.7	4
Bedroom 1	7	20
Bedroom 2	26	12
Bedroom 3	3	10
Kitchen/living room	1	42
Study	1	25
Bathroom	10	9
Laundry	0	26
Hallway	0	7
Total	48	151

5. DIFFERENT MEANS OF IMPROVING NATURAL VENTILATION

The aim is to improve the air exchange in individual rooms and the whole house. A ventilation system should be able to provide outdoor air to the whole house.

Swedish one-family houses built during the seventies with natural ventilation are often reasonably airtight, although they usually do not meet the Swedish Building Code requirement for 3.0 ach at 50 Pa. This means that the ventilation rate (excl. airing) most of the time is too low i.e. below 0,5 ach. Individual rooms, especially with doors closed, can have a very low ventilation rate. One improvement would be to install temperature controlled supply vents in the exterior walls. The maximum opening area of these vents has to be large enough compared with the leakage area of the building envelope. The advantages would be a less varying ventilation rate and a better distribution of outdoor air between individual rooms. The disadvantages would be slightly raised overall ventilation energy losses due to somewhat increased ventilation and no possibility for heat recovery.

Another alternative of improving natural ventilation is to install supply vents in the exterior walls and a temperature controlled fan in the vertical shafts. When it is cold outside the fan will not run and the ventilation will be all natural. During warm and mild periods, when the stack effect is insufficient, the fan will increase the ventilation rate. The advantages would be a raised and more constant ventilation rate and a better distribution of outdoor air between individual rooms. The disadvantages would be raised ventilation energy losses due to increased ventilation and no possibility for heat recovery.

Sofar the suggestions have meant improving on the existing systems for natural ventilation. Another option is to install a completely new ventilation system i.e. mechanical balanced ventilation or exhaust only. A balanced ventilation system should only be installed in a very tight building (Blomsterberg 1990). The advantages would be a raised and constant ventilation rate, a controlled distribution of outdoor air between individual rooms and the possibility to install a heat recovery system e.g. an air-to-air heat exchanger. The main disadvantage would be high costs. New ductwork for supplying and exhausting air has to be installed.

If an exhaust fan ventilation system with supply vents is to be installed the house does not have to be as airtight as for the balanced ventilation system. The recommendation is 3.0 ach at 50 Pa (incl. open supply vents) (Blomsterberg 1991). The advantages would be a raised and constant ventilation rate, a fairly well controlled distribution of outdoor air between individual rooms and the possibility to install a heat recovery system e.g. an exhaust air heat pump. The main disadvantage would be high costs. Using an exhaust air heat pump more heat can be recovered than by an air-to-air heat exchanger. The vertical shafts can to some extent be used for the installation of exhaust air ducts.

For the tested houses the last alternative was chosen. The reason for the choice was that the aim of the project was to make the use of electricity more efficient at the same time as the indoor climate is maintained at the same level or improved.

House # 4 had a total outdoor air ventilation rate of 71 m³/h (0.21 ach) before and 141 m³/h (0.41 ach) after reconstruction (see table 8 for individual rooms).

Table 8. Measured outdoor air ventilation for individual rooms in house # 4 before and after reconstruction, m³/h.

	Before	After
Outdoor temperature, °C	9	4
Wind speed, m/s	1.4	3
Laundry	46	32
Kitchen	13	21
Bedroom	2	24
Living room	6	25
Bedroom upstairs	0	1
Bedroom upstairs	0	5
Living room upstairs	0	10
Bedroom upstairs	0	13
Bathroom upstairs	<u>4</u>	<u>10</u>
Total	71	141

In both houses the overall ventilation and the ventilation of individual rooms have been improved after the reconstruction. The new ventilation system will of course have the problem that the colder the weather the lower the outdoor air and the overall ventilation of the bedrooms and the living room upstairs will be. The stack effect is then more powerful than the exhaust fan. To counteract this effect the building envelope has to be airtighter (Blomsterberg 1991).

In order to determine the ventilation rate during the heating season calculations were made using the LBL-modell (Blomsterberg 1990). The calculations were first made for the tracer gas measuring periods (see table 9). The modell overestimates the ventilation for house # 4. According to the measurements the exfiltration is very low. For colder weather there will most likely be some exfiltration.

Table 9. Calculated (LBL-modell) ventilation rates vs measured ventilation rates.

	House # 1	House # 4
Ceiling leakage arera, cm ²	70	325
Floor leakage area, cm ²	0	0
Total leakage area, cm ²	145	525
Wind speed, m/s	4	3
Outdoor temperature, °C	6	4
Calculated ventilation, m ³ /h (ach)	155 (0.51)	192 (0.56)
Measured ventilation, m ³ /h (ach)	151 (0.50)	141 (0.41)
Measured exhaust air flow, m ³ /h	150	140

Estimates for a heating season during a reference year using the LBL-modell give a ventilation rate of 155 m³/h (0.51 ach) for house # 1 and 205 m³/h (0.64 ach) for house # 4. A reasonable assumption for house # 1 is 0.51 ach as calculated and for house # 4 0.5 ach instead of as calculated 0.64 ach .

A comparison of ventilation heat losses for an entire year show increased and reduced ventilation energy losses (see table 10). The calculated heat losses after reconstruction are based on measured exhaust air temperatures. Degree day values were used.

Table 10. Calculated ventilation heat losses before and after reconstruction, kWh, for the reference year of 1971 from Stockholm.

House	Before	After (actual)	After (feasible)
# 1	2200	3900	450
# 4	4800	4900	950

7. CONCLUSIONS AND RECOMMENDATIONS

Modern one-family houses in Scandinavia built before 1980 are often naturally ventilated and heated by electric baseboard heaters. The overall supply of fresh air is often inadequate during the heating season in many of these houses, and often individual rooms are poorly ventilated. The performance of a natural ventilation system is very much dependant upon the overall airtightness and the distribution of the airtightness of the building and the weather.

Six modern one-family houses were examined before and after the ventilation system was improved. The system for natural ventilation was exchanged for an exhaust fan ventilation system incorporating an exhaust air heat pump. It is obvious from the tested houses that the overall ventilation and the ventilation of individual rooms were improved. The ventilation losses were increased and therefore energy conserving measures had to be taken. The overall costs for the new system were high compared with the energy savings obtained.

For mechanical ventilation with heat recovery to really make sense the house has to have a good level of airtightness. Older houses with natural ventilation are often not airtight enough. There are also practical problems in installing new ventilation systems in existing houses.

8. REFERENCES

1. BLOMSTERBERG, Å. "Ventilation Control Within Exhaust Fan Ventilated Houses". Proceedings of the 12th AIVC Conference, Coventry, Great Britain, 1991.
2. BLOMSTERBERG, Å. "Ventilation and airtightness in low-rise residential buildings - Analyses and full-scale measurements" Ph. d. thesis, Swedish Council for Building Research, D10:1990, Stockholm, Sweden, 1990.
3. LYBERG, M., BOMAN, CA and SKOGSBERG, S. "The actual air change rate in one thousand dwellings". VVS & Energi Journal # 3, Stockholm, Sweden, 1989 (in Swedish).

**Ventilation for Energy Efficiency and Optimum
Indoor Air Quality
13th AIVC Conference, Nice, France
15-18 September 1992**

Paper 10

**An Efficient Enthalpy Exchanger for Economical
Ventilation.**

W.B. Rose

**Building Research Council, University of Illinois,
One E.St.Mary's Rd., Champaign, Illinois 61820,
USA**

Synopsis

A cross-flow polymer membrane enthalpy exchanger has been designed which provides both heat recovery and moisture dissipation in the ventilation of living spaces. The exchanger is of benefit in providing fresh air during both cooling and heating seasons with minimum loss of energy. A prototype of the enthalpy exchanger has been constructed and tested.

The air leakage of the equipment has been found to be negligible; that is, the two air streams are indeed non-mixing. Testing for efficiency of the equipment involved the measurement of dry bulb and wet bulb temperatures in each of the four ports. The measured temperature values were used to calculate the efficiency of the exchanger. The results show a total efficiency of 72%, with 71% sensible heat recovery and 74% latent recovery. These efficiencies were achieved at an air flow rate of 1.7 m³/minute (60 cfm). The measured moisture transfer rates exceed the predicted moisture transfer rates by factors of two and three.

Background

An enthalpy exchanger is a device which allows the beneficial transfer of heat and moisture between two non-mixing air streams. Such devices are useful to reduce the energy penalty (sensible and latent) for providing fresh air to building occupants. Enthalpy exchange is particularly desirable in hot, humid climates, where the difference between indoor and outdoor dry bulb temperature may be small, but the difference in moisture levels may be great. The complaint is often heard "It's not the heat, it's the humidity." Barringer and McGugan (1989) conclude that "when reduction of cooling cost is the main consideration, exchangers with moisture recovery are preferable to sensible HRVs." Enthalpy exchange is desirable in heating climates, as well, in order to reduce the potential for frost closure of the device.

There are several types of air exchange ventilators in use. Most air-to-air exchange ventilators are sensible heat ventilators

that permit no moisture transport between the two air streams. There are several types of enthalpy (sensible + latent) exchangers in use. These include rotary wheel (with and without dessicant), plate, and porous plate.

Description

The apparatus described here is a prototype of a plate-type enthalpy exchanger which uses a spun-bonded polyethylene membrane to separate the two air streams: intake-supply and return-exhaust. The membrane is identical to the membrane in common use as a house-wrap and as a "breathable" envelope material. The product characteristics, derived from available product literature, are given in Table 1. The membrane product was selected because of its high water vapor permeance and its low air leakage characteristics.

The membrane is folded and wrapped in aa fashion to maximize the exposure of the membrane sheet to the passage of air in both directions. The wrapping is schematically illustrated in Figure 1. The sheet is folded in successive loops; then the edges are sealed, creating the separated chambers for air passage. In the prototype which was constructed for this research, the joints are sealed using an adhesive tape; a refinement of the design would involve the use of heat sealing of the joints. This design is a counterflow design, which has inherently higher design efficiencies than tandem flow.

It may be evident from the schematic illustration that the membrane is not maintained in a perfect flat plane but is skewed. This inevitably results in irregularly shaped passages of varying opening width, and offering varied resistance to air movement within the device. It is also evident, given the rectangular shape of the exchanger, that the membrane surface is not of optimally efficient shape. The corners at right angles should not be expected to have uniform air movement. The seams in the membrane were joined using a tape specified for use with the membrane. When taped, the folded and wrapped membrane forms a core.

The membrane core was attached to end chambers of clear rigid acrylic plastic. The apparatus is shown in the illustration

of Figure 2. Axial single-speed fans were attached to the intake and return chambers. The effect of using fans on these two ports is to equalize the air pressures across the membrane and to keep the apparatus in positive pressure with respect to ambient pressure during operation. It was assumed that the apparatus operating in positive pressure would be less likely to cause constricted air passages.

Test methods

In the U.S., heat recovery ventilators (HRVs) are tested by the Home Ventilating Institute, using a standard test method based on Canadian Standards Association CAN/CSA-C439-88 "Standard Methods of Test for Rating the Performance of Heat-Recovery Ventilators" At present, these tests are conducted in only one laboratory. The standard test method involves measurement of:

- temperature and humidity at the four ports,
- cross leakage,
- energy consumption of fans, controllers, etc., and,
- net air flow rates and static pressures developed.

The standard presents a method for using the measured values to calculate the efficiency of the exchanger. There are three sets of environmental conditions for the standard test of heat recovery efficiency according to the HVI standard:

- indoor air at 71.8°F (22.1°C) and 40% relative humidity, "outdoor" air at 32°F (0°C), and,
- indoor air at 71.8°F (22.1°C) and 40% relative humidity, "outdoor" air at -13°F (-25°C), and,
- indoor air at 75°F (23.9°C) and 50% relative humidity, "outdoor" air at 95°F (35°C) at 50% relative humidity (optional).

The first test is intended to measure performance during mild heating climate conditions, the second, under severe heating climate conditions, and the third under hot, humid outdoor conditions (cooling climate).

A facility at the University of Illinois was used to conduct tests on the prototype enthalpy exchanger. This facility was not equipped to maintain the standard conditions. The intended use of

this equipment is primarily for hot, humid climate, so the first two climate conditions were not applied. The following tests were conducted on the prototype equipment:

- dry bulb and wet bulb temperature at the four ports,
- cross leakage, and
- net air flow rates.

The energy consumption was not metered, but rather was estimated from the electrical ratings of the two fans. A static pressure test was not conducted because it was felt that the test deviates significantly from the pressure regimen maintained by the equipment during operation, so that the results would be of little value. It is important to note that the methods used were not HVI standard methods, because the equipment available was not capable of achieving and maintaining the conditions of the standard test.

Dry bulb and wet bulb temperature

Type "T" thermocouples were used to measure temperature. A reference thermistor was used for all eight thermocouples in this test, and the EMF was converted to temperature using a fifth-order polynomial resident in the data acquisition unit.

Wet bulb temperature measurements were taken using aspirated psychrometry; that is, a cotton wick was placed around the junction of each wet bulb thermocouple, and the wick was maintained wet from a nearby water source. The moving air stream in the exchanger itself obviated the need for a separate air flow source. The contribution of moisture from the wet bulb thermocouple to the overall performance of the apparatus was assumed to be negligible. A schematic drawing of the thermocouple placement is shown in **Figure 3**.

Considerable difficulty was encountered in maintaining the wicks so that they neither dried out nor dripped water. Data which showed the wet bulb temperature converging toward the dry bulb temperature were not included in this study. Wet bulb psychrometry may be the source of considerable error. In the data used for calculation, it is assumed that there was sufficient water on the wick for proper aspiration. If indeed the wick lacked proper moisture, then the humidity of the air stream would be seen as erroneously high.

Leakage

Leakage was tested using methods developed in the testing for attic ventilation (Hinrichs 1962), that is, smoke testing. Though the drawbacks to this method are that it is messy and potentially destructive of membrane performance, it has the distinct advantage of allowing continuous concentration measurements at intervals as small as three seconds. A further advantage, in this case, is that the deposit of smoke particles on the membrane allows, after disassembly of the prototype, an inspection of the apparatus for efficiency. The leakage test setup is shown in **Figure 4**. Three solar spectrum pyrgeometers were used as sensitive photovoltaic cells. The test was conducted outdoors in the shade, using illumination from a clear sky. A dense smoke source (from a marine signal flare) was discharged into the return port. Concentrations of smoke in the supply and exhaust ports were measured using voltage output from the pyrgeometers. It is assumed that the reduction in voltage output from the pyrgeometer is directly proportional to the increase in concentration of smoke particles between the light source and the pyrgeometer.

HVI uses Exhaust Air Transfer Ratio (EATR) as the ratio of the leaked air to the total air supplied. In this instance, the EATR that was measured was the ratio of the exhausting air in the supply port to the gross exhausting air flow. It should be noted that the smoke leakage test was assumed to be a test that would damage the membrane, and so it was conducted only after all other tests were completed.

Illumination values were sampled at three-second intervals. Illumination values were gathered for five minutes both before and after the smoke test, and those values were averaged. The values taken during the one-minute test were averaged, and the two sets of values were compared. The opaquing at the return port, into which the smoke was injected, was found to be 42%. The opaquing at the exhaust port was found to be 40%. The opaquing at the supply port was negligible: 0.78%. There was no smoke visibly leaking into the supply port. Of course, there was no leakage into the intake port, which received its air mechanically from the outside. So, for purposes of this report, losses due to leakage into the

supply port are ignored. The test did not measure leakage to the outside. Slight leakage to the outside could be seen, and the same is indicated in comparing the opaquing at the return port where the smoke was injected (42%) with the opaquing at the exhaust port (40%).

The aim of this test was to examine the equipment for gross leakage through cracks in the assembly. Porosity of the membrane to the crossover of air molecules was not tested.

Flow rate

The net flow rate was measured at the supply and exhaust ports using a velometer. The diameter of the port is 3 1/2 inches (89mm). The flow rate, calculated from the velometer reading (length) times the port opening area, is 60 cfm (1.7 m³/min) in each direction. This flow rate may be considered adequate for one person in a dwelling, but would not be considered adequate for meeting the fresh-air requirements of a family of four.

Results

Data were collected during a two day period using environmental conditions limited to the capacity of the university facility. The "indoor" and "outdoor" conditions are shown in **Table 3**. Values for the dry bulb and wet bulb measurements during the test period were averaged. The averages were used to derive other psychrometric values, namely, humidity ratio and total enthalpy. Relations found in *ASHRAE Handbook of Fundamentals* (1989) were used in making these conversions. It may be noted that wet bulb psychrometry was appropriate for this analysis due to the similarity between wet bulb temperatures and enthalpy values, and due also to the uniformly moving air stream.

The output values are shown in **Table 4**. This table also contains the values used in the calculation of three efficiencies: sensible, latent and enthalpy. In each of these three cases, the efficiency is defined to be the ratio between the beneficial contribution by the equipment (Intake - Supply) compared to the range of indoor and outdoor conditions (Intake - Return). The HVI standard requires that these efficiencies be modified to become "net" efficiencies by multiplying the values by the Exhaust Air

Transfer Ratio. In the present test, that reduction was found to be negligible, so the efficiencies stand as calculated from the temperatures.

The findings are represented graphically in **Figures 5** and **6**. Calculation of the humidity ratio permits the results to be posted on a psychrometric chart, allowing the effect of the exchanger on the characteristics of the two air streams to easily illustrated. **Figure 5** shows the process undergone by each air stream. It is apparent in viewing this chart that one cannot maintain the assumption that all heat and all mass being transferred in the apparatus is being transferred to the opposing air stream. Clearly, the moisture loss in the supply air stream is greater than the moisture gain in the exhausting air stream. This is due, most likely, to losses to the outside from the exhausting air stream. It may also be due to errors due to wet bulb psychrometry, as described above.

The same graphical method is applied in **Figure 6**, which illustrates the efficiencies derived from the calculations.

The predicted moisture transfer rate has been compared to the measured transfer rate. The calculations are shown in **Table 5**. It can be seen that the actual rate of moisture transfer exceeds the predicted rate by a factor of two in the exhausting air stream and by a factor of three in the supply air stream. This should not be surprising. Permeance testing of materials takes place under standard low rates of air flow over only one surface of a diffusing membrane. In this instance, there is a high rate of air flow over two surfaces. The difference in moisture transfer rates between the supply and the exhausting air streams is, at present, attributed to air leakage out of the apparatus from the supply air stream.

Discussion

Two concerns are often raised with regard to the performance of air-to-air exchangers with non-metallic cores: fire safety and indoor air quality. Fire safety concerns can often be addressed by separating the flammable core from possible sources of combustion,

often by incorporating it in metal ductwork. Of course, fire movement through the ductwork must be addressed as well.

The core of an enthalpy exchanger should not be a harbor for irritating, allergenic or toxic microorganisms. In the development of an appropriate exchanger, it will be very important to study the conditions under which the membrane material supports the growth of harmful microbes. A long study period should predate any commercial introduction.

Further development of this apparatus should include the use of a replaceable core, which can be removed for testing.

Conclusions

A prototype of a cross-flow plate-type enthalpy exchanger has been constructed and tested. It is shown to be quite free of leakage. It is also shown to be quite efficient in both sensible and latent transfer. An apparatus with such performance may be of considerable benefit in reducing the energy penalty often associated with providing fresh air to occupants in conditioned spaces. This is particularly true in climates where cooling finds frequent use.

References

- ASHRAE
Handbook of Fundamentals 1989
- CANADIAN STANDARDS ASSOCIATION
"Standard methods of test for rating the performance of heat recovery ventilators"
CAN/CSA-C439-88.
- BARRINGER, C.G, and MCGUGAN, C.A.
"Effect of residential air-to-air heat and moisture exchangers on indoor humidity"
ASHRAE Transactions, V. 95, Pt. 2. 1989.
- FISSK, W.J., PEDERSEN, B.S., HEKMAT, D., CHANT, R.E., and KABOLI, H.
"Formaldehyde and tracer gas transfer between airstreams in enthalpy-type air-to-air heat exchangers."
ASHRAE Transactions, Vol. 90, Part 1B, 1985. pp. 173-186.
- HINRICHS, H.S.
"Comparative study of the effectiveness of fixed ventilating louvers."
ASHRAE Transactions, no. 1791. 1962.
- HOME VENTILATING INSTITUTE
"Heat Recovery Ventilator (Ducted) Product Certification Specification"
no date.

Table 1: Membrane properties

Property	standard units	I-P units	Method
Water Vapor Transmission	2755 ng/(s*m ² *Pa)	48 perms	ASTM E-96
Porosity	17.6 sec/100cc-sq.in.		Gurley-Hill

Table 2: Apparatus characteristics

Characteristic	standard units	I-P	units
width	0.60 m	23.75	in.
length	1.14 m	45	in.
slot opening	0.02 m	3/4	in.
no. of openings in height	24 (two thicknesses)		
total membrane area	37.23 m ²	400.8	sq.ft.
flow rate	1.70 m ³ /min	60	cfm

Table 3: Test conditions

Condition	standard units	I-P units
Intake ("outdoor")		
dry bulb temperature	27.1 °C	80.8 °F
wet bulb temperature	20.6 °C	69.0 °F
Return ("indoor")		
dry bulb temperature	16.3 °C	61.4 °F
wet bulb temperature	13.5 °C	56.4 °F

Table 4: Results

Condition	standard units	I-P units
Supply		
dry bulb temperature	19.5 °C	67.1 °F
wet bulb temperature	15.7 °C	60.2 °F
Exhaust		
dry bulb temperature	22.3 °C	72.1 °F
wet bulb temperature	16.8 °C	62.3 °F
Dry bulb _{intake} - dry bulb _{return}	10.8 °C	19.4 °F
Dry bulb _{intake} - dry bulb _{supply}	7.6 °C	13.7 °F
sensible efficiency	70.8%	
Humidity ratio _{intake} - humidity ratio _{return}	.006	
Humidity ratio _{intake} - humidity ratio _{supply}	.004	
latent efficiency	74%	
Enthalpy _{intake} - enthalpy _{return}	4.97 kg cal/kg	8.96 Btu/lb
Enthalpy _{intake} - enthalpy _{supply}	3.60 kg cal/kg	6.49 Btu/lb
enthalpy efficiency	72.4%	

Table 5: Analysis

characteristic	standard units	I-P units
surface area	37.23 m ²	400.8 sf
permeance	2755 ng/(m ² *s*Pa)	48 perms
average vapor pressure difference	290 Pa	.086 inHg
predicted transfer rate	.0297 g/s	1651 grains/hr
volume flow rate	1.7 m ³ /min	60 cfm
mass flow rate	121 kg _{air} /hr	266.7 lb _{air} /hr
humidity ratio loss: supply air stream	.0030	
humidity ratio gain: exhausting air stream	.0012	
measured transfer rate: supply air stream	0.100 g/s	5591 grains/hr
measured transfer rate: exhausting air stream	.0415 g/s	2306 grains/hr

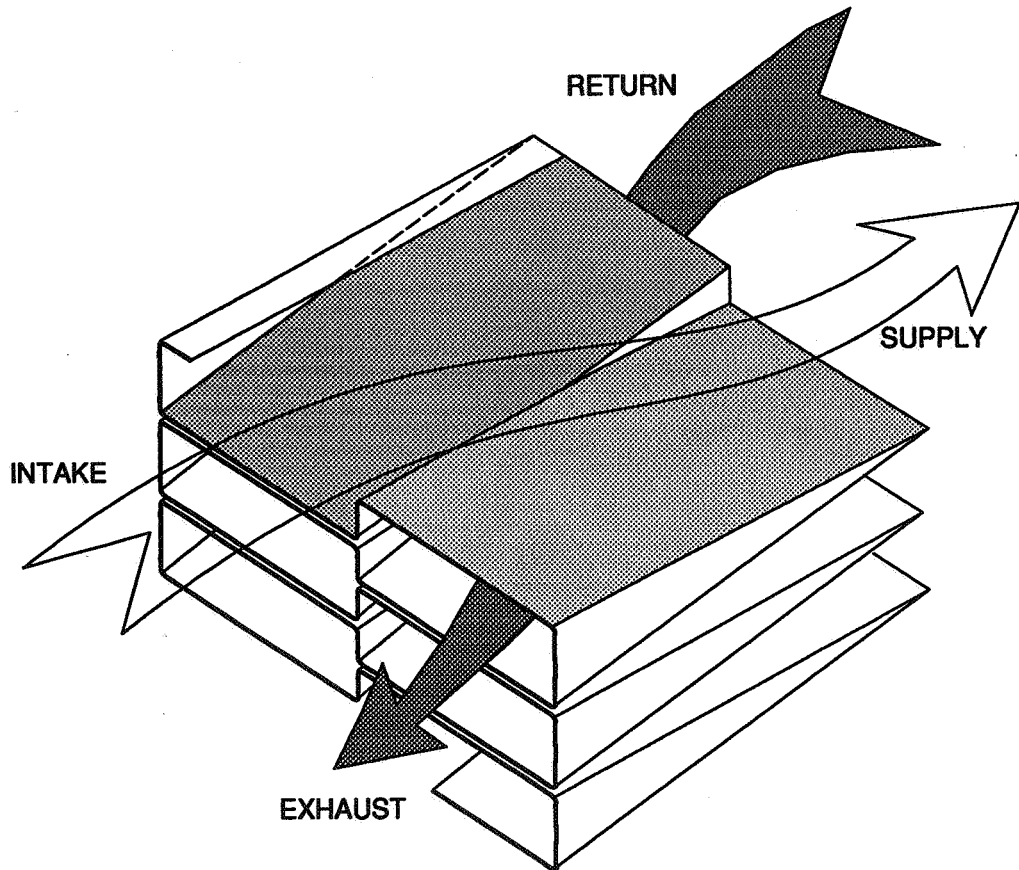


Figure 1. Schematic illustration of wrapping of membrane, showing the cross flow movement of the two non-mixing air streams.

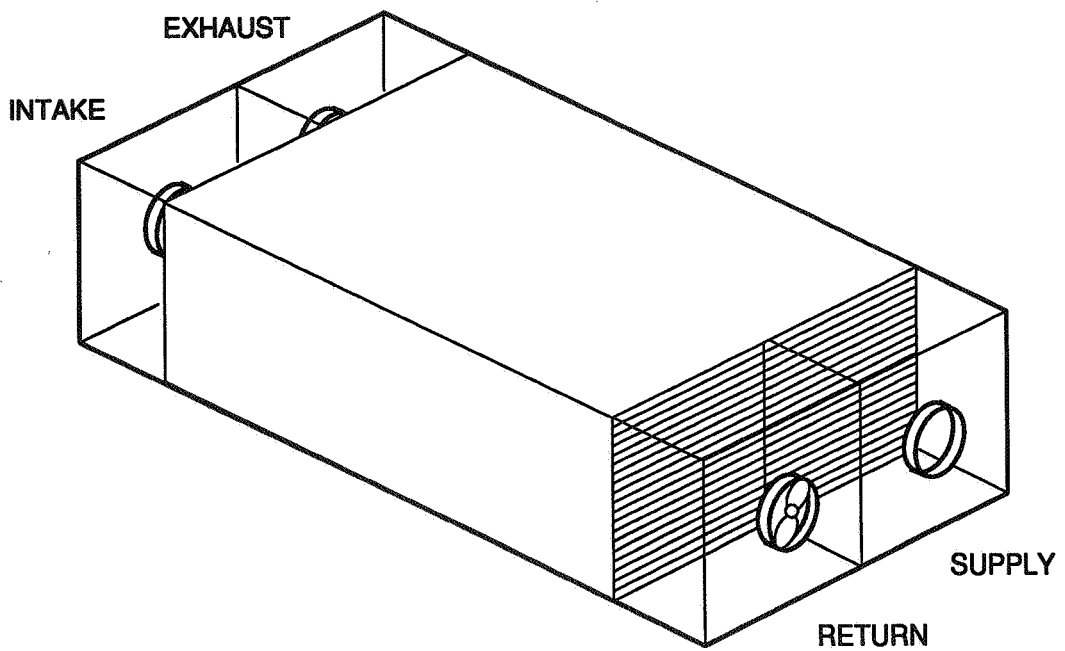


Figure 2. Drawing of enthalpy exchanger construction showing the membrane core, and acrylic plastic end ports.

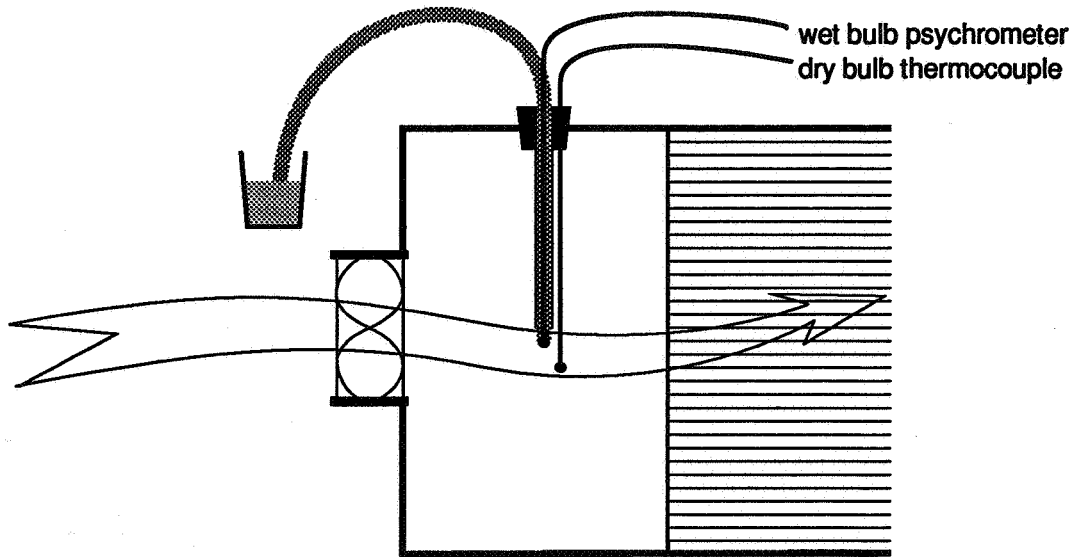


Figure 3. Test setup for measurement of wet bulb and dry bulb temperature. These measurements are used in the calculation of efficiency (sensible, latent and total enthalpy).

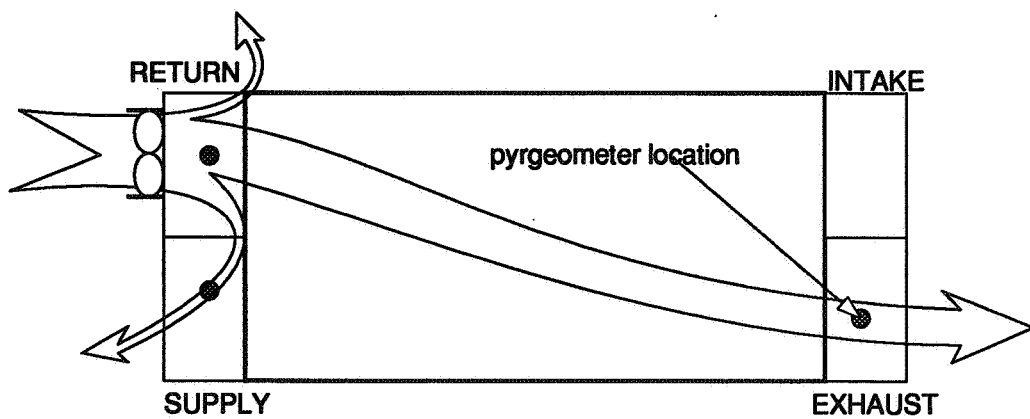


Figure 4. Schematic illustration of test setup for leakage. Smoke is introduced into the return air stream. The amount of opaquing measured by the pyrometers (photocells) is proportional to the concentration of smoke in that port. Leakage from the exhausting air stream into the supply stream was measured. Leakage to the exterior was not.

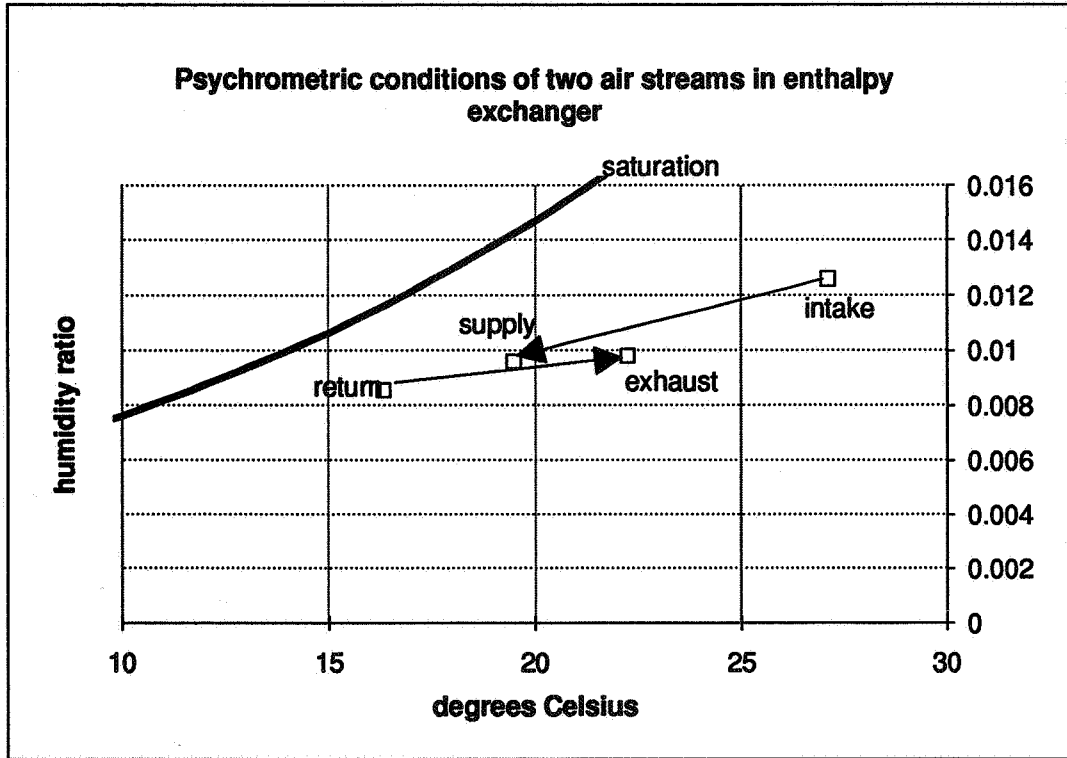


Figure 5. Chart showing psychrometric conditions of the two air streams.

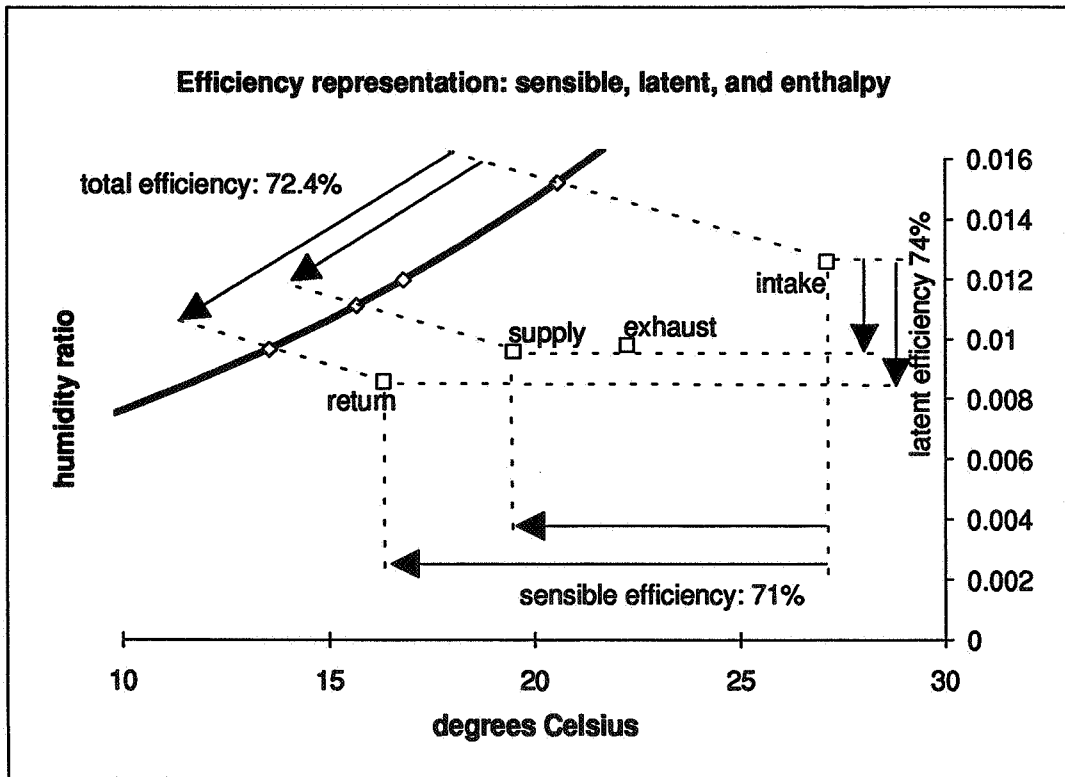


Figure 6. Chart showing the sensible, latent and total efficiencies of the enthalpy exchanger.

**Ventilation for Energy Efficiency and Optimum
Indoor Air Quality
13th AIVC Conference, Nice, France
15-18 September 1992**

Paper 11

**Energy Savings by Balanced Ventilation with Heat
Recovery and Ground Heat Exchanger.**

H. Trümper, K-J Albers, K. Hain

**Universität Dortmund, Fakultät Bauwesen,
Lehrstuhl TGA Technische Gebäudeausrüstung,
August-Schmidt-Str.6, W-4600 Dortmund 50,
Germany.**

Summary

This paper investigates quantitatively the energy conservation achieved by balanced ventilation with heat recovery and upstream ground heat exchanger. The investigations were conducted on an occupied single-family house equipped with such a balanced ventilation system. The heat recovery unit of this system consists of a plate-type heat exchanger with a downstream small air-to-air heat pump. In addition this house is equipped with a ground heat exchanger.

This balanced ventilation system with heat recovery and upstream ground heat exchanger not only covers the entire ventilation heat requirement for the house, but also a part of the transmission heat requirement.

Symbols and abbreviations

EWT	Ground heat exchanger
el. Hzg.	Electrical storage heating units
Gt	Degree days
WGT	Heat recovery unit
$\vartheta_{L,m,Erdrohranfang}$	mean air temperature at the beginning of the ground heat exchanger
$\vartheta_{L,m,Erdrohrende}$	mean air temperature at the end of the ground heat exchanger

Introduction

In low-energy houses, the transmission heat requirement of the building is reduced by the high heat insulation standard to such an extent that the ventilation heat requirement is becoming increasingly significant. An important step in the direction of ventilation heat loss reduction is the installation of a mechanical balanced ventilation system with heat recovery. The heat recovery unit can be a plate-type heat exchanger or a combination of plate-type heat exchanger and downstream small air-to-air heat pump.

An additional option for reducing the ventilation heat losses is to instal a ground heat exchanger. The outdoor air is drawn through a pipe buried in the ground and only passes into the dwelling via the heat recovery unit. In this way the supply air is preheated in winter and partial cooled in summer. In addition, in the summer the outdoor air is partial dehumidified if the temperature falls below the dew point in the ground heat exchanger. This should not be underestimated with regard to comfort, since in summer supply air which is cooler and drier than the outdoor air is experienced as pleasant.

If the ground heat exchanger is correctly designed, the supply air temperature at the end of the ground heat exchanger is, in winter, not lower than 0°C, even with extremely low outdoor air temperatures. This is very important in order to avoid problems regarding any possible icing up of the plate-type heat exchanger in the heat recovery unit. In the summer the cooling of the outdoor air is becoming increasingly important because of the problem of easily achievable overheating in modern, highly insulated low-energy houses.

System of balanced ventilation with heat recovery and upstream ground heat exchanger

The ground heat exchanger set up for a single-family house in southern Germany was designed with regard to practical considerations.

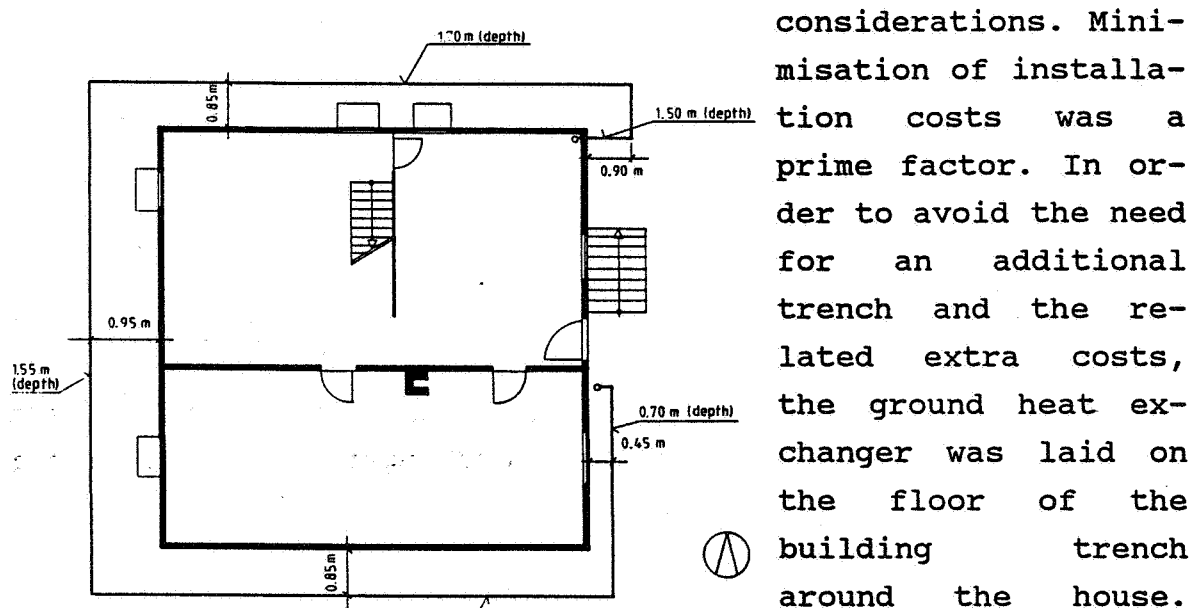


Fig. 1 Scheme of the ground heat exchanger

Minimisation of installation costs was a prime factor. In order to avoid the need for an additional trench and the related extra costs, the ground heat exchanger was laid on the floor of the building trench around the house. This also determined the length of the heat exchanger, name-

ly 42 meters. Because of the need to reliably take off the condensate produced in the summer, a corrugated tube was not used for the ground heat exchanger, but a smooth folded spiral-seam tube, and this was laid at an incline of 2 %. The inside diameter of the tube is 125 mm, the wall thickness 0.8 mm. The position of the ground heat exchanger with details of the laying depth and distance from the house is shown schematically in Figure 1.

Figure 2 shows the scheme of the entire ventilation system. The outdoor air is conveyed through the ground heat exchanger using a tube fan with a measured power consumption of 50 W. The volumetric flow is 140 m³/h. After it has flowed through the ground heat exchanger, the supply air passes through the heat recovery unit and then it passes through a

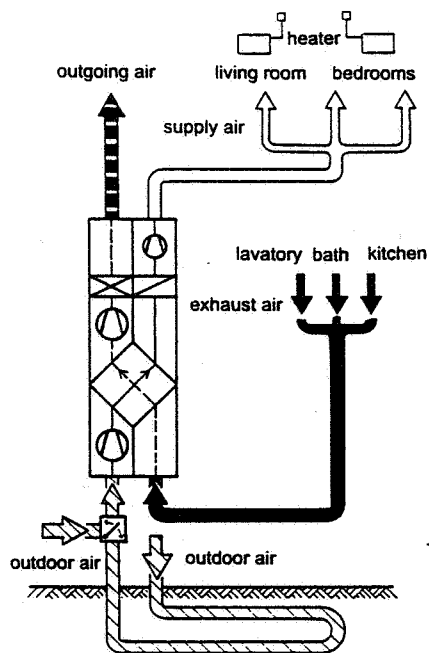


Fig. 2 Scheme of the ventilation system

small tube network into the residential rooms and into the children's and parents' bedrooms in the house. The exhaust air is removed from the bathroom, toilet and kitchen. The heat recovery unit consists of a plate-type heat exchanger and a downstream small air-to-air heat pump. The power consumption of the heat pump compressor is 500 W, that of the supply air fan 20 W and that of the exhaust air fan 16 W. In the summer the small heat pump is not in operation and the plate-type heat exchanger is replaced by a double-duct piece, since the supply air cooled in the ground heat exchanger is not to be subsequently reheated.

Because the heat output of the ground heat exchanger in winter is lower at a certain temperature than the power consumption of the tube fan, and in summer it is not necessary to cool the outdoor air below a certain temperature, suction through the ground heat exchanger can be sealed off using a cap controlled by thermostats. At the same time a second opening is released through which the outdoor air is directly drawn in via the roof. The thermostat is installed under the eaves and adjusted in such a way that the outdoor air is drawn in, at temperatures below 4°C and above 20°C, through the ground heat exchanger, and otherwise directly via the roof. The fact that this ventilation system is not also a room heating system is symbolized in Figure 2 by the heaters needed in addition in winter for room heating. In this case these are electrical storage heating units.

To investigate the thermal technology of the ground heat exchanger, the temperature and relative humidity of the air

drawn in upstream and downstream of the ground heat exchanger and furthermore the wall temperatures of the ground heat exchanger are measured at a distance of 2 meters. For the energy-related evaluation of the heat recovery unit, the temperatures and relative humidities of the supply air and exhaust air are measured upstream and downstream of the system. The measured quantities are registered every five minutes and stored for further evaluation after every hour as hourly mean values. In addition the operating times and power consumptions of the tube fan for the ground heat exchanger, of the compressor and of the supply air and exhaust air fan are registered.

Results for the ground heat exchanger

The ground heat exchanger plays a particularly important role. Thanks to the extremely high heat storage capacity of the ground, supply air is provided at almost constant temperature, regardless of that of the outdoor air. For this purpose, the length of the ground heat exchanger must be

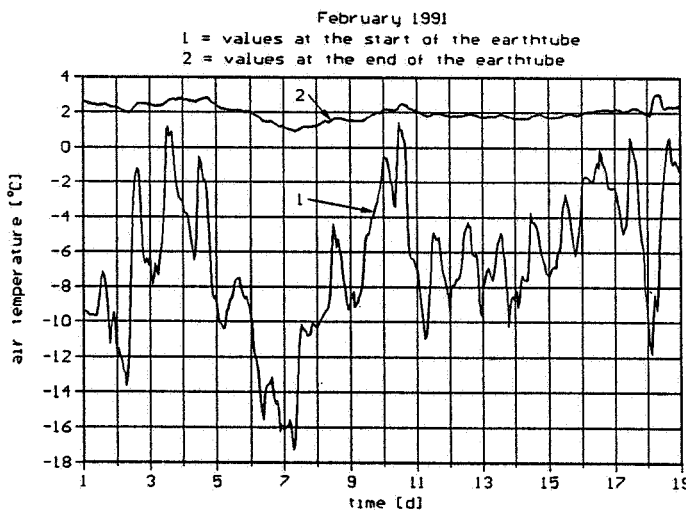


Fig. 3 Temperature curve upstream and downstream of the ground heat exchanger

correctly established as a function of the outdoor air temperature fluctuations /1/. Figure 3 and 4 show the temperature curve for the air upstream and downstream of the ground heat exchanger for a longer period in the winter period 1990/91 and summer period 1991 under investigation here. These temperature curves

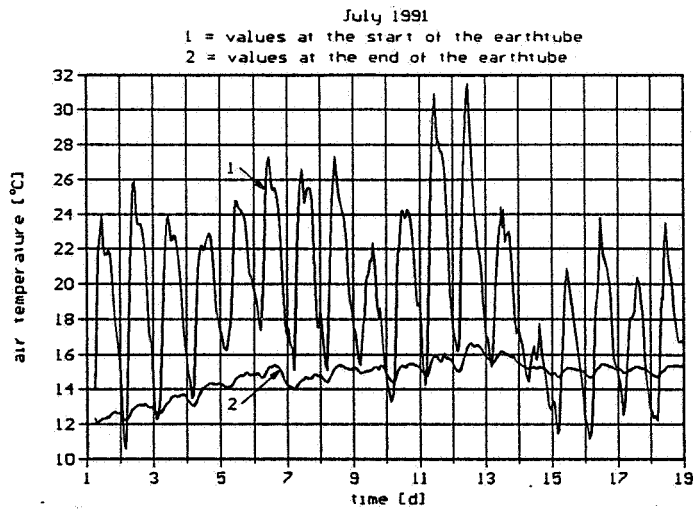


Fig. 4 Temperature curve upstream and downstream of the ground heat exchanger

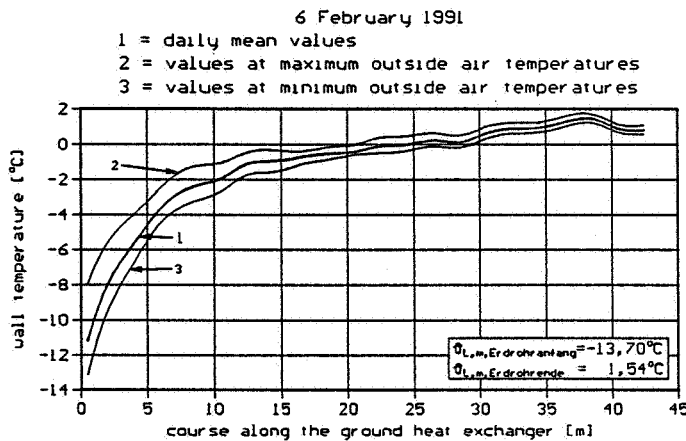


Fig. 5 Temperature curve along the wall of the ground heat exchanger

highlight the very great decaying capacity as against short-term, extreme outdoor air temperature fluctuations. The way in which such short-term temperature fluctuations are reduced along the ground heat exchanger can be seen if we look at the example of a winter day as shown in Figure 5. In addition to the daily mean values for the wall temperatures, the wall temperatures at maximum and minimum outdoor air temperatures are plotted. Furthermore, the daily mean values are given for the air temperatures upstream and downstream of the ground heat exchanger.

In winter the possible icing up of the plate-type heat exchanger as mentioned at the beginning is prevented by the supply air temperature, which is always above 0°C. Furthermore, the almost constant supply air temperature, which is higher than that of the outdoor air, increases the output of the heat pump. In summer, with extremely high outdoor air temperatures and humidities, the clearly cooler and drier supply air leads to greater comfort. The design principles of such ground heat

exchangers were developed in /1/ and presented for the first time at the 12th AIVC Conference /2/.

Results for the entire balanced ventilation system

With the balanced ventilation system with heat recovery and upstream ground heat exchanger as shown here, not only the entire ventilation heat requirement of the house is covered, but also a part of the transmission heat requirement.

The single-family house investigated with a residential area of 150 m² had a heat turnover of 22,150 kWh in 1991, of which a total of 35 % was taken care of by the heat recovery unit (6,710 kWh) and by the ground heat exchanger (1,000 kWh). The remaining 65 % was covered by electrical storage heaters. The compressor and the fans of the heat recovery unit had a power consumption of 1,600 kWh, so that the performance number obtained for this system is 4.2. The tube fan of the ground heat exchanger had a power consumption of 140 kWh during the heating period. The performance number of the ground heat exchanger is thus 7.1. In the months from June to September the ground heat exchanger provided cooled and dried supply air. The perceptible cold gain in this period was 330 kWh and the entire (perceptible and latent) cold gain was 870 kWh. For this purpose 77 kWh electrical energy had to be provided to drive the tube fan, which produces a performance number in relation to the perceptible cold gain of 4.3 and in relation to the total 11.3.

Figure 6 shows the heat turnover in kWh provided by the individual systems and calculated from the degree day numbers (Gt) /3/ determined at the location of the house. Only slight deviations are evident between the heat turnover ac-

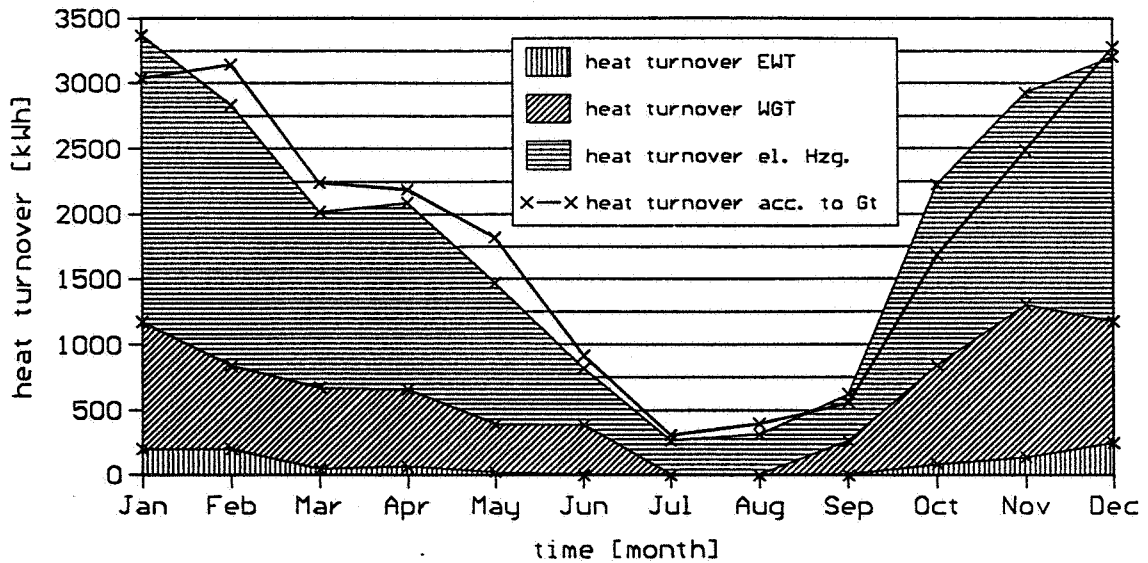


Fig. 6 Heat turnover of the house

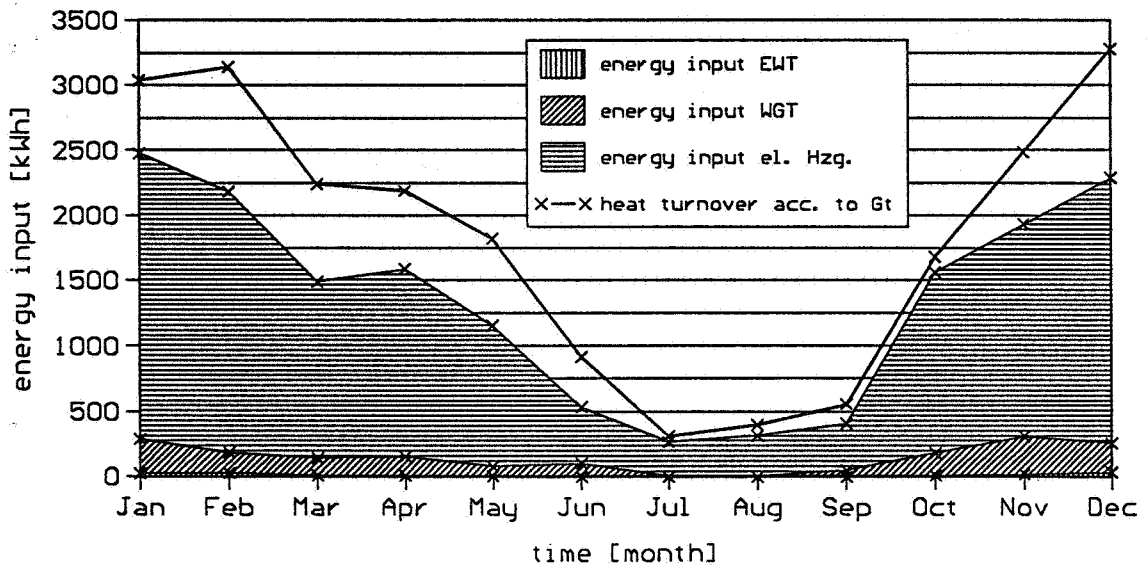


Fig. 7 Energy input to cover the heat turnover according to Figure 6

according to degree day numbers and the actual heat turnover, and so the heat turnover according to degree day numbers can be used very well for the purpose of comparative calculations. Figure 7 plots the energy input over the year under investigations as needed to cover the heat turnover shown in Figure 6. This figure makes clear that balanced ventilation with heat recovery and upstream ground heat exchanger has a considerable energy conservation potential. To cover the

heat turnover of 22,150 kWh needed to heat the house in 1991, an energy input of 16,190 kWh was needed. The energy input thus accounts for only 73 % of the heat turnover, which gives an energy saving of 27 %.

The heat turnover of 22,150 kWh/a seems at first glance to be very high for a modern single-family house with 150 m² residential area. However, this absolute figure is inadequate to evaluate the energy situation of the house. This is made clear by the fact that the location is not taken into account. If the same house were to stand not on its present site, but for example in Essen, it would display a 21 % lower heat turnover, which is caused only by the difference in climate. While at the present location of the house the degree day number for the year under investigation was determined as 4,560, and the normal outdoor temperature is -18°C /3/, in Essen one obtains a degree day number for the same period of 3,634. The normal outdoor temperature for Essen is -10°C /3/.

More informative is an energy-related evaluation of the house, if it is compared with a notional house of the same dimensions whose outer shell still corresponds to the u-values (values for the coefficients of heat transfer) from standards, regulations or generally known recommendations. In Germany, these are the Heat Control Ordinance /4/ or the recommendations for low-energy houses /5/. For this purpose the heat requirement of the house is newly determined with the respective u-values given for the outer shell and the heat turnover is calculated with the help of degree day numbers (Gt). The values thus obtained are shown in Table I.

	Design as is	Design as /5/	Design as /6/
Heat requirement in [W]	11,972	15,446	11,348
Heat turnover acc. to Gt in [kWh/a]	22,055	28,455	20,905

Table I: Heat requirement and turnover for the house in various designs

The comparison shows that the existing house has a 29 % lower heat turnover than a design which just complies with the Heat Control Ordinance. Compared with the design which just meets the recommendations for low-energy houses, however, its heat turnover is 5 % higher. In relation to the transmission heat requirement then the house under investigation does not yet meet the requirements of a low-energy house. This is also made clear by the relatively low proportion of the total heat requirements accounted for by the ventilation heat requirements, namely 31 %. With low-energy houses the proportion of ventilation heat requirement in relation to the total heat requirement is about 35-40 %. If we consider, however, that, as shown above, energy savings of 27 % are achieved by built-in balanced ventilation with heat recovery and upstream ground heat exchanger, this house can be called a low-energy house in spite of the 5 % higher transmission heat losses.

A further variable which influences the heat turnover of buildings but cannot be recorded is the user behavior. All calculations which are used to determine the anticipated heat turnover assume the normal inside temperature /6/. This is for living rooms and bedrooms 20°C. In /7/ it was established for multi-occupation houses that, during the heating period, the room temperatures are over 20°C. The investiga-

tions is also confirmed by this single-family house. Most of the rooms during the heating period had an average temperature of more than 21°C. The higher heat turnover caused by these elevated temperatures can be seen in Figure 6. Since the heat turnover according to degree days does not take into account own-heat or solar heat gains, it always has to be higher than the actual heat turnover. Figure 6, however, shows that the heat turnover according to degree days in the months January and September to November is lower than the actual heat turnover. This indicates an increased heat turnover due to user behavior.

Acknowledgments

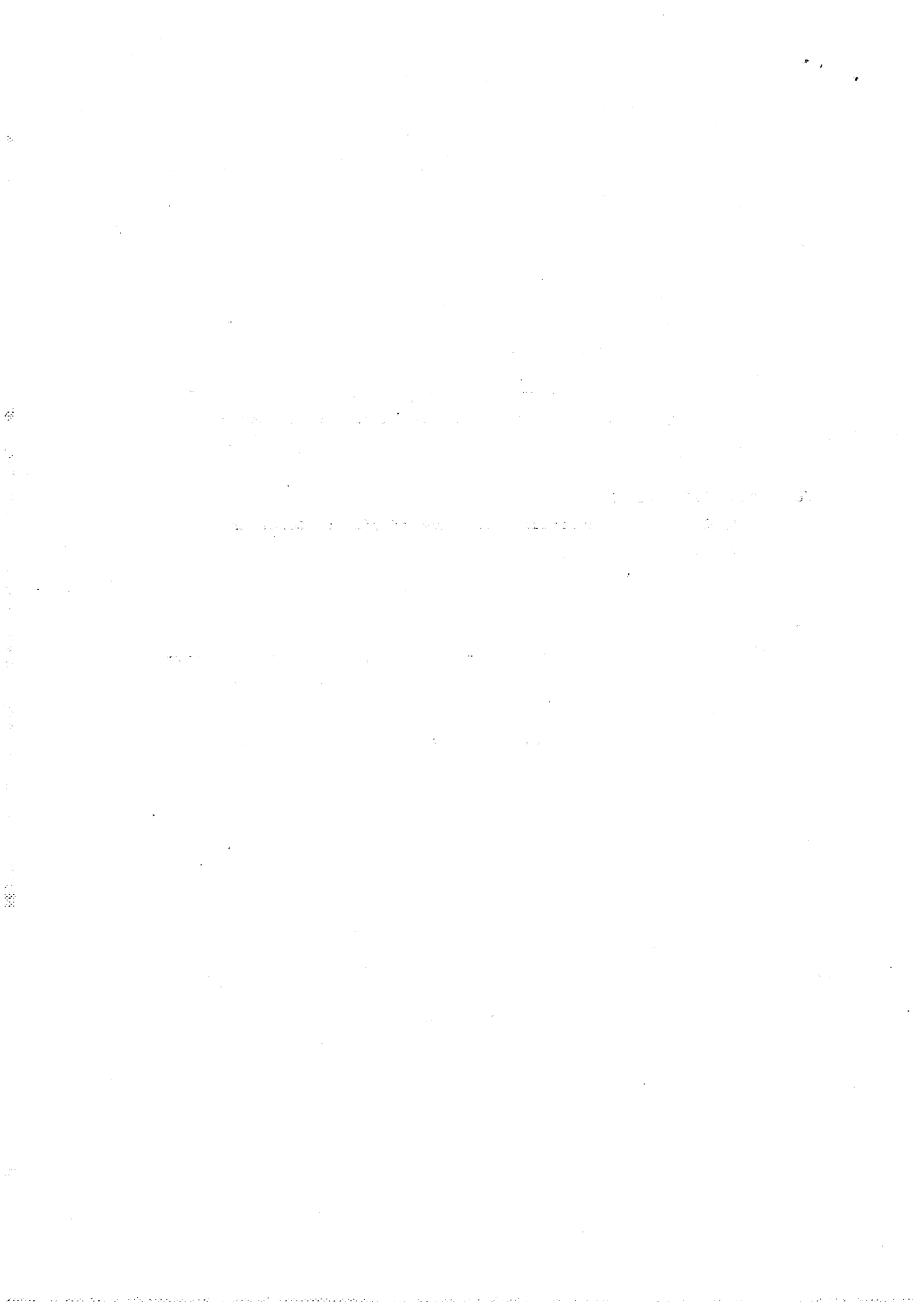
The research product on which this publication is based was financed by funds from the Federal Ministry for Regional Planning, Construction and Urban Development, assistance code B I 5 - 80 01 89 - 108.

References

- /1/ Albers, K.-J.
"Untersuchungen zur Auslegung von Erdwärmeaustauschern für die Konditionierung der Zuluft für Wohngebäude"
Forschungsbericht Nr. 32, Stuttgart, Deutscher Kälte- und Klimatechnischer Verein 1991

- /2/ Trümper, H.; Albers, K.-J.
"Preheating and Cooling of the Incoming Air of Dwellings Using an Earth-Laid Pipe"
Proceedings of the 12th AIVC Conference, Air Movement and Ventilation Control Within Buildings, Ottawa, Canada 24 - 27 September 1991, Volume 2 pp 133-152

- /3/ VDI 2067 Blatt 1
"Berechnung der Kosten für Wärmeversorgungsanlagen
Betriebstechnische und wirtschaftliche Grundlagen"
Düsseldorf, VDI-Gesellschaft für Technische Gebäudeausrüstung 1983
- /4/ N.N.
"Wärmeschutz bei Gebäuden, Wärmeschutzverordnung vom
24. Februar 1982"
Bundesministerium für Wirtschaft, Bonn 1983
- /5/ N.N.
"Wege zum Niedrigenergiehaus"
Bundesministerium für Raumordnung, Bauwesen und Städtebau,
Bonn 1990
- /6/ DIN 4701, Teil 2
"Regeln für die Berechnung des Wärmebedarfs von Gebäuden
Tabellen, Bilder, Algorithmen"
Berlin, Beuth Verlag 1983
- /7/ Trümper, H.; Hain, K.; Schmickler, F.-P.
"Demonstrationsvorhaben Duisburg, Phase II, Vergleichende Unter-
suchung verschiedener Lüftungssysteme in bewohnten Mehrfamilien-
häusern"
Forschungsbericht T 86-239, Bonn, BMFT 1986



**Ventilation for Energy Efficiency and Optimum
Indoor Air Quality
13th AIVC Conference, Nice, France
15-18 September 1992**

Paper 9

METOP - Energy Efficient Office Building

J. Laine and M. Saari

**Technical Research Centre of Finland, Laboratory
of Heating and Ventilation, P O Box 206
(Lämpömiehenkuja 3) SF-02151 Espoo, Finland**

SYNOPSIS

A prototype of a low cost, low energy office building was built using a new Finnish component system building technology.

Thanks to the energy efficient windows, the thermal insulation of the building envelope and the demand-controlled variable outdoor air flow HVAC system with heat recovery and energy-storing structures, the need for heating and cooling energy has been reduced to such a level that a low energy office can be cooled with outdoor air and with the aid of a heat recovery device. The building is kept warm with the support of its own operations almost throughout the year. It is possible to arrange a good individual indoor climate in this way almost without any purchased heating or cooling energy. There is need for heating only during the coldest but short periods in the night and during the weekends. Even during the summer heat periods, cooling energy produced by refrigerators operating on CFC is not needed.

1. INTRODUCTION

The prototype "METOP" for a low energy office was completed in the test house area of VTT in Otaniemi, Espoo /1/, /2/. The prototype was built for testing the function of the new structural, electrotechnical and HVAC solutions which were developed in different studies (EBES, TAT, ETRR, LVIS-2000, RATA-2000) and in the development projects of different companies. The low energy office, whose total costs were quite low, was built using a new Finnish component system building technology and a factory preadjusted variable air volume HVAC system.

A good, individually adjustable indoor climate has been realised by means of a self adjusting demand-controlled HVAC system with variable air flow. The aim is to create an environment in which heating energy needs to be purchased only during the coldest winter days when temperatures fall below -15 °C. Cooling energy produced by refrigerators operating on CFC is not needed. The follow-up studies on the indoor climate, efficiency and energy consumption will continue for two years.

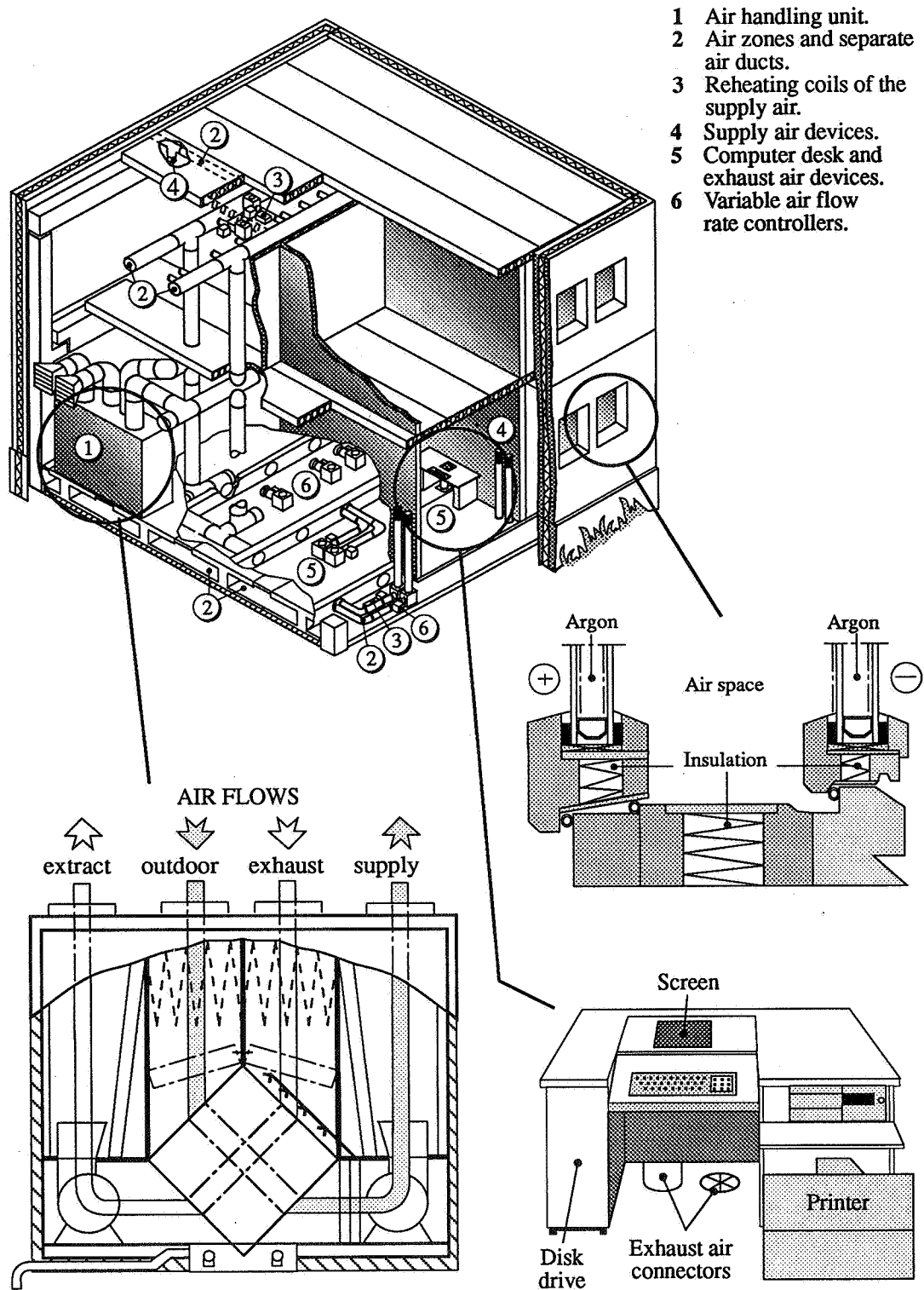


Figure 1. The industrial realization of the METOP low energy office prototype which utilizes the new Finnish component system building technology.

2. NEW WINDOWS PREVENT COLD AND OVERHEATING

In order to obtain a good indoor climate using a simple HVAC system, we must minimize the need for heating and cooling by means of different constructions and control solutions. The windows have an important effect on the heating and cooling need of an office room.

Thanks to a new window solution (U-value $0.5 \text{ W/m}^2\text{K}$), it is possible to reduce the heat losses of the window to a quarter of that of a normal triple glazed window used in Finland. Even during hard frosts (outdoor air temperature $-26 \text{ }^\circ\text{C}$), the lighting alone can compensate the transmission heat losses of the office room (150 - 200 W). Window draughts are eliminated (indoor surface temperature above $17 \text{ }^\circ\text{C}$). In addition, windows reduce the need for cooling extremely well. Only 12 % of the radiation energy of the sun comes through the window. The sun shield does not have any essential effect on the amount of the visible light coming through the window, or on the appearance of the window.

At the beginning of July 1991, there was a heat period of about a week (outdoor temperature $14 - 29 \text{ }^\circ\text{C}$), and at the turn of July and August, there was another hot period of two weeks (outdoor temperature $15 - 27 \text{ }^\circ\text{C}$).

At the end of the first heat period (Figure 2), the indoor temperatures in the late afternoon hours typically rose to $25 \text{ }^\circ\text{C}$ in the office room facing south, and at the end of the second period, it rose to $26 \text{ }^\circ\text{C}$.

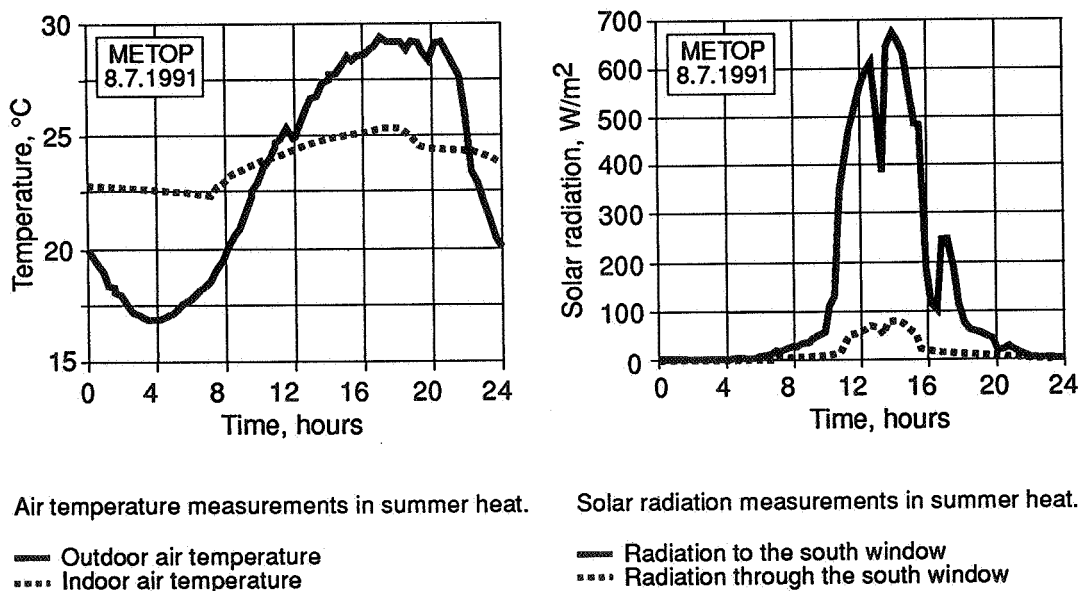


Figure 2. Measurements at summer peaks.

3. SPECIAL STRUCTURES PREVENT AND STORE COLD AND HEAT

The facing elements and double prestressed solid planks of concrete which are used as installation floors and ground slabs are heat insulated with 120 mm thick polyurethane without CFC. The building is founded on foundation elements of concrete. The frame construction is made of pillars and beams of concrete. Hollow core slabs of concrete function as intermediate floors and roofs. The roof is heat insulated with a 350 mm thick layer of loose-fill insulation. The heat insulations of the office are slightly above the requirements of the National Building Code of Finland.

The hollow spaces of the double prestressed solid planks and the hollow core slabs are partly used as installation spaces for building services and as air ducts. When functioning as air ducts, the structures form a short-term storage area for heating and cooling energy which is used by the HVAC system in heating and cooling situations. In winter, the frame structure can be heated with the air handling unit for night, and in summer, it can be cooled in the nighttime with cool outdoor air for daytime cooling.

4. INDIVIDUAL TEMPERATURE AND VENTILATION

The low energy office needs cooling almost continuously also during the winter because of internal heat loads (people, lighting, different machines and devices). There is a small need for heating only during the coldest but short periods in the nighttime and during the weekends.

The outdoor air flow rate of the office room (10 - 40 dm³/s) corresponds to the ventilation in winter, and it is also essentially smaller than in spring, summer or autumn when the excess heat can be removed from the building using outdoor air but without refrigerators using CFC.

The demand-controlled variable air flow HVAC system of the low energy office offers the possibility to choose the level of the room temperature and ventilation separately room by room.

The room air terminal devices, which control the indoor climate individually are equipped with reheating coils and a programmable DDC. The room air terminal devices have been preadjusted at the factory so that the air flows automatically adjust themselves to the right level. There is no need for expensive adjusting operations at the construction site.

The computers of the office room are placed in the computer desk. The computer desk is connected to the HVAC system through the exhaust air terminal device. Temperatures measured inside the computer desk on a typical winter day are shown in Figure 3. When the room requires heating, the heat from the computers automatically heats the room (time 8 - 10 in Figure 3). When the room needs to be cooled (time 10 - 16 in Figure 3), the computer desk automatically removes the heat given off by the computers from the building by means of the exhaust air. Heat recovery is applied to preheat the supply air when the outdoor air is cold. Over 60 % of computer's heat load is removed by means of the computer desk. The task of the computer desk is to function both as a heating and a cooling device either by utilizing or preventing the heat loads according to the circumstances.

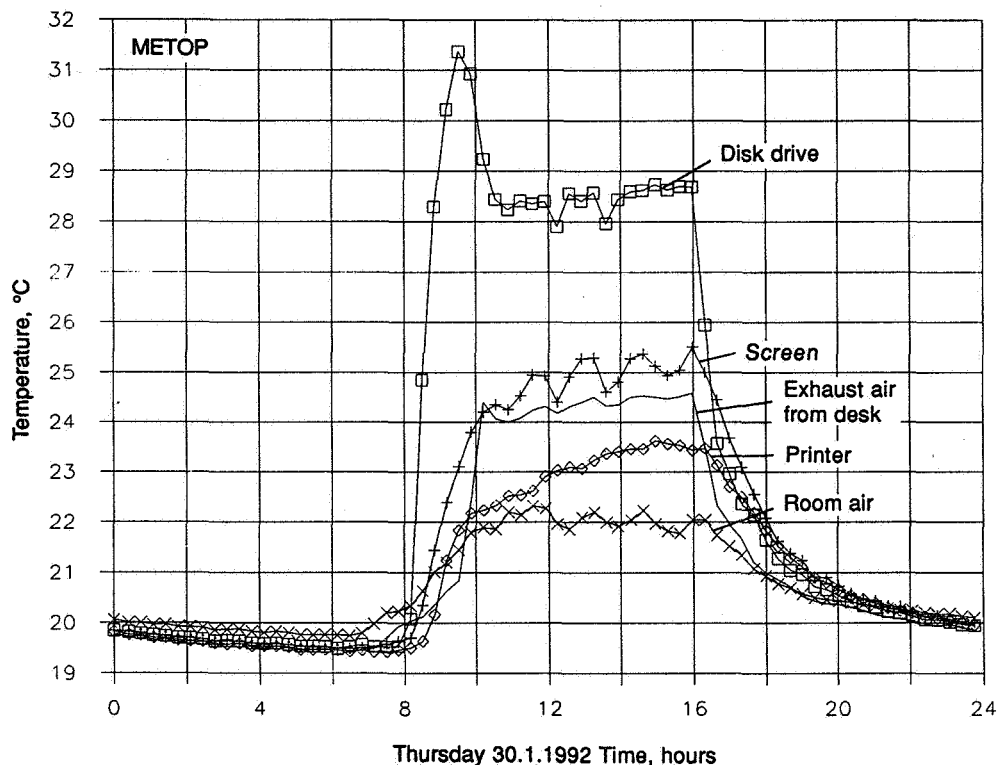


Figure 3. Computer desk temperatures measured in winter.

The HVAC system with a programmable DDC controls the air filtering, the cold and heat recovery, heating, cooling with outdoor air, forced indirect evaporative cooling, pressures and ventilation of the low energy office according to the demands of each room. A communication bus is used between the controller of the room air terminal devices and the air handling unit. The HVAC system has been completed and tested at the factory, and it is ready to operate after pipe and electrical connections. There is no need for expensive adjusting and tuning operations at the construction site. Thanks to its neat appearance, the silent HVAC system does not require any separate machine room.

5. INTELLIGENT CABLING

All rooms of the low energy office have small electric centres of their own, which are equipped with their own power supply. The electric centres control the temperature, ventilation, lighting and energy efficiency individually in each room according to the specific demand so as to minimize the need for cooling. Low energy fluorescent lamps are used for lighting the office. The computer desk as well as direct and indirect lighting are used at the same time to facilitate ergonomical computer work.

6. CONCLUSIONS

6.1 Follow-up study

Two-year follow-up studies on the indoor climate, efficiency and energy consumption will enable us to find out how the new component system building technology has succeeded in realising an ecologically sound low energy office that provides a good indoor climate and low energy use - and which has the advantage of low total costs.

It was noticed during the first heat periods that the control program of the DDC of the air handling unit needed to be developed, and this is why it was impossible to take full advantage of the free cooling effect of the outdoor air. When the effect is fully used next summer, the indoor temperatures of the office rooms can be lowered even further from the present values, which are already quite good.

6.2 A good indoor climate thanks to new technical solutions

Thanks to the energy efficient windows, the thermal insulation of the building envelope, which is slightly above the present level, and the demand-controlled variable air flow HVAC system with heat recovery, the need for heating and cooling energy has been reduced to such a level that the low energy office can be cooled with outdoor air and forced indirect evaporation cooling. The building is kept warm with the support of its own operations almost throughout the year. It is possible to arrange a good individual indoor climate in this way without any purchased heating or cooling energy. In Finland's climatic conditions, a good indoor climate, good energy efficiency and sound ecological principles require the use of demand-controlled, variable outdoor air flows. At the same time, it will be possible to adjust the climatic conditions individually in each room of the office. It is also possible to rearrange the indoor climatic conditions if the structures or the use of the office building are changed.

TECHNICAL SOLUTIONS OF THE METOP-BUILDING

- **Energy economic windows and building envelope.**
- **Air tight structures.**
- **Use of the installation floor and hollow core slabs as installation spaces.**
- **Utilization of the structures as a short time storage of heating and cooling energy by means of an intelligent HVAC system.**
- **Utilization of the external and internal heat loads when heating is needed and their removal when cooling is needed thanks to an intelligent HVAC system and structures.**
- **A new kind of intelligence in the control strategy.**
- **The possibility to choose the quality of indoor climate individually in each room.**
- **Heat recovery in winter and cooling recovery in summer.**
- **Maximum efficiency of heat recovery with a new type of freeze protection.**
- **Heating with return air at night in winter if required.**
- **Cooling with outdoor air at night in summer when needed.**
- **Massive machine rooms for air handling units are unnecessary.**
- **No separate heating and cooling systems are needed.**

ACKNOWLEDGEMENTS

The study is being carried out as a cooperation project involving VTT Technology Inc., the Laboratory of Heating and Ventilation (VTT), The Laboratory of Structural Engineering (VTT), and The Building Materials Laboratory (VTT), and the following building and HVAC-companies, which are financing the study: Lohja Corporation, Partek Concrete, Tietolipasto Oy, Ilmaterä Oy, RC-Linja Ky and NOKIA Cable.

The study is a part of the research programme entitled "Energy Efficient Buildings and Building Components" (ETRR) of the Energy Department of The Ministry of Trade and Industry. In addition, The Ministry of The Environment is supporting experiments which lead to the replacement of HVAC cooling systems using CFC in office buildings.

The authors wish to acknowledge the support of the above-mentioned companies and the authorities.

REFERENCES

- /1/ Laine, J., Prototype for a low energy office building. Caddet Newsletter no. 4, December 1991, p. 11-13.
- /2/ Laine, J., Low-energy office. Industrial Horizons, 1992, p. 24-25. Interview. Technical Research Centre of Finland, VTT Technology Inc.

FURTHER INFORMATION

EBES: The integrated HVAC, piping electrical and building system
TAT: Office and apartment buildings' product development
ETRR: Energy Efficient Buildings and Building Components
LVIS-2000: Future Building Services
RATA-2000: Construction Mode 2000.

**Ventilation for Energy Efficiency and Optimum
Indoor Air Quality
13th AIVC Conference, Nice, France
15-18 September 1992**

Paper 8

**The Energy Benefits of Sunspaces in Houses with
Ventilation Heat Recovery.**

R. Wiltshire and J. Littler

**Research in Building Group, The University of
Westminster, 35 Marylebone Road, London NW1
5LS, United Kingdom**

Summary

A heat recovery system reclaims heat from outgoing stale air, supplying it to incoming fresh air. The energy benefit is greatest if it supplies *all* the fresh air to the house and none enters via uncontrolled openings, hence *ventilation* heat recovery (VHR).

A sunspace (or conservatory) attached to a dwelling will almost always be at some temperature above ambient. Heat losses by conduction through the adjacent building fabric and ventilation losses via cracks will be reduced. This effect is modest; however, Baker [1] has proposed that drawing ventilation air from a sunspace can save substantial amounts of energy, provided ventilation can be preferentially drawn from the conservatory rather than through adventitious openings throughout the dwelling.

In a CEC Demonstration Project, the authors are using a variety of mechanical systems and retrofit conservatories to examine the benefits of such systems.

Data is presented which shows that the combination of VHR with sunspaces does not maximise the benefits of either. A variety of strategies is presented which attempt to optimise this combination - they illustrate the flexibility of the simulation model used; but do not succeed in justifying the sunspace/VHR combination. However, the study has shown that energy is available by heat pumping on the VHR exhaust.

Attention is also devoted to sunspace design parameters; glazing type is shown to have a considerable effect on sunspace temperature.

1 Introduction

Attached sunspaces can reduce the energy requirements of the dwelling to which they are attached. There are 3 distinct mechanisms by which this occurs: the sunspace receives direct solar gains; its presence affords "buffer" protection to the adjacent rooms, reducing conductive and convective losses; it pre-heats ventilation air entering the building via the sunspace.

Unfortunately, conservatories can also be accompanied by an *increase* in energy consumption. This is the result of the conservatory being regarded as extra living space and, accordingly, heated.

There are, therefore, 2 major areas of concern: firstly, to determine how to achieve the available energy savings most effectively; secondly, how best to avoid the sunspace actually *increasing* the energy consumption of the building.

Various approaches have been adopted in order to harness the available energy within sunspaces, and a selection of these are now outlined.

A group of council houses in Newham [2] have been equipped with solar roofspaces. This was done when the houses were being refurbished. Roofspace air is delivered directly to the house (see figure 1). The heated air is drawn down through a vertical duct, by means of a fan. The house has a separate heating system; in order to maximise the benefit of the roofspace air, the central heating setpoint is above the roofspace air setpoint. Monitoring revealed the savings due to the roofspace to be approximately 20% of the total energy requirements, though the savings varied considerably according to how conscientious the

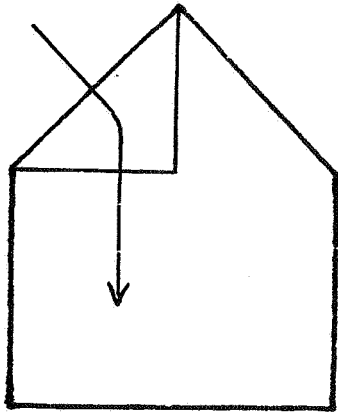


Figure 1 Roofspace air for pre-heat

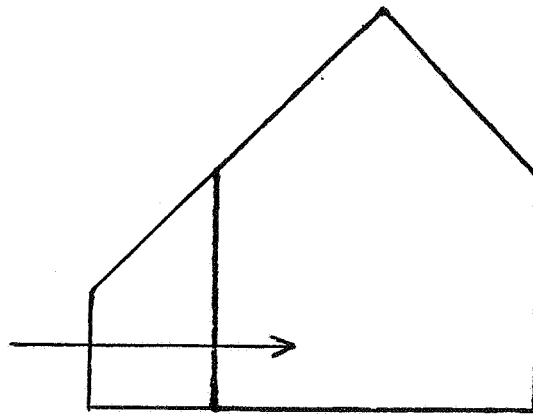


Figure 2 Conservatory air for pre-heat

occupants were, and also whether or not they used the potentially large day-time gains. This system can only use roofspace air advantageously if the roofspace air temperature exceeds that of the house.

Roofspaces have no concurrent amenity value, and are therefore only likely to be economic when roof refurbishment is necessary. A conservatory has amenity value; its contribution is a bonus. This is also its weakness; extracting heat from it reduces this amenity value. Also, it is generally less effective a collector than a roofspace due to its position. However, due to its prevalence this study is primarily concerned with conservatories.

When sunspace air is used directly, benefits can only accrue at times when the conservatory or roofspace temperature exceeds that of the house. However, in the case of tightly sealed dwellings, the heating of ventilation air is a substantial proportion of the energy load. Thus Baker [1] has identified that "the main role for sunspaces attached to well insulated houses is in pre-heating ventilation air". Using sunspaces in this way means that a benefit is gained at all times, because the sunspace always sits at a temperature above ambient.

The single-glazed sunspaces attached to a group of experimental houses in Peterborough [3] reduced the energy consumption by some 15%. The intention was to utilise the air in the sunspace for ventilation pre-heat (see figure 2), as well as anticipating the benefits of buffering. However, zone to zone air movement measurements indicated that much of the available energy could be lost; when the sunspace temperature is high, air is actually drawn from the living space to the sunspace. This suggests a fan is necessary if pre-heated air is to be systematically drawn from sunspace to living area. In these houses the kitchen and bathroom extract fans went some way towards achieving this.

As standards of air-tightness in houses have improved, the heating load due to the ventilation requirement has assumed increasing importance. One effective strategy is to install a warm air heating system with heat recovery. The delivered warm air also constitutes the ventilation to the house; nearly all the fresh air entering the house enters via the heating system.

If there is a sunspace attached to such a tightly sealed house it is possible to draw this fresh air from the sunspace. Air pre-heated in this way will tend to reduce the energy saving potential of the heat recovery unit. The savings from these features are unlikely to be additive, but they may exceed the saving from either feature alone.

A group of well insulated and tightly sealed houses at the Shenley Lodge Estate in Milton Keynes [4] have been constructed with solar roofspaces. Air from the roofspace is used as pre-heat to a Johnson-Starley [5] gas warm-air heating system with heat recovery (see figure 3). By this means solar pre-heat air is used whenever the heating system is operating; the roofspace air need not be warmer than the house air.

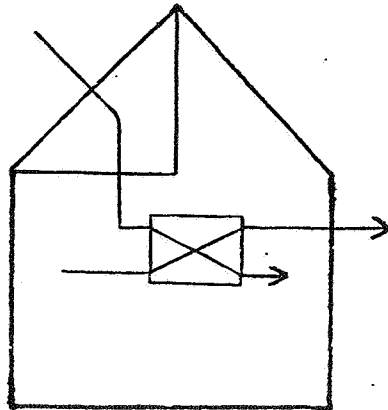


Figure 3 Roofspace air for pre-heat to a VHR

Delivering pre-heated roofspace air directly to the heat recovery unit allows the roofspace air to be used advantageously even when it is cooler than the house temperature, but a different shortcoming is introduced; pre-heated roofspace air is sometimes being cooled down by the outgoing stale air.

This study seeks to determine whether a conservatory, supplying pre-heated air to a VHR system (see figure 4), is capable of supplying useful amounts of heat to the main building. Different systems are examined in an attempt to overcome shortcomings highlighted by previous studies. The results emerging from Shenley Lodge show that the pre-heated sunspace air is sometimes actually *hotter* than the supply air emerging from the heat recovery unit. In order to take full benefit from the energy contained within the sunspace air, it has been suggested that the usual sequence of the air flow should change when this condition applies, so that fresh air first enters the heat recovery unit, then goes to the sunspace, before

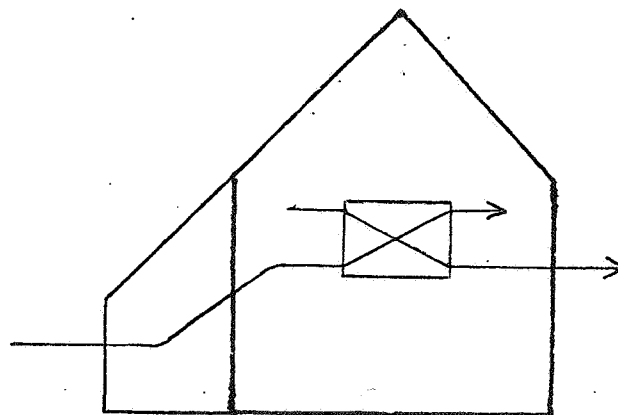


Figure 4 Conservatory air for pre-heat to a VHR

entering the house (see figure 5). When the temperature of the sunspace air falls back below that of the VHR output, the system reverts to the original sequence, air first entering the sunspace and then proceeding to the heat recovery unit.

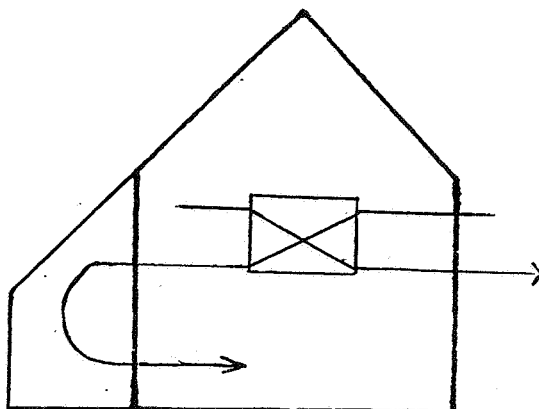


Figure 5 Air stream from VHR to conservatory to house

The impact on conservatory amenity value is also considered; here another issue arises. Sunspaces in the UK are often built to provide extra living space as well as to obtain a "garden in the house" effect. This means they are often heated. The actual construction of the sunspace, and the materials used, are therefore of great importance, whether or not the sunspace is to be used for pre-heated air for the house.

At the Stokkan house in Trondheim [6] the sunspace has been deliberately constructed using high performance glazing, and has been fully integrated with the rest of the house at the design stage. The sunspace is a pleasant area with an outdoor "feel" but with indoor furnishings and comfort expectation. In the relatively cold climate of Trondheim the sunspace is expected to provide worthwhile pre-heat, but at the very coldest times it will be heated. Although such an integrated approach can only be successfully adopted if the house is new-build, the experiences arising from this study can still be heeded for retro-fit applications.

This study is, therefore, also concerned to identify the design factors which influence its impact on the energy consumption of the dwelling.

2 Modelling

The APACHE [7] thermal simulation programme has been widely used throughout this study. APACHE allows a detailed building model to be simulated together with heating plant controlled by almost any control strategy. In particular the modal switching described in section 1 can be simulated, by defining 2 distinct modes of operation. Switching between the modes is controlled according to the setpoint, $(T_{\text{sunspace}} - T_{\text{hrec}}) = 0$. The temperatures T_{sunspace} and T_{hrec} refer to the sunspace and the heat recovery supply to the house. The modes of operation are as follows:

- (i) Air flows first through sunspace, then to the heat recovery unit, when $(T_{\text{sunspace}} - T_{\text{hrec}}) < 0$,
- (ii) Air flows from the heat recovery unit to the sunspace, then to the house warm air ducting system, when $(T_{\text{sunspace}} - T_{\text{hrec}}) > 0$

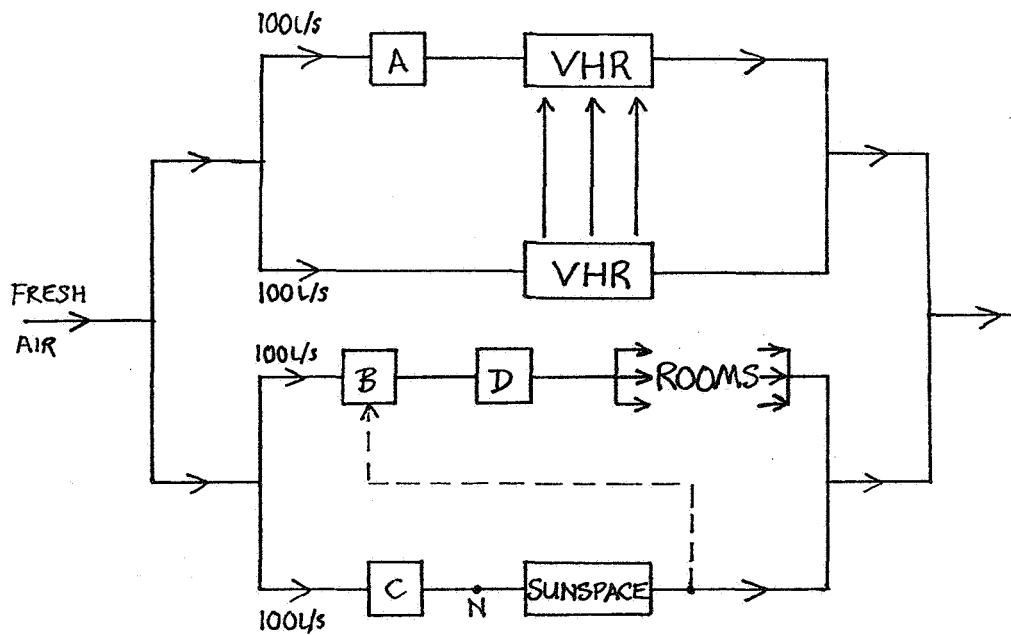


Figure 6 Air flow system diagram for simulating modal switching with APACHE

This situation is represented in APACHE by setting up a system diagram (see figure 6); this includes the air flow, the rooms and the heating components. The modal switching is accomplished by defining dummy heater batteries, which are able to "track" the temperature of any node to which they are referenced. In the first mode air flows into the sunspace from outside, is pre-heated, then enters the VHR unit, before being delivered to the rooms. This mode is in operation when dummy heater battery (A) tracks the temperature of air emerging from the sunspace and when dummy heater battery (B) similarly tracks the temperature at the VHR supply. The air stream, having been successively heated at both sunspace and VHR then proceeds to the rooms. Figure 6 shows the tracking connection for heater battery (B).

When the control condition dictates a change to the second mode, dummy heater batteries (A) and (B) are switched off and (C), tracking the VHR supply, and (D), tracking the sunspace, are activated.

Figure 7, showing temperatures at node (N) in the system, demonstrates the modal switching is occurring as sunspace and heat recovery temperatures cross over.

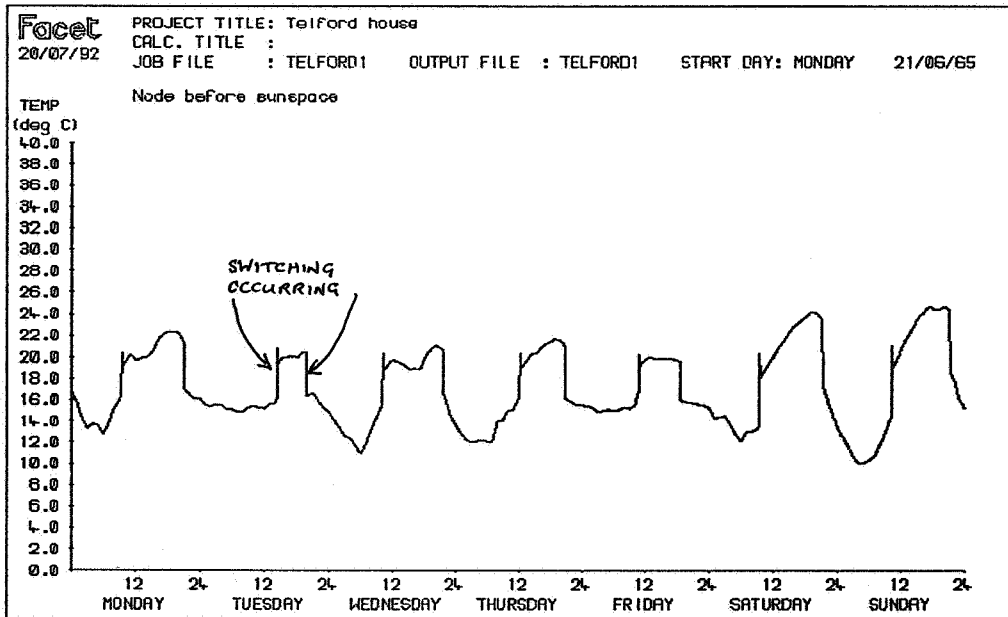


Figure 7 Temperature profile of node (N) showing modal switching

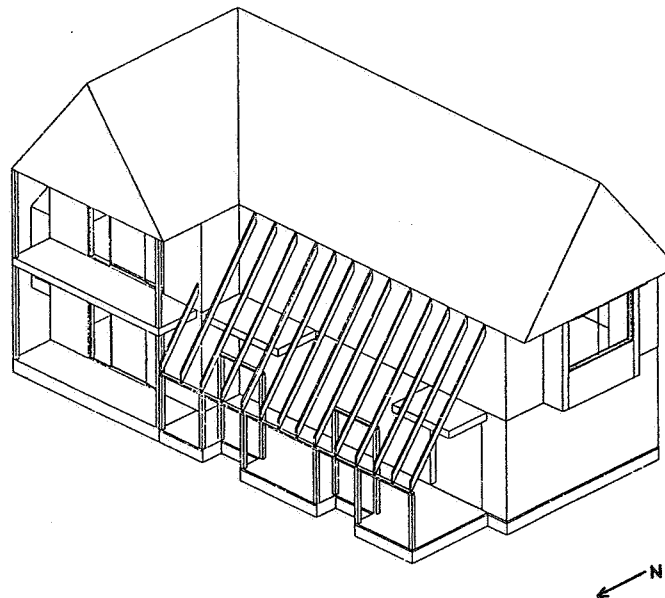


Figure 8 Telford test house

3 Test Houses

3.1 Telford test house

House 1, situated in Telford, is a lightweight, timber frame detached house, with a floor area of 190m². Figure 8 shows a projection of this house, produced using AutoCad. Tracer gas tests, using the Bruel & Kjaer [8] photoacoustic gas analyser for detection, were carried out and indicate an air change rate of 0.15, which increases to 0.31 if the solid fuel fire is lit. The sunspace is comparatively large (20m² floor area, 67m³ volume), is single glazed, and is perceived primarily as an exterior zone for rearing young plants, and a buffer to each of the bedrooms.

The sunspace supplies ventilation pre-heat to a Genvex 315 [9] unit. This unit contains a cross-flow heat exchanger and an air-to-air heat pump. In the heat exchanger stale house air, from extracts in the kitchen and bathroom, surrenders heat to the incoming fresh air. The exhaust airstream then flows directly to the evaporator of the heat pump, and if the thermostat situated on the landing indicates a temperature less than 20°C, the heat pump is switched on. The fresh air is then heated further by passing over the condenser of the heat pump, before being ducted to bedrooms and lounge. If the additional heat available from the heat pump is not required, the Genvex operates in heat exchange mode only.

A damper enables fresh air to be drawn directly from outside when the sunspace temperature is likely to fall below a certain temperature, or when the house temperature is too high and requires only ventilation. Prior to installation of the Genvex unit the solid fuel fire was the only source of heat; consequently winter temperatures in the house have frequently been uncomfortably low.

Table 1 shows APACHE simulations conducted for this house.

TABLE 1: SIMULATED ENERGY CONSUMPTION, TELFORD TEST HOUSE

SUNSPACE PRE-HEAT	VHR	MODAL SWITCH	AUX. HEAT	ENERGY CONS. [kWh]	MIN. MONTHLY BEDROOM TEMP [°C]	MIN. MONTHLY SUNSPACE TEMP [°C]
No	No	No	Yes	15163	20.0	9.4
No	Yes	No	Yes	10846	20.0	9.2
Yes	No	No	Yes	13280	20.0	7.7
Yes	Yes	No	Yes	10353	20.0	7.7
Yes	Yes	Yes	Yes	10855	20.0	9.7
No	Yes	No	No	7302	15.9	7.4
Yes	No	No	No	7297	13.1	6.9
Yes	Yes	No	No	7029	16.4	7.2
Yes	Yes	Yes	No	7089	16.4	7.2

Two sets of results appear in the table; the first compares predicted energy consumption for this house if it is to be maintained at or above 20°C; the second set shows the results of simulations conducted for the installed system alone. Following monitoring of the house the simulation model will be fully calibrated; at present it is the *differences* between each of the results presented which are of interest, and these will now be discussed.

The simulations demonstrate that the savings from using sunspace air for ventilation pre-heat (with the VHR unit switched off), and those for using the VHR unit (with the sunspace left in buffer mode) are not additive.

With neither the VHR unit operating nor the sunspace being used for pre-heat, the projected energy consumption is 15163 kWh. Using the sunspace alone reduces this figure by 1883 kWh. Using the VHR unit alone reduces the figure by 4317 kWh. Using both together the reduction is 4810 kWh; if the savings were wholly additive this figure would be 6200 kWh. Given the presence already of the VHR system, the sunspace in pre-heat mode saves a further 493 kWh, which is approximately one quarter of the saving, had the saving been additive.

The saving produced in this way varies seasonally. Using the sunspace for ventilation pre-heat in preference to leaving it as a buffer zone saves nearly 500 kWh (4.8%). The saving varies from only 2% in January (absolute saving of 34kWh) to 8% in April (absolute saving of 59 kWh), and to 14.5% in July (absolute saving of 40kWh). This causes an average reduction in sunspace temperature of up to 2°C, which will reduce amenity value in the winter. This particular sunspace is not used for sitting, and is seen as an area exterior to the house.

When the VHR unit and sunspace pre-heat are used with no auxiliary heating, the overall reduction of energy consumption is about 3.7%, compared to leaving the sunspace simply as a buffer zone. The savings vary from 1.3% (14 kWh) in January to 7.7% (36 kWh) in April and 11.2% (26 kWh) in July. The total predicted energy saving is about 270 kWh. The pre-heat increases the average temperatures in the house by about 0.3°C in the depths of winter and by 0.8°C in the swing seasons. The sunspace temperature is reduced by 1.3°C - 2.0°C.

The greatest savings are during the swing seasons when the outside temperature may be quite low but the sunspace can be the recipient of large solar gains. Although the savings are small, they are being achieved at a very small extra cost, given the presence already of a sunspace. However, the sunspace temperature is lower, so there is a cost in terms of amenity value. The reduction in temperature is not very great, because this sunspace is quite leaky, so that even if air were not being drawn in for subsequent entry to the warm air heating system, it would suffer a substantial infiltration rate.

The anticipated energy benefit in switching modes, is not apparent from these simulations, although the sunspace is maintained at a higher temperature.

It is noticeable that for auxiliary heating to 20°C the simulation shows a significant *increase* in energy consumption. A possible reason for this is that the simple switching (according to a comparison of VHR output and sunspace temperature) may be causing the system to remain in mode 2 (VHR then sunspace) for longer than was originally intended. When the switch to mode 2 occurs fresh air is no longer drawn into the sunspace, so its temperature will rise, as will the temperature difference between the VHR output (now supplied directly by cold, fresh air) and the sunspace. The corollary of this is that when the sunspace temperature begins to fall, the system will remain in mode 2 substantially beyond a time at which it can more usefully operate in mode 1. If modal switching is to be used, its control needs devising very carefully.

An examination of some weekly profiles of temperatures for a typical week in April shows that, when the sunspace air is not being used for pre-heat (figure 9) the sunspace temperature exceeds that of the VHR supply for more than 40 hours, and the temperature difference is as high as 15°C. When the system is operating in sunspace pre-heat mode (figure 10), however, the times for which the sunspace temperature exceeds the VHR output temperature are reduced by half and the differential is also much less. In general, simulations indicate

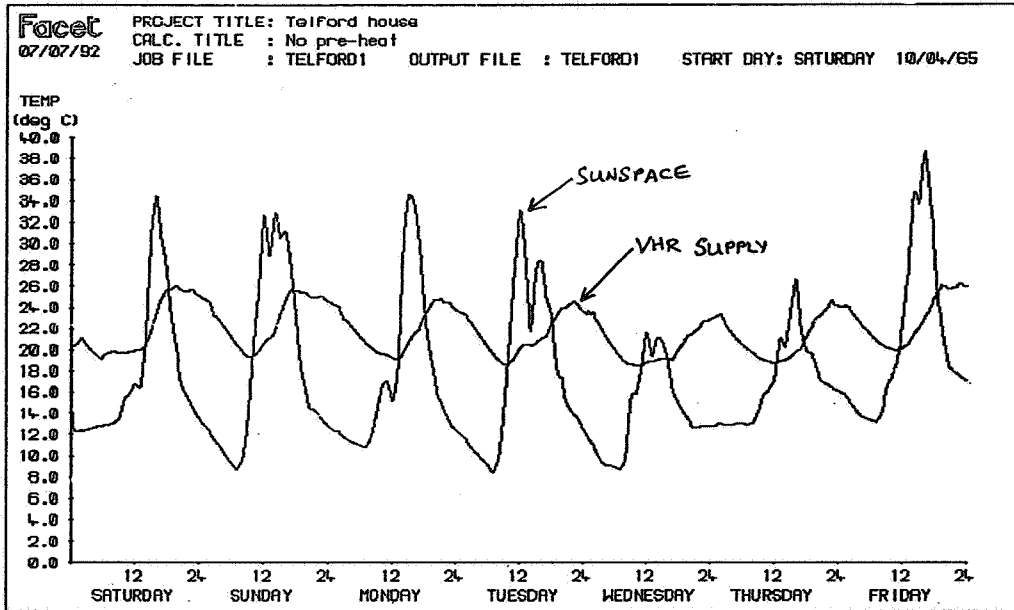


Figure 9 Temperature profile, no pre-heat

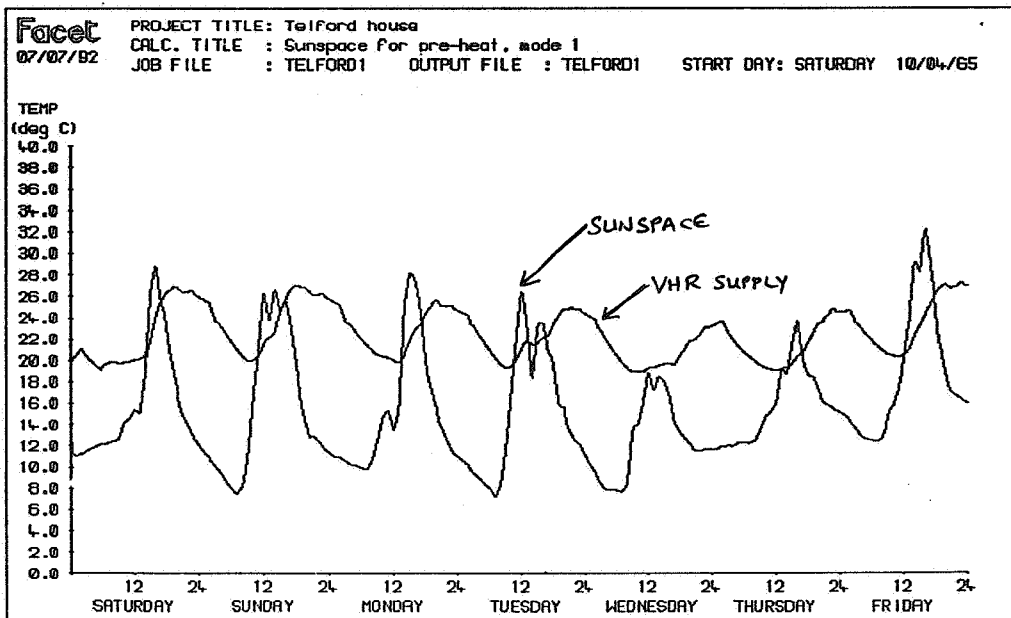


Figure 10 Temperature profile, with pre-heat

that when there is a constant flow of air through the sunspace there are few times when the sunspace temperature significantly exceeds the VHR supply temperature, except when the house temperature is already at a satisfactory level.

Using the sunspace for ventilation pre-heat to this particular house should be worthwhile, but only because the sunspace is not regarded as a sitting area by the occupants. The gains are slight, but they can be achieved at a correspondingly small overcost. The greatest benefit from sunspace ventilation pre-heat is derived when ambient temperature is low, solar radiation high, and heating to the house is required. It is also possible that there are times when the removal of heat from the conservatory not only heats the house but also cools the conservatory to a more comfortable temperature.

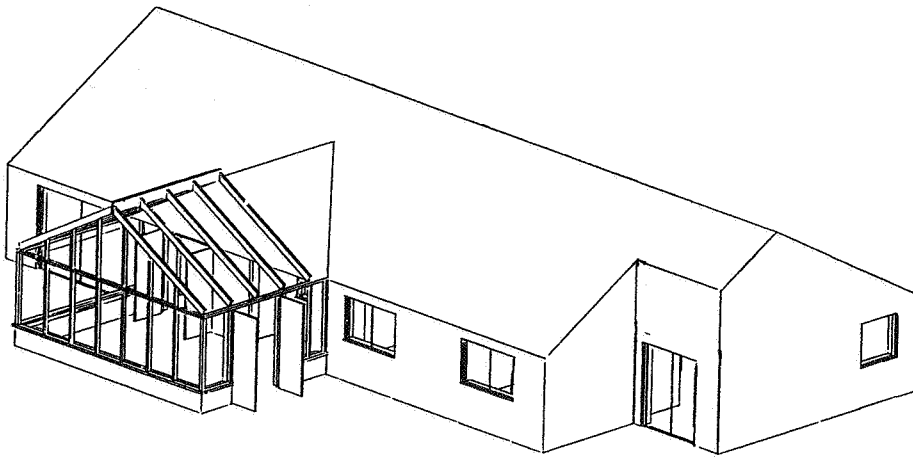


Figure 11 Bath test house, classical shape sunspace

3.2 Bath test house

House 2, situated in Bath, is a large, masonry construction, bungalow. Figure 11 shows an AutoCad projection of this house. It has an air change rate of 0.23, measured using the tracer gas method, together with the photoacoustic gas analyser.

The sunspace supplies ventilation pre-heat to a Johnson-Starley [5] gas warm air central heating system with flue gas heat recovery. The heat recovery unit is supplied partly by recirculation air, with sufficient extra air drawn from ambient or through the sunspace to meet the ventilation requirements of the 2 inhabitants.

The exhaust air from the heat exchanger flows across the evaporator of a heat pump; the compressor supplies heat to water in a closed pipe which runs to, and is embedded within, the sunspace floor. Thus the extra energy available from the heat pump is delivered to a low temperature sink, and helps offset the energy losses from the sunspace due to the pre-heat. The sunspace will not endure such large fluctuations of temperature, and careful control of the times and conditions for which the heat pump is switched on may increase the duration of thermal comfort in the sunspace for a small energy penalty.

An electronically controlled chain mechanism on the windows will be used for cooling. The sunspace is double glazed with a low-e film on one pane; it is perceived as an extra area of living space.

At the design stage, various shapes were considered, each having almost identical floor area and volume (see figures 11,12,13). Simulations indicate that the Wedge shape provides slightly higher winter temperatures (0.6°C warmer than the Upswept version, and 0.7°C warmer than the Classical shape); its major facade is due South whilst the other designs face 20° East of South. There is also slightly less over-heating incurred in the Wedge and Upswept versions, with their "reverse sloping roofs". A comparison of simulated house energy consumption for each sunspace shape reveals a less than 1% overall difference; for reasons of usable floor-space and aesthetic appeal, the Classical shape was chosen.

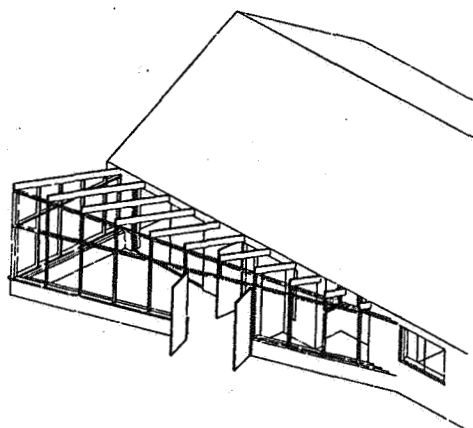


Figure 12 Wedge shape sunspace

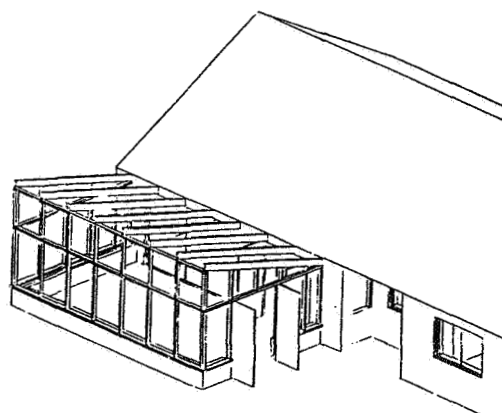


Figure 13 Upswept shape sunspace

Simulations have also been conducted to examine the relative benefits of different glazing types. Table 2 shows the daytime "over-temperatures" (amount by which the sunspace temperature exceeds ambient temperature) for the sunspace at Bath in January.

TABLE 2: SUNSPACE OVER-TEMPERATURES FOR VARIOUS GLAZING OPTIONS

GLAZING TYPE	DAYTIME OVER-TEMPERATURE °C
Single glazing clear float	2°C
Double glazing clear float	5°C
Double with clear float + low-e, air fill	7°C
Double with clear float + low-e, argon fill	8°C
Double with low iron + low-e	8°C

Weekly profiles for early January (figures 14 and 15) show a double glazed low-e coated, tightly sealed sunspace used to supply pre-heat is reduced to a worse thermal environment than a single glazed sunspace not being used. Figure 14 (no pre-heat) shows the double glazed sunspace is about 6°C warmer than the single glazed sunspace. When the double glazed sunspace is used for pre-heat, however, its temperature is reduced to 5°C lower than the single glazed sunspace.

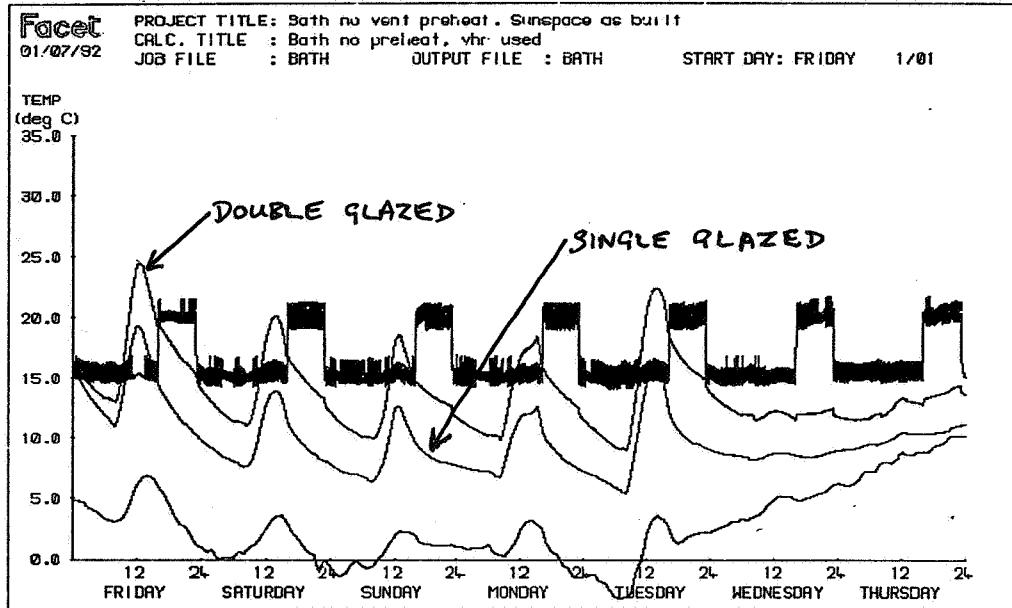


Figure 14 Temperature profile, no pre-heat

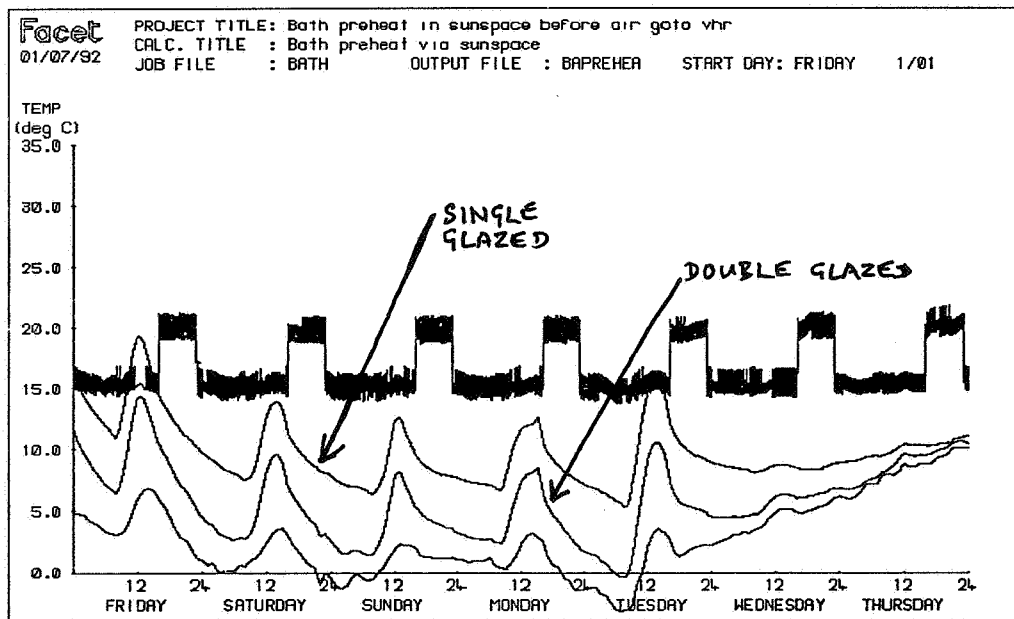


Figure 15 Temperature profile, with pre-heat

The work in progress to identify salient design parameters will continue, so that the influence of, for example, sunspace orientation, and frame and glazing bar construction, will be fully investigated.

4 Conclusion

(i) Simulation results suggest that using sunspace air for ventilation pre-heat to a heat recovery system produces a measurable benefit.

(ii) The simulations suggest that the individual benefits attainable by using sunspace air as ventilation pre-heat, and by using a ventilation heat recovery system are not additive.

(iii) If the sunspace is to be built anyway, and if there is already a warm-air heating system, the overcost to obtain this freely available energy is very small.

(iv) Drawing the air out of the sunspace for pre-heat has an adverse effect on the sunspace environment; the importance of this factor depends on how the owners perceive their sunspace. If it is seen as an area exterior to the house (as in the Telford house where it is used for protection for young plants, general storage area, and active play area), then lowering the temperature may not matter. If the sunspace has been carefully designed to provide a well sealed garden sitting room, then it is not sensible to use it for pre-heat since the temperature within can be lowered to below that of a single glazed sunspace.

(v) If the owners are likely to heat their sunspace, as occurs frequently in UK, then it would not be sensible to extract warm air; indeed, if people demand warm sunspaces, perceiving them as an additional living space, then the sunspace construction, particularly the glazing materials used, and the air-tightness, are matters for utmost care.

5 References

- 1 Baker N. The Use of Passive Solar Gains for the Pre-Heating of Ventilation Air in Houses. ETSU report s1142 DEn, 1985
- 2 Tindale A., Hancock C., Littler J. Hybrid Solar Roofspace Systems in the UK. Final report to CEC, Demonstration Project SE 509/84/UK, 1991
- 3 Martin C., Littler J. The Peterborough Solar Project. Final report to CEC, Demonstration Project SE 216/81/UK, 1988
- 4 Norton B., Lo S.N.G. Roof-space collectors integrated into each of fifteen newly built dwellings of passive solar design in Milton Keynes. Paper presented at ISES Congress, Kobe City, Japan, 1989
- 5 Johnson & Starley Ltd, Rhosili Road, Brackmills, Northampton, NN4 0LZ
- 6 Jacobsen T., Hestnes A.G., Raaen H. The Solar Dwelling at Stokkan: Final Results. Paper presented at NorthSun '92, Trondheim, Norway
- 7 APACHE (Applications Programs for Air Conditioning and Heating Engineers) by FACET, Marlborough House, Upper Marlborough Road, St Albans AL1 3UT
- 8 Brüel & Kjaer (UK) Ltd., 86 East Road, Longsight, Manchester M12 5GY
- 9 Genvex Klimateknik A/S, Roholmsvej 10, DK-2620, Albertslund, Denmark

5965

**Ventilation for Energy Efficiency and Optimum
Indoor Air Quality
13th AIVC Conference, Nice, France
15-18 September 1992**

Paper 7

Heat Recovery in Ventilation Systems.

F.Steimle and S. Schädlich

**Universität Essen, Angewandte Thermodynamik
und Klimatechnik, Universitätsstr.15, W-4300
Essen 1, Germany**

Heat recovery in ventilation systems

Synopsis

In well insulated buildings the ventilation heat is sometimes higher than the heat losses by transmission. For a air change rate of 0,8 per hour the specific heat flux must be calculated with 25 W/m^2 , so heat recovery can save some energy. In all considerations the saving in the heating system must be compared with the additional energy for the fans, because this energy is of a higher quality.

To optimize the heat recovery system, the different designs of the heat exchanger, the annual running hours and the annual hours for heat recovery must be taken into account. Heat recovery heat exchangers can be optimized with an efficiency of about 60%. To reach a higher overall efficiency a heat pump included in the system is a good possibility in special cases. To compare the different systems and combinations an overall COP can be derived not only for the heat pump but also for the heat exchanger. This is very important for the right decisions, because the aim can not be to save heating energy by spending more electricity.

List of symbols

A	[m ²]	-	heat exchanger area
c	[J/kg K]	-	specific heat capacity
\dot{C}	[W/K]	-	heat capacity flux
F _Z	[-]	-	form coefficient
\dot{H}	[W]	-	enthalpy flux
k	[W/m ² K]	-	overall heat transfer coefficient
K _{st}	[-]	-	constant of material
l	[m]	-	length
\dot{M}	[kg/s]	-	mass flow
P	[W]	-	electric power
Δp	[Pa]	-	pressure drop
\dot{Q}	[W]	-	heat flux
t	[K]	-	temperature
v	[m ³ /kg]	-	specific volume
\dot{V}	[m ³ /s]	-	air flow rate

α	[W/m ² K]-	heat transfer coefficient
ϵ^*	[-]	- heat recovery efficiency
η	[kg/m s]	- dynamic viscosity
η_f	[-]	- efficiency of power (fan)
κ	[-]	- number of thermal units, ntu
λ	[W/m K]	- thermal conductivity
ϕ	[-]	- thermal characteristic of heat exchange
ω	[-]	- ratio of heat capacity flux
ϑ	[K]	- temperature difference
ϑ_0	[K]	- maximum temperature difference

1. Introduction

Commonly heat exchanger systems are suited for heat recovery in big buildings, but nowadays energy consumption becomes also important in the domain of dwellings. Especially thermal high insulated buildings have only a transmission heat loss between 10 to 15 W/m², but a constant ventilation heat loss of 25 W/m². For decreasing this first part, different types of air-to-air heat recovery units are used, exhausting the air from the most polluted rooms (kitchen, bathroom, toilet, etc.) and taking it through a heat exchanger. Here the supply air is warmed up and flows into the bedrooms and living rooms.

The heat recovery units can achieve an efficiency of 60% depending on their design. A recuperative system allows only the heat recovery of the sensible heat whereas regenerative systems recover supplementary moisture. Conventional recuperative heat exchangers consist of solid walls like tubes or plates which divide the exhaust and the supply air. A more sophisticated system is the heat pipe system with finned tubes filled with a layer of wick containing a working fluid. One end of the pipes is exposed to the warm exhaust air stream, so that the liquid evaporates and the vapour flows to the other end which is in contact with the cold supply air stream. Here the vapour condenses and the heat is transferred to the cold air with an efficiency of nearly 70%.

One of the regenerative systems is the rotary air-to-air heat exchanger, a large slowly rotating wheel containing a metallic or non-metallic media for heat and moisture recovery which allows the transfer of sensible and

latent heat. This wheel isn't used in dwellings because of the danger of odour transfer.

2. Characteristic numbers of heat exchangers

For a description of the heat exchange process between two fluids some characteristic numbers are useful.

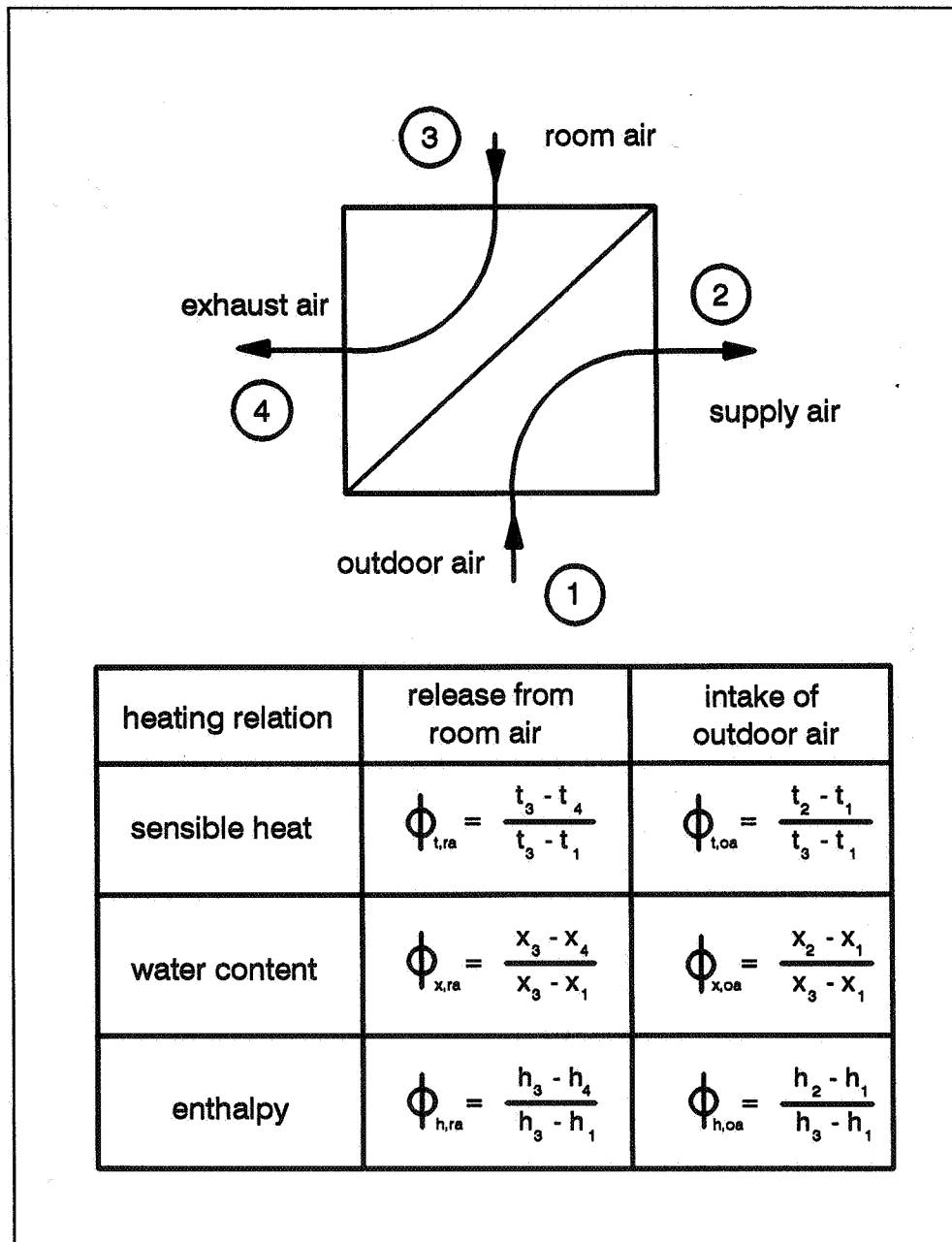


FIG. 2.1: Air flows through a heat exchanger and different thermal characteristic of heat exchanges.

Fig. 2.1 shows the different air flows through a heat exchanger and the different definitions of the thermal characteristic of heat exchange Φ relating to the temperature, the water content and the enthalpy. Considering the maximum temperature difference ϑ_0 of the heat exchanging streams and the temperature difference Δt of one of the fluids between inlet and outlet of the heat exchanger, the thermal characteristic of heat exchange is:

$$\Phi_t = \frac{\Delta t}{\vartheta_0}$$

For recuperative heat exchangers it is also useful to consider the transfer of moisture or of enthalpy. So there are additional thermal characteristics of heat exchange:

$$\Phi_x = \frac{\Delta x}{x_0} \qquad \Phi_h = \frac{\Delta h}{h_0}$$

The heat flux of a mass flow \dot{M} with the specific heat capacity c and temperature decrease Δt is determined by the following relation:

$$\dot{Q} = \dot{M} \cdot c \cdot \Delta t = \dot{M} \cdot c \cdot \Phi \cdot \vartheta_0$$

Assumed there is no heat exchange with the environment, the given heat from the one air stream (1) is completely taken from the other air stream (2). Then the quotient of the temperature difference is the following:

$$\frac{\Delta t_1}{\Delta t_2} = \frac{\Phi_1}{\Phi_2} = \frac{\dot{M}_2 \cdot c_2}{\dot{M}_1 \cdot c_1}$$

Considering the equation for the heat transfer through the wall

$$\dot{Q} = k \cdot A \cdot \vartheta,$$

the number of thermal units κ is defined as:

$$\kappa = \frac{k \cdot A}{\dot{M} \cdot c}$$

Another characteristic number is the relation of the heat capacity flux ω :

$$\omega = \frac{\dot{C}_1}{\dot{C}_2} = \frac{\dot{M}_1 \cdot c_1}{\dot{M}_2 \cdot c_2} = \frac{\Delta t_2}{\Delta t_1} = \frac{\Phi_2}{\Phi_1} = \frac{\kappa_2}{\kappa_1}$$

Here the bigger heat capacity has to be in the denominator of ω , so ω is a number between 0 and 1.

The amount of Φ , κ and ω depends on the type of heat exchanger (parallel, counter or cross flow).

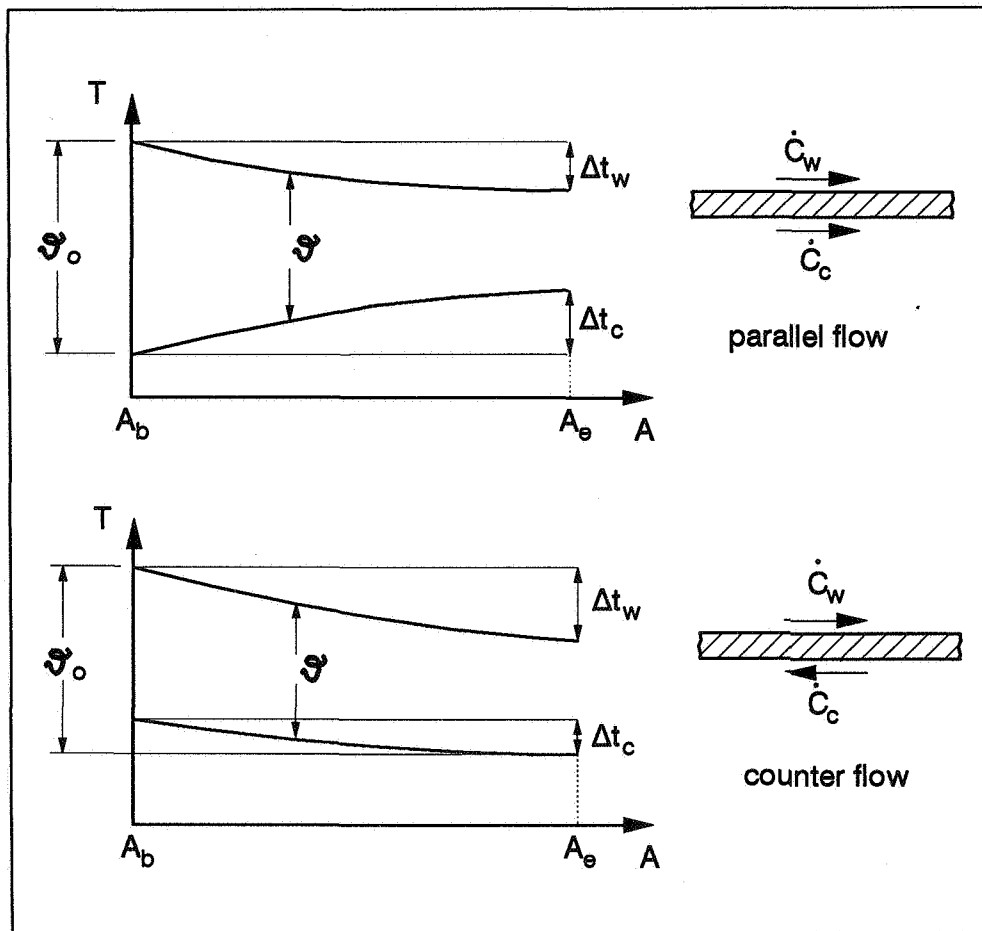


FIG. 2.2: Temperature relations in different types of heat exchangers.

Fig. 2.2. shows the temperature relations between a warm (w) and a cold (c) air flow in parallel and counter flow heat exchangers.

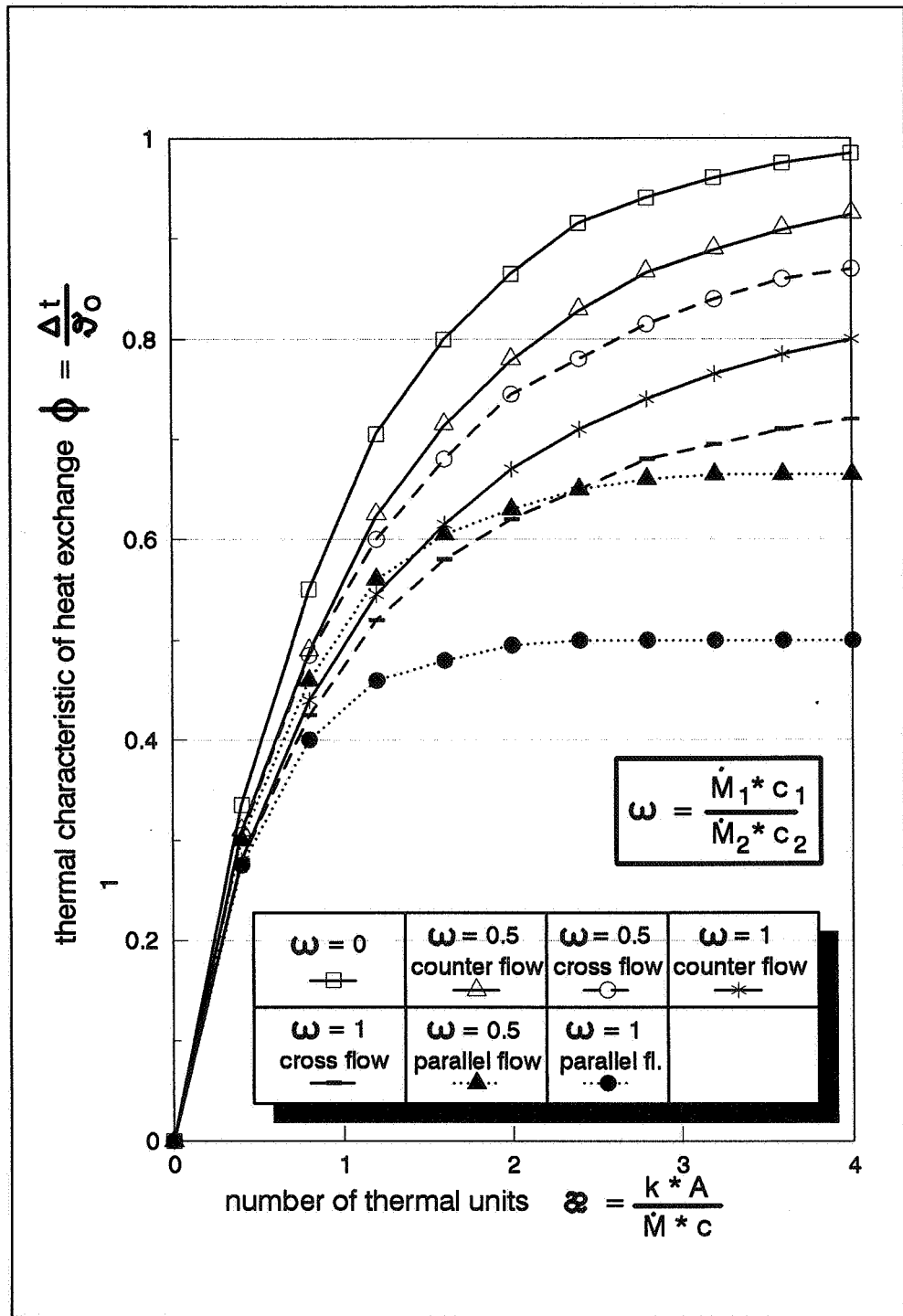


FIG. 2.3: Operating characteristic for different types of heat exchangers.

In FIG. 2.3 the thermal characteristic of heat exchange ϕ is plotted against the number of thermal units κ with the parameter ω for different types of heat exchangers. The relations between ϕ , κ and ω show the highest thermal characteristic of heat exchange for counter flow heat exchangers. Remembering Fig. 2.2 it is evident that parallel flow heat exchangers have

the lowest Φ of only 0.5 ($\omega = 1$) because of the temperature relations between the cold and warm air stream.

But Fig. 2.3 is also useful to optimize heat exchangers. Assuming a counter flow system with an efficiency of 60% and $\omega = 1$, then the thermal characteristic of heat exchange is 1.5. To improve the efficiency factor up to 80%, we get a Φ of 4, so a 2.7 times larger heat exchanger surface is needed. This provides beside higher investments an increasing pressure drop and a higher power consumption of the fans. So there is an optimal operating point for a fan depending on several influences.

3. Material of heat exchangers

For heat exchangers different materials, f. ex. aluminium, glass, plastic, etc. with various thermal conductivities λ are used. The overall heat transfer coefficient k is dependent on the heat transfer coefficient α and the thermal conductivity λ .

$$\frac{1}{k} = \frac{1}{\alpha_w} + \frac{s}{\lambda} + \frac{1}{\alpha_c}$$

Assuming the same α - values for the cold and the warm side of the heat exchanger of for example $\alpha_w = \alpha_c = 17 \text{ W/m}^2\text{K}$ and a thickness of $s = 1 \text{ mm}$ it follows:

aluminium	($\lambda = 200 \text{ W/mK}$)	$k_{al} = 8,5 \text{ W/m}^2\text{K}$
glass	($\lambda = 0,76 \text{ W/mK}$)	$k_{gl} = 8,4 \text{ W/m}^2\text{K}$
plastic	($\lambda = 0,35 \text{ W/mK}$)	$k_{pl} = 8,3 \text{ W/m}^2\text{K}$

So it is evident that the impact of material is of secondary order and the most important value for the overall heat transfer coefficient is the α - value which increases with the mass flow. But at the same time the number of thermal units κ and also the thermal characteristic of heat exchange Φ decreases, because M is in the denominator of κ .

Beyond that, the time for passing the heat exchanger is too short to produce a real improvement of heat flux. In addition an increasing velocity provokes a higher pressure drop, so that a higher power consumption is required. To estimate the impact of all influences, a theoretical treatment of heat transfer and fan power is useful.

4. Theoretical treatment

Based on theoretical knowledge of the heat transfer mechanism and the influences on the fan power consumption, various equations are derived to determine the relation between the different characteristic numbers. The precise mathematical formulation of the heat transfer problem is the Nusselt number:

$$\text{Nu} = \frac{\alpha \cdot l}{\lambda} = \frac{\alpha \cdot \dot{M}}{\lambda \cdot \eta} = F_z \cdot \left(\frac{(\Delta p/l) \cdot \dot{M}^3}{a \cdot \eta^4} \right)^{0.37}$$

Under consideration of the fan power

$$P = \frac{\Delta p \cdot \dot{V}}{\eta_f} = \frac{\Delta p \cdot \dot{M} \cdot v}{\eta_f}$$

we get the following equation:

$$P = \frac{1}{\eta_f} \cdot \dot{M}^{3.4} \cdot \left(\frac{2 \cdot \kappa}{K_{St} \cdot A \cdot F_z} \right)^{2.7}$$

with K_{St} depending only from the material and the fluid:

$$K_{St} = \frac{\lambda \cdot \eta}{c} \cdot \left(\frac{1}{a \cdot \eta^4 \cdot v} \right)^{0.37}$$

5. Boundary conditions and optimization

Under consideration of the efficiency of electrical generation in power stations the boundary condition for useful heat recovery is:

$$3 \cdot P = Q$$

$$\frac{3 \cdot \Delta p \cdot \dot{M} \cdot v}{\eta_f} = \dot{M} \cdot c \cdot \Phi \cdot \vartheta_0$$

So the pressure drop additionally provoked by the heat exchanger is limited by the following equation:

$$\Delta p = \frac{c \cdot \Phi \cdot \vartheta_0 \cdot \eta_f}{3 \cdot v}$$

To optimize the heat exchanging process, the required electrical power and the non-transferred heat flux has to be a minimum value:

$$3 \cdot P + \Delta\dot{Q} = \text{minimum}$$

The non-transferred heat flux is:

$$\Delta\dot{Q} = \dot{M} \cdot c \cdot \vartheta_0 \cdot (1 - \Phi) = \dot{M} \cdot c \cdot \vartheta_0 \cdot \frac{1}{1 + \kappa}$$

Then it follows:

$$\frac{3 \cdot 1}{\eta_f} \cdot \dot{M}^{3,4} \cdot \left(\frac{2 \cdot \kappa}{K_{St} \cdot A \cdot F_z} \right)^{2,7} +$$

$$\dot{M} \cdot c \cdot \vartheta_0 \cdot \frac{1}{1 + \kappa} = \text{minimum}$$

This equation allows only a qualitative judgement of the impact of the different influences like the area and the length of the heat exchanger, the mass flow, the kind of fluids, etc..

6. Investigations

In order to determine the efficiency of a special heat pipe system of a ventilation window, a ϵ^* -value is defined as the relation of the enthalpy flux difference between the room air and the exhaust air to the required fan power.

$$\epsilon^* = \frac{\dot{H}_{\text{room air}} - \dot{H}_{\text{exhaust air}}}{P_{\text{fan}}}$$

Fig. 6.1 shows the fan power increasing with the mass flow and its impact on the heat recovery efficiency ϵ^* . Under consideration of the factor 3 for the generation of electrical power for this system only a fan power up to 40 W is economical for heat recovery.

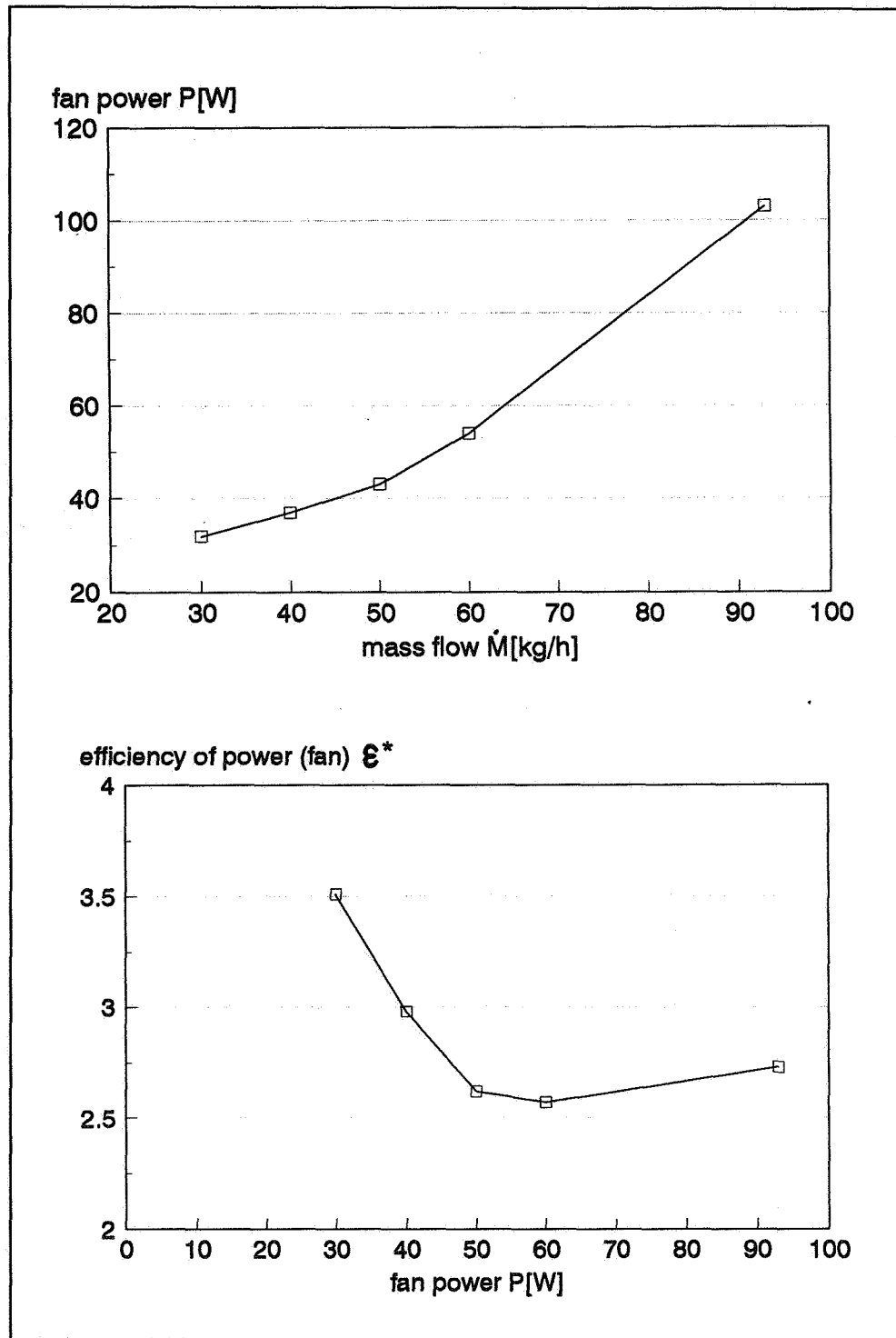


FIG. 6.1: Mass flow and efficiency of a heat pipe system as a function of the fan power.

7. Annual running hours

A heat exchanger in a ventilation system represents an additional pressure drop, so the fan power increases. In order to calculate a realistic efficiency for a heat recovery system, the annual hours for the heat recovery in relation to the total annual running hours of the system with the higher pressure drop must be taken into account.

Here some ventilation systems offer the possibility to take off the heat recovery unit in times where it isn't needed, so the required fan power decreases.

8. Summary

The impact of ventilation heat losses are increasing because of the improved insulation of buildings, so heat recovery systems are used to save more energy. But the higher pressure drop of the heat exchangers causes additional power consumption of supply and exhaust fans. This must be offset against the energy reclaimed from the air streams under consideration that electricity is of a higher quality than heating energy.

Under consideration of all influences on heat exchanger efficiency taken by theoretical and practical estimations as well as calculations of the annual running hours and the required additional fan power, it is possible to design a economical heat recovery system for different applications.

8. References

- /1/ Steimle, F.
"A general analogy between heat transfer and pressure drop in turbulent flows"
Commissions II & III, London 1970, Annex 1970-1, Supplement of the Bulletin of the International Institute of Refrigeration (Extract)
- /2/ Steimle, F.
"The effect of superimposed free and forced convection on heat transfer and pressure drop correlation"

Commissions B-1, B-2 and E-1, Freudenstadt 1972, Annex 1972-1
Supplement of the Bulletin of the International Institute of
Refrigeration (Extract)

/3/ Steimle, F., Gräff, B.

"Investigation about heat recovery of ventilation windows"

Institut für Angewandte Thermodynamik und Klimatechnik
Universität Essen, 1979

**Ventilation for Energy Efficiency and Optimum
Indoor Air Quality
13th AIVC Conference, Nice, France
15-18 September 1992**

Paper 6

**Modelling Fluctuating Airflow Through Large
Openings.**

F. Haghightat^{*}, J.Rao^{*}, J. Riberon^{}**

*** Centre for Building Studies, Concordia
University, 1455 de Maisonneuve Blvd. W.,
Montreal, Canada.**

**** CSTB (Centre Scientifique et Technique du
Bâtiment) 02-77421 Marne La Vallée, France.**

SYNOPSIS

Fluctuating airflow through buildings is caused by temporal and spatial variations of wind-induced pressures around building envelopes, and include pulsating airflow and eddy penetrations. Two approaches using a multi-zone pulsating airflow model are introduced in this paper to study the eddy penetration and multi-way airflow through large openings. In the first approach, the eddy flow is considered to be caused by imperfect correlations among pressures at different points of an opening. The concept of aerodynamic admittance functions is employed to modify the wind pressure spectra to represent the net effect of fluctuating pressures over the area of the opening. The other approach considers a large opening as composed of a number of smaller airflow paths, each permitting only pulsating airflow. Theoretical solutions are compared with field experimental results from the BOUIN test-house at CSTB, France.

LIST OF SYMBOLS

A_1, L_1, A_2, L_2 : effective opening areas and opening depths,

K_1, n_1, K_2, n_2 : power law coefficients and exponents,

$\bar{P}_1^w, \bar{P}_2^w, \bar{P}^i, \bar{Q}_1, \bar{Q}_2$: mean values of wind-induced pressures, internal pressure and airflow rates ,

$P_1^w(t), P_2^w(t), P^i(t), q_1(t), q_2(t), q^i(t)$: fluctuating components of wind pressures, internal pressure, airflow through openings, and compressibility airflow,
 f, ω : frequency and angular frequency, $f = 2\pi\omega$

$P_1^w(\omega), P_2^w(\omega), P^i(\omega), Q_1(\omega), Q_2(\omega), Q^i(\omega)$: Fourier transform of corresponding variables,

$S_{P_1^w}(\omega), S_{P_2^w}(\omega), S_{P_1^w P_2^w}^{(c)}(\omega), S_{P^i}(\omega)$: spectra and co-spectrum of two wind-induced pressures, and internal pressure spectrum,

$H_{P^i P_1^w}(\omega), H_{P^i P_2^w}(\omega)$: transfer functions between external and internal pressure,

$\chi_1(\omega)$: aerodynamic admittance function,

ρ air density, P_a atmosphere pressure, $\gamma=1.4, j = \sqrt{-1}$.

1. INTRODUCTION

Airflow through openings in building envelopes and internal walls is caused by the combined effects of three driving forces: wind-induced pressures, thermal buoyancy and mechanical systems. This airflow can be divided into steady-state airflow and fluctuating airflow. Steady-state or mean airflow is generated by mean pressure differences due to driving forces. The primary unsteady variables that cause fluctuations in airflow are temporal variations in wind-induced pressures.

Fluctuating airflow through individual openings caused by temporal variations in pressure differences can be divided into two types: the pulsating flow and the penetration of eddies. The pulsating flow results from the wind fluctuation and the compressibility of air in the building internal space. Fluctuations in the wind causes simultaneous positive or negative pressure variations at an opening.

The inside air is thus either pressurized or depressurized. The eddy flow is due to the turbulence in the air stream. They create a rotational effect on the inside air. This leads to an exchange between the inside air and the outside air through openings.

A model has been developed for predicting pulsating airflow in multi-zone buildings [1,2]. Inputs to the model include: the building airflow system (rooms, openings, and connections), the frequency characteristics of wind-induced pressures and their correlations, and output from a steady-state airflow model. In this paper, this model is extended to account for the effect of eddy flow, and is compared to field experimental data.

2. BOUIN TEST HOUSE AT CSTB, FRANCE

Field experiments were conducted in France by CSTB to study single sided ventilation [3]. The test house at Bouin (Figure 1a) was a single zone building on an exposed site near the Atlantic coast. The volume of the test house was 93.6 m^3 . The equivalent air leakage area of the house was measured and was less than 5 cm^2 . The building was mounted on a turntable that can be rotated during an experiment.

A sharp edged slot of 40 cm wide, 2.5 cm high and 1 cm thick was located in the building envelope. During the experiment, this opening was positioned to face the wind direction. The wind-induced external pressures, internal pressures, wind speed and direction, and tracer gas concentration were measured simultaneously at a rate of 10 Hz.

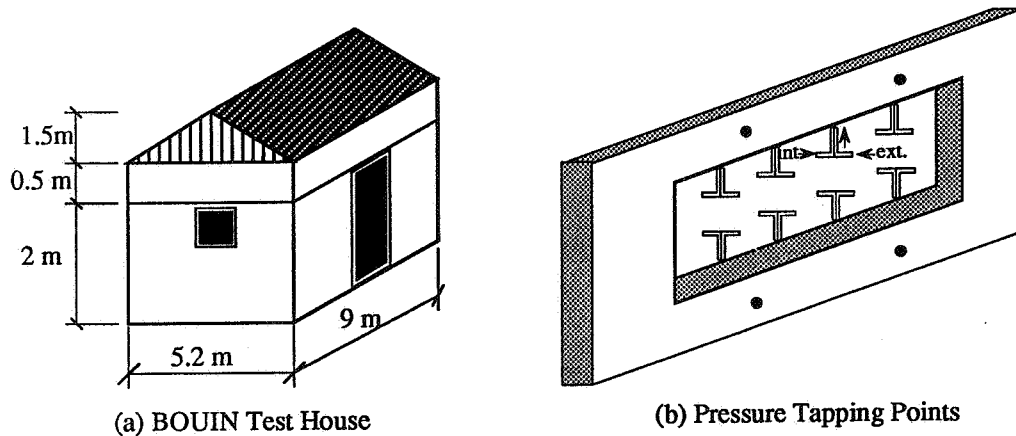


Figure 1. BOUIN Test House and Slot Opening

The wind pressure was measured close to the opening. This pressure was equal to the difference between the total pressure and the external static pressure. The pressures were also measured at eight points within the opening (Figure 1b), both inside and outside the building, allowing the direction of flow to be known locally. Full details of the site and the measurement used can be found in Riberon and Villain [4].

3. PULSATING AIRFLOW MODEL

In the pulsating airflow model presented in [1,2], the analysis is performed in the frequency domain. The task of calculating the pulsating airflow due to temporal variations in wind-induced pressures is decomposed into an infinite series of simple problems. Each problem calculates the corresponding portion of airflow caused by the simple sine wave pressure at a single frequency. The total airflow is then obtained by summing up all these infinitesimal portions of airflow at single frequencies. The formulation procedure for nodal governing equations of fluctuating airflow is demonstrated in the following using the BOUIN test house as an example.

In the steady-state calculation, the test house is modelled as a single-zone building with two openings. Opening 1 is the purpose-provided slot opening, and opening 2 represents the total leakage of the house envelope (Figure 2). The air mass balance for this building is written as:

$$K_1(\bar{P}_1^w - \bar{P}^i)^{n_1} + K_2(\bar{P}_2^w - \bar{P}^i)^{n_2} - 0 \quad (1)$$

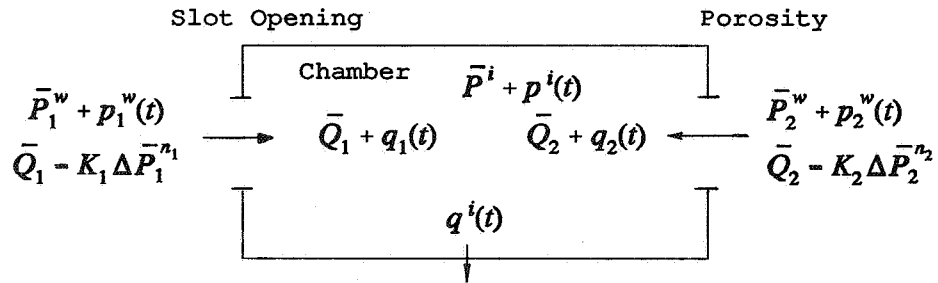


Figure 2. Modelling BOUIN House

For fluctuating airflow through the openings, the pressure differences are balanced by the forces required to overcome the flow resistance and the inertia of air in the openings, i.e.:

$$K_i^{-\frac{1}{n_i}} \left\{ (\bar{Q}_i + q_i)^{\frac{1}{n_i}} - \bar{Q}_i^{\frac{1}{n_i}} \right\} + M_i \frac{dq_i}{dt} = p_i^w - p^i \quad (2)$$

where $M_i = \rho L_i / A_i$, the subscripts $i = 1, 2$ and is the same for the following equations.

The nonlinear terms in the above equations are approximated to linear relations using a statistical linearization method. The linear fluctuating airflow equation for the openings can be expressed as:

$$M_i \frac{dq_i}{dt} + \lambda_i q_i = p_i^w - p^i \quad (3)$$

The coefficients λ_i are assigned to values such that the statistical variances of the nonlinear terms and the linear relations are the same. Equation (3) is then Fourier transformed into the frequency domain, and the fluctuating airflow equations in the frequency domain can be expressed as:

$$Q_i(\omega) = \frac{1}{\lambda_i + j\omega M_i} [p_i^w(\omega) - P^i(\omega)] \quad (4)$$

The compressibility of air in the room influences the fluctuating airflow through the building. The air mass increments due to pressurizations of the air volume in the building and decrements due to depressurizations are modelled by an imaginary airflow path which connects the room with the atmosphere. This compressibility airflow, $q^i(t)$, is related to the fluctuating internal pressure by:

$$p^i(t) = -\frac{\gamma P_a}{V} \int_0^t q^i(v) dv = -B \int_0^t q^i(v) dv \quad (5)$$

Applying a Fourier transformation, the fluctuating airflow equation for the imaginary compressibility airflow path can be written in the frequency domain as:

$$Q^i(\omega) = -\frac{j\omega}{B} P^i(\omega) \quad (6)$$

The airflow system of the BOUIN house, therefore, can be modelled by three openings in the frequency domain: the purpose provided slot opening, the porosity, and the imaginary airflow path for air compressibility. The governing equation can be obtained from the air mass balance:

$$Q_1(\omega) + Q_2(\omega) - Q^i(\omega) = 0 \quad (7)$$

Applying fluctuating airflow equations (4 & 6), the governing equation with the internal pressure as the unknown variable is obtained. Transfer functions for the internal pressure can be calculated as:

$$H_{p^i}(\omega) = \frac{P^i(\omega)}{P_i^w(\omega)} = \left\{ \frac{1}{\lambda_i + j\omega M_i} \right\} / \left\{ -\frac{j\omega}{B} + \sum_{i=1,2} \frac{1}{\lambda_i + j\omega M_i} \right\} \quad (8)$$

When the spectra and co-spectrum of the wind pressures are known, the spectrum for the fluctuating internal pressure is calculated by the spectral relation:

$$S_{p^i}(\omega) = \|H_{p^i1}\|^2 S_{p_1^w}(\omega) + \|H_{p^i2}\|^2 S_{p_2^w}(\omega) + 2\|H_{p^i1}\| \|H_{p^i2}\| S_{p_1^w p_2^w}^{(c)}(\omega) \quad (9)$$

In turn, the RMS (root-mean-square) value and other statistical information of the fluctuating internal pressure can be derived from the spectrum.

4. MODIFIED FLUCTUATING AIRFLOW MODEL

The mean and RMS values for variables of interest are displayed in Table 1. Figure 3 shows the magnitude and phase plots of the transfer function $H_{p^i}(\omega)$ for both experimental estimation and theoretical calculation based on the pulsating airflow model.

The discrepancy between theoretical and experimental results shown in Figure 3 can be attributed to the fact that the pulsating airflow model does not consider the eddy flow due to the spatial variations of wind pressures over the opening. The pressures on the area of the opening are assumed to be simultaneously pushing in or pulling out the air through the opening at all points. In reality, however, the pressures at different points on the opening are not perfectly synchronized or correlated due to the presence of eddies. Although these pressures have (or are assumed to have) the same statistical and stochastic properties, there are differences between these pressures. The differences are influenced by the distance between the two points, the turbulence characteristics, and eddy sizes.

Table 1. Experimental and Pulsating Airflow Model

		Experimental		Theoretical		
		Mean	RMS	Mean	RMS	Flow Reversal
Opening		$K_1=7.6771 \times 10^{-3}$ $n_1=0.5$		input		NA
Porosity		$K_2=8.3424 \times 10^{-4}$ $n_2=0.5$		input		NA
P_1^w		14.45	5.02	input		NA
P_2^w		-4.35	1.51	input		NA
Pulsating Model	P^i (Pascal)	13.60	4.53	14.23	4.72	NA
	Q_1 (l/s)	4.93	6.24	3.60	4.72	22.3%
	Q_2 (/s)	3.02	0.59	3.60	0.66	0
Aerodynamic Admittance Approach	P^i (Pascal)	13.60	4.53	14.23	4.50	NA
	Q_1 (l/s)	4.93	6.24	3.60	5.17	24.3%
	Q_2 (m ³ /s)	3.02	0.59	3.60	0.66	0
Multi-Path Approach	P^i (Pascal)	13.60	4.53	14.23	4.60	NA
	Q_1 (l/s)	4.93	6.24	3.60	5.50	25.7%
	Q_2 (l/s)	3.02	0.59	3.60	0.31	0

Note: NA: not available or not applicable.

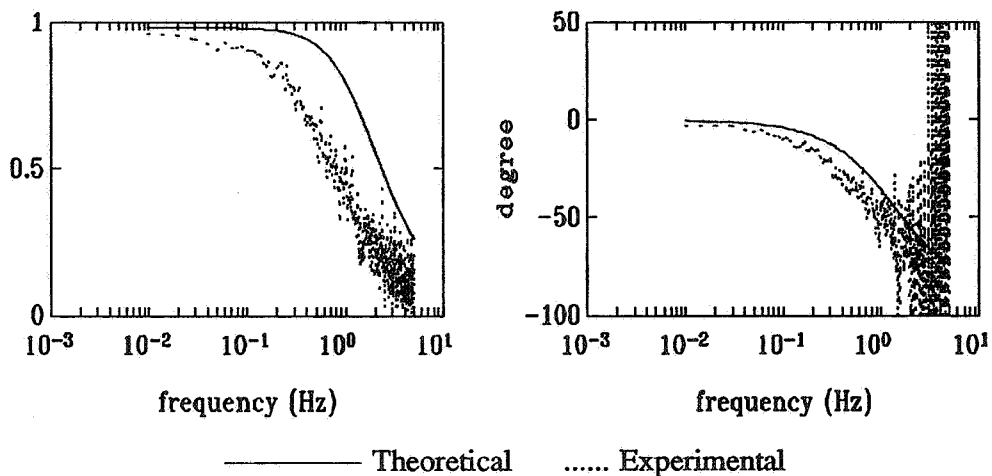


Figure 3. Results of Pulsating Model: (a) Magnitude and (b) Phase Plots of Transfer Function Between External and Internal Pressures

As a solution, a function is introduced to obtain the net effect of the imperfectly correlated pressures. Since the net force is always less than the "point" pressure (multiplied by the opening area), the function should be bounded from above by a value of 1. Because the differences are related to eddy sizes or the frequency, this function is related to the frequency. The concept of this function has been utilized in wind engineering to calculate the dynamic wind loading on building envelopes [5]. The function is referred to as an aerodynamic admittance function.

In the proposed approach to account for the eddies in the airflow through the opening, the aerodynamic admittance function is chosen to be the coherence function of wind-induced pressures at two representative points. Figure 4 shows the experimental estimation of the coherence function and fitting. The fitting curve will be used for later calculation.

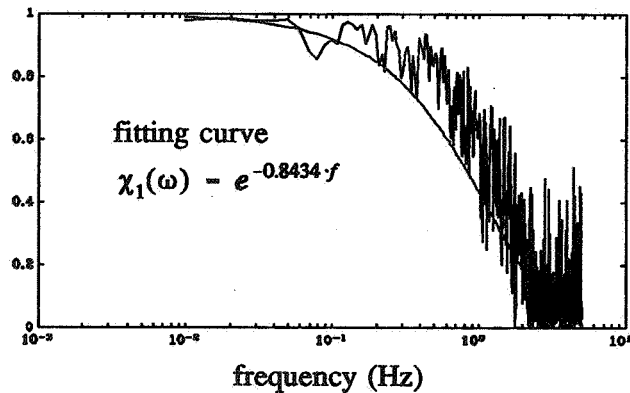


Figure 4. Coherence Function as Aerodynamic Admittance Function

Once the aerodynamic admittance function is obtained, the net effect should equal to the "point" value modified (multiplied) by the aerodynamic admittance function. In the theoretical calculation the "point" force is the power spectrum of the external pressure at the opening. Therefore, the calculation will take:

$$\hat{S}_{p_1^*}(\omega) = S_{p_1^*}(\omega) \cdot \chi_1^2(\omega) \quad (10)$$

as the input force. A further analysis shows this is equivalent to using a modified transfer function:

$$\hat{H}_{p_1^*}(\omega) = H_{p_1^*}(\omega) \cdot \chi_1(\omega) \quad (11)$$

in the theoretical calculation.

The comparison between experimental estimations and theoretical calculations by the modified model is shown in Figure 5. The plots show an improvement of the modified model over the pulsating model in predicting the transfer function. Table 1 also shows that the predicted RMS value of the internal pressure by the modified model is closer to the experimental results. The new approach also results in a larger RMS of airflow at the slot opening.

The second approach for modelling large openings is to consider airflow through an opening as composed of several separate airflows (sub-flows). Each sub-flow is a pulsating airflow and is modelled as one distinct airflow path using the pulsating airflow model. In this way, the limitation to pulsating airflow is overcome, and eddy flow or multi-way airflow through large openings can be accounted for in the prediction.

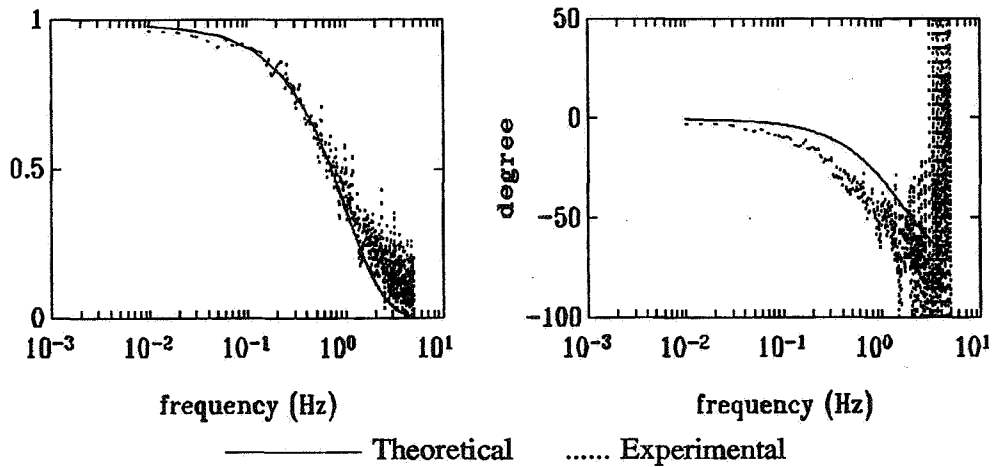


Figure 5. Results of Modified Model: (a) Magnitude and (b) Phase Plots of Transfer Function Between External and Internal Pressures

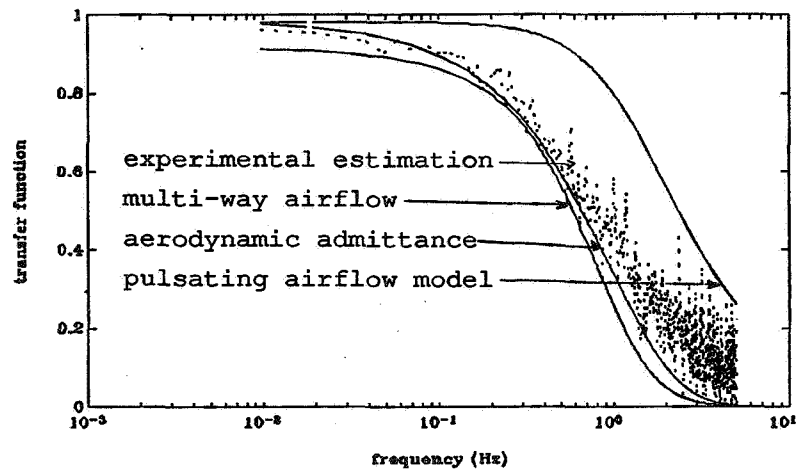


Figure 6. Results of Multi-Path Model: Magnitude Plot of Transfer Function Between External Pressure and Internal Pressure

The slot opening of the BOUIN house is modelled as two flow paths. The theoretical results based on this modified model is shown in Table 1 and Figure 6. The predictions of the transfer function and RMS value for the internal pressure, as well as for the fluctuating airflow, show an improvement over the original pulsating airflow model.

The total air exchange across an opening is determined by both the mean and fluctuating airflow rates. The amount of flow reversal due to contributions from fluctuating components can be calculated from the RMS values and by assuming normal distributions for the temporal variations in the airflow rates. The last column of Table 1 shows the percentage of fluctuating airflow that is involved in flow reversal through the slot opening. Let this percentage be β , the total air exchange across the opening is the summation of the mean airflow rate (\bar{Q}) and 3/2 of its fluctuating component (σ_q). Calculations (Table 2) show that due to fluctuations in the airflow, the air exchange across the slot opening is approximately 40 to 60 percent more than the mean value.

Table 2. Airflow Rate (l/s) Through Slot Opening

	\bar{Q}	σ_q	β	$\bar{Q} + \frac{3}{2}\beta\sigma_q$	$[\frac{3}{2}\beta\sigma_q]/\bar{Q}$
Pulsating	3.60	4.72	0.223	5.18	43.9%
Aerodynamic Admittance		5.17	0.243	5.48	52.4%
Multi-Path		5.50	0.257	5.72	58.8%

5. CONCLUSION

The pulsating airflow model and its modified versions for large openings perform analyses in the frequency domain, and take the spectra and co-spectra as input. The model provides predictions on statistical characteristics of the resultant airflow. The frequency analyses have the advantage of less computations over other models based on time domain simulations. The greater stability of the wind-induced pressure spectral information compared to the time signals also makes the model easier to apply in other general situations.

In accounting for fluctuating airflow through large openings, two approaches are employed. One approach utilizes the concept of aerodynamic admittance function. The net force that is pushing in or pulling out the air through the opening is considered to be the "point" pressure multiplied by the aerodynamic admittance function. The coherence function is chosen as the modifying function. The other approach considers airflow through a large opening as composed of multi-way flows and models the opening by several flow paths. The new approaches are applied to field experimental data from BOUIN test house in France. The comparison shows that both approaches are quite effective in explaining the experimental results.

References

1. Haghghat, F., Rao, J., and Fazio, P. (1991), "The Influence of Turbulent Wind on Air Change Rates - a Modelling Approach", *Building and Environment*, vol. 26, No. 2, pp. 95-109.
2. Rao, J. and Haghghat, F. (1991), "Wind Induced Fluctuating Airflow in Buildings", *Proc. of the 12th AIVC Conference*, Ottawa, Canada.
3. Bienfait, D., Phaff, H., Vandaele, L. Van der Maas, J. and Walker, R. (1991), "Single Sided Ventilation", *Proc. of the 12th AIVC Conference*, Ottawa, Canada, vol. 1, pp. 73-98.
4. Riberon, J. and Villain, J. (1990), "Etude en vraie grandeur des débits effectifs de renouvellement d'air", CSTB GEC/DAC-90.101R, Champs-Sur-Marne.
5. Simiu, E. and Scanlan, H. (1986), *Wind Effects on Structures - An Introduction to Wind Engineering*, Wiley, New York.

**Ventilation for Energy Efficiency and Optimum
Indoor Air Quality
13th AIVC Conference, Nice, France
15-18 September 1992**

Paper 5

**A New Method For Linking Results of Detailed Air
Flow Pattern Calculation With Multizone Models.**

A. Schälin^{*}, V. Dorer^{}, J. Van der Maas^{***}, A.
Moser^{*}**

*** Energy Systems Laboratory (LESO), Swiss
Federal Institute of Technology of Zurich
(ETHZ), ETH-Zentrum, CH-8092 Zurich,
Switzerland**

**** EMPA, Section 175, CH-8600 Dübendorf,
Switzerland**

***** LESO-PB, Ecole Polytechnique Fédérale de
Lausanne, CH-1015 Lausanne, Switzerland**

Synopsis

Multi-zone models are a common tool for calculating air and contaminant exchange within rooms of a building and between building and outdoors. Usually a whole room is then modelled by one calculation node with the assumption of homogeneously mixed conditions within this room whereas in real cases temperature and contaminant concentrations vary in space. The exchange to the neighbouring nodes via the flow paths is then a function of the local values of these variables. Detailed knowledge can be obtained from the solution of the transport equations for the air flow pattern within the room at the expense of far higher computation cost.

This work shows a new approach called "method of detailed node values" to include results from detailed calculations in multi-zone models to give a better description of the real cases. Parameter transfer between a multi-zone program and a detailed air flow simulation program is discussed for different flow paths of practical importance.

The method is demonstrated in an example case with air in/exfiltration, ventilation and contaminant propagation, and discussed in a second example with large openings. This new method promises to improve the multizone model predictions with few additional CFD computations.

1. Introduction

Multizone models are computer tools for calculating air and contaminant exchange between rooms of a building and between the building and outdoors. Usually a whole room is modeled by one calculation node (a zone) under the assumption of homogeneous conditions within this room.

In real cases, however, temperature and contaminant concentrations vary in space. The exchange to the neighbouring nodes is then a function of the local values of these variables near the flow paths within each zone. Examples where detailed results are important for the multizone problem include:

- detailed multizone indoor air quality and detailed multizone ventilation efficiency simulations
- pollutant spread from a zone with a non-homogeneous concentration (i.e. a local source) into other rooms and therefore a complex room concentration pattern
- rooms with thermal stratification (e.g. displacement ventilation, open doors and windows)

Detailed knowledge can be obtained from the field solution of the transport equations for the air flow pattern within the room, at the expense of relatively high computation cost. Methods to include detailed results in multizone pro-

grams are therefore desirable to improve the predictions of the whole building transport behaviour.

On the other hand, it can quite generally be useful to calculate the boundary conditions for a specific ventilation problem and for desired climatic conditions with the multizone program. This holds especially for cases with a combined mechanical/natural ventilation system, i.e. small mechanical exhaust systems with inlets and infiltration paths considerably influenced by stack and wind pressures.

This work shows a new approach to include results from detailed single-room calculations in multizone models to give a better description of the real cases. Parameter transfer between a multizone program and a detailed air flow simulation program is discussed. The method is then applied to an example case with air infiltration and exfiltration, ventilation and contaminant propagation. For the case of an open door or window, detailed information on the risk for cold draughts and uncomfortable temperature gradients can be obtained.

The presented method may thus be very helpful in the conceptual and the design stages of advanced ventilation systems for residential and small office buildings.

2. Method for linking results of detailed air flow pattern calculation with multizone models

2.1. Brief description of multizone models

In a multizone model a building is represented by a network of nodes and links (flow paths) between nodes. Usually a whole room is modeled by one calculation node (a zone) with the assumption of homogeneous conditions within this room. Different connections (flow paths) between zones are described by functional relationships between mass flow and pressure difference. Figure 1a shows a simple example of a house, and Figure 1b its network representation for the multizone modeler.

A system of algebraic equations derived from mass continuity is then set up. The equations are explicitly solved for pressure, and mass flow; humidity and concentrations of contaminants are then derived from the calculated mass flow rates. Temperature is used as a known input for the calculation of the mass flow between two nodes; even stratification profiles can be provided as input to the presently used program COMIS [Feustel et al. 1990, 1992].

In the example of Figure 1b the node values 1 and 2 are calculated; the other nodes serve as boundary conditions. The results are in general time-dependent in accordance to the climatic data used in the input.

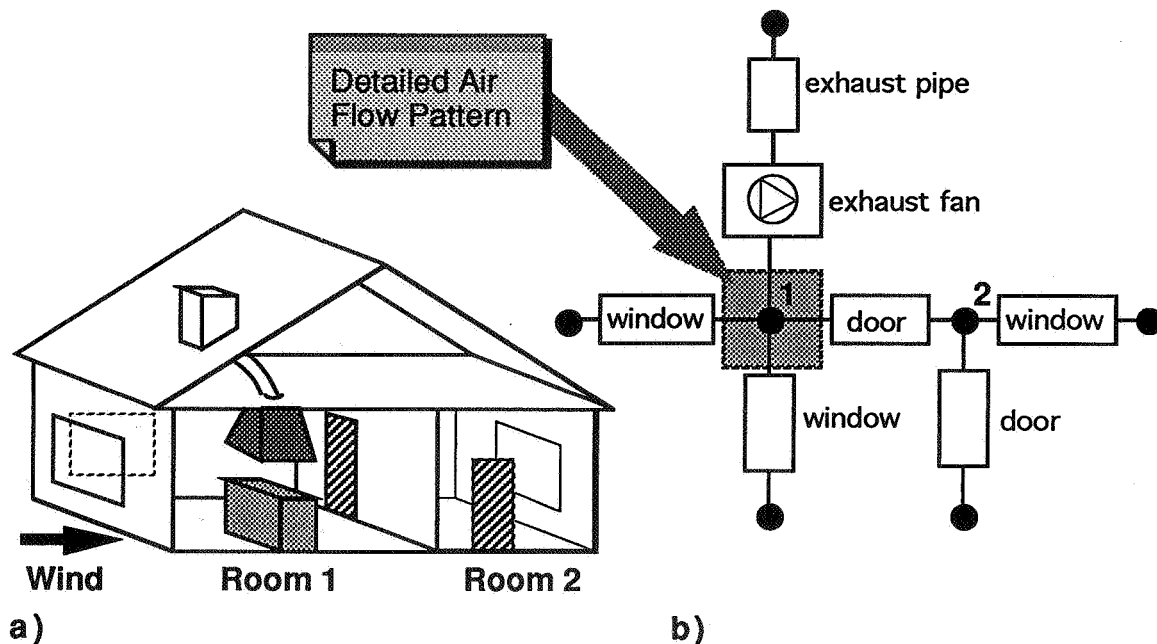


Figure 1: a) Example house with two rooms. The left room with internal details shown is the one chosen for the CFD calculation. b) Multizone network of the whole building.

The case of an open door or window is traditionally treated by keeping the inside temperature fixed. New modules under development for COMIS provide estimates for the time dependence of temperature and temperature gradients, and CFD can give a detailed picture of the velocity and temperature field.

2.2. Brief description of a CFD program

In a CFD (Computational Fluid Dynamics) program for the calculation of a single-room air flow pattern, the room is divided into a large number of cells (typically 10'000) and for each cell transport equations for mass, momentum, energy, turbulence quantities and concentrations of contaminants are solved. Variables solved for and under discussion for this application are: pressure, velocity components, temperature and contaminant concentrations. Turbulence variables depend on the turbulence model used and are not of concern for the present application.

In the present example the commercial code PHOENICS was used [Rosten and Spalding 1987, Chen et al. 1990]. The calculations have been performed in steady state, but could also be solved for time-varying boundary conditions. In most cases it is usually preferred to calculate stationary solutions for three or four different boundary conditions rather than the dynamical behaviour of the room air flow.

2.3. Evaluation of a method

A new method had to be worked out for combining detailed air flow pattern results with multizone programs, because no previous work is known for such an application.

At first an approach was considered to enhance the resolution of the multizone program itself by including several horizontally and vertically divided subzones with appropriate flow paths between them. The subdivision of a room in subzones should be done depending on the characteristic flow patterns. Figure 2a shows an example of a room with a radiator (after Inard et al. 1991) with 5 subzones and a predominant flow pattern in each subzone. The detailed air flow pattern calculation should then give details for each subzone.

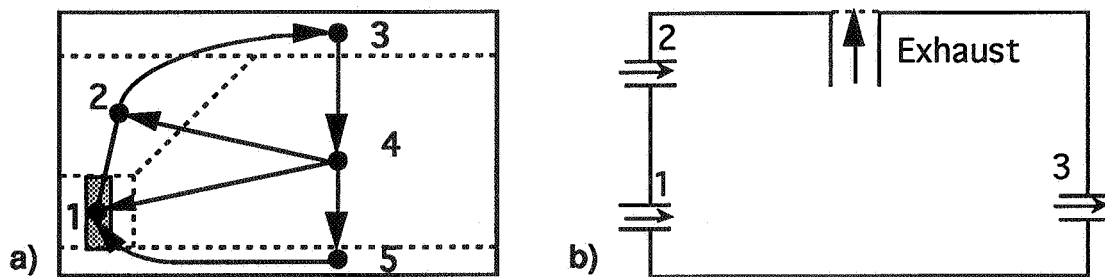


Figure 2: a) Substructuring in subzone model for a room with radiator (after C. Inard, 1991). b) Interface of new method for example room 1 of Figure 1: 1,2 window infiltration paths, 3 door exfiltration path, and kitchen exhaust.

For this situation Inard et al. (1991) obtained good agreement with measured data, but the flow pattern had to be known in advance. In a general case it is difficult to divide a room in such subzones. Even if it is possible in one case, a moderate parameter variation can change the flow pattern of the whole room and the division in ordered subzones has to be modified. As a further problem the available COMIS code cannot handle the desired subzones.

So another approach deferring all the detailed calculation to the CFD code was chosen. The complete room air flow pattern of one zone or node is calculated by CFD with appropriate boundary conditions at the connections to the other nodes. The remaining problem is then basically a discussion of the interface values at the connections to other nodes between the multizone program and the CFD program.

A suggested preliminary name of the whole method is "method of detailed node values". Instead of one average variable value (C_1 and C_2 for the nodes 1 and 2 in the example of Figure 1b and 2b), a different variable value is provided for each flow path connected to the considered node(s) (as indicated in Figure 2b).

3. Interface parameters

3.1. Flow paths considered

Multizone programs like COMIS provide many flow paths which the user can choose for his particular needs. We discuss here only those of practical importance for the present connection to air flow calculations:

- Fans (ventilation supply, exhaust), flow controller
- Leakage flow paths with infiltration or exfiltration
- Large openings (open doors, open windows)

In the example case the method is applied to some of these flow paths. An application to cases with large openings is shortly outlined in principle.

3.2. Input and output parameters

All the variables mentioned in Sections 2.1 and 2.2 can be transferred from one program to the other but will be handled differently. For each of the two programs they can be either input value (i.e. boundary condition) or output value (i.e. a result) or irrelevant, depending on the flow direction and the type of flow path.

- Pressure: The node pressure as a result of the multizone program can be given to the CFD code, but is irrelevant in the case of a single-room calculation as discussed here. In a case where a flow path like an exhaust pipe would be included in the calculation domain it could be used. However it is generally preferred to use velocity boundary conditions rather than pressure boundary conditions for numerical reasons. However it is possible to transfer local pressure differences due to temperature or air velocity differences to the multizone program allowing for higher accuracy (Figure 6c gives an impression of the local pressure field in a room).
- Velocities or mass flow belong to the main variables of concern here. Usually the multizone model will calculate first the whole network and therefore the resulting mass flows provide the boundary conditions for the CFD code. In some cases however (e.g. in a room with several large openings) it can also depend on the local air flow pattern and therefore be an unknown.
- Temperature and gradients as a result of the CFD calculation can in some cases be given back to the multizone program and be used as input for a calculation with higher accuracy.
- Concentrations are the other main variables of concern. They will be input or output variable depending on the flow direction.

	Velocity	Temperature	Concentrations
Ventilation inlet	i	i	i
Ventilation outlet	i	o	o
Leakage infiltration	i	i	i
Leakage exfiltration	i	o	o
Large opening	i/o	i/o	i/o

Table 1: Input(i) and output(o) parameters for CFD program for different flow paths.

Table 1 shows an overview of input and output parameters for different flow paths, as seen from the CFD program. The role of the different variables depends mainly on the flow direction. The case of the large opening must be treated specially because bi-directional flow is possible and often occurs.

All the output parameters which are results from CFD calculations will then be fed back to the multizone program. In some cases it is even possible that the mass flow depends strongly on the local conditions (e.g. in a room with two large openings). In such cases the whole procedure can be repeated two or three times, i.e. the CFD results are fed back into the multizone program which is run another time, and the new results put again into the CFD program and so on. This procedure could be called an external iteration.

For the contaminant transport the new concentrations (the above-mentioned output parameters) can be fed directly into the contaminant modules of the multizone program without a second run. The Swiss version of COMIS (called COMERL) which was actually used for this application was adapted for this special type of input. With such local values, also time-dependent contaminant concentrations can be calculated under the assumption that the room air flow pattern remains unchanged.

4. Example cases

The first example (sections 4.1 to 4.4) shows how the air flow pattern in a room in a simple building is calculated with a CFD program while most boundary conditions are given from the output of a multizone program. From the CFD results temperature and concentrations at those locations where outflow occurs can be fed back to the multizone program. The contaminant transport can be calculated with the new input values.

The second example (in section 4.5) gives a short discussion on cases with large openings.

4.1. Case description

We consider the typical residential building from Figure 1. The situation represents a living room and kitchen combination, as seen in more details in Figure 3. The kitchen ventilation is mechanically forced by an exhaust system above the cooking plate running at $200 \text{ m}^3/\text{h}$. The cooking plates are assumed to have a convective heat transfer of 500 W to the air. For the cooking process a unit contaminant source of $S=0.01 \text{ ml/s}$ is assumed (For a weight factor of 1.0, it corresponds to an olfactory source of 1 olf [Fanger 1989]). For higher source strengths, the concentration results (given in ppm) can be scaled up by the same factor. The walls are treated as adiabatic.

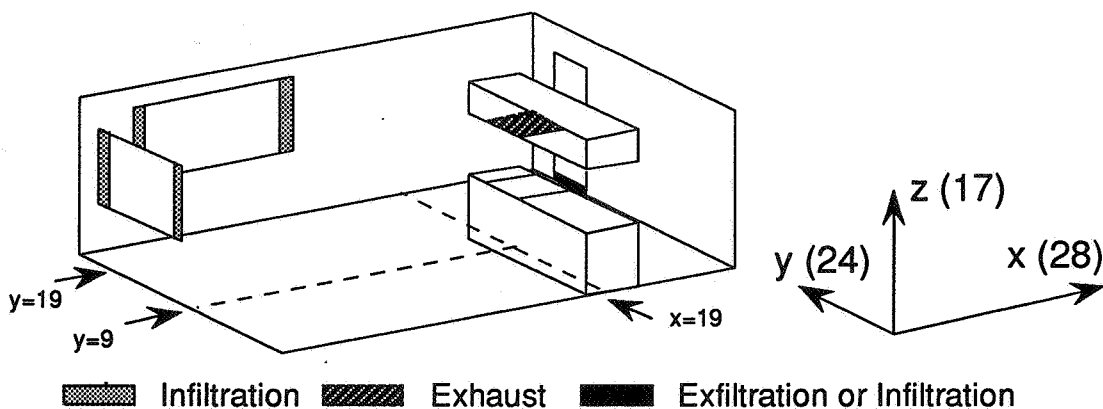


Figure 3: Sketch of the living room & kitchen, with two windows and infiltration area, kitchen combination and exhaust, and door and exfiltration area. To the right the number of cells in each direction are given, with a total of 11424 cells for the CFD program.

4.2. Input from multizone program

The values for the crack flow through the windows and the internal door into the adjacent room have been calculated with the multizone program for two meteorological wind conditions assuming typical building wind pressure and leakage data, and exhaust fan characteristics. The cracks have been modeled by rather large areas because of the coarse grid resolution chosen; a finer grid would only change the resulting air flow pattern in the near-crack region, and is not needed in the present example.

In the first situation (case K4) without wind, half of the exhaust volume flow is infiltrated from the windows, the other half from the adjacent room (through the door). In the second situation (case K5) a strong wind (10 m/s) has been assumed from the left which leads to a total infiltration through the window cracks of $240 \text{ m}^3/\text{h}$, and therefore to an exfiltration of $40 \text{ m}^3/\text{h}$ through the door crack to the adjacent room.

The temperature of the outside air was assumed to be 20°C, and of the air from the second room 22°C; contaminant concentration of inflowing air is 0. A list of these parameters is contained in Table 2.

4.3. CFD results

Figure 4 shows as an illustration, for case K5, the resulting air flow pattern, temperature and contaminant concentration contour lines in the planes $y=9$ and 19, and $x=9$. The position of these planes (in units of cell numbers) is indicated in Figure 3. The air inflow at the window cracks and outflow at the exhaust and near the bottom of the door, temperature stratification in the room (21°C near the bottom, and +1K/m) and contaminant distribution can be nicely seen. The stratification would be important for the multizone problem specially in connection with large openings.

Table 2 gives also the results (bold face) of the variable values at the flow paths to the neighboured nodes (exhaust and door crack) for cases K4 and K5.

Case K4 (no wind)	Volume flow	Velocity	Temperature	Concentration
Window, Inf.	100 m ³ /h	0.03 m/s	20°C	0
Door, Inf.	100 m ³ /h	0.35 m/s	22°C	0
Exhaust	- 200 m ³ /h	0.09 m/s	24.5°C	0.18

Case K5 (wind)	Volume flow	Velocity	Temperature	Concentration
Window, Inf.	240 m ³ /h	0.07 m/s	20°C	0
Door, Exf.	- 40 m ³ /h	0.14 m/s	21°C	0.09
Exhaust	- 200 m ³ /h	0.09 m/s	24.5°C	0.185

Table 2: Input parameters and results (bold) for the two cases K4 and K5.

4.4. Results of the detailed node value method

In the present example, the most interesting results are those for the contaminant concentrations. Table 3 compares the results of the multizone program a) under the usual assumption of homogeneous mixing, and b) with the CFD result as additional input. Figure 5 illustrates the terminology of the following analytical discussion.

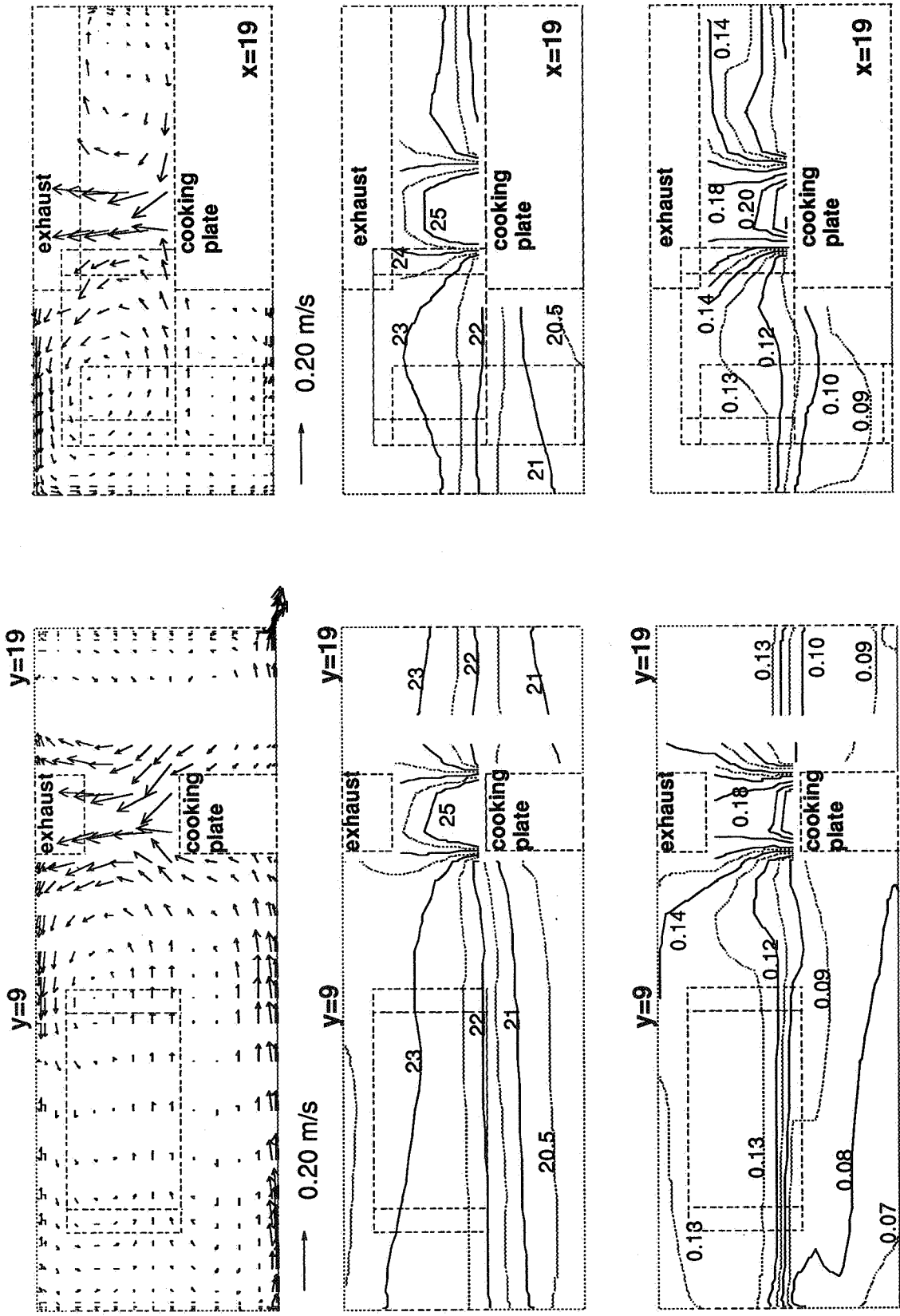


Figure 4: Case K5. Left column: y-planes y=9 and y=19 (see Figure 3). Right column: x-plane x=19. Top row: Air flow field. Medium row: Temperature contour lines. Bottom row: Contaminant concentration contour lines. The source is situated above the cooking plate.

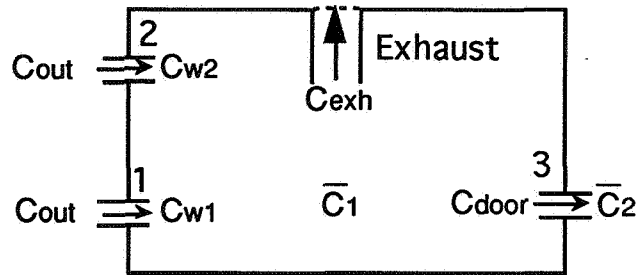


Figure 5: Terminology for case K5.

In the no-wind case (K4) also the door is an inflow path. The balance for node 1 (our example room) states then for the volume flow rates ($\dot{V} = \dot{m} / \rho$):

$$\dot{V}_{w1} + \dot{V}_{w2} + \dot{V}_{door} = \dot{V}_{exh} \quad (1)$$

For the contaminant concentration (we consider one contaminant species) we get for the multizone model:

$$\dot{V}_{w1} C_{outdoor} + \dot{V}_{w2} C_{outdoor} + \dot{V}_{door} C_2 + S = \dot{V}_{exh} C_1 \quad (2)$$

The outdoor concentration $C_{outdoor}$ and the concentration in the adjacent room C_2 are 0 because the contaminant source is inside of Room 1. C_1 is the average concentration in Room 1, which is in this simple case calculated by

$$C_1 = \frac{S}{\dot{V}_{exh}} = 0.18 \text{ ppm} \quad (3)$$

The detailed node value method leads to the same concentration result at the exhaust because there is only one outflow port. Note that in this case the concentration in the typical occupied area in Room 1 is 0.11 ppm, also lower than the calculated C_1 .

Case K4 (no wind)	Room 1	Room 2	Exhaust
a) Multizone only (perfect mixing)	0.18 ppm	0	0.18 ppm
b) Detailed node value method	0.11 ppm	0	0.18 ppm

Case K5 (wind)	Room 1	Room 2	Exhaust
a) Multizone only (perfect mixing)	0.15 ppm	0.15 ppm	0.15 ppm
b) Detailed node value method	0.12 ppm	0.09 ppm	0.185 ppm

Table 3: Node value concentrations for the nodes living room & kitchen (Room 1), adjacent room (Room 2) and exhaust, in the two cases K4 and K5. For Room 1 typical values in a height of 1.6 m have been taken.

In the wind-case (K5) Equation 2 for the multi-zone model, again with $C_{out} = 0$, is changed to:

$$S = \dot{V}_{exh} C_1 + \dot{V}_{door} C_1 \quad (4)$$

The multizone average value C_1 is then 0.15 ppm, whereas the detailed node value method equation reads as

$$S = \dot{V}_{exh} C_{exh} + \dot{V}_{door} C_{door} \quad (5)$$

The concentrations are $C_2 = C_{door} = 0.09$ ppm in the adjacent room near the door and $C_{exh} = 0.185$ ppm for the exhaust from the CFD results (the values can be read approximately from Figure 4).

In this simple example, which was chosen to illustrate the essential features, no additional multizone run was necessary to produce the desired results, but in a general case the procedure would go on as described in Section 3. For a time-dependent multizone calculation, e.g., of a time-dependent source $S(t) = S_0 f(t)$, the above results could also be applied, e.g., to the concentration in Room 2 being $C_2(t) = C_{door} f(t)$. This is based on the assumption that the room air flow pattern is still the same. This is fulfilled in the present example, but must be verified in a general case; otherwise more CFD runs are needed to give additional informations.

4.5. Open doors and windows

A multizone program calculates mass and heat flow through open doors and windows by using simplified algorithms based on the Bernoulli equation (Schaelin et al. 1992). The algorithm uses the average zone temperatures (both air and wall temperatures can be used) and an estimated linear zone temperature gradient. Also estimates for the velocities in the opening plane can be made available. However no information is available on the vertical and horizontal variation of the air temperature gradient as a function of the opening arrangement.

A link to a CFD program should be very helpful to predict the ventilation efficiency as a function of the position of the openings, and could indicate when cold draughts at floor level become a problem (CFD can help finding comfort problems with open doors and windows), e.g. as a function of the opening angle or when more than one window are opened.

Figure 6 shows air flow pattern, temperature and pressure contour lines of a twodimensional calculation of a room with an open door and a heater inside. The CFD computation domain includes the outdoor environment in this case. This example serves as an illustration how the temperature and pressure vary

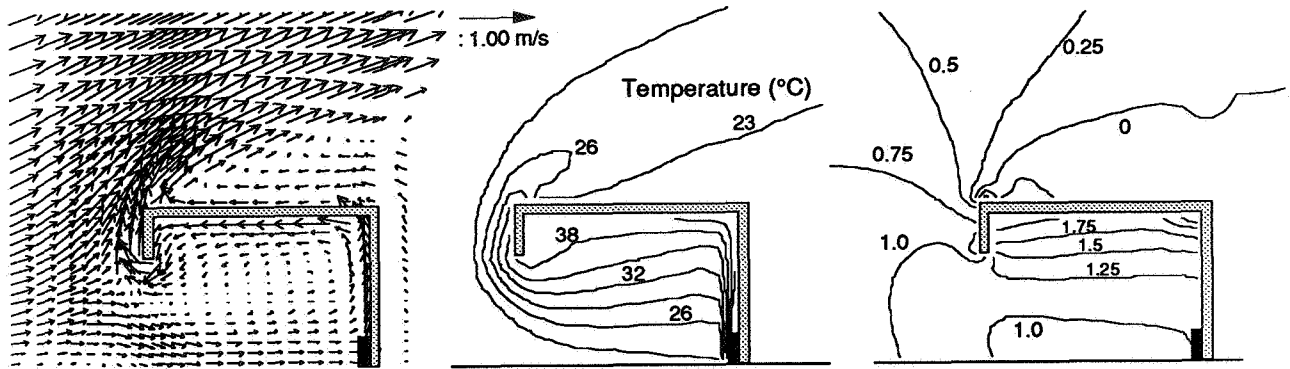


Figure 6: Air flow pattern, temperature and pressure contour lines of a room with an open door and a heater inside (calculation from Schaelin et al. 1992).

inside the room. The pressure varies in this example due to stagnation pressure of the wind, due to the temperature stratification and, in the corners, due to the deceleration of the air flow.

5. Conclusions

- A new method for linking CFD detailed air flow pattern results with multizone models has been presented. The accuracy of results of multizone simulations is limited by the assumption of homogeneously mixed conditions in each node. This condition is violated in many cases of practical importance. Therefore the accuracy can be considerably enhanced by the presented method.
- The proposed name of the method is "method of detailed node values". Instead of one variable value used for each node, a different value is provided for each flow path connected to that node.
- The method is demonstrated with a simple example and shows a more accurate prediction of the contaminant spread. The method can and will be expanded to more complicated cases. It can be used to determine detailed transfer values of all the variables solved in the multizone program like pressure, mass flows, temperature and contaminant concentrations.
- The method so far is suited for applications to cases where detailed air flow knowledge in a few rooms or only one room (in the important ones) is sufficient to give a better prediction of the overall air and contamination transport. In these cases, the method promises to improve the multizone model predictions with few additional CFD computations.

Acknowledgements

This work was financially supported by the Swiss Federal Office of Energy (BEW). The authors are grateful to Q. Chen, now at the Institute of Applied Physics, TNO Industrial Research, Delft, Netherlands, for preliminary discussions.

References

- Chen, Q.; A. Moser; and A. Huber. 1990. Prediction of buoyant, turbulent flow by a Low-Reynolds-number $k-\epsilon$ model. ASHRAE Trans., Vol. 96, pp. 3366-3375.
- Fanger P.O. 1989. The new equation for indoor air quality - The Human Equation: Health and Comfort. Proc. Indoor Air Quality 89, San Diego, Ca., ASHRAE, pp. 1-9.
- Feustel, H.E.; and A. Rayner-Hooson. 1990. Fundamentals of the multizone air flow model - COMIS. Technical Note AIVC 29. AIVC, Coventry, GB..
- Feustel, H.E.; and A. Rayner-Hooson. 1992. COMIS 1.0 - User Guide. AIVC, Coventry, GB.
- Inard C.; and D. Buty. 1991. Simulation of thermal coupling between a radiator and a room with zonal models. Proc. 12th AIVC Conference, Ottawa, Canada, 24-27 Sept. 1991.
- Rosten, H.I.; and D.B. Spalding. 1987. The PHOENICS reference manual, for Version 1.4, Report No. TR/200. London: CHAM Ltd.
- Schaelin, A.; van der Maas, J.; and A. Moser. 1992. Simulation of Airflow through Large Openings in Buildings. ASHRAE Trans., Vol. 98, BA-92-2-4.